Numerical Evaluation of Pre-Damaged Beams Using Recycled Concrete Aggregate Strengthened by FRP Sheets

التقييم العددي للجسور الخرسانية التي تعرضت للتلف باستخدام ركام الخرسانة المعاد تدويره المعزز بألواح البوليمر المقوى بالألياف

by

MOHAMMED ASHRAF MOUSTAFA MOHAMMED

Dissertation submitted in partial fulfilment
of the requirements for the degree of
MSc STRUCTURAL ENGINEERING at
at
The British University in Dubai

September 2022

DECLARATION

I warrant that the content of this research is the direct result of my own work and that any use made in it of published or unpublished copyright material falls within the limits permitted by international copyright conventions.

I understand that a copy of my research will be deposited in the University Library for permanent retention.

I hereby agree that the material mentioned above for which I am author and copyright holder may be copied and distributed by The British University in Dubai for the purposes of research, private study or education and that The British University in Dubai may recover from purchasers the costs incurred in such copying and distribution, where appropriate.

I understand that The British University in Dubai may make a digital copy available in the institutional repository.

I understand that I may apply to the University to retain the right to withhold or to restrict access to my thesis for a period which shall not normally exceed four calendar years from the congregation at which the degree is conferred, the length of the period to be specified in the application, together with the precise reasons for making that application.

____

Signature of the student

COPYRIGHT AND INFORMATION TO USERS

ABSTRACT

Fiber reinforced polymers (FRPs) are being increasingly used nowadays as an effective rehabilitation method to repair beams, columns, slabs caused by structural flaws that are a result of the aging of the service life of building structures. Numerical evaluation were conducted to evaulate the behaviour of recycled reinforced concrete (RCA) beam samples; additionally, normal weigh aggregate (NWA) beam as control sample strengthened by carbon fiber reinforced polymer (CFRP). Th research aims to try and predict the effect of strengthening (RCA) reinforced beam samples with (CFRP) or without shear reinforcement on the shear capacities, deflections and damage mode types (Shear- Moment). To conduct this research, four numerical models were investigated, two models of (RCA) and two models of ($NWA\text{-}_{Control\ Samples}$) un-strengthened beams and strengthened beams with (CFRP-U) wrapping. The behaviour of strengthening the reinforced concrete beam with (RCA) without shear reinforcement is examined using three main parameters. The first parameter is type of loading, loads ranges from 81.7-130.9 KN for static and dynamic load. The second parameter is type of (FRP) carbon fiber, which has been used “Master Brace FIB 600/50 CFS” types. The third parameter is the concrete strength with different strengths varies from 64.5-77.00 MPa. All parameters mentioned above have been considered carefully in the numerical analysis of FRP strengthened the (RCA) beam samples.

The (RCA) beam type has been modelled using two models, one with 0.75% (5D) steel fibers in self-consolidating concrete matrix (SCC) and the other without it, but both models consist of 100 % coarse recycled aggregate (RCA), while (NWA) beam types are modelled without steel fibres with compressive strength 70.50 MPa and loads ranges from 120.1-130.1 KN. Using (SCC) and steel fibers are to enhance shear capacity by achieving the best performance of structure integrity. The analytical model cross-section of the beam is 200mm in depth, 150mm in width and 1600mm in length; three 12mm diameters rebars as bottom reinforcement. For more additional checking, two rebars of 12mm as top reinforcement for the cross section with all rebars having length of 1540mm. The longitudinal percentage of reinforcement was 1.45% , has been selected to warranty the shear failure of the experimental beam samples. This means that, no shear steel rebars have been used along the horizontal cross section of the beam, except for three closed stirrup rebars with 10mm diameter used at support locations with 300mm distance from each support, to prevent the concertation of stress and act as steel rebar hangers.

The research demonstrates the load path with distribution of stress/strain and deflection through both models under different values and types of loads using (FE) software which is represented through (ANSYS Workbench). The results show that the 3D modelling reflects some differences in deflection values between (RCA) by and (NWA) samples when un-strengthened or strengthened by (CFRP) laminates, and when using compression rebars as well. Nevertheless, no differences have been detected in shear load values under diverse types of experimental loadings. Likewise, 3D-(FE) model (ANSYS Workbench) illustrates the type and location of failure which confirms where retrofitting is needed. The numerical analysis and strengthening calculations are completed using (ACI 318-19& ACI 440-17) standards through (MIDAS Gen and MIDAS design plus); these calculations are then compared to experimental results. To close, numerical evaluations conducted via the finite element and Midas Design software present good prediction of stress, load path, and failures especially shear failure of (RCA) reinforced beam strengthened by external-bonded (CFRP) laminates and identical strengthening calculations.

Keywords:

Recycled concrete aggregate (RCA), fiber reinforced Polymer (FRP), Carbon fiber reinforced Polymer (CFRP), Carbon fiber reinforced Polymer U-Wrapping (CFRP-U), reinforced concrete beam (RC), Normal weight aggregate (NWA), Shear Strengthening, Retrofitting, self-consolidating concrete matrix (SCC), ACI318-19, ACI 440-17R, Finite element (FE), Ansys Workbench, Midas Design Plus, Midas Gen.

الملخص

تم استخدام البوليمر المقوى بالألياف بشكل متزايد في الوقت الحاضر كطريقة فعالة لإعادة التأهيل في المباني، بسبب العيوب الهيكلية وتقادم هياكل المباني، لذلك فهي طريقة فعالة لإصلاح الكمرات والأعمدة والأسقف الإنشائية.

يقوم البحث بإجراء تقييماً عددياً لمعرفة سلوك عينات الكمرات الخرسانة المسلحة بالركام المعاد تدويره، بالإضافة إلى العينات ذات الركام العادي كعينة تحكم (بدون استخدام حديد تسليح لمقاومة القص)، عند تقويتها بالبوليمر المقوى بألياف الكربون. الغرض من إجراء هذا النوع من البحث هو محاولة التنبؤ بتأثير التقوية باستخدام بالبوليمر المقوى بألياف الكربون على عينات الكمرات الخرسانة المسلحة بالركام المعاد تدويره بدون تقوية القص على أنماط الهبوط والتلف الناتج عن (العزوم - القص). نتيجة لذلك، سيتم فحص أربعة نماذج عددية، نموذجان من عينات ركام الخرسانة المعاد تدويره، ونموذجان من الخرسانة ذات الركام العادي مثل (عينات التحكم) في حالة انها غير مقواه ومعززة ومن ناحية أخرى مقواه ومعززة بلفائف البوليمر المقوي بألياف الكربون على شكل حرف (U).

تمت دراسة سلوك تقوية الكمرات الخرسانية المسلحة المستخدم بها الركام المعاد تدويره بدون تقوية القص، باستخدام ثلاث عوامل رئيسية. العامل الاول هو نوع التحميل، وتتراوح الأحمال من 81.7-130.9 كيلو نيوتن للحمل الثابت والديناميكي. العامل الثاني هو نوع البوليمر (الياف الكربون)، وقد تم استخدام نوع FIB 600/50 CFS من شركة Master Brace. العامل الثالث وهو إجهاد الخرسانة المستخدمة بأنواع مختلفة، وتتراوح من 64.5-77.00 ميجا باسكال. تم أخذ جميع العوامل التي تم ذكرها في الاعتبار بعناية أثناء القيام بالتحليل العددي لعينات الكمرات الخرسانية المسلحة المستخدم بها الركام المعاد تدويره المعززة بألياف البوليمر.

تم نمذجة عينات الكمرات الخرسانية المسلحة المستخدم بها الركام المعاد تدويره في نموذجين، أحدهما يحتوي على 0.75٪ من الألياف الفولاذية من نوع (5D) في مصفوفة خرسانية ذاتية الدمك والنموذج الاخر بدونها، ولكن كلا النموذجين يستخدمان مع ركام خشن معاد تدويره بنسبة 100٪ ، بينما تم نمذجة أنواع من الخرسانة ذات الركام العادي بدون ألياف فولاذية بقوة ضغط 70.50 ميجا باسكال وتتراوح الأحمال من 120.1-130.1كيلو نيوتن. تتمثل مزايا استخدام ألياف الصلب والألياف الفولاذية في تعزيز قدرة القص من خلال تحقيق أفضل أداء لسلامة الهيكل. علاوة على ذلك، سيتم تحسين ليونة وتشقق عينات الكمرات الخرسانية المسلحة المستخدم بها الركام المعاد تدويره. من ناحية أخرى، القطاع العرضي للنموذج التحليلي للعينه يبلغ عمقه 200 مم وعرض 150 مم وطول 1600 مم مع ثلاثة قضبان من حديد التسليح ذات القطر 12 مم كتدعيم سفلي

وللمزيد من الفحص الإضافي، فقد تمت إضافة عدد اثنان قضبان من حديد التسليح ذات القطر 12 مم كتعزيز علوي للقطاع العرضي، مع العلم ان جميع قضبان حديد التسليح يبلغ طولها 1540 ملم. من ناحية أخرى، نسبة حديد التسليح الطولية للتعزيز 1.4% والتي تم اختيارها لضمان فشل القص. بمعنى آخر، لم يتم استخدام قضبان حديدية لمقاومة تأثير القص على طول الكمرة الخرسانية؛ على الرغم من ذلك، تم استخدام ثلاثة كانات مغلقة بقطر 10 مم في مواقع بطول 300 مم من الركائز لمنع تضافر الضغط وكونها أيضا حاملات حديدية فولاذية لقضبان الحديد العلوية والسفلية.

يوضح البحث مسار الحمل مع توزيع الإجهاد / الانفعال والهبوط من خلال كلا النموذجين تحت قيم وأنواع مختلفة من الأحمال باستخدام برنامج العناصر المحدودة والمتمثل في(ANSYS Workbench) حيث توضح النتائج أن النمذجة ثلاثية الأبعاد تظهر بعض الاختلافات في قيم الانحراف بين عينات الكمرات الخرسانية المسلحة المستخدم بها الركام المعاد تدويره وعينات الخرسانة ذات الركام العادي عندما لا تكون مقواه أو مقواه بواسطة رقائق البوليمر المقوي بألياف الكربون، وعند استخدام قضبان الضغط أيضًا، بينما لم يتم العثور على فروق في قيم أحمال القص تحت أنواع مختلفة من الأحمال التجريبية التي استخدمت في التحليل العددي وبين التي استخدمت في المختبر عند اجراء التجارب. بالإضافة إلى ذلك، يوضح نموذج ثلاثي الابعاد باستخدام برنامج (ANSYS Workbench) نوع وموقع الانهيار او التشقق الذي يؤكد أن هناك حاجة إلى التعزيز والتقوية. أيضا تم إجراء التحليل العددي الحسابي وحسابات التقوية وفقًا لمعايير الكود الأمريكي لتصميم المنشآت الخرسانية باستخدام برنامج (Midas Gen) والكود الأمريكي لترميم القطاعات الخرسانية باستخدام البوليمر المعزز بالألياف باستخدام برنامج (Midas Design Plus) ومقارنتها بالنتائج التي تم إجراؤها في المختبر. بشكل عام، أوضحت التقييمات العددية باستخدام برامج العناصر المحدودة تنبؤًا جيدًا بالإجهاد ومسار الحمل ونوع الانهيار، وخاصة انهيار القص للكمرات المستخدم فيها الركام المعاد تدويره من الخرسانة المعززة والمدعومة بشرائح لفائف البوليمر المقوي بألياف الكربون على شكل حرف (U).، بالإضافة إلى حسابات تقوية مماثلة وفقا لاشتراطات الكود الأمريكي للخرسانة المسلحة والكود الأمريكي الخاص بالتدعيم باستخدام البوليمر المعزز بالألياف.

DEDICATION

I dedicated my work to my parents, who taught me to trust first in Allah and then in myself in order to pursue my objectives in life with confidence and faith.

I also dedicated this work to my F.P, who helped me complete it and encouraged me to reach my objectives, as well as to the rest of my family and friends.

ACKNOWLEDGEMENT

Preparing this dissertation was a tremendous task. I'd want to offer my heartfelt appreciation to everyone who has helped and encouraged me to accomplish my high graduate studies.

Prof. Abid Abu Tair and Dr. Gul Ahmed Jokhio deserve special thanks for their guidance and advice during the whole process of completing the job.

I'd like to thank Prof. Sherif Yahia and Dr. Ghanim Kashwani for their encouragement and assistance.

Sincere gratitude is extended to my instructors and the whole team at the British University in Dubai for their assistance.

Special thanks to **Midas Research and Development Centre- India** for their assistance and for supporting me with all of the necessary material and software to finish the study.

TABLE OF CONTENTS

NOTATIONS

Scope

-All notations used in this dissertation will be defined in this chapter.

$A_c =$ cross-sectional area of concrete in compression member, (mm^2)

$A_{cw} =$ area of concrete section of individual vertical wall, (mm^2)

$A_e =$ cross-sectional area of effectively confined concrete section, (mm^2)

$A_f =$area of FRP external reinforcement, (mm^2)

$A_{fanchor} =$ area of transverse FRP U-wrap for anchorage of flexural FRP reinforcement, (mm^2)

$A_{fv} =$ area of FRP shear reinforcement with spacing *s*, (mm^2)

$A_g =$ gross area of concrete section, (mm^2)

$A_{sc} =$area of the longitudinal reinforcement within a distance of w_f in the compression region, (mm^2)

$A_{sw} =$area of longitudinal reinforcement in the central area of the wall, (mm^2)

$b =$ width of compression face of member, in. (mm)

$C_E =$ environmental reduction factor

$d =$ distance from extreme compression fiber to centroid of tension reinforcement, (mm)

$d' =$distance from the extreme compression fiber to the center of A_{sc}, (mm)

$E_c =$modulus of elasticity of concrete, (MPa)

$E_f =$tensile modulus of elasticity of FRP, (MPa)

$E_s =$modulus of elasticity of steel, (MPa)

$f_C =$compressive stress in concrete, (MPa)

$f'_C =$specified compressive strength of concrete, (MPa)

$f_{CC}' =$compressive strength of confined concrete, (MPa)

$f_f =$stress in FRP reinforcement, (MPa)

f_{dh} =design stress of externally bonded FRP reinforcement, (MPa)

f_{fe} = effective stress in the FRP; stress attained at section failure, (MPa)

f_{fu} = design ultimate tensile strength of FRP, (MPa)

$f_{fu}{}^{*}$ = ultimate tensile strength of the FRP material as reported by the manufacturer, (MPa)

K =ratio of depth of neutral axis to reinforcement depth measured from extreme compression fiber

K_1 = modification factor applied to κ_v to account for concrete strength

K_2 = modification factor applied to κ_v to account for wrapping scheme

K_f = stiffness per unit width per ply of the FRP reinforcement, (N/mm); $k_f = E_f t_f$

L_e = active bond length of FRP laminate, (mm)

N = number of plies of FRP reinforcement

n_f = modular ratio of elasticity between FRP and concrete = E_f/E_c

n_s = modular ratio of elasticity between steel and concrete = E_s/E_c

s_f = center-to-center spacing of FRP strips, (mm)

T_f = tensile force in FRP, (N)

T_g = glass-transition temperature, (°C)

T_{gw} = wet glass-transition temperature, (°C)

T_{st} = tensile force in A_{st}, (N)

T_{sw} = tensile force in A_{sw}, (N)

t_f = nominal thickness of one ply of FRP reinforcement, (mm)

t_w = thickness of the existing concrete shear wall, (mm)

V_c =nominal shear strength provided by concrete with steel flexural reinforcement, (N)

V_f = nominal shear strength provided by FRP stirrups, (N)

V_s = nominal shear strength provided by steel stirrups, (N)

w_f = width of FRP reinforcing plies, (mm)

ε_f = strain in the FRP reinforcement, (mm/mm)

ε_{fd} = debonding strain of externally bonded FRP reinforcement, (mm/mm)

ε_{fe} = effective strain in FRP reinforcement attained at failure, (mm/mm)

ε_{fu} =design rupture strain of FRP reinforcement, (mm/mm)

$\varepsilon_{fu}{}^*$ =ultimate rupture strain of FRP reinforcement, (mm/mm)

ε_{ccu} =ultimate axial compressive strain of confined concrete corresponding to 0.85fcc′ in a lightly confined member (member confined to restore its concrete design compressive strength), or ultimate axial compressive strain of confined concrete corresponding to failure in a heavily confined member

V_f = nominal shear strength provided by FRP stirrups, (N)

$\emptyset$ =strength reduction factor

k_a = efficiency factor for FRP reinforcement in determination of f_{cc}' (based on geometry of cross section)

k_b = efficiency factor for FRP reinforcement in determination of ε_{ccu} (based on geometry of cross section)

k_v = bond-dependent coefficient for shear

ψ_f =FRP strength reduction factor

LISTS OF EQUATIONS

LIST OF FIGURES

LISTS OF TABLES

CHAPTER 1

1. INTRODUCTION

1.1 Fiber Reinforced Polymer in Construction Repairing

Many problems have recently been discovered in structures, causing damage and deterioration. In other words, deteriorations such as cracks and concrete spalling are caused by reasons such as the end of a building's service life, unintentional impacts, corrosion of steel due to environmental threats, and in certain circumstances, poor engineering design. It's now more important than ever to find low-cost, quick-to-process repair options. It is now vital to identify repair solutions that are both low-cost and quick to process. Because of its high tensile strength, lightweight, corrosion resistance, high durability, and ease of installation, externally bonded FRP(Cao et al., 2005) has arisen as a novel structural strengthening technology in response to the rising demand for repair and strengthening of reinforced concrete structures. High-strength fibers incorporated in polymer resin characterize FRP. Carbon (CFRP), aramid (AFRP), or glass (GFRP) fibers are the most prevalent types of FRP used in the industry in different methods varies from Full to U-wrapping, Post-Tensioned Rods, Ropes-Strips and Grids. Externally bonded FRP composites (Abdalla Ghoneim, 2019) are used to repair beam constructions by attaching FRP laminates to the tensile face of the beam.

The application of FRP to reinforce and repair concrete beams has garnered the greatest attention among various forms of FRP. The research community analysed the test methodologies for evaluating FRP-concrete bond properties(Mukhtar FM, 2018).

1.2 Recycled Concrete Aggregate

In terms of low cost, environment and sustainability aspects, the needs to use recycled concrete aggregate (RCA)(Mohamed Ghoneim, 2020) increased. In other words, concrete waste makes up a large amount of landfills, and many of them are unable to handle its size and volume. Recycling these materials keeps them out of landfills and allows them to be utilised in various ways. Recycling also helps the environment by conserving energy that would otherwise be required to mine, process, or transport new aggregates. Despite that, the use of recycled aggregate in structural applications has been limited due of concerns regarding the diversity of recycled aggregate characteristics. Several studies were conducted to evaluate the characteristics of fresh and cured concrete with various amounts of coarse recycled material (Yehia, Crystals 2020, Silva, 2018). Moreover, studies conducting on recycled aggregate with self-consolidated concrete and fibers (Mohamed Ghoneim, 2020), shows improvement of the concrete's mechanical properties, flexure strength, and shear capacity, as well as helping to resist brittleness shear failure and providing a more ductile behaviour, including post-cracking tensile strength (Meddah, 2009, Gao et al., 2017). On the contrast, researches shows that using of recycled aggregate will leads to pre-damaged shear failure which needs strengthening like FRP wraps to enhance shear capacity(Mohamed Ghoneim, 2020).

1.3 Numerical Evaluation

Lately, numerical analysis is used as a preliminary method to estimate stress, straining actions, homogeneity of mix design, crack locations, and safety for any structure(Nawal K. Banjara, 2017). Therefore, in this study modelling of matrix of self-consolidated concrete beam containing coarse recycled material and fibers will be simulating to estimate stress, straining actions, crack locations, and then strengthening using FRP sheets in trying to match and comparing the lab experiment results conducted by (Mohamed Ghoneim, 2020) with numerical results .

1.4 Research Significance

The FRP strengthening are widely used in construction specially for pre-damaged structural members due to deterioration in order to increase structural member's capacity like beams. The use of FRP with self-consolidated concrete and steel fibers for structural members will enhance not only capacity but durability and corrosion resistance and long-time service life.

The research is quite needed to understand the behaviour of strengthened RCA beam by CFRP when no shear reinforcement is provided under different type of loading and parameters.

Moreover, comparison will be conducting between detailed model of pre-damaged beam samples strengthened/unstrengthen by CFRP in infinite element approach with actual study results done by (Mohamed Ghoneim, 2020) in lab on same sample, consequently; it allows the engineer to understand the stress distribution, load path and failure type with possible damaged areas along beam when no shear reinforced provided with CFRP laminates .

1.5 Research Challenge

In this research, the task is to develop a 3D model with boundary conditions that are consistent with the real case study and to guarantee that the load route is accurate and identical with applied load in the case study.

The 3D finite element model has been developed to study the behaviour of pre-damaged RCA concrete beam with CFRP laminates and without it when no shear reinforcement exists. With this process, it could be possible to predict the type of failure and weak points when strengthening this type of beams, in addition to the impact of RC matrix with RCA beam in order to enhance shear capacity of beams.

The strengthening with CFRP on reinforced concrete beams has been widely studied with different configuration of strengthening methods in experimental works and numerically as well, but pre-damaged recycled aggregate with self-consolidating concrete and steel fibers in beam strengthened by CFRP modelling numerically is a significant challenge for the engineer, and it necessitated further analysis and testing to guarantee that the shear capacity corresponded to the experimental results and codes.

1.6 Research Objectives

The objectives of this research have been clarified as following:

1-Study the behaviour of RCA beam samples before and after strengthening with CFRP laminates in terms of stresses and strains under different types of loadings and comparing with experimental values.

2-Study deflections, shear values and moment as linear analysis for RAC and NWA beam samples by using (Midas Gen) software and comparing with experimental values.

3- Study the deflection before/ after strengthening with CFRP laminates and with compression rebars or without it under different types of loadings using (ANSYS Workbench) software and comparing with experimental values.

4-Study the shear capacity values for RCA and NWA beam samples before/ after strengthening with CFRP laminates and with compression rebars or without it as per ACI 40-17R using (MIDAS Design Plus) software.

5- Study the damage and failure modes for RCA and NWA under different types of dynamic loadings before/ after strengthening with CFRP laminates and with compression rebars or without it under different types of loadings using (ANSYS Workbench) software and comparing with experimental values.

6- Checking the ductility index of RCA and NWA each beam sample before/ after strengthening with CFRP laminates and with compression rebars or without it under different types of loadings using (ANSYS Workbench) software and comparing with experimental values.

1.7 Software Used

The analytical evaluation in this research will be used by three software, which will be clarified as the following:

1. ANSYS Workbench Vr. 2021

The Ansys workbench is a platform works with finite element method, which used in any analysis with three component including geometries, differential equations, and boundary conditions. The approach begins by breaking up the geometry or issue area into a number of little components. The nodes that link these components are where the unknowns must be identified. The finite element equations for each element are obtained from the governing differential equations that describe physics. A sizable collection of algebraic equations is created from these finite element equations. The collection of algebraic equations is then subjected to boundary conditions in order to find solutions at each node.

1.1 Ansys Workbench Analysis Systems

In this research two types of analysis systems will be used, the first one is:

1.1.1 The Static Structural Analysis System

This analysis will be used for modelling the nonlinear analysis and divided in to 6 sections as in Figure 1.

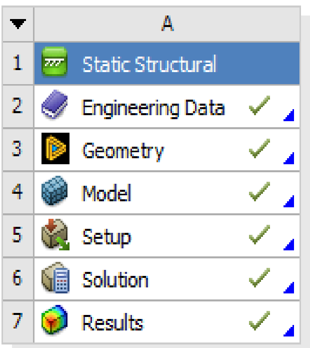

Figure 1(Static Structural Analysis System Window- ANSYS Workbench)

1-The Engineering data section verifies all material like compressive strength of concrete and strengthening fibers, rebars and bearing pads mechanical properties used in this analysis as in Figure 2.

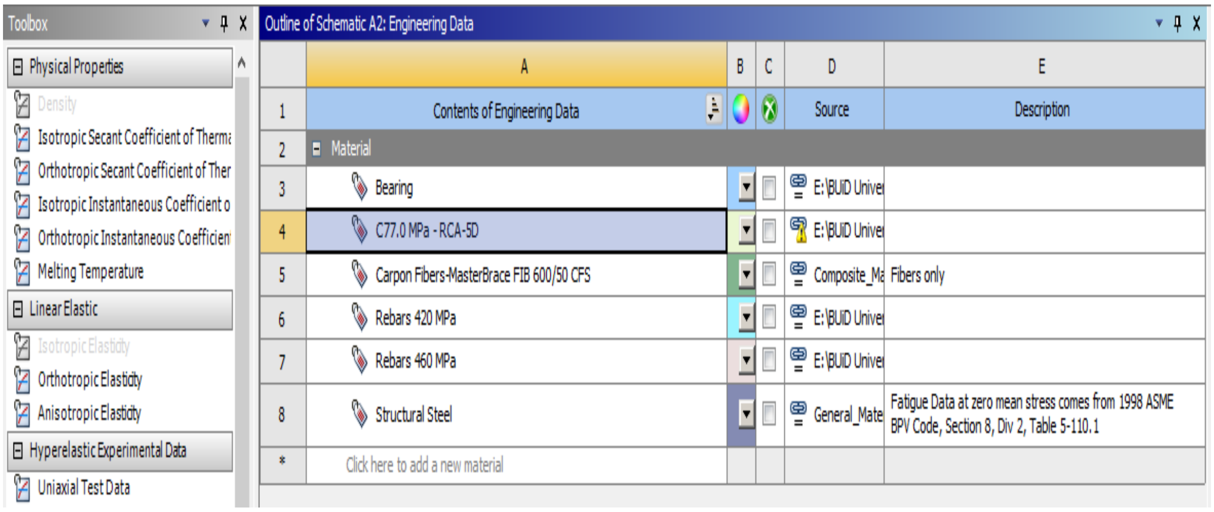

Figure 2(Engineering Data Panel Window- ANSYS Workbench)

2- Geometry

This part identifies the geometry will be used in the analysis section see.Figure 3 .

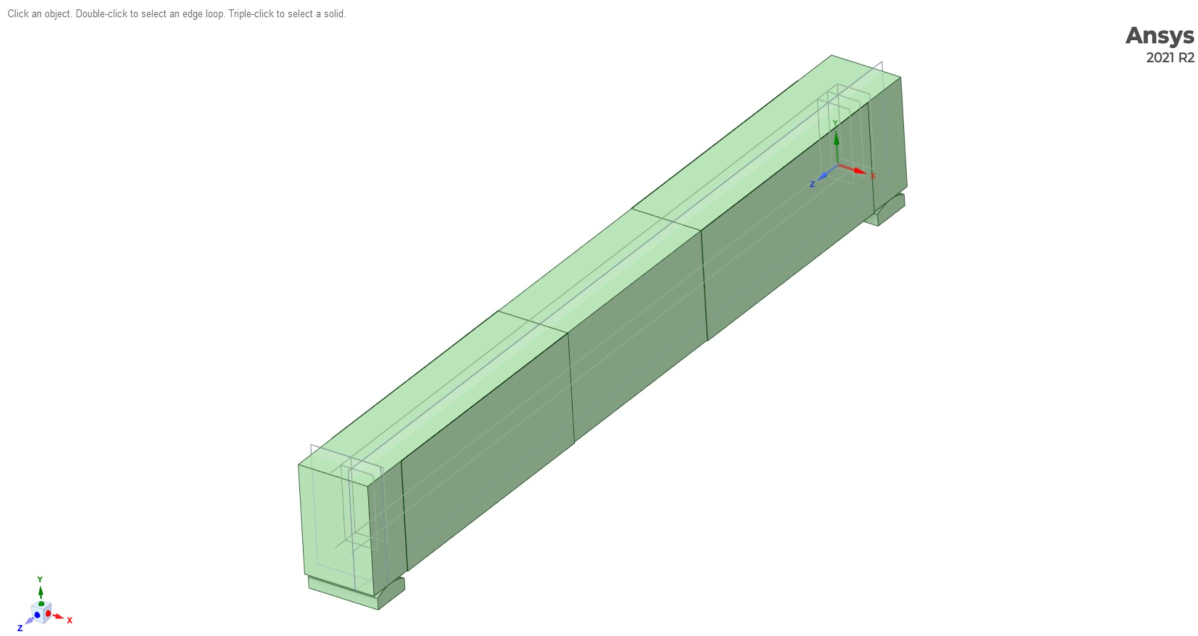

Figure 3(Geometry Panel Window-Static Non-Linear Analysis- ANSYS Workbench)

3-Model

This part identifies all analytical parameters like loads, meshing (Linear) and boundary conditions and type of analysis see.Figure 4 & Figure 5 .

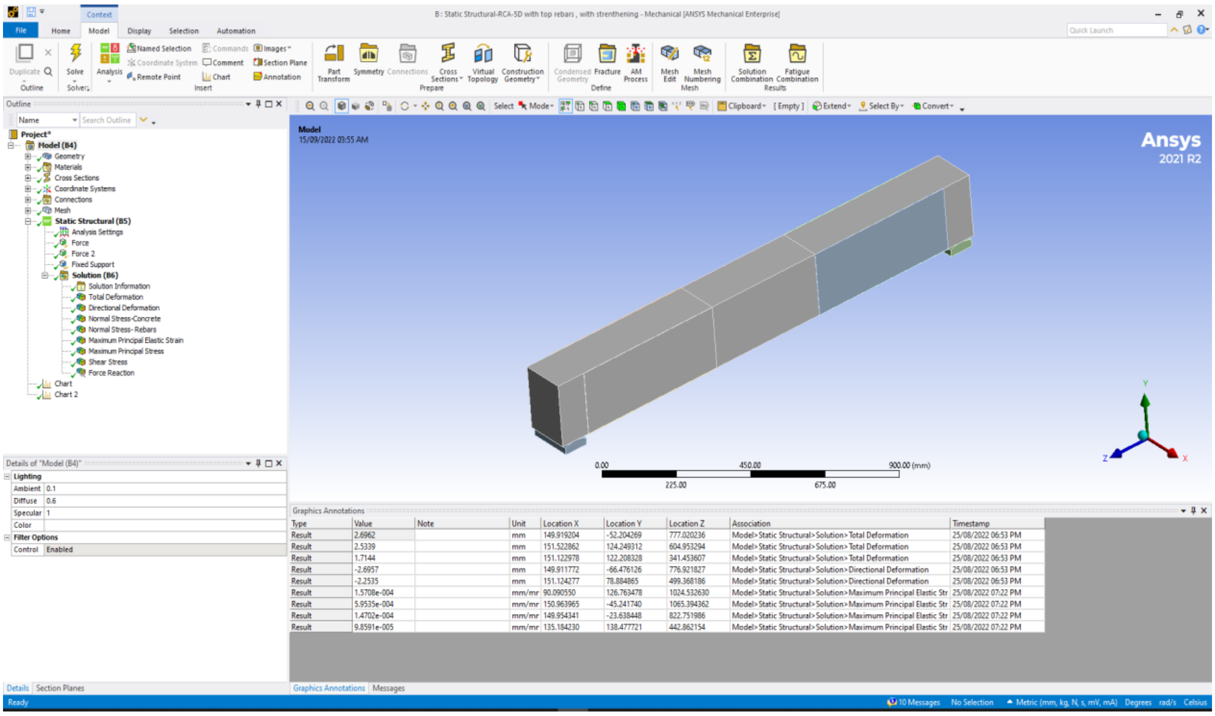

Figure 4(Model Window-Static Structural Analysis (including Setup, Solution and Results panels) - ANSYS Workbench)

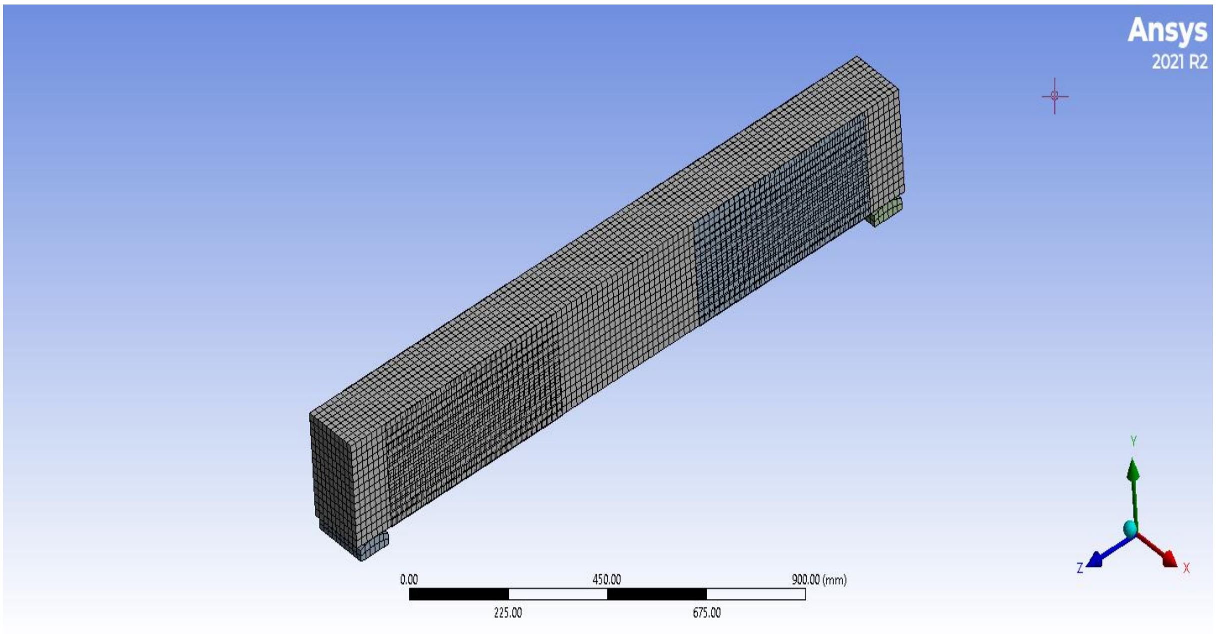

Figure 5(Meshing beam sample with strengthening view - ANSYS Workbench)

4- Setup, Solution and Results

These sections follow the model section see. Figure 6. The setup and solution showing in red arrows, while results showing in the black box as following.

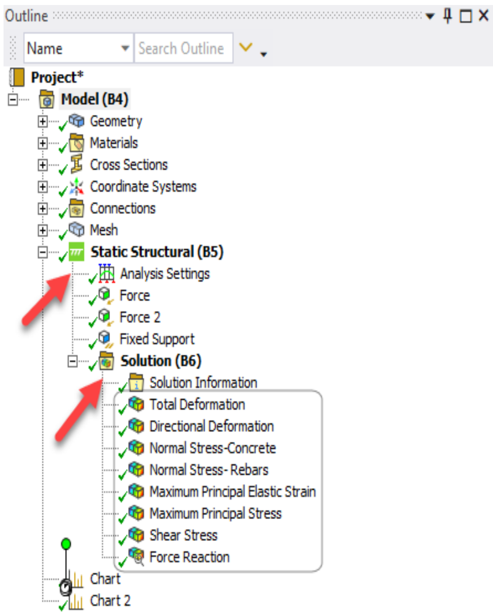

Figure 6(Setup, Solution and Results panels locations- ANSYS Workbench)

1.1.2 The Explicit Dynamic Analysis System

The second analysis system will be used for failure and damage modes. Furthermore, dynamic analysis will be employed in this type of analysis system. This section is divided in to six sections as the **Static Structural** Analysis system Figure 7.

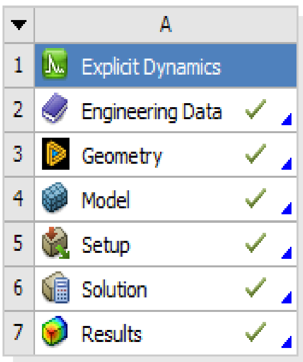

Figure 7(Explicit Dynamic Analysis System Window- ANSYS Workbench)

All sections are the same as **Static Structural** platform, from Engineering Data, Model, Setup, Solution and Results except geometry see.Figure 8 & Figure 9 .

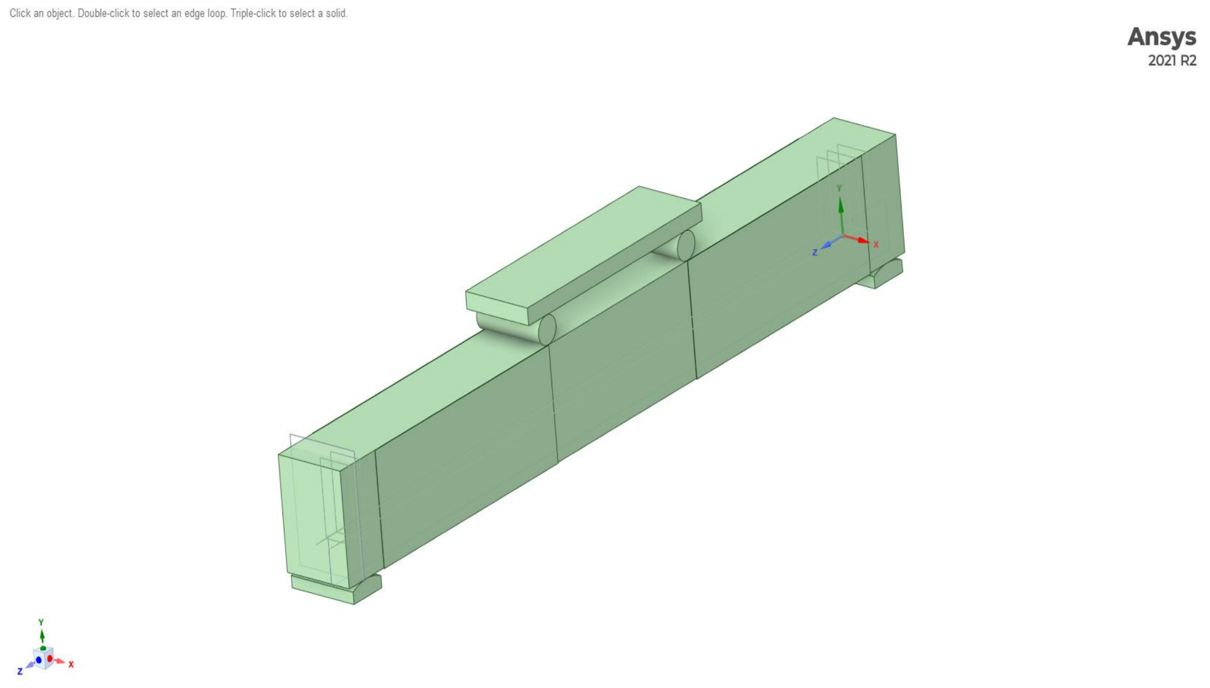

Figure 8(Geometry Panel Window-Explicit Dynamic Analysis- ANSYS Workbench)

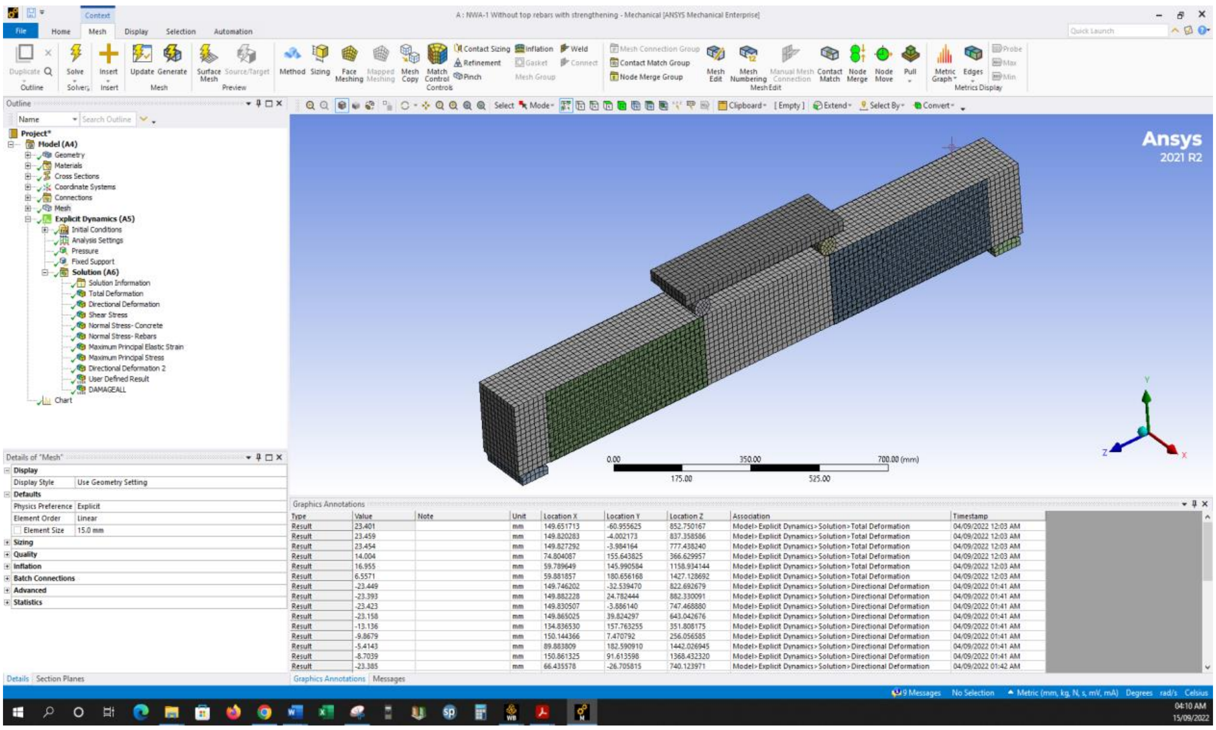

Figure 9(Model Window-Static Structural Analysis (including Setup, Solution and Results panels) - ANSYS Workbench)

2. Midas Vr.2021 platforms

These platforms are using building information technology (BIM) to model structural elements. This section is divided in two sub-software as following:

2.1 Midas Gen Vr.2021

In this research, Midas Gen will be used for linear analysis of RCA and NWA beam samples to get the straining actions like deflections, shear and moment values, and the graphical user interface (GUI) shown tree menu which will be illustrated as following:

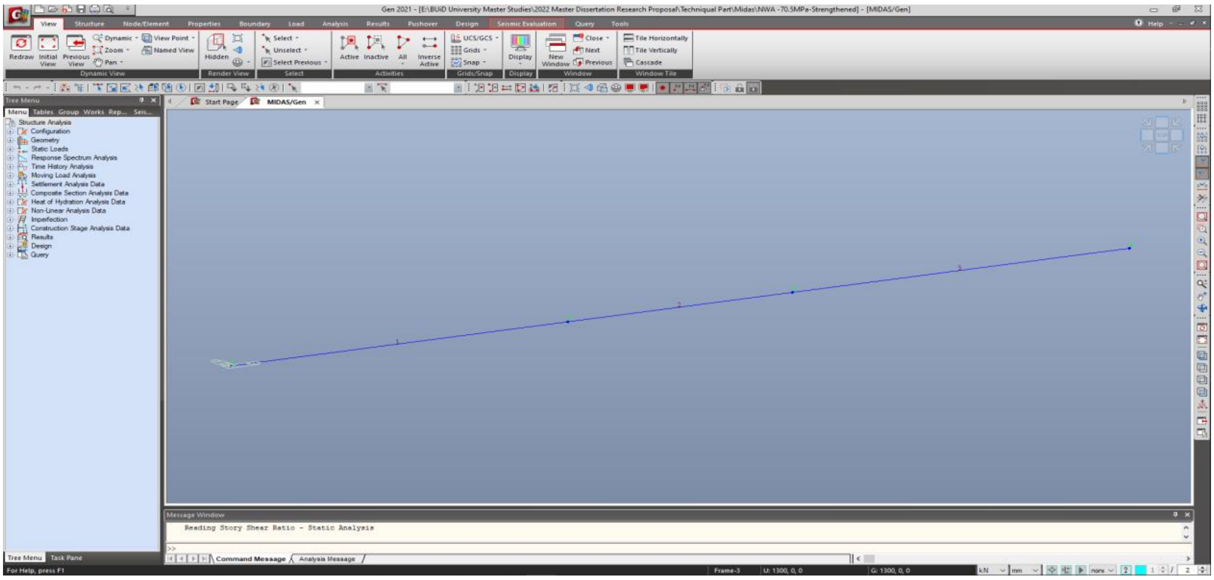

Figure 10(Graphical User Interface (GUI)- Midas Gen)

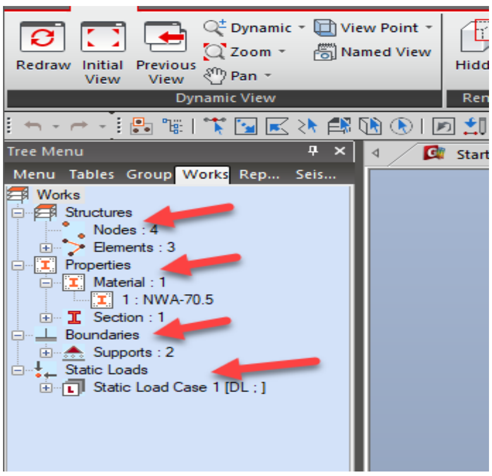

Figure 11(Tree Menu View-Static Analysis- Midas Gen)

-As we can see above, that tress menu shown a full menu as in Figure 10 and sub-divided menus, which allow the beam samples to be modelled by using the menus pointed with red arrows red arrows as shown in Figure 11. The mechanical properties can be defined as shown in Figure 12 .

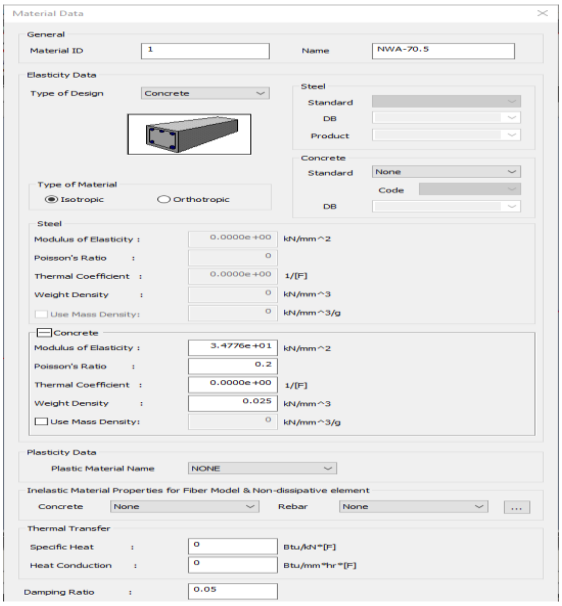

Figure 12(Material Data Assign- Midas Gen)

-The cross section of the beam sample can be identified as following see. Figure 13:

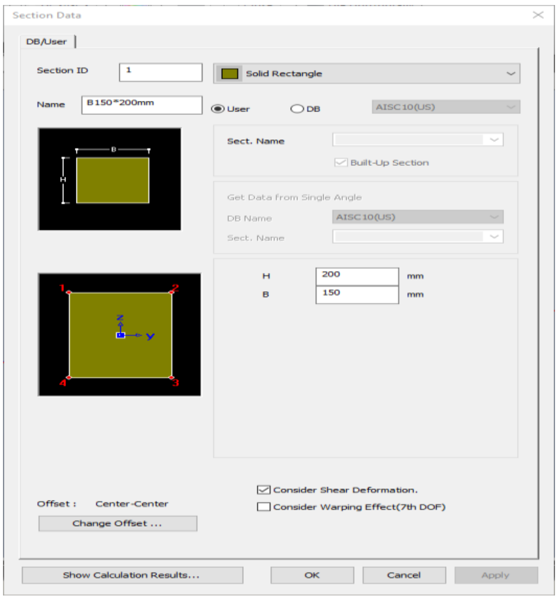

Figure 13(Section Data Assign - Midas Gen)

Moreover, same experimental loads will be used in 6.2.2.1 Stage 1 - Structural Analysis Stage Using (Midas Gen 2021) and Appendix B .

2.2 Midas Design Plus Vr.2021

In this research, Midas Design Plus has been used for strengthening technique using CFRP laminates (U-Wrapping) as per ACI440-2R-17 standards for RCA and NWA beam samples, to check the shearing capacity before and after strengthening. The graphical user interface (GUI) see. Figure 14 shown tree menu and other panels pointing in red arrows and will be illustrated as following:

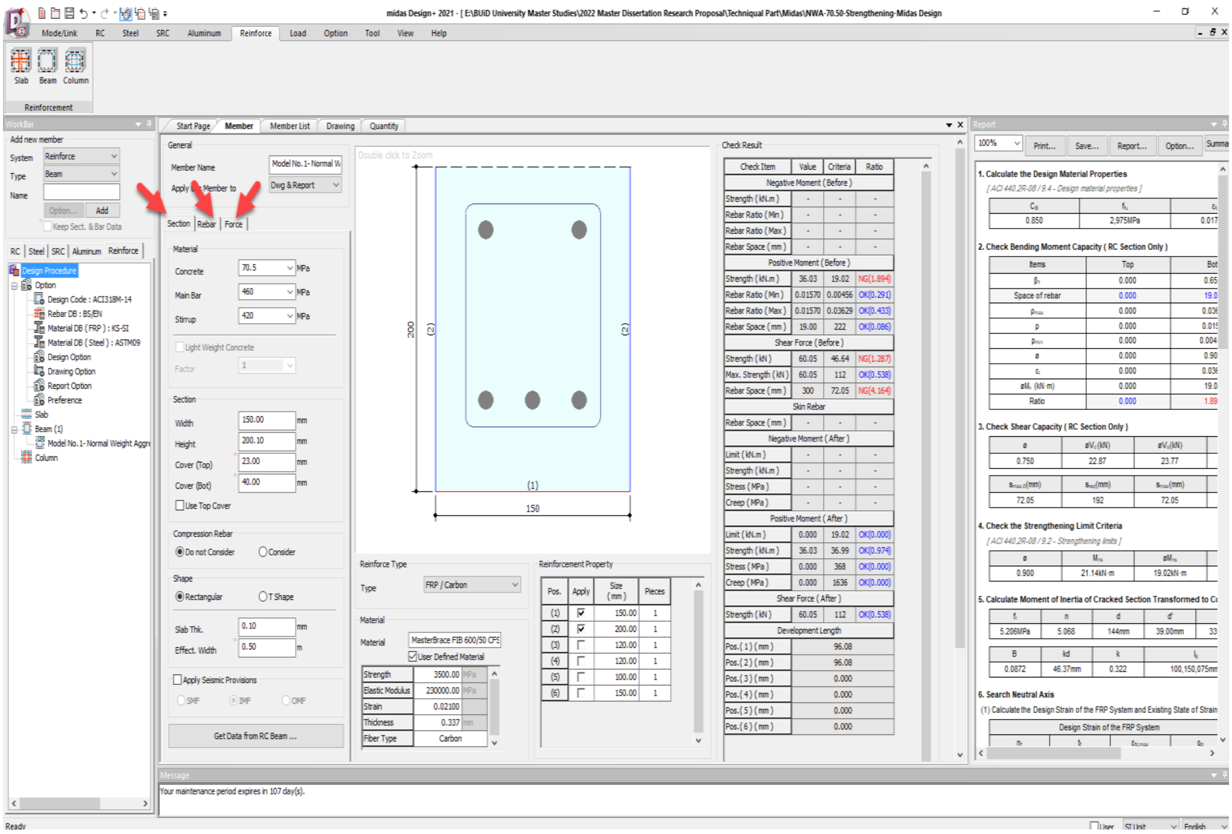

Figure 14(Graphical User Interface (GUI)- Reinforce Panel- Midas Design Plus)

The panels used in the modelling as following:

- Section

The cross section can be identified as the following see. Figure 15

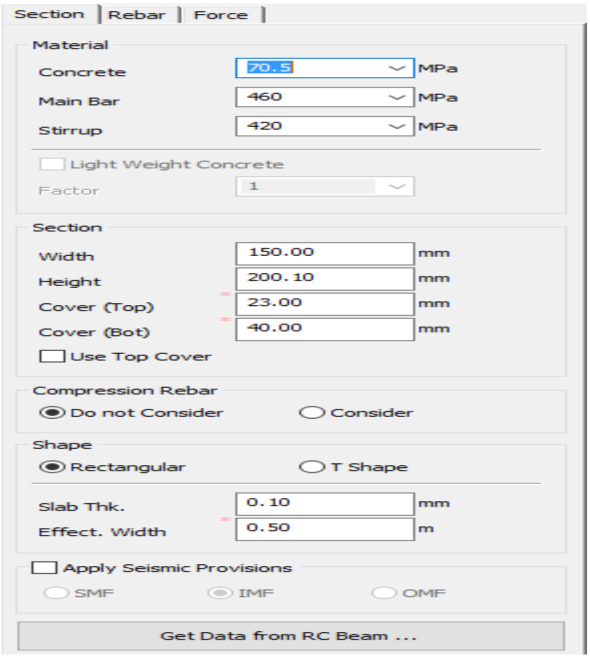

Figure 15(Section Part/ Reinforce-Midas Design Plus)

2- Rebars

The rebars of the cross section used can be identified as following see.<u>Figure 16</u> .

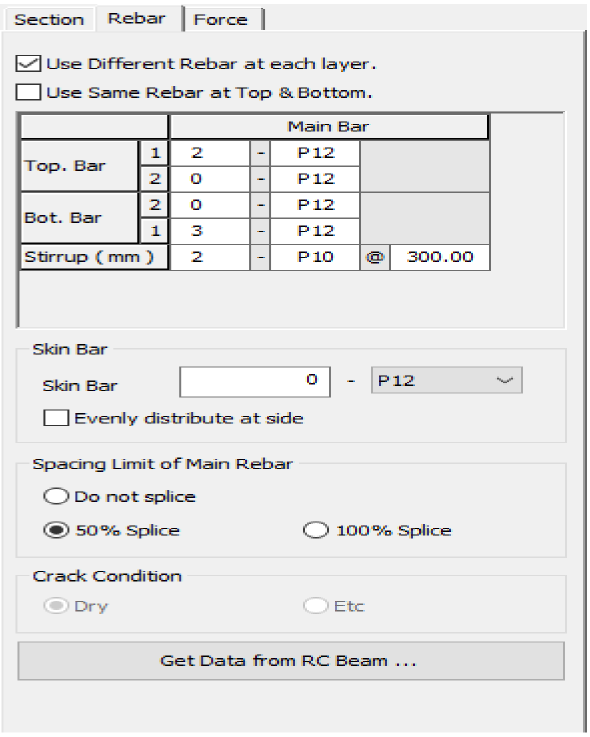

Figure 16(Rebars Part/Reinforce-Midas Design Plus)

3- Forces

The forces and loads used for each sample can be identified as the following see.Figure 17 .

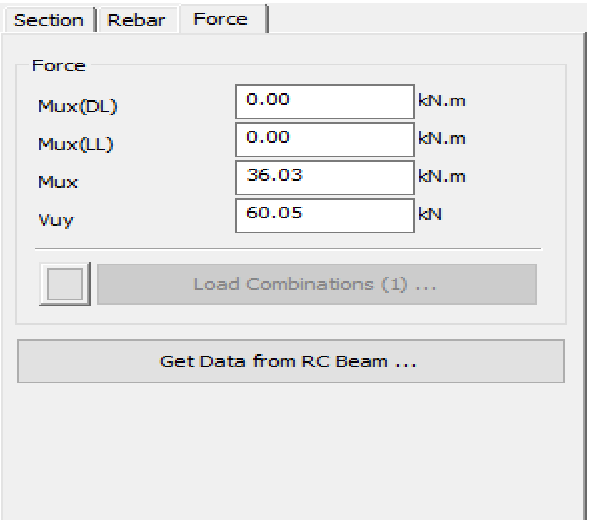

Figure 17(Force Part/Reinforce-Midas Design Plus)

- Reinforcement using CFRP Laminates

Reinforce Type, Material, Exposure Condition as the following see.Figure 18 .

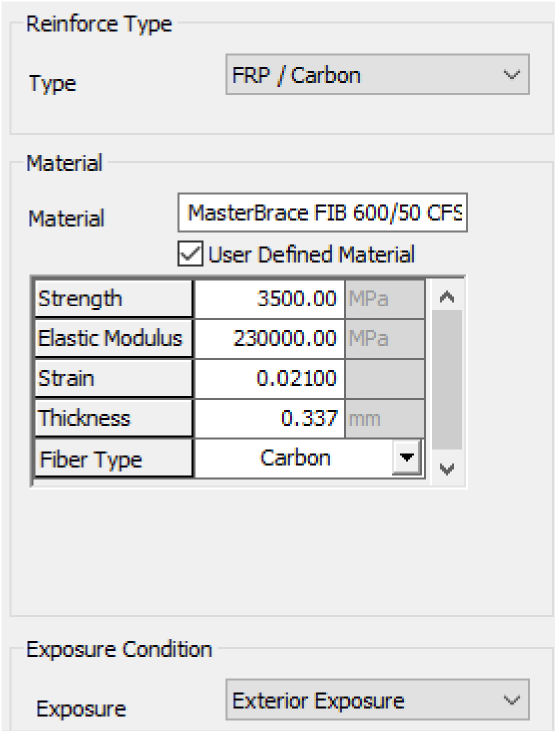

Figure 18(Reinforce Type and Exposure Condition Parts/Reinforce-Midas Design Plus)

- Reinforcement Property and Shear Reinforcement as the following see.Figure 19 .

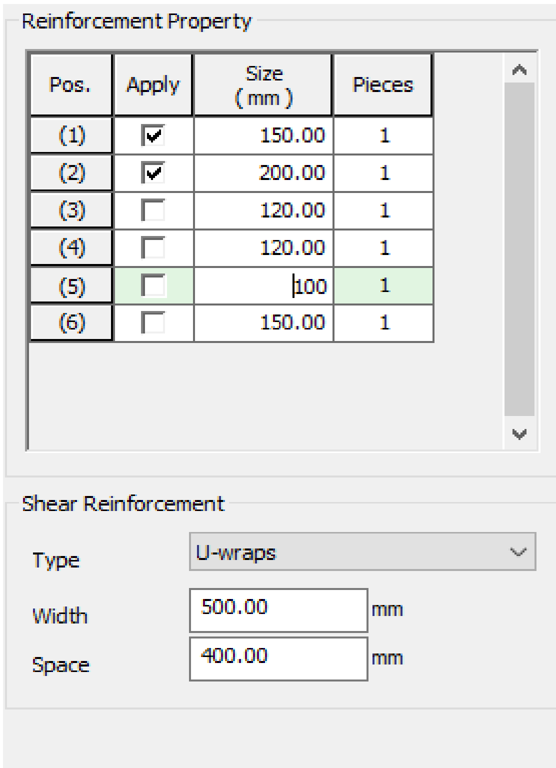

Figure 19(Reinforcement Property/Reinforce-Midas Design Plus)

Moreover, other experimental loads for other samples will be used in 6.2.2.2 Stage 2 - ACI440.2R-17 Code Check Using (Midas Design Plus 2021) and Appendix C .

1.8 Scope

The next chapters provide a thorough description of prior research for recycled concrete aggregate (RCA), fiber reinforced polymer (FRP), shear strengthening and mending approaches, and case study findings analysed using a precise finite element methodology.

Chapter (2) illustrates the literature review on recycled concrete aggregate (RCA)including utilization forms, properties, and pros& cons.

Chapter (3) demonstrates the literature review on fiber reinforced polymer (FRP) including types, importance, properties, and selection.

Chapter (4) demonstrates the literature review on repairing and strengthening techniques for the shear.

Chapter (5) describe the research methodology, code provisions and data collection in this research.

Chapter (6) illustrates the numerical evaluation results and comparing to experimental results using specified software (ANSYS Workbench, Midas Gen and Midas Design Plus).

Chapter (7) demonstrates technical discussion of the results for the research.

Chapter (8) provides the conclusion and recommendation for the research.

CHAPTER 2

2. RECYCLED CONCRETE AGGREGATE (RCA)

It is commonly believed that concrete trash accounts for the highest share of total construction waste in many countries(Kim, 2021, Muluken Yeheyis, 2013).In Other words, debris from demolition and construction, often known as (D&C) debris, is a type of waste material that is generated in large quantities during the building, repairing, renovating, and demolishing of different structures as part of civil engineering projects all over the world.

Recovery and utilization of demolition and construction (D&C) waste are on the rise in the modern era due to the trash's apparent durability, ready availability, and cost-effectiveness. The volume of construction and demolition waste has been steadily declining as a direct result of this rising use. Every day, tons of construction and demolition waste go unused. It was estimated that the amount of waste produced each day in inner-city regions was approximately 2.5 tons. (D&C) waste significantly subsidizes the growing manufacture of solid waste worldwide, particularly in developing countries, with only approximately 30 percent, and less of such debris is only subjected to recycling(Bakri, 2011). This is particularly true in light of the fact that recycling only accounts for a smaller portion of such debris. Because natural processes are unable to degrade most of these materials into useable resources, the disposal of debris from construction and demolition can be a source of numerous problems that hurt any society. These difficulties can be caused by the construction and demolition debris. The utilization of construction and demolition debris is an important part of the problem-solving process in landfills, but it also has a detrimental impact on environmental concerns. Therefore, there ought to be a process that is optimal for turning this (D&C) garbage into recycled aggregate materials see. Figure 20 that can be utilized for producing concrete materials for a variety of uses (Ashraf M. Wagih, 2019). This is despite the fact that the amount of waste created from construction is steadily rising year after year. In addition to recycling, potential disposal routes for construction debris include the landfill, being ignored, and dumping. These choices have a detrimental effect on the environment because they lead to an even greater depletion of natural resources and an upset in the delicate balance of ecosystems. As a result, the recycling of waste concrete is absolutely necessary for the continued growth of the building sector in a sustainable manner.

Figure 20(Recycled aggregate materials derived from construction and demolition rubble)(Abera, 2022)

Many experts have examined the potential for recycling concrete waste during the past few decades. Researchers have concluded that recycled aggregate (RA) concrete is inferior to that made with natural aggregates. Workability(Anna M. Grabiec 2020), density(Haitham Al Ajmani 2019), permeability (G.L. Vieira, 2020), mechanical strength(Haitham Al Ajmani 2019), and elastic modulus(M.Etxeberria, 2007) all decrease with increasing (RA) replacement rate, whereas bleeding(C. S. Poon, 2007) , drying shrinkage(Huan Zhang, 2020), and creep deformation(R.V.Silva, 2015) all increase. Adhered mortar in (RA) is responsible for these altered concrete characteristics (Jeonghyun Kim, 2015, P.Saravanakumar, 2016). As a result, efforts have been ongoing to enhance the mechanical strength and durability performance of recycled aggregate concrete by eliminating or reinforcing the adhering mortar.

2.1 Recycled Concrete Aggregate Utilization Forms

In concrete material and other uses, recycled aggregate (RA) and recycled concrete aggregate (RCA) derived from construction and demolition waste may serve as suitable replacements for fine and coarse aggregate materials, respectively. A major undertaking in the fields of building, civil engineering, and construction engineering is the production of recycled concrete aggregate. RCA is a sort of concrete that is produced through the recycling process for D&C waste from waste material that was once concrete. It has an intensifying ingredient in it, which raises the mix's capacity while also having additional potentials, such lowering the dead load.

In several civil engineering projects, recycled aggregate materials derived from mixed construction waste and recycled concrete aggregate materials created from demolished concrete rubble are employed(ACI-AC, 2007) . It may be utilized in bare cement concrete to replace up to 25% of the coarse aggregate and 20% of the coarse aggregate in reinforced cement concrete (FatihÖzalp, 2016). It is feasible to use recycled aggregates in lean concrete to completely replace natural aggregate resources with 100 % as research conducted by (Mohamed Ghoneim, 2020).

2.2 Recycled Concrete Aggregate Properties

2.2.1 Surface Condition and Gradation

With recycled aggregate, almost any gradation is possible. Crushing may produce leftover dust on aggregate surfaces. Usually this is not a problem, but there are cases when cleaning the aggregate is necessary before it may be put to good use (ACI-AC, 2007)

2.2.2 Specific gravity

Crushed recycled aggregate has a lower specific gravity than otherwise comparable virgin aggregate, often ranging from 2.2 to 2.5 in the saturated surface-dry (SSD) state. Specific gravity reduces as particle size decreases. The specific gravity of recycled sand ranges between 2.0 and 2.3. (SSD)(ACI-AC, 2007).

2.2.3 Recycled Concrete Aggregate Absorption

The absorption of recycled aggregates is substantially greater than that of otherwise equivalent fresh aggregates due to the cement mortar bonded to the particles, approximately 2 to 6 percent for coarse aggregate and more for tiny aggregate. Because of the high absorption, the resultant new concrete may be less workable. To make up for it, either spray the recycled aggregate with water before incorporating it into the concrete, or add extra water to the mixture. Because fine aggregate produced by crushing concrete is highly angular and absorbs a lot of water, it is usually limited to 10 to 20% of the total quantity of fine aggregate in the mixture (ACI-AC, 2007).

2.2.4 Recycled Concrete Aggregates' Durability

For recycled aggregate, abrasion loss and sulfate soundness are typically unimportant. Residual chlorides in a mixture, such as those produced by the application of deicing salts to a pavement, are typically below threshold levels for both fine and coarse aggregates and are thus not a problem. However, recycled aggregates derived from salt-water-exposed concrete should be subjected to further chemical and physical testing before being used in concrete. Concretes containing D-cracking aggregates should be examined before being utilized as recycled aggregates in concrete exposed to freezing and thawing. While recycled concrete may be utilized as coarse aggregate in new concrete pavements, the Alkali Silica Reaction (ASR) potential of the material should be assessed before usage. Several variables may assist determine this aggregate's capacity to operate without causing detrimental ASR throughout the pavement's life. The alkali levels of both recycled and new concrete might impact the finished concrete's expansion. The following recycled aggregate parameters should be evaluated to estimate ASR potential; factors such as the new concrete's alkalinity, the old concrete's expansion, the old concrete's remaining expansion capacity, and the new concrete's starting alkalinity. Alkali-silica reactivity in concrete using ASR reactive recycled materials may be reduced in many of the same methods as in concrete built with virgin aggregates.

2.3 Recycled Concrete Aggregate (Pros & Cons) In Terms of Properties

Research has been conducted by (Ashraf A.Bahraq, 2022) of up-to-date assessment of the factors influencing RCA's longevity, including permeability, carbonation, reinforcement corrosion, and shrinkage. The results illustrated that;

1- (RCA) is a porous concrete having a greater chloride migration propensity than natural aggregate concrete (NAC).

2- (RCA) has a higher water absorption rate than (NAC).

3- (RCA) has about double the water permeability of (NAC).

4- The presence of (RA) in concrete has a considerable impact on shrinkage because (RA) has a lower stiffness than (NA).

5- The presence of (RA) in concrete enhances the depth of carbonation by 1.8-2.5 times, depending on the amount of (RA).

6- (RA) produces additional interfaces in concrete, which accelerates the steel corrosion process and the spread of corrosion-induced cracks in the cover concrete.

Despite the weaker qualities of (RA) indicated above, a durable (RAC) may be developed with adequate treatment of the former see Figure 21 . The treatment procedures are as follows:

1-Removal of attached mortar from (RA).

2-Strengthening of adhering mortar on (RA) using physical and/or chemical approaches.

3- Using updated mix design methods.

4-Integrating fine materials that will physically and chemically alter the (RAC).

Figure 21(Proposed treatment approach augmentation strategies in terms of durability)(Ashraf A.Bahraq, 2022)

CHAPTER 3

3. FIBER REINFORCED POLYMER (FRP)

In past few years, the construction industry has emerged as a large prospective market for the consumption of fiber-reinforced polymers (FRP), which are used in a variety of civil engineering applications. Many different types of research have been carried out in order to investigate the use of FRP composites in structures due to the fact that they are lightweight, resistant to corrosion, nonmagnetic, have low electric and thermal conductivity for aramid and glass fibers, have high strength and stiffness in comparison to their weight ratios, and have the potential to last for a long time (Y.H.Mugahed Amran, 2018). Advanced polymer composites, or FRP for short, are a type of composite material that are primarily made up of polymer matrix resins like polyester, vinyl esters and epoxy which are then reinforced with fibers like glass, basalt, carbon, and aramid. FRP are also known as advanced polymer composites (APC). Glass fiber reinforced polymer, also known as (GFPP), basalt fiber reinforced polymer, also known as (BFRP), carbon fiber reinforced polymer, also known as (CFRP), and aramid fiber reinforced polymer are the most prevalent forms of FRP reinforcement (AFRP). The use of FRP composites in construction applications ranges from the rehabilitation of existing structures, which includes strengthening, retrofitting, and repairing of the structures, to the use of FRP composites in new projects either by total use of FRP or partial use like concrete-FRP system (Asifuz Zaman, 2013). The rehabilitation of existing structures includes strengthening, retrofitting, and repairing of the structures. The use of FRP composites in new projects either by total use of FRP or partial However, the elastic modulus of GFRP is four to five times lower than structural steel, which leads to an increase in the amount of deformations in GFRP reinforced elements (Eugenijus Gudonis, 2014). GFRP is the most popular category of FRP bars due to its high tensile strength in comparison to steel and its relatively low cost in comparison to CFRP and BFRP. The tensile strength of CFRP may reach up to 3,690 MPa, making it the FRP with the highest possible value. When compared to other types of FRP, CFRP has a high modulus of elasticity, which helps to limit the amount of deformation that occurs in parts that are reinforced with CFRP (Eugenijus Gudonis, 2014).

3.1 Types of Composite Fiber Reinforced Polymer Materials

When two or more elements are combined, a material is created that has unique features that are entirely distinct from those of the individual components included (Sardasht S Weli, 2020). Composite materials may be created by mixing two or more materials. The fiber in FRP composite has a high elastic modulus, which contributes to the material's overall mechanical qualities. FRP composite is designed from fibers and resins. While the resins assist in the transmission or distribution of stresses from one fiber to another in order to protect the fibers from damage caused by mechanical forces and the environment, it is well known that the interface between the fibers and the matrix may safely alter the behavior of the material, which can help reduce shrinkage and cost. In addition to improving the workability of composites, additives may also enhance the material's physical and mechanical qualities(Eugenijus Gudonis, 2014). Carbon, glass, aramid, and basalt are the four primary materials that are employed in order to generate fibers that are mostly used in the civil engineering sector (Ayesha Siddika, 2020, Eugenijus Gudonis, 2014, Y.H.Mugahed Amran, 2018). These four elements combine to form CFRP, GFRP, AFRP, and BFRP.

In contrast to steel, FRP composites are impervious to the corrosion caused by chloride because they are inherently non-corrosive and non-metallic. This property, which has the potential to significantly improve the corrosion resistance of structures, makes FRP composites an excellent choice. Table 1 provides an overview of the characteristics shared by FRP materials in addition to those of traditional steel. In contrast to conventional steel, fiber reinforced plastics (FRP) have a low weight yet a high strength. However, its mechanical properties may be characterized as having linear strength. However, its mechanical properties may be characterized as having linear strength. Despite this, its mechanical properties are linear elastic, and it does not exhibit an evident yielding stage; as a consequence, its failure strain and elongation rates are lower. In addition, the elastic modulus of FRP is often lower than that of steel, with the exception of some CFRP materials, which have a high Young's modulus. The FRP composites might be applied as reinforcing with concrete in a variety of forms, including rebar, rod, tube, sheet, beam stirrup, plate, roving, as well as textile and mesh fabric. In particular, the FRP bars might be used as a potential substitute for steel rebars, which are manufactured by the pultrusion process using impregnated thermoset resin fibers (Azzam Ahmed, 2020).

3.1.1 Carbon Fiber Reinforced Polymer (CFRP)

Manufactured at a temperature of 1300 C, carbon fiber has a naturally anisotropic structure. The main benefits of this fiber are its low density, low conductivity, high fatigue strength, high elastic modulus, excellent creep level, resistance to chemical impacts, and lack of water absorption Table 2. In contrast, carbon fiber's poor compressive strength and anisotropy (reduced radial strength) are its Achilles' heels. Another drawback is the high cost of production due to the large amount of energy needed to create carbon fiber (Eugenijus Gudonis, 2014).

3.1.2 Armid Fiber Reinforced Polymer

Aramid fiber is not the same in all directions and is usually yellow.

As Table 3 shows, Aramid fiber is often called Kevlar fiber on the market. Aramid fibers are more expensive than glass fibers, but they are strong enough for tension applications like tendons and cables, but not strong enough for compression. It is light, has a high tensile strength, a high elasticity modulus, and is stiff enough.

3.1.3 Glass Fiber Reinforced Polymer

Because of its isotropic structure, glass fiber is a widely used filament material. Glass fibers of the E-, S-, C-, and AR varieties are among the most widely used Table 4 . Glass fiber has a high strength-to-weight ratio, is chemical and water resistant, and is inexpensive.

Compared to other FRPs, glass fiber's cheap price makes it the material of choice for most building projects. However, the main limitations of glass fiber are its poor long-term strength owing to stress rupture and its relatively low elastic modulus and resistance to alkalinity. There may be a use for this so-called AR-glass in situations where increased resistance to alkaline is necessary (R. Sonnenschein, 2016).

3.1.4 Basalt Fiber Reinforced Polymer

The rapid cooling of molten rock, known as lava, on the surface of the earth results in the formation of the igneous rock known as basalt fiber. The process of creating basalt fiber is quite similar to the process of making glass fiber. The sole raw materials that are required for the production of fiber are basalt rocks that have been crushed. The use of basalt fibers in FRP composites and structural materials is a relatively recent development. These fibers have an excellent tensile strength, are resistant to high temperatures in exact measure, and also have a good durability Table 1. Having strong electromagnetic qualities and being resistant to corrosion, acid, radiation, ultraviolet light, and vibration are two additional benefits of this material. The use of BFRP in the area of civil construction is fairly restricted when compared to that of FRP composites, which are formed from glass, carbon, and aramid fibers (Banibayat, 2011, Eugenijus Gudonis, 2014)

Property	FRP				
	CFRP	GFRP	AFRP	BFRP	Steel
Density (gm/cm^3)	1.50–2.10	1.25–2.50	1.25–1.45	1.90–2.10	7.85
Tensile Strength (MPa)	600–3920	483–4580	1720–3620	600–1500	483–690
Young's Modulus (GPa)	37–784	35–86	41–175	50–65	200
Elongation (%)	0.5–1.8	1.2–5.0	1.4–4.4	1.2–2.6	6.0–12.0
Coefficient of Linear Expansion (10^{-6}/°C)	–9.0–0.0	6.0–10.0	–6.0–2.0	9.0–12.0	11.7

Table 1(FRP Mechanical Properties)(Azzam Ahmed, 2020, Imad Shakir Abbood, 2021)

Property	CFRP			
	Polyacrylic Nitril Carbon		Pitch Carbon	
	High Strength	High Modulus	Ordinary	High Modulus
Density (gm/cm^3)	1.7–1.8	1.8–2.0	1.6–1.7	1.9–2.1
Tensile Strength (MPa)	3430	2450–3920	764–980	2940–3430
Young's Modulus (GPa)	196–235	343–637	37–39	392–784
Elongation (%)	1.3–1.8	0.4–0.8	2.1–2.5	0.4–1.5
Coefficient of Linear Expansion (10^{-6}/°C)	–0.6 up to –0.2	–1.2 up to –0.1	–0.6 up to –0.2	–1.2 up to –0.1

Table 2(CFRP Mechanical Properties)(Eugenijus Gudonis, 2014, Imad Shakir Abbood, 2021)

Property	AFRP					
	Kevlar 29	Kevlar 49	Kevlar 149	Technora H	Twaron	Twaron HM
Density (gm/cm^3)	1.44	1.44	1.44	1.39	1.44	1.45
Tensile Strength (MPa)	2760	3620	3450	3000	3000	3000
Young's Modulus (GPa)	62	124	175	70	80	124
Elongation (%)	4.4	2.2	1.4	4.4	3.3	2.0
Coefficient of Linear Expansion (10^{-6}/°C)	–2.0 long. 59 radil	–2.0 long. 59 radil	–2.0 long. 59 radil	–2.0 long. 59 radil	–2.0 long. 59 radil	–2.0 long. 59 radil

Table 3(AFRP Mechanical Properties)(Eugenijus Gudonis, 2014, Imad Shakir Abbood, 2021)

Property	GFRP			
	E-glass	S-glass	C-glass	Ar-Glass
Density (gm/cm^3)	2.5	2.5	2.5	2.5
Tensile Strength (MPa)	3450	4580	3300	1800-3500
Modulus of Elasticity (GPa)	72.4	85.5	69	70-76
Extension to Break (%)	2.4	3.3	2.3	2.0-3.0
Coefficient of Linear Expansion (10^{-6}/°C)	5.0	2.9	N/A	N/A

Table 4(GFRP Mechanical Properties)(Eugenijus Gudonis, 2014, Imad Shakir Abbood, 2021)

3.2 Importance of Using Fiber Reinforced Polymer

Research review has been conducted by(Sallal R. Abid, 2018), illustrated that AFRP has exceptional corrosion resistance and fatigue characteristics. However, its weak resistance to acids and alkalis moved attention to CFRP. In addition to its high strength-to-weight ratio, CFRP offers superior chemical resistance, temperature resistance, and fatigue resistance in contrast to other forms of FRPs. These qualities make CFRP the material of choice for strengthening applications. However, CFRP has poor ductility. To make the most of the high strength of CFRPs and the excellent ductility of GFRP, they are used as mixed layers to reinforce structures. On other hand, (Paweł Grzegorz Kossakowski, 2022) performed a another study on using FRP in bridges construction and illustrated that, Glass fibers have a great resistance to corrosion and a low temperature effect on their mechanical qualities. Some of its biggest drawbacks include a low modulus of longitudinal elasticity and a susceptibility to moisture. Despite its high fatigue strength, aramid fibers are seldom employed in construction because of their creep susceptibility, expensive cost, and complex manufacturing technique. Among FRP's many desirable properties are its high corrosion resistance, increased durability, reduced maintenance needs, superior tensile strength, high fatigue strength, low weight, extended service life, and superior electrical insulation.

3.3 Degradation and Material Characteristics

3.3.1 Fiber Reinforced Polymer Humid Environment

Existing research (Park, 2012) reveal that when exposed to moisture, the Si–O bonds present in FRP bars react with OH- and water molecules to form micro-cracks. As a result, several research has attempted to replicate corrosion by immersing FRP bars in artificial solutions. The retention rate (the ratio of the index after the long-term test to the index at the beginning of the test) and tensile strength (the ratio of the index after the long-term test to the index at the beginning of the test) of various FRP in different solutions are shown as shown in Figure 23 (pH, temperature). According to the findings, the rate of deterioration differs across different types of FRP. Compared to other FRPs, CFRP maintains its superior mechanical qualities both immediately upon installation and after extensive use in a wide range of conditions. Although GFRP and BFRP deteriorate very slowly in salt solutions, they disintegrate very rapidly in neutral solutions, sea water, and alkaline solution. Also, whereas both GFRP and BFRP disintegrate when exposed to acid solutions, the latter does so far more quickly (Viet Quoc Dang, 2021) . It's important to note that the mechanical characteristics of FRP degrade at varying rates, and that the failure modes frequently rely on the mechanical property that degrades the most. As a result, the design of FRP must take into account the possibility of mechanical property deterioration over time. Figure 29 shows a scatter plot of the mechanical characteristics of the same batch of GFRP bars when exposed to an alkaline environment (pH 12.7). Since direct comparisons of compressive strength would be flawed due to its close link with the slenderness ratio, the strength retention rate was used instead. Mechanical characteristics of FRP degrade differently even when exposed to the same conditions. Compressive strength is decreasing at a faster rate than flexural, shear, and tensile strengths. This may help to shed light on why FRP beams' failure mode changes over time.

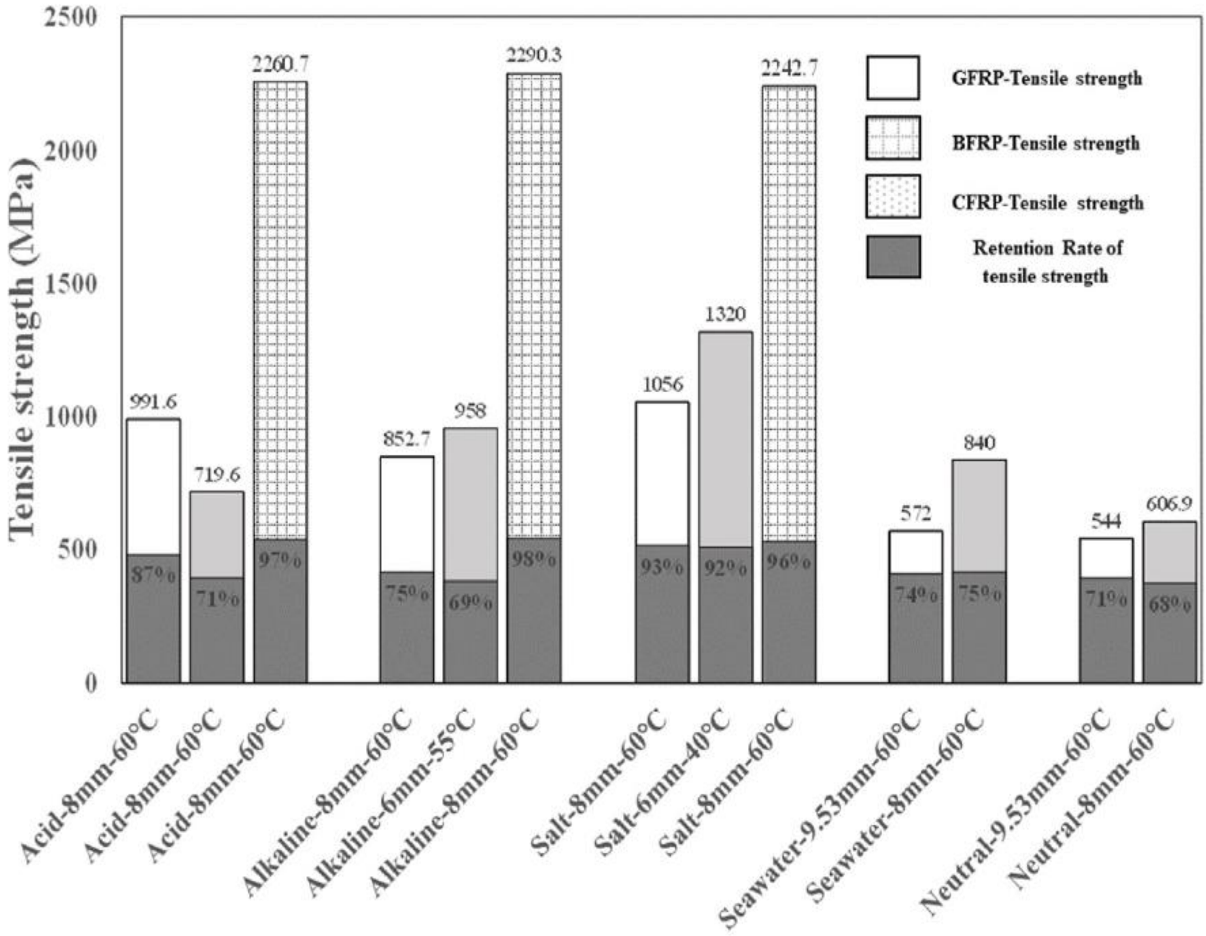

Figure 22(Comparison of the tensile strength and retention rates of several FRPs over a range of conditions)(Xiaolong Hu, 2022)

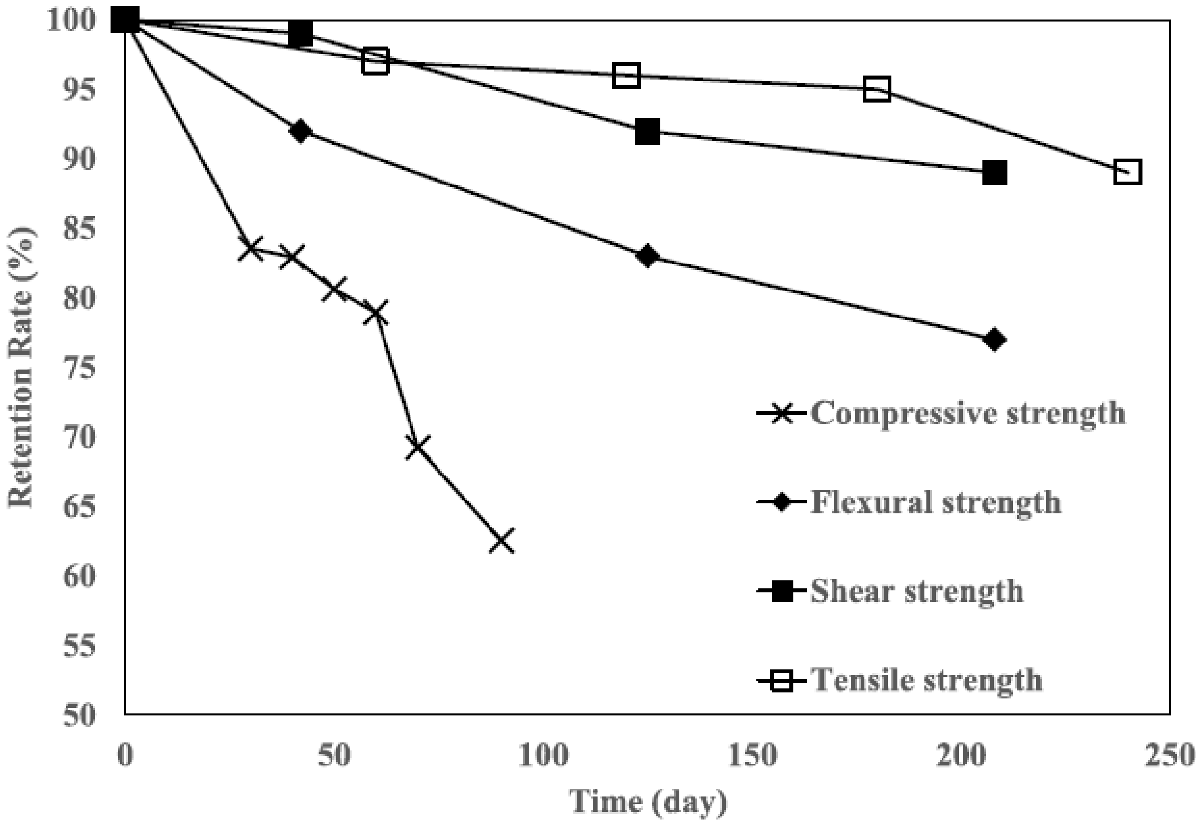

Figure 23(Mechanical property degradation variations in FRP)(Xiaolong Hu, 2022)

3.3.2 UV (Ultraviolet) Radiation

More and more construction projects are opting to employ FRP as a protective material, wrapping it around components after they have been reinforced with FRP bars. UV light will be shown on FRP. The deterioration of FRP bars is caused by ultraviolet light, which alters the molecular structure of the resin used to make them. Four sheet materials (CFRP, BFRP, E-type GFRP, and S-type GFRP) were UV-irradiated by (Jun Zhao 2017). The four FRP bars retain 81.3%, 84.7%, 76%, and 92.4% of their initial tensile strength after 90 days of exposure to UV radiation (slight increase was probably observed in a short period of time due to shrinkage or hardening of the resin). UV rays mostly damage the molecular structure of the resin, but have minimal impact on the resin itself, as shown by the fact that S-type GFRP bars retain their tensile strength at the greatest rates and E-type GFRP bars retain it at the lowest rates.

3.3.3 Cycles of Wet and Dry

The effects of tides on marine ecosystems may be simulated by a wet-dry cycle. CFRP and GFRP were exposed to air and a 5% NaCl solution for 12 hours by (Hongjun Liang, 2018). After 360 cycles, CFRP retains 90.6% of its initial tensile strength, while GFRP bars retain 88.95% of theirs; nonetheless, both show little change in elongation and elasticity. Wet and dry cycling significantly reduced the material's tensile strength but had no effect on its elongation or elastic modulus. Furthermore, CFRP exhibits greater resilience in the face of repeated exposure to damp and dry environments than GFRP does. The GFRP bars were subjected to a wet and dry cycle test using various water and salt solutions, as well as a strong alkaline solution (pH = 13.6) and an alkaline solution (pH = 12.7). After 9 cycles, the bars were exposed to air at 20 degrees Celsius after being soaked in the aforementioned solutions at 60 degrees Celsius for 4 days. The percentages of tensile strength retained by GFRP bars after being immersed in four different solutions are 84%, 86%, 73%, and 80%, respectively. This fits with what we know about how the aforementioned remedies affect FRP bars.

3.4 Fiber Reinforced Polymer Durability

3.4.1 Environment of Humid

Shear strength of concrete beams reinforced with BFRP bars is worse than that reinforced with steel bars after long-term immersion in marine environment, according to a study by (Zhongyu Lu, 2020), who immersed BFRP bars and steel reinforced concrete beams in seawater for 6 months and found that the failure mode of BFRP bars reinforced concrete beam was shear compression failure. Sandblasted GFRP and spiral ribbed GFRP reinforced concrete beams with cracks were first soaked, and then exposed to a steady load for 300 days in (Yeonho Park, 2014) study. Ultimate flexural capacity of beams reinforced by sandblasted GFRP bars and spiral ribbed GFRP bars reduced by 0.5% and 9.1%, respectively, indicating that sandblasted GFRP bars had greater resistance to salt solution owing to the protection of extra resin layer.

3.4.2 Dry and Wet Cycles

Natural environment, tap water, 40 C saltwater (immersion), and 40 C seawater (dry-wet cycle) were tested on GFRP bars reinforced concrete beams for 300 days by (Yousef A. Al-Salloum, 2013), with a constant load of 23% of the ultimate load. The long-term test results showed that the dry-wet cycle was more damaging than the soaking environment, with the mid-span deflection being 113%, 120%, 130%, and 136% of initial deformation for the four groups (Milad Bazli, 2020b).

3.4.3 The Cycle of Freeze-Thaw

GFRP reinforced concrete beams were subjected to freeze-thaw cycle testing by (Kader Laoubi, 2006) at temperatures between 20 C and 20 C. Mid-span deflections under the same load rose by 3.6% after 100 freeze-thaw cycles and by 0.1% after 200 such cycles. Following 360 freeze-thaw cycles, the beam's mid-span deflection decreased by 2.5%, while the ultimate flexural capacity of the GFRP reinforced concrete beam rose by 2.8%-5.3%. The freeze-thaw cycle had minimal influence on concrete beams reinforced with FRP bars, however there were some minor irregularities and shifts that may be attributed to knot mistakes.

3.4.4 Fibre Reinforced Polymer Failure Modes (Sea Sand and See Water Concrete- SSC)

Failure of FRP-SSC beams often occurs in one of three ways: bending, bending shear, or shear compression. Existing study like (Brahim Benmokrane, 2017), shown that the failure modes of FRP-SSC beams were defined by the FRP bars and environments, and that the addition of sea water and sea sand had little influence on these failure modes. Figure 24 depicts the failure modes of steel bar, GFRP bar, BFRP bar, and CFRP bar reinforced beams after being submerged in salt water for an extended period of time. There were no obvious variations between the flexural failure and crushed concrete failure modes of beams reinforced with various FRP bars in the early stages of the test. However, the difference between FRP bars reinforced beams and steel bars reinforced beams revealed with the corrosion. For steel-reinforced beams, the fact that concrete crushing failure modes dominated indicates that the bonding strength between the steel and concrete rarely altered over time. In a 270-day seawater test, the steel-ordinary concrete (OC) beam showed no signs of instability. A lengthier test is required to validate the steel-OC beam's longevity in a maritime environment, since it was discovered that all of the steel bars in the test beam had rusted following the test. For FRP-OC beams, concrete crushing was the failure mechanism in the control group, but exposure to salt water caused the FRP bars to break before the concrete could. As for FRP-SSC beams, the failure mechanism of the control group was concrete crushing. After extensive testing in a maritime setting, the beams' failure mechanism shifted from tension to compression failure. Long-term tests showed that the interaction between FRP and saltwater caused the FRP bars to deteriorate significantly and break before the concrete was crushed. In addition, it must be noted out that the most FRP bars in FRP-OC beams damaged after long-term testing, but most of the FRP bars in FRP-SSC were not broken, which suggested that SSC can withstand the erosion of the marine environment better than OC owing to the high concentration of ions in SSC. After being subjected to long-term testing, the bond strength between CFRP bars and concrete was shown to be inferior to that of GFRP and BFRP bars. Along the stirrups, fractures in CFRP-reinforced SSC beams narrowed and spread. So, in a corrosive environment, strengthening concrete components using BFRP bars or GFRP bars is preferable.

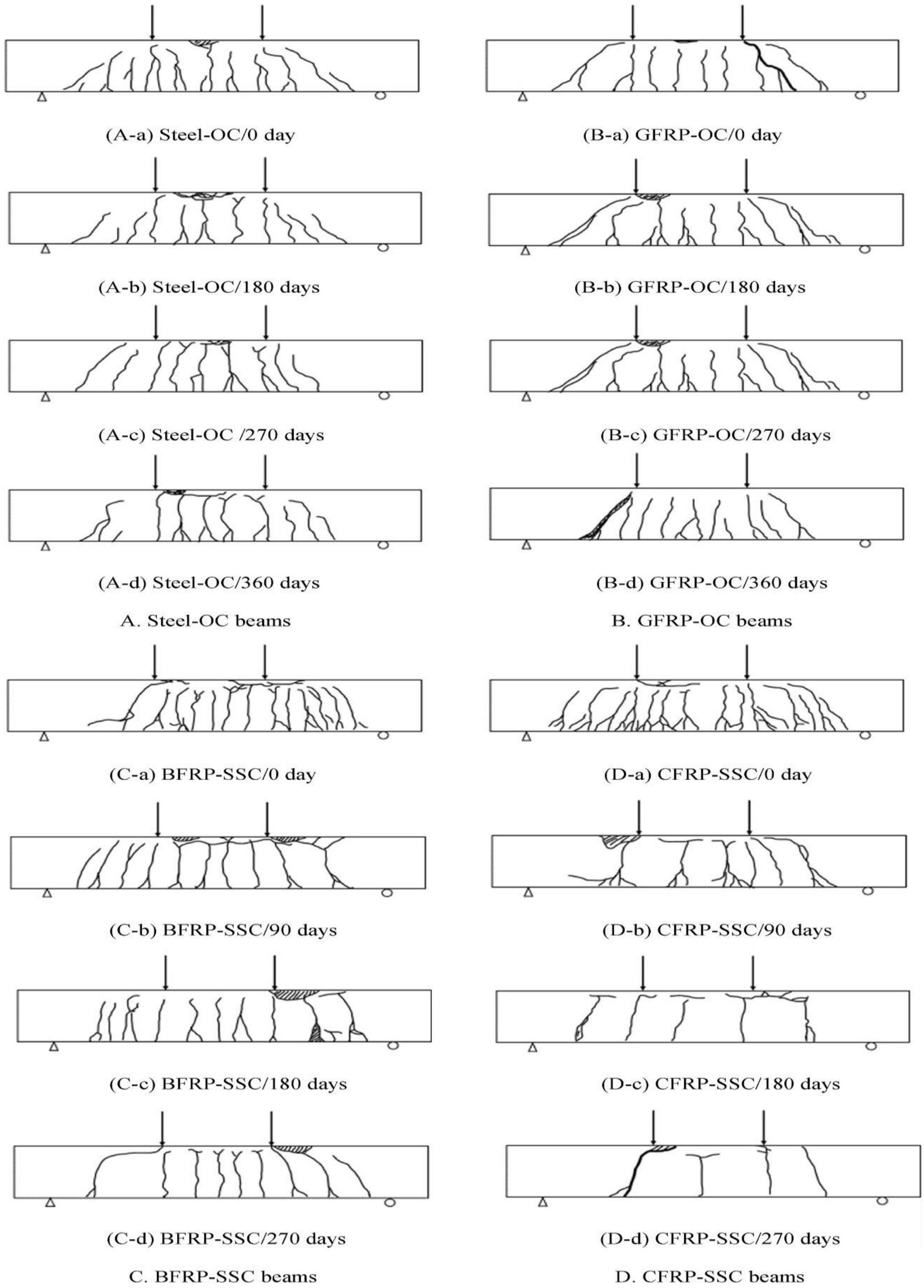

Figure 24(Different failure modes shapes of beams reinforced with steel/GFRP/BFRP/CFRP bars)(Xiaolong Hu, 2022)

3.4.5 High Temperatures

After being subjected to extreme heat, such as in a fire, FRP composites reach a temperature known as the glass transition temperature (Tg), at which point the resin transforms from a glassy state to a leathery one. At a higher temperature, known as the resin decomposition temperature (Td), the chemical bonds, modular chains of the resin, and links between the fibers are broken. Finally, the ignition and combustion of the composite occur at greater temperatures. The polymer matrix generally had a glass transition temperature (Tg) between 65 and 120 degrees Celsius and a decomposition temperature (Td) between 300 and 400 degrees Celsius. When subjected to temperatures in this range (i.e., the resin breakdown temperature Td), the chemical bonds, modular chains of the resin, and linkages between the fibers all decompose (Rami J.A.Hamad, 2017). According to (Y.C.Wang, 2005), the critical temperature is the point at which the reinforcement loses about half of its strength and can no longer bear the applied stress. Given this definition, the critical temperature (Tc), in this research, it is defined as the temperature at which FRP composite, independent of the type and design, loses 50 percent of its mechanical strength. The idealized link between temperature and the mechanical characteristics of FRP composite is shown in Figure 25. Until the softening temperature, Ts, is reached, the model assumes that the mechanical properties remain unchanged from the original room temperature. When the temperature of the composite rises over its melting point (Tm), the mechanical properties begin to degrade until they reach a residual value of Pre-sidual. It is vital to note that the transition range of resin glass is the temperature range at which the rein matrix goes from brittle to rubbery (i.e., the softening temperature). It is also important to note that the distinction between (Tg) and (Tm) is not always clearly drawn in the reseach (Friederike Fleischhaker, 2014). To determine the (Tg) of the resin matrix, either differential thermal analysis

(DSC) or dynamic mechanical thermal analysis (DMTA) might be used. Beyond Tm, the mechanical property declines progressively (E. U. Chowdhury, 2009).

In other terms, the tensile characteristics of carbon fiber reinforced plastic (CFRP) sheets, hybrid carbon/glass fiber-reinforced polymer (C/GFRP) sheets, and hybrid carbon/basalt fiber-reinforced polymer (C/BFRP) sheets were measured at temperatures ranging from 16 to 200°C(Shenghu Cao, 2009). The tensile strength of carbon fibers in different FRP sheets fell significantly as temperature climbed from 16 to 55°C, and remained virtually steady at retention 67 percent when the polymer reaches its (Tg) 55°C. Furthermore, hybridization of carbon fibers with glass or basalt fibers showed the same variation in tensile strength as CFRP sheets at temperatures between 16 and 200°C, with lower scatter Figure 26. (Saleh Alsayed, 2012) studied the effects of 100, 200, and 300 degrees Celsius on the strength and durability of GFRP bars (E-glass/vinylester) and GFRP-reinforced concrete parts (1, 2 and 3 h). Exposure to higher temperatures and longer times resulted in greater reductions in tensile strength. The residual tensile strength of the bars that were coated with concrete was greater than that of their uncovered counterparts, particularly after being heated to 100 degrees Celsius for 1 hour. (Wang YC, 2007)examined the mechanical characteristics of GFRP and CFRP bars at extreme temperatures. Once the desired temperature was reached, it was maintained for around 30 minutes. The strength test continued until the failure load was reached while the temperature was maintained at the set point. Figure 27 displays that at high temperatures, the stress–strain relation-ships of both GFRP and CFRP bars remained nearly linear up to failure. Carbon, glass, and hybrid carbon-glass-reinforced epoxy composites were subjected to temperatures ranging from 25 to 300C for 45 minutes, and their failure mechanisms were studied by (Wang YC, 2007). In Figure 14, we can see that three distinct failure modes emerged, each correlated to a certain temperature range and FRP laminate type. The CFRP, GFRP, and C/GFRP specimens all failed in the same way as the room temperature specimens, with brittle fiber ruptures at various locations along the gauge length; the epoxy adhesives softened at temperatures between 200 and 250 degrees Celsius, and the specimens failed primarily due to partial loss of the epoxy adhesives followed by sheet splitting; and at 300 degrees Celsius, the epoxy adhesives were burnt. Epoxy resin's thermal resilience worsened with increasing temperature, as shown by the varying failure modes, leading to the debonding of the FRP/matrix interface. When fibers are exposed to temperatures over the resin's ignition point, the mechanical behavior and service life of the fibers degrade. (Atsushi Sumida, 2008) looked into the mechanical characteristics of FRP bars made from resol type phenolic (PH) and M type cross-linked polyester-amide (CP) resins with the goal of creating heat-resistant FRP bars. The remaining findings demonstrated that the FRP bar specimens with PH or CP matrix had greater heat resistance than the epoxy resin specimens. In instance, FRP bars constructed with carbon fiber and PH matrix resin have almost the same heat resistance as steel bars.

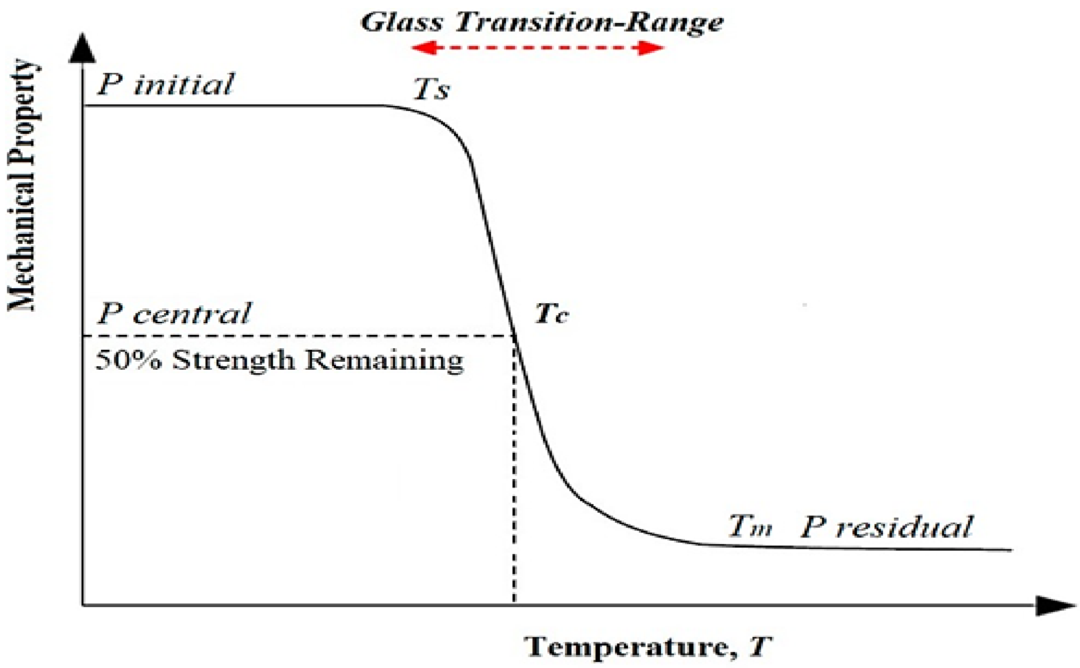

Figure 25(Correlation between heat and changes in FRP mechanical qualities)(Milad Bazli, 2020a) (E. U. Chowdhury, 2011)

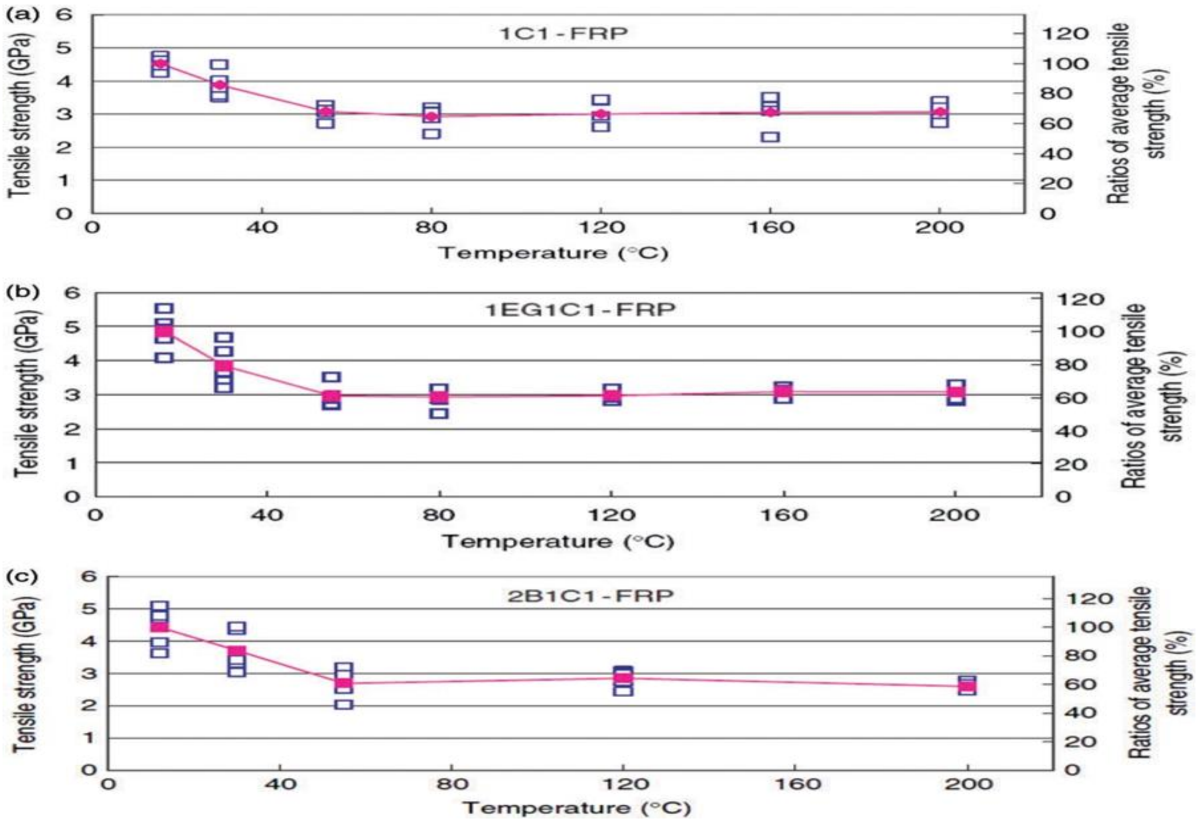

Figure 26(Ratios of tensile strengths to average strengths)(Jun Wang, 2015, Shenghu Cao, 2009)

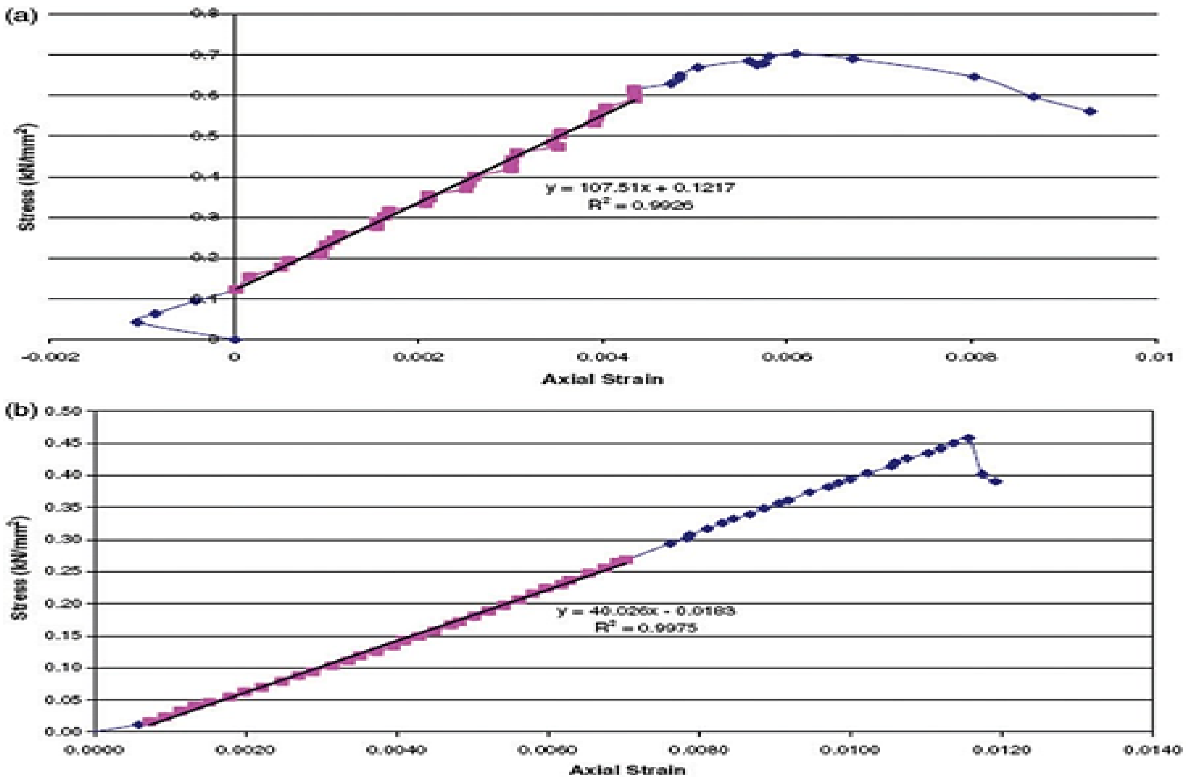

Figure 27((a) CFRP bar at 200C and (b) GFRP bar at 100C stress–strain diagrams)(Jun Wang, 2015, Wang YC, 2007)

3.4.6 Fiber Reinforced Polymer Fatigue

Several factors, including RC, steel, fiber reinforced polymer, loading rate, beam shape, etc., must be taken into account in order to fully understand the fatigue behaviour of an RC beam enhanced with FRP. Some research, particularly those that relied heavily on experimental investigations, found that strengthening an RC beam with FRP increased its fatigue life . Carbon fiber-reinforced polymer (CFRP) may dramatically enhance the fatigue performance of corroded and defective RC beams . As a result of using FRP, reinforcing steel stress is reduced, which is the primary factor. However, the most common types of fatigue failure, such as FRP debonding, steel fracture, and concrete crush, were also included (Jia-Xiang Lin, 2020).

Several experimental programs have investigated the effects of several variables on fatigue performance (Cheng Chen, 2019). These variables include fatigue loading circumstances, prestress levels, beam type, and others. Several scholars have created analytical fatigue models to explore the impact of FRP on the fatigue performance of RC beams, complementing the results of actual study. By examining the residual life and residual strength,(Rongwei Lin, 2008) were able to create two techniques for forecasting the fatigue life of RC beams reinforced with CFRP under random loading. S-N curves might be determined depending on the residual life.

3.4.6.1 FRP Fatigue Numerical Models Predictions

Deterioration in stiffness of RC beam reinforced with FRP during fatigue loading was examined by (Miao Lu, 2007, Papakonstantinou CG, 2002).Using the plane section and perfect bond assumptions, an analytical fatigue model was developed. The fatigue performance of RC beams reinforced with CFRP was simulated using a model (Sherif El-Tawil, 2001), who took into consideration the fatigue behaviour of component materials. In addition, the plane section and perfect bond assumptions has been taken into consideration in this model. In order to foretell the fatigue life of flawed RC reinforced with CFRP using the finite element (FE) approach, (Nawal KishorBanjara, 2019) created computational models. The plane section and perfect bond assumptions were also included into the model. Although complete bond was assumed in the aforementioned analytical fatigue models, the impact of interfacial slip between the FRP and concrete on the reinforced beams was not taken into account. It is crucial to understand how FRP and concrete connect at the interface. Studies of the static behaviour of RC beams reinforced with CFRP have been conducted, and the bond behaviour of the CFRP-concrete interface has been investigated in numerical model. By plugging in data from the bi-linear bond-slip model of the FRP-concrete interface into equilibrium equations, (M.L.Bennegadi, 2016) developed a model.

Flexural fracture in RC beams reinforced with FRP may be characterized by measuring the interfacial shear stresses and normal stresses induced by the crack. Research Conducted by (Ricardo P., 2010), who computed the interfacial shear stress and the load–displacement response of FRP-strengthened RC beams subjected to static loading using the bilinear bond-slip equation.(A.G.Razaqpur, 2020) developed equations that account for the slide of the FRP-concrete contact and yet satisfy the compatibility and equilibrium requirements. Under static loading, it is also possible to measure the load-deflection relationship, the shear stress at the FRP-concrete interface, the FRP strain, and the debonding load in RC beams that have been retrofitted with externally bonded FRP. To investigate the performance of RC beams when reinforced with FRP, (C.Faella, 2008) devised a mechanical model. Vertical deflection of RC beams was found via modelling the interaction of FRP-concrete interface using a continuous elastic layer with no thickness. . Due to the difficulty of bond behaviour of CFRP-concrete interface and the fatigue behaviour of RC beam enhanced with FRP, analytical fatigue models addressing the slip of CFRP-concrete interface is quite restricted. In order to investigate the fatigue behaviour of RC beams reinforced with externally bonded FRP, (Kam Yoke M. Loo, 2012) created a FE model. In spite of this, the numerical model included the fatigue behaviour of steel and concrete, in addition to the constitutive mode of the FRP-concrete interface. (Xiaodan Teng, 2015) carried out a nonlinear finite element study. This study used the bond-slip model of the FRP-concrete interface, and the FE model was used for the analysis of RC slabs subjected to cyclic stress, which accounted for the degradation of concrete, FRP, and steel reinforcement.. By using the bilinear model to explain the strength degradation of the CFRP-concrete interface during cyclic loading, (Xinyan Guo, 2019) established a FE model to investigate the fatigue behaviour of RC beams enhanced with prestressed CFRP.

Fatigue behaviour of FRP-strengthened RC beams with bond-slip connections and intermediate crack-induced are combined into one model by (Xinyan Guo, 2021)'s analysis, which includes two significant failure modes see. Figure 28, rupture of steel reinforcement and central crack-induced debonding failure. The central flexural fracture was discovered between the 1st and 500th cycles of the fatigue test. High peak load increased the shear stress at the CFRP-concrete interface, causing the fracture to propagate and the deflection of FRP-strengthened RC beams to steadily grow during fatigue loading. The peak load determines how likely it is that an integrated circuit may fail due to debonding. If the associated failure modes were taken into account, predictions of fatigue life would be more precise. Thus, taking into account the relevant failure modes improves the accuracy of the fatigue life forecast.

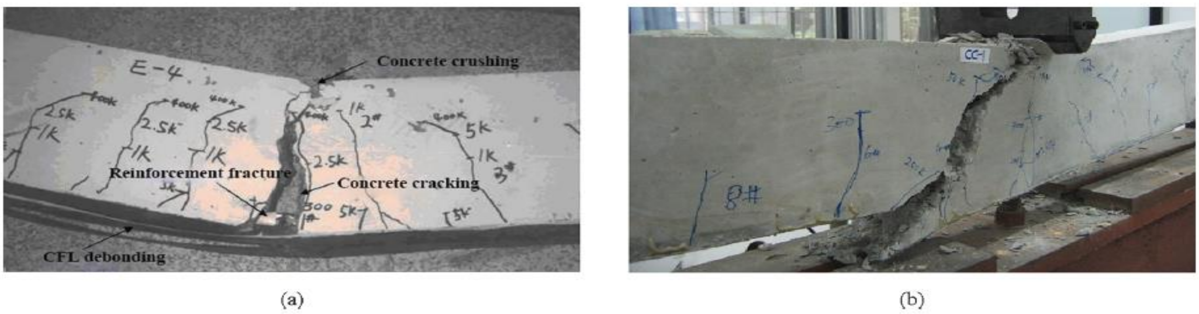

Figure 28(Failure mechanisms of a CFL-reinforced RC beam are (a) reinforcement rupture and (b) Debonding of Central Flexure Crack-CFL)

3.5 Fiber Reinforced Polymer Systems Selection

3.5.1 Considerations for the environment

Resins and fibers of different FRP systems react differently to the elements. Some conditions, such as alkalinity, salt water, chemicals, UV radiation, high temperatures, high humidity, and freezing and thawing cycles, damage the mechanical characteristics (such as tensile strength, ultimate tensile strain, and elastic modulus) of some FRP systems.

1- Alkalinity/Acidity

Matrix material and reinforcing fiber determine how well a FRP system will hold up over time in an alkaline or acidic climate. In contrast to exposed glass fiber, which degrades over time in alkaline and acidic environments, bare carbon fiber can withstand these conditions. However, the fiber should be isolated from the alkaline/acidic environment and protected by a resin matrix that has been carefully chosen and applied to prevent degradation. Carbon fiber systems are more preferable than glass-fiber systems in environments with high alkalinity and high moisture or relative humidity.

2-Thermal Expansion

It's possible that FRP systems' thermal expansion characteristics are different from concrete's. The fiber and polymer components of a FRP system might also have different thermal expansion characteristics. Glass fibers have a coefficient of thermal expansion close to concrete, whereas carbon fibers have an almost negligible value. As a rule of thumb, the coefficient of thermal expansion of polymers employed in FRP strengthening systems is around five times that of concrete. Variations in fiber orientation, fiber volume percentage, and adhesive layer thickness add complexity to strain differential calculations caused by temperature changes.

However, previous research and experiments have shown that for moderate changes in temperature (+/-28℃), the bond is unaffected by thermal expansion fluctuations.

3- Conductivity to electricity

Carbon FRP (CFRP) is conductive, whereas glass FRP (GFRP) and aramid FRP (AFRP) serve as effective electrical insulators. Carbon-based FRP materials should not come into direct touch with steel to prevent the possibility of galvanic corrosion of steel parts.

3.5.2 Loading factors

1-The impact tolerance:

The (AFRP) and (GFRP) systems is higher than that of (CFRP) systems in terms of impact tolerance.

2- Creep rupture and fatigue

The carbon fiber reinforced plastic (CFRP) systems are very resistant to creep rupture and fatigue. It has been shown that (GFRP) systems are more vulnerable to the combined effects of these loads.

3.5.3 Durability factors to consider

Freezing and thawing, steel corrosion, alkali and silica aggregate reactions, water entrapment, vapor pressures, and moisture vapor transfer are only some of the climatic factors that should be studied in relation to any FRP system that fully encases or covers a concrete portion.

3.5.4 Selection of protective coating factors

The installed FRP system may be safeguarded against certain forms of environmental damage with the help of a coating or insulation system. The composite repair's needs, as well as the coating's thickness and kind, should inform the decision to protect against moisture, sea water, temperature extremes, fire, impact, UV rays, and other environmental hazards as well as site-specific impacts and vandalism. To delay the loss of the FRP systems' mechanical qualities, coatings are used. It is important to examine and maintain the coatings on a regular basis to keep them performing as intended. Fibers may be shielded against impact and abrasion by applying an external coating or a thicker layer of resin. It may be required to install extra safeguards in high-traffic or high-impact locations. Plaster made of Portland cement and polymer coatings are often used for protection against light impact and abrasion

CHAPTER 4

4. SHEAR REPAIR AND STRENGTHENING TECHNIQUES REVIEW

4.1 Unbonded or Bonded Fiber Reinforced Polymer Wraps

Figure 29(FRB Material Types)(Izat, 2004)

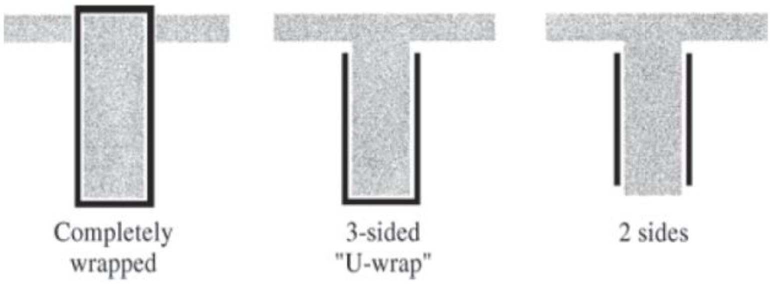

Figure 30(FRP laminates types for shear strengthening)(ACI-440, 2017)

Many experimental researches have established the technique of shear strengthening using fiber reinforced polymer FRP to RC beams. There are different types of FRP (GFRP, CFRP and AFRP) see. Figure 29 and shapes of FRP shear strengthening like (U-Jackets, Full Wraps and Side Strips) see. Figure 30, as with bonded (BF) FRP wraps. Experiments illustrated that flexural cracks, flexural/shear cracks, or both, around the instant of maximum moment may be the starting point of the cracking process which causes FRP de-ponding see. Figure 31. In addition, when beams loaded, these fractures widen and provide significant local interfacial shear stress, which triggers FRP debonding, which spreads over the shear span in the direction of decreasing moment decreases. While the aggregate is often not affected by this failure, it typically progresses through the thin mortar-rich layer that covers the surface of the concrete substrate. In places with a high shear-moment ratio, this failure mode is intensified mechanical anchorage methods, like U-wraps ACI(ACI-318, 2019)

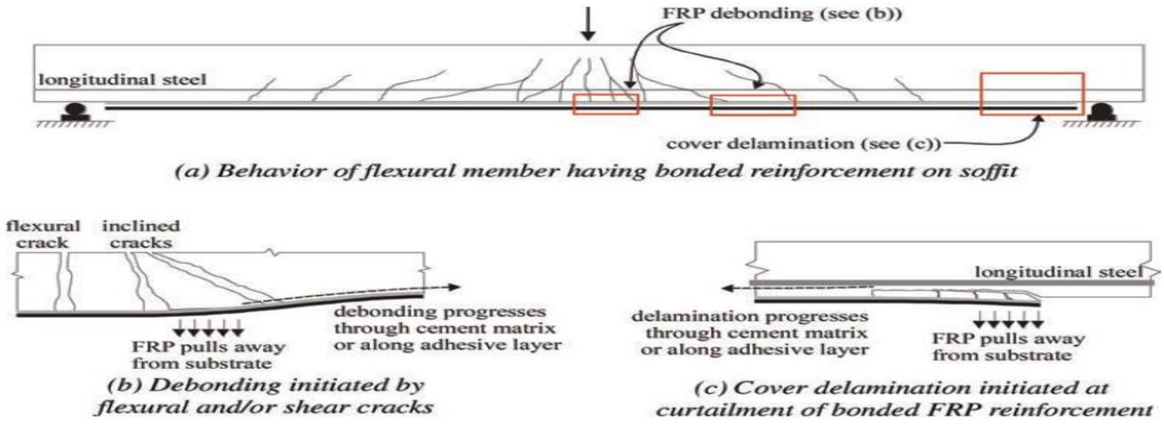

Figure 31(Delamination and Debonding of externally bonded FRP systems)(ACI-440, 2017)

As research done by J.G.Teng(Teng, 2009), reveals that bonded fibers BF and unbonded wraps UBF means (No shear strengthening used), effects in ductility when shear failure happened. The FRP-wrapped beams can be controlled by FRP rapture in the direction of the hoop and can be tested by two different tests (split-disk tests and tensile test of flat coupons) to get FRP rapture strain ε_{fu} and strength of the hoop see. Figure 32. On the contrary, split-disk tests often provide lower FRP rupture strains than flat coupon tests, but there is no clear correlation between the two, and no thorough explanation for why they are different is available either. As an assessment of FRP hoop strains using finite element analysis (FEA) in the split-disk test done by J.F Chen (J.F. Chen 2011), presented an effort to understand why FRP rupture strain was reduced in the test.

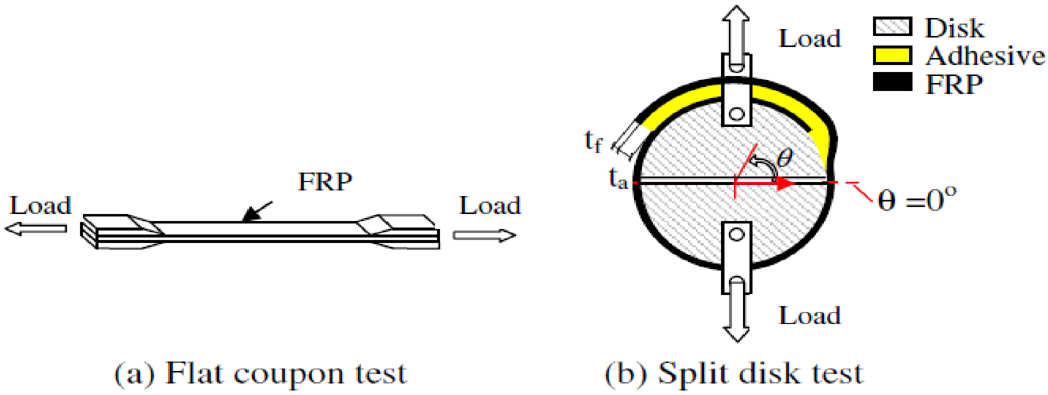

Figure 32(FRB Rapture Strain, Hoop strength Tests)

The FEA findings demonstrate that discontinuities of geometric at the ends of the FRP ring and circumferential bending of the FRP ring at the gap generated by the relative moment of the two half disks enhance local stresses in a split-disk test. Therefore, due to FRP's tendency to rupture when subjected to a load greater than that required to cause FRP coupon rupture, flat coupon tests provide lower apparent tensile strengths. In Other hand, UBF wrap used to estimate the bonding effects and FRP contribution to the sides of the tested beams, it also provide somewhat more shear strength than BF wraps(Teng, 2009). At the point of the view of strain, both types exhibited a significant rise only after the emergence of the shear fracture spanning the FRP wraps, prior to which the stresses were rather low. Due to dynamic debonding and FRP wrap deformation as a result of relative displacement of the critical shear fracture, the FRP for BF and UBF rupture strain was 11% and 29% of the reinforced beams which is much lower than that obtained in tensile testing of flat coupons(Teng, 2009). Even if internal steel stirrups are fully used at beam shear failure owing to FRP rupture ε_{fu} , the concrete contribution to shear capacity may be substantially damaged at high tensile strain $\varepsilon_{fu}{}^*$ values in FRP wraps. As a result for that, the test conducting by J.G.Teng (Teng, 2009) shows that the average values of effective FRP Strain ε_{fe} is a little bit above than recommended value which is 4000 $\mu\varepsilon$ as per ACI440.2R-17(ACI-440, 2017) in order to avoid the loss of aggregate interlock.

4.1.2. Carbon Fiber Reinforced Polymer (CFRP)

Figure 33(Beam Strengthening using CFRP Laminates-Strips)(Construction)

Carbon fiber-reinforced polymer (CFRP) see. Figure 33 is a new reinforcement in concrete materials with numerous appealing mechanical and physical properties. CFRP has strong compressive, flexural, and shear strengths, among other mechanical qualities, and its use enhanced ductility and appropriateness for crack prevention. As a result, the use of CFRP in the building sector is growing.

There are different methods for strengthening using CFRP see. Figure 34 :

1-CFRP Full Wrapping

2-CFRP U-Wrapping

3-CFRP Post-Tensioned Rods

4-CFRP Ropes and Strips

5- CFRP Grids.

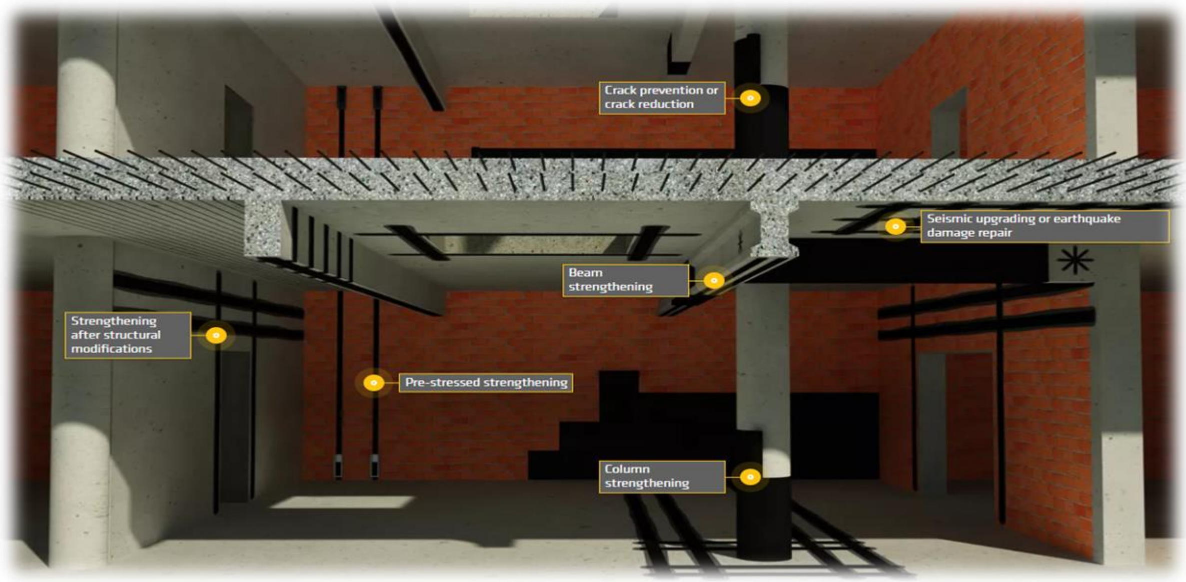

Figure 34(Different Strengthening methods and Types of CFRP)(SIKA)

4.1.1 CFRP Full Wrapping

Full wrapping may be utilized in projects prone to progressive collapse and corrosion to reinforce structural components such as beams, columns, and slabs... and so on. In certain circumstances, complete wrapping may be employed to strengthen particular areas of beams or columns that fail or are on the verge of collapsing owing to increased. Experimental study done by Piya Cho.(Piya Chotickai, 2021) to investigate columns strengthened with (CFRP Full Wrapped) composites under axial eccentric stress of corrosion-corroded reinforced concrete (RC), the result proved the ability of CFRP jacket to reduce columns' confinement effect, moreover under relatively high-eccentricity stress , the ductility and ultimate load for columns rose dramatically for uncorroded specimens. In terms of shear damage, Yanhui said(Yanhui Liu, 2021) that CFRP shown mitigation effectively to avoid brittle shear failure on circular RC columns. In contrast, in order to maximize the strengthening system's performance, the volumetric CFRP ratio had to be high. In badly corroded columns, the confinement effect was recovered at a rather high volumetric CFRP ratio.

4.1.2 CFRP U-Wrapping

U-CFRP wrapping can be used to enhance shear strengths against shear failure to RC beams. It also may be employed to strengthen particular areas of beams like experimental study done by Abdalla G.(Abdalla Ghoneim, 2019) on pre-damaged RC beams. Those beams with no shear reinforcement, which led to be strengthened by bonded CFRP see. Figure 35. The research proved that CFRP improved the shear capacity by 77% from the original value of shear capacity with stiffness and deflection enhancement as well by 32 and 76 % respectively.

Figure 35(Pre-damaged beam with CFRP Strengthening)(Abdalla Ghoneim, 2019)

4.1.3 CFRP Post-Tensioned Rods

This repair approach may be used to repair and maintain old infrastructure such as bridges. Cracks, deformation, and corrosion of reinforcement due to environmental and loads impacts may cause deterioration to bridge girders, so proper repairing technique should be follow to strength this type of structural elements. Research conducted by Clayton A.(Clayton A. Burningham, 2015) on pre-damaged RC deep beam(Girder with diagonal cracks which strengthened by post-tensioned CFRP rods (Unbonded) see. Figure 36. The results illustrated, enhancements in load capacity for the girder comparing with un-repaired one. On the contrary, deflection has no change after strengthened with CFRP post-tensioned rods.

Figure 36(Strengthening using Post-tensioned CFRP Rods)(Clayton A. Burningham, 2015)

4.1.4 CFRP Ropes and Strips

Due to aging of structures some parts of structural elements are weak and needs to reinforced it, so we can use carbon fibres reinforced polymer laminate (Strips) which comes in a form of Plates (SIKA) . When using FRP plates that have been externally bonded, the plates are susceptible to FRP debonding and weathering at relatively modest stresses. Near surface mounted (NSM) was employed as a novel strengthening technology to address the constraint of the externally bonded technique, in which CFRP is inserted in grooves that are produced beneath the concrete cover of reinforced concrete structures see. Figure 37. NSM The application of NSMCFRP in reinforcing concrete structures under compression, flexure, and shear has been researched by a large number of researchers (Hong K, 2018, Obaidat YT, 2020). They discovered that utilizing NSM improves the flexural and shear capacity of RC structures by taking into account numerous aspects such as the quantity, orientation, and type of FRP, groove dimensions, size, and position of NSM, and kind of adhesive. On the other hand, the unique flexible NSM-CFRP material CFRP-Rope may be utilized to repair structural parts. It consists of a bundle of unidirectional, flexible carbon fibers. Although the unit cost of CFRP ropes is about half that of CFRP strips, the research on the use of NSM CFRP ropes for shear strengthening of RC beams is sparse. Research conducting by Marwa s.(Marwa Saadah, 2021) on concrete beams to evaluate the impact of NSM strips and rope see. Figure 38 in shear capacity. As a consequence of the research, it was discovered that NSM CFRP rope is a very successful technology for reinforcing reinforced concrete beams. When compared to all other configurations, the use of inclined CFRP ropes or strips has the highest load bearing capability, with the final load capacity increasing by (150–170 %), in addition of significantly postpone the onset of the initial crack and failure type changing from shear cracking to flexure failure.

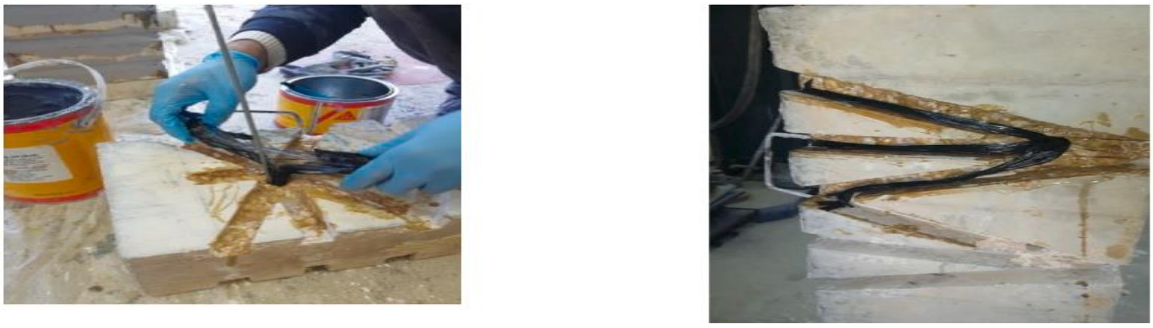

Figure 37 (Installation of CFRP in to Grooves of RC Beam)

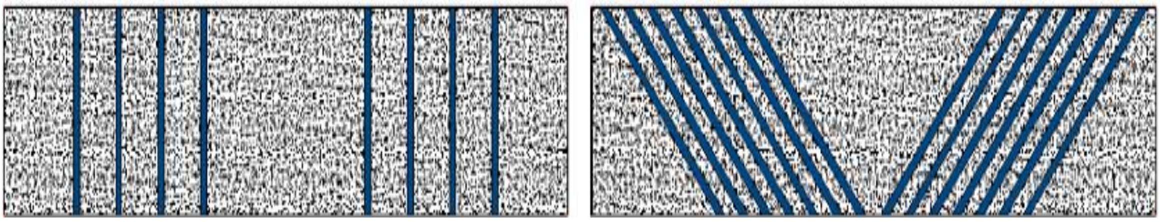

Figure 38(CFRP strengthening using ropes and strips)(Marwa Saadah, 2021)

4.1.5 CFRP Grids

The carbon fiber reinforced plastic grid see. Figure 39, along with cementitious materials, is the innovative approach of reinforcing RC structures that has been developed during the last decade (Yu-Zhou Zheng 2016, Wang WW, 2015).Therefore, carbon fiber reinforced plastic (CFRP) grid is a novel kind of fiber-reinforced plastic (FRP) composite, which is made up of high-strength fiber infused into the resin to produce a grid pattern that has a specific degree of stiffness. Cementitious materials, such as epoxy mortar, polymer cement mortar (PCM), and engineered cementitious composite (ECC), are used to serve as both inorganic bonding agents and protective layers of CFRP grid, epoxy mortar is employed to play these roles. Other cementitious materials, such as polymer cement mortar (PCM) and engineered cementitious composite (ECC), are also used. Research conducted by Lianheng (Lianheng Cai 2021), approved that CFRP grid with epoxy mortar for RC beams under shear may effectively delay the establishment of the key diagonal fractures and improve both shear capacity and deformation ability. As the reinforcement ratio rises, the shear contribution increases; on the contrary, the concrete strength or the shear span ratio decreases. However, even with the premature debonding that occurs during the loading process, the shear capacity of strengthened beams has increased from 22.4% to 56.3%; in addition, the gain in shear capacity is primarily provided by vertical CFRP grids, while horizontal grids inhibit cracking development and also improve bond behaviour.

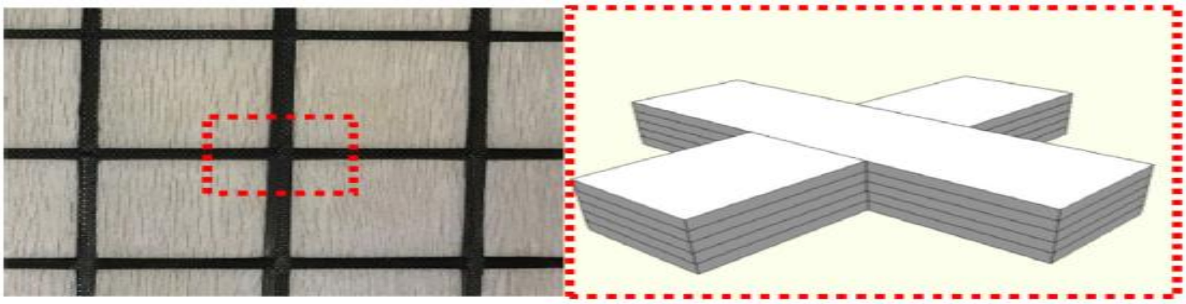

Figure 39(CFRP Grids)(Lianheng Cai 2021)

4.2 Epoxy Injection

Epoxy resin has been extensively utilized across the globe for the restoration of damaged reinforced concrete (RC) structures. It has been widely utilized by contractors in the United Arab Emirates to fix concrete bridges, walls, decks, beams, columns, and other concrete constructions. Repairing fractured concrete buildings has become a standard practice in the civil engineering sector. Epoxy injection offers the potential for durability if the broken reinforced concrete structure is subjected to corrosion, as mentioned by many researchers that have studied the usage of epoxy injection for different applications of RC construction, such as Ekenel and Myers(M. Ekenel, 2007). It's because epoxy injection may raise the initial stiffness of the beam since the bond performance of the epoxy injection is directly connected to the strength of the restored structure. The effects of epoxy injection on fatigue-cracked mortar and concrete have been studied by H.C. Shin(H.C. Shin, 2011) .

Higher temperatures caused the mode of failure to change, according to the findings of the inquiry. Instead of mortar failing, a failure of the epoxy and the interface happened together. Crack movement was found in epoxy-repaired concrete. Due to the epoxy's restraining action, the movement of the fracture was reduced. Another investigation on the use of epoxy injection to repair concrete fractures has been undertaken by C.A. Issa and P.Debs(C.A. Issa, 2007). Concretes' compressive strengths might decrease by as much as 40.93 percent after cracking. However, they discovered that this figure dropped to 8.23% when fractures in concrete were fixed with epoxy.

This exemplifies its usefulness in restoring the original strength of damaged concrete. Based on the reviewed literature, it is clear that prior research has only investigated how well epoxy injection works for structural connections. On the other hand, Soffian and Noorsu.(Soffian Noor Mat Saliah 2021) conducted another study for using acoustic emission (AE) technique with epoxy injection. The study used two different beams (un-repaired reference beam and repaired beam with epoxy injection). The research analyzes and discusses the restoration and repair of reinforced concrete beams that have been damaged by monotonic loading. Epoxy injection strengthened the damaged RC beam by up to 15% relative to the reinforced beam.

This finding suggests that the repaired RC beam's strength may be enhanced using the method described. Beams exposed to three-point stress were analyzed for crack mode classification using (AE) signal strength and load versus time. Results for the (AE) signal strength of the reference beam are also found to be greater than that of the repaired beam. Injecting epoxy into cracks with in an RC beam with (AE) restores the beam's structural integrity and boosts its strength, performance and shear, tensile cracks modes can be identified to be matched with patterns of crack.

4.3 Prestressed Fiber Reinforced Polymer Deep Embedded Bars

Externally applied reinforcement to the shear span of a structure gave rise to the modern practice of shear retrofitting of RC buildings. Due to their resistance to environmental factors, fibre reinforced polymer (FRP) materials have found widespread use in retrofitting applications. An early form of FRP shear retrofitting was the externally bonded (EB) method. The shear span of an RC member is where the retrofitting material is bonded. Premature de-bonding of the unanchored retrofitting material is an inherent downside (Chaallal O, 2011, Godat, 2012) of the EB FRP shear strengthening technology, despite its well-documented efficacy(Bousselham A, 2008) .

One relatively new shear strengthening technology is the deep embedment (DE) method (also known as the embedded through-section (ETS) method) (Manjola Caro, 2021). Because the retrofitting element is embedded into the RC member's core, this method, devised by P.Valerio and T.J.Ibell (P. Valerio, 2003), stands apart from the aforementioned methods. It was shown that steel and FRP reinforcement give equal shear strength augmentation (P. Valerio, 2003), and because the retrofitting element is internal and shielded, steel may also be used in the system without worries about corrosion. For the DE technique, holes are drilled at an angle or straight up from the slab's soffit. Injection of high viscosity epoxy resin followed by embedding of FRP or steel bars see. Figure 40

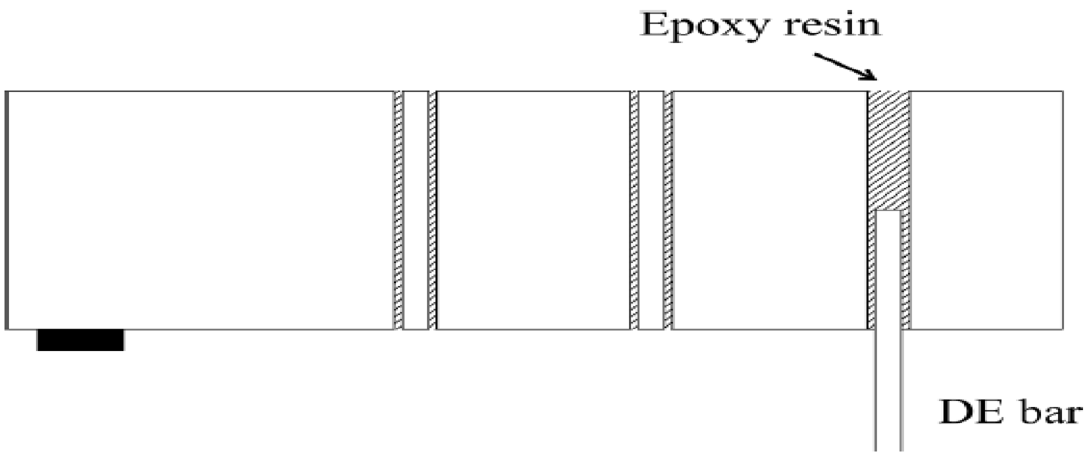

Figure 40(Deep Embedded FRP Prestressed Bars with Epoxy Injection)(Maheshwaran Bhanugoban, 2021)

The DE system's primary benefit is improved truss action inside the beam as a result of the retrofitting bars' tying of the top chord to the bottom chord (Raicic V, 2017). Because the DE technique uses the concrete core to transmit stresses to the retrofitting part, the resulting confinement improves bond performance(P. Valerio, 2003). Experiments by P.Valerio (P. Valerio, 2009) demonstrated the system's effectiveness by achieving shear enhancement values close to or equal to 100%. For buildings where access is limited to the soffit, DE is a great option. There are other benefits, such as resistance to fire and vandalism, less epoxy usage, and less time spent on beam surface preparation (P. Valerio, 2003). On the other hand, numerical study has been conducted by Maheshwaran Bh.(Maheshwaran Bhanugoban, 2021) illustrated that, The prestress used in the DE shear retrofitting method was shown to be very effective via non-linear numerical simulations. Prestressing the normal and high-tensile concrete by 40% was shown to increase their respective contributions to the structure. Additionally, the use of prestress reduced the amount of undesired straining of the internal shear reinforcement. The DE system also reduced crack propagation in the shear span and increased the beam's stiffness after breaking. As a result, the prestress treatment also improved the beams' durability and serviceability.

4.4 Hybrid Composite Plates

Structures made of reinforced concrete (RC) often need to be repaired and strengthened because of shifts in the load or support conditions, degradation of the materials, or structural damage brought on by earthquakes or other types of intense loading events. Externally bonded steel plates(M. S. Abdel-Jaber, 2003), embedded through section (ETS) (Darby, 2009) and fiber reinforced polymers (FRP), to name a few, are only a few of the various methods and materials that may be used to repair or enhance RC structures.

The weight of the steel plates makes it difficult to manipulate them on the construction site, which is one of the disadvantages of bonded steel plates externally (M. S. Abdel-Jaber, 2003) . There are also concerns regarding durability associated with a reduction in the bond between the surface of the steel plates and the adhesive, as well as a susceptibility to corrosion. One of the limitations of the ETS approach is that it might be difficult to execute the holes at the optimal angle, find the location of the longitudinal steel bars, and have sufficient room to produce the holes through section.

Strain Hardening Cementitious Composite, also known as (SHCC), may be used as the support material for fiber reinforced plastic (FRP) reinforcements in order to provide an efficient strengthening solution that may be anchored to concrete structures using various types of anchoring systems. In more recent times, SHCC has been used in the production of thin plates with the purpose of enhancing the ability to shear of RC beams(Baghi, 2015) . A ductile shear response, a high energy absorption capacity, stable hysteretic loops even at large drifts, and structural integrity are all shown by the reinforced SHCC. (V. Mechtcherine, 2012).

The Hybrid Composite Plates (HCPs) method used a thin plate of strain hardening Cementitious composite (SHCC) strengthened with Carbon Fiber Reinforced Polymer (CFRP) laminates see. Figure 41.

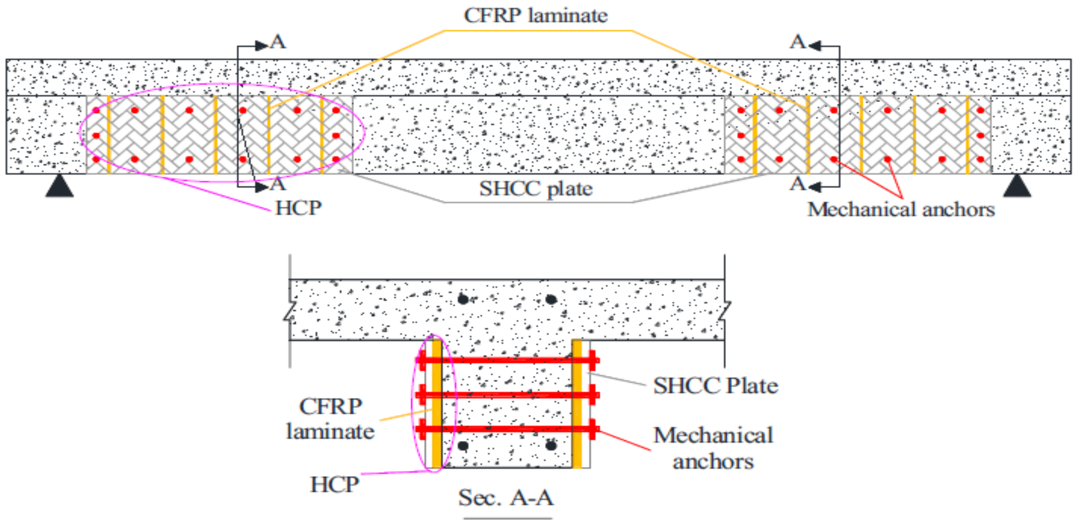

Figure 41(Shear Strengthening using HCPs)(Hadi Baghi 2017)

According to research done by Hadi B.(Hadi Baghi 2017) , when (HCPs) technique has been applied to the beams' end faces using epoxy resin and mechanical fasteners. A certain tension was given to the fasteners to improve concrete confinement. As a result, the (HCPs) illustrated see. Figure 41 the ability to stop the shear failure crack from spreading while new fractures developed in another area of the beam under loading, the reinforced beams behaved similarly to their undamaged counterparts(Hadi Baghi 2017). The SHCC was able to maintain 50 percent of the average shear strength for an average slip that was two times bigger than the average slip at peak load, which demonstrates the composite material ductility when it is subjected to shear deformations. Higher confinement of the concrete increases the load-carrying capacity and deformability performance of these reinforced beams with increasing torque applied to the mechanical fasteners(Hadi Baghi 2017). When compared to a beam where a bond material is employed to guarantee perfect (no sliding between HCPs and substrate), the load bearing capability of the beam without adhesive is around 65% of the beam where a bond material is applied. For the purpose of this investigation Another study has been carried out by Matheus Pi.(Matheus Pimentel Tinoco 2021), polyvinyl alcohol (PVA), polyethylene, and steel fibers were used, and hybrid combinations were generated by substituting steel fibers for PVA and polyethylene fibers. The composites were subjected to uniaxial strain tests in order to investigate their mechanical performance, and a high-resolution picture capture approach was used in order to investigate the fracture pattern. The findings have indicated that the hybridization decreases the strain capacity of the composites but enhances their strength and post-crack stiffness. In addition to this, the load-bearing capability of the beams was enhanced, and the expansion of any pre-existing cracks was slowed down. When it came to managing the existing cracks, the performance of the hybrid composites was on par with that of the non-hybrid composites. Moreover, it was discovered that hybrid composites are potential materials for increasing the performance of structural elements in serviceability limit states as well as at low strain values.

4.5 Self-Compacting Concrete Jacketing (SCC)

Applying jackets around reinforced concrete (RC) structural parts is a typical rehabilitation treatment for members with inadequate detailing or damage. It is common knowledge that RC jacketing is an established and reliable upgrade option. It's common knowledge that RC jackets improve structural performance in terms of rigidity, strength, and pliability. Despite its drawbacks, typical RC jacketing is widely used either before or after damage to RC parts such beams, columns, and joints (G. E. Thermou, 2007, Dritsos, 2008).

Strengthening an existing RC component with a shotcrete overlay and an exterior constructed reinforcement cage has also been shown to be effective. Shotcrete jacketing has the potential to produce strong bond strength and low permeability, making it an alternative to traditional cast-in-place concrete jackets. Shotcrete is more adaptable than traditional concrete installation and may be used in areas where using traditional concrete formwork would be time-consuming, expensive, or impossible (Tsonos, 2010).

Lately, thin locally applied RC jacket used to repair weakened RC beam-column connections. Since this jacketing method very little alters the original size of the components, the building's seismic behaviour is hardly impacted, and it may be used even in limited spaces where traditional RC jackets cannot. This thin jacket is comprised of a premixed, non-shrink, flowable, fast, and high-strength cement based mortar, and it is reinforced with steel bars with tiny diameters.

SCC is a non-segregating concrete that flows easily and fills in formwork, enclosing even the densest reinforcement without the need for mechanical vibration (A. S. Georgiadis, 2010). For the restoration of element continuity and homogeneity after damage to concrete, SCC is the material of choice because to its high workability, amazing filling and passing ability. In addition, SCC flows through reinforcements without creating vacuums in the element or a break between the old and new concrete. Because of the constraints of the jacket, SCC combinations with high fluidity, small diameter aggregate, shrinkage offset, and high strength are often needed.

Research undertaken by (Pourzitidis, 2012) addressed and investigated the use of a thin jacket composed of self-compacting-concrete (SCC) for the rehabilitation of shear-damaged RC beams see. Figure 42. As a results of using this retrofitting technique; the applied jacket capacity improved the structural performance of the analysed beams, as is the possibility that the beams' shear failure mode may be changed to a more ductile one. In addition, significant increase of the loading bearing capacity of retrofitting RC beam that varied from 35% to 200%.

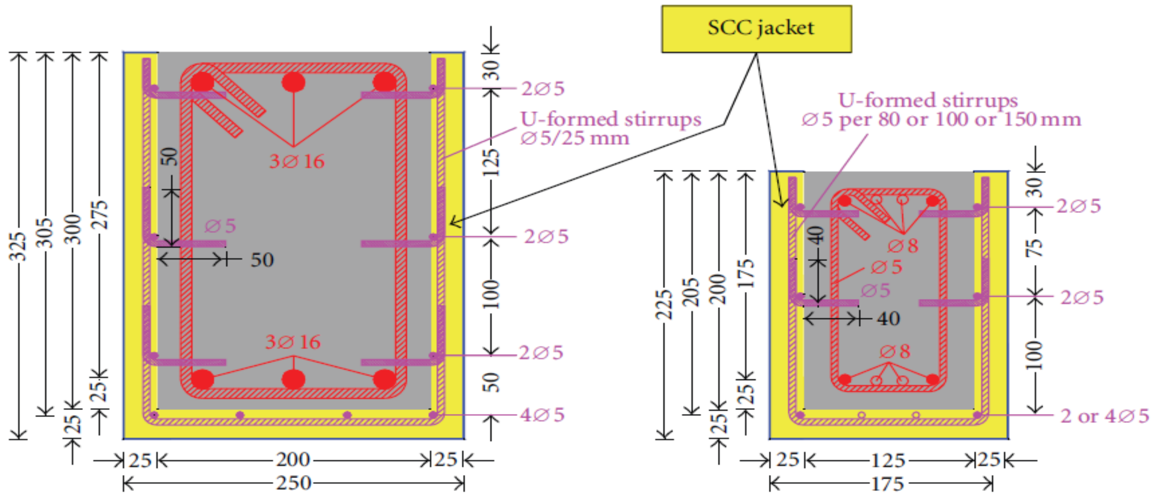

Figure 42(The jacketed beams' cross-sectional size and steel reinforcing layout)(Pourzitidis, 2012)

4.6 Slurry Infiltrated Fiber Concrete (SIFCON) Jacketing

One catastrophic failure mechanism is shear failure of a reinforced concrete beam. Unlike flexural failure, which happens gradually (if the beam is inadequately reinforced) with huge deflections and cracks providing enough notice, shear failure may occur rapidly without prior warning if an overloaded reinforced concrete beam is weak in shear strength. Therefore, in order to guarantee ductile flexural failure, reinforced concrete beams need enough protection, strengthened, in the shear zone(MSai Krishna, 2021, Rawan Al-Shamayleh, 2022).Rehabilitating structural parts to resist shear is now the industry's biggest problem. To begin, various models were created to determine how much shear force could be carried inside an RC beam before it failed. In other words, the shear strength of reinforced concrete elements was improved by the introduction of novel materials and methods (Triantafillou, 1998).

High Performance Fiber Reinforced Composites (HPFRC) are an innovative cement-based composite that has recently emerged as a dependable and cost-effective means of modernizing reinforced concrete buildings. The upgrading process has the potential to provide significantly improved strengths, ductility, and durability, and it is less expensive to build than traditional approaches. There are now three different HPFRC varieties on the market, using Slurry Infiltrated Fiber Concrete (SIFCON) (B.Abdollahi, 2012) as an example, using concrete is infiltrated with a slurry is called slurry infiltrated mat concrete (SIMCON) (Neven Krstulovic, 1999) and using (SFRC) (WassimBen Chaabene, 2021) Steel Fiber Reinforced Concrete. Composite material SIFCON consists of short steel fibers embedded in a Portland cement matrix. It's not like traditional FRC, where steel fibers are blended with regular concrete at a rate of 1% by volume. However, SIFCON begins with a bed of preplaced steel fibers, typically between 8% and 12% by volume. A cementitious slurry of low viscosity is injected into the fiber bed. Compressive strength, toughness, and ductility are all enhanced in the final composite material. SIFCON typically has compressive strengths between 80 and 200 MPa (B.Abdollahi, 2012).Identical steel fibers as those used in regular fiber concrete are utilized in SIFCON. Different types of deformation on the fibers help with mechanical bonding (B.Abdollahi, 2012). The fibers also vary in length and diameter. Large stresses in the cement matrix are when fibers really shine. The matrix's limited ability to withstand tensile strain precludes this from occurring without the emergence of fractures. Because fibers are able to withstand tensile pressures that the softening cement matrix can no longer handle, their inclusion should help keep fracture widths to a minimum.

Study conducted by (Rajai Z. Al-Rousan, 2018) who used Slurry Infiltrated Fiber Concrete (SIFCON) as shear strengthening and repair materials for reinforced concrete (RC) beams of normal strength. The primary goal was to providing innovative and effective building materials for reinforcing defective RC beams. According to the test findings, all of the beams reinforced with SIFCON jackets had a good shear capability. The use of SIFCON jackets as external shear reinforcement eliminated brittle shear failure and increased the ultimate shear strength of strengthened beams from 37 to 53 percent; additionally, it was more effective than repaired beam in improving ultimate load capacity and post peak deformability due to the fiber mechanism at early and late stages of loading. As a result, SIFCON jacket may be regarded as a potential material for RC structure strengthening and repair. With an acceptable error of less than 30%, an analytical model was given for forecasting the shear behavior of reinforced RC beams with SIFCON Jackets.

4.6.1 SIFCON Jackets Effectiveness in shear Strengthening

Calculating the energy absorption ratio for each of the beams with SIFCON jackets is a more concrete way to show the efficacy of SIFCON jackets in enhancing the ultimate load capacity and the post-peak deformability. The energy absorption ratio is calculated by dividing the energy absorbed by the beam with SIFCON jackets by the energy absorbed by a reference beam without shear reinforcement. There are three processes through which the SIFCON jackets increase the shear strength of reinforced concrete beams. At first, SIFCON jackets secure the longitudinal bars and boost their dowel capacity. Second, the fibers' capacity to bridge and transmit pressures across the diagonal fracture limits the cracks' expansion. As a result, reinforced concrete beams perform better under service load circumstances, and their ultimate strength is increased and they are able to attain their maximum flexural capacity with less cracking(Rajai Z. Al-Rousan, 2018) .

4.7 Textile-Reinforced Mortar (TRM)

Of most cases, the results of a shear failure in a building's RC beams are catastrophic. Existing RC beams may have varying degrees of shear insufficiency due to accidents and mistakes during the design or construction stage, natural catastrophes, increases in applied loads, aging, and lack of maintenance (Lindung Zalbuin Masea, 2020, Tidarut Jirawattanasomkul, 2020). Therefore, existing shear-deficient RC beams need to be repaired and their structural performance enhanced using a cost-effective strengthening strategy. Textile-reinforced mortar

(TRM) is a potential strengthening technique launched in recent years to enhance existing buildings due to its high temperature resistance, excellent compatibility with concrete structures, worker friendliness, and little size change compared to the original structure (Leonidas Alexandros S.Kouris, 2018). A fiber textile and an inorganic matrix made up the TRM system. Fabric-reinforced cementitious matrix (FRCM) (Adel Younis, 2017) and textile-reinforced concrete (TRC) (Li Yao, 2019) are other names for TRM. There have been studies in which TRM was used to reinforce RC beams against shear (Aohan Zheng, 2021). After being strengthened, the RC beams' shear capacity improved, and their failure mode shifted from brittle to ductile, as shown by the findings. However, debonding between the interface of the TRM and the concrete substrate was commonly seen (Zoi C.Tetta, 2016). This was attributed to textile slippage in the mortar. Low textile efficiency (Rui Guo, 2019) was a direct outcome of the poor matching performance between mortar and textile and the low elongation of mortar. There is a correlation between the matrix's ductility and fracture toughness and the efficiency with which textiles are used, as well as the shear strengthening efficacy of TRM, as was determined in (XuYang, 2020). Short polyvinyl alcohol (PVA) fibers were shown to increase the toughness of the matrix and the interface performance between the textile and the matrix (Zhifang Dong, 2020). Incorporating short PVA fibers into the TRM is a practical and widely accessible way to improve textile performance. Most prior research focused on the material ingredients of TRM (XuYang, 2020), structural features of RC beams (Zoi C.Tetta, 2018), strengthening forms (Zoi C.Tetta, 2015)and end-anchorage methods (E. Tzoura, 2016). These TRM shear strengthening studies only included beams that were neither damaged or preloaded. However, in fact, most RC structures that need reinforcing are in a deteriorated condition. Some RC parts, nevertheless, can't be fully de-stressed before being strengthened. The effects of initial damage and sustaining load levels on TRM's ability to strengthen against shear have not been taken into account in previous investigations. Therefore, research into TRM's practical engineering use is necessitated by the need to better understand its applicability to shear-damaged RC beams.

Research on the shear behavior of reinforced concrete (RC) beams with a U-shaped thermoplastic resin (TRM) jacket has been undertaken by (Liying Guo, 2022). The efficiency of the TRM was enhanced by using short PVA fibers. Carbon textile reinforcement ratios, RC beam degrees of pre-damage, and sustaining loads were the variables studied. Steel bars and textiles were analyzed for their failure mechanism, load–deflection curve, and strain development. As a result of this study, TRM raised the shear capacity and ultimate deflection of undamaged beams by 53.42-67.35% and 18.37-35.54%, respectively. Increases of 18.32%-53.78% in shear capacity and 12.24%-14.12% in ultimate deflection were seen in pre-damaged beams after being reinforced with the TRM. The shear capacity of RC beams may be greatly improved by using the TRM strengthening system, which can also repair any damage they may have sustained. Increase in shear capacity of pre-damaged beams reinforced with TRM was equivalent to that of the nondamaged strengthened beam when the pre-damaged degree was not over the yield of the stirrups. However, the increase in shear capacity of the pre-damaged beam reinforced with TRM was much smaller than that of the non-damaged strengthened beam when the pre-damaged degree reached up to the shear failure. As a result of shear cracking, the beams' internal stress was also redistributed.

4.8 Externally Bonded Steel Plates

The ultimate flexural or shear capacity, or the ability to regulate deflections and cracks, may need to be increased in preexisting concrete structures, which may need reinforcing or stiffening. Adhesively bonding steel plates to the concrete surface is one approach to achieving this increased strength. In use for almost 30 years globally, and in the UK since 1975, the method of employing externally bonded steel plates is not new. The benefits of external reinforcement over other techniques include a less impact on available headroom, a lower overall cost, simplified maintenance, and the possibility to strengthen a portion of the building while it is in use.

(R.A.Barnes, 2001) shown that bolts may be used to fasten steel plates to the sides of reinforced concrete beams for strengthening reasons, adding to the growing body of evidence that connecting steel plates to the side of reinforced concrete beams can increase their load capacity in shear. Steel plates are bonded to the beam's side faces in certain plate bonding operations to increase the beam's shear capacity; (G C Mays, 1992) document an empirical method to the design of the steel plates.

For shear and flexural strengthening of reinforced concrete buildings, however, the externally bonded (EB) approach utilizing steel plate has been the most prevalent and popular owing to its superior benefits (H. M. Elsanadedy, 2014). The main drawback of this approach, however, is that EB plates might break prematurely due to debonding, preventing the beams from reaching their full flexural and shear strength potential. Debonding of strips at the concrete-adhesive interface was seen for shear strengthened beams (Sinan Altin, 2005), whereas end peeling was observed for flexural strengthened beams (H. M. Elsanadedy, 2014) and intermediate crack (IC) induced debonding of plates (Richard Andrew Barnes, 2006b). As a result of inadequate bonded area of plates and shear fractures, the shear strip of the reinforced beam would have deboned. Shorter shear strips are the norm since beam depth is often lower. Furthermore, shear cracks hasten the strain of plate and cause stress concentration around the fracture to be larger, which might lead to the initiation of debonding of the plate. Therefore, in shear strengthening of RC beam, debonding of EB steel plate, FRP wrap, and CFRP laminate is typical(Richard Andrew Barnes, 2006b).

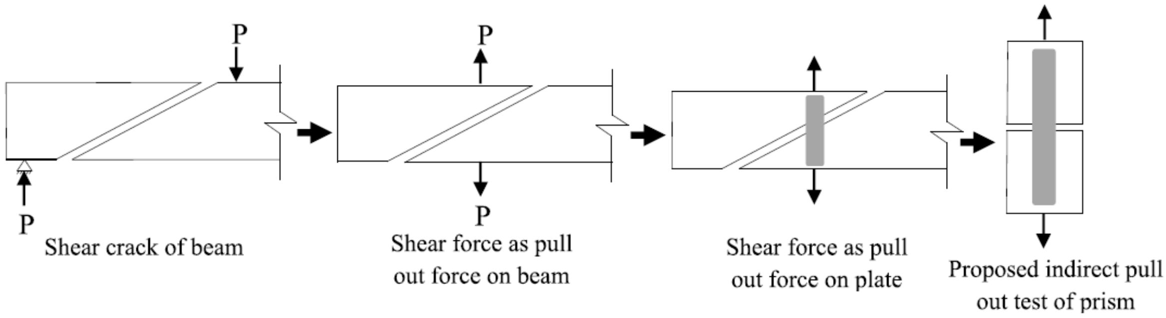

Figure 43(Schematic depiction of the relationship between the beam's shear force and the prism's tensile force)(Md Ashraful Alam, 2020)

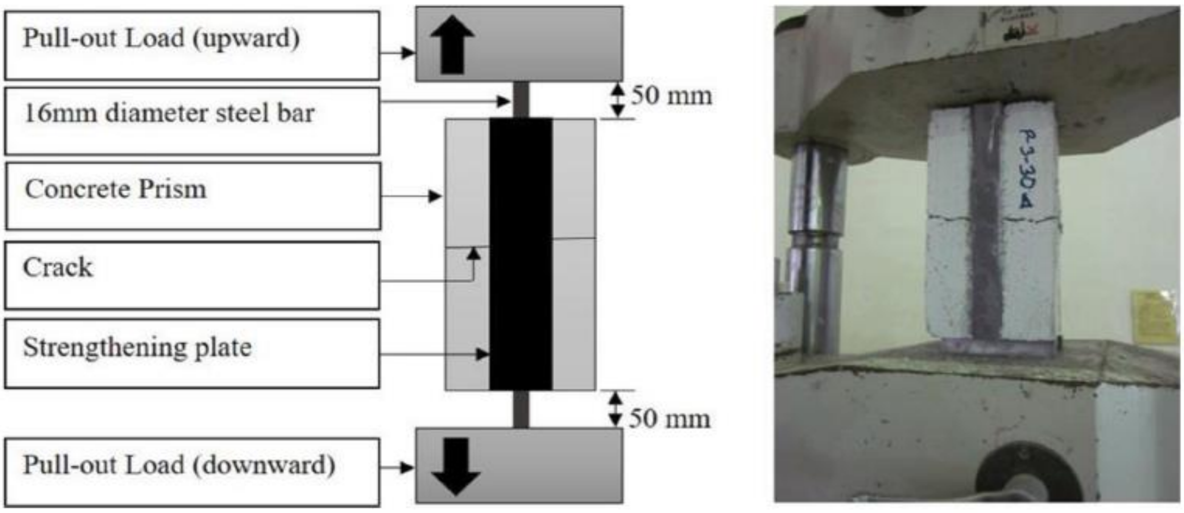

Figure 44(RC Prism Pull out Test Considering Cracking)(Md Ashraful Alam, 2020)

Researchers have developed anchor solutions for preventing debonding failure(A. Mofidi, 2012) due to the prevalence of this problem in shear-strengthened RC beams. Since this is the case, theoretical prediction of debonding failure is necessary for both anchor system design and shear reinforced RC beam analysis. Debonding failure of a shear reinforced RC beam may be predicted using existing research and algorithms. The interfacial bond strength of externally joined plates is the primary parameter in determining the likelihood of debonding failure, as stated by the recommendations (Md Ashraful Alam, 2016). Pull out testing of prisms provided information on the interfacial binding strength of EB plates Figure 44 . However, as can be shown in Figure 43, the process of shear force transmission to the EB strip of the reinforced beam should inform the approach used for the pull out test of the externally bonded shear strip.

The beam is now in halves due to the shear fracture. When a beam cracks in two, the two halves may exert a pulling force on the EB shear strip seen in Figure 43.

Debonding failures of shear reinforced RC beams may be predicted with the use of bond strength models of EB steel plates, as described by (Md Ashraful Alam, 2020) research. The findings showed that the interfacial bond strengths of EB steel plate were drastically reduced by the existence of fractures, and that the bond strength was also diminished due to increasing length and breadth of EB steel plate. Debonding failure loads predicted by the suggested models for steel plate shear reinforced RC beams differed from actual data by 3.4% and 4.7%, respectively. However, prior studies' models had shown far greater debonding failure loads than those of experimental data.

In contrast to (Md Ashraful Alam, 2020) suggested adhesively EB vertical strips, which rely on traditional internal shear linkages, a different research by (Richard Andrew Barnes, 2006a) showed that employing continuous adhesively EB vertical steel plates was more advantageous. The plated beams failed at higher loads than expected, shear strains, in addition to tensile and compressive strains from bending, were detected in the plated RC beams by the use of primary stress measurement techniques. Thus, the plates prevent cracking and catastrophic shear failure up to the load level at which bond failure occurred in the concrete. Strain patterns close to the shear fracture matched those anticipated by the model. Shear strength contributions of continuously externally bonded steel plates to various concrete sections may be determined using the equation published by (Richard Andrew Barnes, 2006c)

CHAPTER 5

5. RESEARCH METHODOLOGY

5.1 Introduction

This chapter describes the research technique, methodology, and strategy used to achieve the study's purpose.

It illustrates a case study taken into consideration for this research by (Mohamed Ghoneim, 2020) and provides a numerical assessment to understand how a RECYCLED CONCRETE AGGREGATE (RCA) beam would behave when reinforced with carbon fiber reinforced polymer (CFRP) without shear reinforcement (CFRP) and to compare the experimental method vs the theoretical method. This kind of study aims to forecast the outcome of reinforcing an RCA beam using CFRP without shear reinforcement using numerical evaluations. Moreover, American standards code based check for strengthening using FRP (ACI-440, 2017) will be conducting in this study using (MIDAS Design +) software to compare the experimental results with numerical calculations.

5.2 Code Provision of FRP Strengthening in Accordance with ACI Standards

One of the important objectives in this research is to confirm the quality and accuracy of the results using the American Code for (4.1 Unbonded or Bonded Fiber Reinforced Polymer Wraps) FRP Strengthening Concrete Structural Elements (ACI-440, 2017).The steps which code follows to calculate shear reinforcement's shear contribution of FRP strengthening using CFRP as below:

Step 1: Determine the design material characteristics.

Table 1 illustrates how can I choose the right type of FRP based on environmental exposure

Exposure conditions	**Fiber type**	**Environmental reduction factor C_E**
	Carbon	0.95
	Glass	0.75

Interior exposure	Aramid	0.85
Exterior exposure (bridges, piers, and unenclosed parking garages)	Carbon	0.85
	Glass	0.65
	Aramid	0.75
Aggressive environment (chemical plants and wastewater treatment plants)	Carbon	0.85
	Glass	0.50
	Aramid	0.70

Table 5(Factor of environmental reduction for different FRP systems and exposure situations)(ACI-440, 2017)

-By using equations to get

$$\left[f_{fu} = C_E\, f_{fu}^{*}\right] \text{MPa}$$

Equation 1(Ultimate Tensile Strength FRP)

$$\left[\varepsilon_{fu} = C_E \varepsilon_{fu}^{*}\right] \text{mm/mm}$$

Equation 2(Design Rupture Strain of FRP Reinforcement)

Where:
f_{fu} = design ultimate tensile strength of FRP, (MPa)
C_E = environmental reduction factor
f_{fu}^{*} = ultimate tensile strength of the FRP material as reported by the manufacturer, (MPa)
ε_{fu} =design rupture strain of FRP reinforcement, (mm/mm)
ε_{fu}^{*} =ultimate rupture strain of FRP reinforcement, (mm/mm)

Step 2: Determine the effective strain level in the shear reinforcement of FRP.

-Calculate the Following

$$\left[L_e = \frac{23300}{(nt_f E_f)^{0.58}}\right] \text{mm}$$

Equation 3(FRP Laminates Active Bond Length)

$$\left[k_1 = \left(\frac{f'_c}{27}\right)^{\frac{2}{3}}\right]$$

Equation 4(Concrete Strength Modification Factor)

$$\begin{bmatrix} k_2 = \left(\dfrac{d_{fv} - L_e}{d_{fv}}\right) & for\ U - Wraps \\ = \left(\dfrac{d_{fv} - 2L_e}{d_{fv}}\right) & for\ Two\ Sides\ Bonded \end{bmatrix}$$

Equation 5(Wrapping Scheme Modification Factor)

$$\left[k_v = \frac{k_1 k_2 L_e}{11900\varepsilon_{fu}} \le 0.75\right]$$

Equation 6(Coefficient of Bond Reduction)

- If members are wrapped completely

Where:
L_e = active bond length of FRP laminate, (mm)
K_1 = modification factor applied to κv to account for concrete strength
K_2 = modification factor applied to κv to account for wrapping scheme
k_v = bond-dependent coefficient for shear
ε_{fe} = effective strain in FRP reinforcement attained at failure, (mm/mm)
ε_{fu} =design rupture strain of FRP reinforcement, (mm/mm)

$\left[\varepsilon_{fe}\ = 0.004 \leq 0.75\ \varepsilon_{fu}\ \right]$ mm/mm

Equation 7(Effective Strain attained by failure in FRP Reinforcement-Full Wrapped)

-If members are Bonded face plies or Bonded U-wraps

$\left[\varepsilon_{fe}\ =\ K_v \varepsilon_{fu} \leq 0.004\ \right]$ mm/mm

Where:
k_v = bond-dependent coefficient for shear
ε_{fe} = effective strain in FRP reinforcement attained at failure, (mm/mm)
ε_{fu} =design rupture strain of FRP reinforcement,

Equation 8(Effective Strain attained by failure in FRP Reinforcement- Bonded Face Plies or U-Wraps)

Step 3: Determine the FRP reinforcement's contribution to shear strength.

-By Using the following equations:

$\left[A_{fv}\ =\ 2nt_f w_f\ \right]$mm^2

Equation 9(FRP Shear Reinforcement Area- Rectangular Sections)

$\left[f_{fe}\ =\ \varepsilon_{fe} E_f\ \right]$ KN/mm^2

Equation 10(FRP Effective Stress at Section Failure)

$$\left[V_f\ =\ \frac{A_{fv}F_{fe}(sin\alpha + cos\alpha)d_{fv}}{s_f}\right] \text{KN}$$

Equation 11(FRP Shear Reinforcement's Shear Contribution)

Where:
A_{fv} = area of FRP shear reinforcement with spacing s, (mm^2)
t_f = nominal thickness of one ply of FRP reinforcement, (mm)
w_f = width of FRP reinforcing plies, (mm)
f_{fe} = effective stress in the FRP; stress attained at section failure, (MPa)
ε_{fe} = effective strain in FRP reinforcement attained at failure, (mm/mm)
E_f =tensile modulus of elasticity of FRP, (MPa)
V_f = nominal shear strength provided by FRP stirrups, (N)
s_f = centre-to-centre spacing of FRP strips, (mm)
N =Number of plies of FRP reinforcement

Step 4: Sections Shear Strength

$\left[\phi V_n = \phi(V_c + V_s + \psi_f V_f\ \right]$ KN

Equation 12(Section Nominal Sear Strength)

Where:
V_c =nominal shear strength provided by concrete with steel flexural reinforcement, (N)
V_f = nominal shear strength provided by FRP stirrups, (N)
V_s = nominal shear strength provided by steel stirrups, (N)

To get (φ) use the following Table 6

$\varphi_f = 0.95$	Completely wrapped members
$\varphi_f = 0.85$	Three-side and two-opposite-sides schemes

Table 6(FRP Shear Reinforcement Additional Reduction Factors)(ACI-440, 2017)

5.3 Research Approach

The state-of-the art review introduced in this research has displayed more details on RCA, FRP and repair techniques for shear failure under different types of loadings with various types of concrete grades and characteristics.

The research approach concentrates on the behaviour of CFRP laminates when used to strengthen RCA beams with (SCC) and fibers in concrete matrix without shear reinforcements under concentrated loads, as per a case study published by (Mohamed Ghoneim, 2020).

5.4 Research Strategy

This study aims to investigate the performance of RC samples strengthened by CFRP with concentrated applied loads to check the shear capacity before and after strengthening.
Data and information used in lab been carried out by (Mohamed Ghoneim, 2020) such like mechanical properties of recycled aggregate, fibers, concrete type and FRP strengthening type. All information provided from study by (Mohamed Ghoneim, 2020) interprets in to ANSYS software to simulate a three beam models (3D Models) with the same applied loads as per study conducted by (Mohamed Ghoneim, 2020). The models will be stated as follows; one with normal aggregate concrete without fibers as control sample, one with (5D) steel fibers in concrete matrix and the last RC with (5D) steel fibers. All samples consist of RA and SCC in concrete matrix.5.5 Modeling Samples Specifications

5.5 Modelling Samples Specifications

The information presented in the case study obtained from research conducted by (Mohamed Ghoneim, 2020, Abdalla Ghoneim, 2019), based on lab testing experiments .

All beams models' dimensions are 150 mm in width and 200 mm in depth and 1600 mm in length; with three bars of 12mm diameters and three stirrups spaced by each 100mm from each support see.Figure 45 (Mohamed Ghoneim, 2020). All beam without shear reinforcement need to evaluate the concrete contribution to the shear capacity by carrying out stress results. Strengthening of externally bonded (EB) CFRP will be used as retrofitting for normal weight aggregate (NWA) sample as per study conducted by conducted by (Abdalla Ghoneim, 2019) to overcome the absence of shear reinforcement .

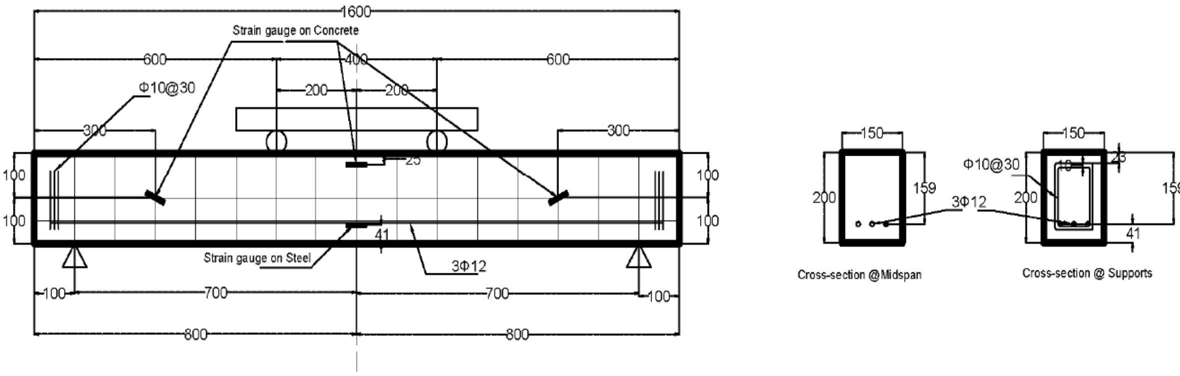

Figure 45(Beam samples with cross-sectional details)(Mohamed Ghoneim, 2020)

5.6 Modeling Procedures

The purpose of using numerical evaluation is trying to figure out all possible straining actions and stresses of different types of beams samples with and without strengthening to study the differences and conducting comparison between modeling software as numerical evaluations and experimental results.

The [ANSYS] model will be used for figuring out the stresses like shear and moment on beam models with proper meshing type and will be compared to lab results. [MIDAS GEN] software will be used for simulating NWA & RCA beams without retrofitting as simple beams (frame elements) with same loads taken in [ANSYS]; then check the stress results (Shear & Moment). After that, exporting the analysis file to [MIDAS Design plus] software and details shear capacity calculation based on ACI-318-19M code (ACI-318, 2019). For NWA sample the strengthening calculations for shear will be carried out using same characterises of (Abdalla Ghoneim, 2019) and results will be checked as per (ACI-440, 2017) code . To close, comparison will be carried out between lab results see. Table 7 and numerical evaluation for shear capacity carried out by software.

<table>
<tr><th>Beam Type</th><th>Compressive Strength ($f'c$) (KN)</th><th>Ultimate Load (KN)</th><th>Failure Load (KN)</th><th>Shear Load (KN)</th><th>Has been Strengthened</th></tr>
<tr><td>NWA(1)
(Normal Weight Aggregate)</td><td rowspan="2">70.50</td><td>120.1</td><td>120.1</td><td>60.05</td><td>No</td></tr>
<tr><td>NWA(2)
(Normal Weight Aggregate)</td><td>126.27</td><td>110.92</td><td>63.14</td><td>Yes</td></tr>
<tr><td>(RCA)
(RECYCLED CONCRETE AGGREGATE (RCA)</td><td>64.50</td><td>81.7</td><td>65.39</td><td>40.85</td><td>No</td></tr>
<tr><td>(RCA-5D$_{(Fibers)}$)
(RECYCLED CONCRETE AGGREGATE (RCA)-5D(Fibers)</td><td>77.00</td><td>130.09</td><td>121.51</td><td>65.05</td><td>No</td></tr>
<tr><td colspan="6">All beams are tested for four-point loading test using Instron servo-hydraulic load frame, with rate of 0.6 mm/min for loading in displacement control</td></tr>
</table>

Table 7(Lab Results for different types of RCA beams)(Mohamed Ghoneim, 2020, Abdalla Ghoneim, 2019)

CHAPTER 6

6. RESEARCH RESULTS (MODELLING)

6.1 Introduction

This chapter outlines the numerical evaluation of pre-damaged recycled aggregate reinforced concrete strengthened by carbon fiber reinforced polymer under the four-point loading test. The research study has been carried out by (Mohamed Ghoneim, 2020, Abdalla Ghoneim, 2019) using experiential lab testing at The American university in Sharjah-UAE.

On the other hand, the modelling results from 3D-Finite elements (ANSYS) and (MIDAS Design+), will be compared to the experimental results and ACI440.2R-17 (ACI-440, 2017).

As mentioned in paragraph (This study aims to investigate the performance of RC samples strengthened by CFRP with concentrated applied loads to check the shear capacity before and after strengthening.

Data and information used in lab been carried out by (Mohamed Ghoneim, 2020) such like mechanical properties of recycled aggregate, fibers, concrete type and FRP strengthening type. All information provided from study by (Mohamed Ghoneim, 2020) interprets in to ANSYS software to simulate a three beam models (3D Models) with the same applied loads as per study conducted by (Mohamed Ghoneim, 2020). The models will be stated as follows; one with normal aggregate concrete without fibers as control sample, one with (5D) steel fibers in concrete matrix and the last RC with (5D) steel fibers. All samples consist of RA and SCC in concrete matrix.5.5 Modeling Samples Specifications) of the methodology chapter, the case study information that will be utilized to perform this assessment are divided into two sections. The first section will be titled "The Analysis Evaluation Part", and it will employ (ANSYS) to depict stress, strains, deflection, and damage. The second section will be titled "The Strengthening Code Evaluation Part", and it will be executed using (Midas Design Plus) to demonstrate the validity and correctness of employing CFRP to strengthen the (RCA-RC) section based on the ACI440.2R-17 standard.

6.2 Numerical Evaluation

6.2.1 Section 1- The Analysis Evaluation (ANSYS)

In this section ANSYS Workbench 2021/R2 will be employed to evaluate the different types of stress, strain, deflection and expected damage to (RCA-RC) beam with CFRP laminates.

6.2.1.1 Analysis Forms

This part will include two separate forms of analysis: "Static structural with non-linear analysis" for various strain, stress, and deflection types, and "Explicit dynamic analysis" for anticipated damage behaviour.

6.2.1.2 Analysis data

6.2.1.2.1 Engineering Data (Mechanical Properties)-For Static Non-Linear Analysis

*Model No.1- Normal Weight Aggregate Sample (NWA).

Mechanical Properties of Normal Weight Aggregate Sample (NWA), $f'c$ =70.50MPa			
Linear Elastic Isotropic Elasticity	Equations	Value	Reference Code
Young's Modulus E_c	$E_c = 3320\sqrt{f'c} + 6900$	34776.14MPa	ACI363R-10-(Eq.6-1) For $f'c > 55MPa$
Poisson's Ration V_c	--	0.2	ACI363R-10-(Sec.6.4)
Bulk Modulus	--	19320 MPa	Software Calculated
Shear Modulus G	0.4 E_c (ACI318-19)	14490 MPa	Software Calculated& ACI318-19-R6.6.3.1
Using Menetrey-Willam Base (Geomechanical Properties)			
Uniaxial Compressive Strength	---	70.5 MPa	ACI318-19 Specified compressive strength of concrete
Uniaxial Tensile Strength	$f_r = 0.62\lambda\sqrt{f'_c}$	5.038 MPa	ACI 318-19 (Eq. 19-2-3)

Biaxial Compressive Strength	$f_{c2c} = \left(1.2 - \frac{f'_c}{1000}\right).f'_c$	79.629 MPa	fib-Bulletin55 Model Code 2010 Section 5.1.6 Commentary
Dilatancy Angle	--	30°	Assumed
Using Menetrey-Willam Base (Geomechanical Properties)-Softening			
Plastic Strain at Uniaxial Compressive Strength	$K_{cm} = \varepsilon_{c1} - \frac{f'_c}{E_c}$	0.000672	fib-Bulletin55 Model Code 2010 Section 5.1.6 Commentary
Ultimate Effective Plastic Strain in Compression	--	0.01	Assumed
Relative Stress at Start of Non-linear Hardening	--	0.4	Assumed
Residual Compressive Relative Stress	--	0.2	Assumed
Plastic Strain Limit in Tension	--	0.01	Assumed
Residual Tensile Relative Stress	--	0.2	Assumed
Strain at Peak Compression	$\varepsilon_{c1} = 0.0027$		Fib-Bulletin,42 Constitutive Modelling of HPC

Table 8(Mechanical Properties of Normal Weight Aggregate Sample (NWA), f^' c =70.50MPa)

*Model No. 2- Mechanical Properties of Recycled Aggregate Concrete with Self Consolidating Concrete Sample (RCA).

Mechanical Properties of Recycled Aggregate Concrete with Self Consolidating Concrete Sample (RCA), $f'c$ =64.50MPa			
Linear Elastic Isotropic Elasticity	Equations	Value	Reference Code
Young's Modulus E_c	$E_c = 3320\sqrt{f'c} + 6900$	33563.55MPa	ACI363R-10-(Eq.6-1) For f'$c > 55MPa$
Poisson's Ration V_c	--	0.2	ACI363R-10-(Sec.6.4)
Bulk Modulus	--	18646 MPa	Software Calculated
Shear Modulus G	0.4 E_c (ACI318-19)	13985 MPa	Software Calculated& ACI318-19-R6.6.3.1
Using Menetrey-Willam Base (Geomechanical Properties)			
Uniaxial Compressive Strength	---	64.5 MPa	ACI318-19 Specified compressive strength of concrete
Uniaxial Tensile Strength	$f_r = 0.62\lambda\sqrt{f'_c}$	4.979 MPa	ACI 318-19 (Eq. 19-2-3)

Biaxial Compressive Strength	$f_{c2c} = \left(1.2 - \frac{f'_c}{1000}\right) . f'_c$	73.24 MPa	fib-Bulletin55 Model Code 2010 Section 5.1.6 Commentary
Dilatancy Angle	--	30°	Assumed
Using Menetrey-Willam Base (Geomechanical Properties)-Softening			
Plastic Strain at Uniaxial Compressive Strength	$K_{cm} = \varepsilon_{c1} - \frac{f'_c}{E_c}$	0.000703	fib-Bulletin55 Model Code 2010 Section 5.1.6 Commentary
Ultimate Effective Plastic Strain in Compression	--	0.01	Assumed
Relative Stress at Start of Non-linear Hardening	--	0.4	Assumed
Residual Compressive Relative Stress	--	0.2	Assumed
Plastic Strain Limit in Tension	--	0.01	Assumed
Residual Tensile Relative Stress	--	0.2	Assumed
Strain at Peak Compression	$\varepsilon_{c1} = 0.002625$		fib-Bulletin,42 Constitutive Modelling of HPC

Table 9(Mechanical Properties of Recycled Aggregate Concrete with Self Consolidating Concrete Sample (RCA), f' c =64.50MPa)

*Model No. 3- Mechanical Properties of Recycled Aggregate Concrete with Self Consolidating Concrete Sample (RCA-5D).

Mechanical Properties of Recycled Aggregate Concrete with Self Consolidating Concrete and Fibers (RCA-5D Fibers), $f'c$ =77.0MPa			
Linear Elastic Isotropic Elasticity	Equations	Value	Reference Code
Young's Modulus E_c	$E_c = 3320\sqrt{f'c} + 6900$	36032.88MPa	ACI363R-10-(Eq.6-1) For $f'c > 55MPa$
Poisson's Ration V_c	--	0.2	ACI363R-10-(Sec.6.4)
Bulk Modulus	--	20018 MPa	Software Calculated
Shear Modulus G	0.4 E_c (ACI318-19)	15014 MPa	Software Calculated& ACI318-19-R6.6.3.1
Using Menetrey-Willam Base (Geomechanical Properties)			
Uniaxial Compressive Strength	---	77.0 MPa	ACI318-19 Specified compressive strength of concrete
Uniaxial Tensile Strength	$f_r = 0.62\lambda\sqrt{f'_c}$	5.44 MPa	ACI 318-19 (Eq. 19-2-3)

Biaxial Compressive Strength	$f_{c2c} = \left(1.2 - \frac{f'_c}{1000}\right).f'_c$	86.471 MPa	fib-Bulletin55 Model Code 2010 Section 5.1.6 Commentary
Dilatancy Angle	--	30°	Assumed
Using Menetrey-Willam Base (Geomechanical Properties)-Softening			
Plastic Strain at Uniaxial Compressive Strength	$K_{cm} = \varepsilon_{c1} - \frac{f'_c}{E_c}$	0.000593	fib-Bulletin55 Model Code 2010 Section 5.1.6 Commentary
Ultimate Effective Plastic Strain in Compression	--	0.01	Assumed
Relative Stress at Start of Non-linear Hardening	--	0.4	Assumed
Residual Compressive Relative Stress	--	0.2	Assumed
Plastic Strain Limit in Tension	--	0.01	Assumed
Residual Tensile Relative Stress	--	0.2	Assumed
Strain at Peak Compression	$\varepsilon_{c1} = 0.00273$		Fib-Bulletin,42 Constitutive Modelling of HPC

Table 10(Mechanical Properties of Recycled Aggregate Concrete with Self Consolidating Concrete and Fibers (RCA-5D Fibers), f' c =77.0MPa

6.2.1.2.2 Engineering Data (Mechanical Properties)- For Explicit Dynamic Analysis

*Model No.1- Normal Weight Aggregate Sample (NWA)- Dynamic.

Mechanical Properties of Normal Weight Aggregate Sample (NWA), $f'c$ =70.50MPa-Dynamic			
Physical Properties	Units	Value	Reference Code
Density	MPa	25	Experimental Data
Thermal Properties			
Specific Heat Constant Pressure	J/Kg-C	654	Assumed Value
RHT Concrete Strength Properties (Brittle/Granular)			
Bulk Modulus	MPa	19320	Software Calculated
Shear Modulus G	MPa	14490	Software Calculated
Compressive Strength $f'c$	MPa	70.5	Experimental Data
Tensile Strength f_t/f_c	--	0.1	Assumed Value
Shear Strength f_s/f_c	--	0.18	Assumed Value
Intact Failure Surface Constant A	--	1.6	Assumed Value
Intact Failure Surface Constant n	--	0.61	Assumed Value
Tension/Compression Meridian Ration Q2.0	--	0.6805	Assumed Value
Brittle to Ductile Transition BQ	--	0.0105	Assumed Value

Hardening Slope	--	2	Assumed Value
Elastic Strength/ft	--	0.7	Assumed Value
Elastic Strength/fc	--	0.53	Assumed Value
Fracture Strength Constant B	--	1.6	Assumed Value
Fracture Strength Exponent m	--	0.61	Assumed Value
Compression Strain Rate Exponent	--	0.032	Software Calculated
Tensile Strain Rate Exponent	--	0.0375	Software Calculated
Maximum Fracture Strength Ration SFMAX	--	1.0E+20	Assumed Value
Damage Constant D1	--	0.04	Assumed Value
Damage Constant D2	--	1	Assumed Value
Minimum Strain to Failure	--	0.001	Assumed Value
Residual Shear Modulus Fraction	--	0.13	Assumed Value
Plastic Strain Failure Properties			
Maximum Equivalent Plastic Strain EPS	--	0.75	Assumed Value
Tensile Pressure Failure Properties			
Maximum Tensile Pressure-(Concrete Spalling)	MPa	4.0	Calculated Value
Crack Softening Failure			
Flow Rule	No Bulking		Assumed Value
Fracture Energy Gf	J/m^2	100	Assumed Value

Table 11(Mechanical Properties of Normal Weight Aggregate Sample (NWA), f' c =70.50MPa Explicit Dynamic)

*Model No. 2- Mechanical Properties of Recycled Aggregate Concrete with Self Consolidating Concrete Sample (RCA)- Dynamic.

Mechanical Properties of Recycled Aggregate Concrete with Self Consolidating Concrete Sample (RCA), $f'c$ =64.50MPa-Dynamic			
Physical Properties	Units	Value	Reference Code
Density	MPa	25	Experimental Data
Thermal Properties			
Specific Heat Constant Pressure	J/Kg-C	654	Assumed Value
RHT Concrete Strength Properties (Brittle/Granular)			
Bulk Modulus	MPa	18646	Software Calculated
Shear Modulus G	MPa	13985	Software Calculated
Compressive Strength $f'c$	MPa	64.5	Experimental Data
Tensile Strength f_t/f_c	--	0.1	Assumed Value
Shear Strength f_s/f_c	--	0.18	Assumed Value
Intact Failure Surface Constant A	--	1.6	Assumed Value
Intact Failure Surface Constant n	--	0.61	Assumed Value
Tension/Compression Meridian Ration Q2.0	--	0.6805	Assumed Value
Brittle to Ductile Transition BQ	--	0.0105	Assumed Value
Hardening Slope	--	2	Assumed Value

Elastic Strength/ft	--	0.7	Assumed Value
Elastic Strength/fc	--	0.53	Assumed Value
Fracture Strength Constant B	--	1.6	Assumed Value
Fracture Strength Exponent m	--	0.61	Software Calculated
Compression Strain Rate Exponent	--	0.032	Software Calculated
Tensile Strain Rate Exponent	--	0.0375	Software Calculated
Maximum Fracture Strength Ration SFMAX	--	1.0E+20	Assumed Value
Damage Constant D1	--	0.04	Assumed Value
Damage Constant D2	--	1	Assumed Value
Minimum Strain to Failure	--	0.001	Assumed Value
Residual Shear Modulus Fraction	--	0.13	Assumed Value
Plastic Strain Failure Properties			
Maximum Equivalent Plastic Strain EPS	--	0.75	Assumed Value
Tensile Pressure Failure Properties			
Maximum Tensile Pressure-(Concrete Spalling)	MPa	2.18	Calculated Value
Crack Softening Failure			
Flow Rule	No Bulking		Assumed Value
Fracture Energy Gf	J/m^2	100	Assumed Value

Table 12(Mechanical Properties of Recycled Aggregate Concrete with Self Consolidating Concrete Sample (RCA), $f'c$ =64.50MPa Explicit Dynamic)

*Model No. 3- Mechanical Properties of Recycled Aggregate Concrete with Self Consolidating Concrete Sample (RCA-5D) Dynamic

Mechanical Properties of Recycled Aggregate Concrete with Self Consolidating Concrete and Fibers ($RCA\text{-}5D_{Fibers}$), $f'c$ =77.0MPa-Dynamic			
Physical Properties	Units	Value	Reference Code
Density	MPa	25	Experimental Data
Thermal Properties			
Specific Heat Constant Pressure	J/Kg-C	654	Assumed Value
RHT Concrete Strength Properties (Brittle/Granular)			
Bulk Modulus	MPa	20018	Software Calculated
Shear Modulus G	MPa	15014	Software Calculated
Compressive Strength $f'c$	MPa	77.0	Experimental Data
Tensile Strength f_t/f_c	--	0.1	Assumed Value
Shear Strength f_s/f_c	--	0.18	Assumed Value
Intact Failure Surface Constant A	--	1.6	Assumed Value
Intact Failure Surface Constant n	--	0.61	Assumed Value
Tension/Compression Meridian Ration Q2.0	--	0.6805	Assumed Value
Brittle to Ductile Transition BQ	--	0.0105	Assumed Value
Hardening Slope	--	2	Assumed Value

Elastic Strength/ft	--	0.7	Assumed Value
Elastic Strength/fc	--	0.53	Assumed Value
Fracture Strength Constant B	--	1.6	Assumed Value
Fracture Strength Exponent m	--	0.61	Assumed Value
Compression Strain Rate Exponent	--	0.032	Software Calculated
Tensile Strain Rate Exponent	--	0.0375	Software Calculated
Maximum Fracture Strength Ration SFMAX	--	1.0E+20	Assumed Value
Damage Constant D1	--	0.04	Assumed Value
Damage Constant D2	--	1	Assumed Value
Minimum Strain to Failure	--	0.001	Assumed Value
Residual Shear Modulus Fraction	--	0.13	Assumed Value
Plastic Strain Failure Properties			
Maximum Equivalent Plastic Strain EPS	--	0.75	Assumed Value
Tensile Pressure Failure Properties			
Maximum Tensile Pressure-(Concrete Spalling)	MPa	4.05	Calculated Value
Crack Softening Failure			
Flow Rule	No Bulking		Assumed Value
Fracture Energy Gf	J/m^2	100	Assumed Value

Table 13(Mechanical Properties of Recycled Aggregate Concrete with Self Consolidating Concrete and Fibers (RCA-5D Fibers), f' c =77.0MPa Explicit Dynamic)

6.2.1.2.3 Engineering Data (Mechanical Properties)- For (CFRP)

Mechanical Properties of Carbon fiber Reinforced Polymer (CFRP)-Sheets (MasterBrace FIB 600/50 CFS)			
Linear Elastic Orthotropic Elasticity	Units	Value	Refences
Density	Kg/m^3	1800	(MasterBrace FIB 600/50 CFS)
Elasticity Young's Modulus X Dir.	MPa	230000	
Elasticity Young's Modulus Y Dir.	MPa	23000	
Elasticity Young's Modulus Z Dir.	MPa	23000	
Poisson's Ratio XY	--	0.2	
Poisson's Ratio YZ	--	0.4	
Poisson's Ratio XZ	--	0.2	
Shear Modulus XY	MPa	9000	Software Calculation (ANSYS)
Shear Modulus YZ	MPa	8214.3	
Shear Modulus XZ	MPa	9000	
Tensile Strength	MPa	3500	(MasterBrace FIB 600/50 CFS)
Thickness	mm	0.337	
Fiber Weight	MPa	600	
Elongation at Break %	--	2.1	
Width	MPa	500	

Table 14(Mechanical Properties of Carbon fiber Reinforced Polymer(CFRP)-Sheets)

6.2.1.2.4 Engineering Data (Mechanical Properties)- For Bearing Pads

Mechanical Properties of Bearing Pads			
Linear Elastic Isotropic Elasticity	Units	Value	Refences

Density	Kg/m^3	7850	Assumed
Young's Modulus E_c	MPa	70	
Poisson's Ration V_c	MPa	0.49999	
Bulk Modulus	MPa	23000	Software Calculation (ANSYS)
Shear Modulus	--	0.2	

Table 15(Mechanical Properties of Bearing Pads)

6.2.1.2.5 Engineering Data (Mechanical Properties)- For Main & Stirrups Rebars

Mechanical Properties of Steel Rebars			
Linear Elastic Isotropic Elasticity	Units	Value	References
Density	Kg/m^3	7850	ACI318-19 Code
Young's Modulus E_c	MPa	200000	
Poisson's Ration V_c	MPa	0.3	
Bulk Modulus	MPa	23000	Software Calculation (ANSYS)
Shear Modulus	MPa	0.2	
Bilinear Isotropic Elasticity (Main Bars)	Units	Value	References
Yield Strength	MPa	460	ACI318-19 Code
Tangent Modulus	MPa	2100	
Bilinear Isotropic Elasticity (Stirrups)	Units	Value	References
Yield Strength	MPa	420	ACI318-19 Code
Tangent Modulus	MPa	2100	

Table 16(Mechanical Properties of Steel Rebars)

6.2.1.3 Analysis Results

6.2.1.3.1 Model Sample No.1 (NWA-1/70.5 MPa)

More study cases of NWA-1 from 1-8 can be found in Appendix A

*The applied load is 120.1 KN which is the ultimate load see.Table 7

6.2.1.3.1.1 Static Non-Linear Analysis – Without Top Rebars and Strengthening

Deformations

Total Deformations

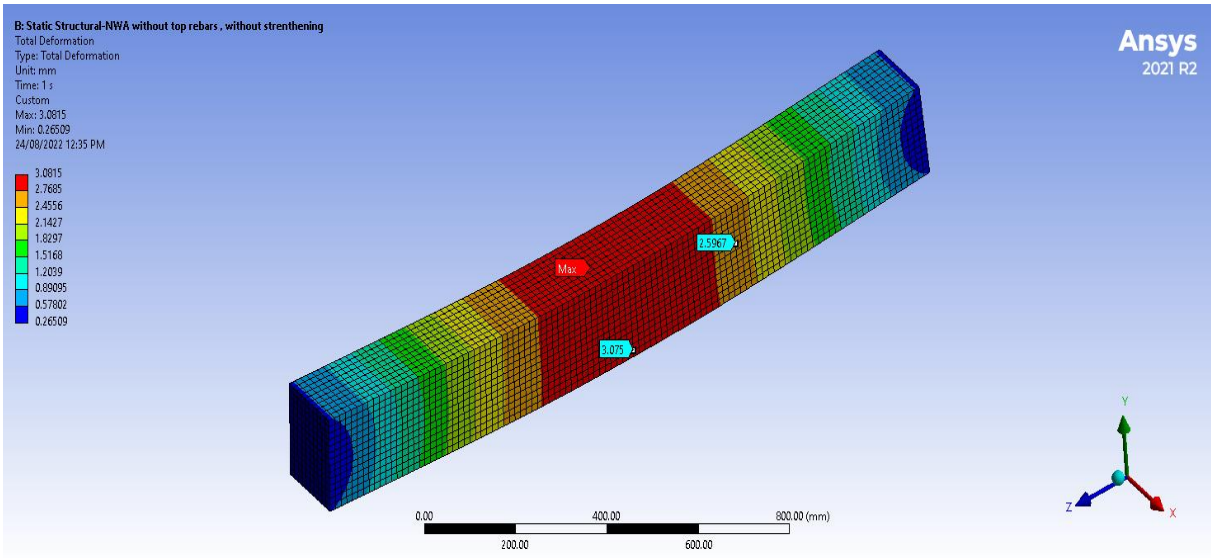

Figure 46((NWA-1/70.5MPa – Total deflections of beam sample without strengthening and top rebars- Static Nonlinear Analysis)

The value is 3.0815 mm

Directional Deformation (Y-Direction)

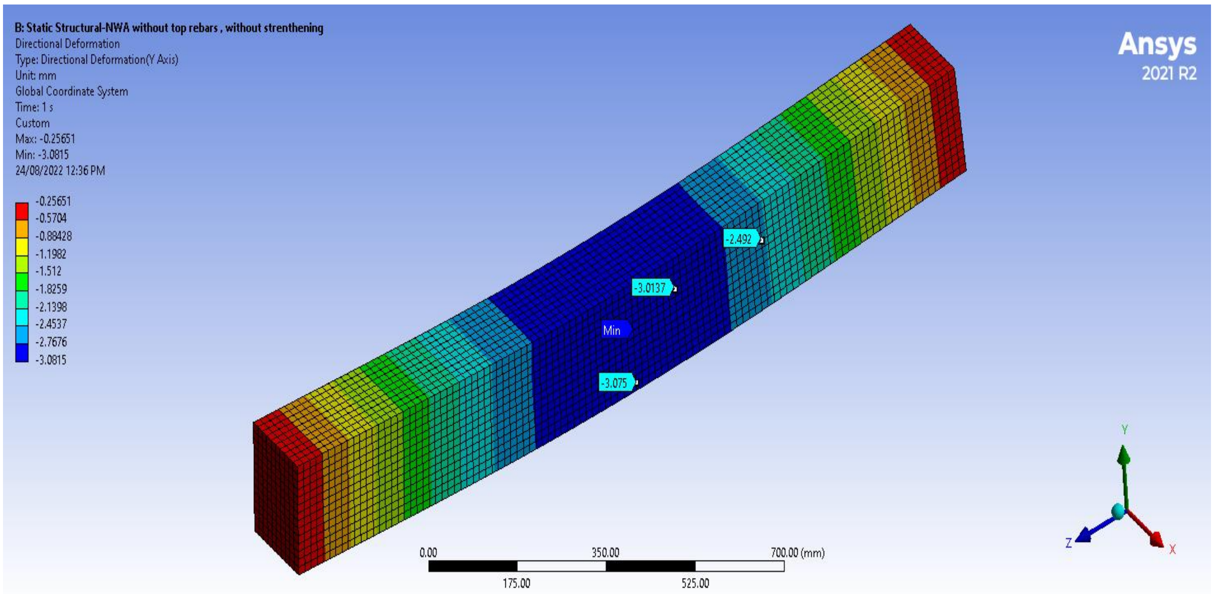

Figure 47(NWA-1/70.5MPa – Directional deflections (Y-Dir.) of beam sample without strengthening and top rebars- Static Nonlinear Analysis)

The value is 3.0815 mm.

Elastic Strain

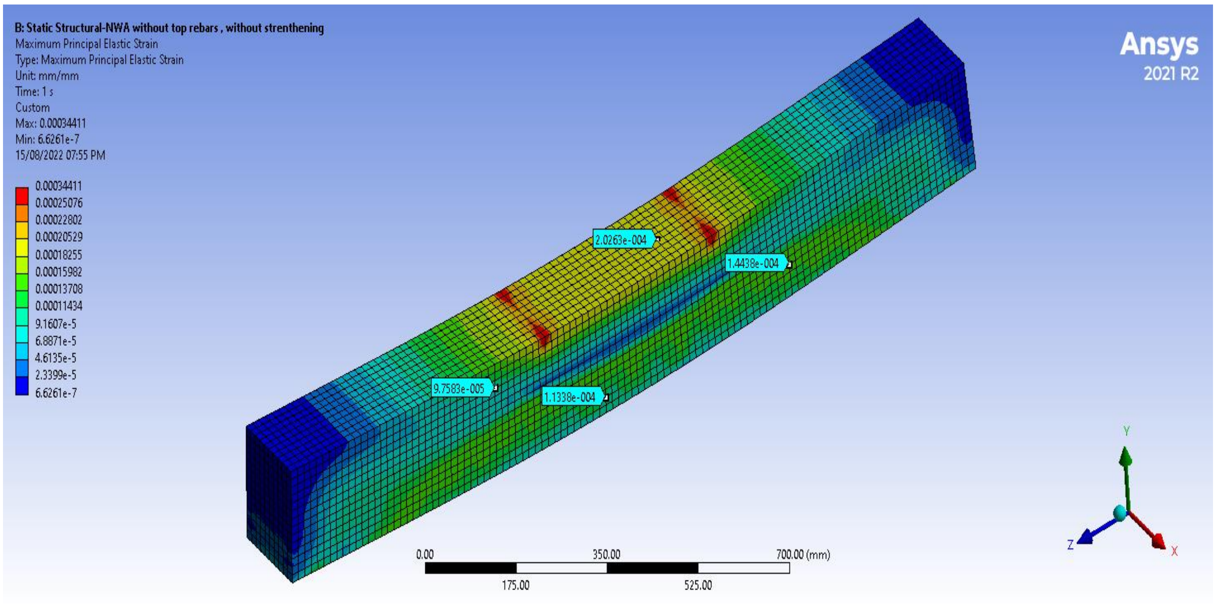

Figure 48(NWA-1/70.5MPa – Elastic strain of beam sample without strengthening and top rebars- Static Nonlinear Analysis)

Detailed Calculations in Appendix A (3-Static Non-Linear Analysis - Without Strengthening and Top Rebars)

6.2.1.3.1.2 Explicit Dynamic-Without Top Rebars & Strengthening

Deformations

Total Deformations

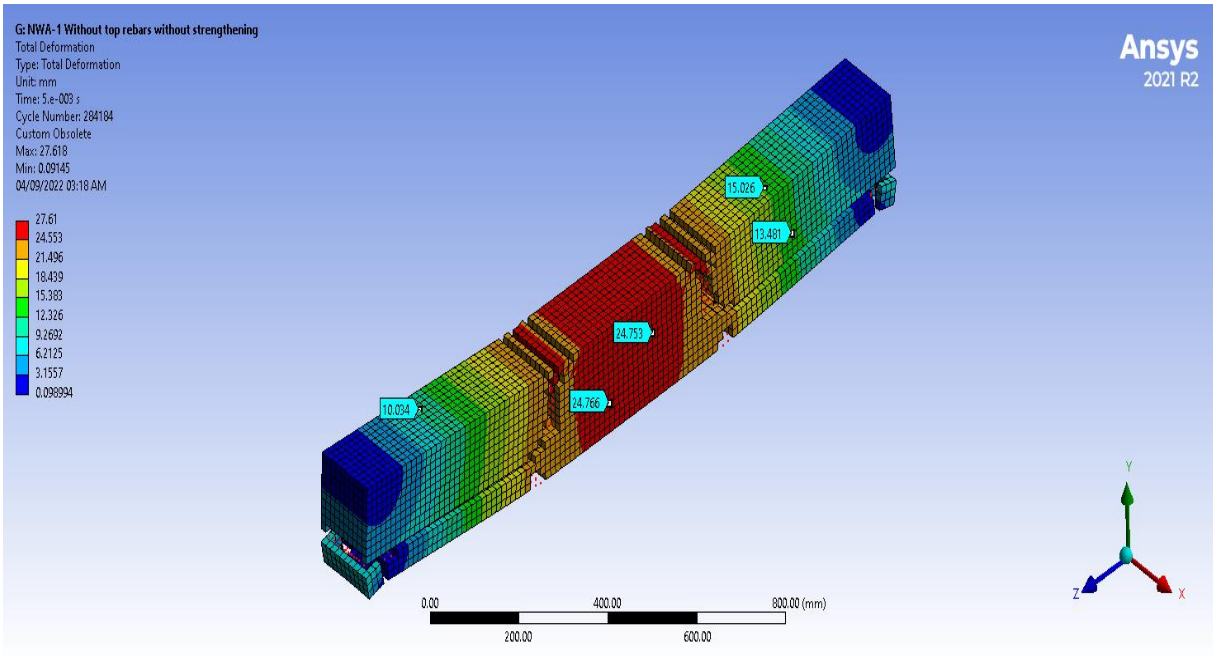

Figure 49(NWA-1/70.5MPa – Total deflections of beam sample without strengthening and top rebars- Explicit Dynamic Analysis)

The value is 24.766 mm.

Directional Deformation (Y-Direction)-Concrete

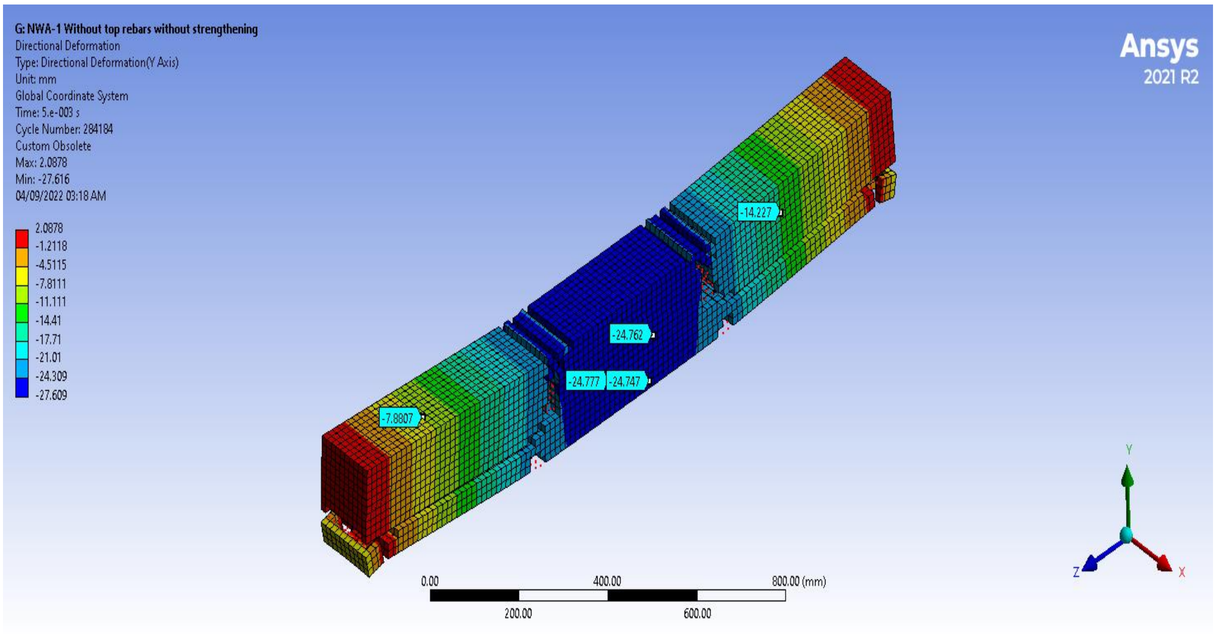

Figure 50(NWA-1/70.5MPa – Directional deflections (Y-Dim.) of beam sample without strengthening and top rebars- Explicit Dynamic Analysis)

The value is 21.063 mm.

The Damage Pattern

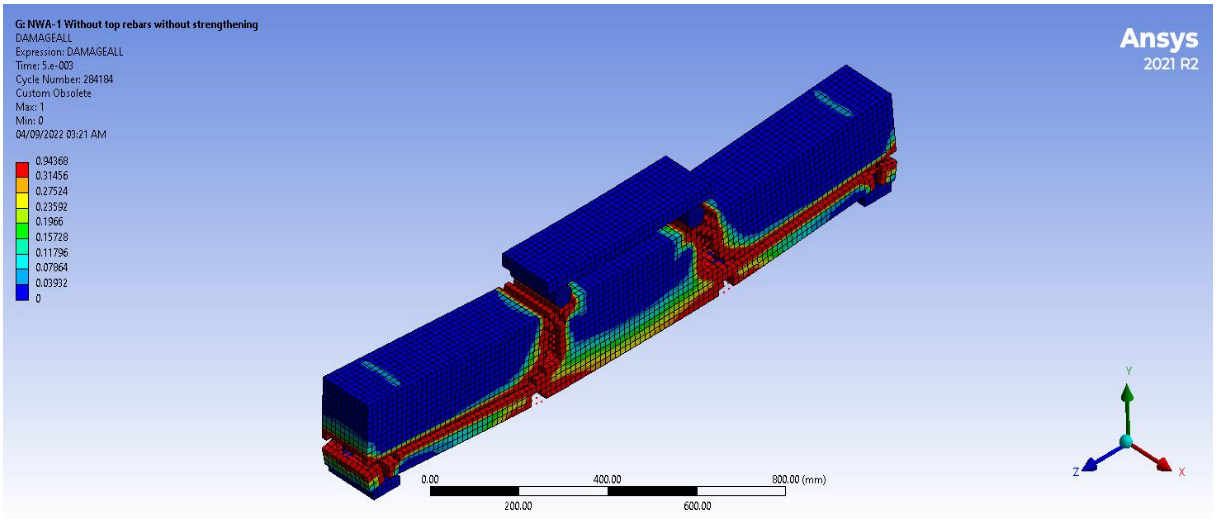

Figure 51(NWA-1/70.5MPa – Damage Pattern of beam sample without strengthening and top rebars- Explicit Dynamic Analysis)

As we can see the shear damage cracks and concrete failures.

<u>Detailed Calculations in Appendix A (4- Explicit Dynamic-Without Top Rebars & Strengthening)</u>

6.2.1.3.1.3 Static Non-Linear Analysis – Without Top Rebars and With Strengthening

Deformations

Total Deformations

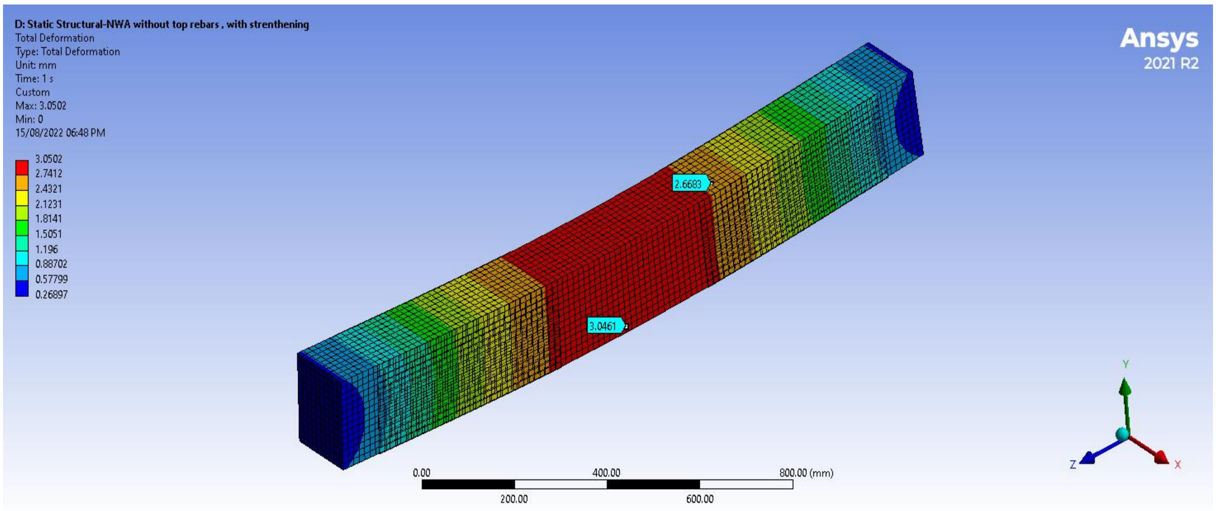

Figure 52(NWA-1/70.5MPa – Total deflections of beam sample with strengthening and without top rebars- Static Nonlinear Analysis)

The value is 3.050 mm.

Directional Deformation (Y-Direction)

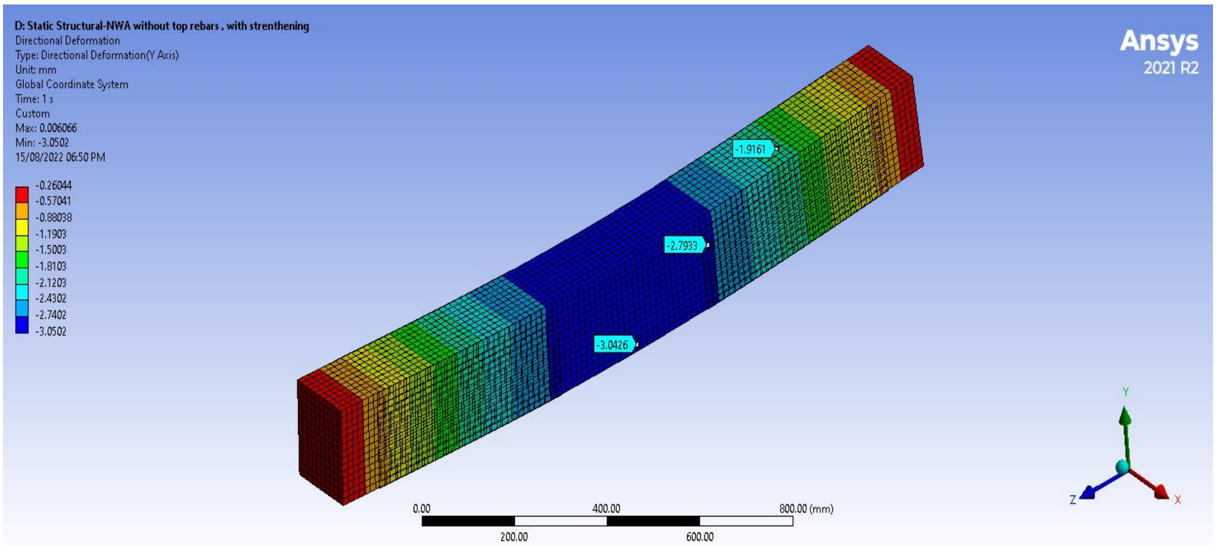

Figure 53(NWA-1/70.5MPa – Directional deflections (Y-Dim.) of beam sample with strengthening and without top rebars- Static Nonlinear Analysis)

The value is 3.050 mm.

Elastic Strain

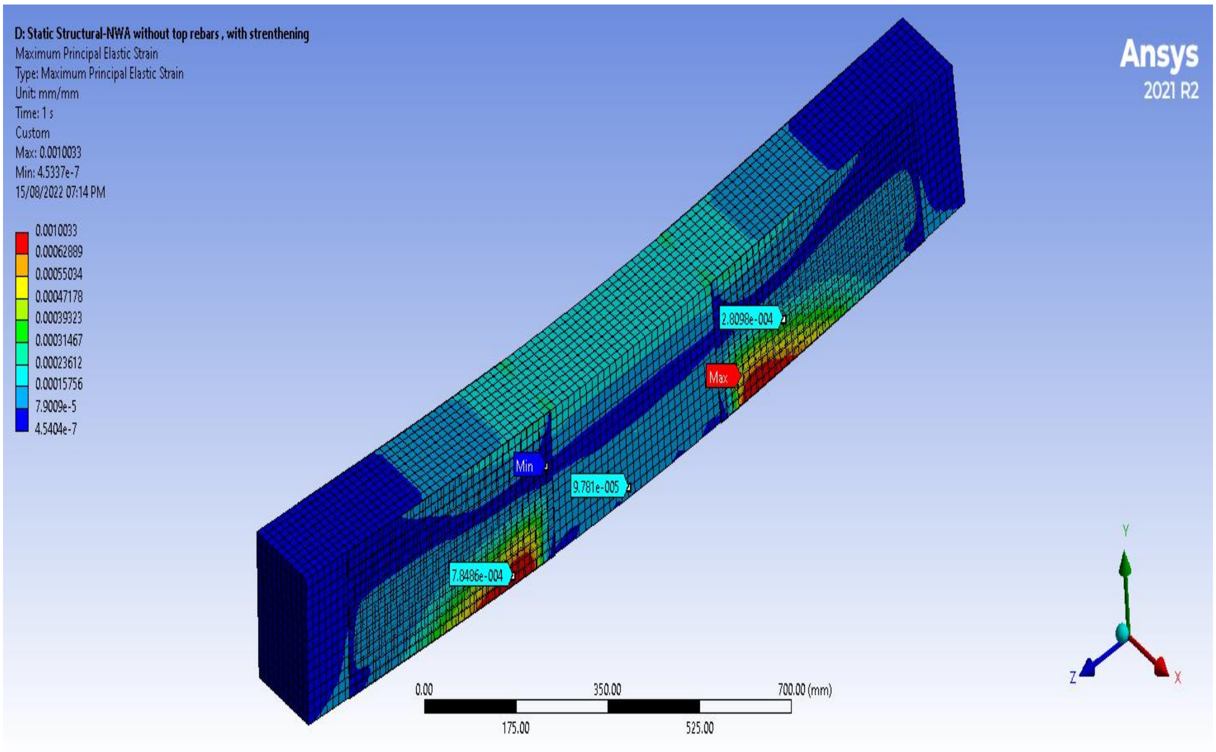

Figure 54(NWA-1/70.5MPa – Elastic strain of beam sample with strengthening and without top rebars- Static Nonlinear Analysis)

<u>Detailed Calculations in Appendix A (7-Static Non-Linear Analysis - Without Top Rebars and With Strengthening)</u>

6.2.1.3.1.4 Explicit Dynamic-Without Top Rebars & With Strengthening

Deformations

Total Deformations

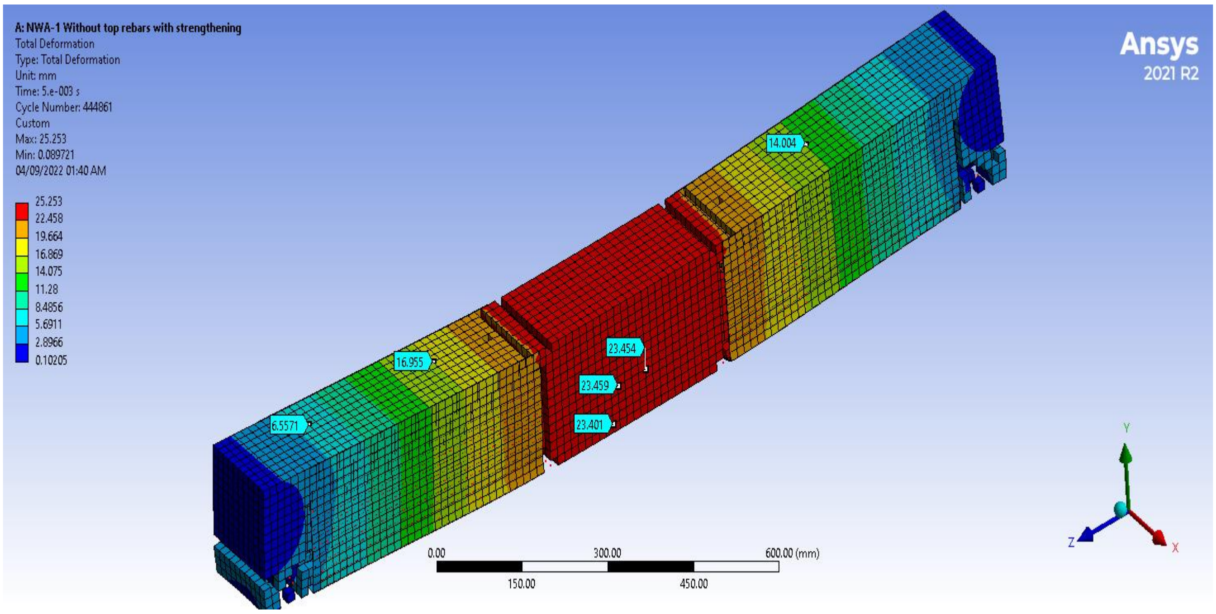

Figure 55(NWA-1/70.5MPa – Total deflections of beam sample with strengthening and without top rebars- Explicit Dynamic Analysis)

The value is 23.459 mm.

Directional Deformation (Y-Direction)-Concrete

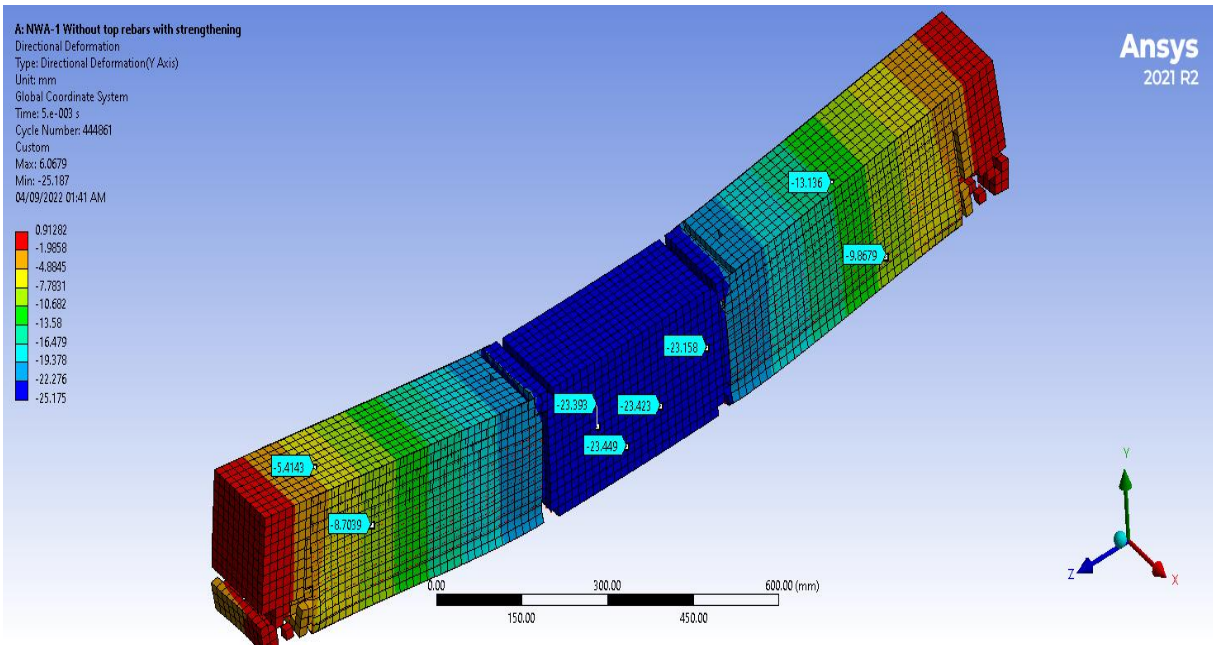

Figure 56(NWA-1/70.5MPa – Directional deflections (Y-Dim.) of beam sample with strengthening and without top rebars- Explicit Dynamic Analysis)

The value is 23.449 mm

The Damage Pattern

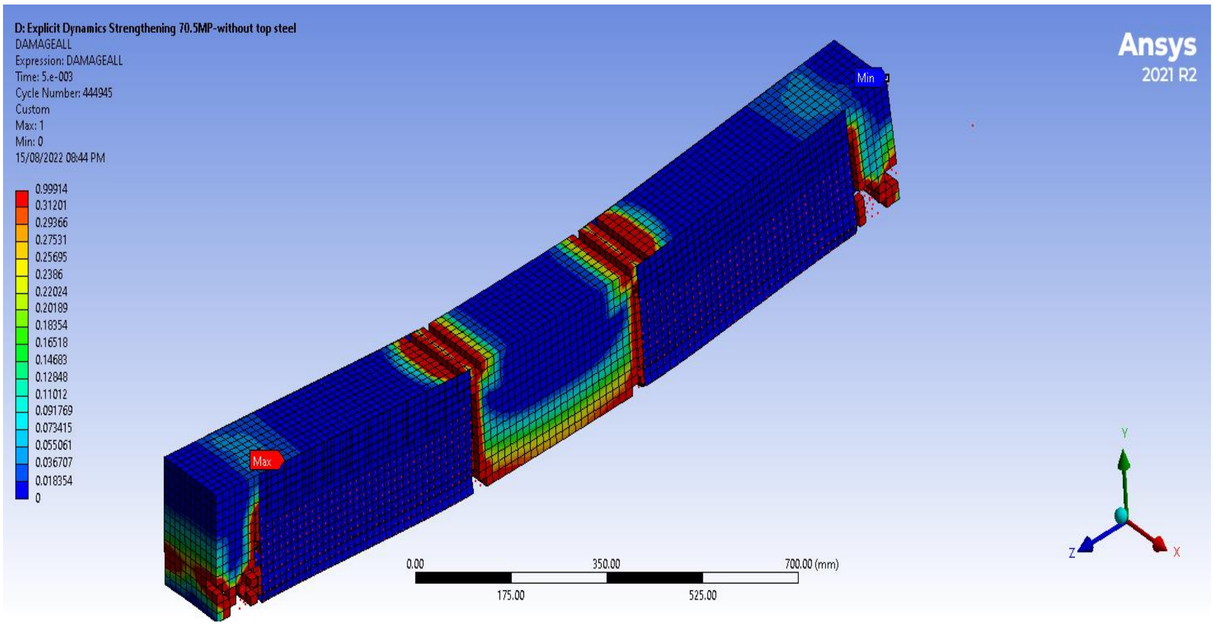

Figure 57(NWA-1/70.5MPa – Damage pattern-1 of beam sample with strengthening and without top rebars- Explicit Dynamic Analysis)

As we can see the shear damage cracks in red and CFRP debonding on edges of concrete failure.

Detailed Calculations in Appendix A (8- Explicit Dynamic-Without Top Rebars & Strengthening)

6.2.1.3.2 Model Sample No.2 (RCA-64.5 MPa)

More study cases of RCA from 9-16 can be found in **Appendix A**

*The applied load is 81.7 KN which is the ultimate load see.Table 7

6.2.1.3.2.1 Static Non-Linear Analysis - Without Strengthening and Top Rebars

Deformations

Total Deformations

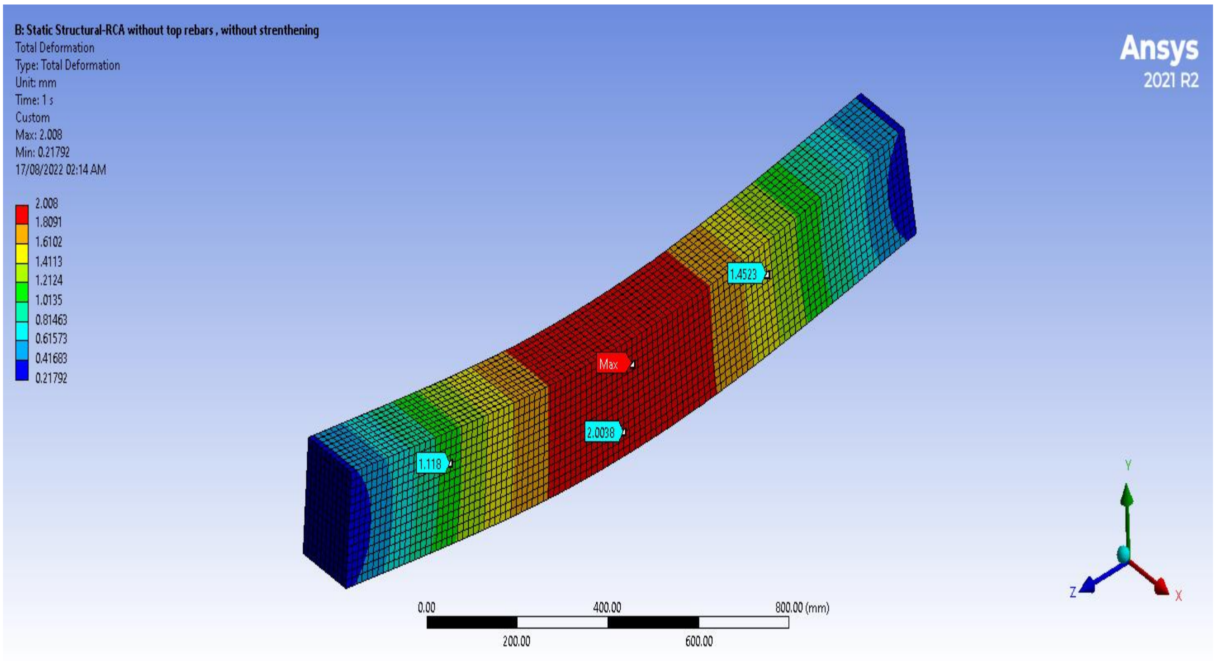

Figure 58(RCA-64.50MPa –Total deflections of beam sample without strengthening and top rebars- Static Nonlinear Analysis)

The value is 2.008 mm.

Directional Deformation (Y-Direction)

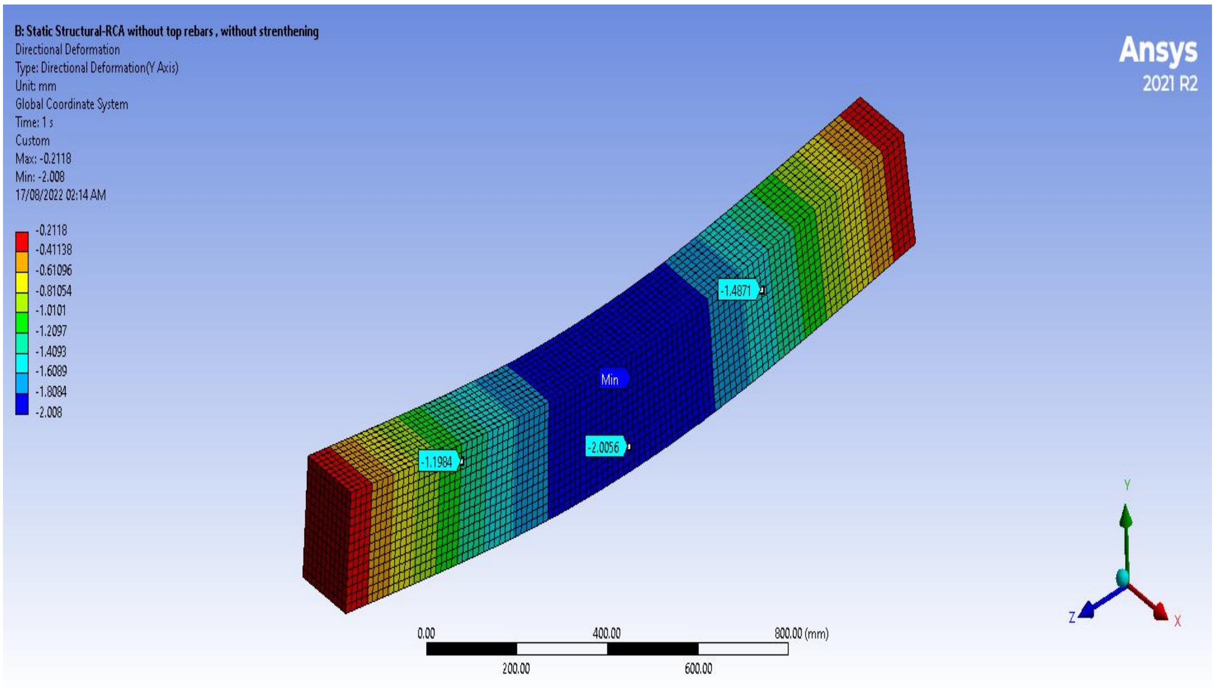

Figure 59(RCA-64.50MPa – Directional deflections (Y-Dir.) of beam sample without strengthening and top rebars- Static Nonlinear Analysis)

The value is 2.008 mm.

Elastic Strain

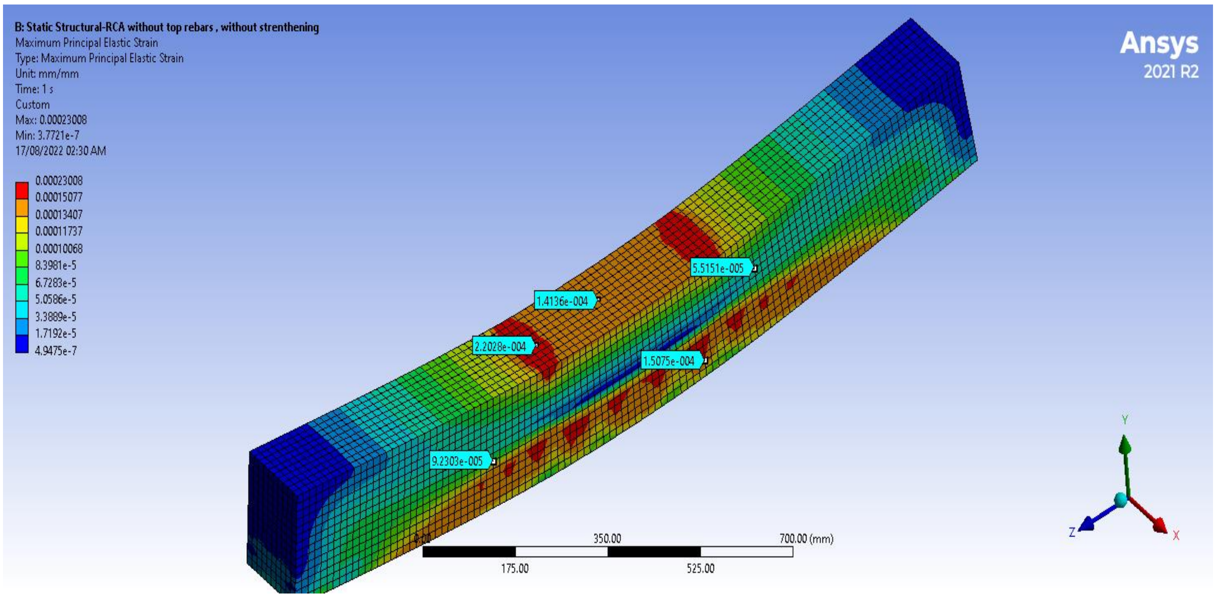

Figure 60(RCA-64.5MPa – Elastic strain of beam sample without strengthening and top rebars- Static Nonlinear Analysis)

<u>Detailed Calculations in Appendix A (11-Static Non-Linear Analysis - Without Top Rebars and With Strengthening)</u>

6.2.1.3.2.2 Explicit Dynamic-Without Top Rebars & Strengthening

Deformations

Total Deformations

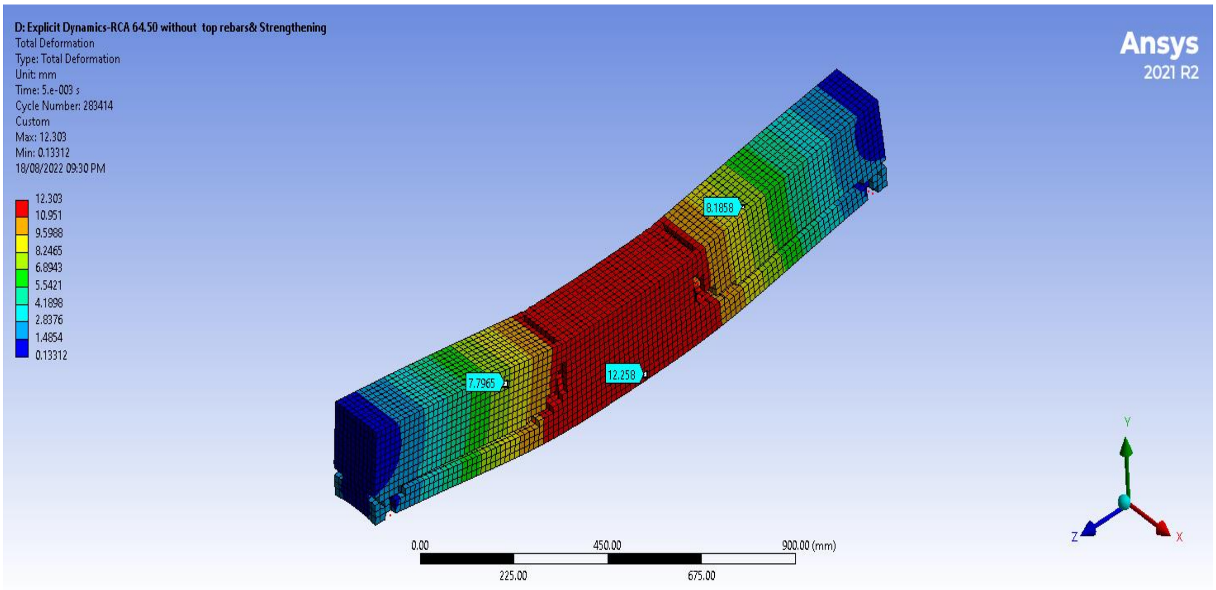

Figure 61(RCA-64.5MPa – Total deflections of beam sample without strengthening and top rebars- Explicit Dynamic Analysis)

The value is 12.303 mm.

Directional Deformation (Y-Direction)-Concrete

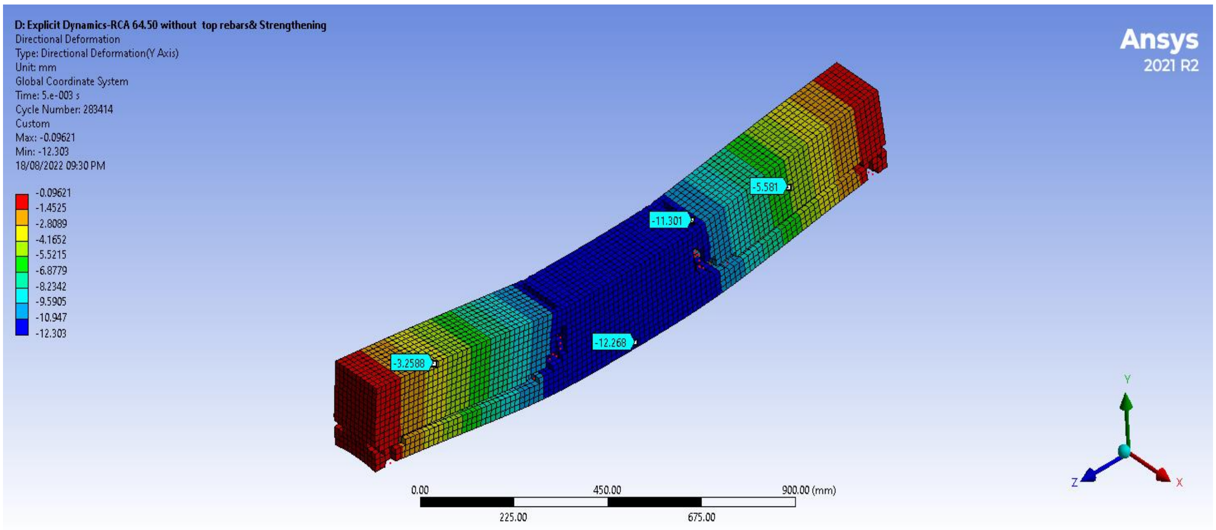

Figure 62(RCA-64.5MPa – Directional deflections (Y-Dim.) of beam sample without strengthening and top rebars- Explicit Dynamic Analysis)

The value is 12.303 mm.

The Damage Pattern

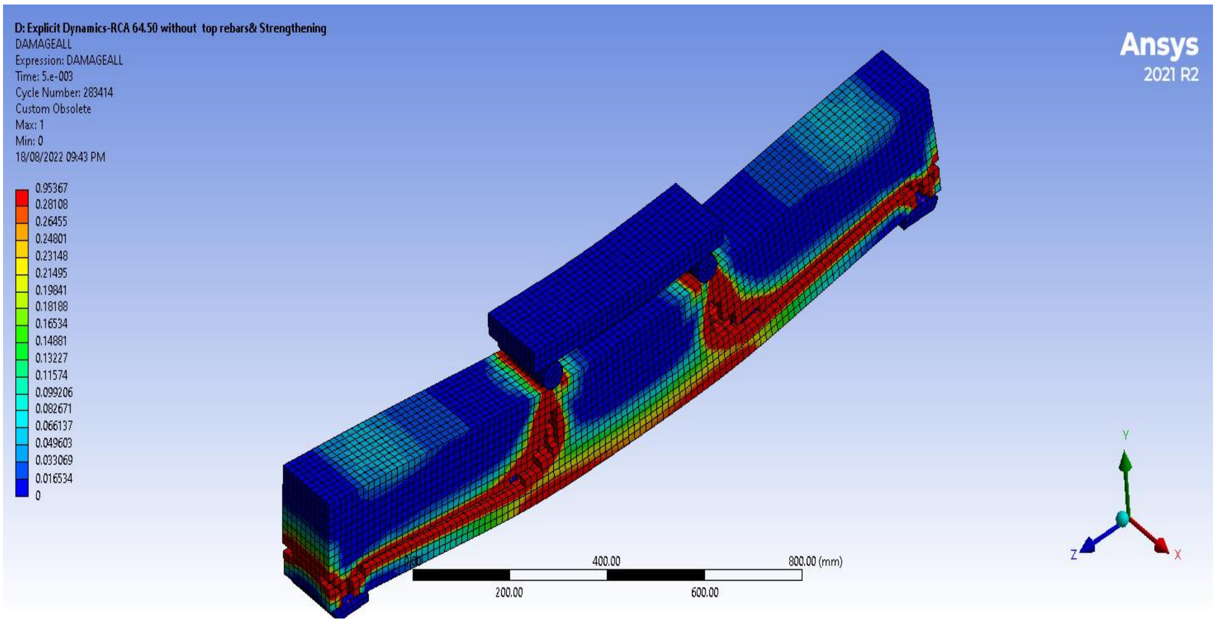

Figure 63(RCA-64.50MPa – Damage Pattern-1 of beam sample without strengthening and top rebars- Explicit Dynamic Analysis)

<u>Detailed Calculations in Appendix A (12- Explicit Dynamic-Without Top Rebars & Strengthening)</u>

6.2.1.3.2.3 Static Non-Linear Analysis - With Strengthening and Without Top Rebars

Deformations

Total Deformations

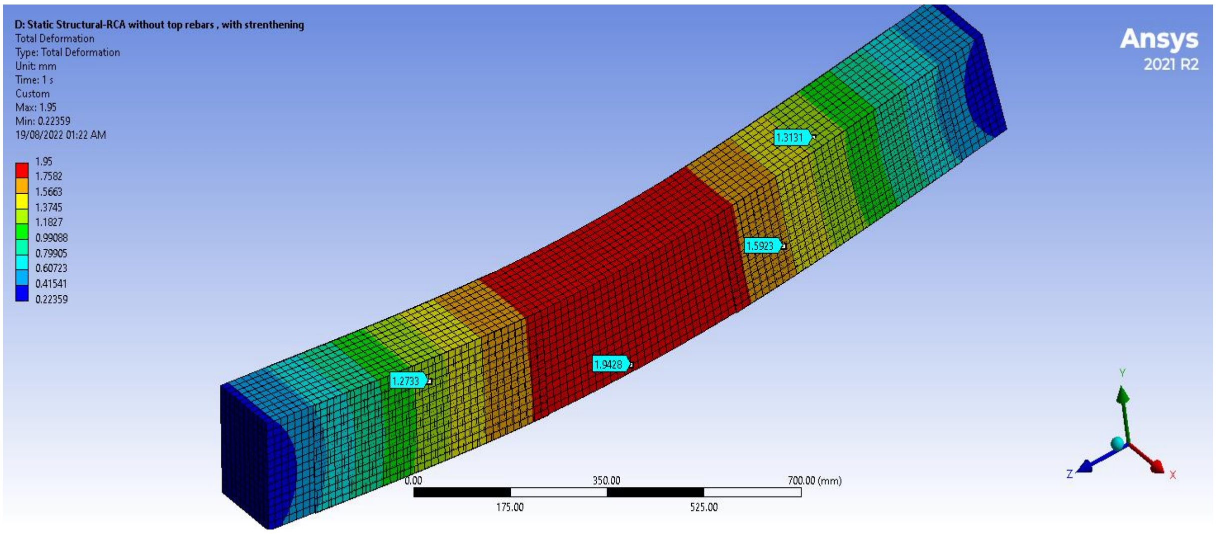

Figure 64(RCA-64.5MPa – Total deflections of beam sample with strengthening and without top rebars- Static Nonlinear Analysis)

The value is 1.95 mm.

Directional Deformation (Y-Direction)

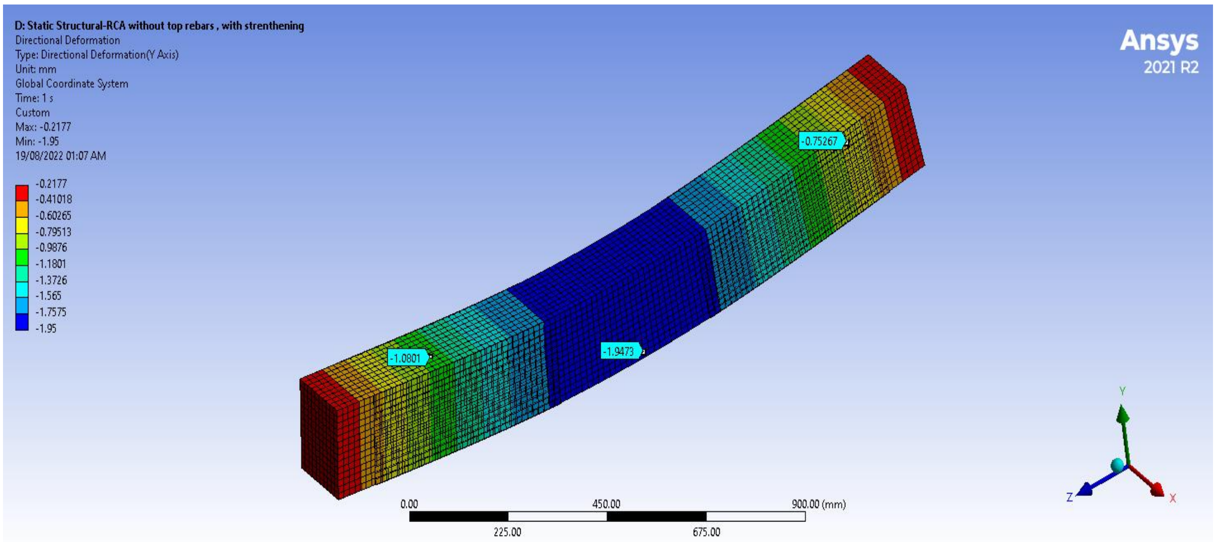

Figure 65(RCA-64.5MPa – Directional deflections (Y-Dim.) of beam sample with strengthening and without top rebars- Static Nonlinear Analysis)

The value is 1.95 mm.

Elastic Strain

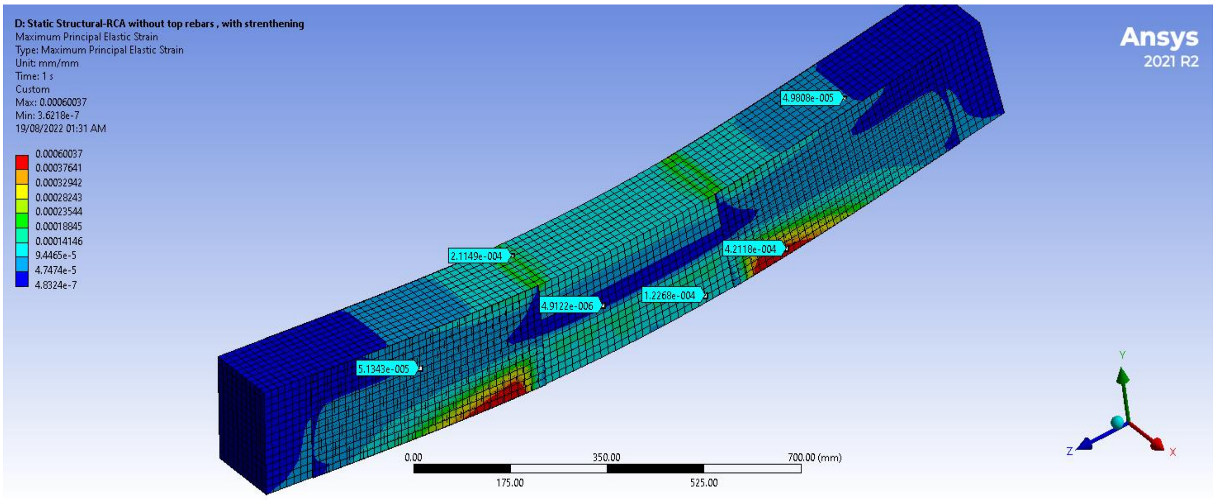

Figure 66(RCA-645MPa – Elastic strain of beam sample with strengthening and without top rebars- Static Nonlinear Analysis)

<u>Detailed Calculations in Appendix A (15-Static Non-Linear Analysis - Without Top Rebars and With Strengthening)</u>

6.2.1.3.2.4 Explicit Dynamic-Without Top Rebars & With Strengthening

Deformations

Total Deformations

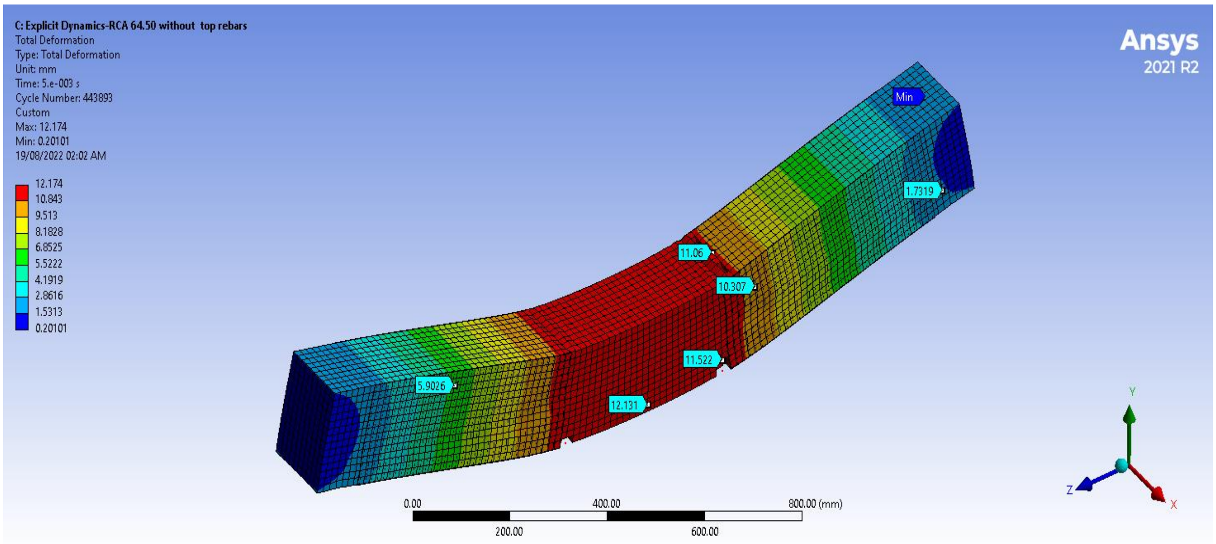

Figure 67(RCA-64.5MPa – Total deflections of beam sample with strengthening and without top rebars- Explicit Dynamic Analysis)

The value is 12.174 mm.

Directional Deformation (Y-Direction)-Concrete

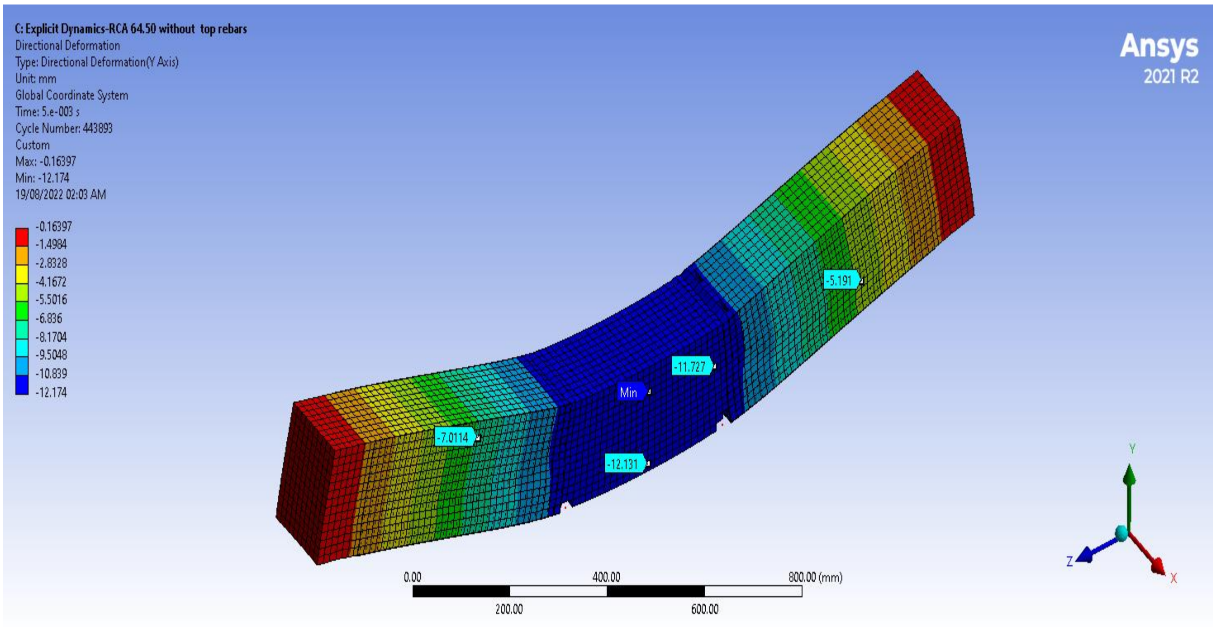

Figure 68(RCA-64.5MPa – Directional deflections (Y-Dim.) of beam sample with strengthening and without top rebars- Explicit Dynamic Analysis)

The value is 12.174 mm.

The Damage Pattern

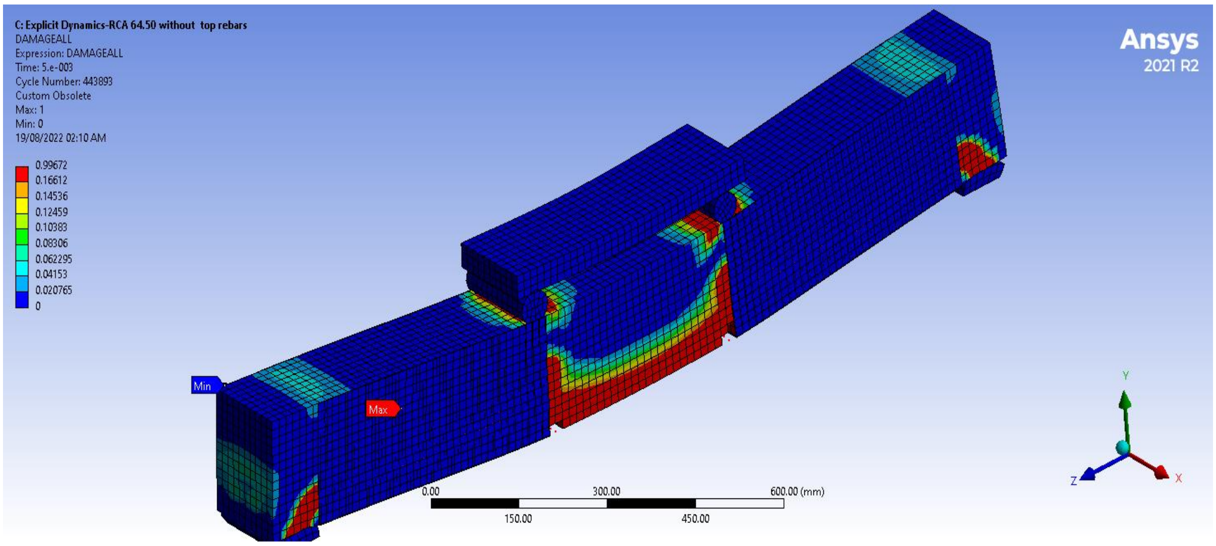

Figure 69(RCA-64.5MPa – Damage pattern-1 of beam sample with strengthening and without top rebars- Explicit Dynamic Analysis)

As we can see the shear damage cracks in red and CFRP debonding on edges of concrete failure.

<u>Detailed Calculations in Appendix A (16- Explicit Dynamic-Without Top Rebars & with Strengthening)</u>

6.2.1.3.3 Model Sample No.2 (RCA-5D $_{\text{Fibers}}$-77.0 MPa)

More study cases of RCA-5D from 17-25 can be found in Appendix A

*The applied load is 130.09 KN which is the ultimate load see.Table 7

6.2.1.3.3.1 Static Non-Linear Analysis – Without Top Rebars and Strengthening

Deformations

Total Deformations

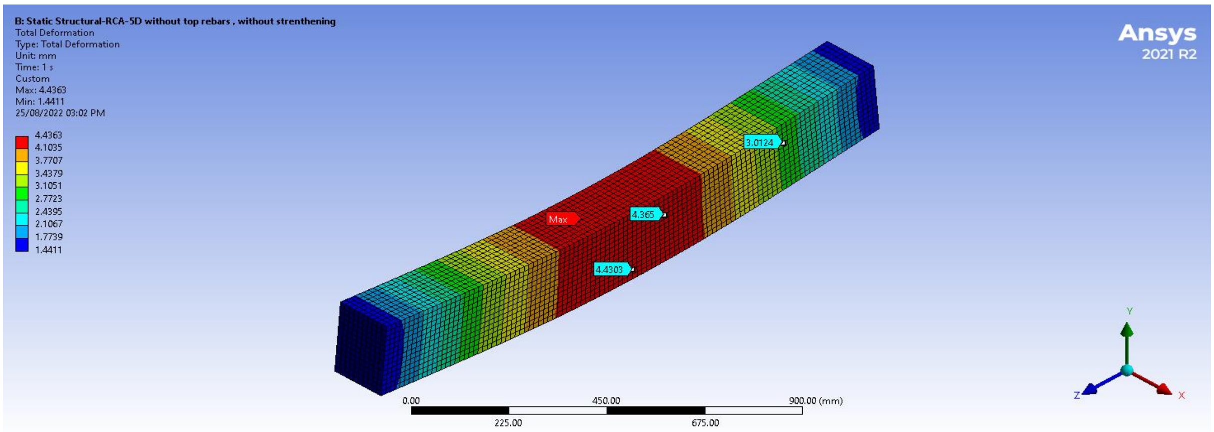

Figure 70(RCA-5D$_{Fibers}$-77.0MPa – Total deflections of beam sample without strengthening and top rebars- Static Nonlinear Analysis)

The value is 4.4363 mm.

Directional Deformation (Y-Direction)

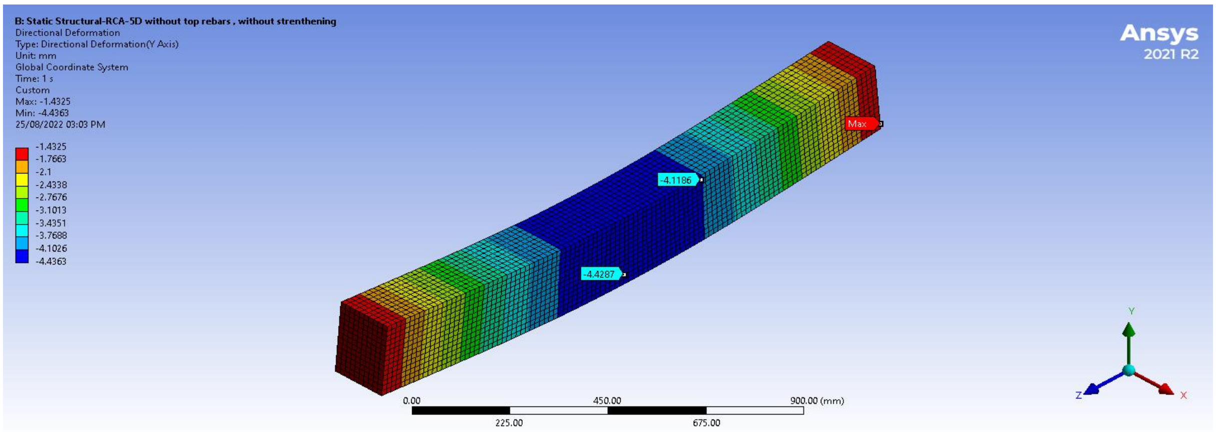

Figure 71(RCA-5D$_{Fibers}$-77.0MPa – Directional deflections (Y-Dir.) of beam sample without strengthening and top rebars- Static Nonlinear Analysis)

The value is 4.4363 mm.

Figure 72(RCA-5D$_{Fibers}$-77.0MPa – Directional deflections (Y-Dir.) graph of beam sample without strengthening and top rebars- Static Nonlinear Analysis)

Elastic Strain

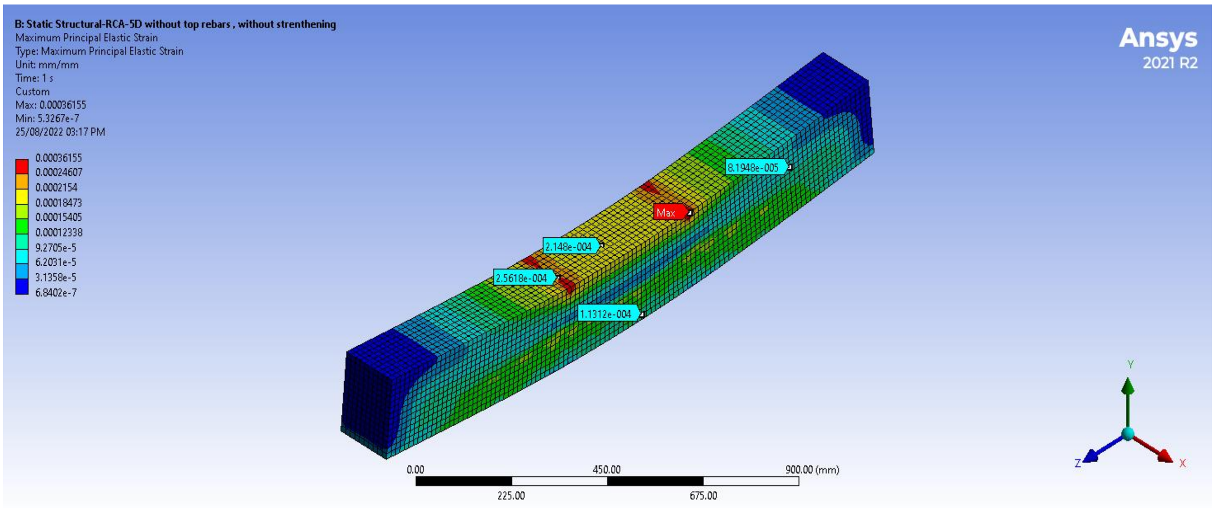

Figure 73(RCA-5D$_{Fibers}$-77.0MPa – Elastic strain of beam sample without strengthening and top rebars- Static Nonlinear Analysis)

<u>Detailed Calculations in Appendix A (20-Static Non-Linear Analysis - Without Top Rebars and With Strengthening)</u>

6.2.1.3.3.2 Explicit Dynamic-Without Top Rebars & Strengthening

Deformations

Total Deformations

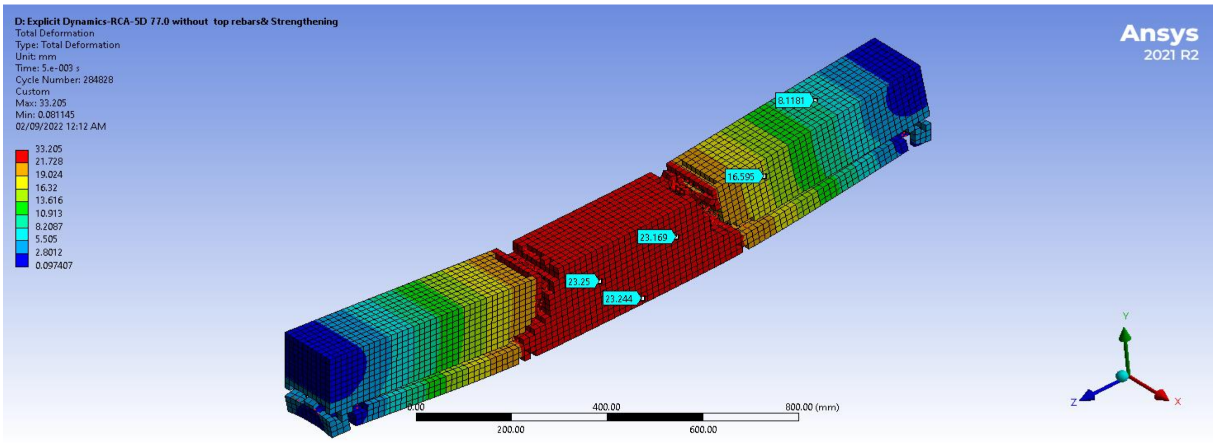

Figure 74(RCA-5D$_{Fibers}$-77.0MPa – Total deflections of beam sample without strengthening and top rebars- Explicit Dynamic Analysis)

The value is 23.25 mm.

Directional Deformation (Y-Direction)-Concrete

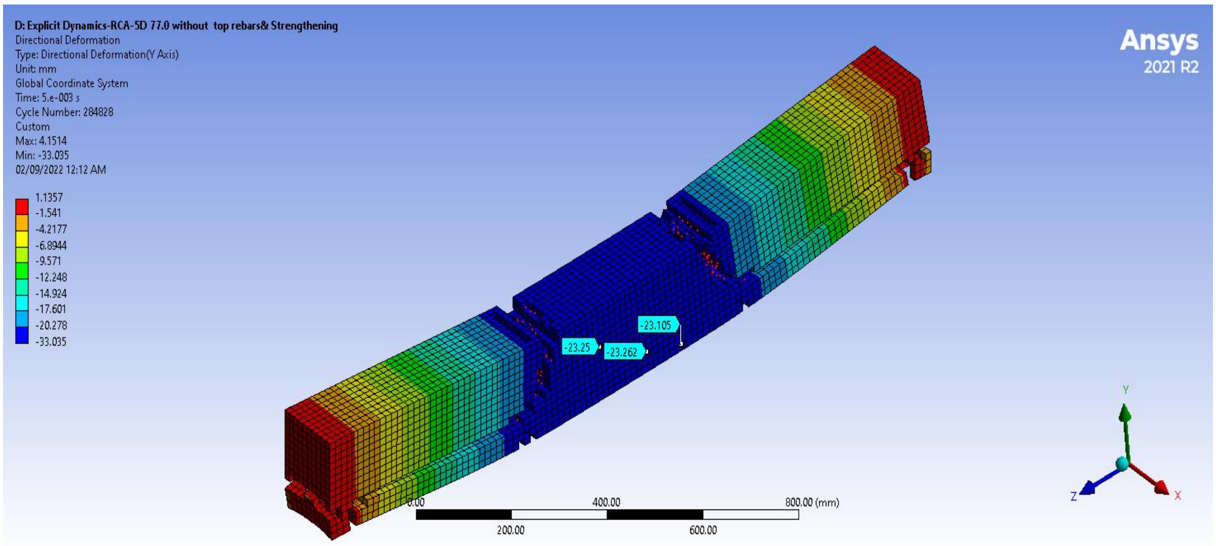

Figure 75(RCA-5D$_{Fibers}$-77.0MPa – Directional deflections (Y-Dim.) of beam sample without strengthening and top rebars- Explicit Dynamic Analysis)

The value is 23.262 mm.

The Damage Pattern

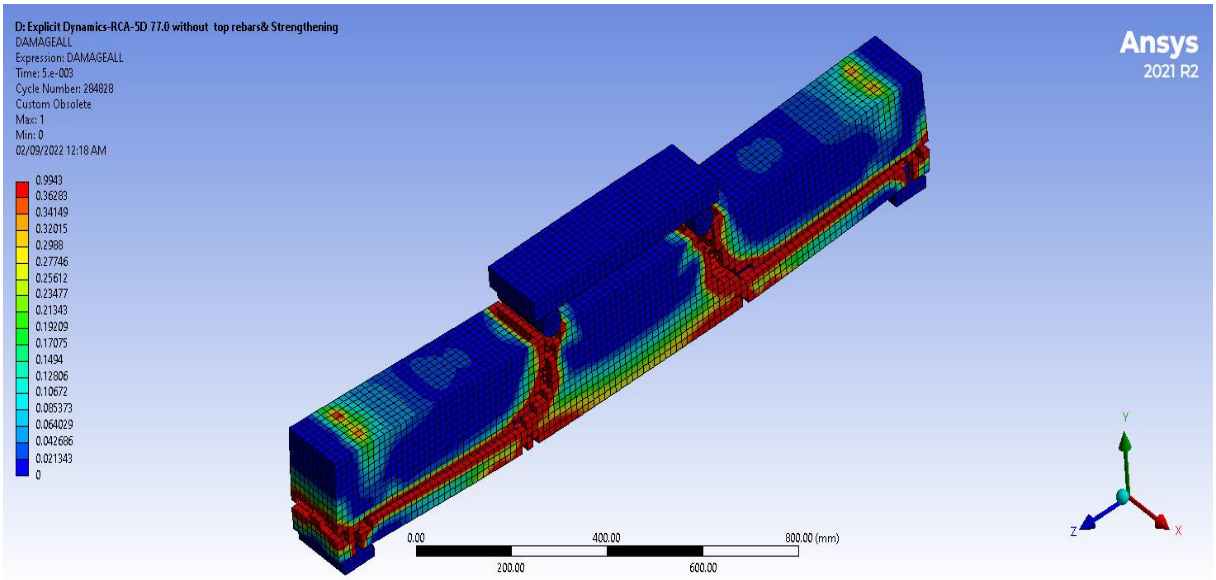

Figure 76(RCA-5D$_{Fibers}$-77.0MPa – Damage Pattern-1 of beam sample without strengthening and top rebars- Explicit Dynamic Analysis)

As we can see the shear damage cracks and concrete failures.

<u>Detailed Calculations in Appendix A (21- Explicit Dynamic-Without Top Rebars & Strengthening)</u>

6.2.1.3.3.3 Static Non-Linear Analysis – Without Top Rebars and With Strengthening

Deformations

Total Deformations

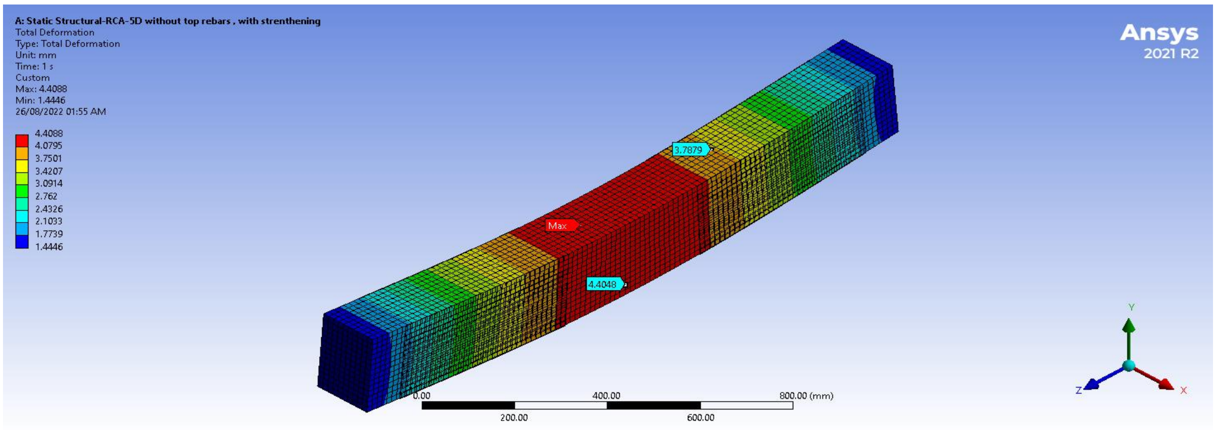

Figure 77(RCA-5D$_{Fibers}$-77.0MPa – Total deflections of beam sample with strengthening and without top rebars- Static Nonlinear Analysis)

The value is 4.4088 mm.

Directional Deformation (Y-Direction)

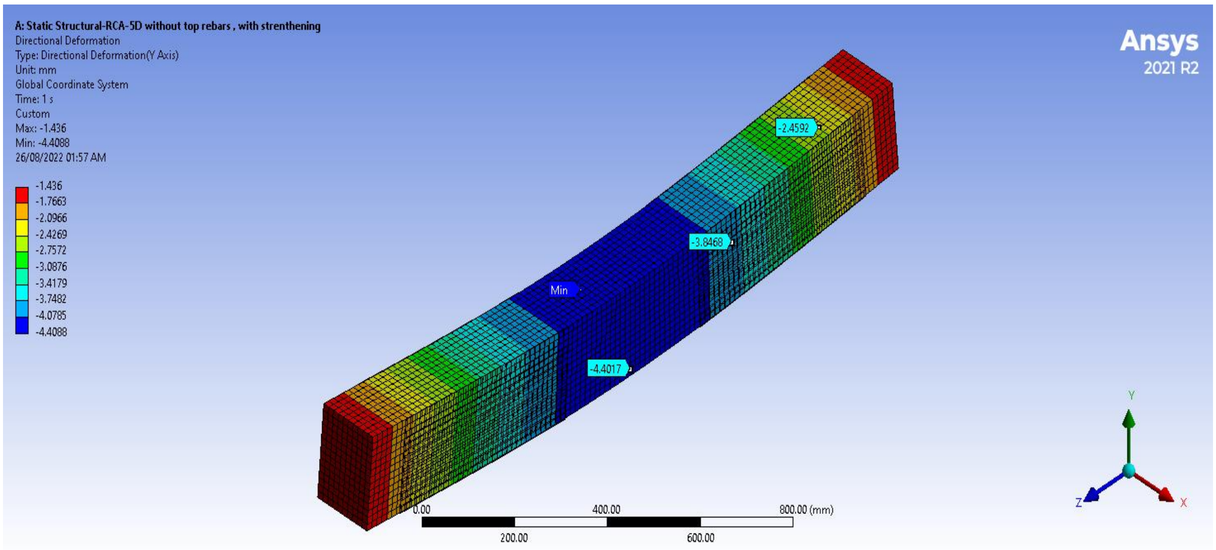

Figure 78(RCA-5D$_{Fibers}$-77.0MPa – Directional deflections (Y-Dim.) of beam sample with strengthening and without top rebars- Static Nonlinear Analysis)

The value is 4.4088 mm.

Elastic Strain

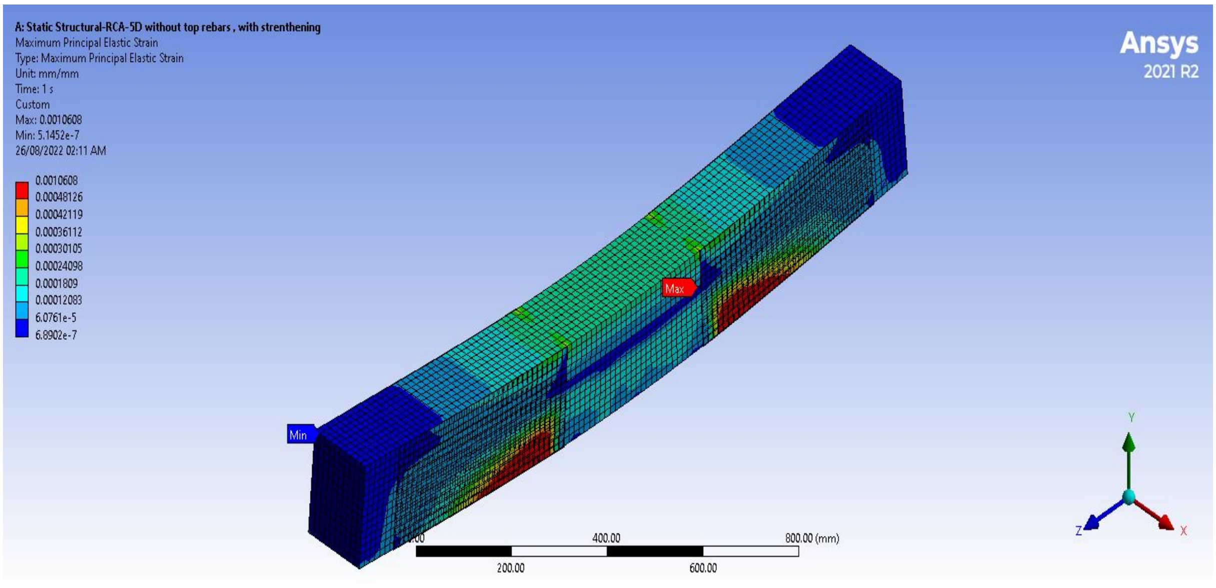

Figure 79(RCA-5D$_{Fibers}$-77.0MPa – Elastic strain of beam sample with strengthening and without top rebars- Static Nonlinear Analysis)

<u>Detailed Calculations in Appendix A (24-Static Non-Linear Analysis - Without Top Rebars and With Strengthening)</u>

6.2.1.3.3.4 Explicit Dynamic-Without Top Rebars & With Strengthening

Deformations

Total Deformations

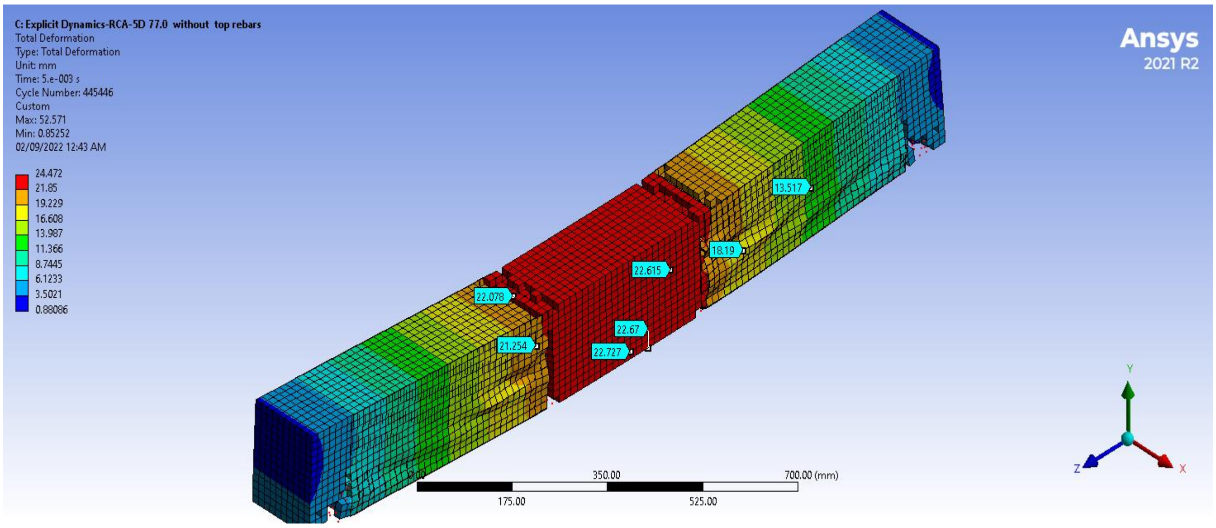

Figure 80(RCA-5D$_{Fibers}$-77.0MPa – Total deflections of beam sample with strengthening and without top rebars- Explicit Dynamic Analysis)

The value is 22.727 mm.

Directional Deformation (Y-Direction)-Concrete

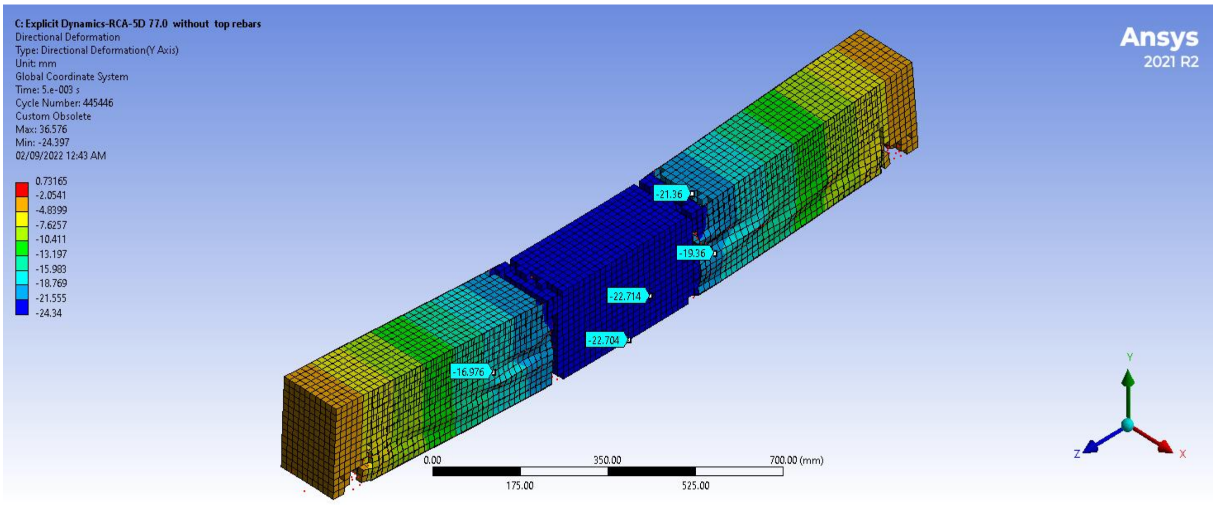

Figure 81(RCA-5D$_{Fibers}$-77.0MPa – Directional deflections (Y-Dim.) of beam sample with strengthening and without top rebars-Explicit Dynamic Analysis)

The value is 22.704 mm

The Damage Pattern

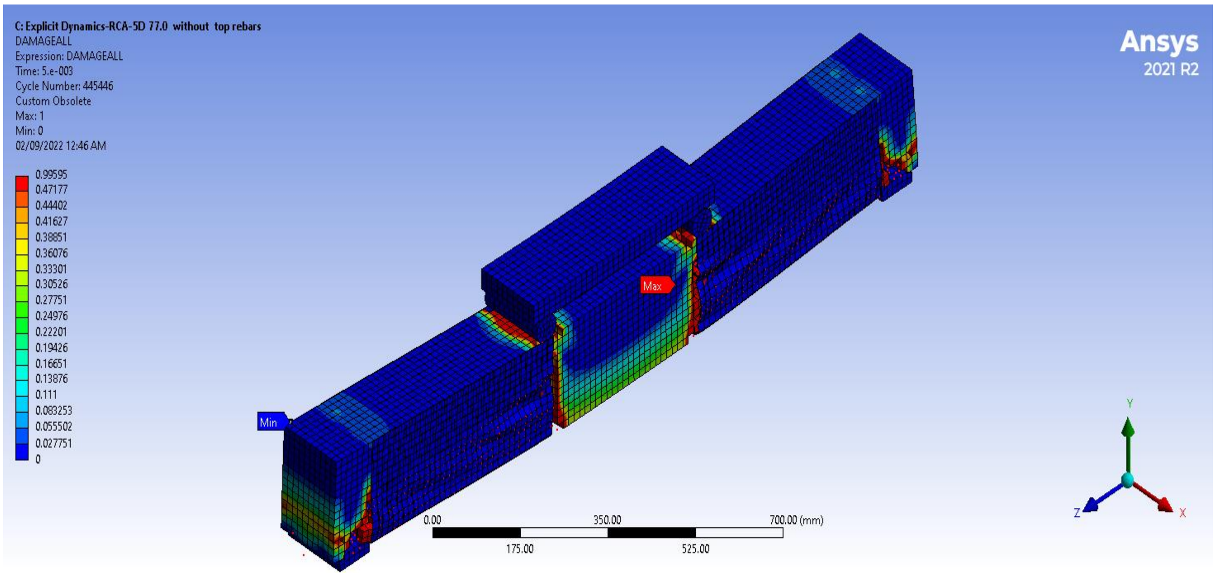

Figure 82(RCA-5D$_{Fibers}$-77.0MPa – Damage pattern-1 of beam sample with strengthening and without top rebars- Explicit Dynamic Analysis)

As we can see the shear damage cracks in red and CFRP debonding on edges of concrete failure.

<u>Detailed Calculations in Appendix A (25- Explicit Dynamic-Without Top Rebars & with Strengthening)</u>

6.2.1.3.4 Model Sample No.2 (NWA-2 /70.5 MPa)

More study cases of NWA-2 from 26-33 can be found in Appendix A

*The applied load is 126.27 KN which is the ultimate load see.Table 7

6.2.1.3.4.1 Static Non-Linear Analysis - Without Strengthening and Top Rebars

Deformations

Total Deformations

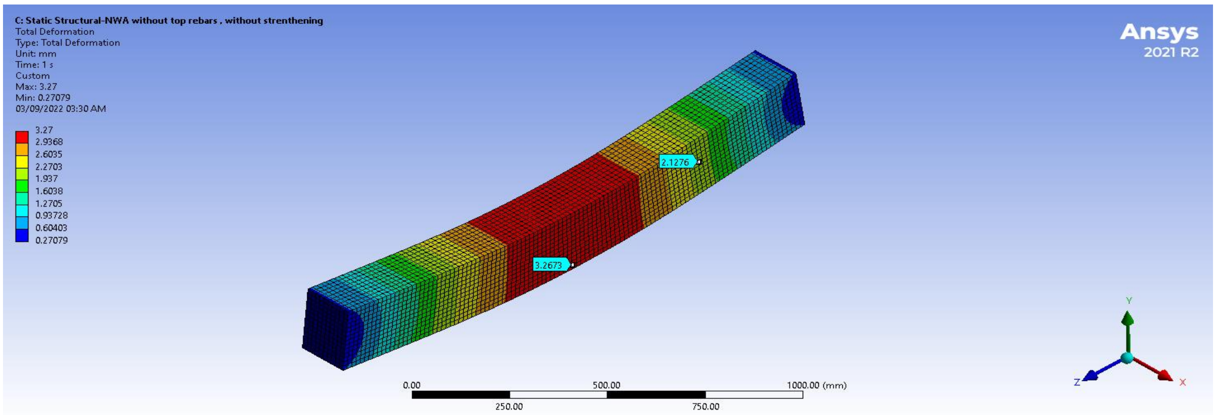

Figure 83(NWA-2/70.5MPa – Total deflections of beam sample without strengthening and top rebars- Static Nonlinear Analysis)

The value is 3.27 mm.

Directional Deformation (Y-Direction)

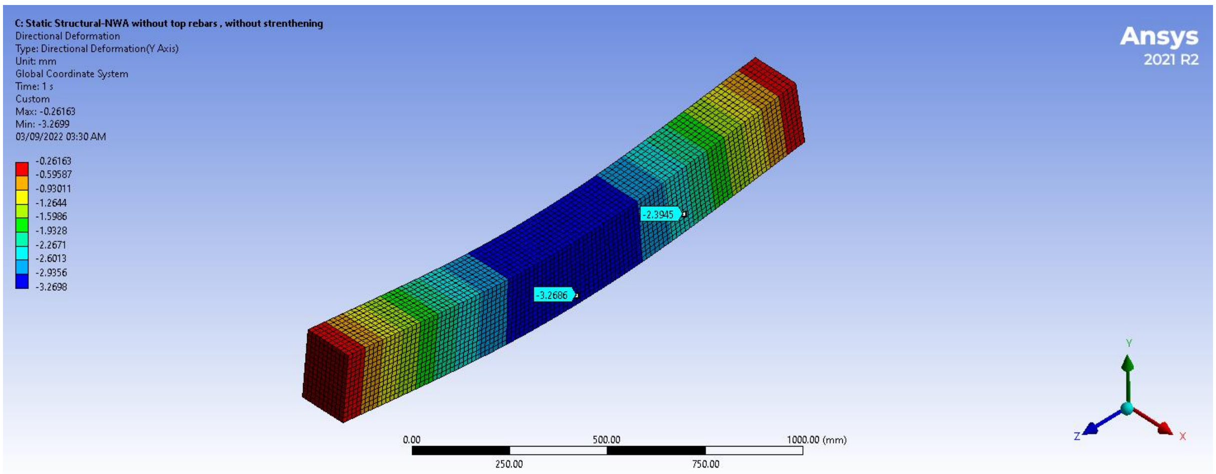

Figure 84(NWA-2/70.5MPa – Directional deflections (Y-Dim.) of beam sample without strengthening and top rebars- Static Nonlinear Analysis)

The value is 3.27 mm.

Elastic Strain

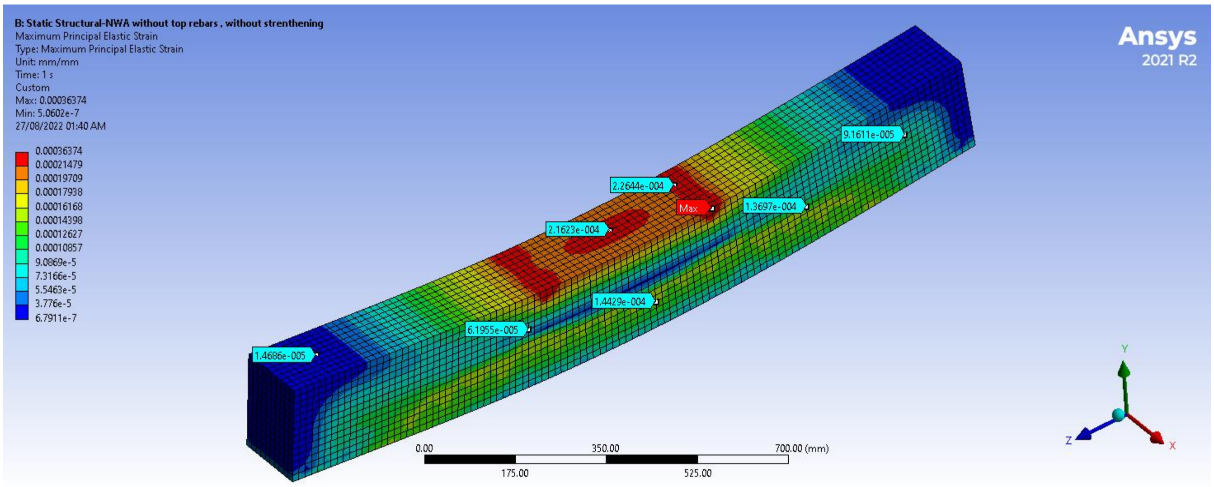

Figure 85(NWA-2/70.5MPa – Elastic Strain of beam sample without strengthening and top rebars - Static Nonlinear Analysis)

<u>Detailed Calculations in Appendix A (28-Static Non-Linear Analysis - Without Top Rebars and With Strengthening)</u>

6.2.1.3.4.2 Explicit Dynamics-With Top Rebars & Without Strengthening

Deformations

Total Deformations

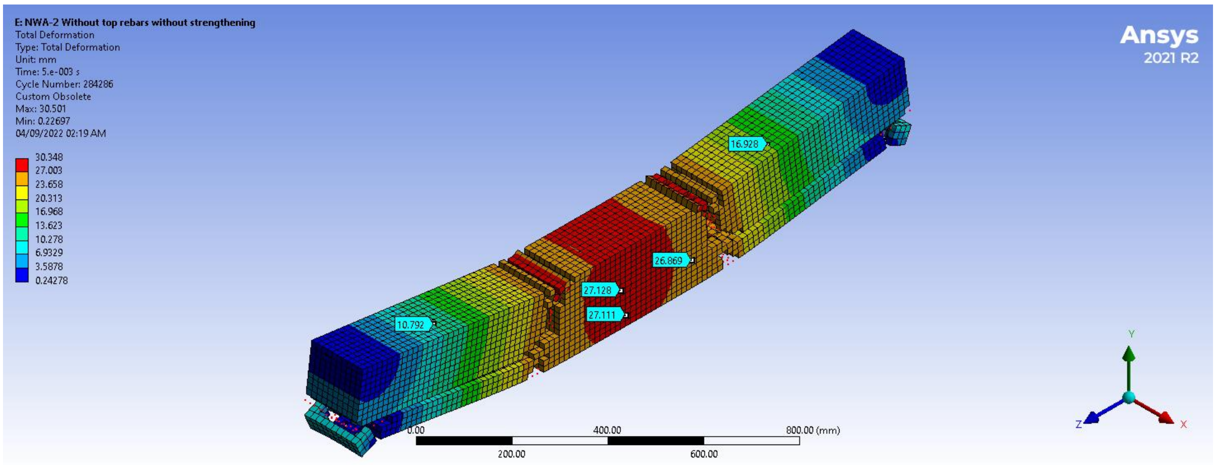

Figure 86(NWA-2/70.5MPa – Total deflections of beam sample without strengthening and top rebars- Explicit Dynamic Analysis)

The value is 27.128 mm.

-Directional Deformation (Y-Direction)-Concrete

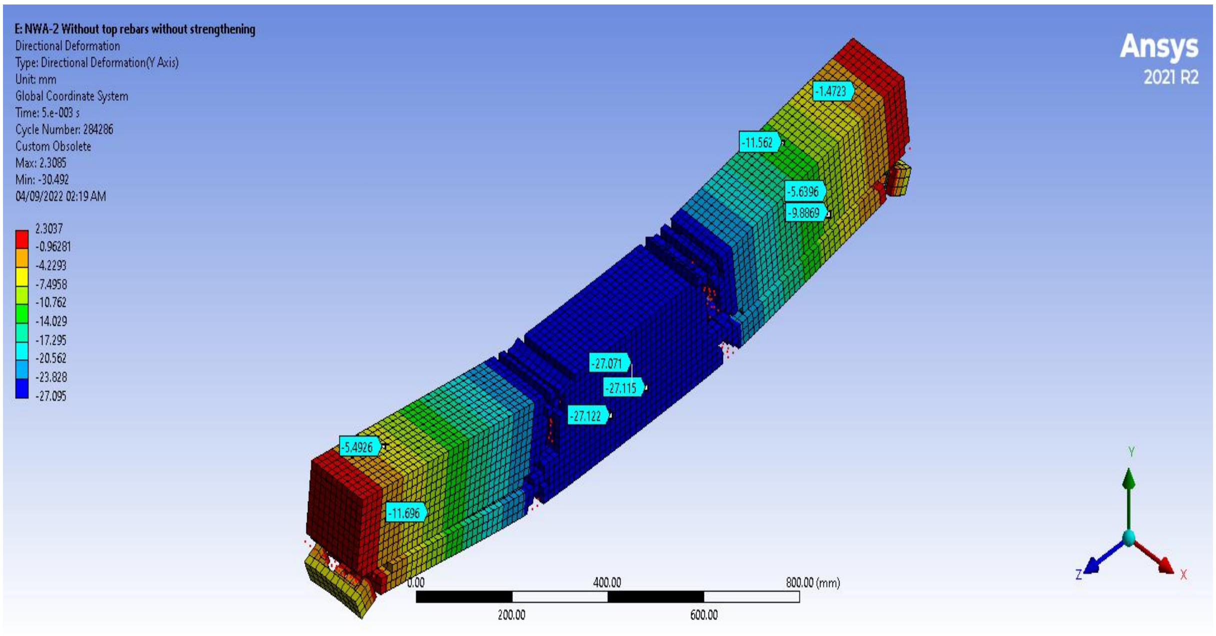

Figure 87(NWA-2/70.5MPa – Directional deflections (Y-Dir.) of beam sample without strengthening and top rebars- Explicit Dynamic Analysis)

The value is 23.35 mm.

The Damage Pattern

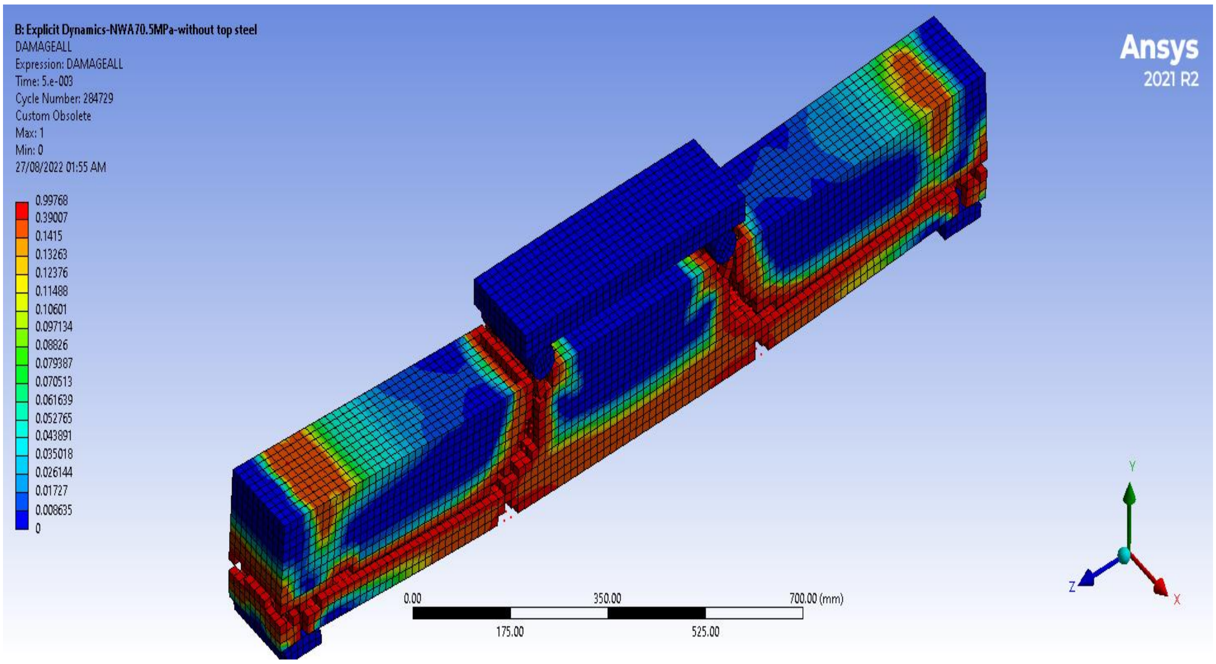

Figure 88(NWA-2/70.5MPa – Damage pattern-1 of beam sample without strengthening and top rebars- Explicit Dynamic Analysis)

As we can see the shear damage cracks and concrete failures.

<u>Detailed Calculations in Appendix A (29- Explicit Dynamic-Without Top Rebars & with Strengthening)</u>

6.2.1.3.4.3 Static Non-Linear Analysis – Without Top Rebars and With Strengthening

Deformations

Total Deformations

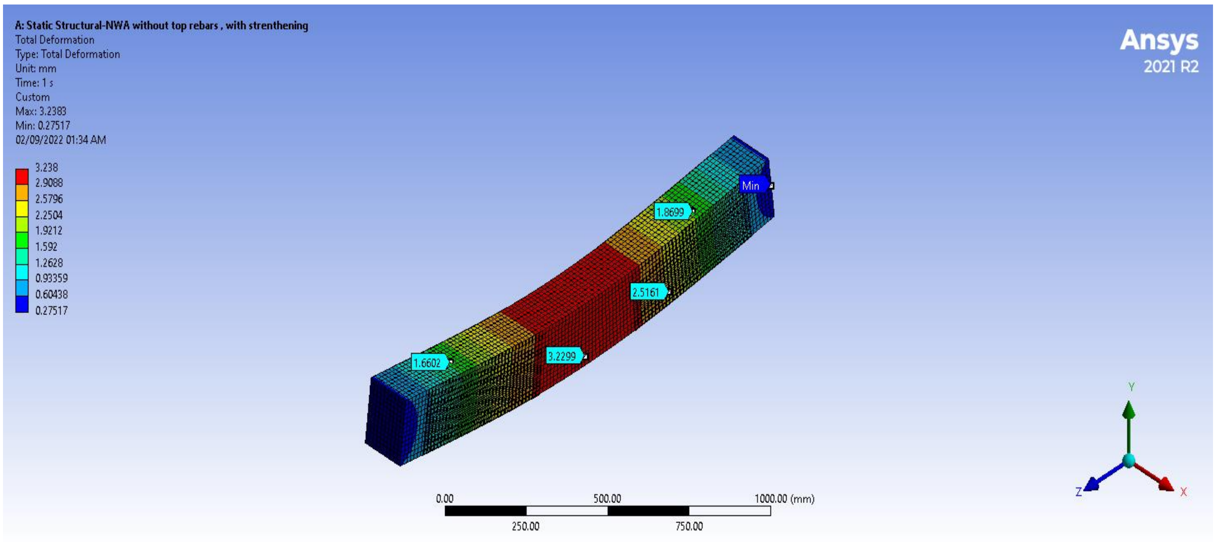

Figure 89(NWA-2/70.5MPa – Total deflections of beam sample with strengthening and without top rebars- Static Nonlinear Analysis)

The value is 3.238 mm.

Directional Deformation (Y-Direction)

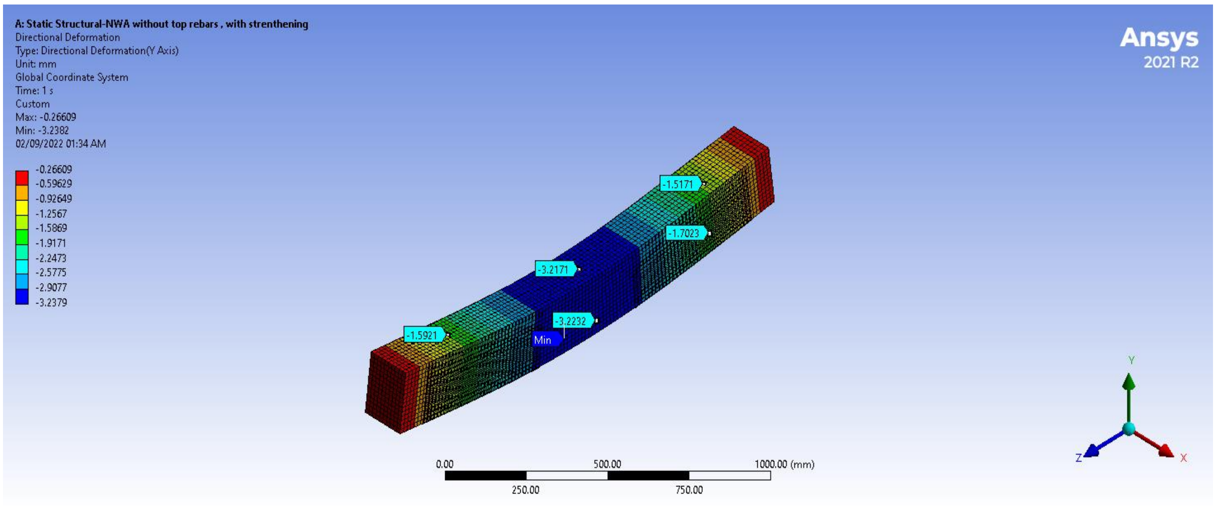

Figure 90(NWA-2/70.5MPa – Directional deflections (Y-Dim.) of beam sample with strengthening and without top rebars- Static Nonlinear Analysis)

The value is 3.238 mm.

Elastic Strain

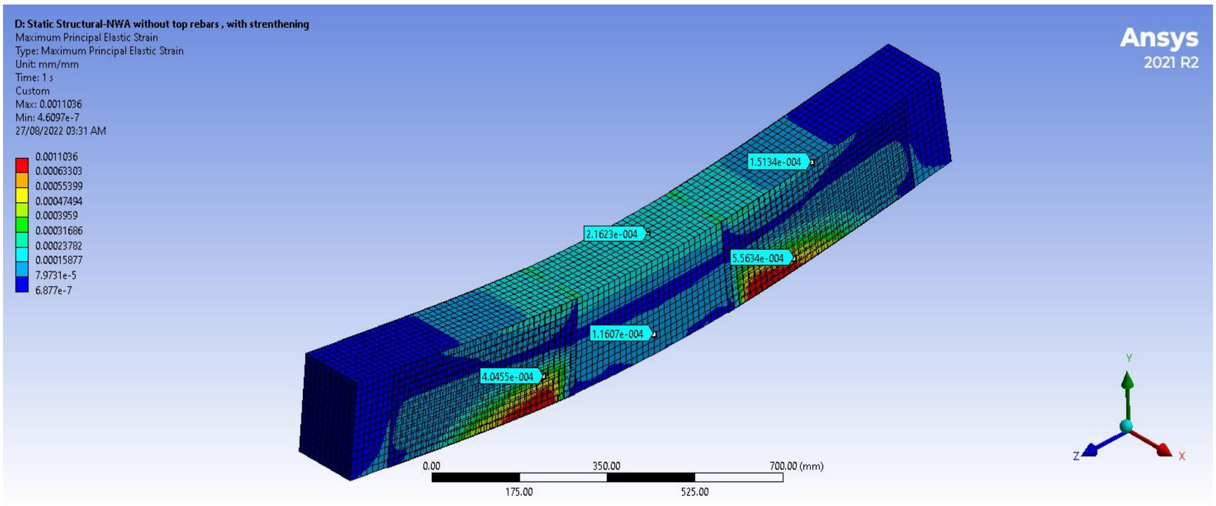

Figure 91(NWA-2/70.5MPa – Elastic strain of beam sample with strengthening and without top rebars- Static Nonlinear Analysis

Detailed Calculations in Appendix A (32-Static Non-Linear Analysis - Without Top Rebars and Strengthening)

6.2.1.3.4.4 Explicit Dynamic-Without Top Rebars & With Strengthening

Deformations

Total Deformations

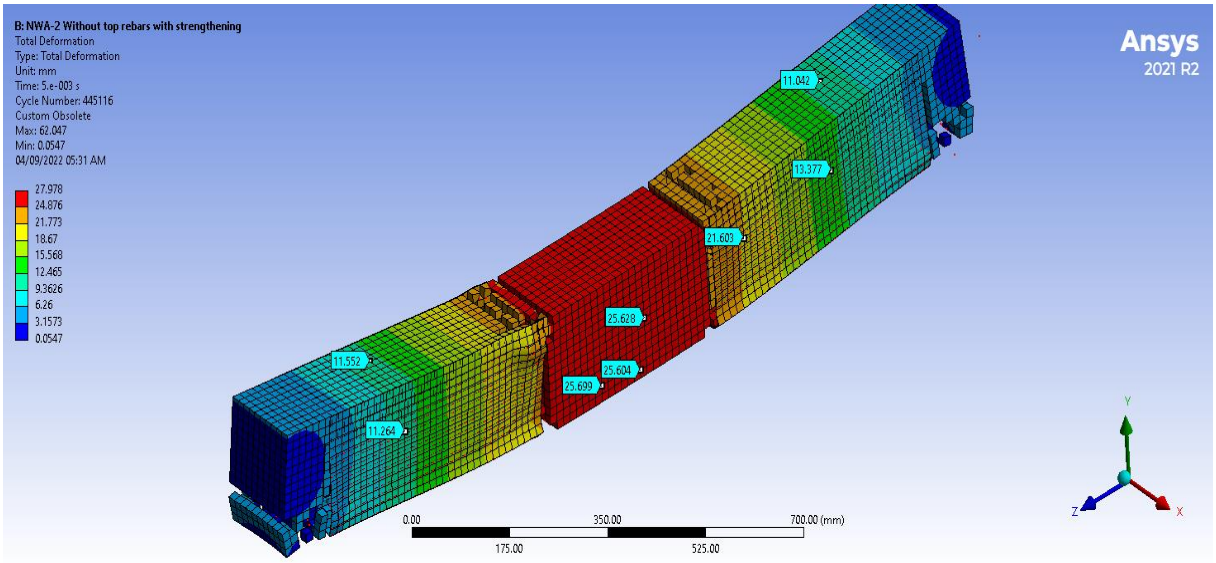

Figure 92(NWA-2/70.5MPa – Total deflections of beam sample with strengthening and without top rebars- Explicit Dynamic Analysis)

The value is 25.699 mm.

Directional Deformation (Y-Direction)-Concrete

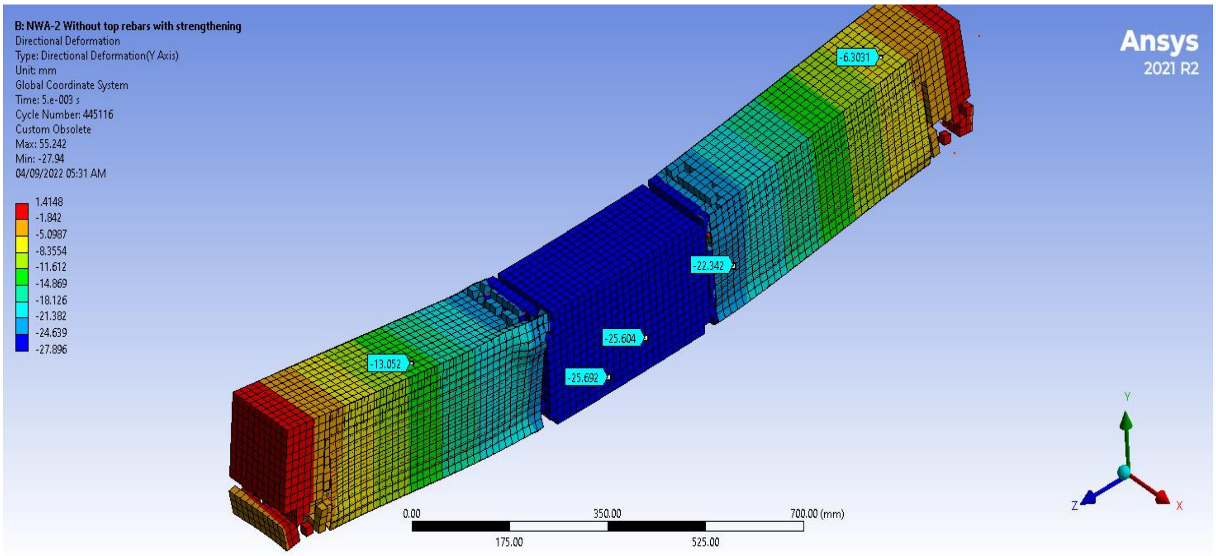

Figure 93(NWA-2/70.5MPa – Directional deflections (Y-Dim.) of beam sample with strengthening and without top rebars-Explicit Dynamic Analysis)

The value is 25.699 mm

The Damage Pattern

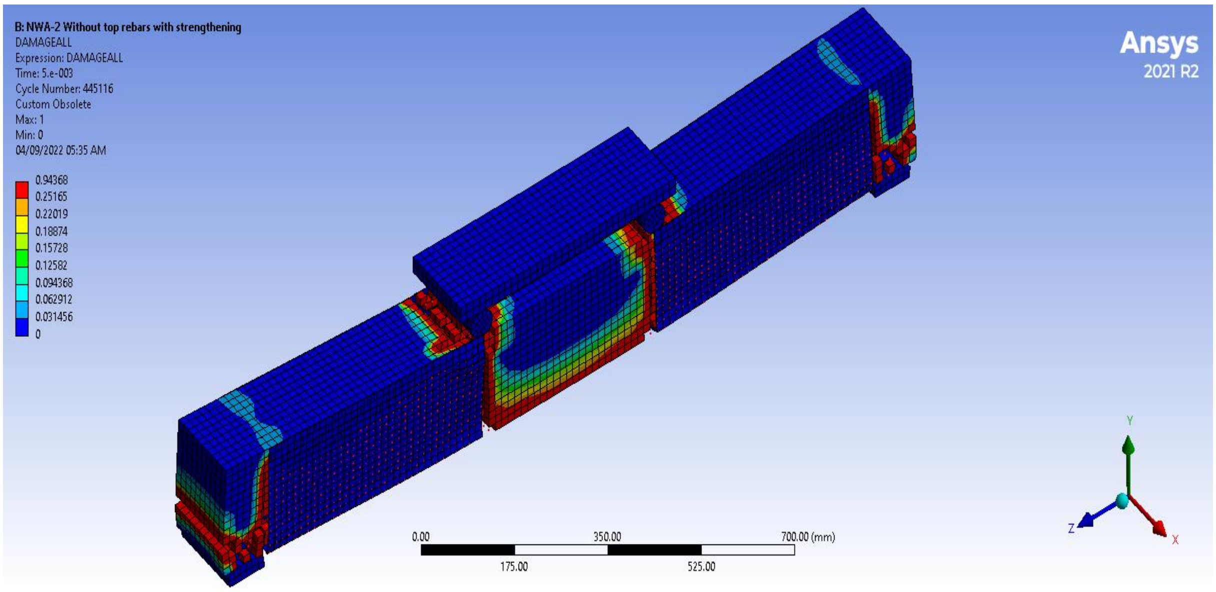

Figure 94(NWA-2/70.5MPa – Damage pattern-1 of beam sample with strengthening and without top rebars- Explicit Dynamic Analysis)

As we can see the shear damage cracks in red and CFRP debonding on edges of concrete failure.

Detailed Calculations in Appendix A (32- Explicit Dynamic-Without Top Rebars & with Strengthening)

6.2.2 Section 2- The Structural Analysis and Code Based Evaluations Using (Midas Gen & Midas Design Plus 2021)

This section will involve the execution of two stages. The first stage is "Structural Analysis," which will be carried out by (Midas Gen 2021) in order to check reactions, deformations, shear, and moment values for each sample (NWA, RCA and RCA-5D$_{fibers}$). The second stage is "ACI440 Code Check," which will be performed by (Midas Design Plus 2021) to ensure that the strengthening using CFRP adheres to (ACI-440, 2017) standard .

6.2.2.1 Stage 1 - Structural Analysis Stage Using (Midas Gen 2021)

6.2.2.1.1 Model No.1- Normal Weight Aggregate Sample (NWA-1).

Case in details check No.1 in **Appendix B**

Mechanical Properties of Normal Weight Aggregate Sample (NWA-1), $f'c$ =70.50MPa Not Strengthened			
Linear Elastic Isotropic Elasticity	Equations	Value	Reference Code
Young's Modulus E_c	$E_c = 3320\sqrt{f'c} + 6900$	34776.14MPa	ACI363R-10-(Eq.6-1) For f'$c > 55MPa$
Poisson's Ration V_c	--	0.2	ACI363R-10-(Sec.6.4)
Density	--	25 MPa	Software Calculated

Table 17(Mechanical Properties of Normal Weight Aggregate Sample (NWA-1), f' c =70.50MPa, Not Strengthened -Midas Gen)

6.2.2.1.1.1 Summarized Analysis Data (Deformations-Deflection)

	Node	Load	DX (mm)	DY (mm)	DZ (mm)	RX ([rad])	RY ([rad])	RZ ([rad])
	1	DL	0	0	0	0	0.00518	0
	2	DL	0	0	-2.586004	0	0.002072	0
	3	DL	0	0	-2.586004	0	-0.002072	0
	4	DL	0	0	0	0	-0.00518	0

Table 18(NWA-1/70.5MPa Deformations-Deflection Values-Midas Gen)

6.2.2.1.1.2 Summarized Analysis Data (Shear-Moment)

	Elem	Load	Part	Axial (kN)	Shear-y (kN)	Shear-z (kN)	Torsion (kN*m)	Moment-y (kN*m)	Moment-z (kN*m)
	1	DL	I[1]	0	0	-60.05	0	0	0
	1	DL	J[2]	0	0	-60.05	0	36.03	0
	2	DL	I[2]	0	0	0	0	36.03	0
	2	DL	J[3]	0	0	0	0	36.03	0
	3	DL	I[3]	0	0	60.05	0	36.03	0
	3	DL	J[4]	0	0	60.05	0	0	0

Table 19(NWA-1/70.5MPa shear-Moment Values-Midas Gen)

Detailed Calculations Report in Appendix B (1- Normal Weight Aggregate Sample (NWA-1))

6.2.2.1.2 Model No.2- Mechanical Properties of Recycled Aggregate Concrete with Self Consolidating Concrete Sample (RCA).

Case in details check No.2 in **Appendix B**

Mechanical Properties of Recycled Aggregate Concrete with Self Consolidating Concrete Sample (RCA), $f'c$ =64.50MPa-Not Strengthened			
Linear Elastic Isotropic Elasticity	Equations	Value	Reference Code
Young's Modulus E_c	$E_c = 3320\sqrt{f'c} + 6900$	33563.55MPa	ACI363R-10-(Eq.6-1) For $f'c > 55MPa$
Poisson's Ration V_c	--	0.2	ACI363R-10-(Sec.6.4)
Density	--	25 MPa	Software Calculated

Table 20(Mechanical Properties of Recycled Aggregate Concrete with Self Consolidating Concrete Sample (RCA), f' c =64.50MPa, Not Strengthened -Midas Gen)

6.2.2.1.2.1 Summarized Analysis Data (Deformations-Deflection)

	Node	Load	DX (mm)	DY (mm)	DZ (mm)	RX ([rad])	RY ([rad])	RZ ([rad])
	1	DL	0	0	0	0	0.003651	0
	2	DL	0	0	-1.811036	0	0.001461	0
	3	DL	0	0	-1.811036	0	-0.001461	0
	4	DL	0	0	0	0	-0.003651	0

Table 21(RCA-64.50MPa Deformations-Deflection Values-Midas Gen)

6.2.2.1.2.2 Summarized Analysis Data (Shear- Moment)

	Elem	Load	Part	Axial (kN)	Shear-y (kN)	Shear-z (kN)	Torsion (kN*m)	Moment-y (kN*m)	Moment-z (kN*m)
	1	DL	I[1]	0	0	-40.85	0	0	0
	1	DL	J[2]	0	0	-40.85	0	24.51	0
	2	DL	I[2]	0	0	0	0	24.51	0
	2	DL	J[3]	0	0	0	0	24.51	0
	3	DL	I[3]	0	0	40.85	0	24.51	0
	3	DL	J[4]	0	0	40.85	0	0	0

Table 22(RCA-64.50MPa shear-Moment Values-Midas Gen)

Detailed Calculations Report in Appendix B (2- Mechanical Properties of Recycled Aggregate Concrete with Self Consolidating Concrete Sample (RCA))

6.2.2.1.3 Model No. 3- Mechanical Properties of Recycled Aggregate Concrete with Self Consolidating Concrete Sample (RCA-5D).

Case in details check No.3 in Appendix B

Mechanical Properties of Recycled Aggregate Concrete with Self Consolidating Concrete and Fibers (RCA-5D $_{\text{Fibers}}$), f' c =77.0MPa, Not Strengthened			
Linear Elastic Isotropic Elasticity	Equations	Value	Reference Code
Young's Modulus E_c	$E_c = 3320\sqrt{f'c} + 6900$	36032.88MPa	ACI363R-10-(Eq.6-1) For $f'c > 55MPa$
Poisson's Ration V_c	--	0.2	ACI363R-10-(Sec.6.4)
Density	--	25 MPa	Software Calculated

Table 23(Mechanical Properties of Recycled Aggregate Concrete with Self Consolidating Concrete and Fibers (RCA-5D $_{\text{Fibers}}$), f' c =77.0MPa, Not Strengthened -Midas Gen)

6.2.2.1.3.1 Summarized Analysis Data (Deformations-Deflection)

	Node	Load	DX (mm)	DY (mm)	DZ (mm)	RX ([rad])	RY ([rad])	RZ ([rad])
	1	DL	0	0	0	0	0.005416	0
	2	DL	0	0	-2.686280	0	0.002166	0
	3	DL	0	0	-2.686280	0	-0.002166	0
	4	DL	0	0	0	0	-0.005416	0

Table 24(RCA-5D $_{\text{Fibers}}$- 77.0MPa Deformations-Deflection Values-Midas Gen)

6.2.2.1.3.2 Summarized Analysis Data (Shear- Moment)

	Elem	Load	Part	Axial (kN)	Shear-y (kN)	Shear-z (kN)	Torsion (kN*m)	Moment-y (kN*m)	Moment-z (kN*m)
	1	DL	I[1]	0	0	-65.05	0	0.00	0
	1	DL	J[2]	0	0	-65.05	0	39.03	0
	2	DL	I[2]	0	0	0	0	39.03	0
	2	DL	J[3]	0	0	0	0	39.03	0
	3	DL	I[3]	0	0	65.05	0	39.03	0
	3	DL	J[4]	0	0	65.05	0	0.00	0

Table 25(RCA-5D $_{Fibers}$- 77.0MPa shear-Moment Values-Midas Gen)

<u>Detailed Calculations Report in Appendix B (3- Mechanical Properties of Recycled Aggregate Concrete with Self Consolidating Concrete Sample (RCA-5D))</u>

6.2.2.1.4 Model No. 4- Normal Weight Aggregate Sample (NWA-2)- Strengthened

Case in details check No.4 in **Appendix B**

Mechanical Properties of Normal Weight Aggregate Sample (NWA-2), f' c =70.50MPa - Strengthened			
Linear Elastic Isotropic Elasticity	Equations	Value	Reference Code
Young's Modulus E_c	$E_c = 3320\sqrt{f'c} + 6900$	34776.14MPa	ACI363R-10-(Eq.6-1) For $f'c > 55MPa$
Poisson's Ration V_c	--	0.2	ACI363R-10-(Sec.6.4)
Density	--	25 MPa	Software Calculated

Table 26(Mechanical Properties of Normal Weight Aggregate Sample (NWA-2), f' c =70.50MPa-Strengthened- Midas Gen)

6.2.2.1.4.1 Summarized Analysis Data (Deformations-Deflection)

	Node	Load	DX (mm)	DY (mm)	DZ (mm)	RX ([rad])	RY ([rad])	RZ ([rad])
	1	DL	0	0	0	0	0.005446	0
	2	DL	0	0	-2.718857	0	0.002179	0
	3	DL	0	0	-2.718857	0	-0.002179	0
	4	DL	0	0	0	0	-0.005446	0

Table 27(NWA-2/ 70.5MPa-Deformations-Deflection Values-Midas Gen)

6.2.2.1.4.2 Summarized Analysis Data (Shear- Moment)

	Elem	Load	Part	Axial (kN)	Shear-y (kN)	Shear-z (kN)	Torsion (kN*m)	Moment-y (kN*m)	Moment-z (kN*m)
	1	DL	I[1]	0	0	-63.14	0	0.00	0
	1	DL	J[2]	0	0	-63.14	0	37.88	0
	2	DL	I[2]	0	0	0	0	37.88	0
	2	DL	J[3]	0	0	0	0	37.88	0
	3	DL	I[3]	0	0	63.14	0	37.88	0
	3	DL	J[4]	0	0	63.14	0	0.00	0

Table 28(NWA 70.5MPa shear-Moment Values-Midas Gen)

<u>Detailed Calculations Report in Appendix B (4-Normal Weight Aggregate Sample (NWA-2)- Strengthened)</u>

6.2.2.2 Stage 2 - ACI440.2R-17 Code Check Using (Midas Design Plus 2021)

6.2.2.2.1 Model No.1- Normal Weight Aggregate Sample (NWA-1).

Case 1: Strengthening the Beam Cross section with U-Wraps (3Sides), without Compression Rebars.

For more details check case 1 in **Appendix C**

General Information

Design Code	Reference Code	Code Unit
ACI318M-14	ACI 440.2R-08	N, mm

Material

Concrete / Rebar

f_{ck}	E_c	f_y	f_{ys}	E_s	λ
70.50MPa	39,463MPa	460MPa	420MPa	200,000MPa	-

/ Carbon (Table 14)

Name	f^*_{fu}	E^*_{fs}	t_f	ε^*_{fu}	Fiber Type
MasterBrace FIB 600/50 CFS	3,500MPa	230,000MPa	0.337mm	0.021000	Carbon

Section

Beam

Section	Slab Thickness	Effective Width	Cover	Compression	Splicing Limit
150 x 200mm	0.0mm	0.0mm	23.00 / 40.00mm	**Not Considered**	50%

FRP / Carbon

POS.	Apply	Size(mm)	Pieces	Description
(1)	**Yes**	**150**	**1**	**Bottom of Beam**
(2)	**Yes**	**200**	**1**	**Side of Beam (Shear)**
(3)	No	120	1	Side of Beam (Bottom)
(4)	No	120	1	Side of Beam (Top)
(5)	No	100	1	Bottom of Slab
(6)	No	150	1	Top of Beam

FRP / Carbon (Shear)

Wrapping Schemes	w_f	s_f
U-Wraps (3 Sides Bonded)	500mm	400mm

Rebar

Top Bar	Bot Bar	Stirrup	Skin Bar
2-P12(Not Considered)	3-P12	2-P10@300	-

Case 1 Results:

Check Item	Value	Criteria	Ratio
Negative Moment (Before)			
Strength (kN.m)	-	-	-
Rebar Ratio (Min)	-	-	-
Rebar Ratio (Max)	-	-	-
Rebar Space (mm)	-	-	-
Positive Moment (Before)			
Strength (kN.m)	36.03	19.02	NG(1.894)
Rebar Ratio (Min)	0.01570	0.00456	OK(0.291)
Rebar Ratio (Max)	0.01570	0.03629	OK(0.433)
Rebar Space (mm)	19.00	222	OK(0.086)
Shear Force (Before)			
Strength (kN)	60.05	46.64	NG(1.287)
Max. Strength (kN)	60.05	112	OK(0.538)
Rebar Space (mm)	300	72.05	NG(4.164)
Skin Rebar			
Rebar Space (mm)	-	-	-
Negative Moment (After)			
Limit (kN.m)	-	-	-
Strength (kN.m)	-	-	-
Stress (MPa)	-	-	-
Creep (MPa)	-	-	-
Positive Moment (After)			
Limit (kN.m)	0.000	19.02	OK(0.000)
Strength (kN.m)	36.03	36.99	OK(0.974)
Stress (MPa)	0.000	368	OK(0.000)
Creep (MPa)	0.000	1636	OK(0.000)
Shear Force (After)			
Strength (kN)	60.05	112	OK(0.538)

Figure 95(Case 1 Results-Midas Design Plus)

Detailed Calculations Report in Appendix C (Case 1- FRP Strengthening Detailed Calculations-Midas Design Plus 2021)

Case 2: Strengthening the Beam Cross section with U-Wraps (3Sides), with Compression Rebars.

For more details check case 2 in **Appendix C**

General Information

Design Code	Reference Code	Code Unit
ACI318M-14	ACI 440.2R-08	N, mm

Material

Concrete / Rebar

f_{ck}	E_c	f_y	f_{ys}	E_s	λ
70.50MPa	39,463MPa	460MPa	420MPa	200,000MPa	-

FRP / Carbon (Table 14)

Name	f^*_{fu}	E^*_{fs}	t_f	ε^*_{fu}	Fiber Type
MasterBrace FIB 600/50 CFS	3,500MPa	230,000MPa	0.337mm	0.021000	Carbon

Section
Beam

Section	Slab Thickness	Effective Width	Cover	Compression	Splicing Limit
150 x 200mm	0.0mm	0.0mm	23.00 / 40.00mm	**Considered**	50%

FRP / Carbon

POS.	Apply	Size(mm)	Pieces	Description
(1)	**Yes**	**150**	**1**	**Bottom of Beam**
(2)	**Yes**	**200**	**1**	**Side of Beam (Shear)**
(3)	No	120	1	Side of Beam (Bottom)
(4)	No	120	1	Side of Beam (Top)
(5)	No	100	1	Bottom of Slab
(6)	No	150	1	Top of Beam

FRP / Carbon (Shear)

Wrapping Schemes	w_f	s_f
U-Wraps (3 Sides Bonded)	500mm	400mm

Rebar

Top Bar	Bot Bar	Stirrup	Skin Bar
2-P12(Considered)	3-P12	2-P10@300	-

Case 2 Results:

Check Item	Value	Criteria	Ratio
Negative Moment (Before)			
Strength (kN.m)	-	-	-
Rebar Ratio (Min)	-	-	-
Rebar Ratio (Max)	-	-	-
Rebar Space (mm)	-	-	-
Positive Moment (Before)			
Strength (kN.m)	36.03	19.58	NG(1.840)
Rebar Ratio (Min)	0.01570	0.00456	OK(0.291)
Rebar Ratio (Max)	0.01570	0.04341	OK(0.362)
Rebar Space (mm)	19.00	222	OK(0.086)
Shear Force (Before)			
Strength (kN)	60.05	46.64	NG(1.287)
Max. Strength (kN)	60.05	112	OK(0.538)
Rebar Space (mm)	300	72.05	NG(4.164)
Skin Rebar			
Rebar Space (mm)	-	-	-
Negative Moment (After)			
Limit (kN.m)	-	-	-
Strength (kN.m)	-	-	-
Stress (MPa)	-	-	-
Creep (MPa)	-	-	-
Positive Moment (After)			
Limit (kN.m)	0.000	19.58	OK(0.000)
Strength (kN.m)	36.03	36.99	OK(0.974)
Stress (MPa)	0.000	368	OK(0.000)
Creep (MPa)	0.000	1636	OK(0.000)
Shear Force (After)			
Strength (kN)	60.05	112	OK(0.538)

Figure 96(Case 2 Results-Midas Design Plus)

Detailed Calculations Report in Appendix C (Case 2- FRP Strengthening Detailed Calculations-Midas Design Plus 2021)

6.2.2.2.2 Model No.2- Recycled Aggregate Concrete with Self Consolidating Concrete Sample (RCA).

Case 3: Strengthening the Beam Cross section with U-Wraps (3Sides), without Compression Rebars.

For more details check case 3 in Appendix C

General Information

Design Code	Reference Code	Code Unit
ACI318M-14	ACI 440.2R-08	N, mm

Material
Concrete / Rebar

f_{ck}	E_c	f_y	f_{ys}	E_s	λ
64.50MPa	37,746MPa	460MPa	420MPa	200,000MPa	-

FRP / Carbon (Table 14)

Name	f^*_{fu}	E^*_{fs}	t_f	ε^*_{fu}	Fiber Type
MasterBrace FIB 600/50 CFS	3,500MPa	230,000MPa	0.337mm	0.021000	Carbon

Section
Beam

Section	Slab Thickness	Effective Width	Cover	Compression	Splicing Limit
150 x 200mm	0.0mm	0.0mm	23.00 / 40.00mm	**Not Considered**	50%

FRP / Carbon

POS.	Apply	Size(mm)	Pieces	Description
(1)	**Yes**	**150**	**1**	**Bottom of Beam**
(2)	**Yes**	**200**	**1**	**Side of Beam (Shear)**
(3)	No	120	1	Side of Beam (Bottom)
(4)	No	120	1	Side of Beam (Top)
(5)	No	100	1	Bottom of Slab
(6)	No	150	1	Top of Beam

FRP / Carbon (Shear)

Wrapping Schemes	w_f	s_f
U-Wraps (3 Sides Bonded)	500mm	400mm

Rebar

Top Bar	Bot Bar	Stirrup	Skin Bar
2-P12(Not Considered)	3-P12	2-P10@300	-

Case 3 Results:

Check Item	Value	Criteria	Ratio
Negative Moment (Before)			
Strength (kN.m)	-	-	-
Rebar Ratio (Min)	-	-	-
Rebar Ratio (Max)	-	-	-
Rebar Space (mm)	-	-	-
Positive Moment (Before)			
Strength (kN.m)	24.51	18.91	NG(1.296)
Rebar Ratio (Min)	0.01570	0.00436	OK(0.278)
Rebar Ratio (Max)	0.01570	0.03320	OK(0.473)
Rebar Space (mm)	19.00	222	OK(0.086)
Shear Force (Before)			
Strength (kN)	40.85	45.90	OK(0.890)
Max. Strength (kN)	40.85	108	OK(0.378)
Rebar Space (mm)	300	72.05	NG(4.164)
Skin Rebar			
Rebar Space (mm)	-	-	-
Negative Moment (After)			
Limit (kN.m)	-	-	-
Strength (kN.m)	-	-	-
Stress (MPa)	-	-	-
Creep (MPa)	-	-	-
Positive Moment (After)			
Limit (kN.m)	0.000	18.91	OK(0.000)
Strength (kN.m)	24.51	40.12	OK(0.611)
Stress (MPa)	0.000	368	OK(0.000)
Creep (MPa)	0.000	1636	OK(0.000)
Shear Force (After)			
Strength (kN)	40.85	108	OK(0.378)

Figure 97(Case 3 Results-Midas Design Plus)

Detailed Calculations Report in Appendix C (Case 3- FRP Strengthening Detailed Calculations-Midas Design Plus 2021)

Case 4: Strengthening the Beam Cross section with U-Wraps (3Sides), with Compression Rebars.

For more details check case 4 in **Appendix C**

General Information

Design Code	Reference Code	Code Unit
ACI318M-14	ACI 440.2R-08	N, mm

Material

Concrete / Rebar

f_{ck}	E_c	f_y	f_{ys}	E_s	λ
64.50MPa	37,746MPa	460MPa	420MPa	200,000MPa	-

FRP / Carbon (Table 14)

Name	f^*_{fu}	E^*_{fs}	t_f	ε^*_{fu}	Fiber Type
MasterBrace FIB 600/50 CFS	3,500MPa	230,000MPa	0.337mm	0.021000	Carbon

Section

Beam

Section	Slab Thickness	Effective Width	Cover	Compression	Splicing Limit
150 x 200mm	0.0mm	0.0mm	23.00 / 40.00mm	**Considered**	50%

FRP / Carbon

POS.	Apply	Size(mm)	Pieces	Description
(1)	**Yes**	**150**	**1**	**Bottom of Beam**
(2)	**Yes**	**200**	**1**	**Side of Beam (Shear)**
(3)	No	120	1	Side of Beam (Bottom)
(4)	No	120	1	Side of Beam (Top)
(5)	No	100	1	Bottom of Slab
(6)	No	150	1	Top of Beam

FRP / Carbon (Shear)

Wrapping Schemes	W_f	S_f
U-Wraps (3 Sides Bonded)	500mm	400mm

Rebar

Top Bar	Bot Bar	Stirrup	Skin Bar
2-P12(Considered)	3-P12	2-P10@300	-

Case 4 Results:

Check Item	Value	Criteria	Ratio
Negative Moment (Before)			
Strength (kN.m)	-	-	-
Rebar Ratio (Min)	-	-	-
Rebar Ratio (Max)	-	-	-
Rebar Space (mm)	-	-	-
Positive Moment (Before)			
Strength (kN.m)	24.51	19.30	NG(1.270)
Rebar Ratio (Min)	0.01570	0.00436	OK(0.278)
Rebar Ratio (Max)	0.01570	0.04032	OK(0.389)
Rebar Space (mm)	19.00	222	OK(0.086)
Shear Force (Before)			
Strength (kN)	40.85	45.90	OK(0.890)
Max. Strength (kN)	40.85	108	OK(0.378)
Rebar Space (mm)	300	72.05	NG(4.164)
Skin Rebar			
Rebar Space (mm)	-	-	-
Negative Moment (After)			
Limit (kN.m)	-	-	-
Strength (kN.m)	-	-	-
Stress (MPa)	-	-	-
Creep (MPa)	-	-	-
Positive Moment (After)			
Limit (kN.m)	0.000	19.30	OK(0.000)
Strength (kN.m)	24.51	40.12	OK(0.611)
Stress (MPa)	0.000	368	OK(0.000)
Creep (MPa)	0.000	1636	OK(0.000)
Shear Force (After)			
Strength (kN)	40.85	108	OK(0.378)

Figure 98(Case 4 Results-Midas Design Plus)

Detailed Calculations Report in Appendix C (Case 4- FRP Strengthening Detailed Calculations-Midas Design Plus 2021)

6.2.2.2.3 Model No. 3- Recycled Aggregate Concrete with Self Consolidating Concrete Sample (RCA-5D).

Case 5: Strengthening the Beam Cross section with U-Wraps (3Sides), without Compression Rebars.

For more details check case 5 in Appendix C

General Information

Design Code	Reference Code	Code Unit
ACI318M-14	ACI 440.2R-08	N, mm

Material

Concrete / Rebar

f_{ck}	E_c	f_y	f_{ys}	E_s	λ
77.00MPa	41,242MPa	460MPa	420MPa	200,000MPa	-

FRP / Carbon (Table 14)

Name	f^*_{fu}	E^*_{fs}	t_f	ε^*_{fu}	Fiber Type
MasterBrace FIB 600/50 CFS	3,500MPa	230,000MPa	0.337mm	0.021000	Carbon

Section

Beam

Section	Slab Thickness	Effective Width	Cover	Compression	Splicing Limit
150 x 200mm	0.0mm	0.0mm	23.00 / 40.00mm	**Not Considered**	50%

FRP / Carbon

POS.	Apply	Size(mm)	Pieces	Description
(1)	**Yes**	**150**	**1**	**Bottom of Beam**
(2)	**Yes**	**200**	**1**	**Side of Beam (Shear)**
(3)	No	120	1	Side of Beam (Bottom)
(4)	No	120	1	Side of Beam (Top)
(5)	No	100	1	Bottom of Slab
(6)	No	150	1	Top of Beam

FRP / Carbon (Shear)

Wrapping Schemes	w_f	s_f
U-Wraps (3 Sides Bonded)	500mm	400mm

Rebar

Top Bar	Bot Bar	Stirrup	Skin Bar
2-P12(Not Considered)	3-P12	2-P10@300	-

Case 5 Results:

Check Item	Value	Criteria	Ratio
Negative Moment (Before)			
Strength (kN.m)	-	-	-
Rebar Ratio (Min)	-	-	-
Rebar Ratio (Max)	-	-	-
Rebar Space (mm)	-	-	-
Positive Moment (Before)			
Strength (kN.m)	39.03	19.13	NG(2.041)
Rebar Ratio (Min)	0.01570	0.00477	OK(0.304)
Rebar Ratio (Max)	0.01570	0.03964	OK(0.396)
Rebar Space (mm)	19.00	222	OK(0.086)
Shear Force (Before)			
Strength (kN)	65.05	46.64	NG(1.395)
Max. Strength (kN)	65.05	112	OK(0.582)
Rebar Space (mm)	300	72.05	NG(4.164)
Skin Rebar			
Rebar Space (mm)	-	-	-
Negative Moment (After)			
Limit (kN.m)	-	-	-
Strength (kN.m)	-	-	-
Stress (MPa)	-	-	-
Creep (MPa)	-	-	-
Positive Moment (After)			
Limit (kN.m)	0.000	19.13	OK(0.000)
Strength (kN.m)	39.03	38.17	NG(1.022)
Stress (MPa)	0.000	368	OK(0.000)
Creep (MPa)	0.000	1636	OK(0.000)
Shear Force (After)			
Strength (kN)	65.05	112	OK(0.582)

Figure 99(Case 5 Results-Midas Design Plus)

Detailed Calculations Report in Appendix C (Case 5- FRP Strengthening Detailed Calculations-Midas Design Plus 2021)

Case 6: Strengthening the Beam Cross section with U-Wraps (3Sides), with Compression Rebars.

For more details check case 6 in **Appendix C**

General Information

Design Code	Reference Code	Code Unit
ACI318M-14	ACI 440.2R-08	N, mm

Material

Concrete / Rebar

f_{ck}	E_c	f_y	f_{ys}	E_s	λ
77.00MPa	41,242MPa	460MPa	420MPa	200,000MPa	-

FRP / Carbon (Table 14)

Name	f^*_{fu}	E^*_{fs}	t_f	ε^*_{fu}	Fiber Type
MasterBrace FIB 600/50 CFS	3,500MPa	230,000MPa	0.337mm	0.021000	Carbon

Section

Beam

Section	Slab Thickness	Effective Width	Cover	Compression	Splicing Limit

150 x 200mm	0.0mm	0.0mm	23.00 / 40.00mm	**Considered**	50%

FRP / Carbon

POS.	Apply	Size(mm)	Pieces	Description
(1)	**Yes**	**150**	**1**	**Bottom of Beam**
(2)	**Yes**	**200**	**1**	**Side of Beam (Shear)**
(3)	No	120	1	Side of Beam (Bottom)
(4)	No	120	1	Side of Beam (Top)
(5)	No	100	1	Bottom of Slab
(6)	No	150	1	Top of Beam

FRP / Carbon (Shear)

Wrapping Schemes	w_f	s_f
U-Wraps (3 Sides Bonded)	500mm	400mm

Rebar

Top Bar	Bot Bar	Stirrup	Skin Bar
2-P12(Considered)	3-P12	2-P10@300	-

Case 6 Results:

Check Item	Value	Criteria	Ratio
Negative Moment (Before)			
Strength (kN.m)	-	-	-
Rebar Ratio (Min)	-	-	-
Rebar Ratio (Max)	-	-	-
Rebar Space (mm)	-	-	-
Positive Moment (Before)			
Strength (kN.m)	39.03	19.86	NG(1.965)
Rebar Ratio (Min)	0.01570	0.00477	OK(0.304)
Rebar Ratio (Max)	0.01570	0.04676	OK(0.336)
Rebar Space (mm)	19.00	222	OK(0.086)
Shear Force (Before)			
Strength (kN)	65.05	46.64	NG(1.395)
Max. Strength (kN)	65.05	112	OK(0.582)
Rebar Space (mm)	300	72.05	NG(4.164)
Skin Rebar			
Rebar Space (mm)	-	-	-
Negative Moment (After)			
Limit (kN.m)	-	-	-
Strength (kN.m)	-	-	-
Stress (MPa)	-	-	-
Creep (MPa)	-	-	-
Positive Moment (After)			
Limit (kN.m)	0.000	19.86	OK(0.000)
Strength (kN.m)	39.03	38.17	NG(1.022)
Stress (MPa)	0.000	368	OK(0.000)
Creep (MPa)	0.000	1636	OK(0.000)
Shear Force (After)			
Strength (kN)	65.05	112	OK(0.582)

Figure 100(Case 6 Results-Midas Design Plus)

Detailed Calculations Report in Appendix C (Case 6- FRP Strengthening Detailed Calculations-Midas Design Plus 2021)

6.2.2.2.4 Model No. 4- Model No.2- Normal Weight Aggregate Sample (NWA-2).

Case 7: Strengthening the Beam Cross section with U-Wraps (3Sides), without Compression Rebars.

For more details check case 7 in **Appendix C**

General Information

Design Code	Reference Code	Code Unit
ACI318M-14	ACI 440.2R-08	N, mm

Material

Concrete / Rebar

f_{ck}	E_c	f_y	f_{ys}	E_s	λ
70.50MPa	39,463MPa	460MPa	420MPa	200,000MPa	-

FRP / Carbon (Table 14)

Name	f^*_{fu}	E^*_{fs}	t_f	ε^*_{fu}	Fiber Type
MasterBrace FIB 600/50 CFS	3,500MPa	230,000MPa	0.337mm	0.021000	Carbon

Section

Beam

Section	Slab Thickness	Effective Width	Cover	Compression	Splicing Limit
150 x 200mm	0.0mm	0.0mm	23.00 / 40.00mm	**Not Considered**	50%

FRP / Carbon

POS.	Apply	Size(mm)	Pieces	Description
(1)	**Yes**	**150**	**1**	**Bottom of Beam**
(2)	**Yes**	**200**	**1**	**Side of Beam (Shear)**
(3)	No	120	1	Side of Beam (Bottom)
(4)	No	120	1	Side of Beam (Top)
(5)	No	100	1	Bottom of Slab
(6)	No	150	1	Top of Beam

FRP / Carbon (Shear)

Wrapping Schemes	w_f	s_f
U-Wraps (3 Sides Bonded)	500mm	400mm

Rebar

Top Bar	Bot Bar	Stirrup	Skin Bar
2-P12(Not Considered)	3-P12	2-P10@300	-

Case 7 Results:

Check Item	Value	Criteria	Ratio
Negative Moment (Before)			
Strength (kN.m)	-	-	-
Rebar Ratio (Min)	-	-	-
Rebar Ratio (Max)	-	-	-
Rebar Space (mm)	-	-	-
Positive Moment (Before)			
Strength (kN.m)	37.88	19.02	NG(1.991)
Rebar Ratio (Min)	0.01570	0.00456	OK(0.291)
Rebar Ratio (Max)	0.01570	0.03629	OK(0.433)
Rebar Space (mm)	19.00	222	OK(0.086)
Shear Force (Before)			
Strength (kN)	63.14	46.64	NG(1.354)
Max. Strength (kN)	63.14	112	OK(0.565)
Rebar Space (mm)	300	72.05	NG(4.164)
Skin Rebar			
Rebar Space (mm)	-	-	-
Negative Moment (After)			
Limit (kN.m)	-	-	-
Strength (kN.m)	-	-	-
Stress (MPa)	-	-	-
Creep (MPa)	-	-	-
Positive Moment (After)			
Limit (kN.m)	0.000	19.02	OK(0.000)
Strength (kN.m)	37.88	36.99	NG(1.024)
Stress (MPa)	0.000	368	OK(0.000)
Creep (MPa)	0.000	1636	OK(0.000)
Shear Force (After)			
Strength (kN)	63.14	112	OK(0.565)

Figure 101(Case 7 Results-Midas Design Plus)

Detailed Calculations Report in Appendix C (Case 7- FRP Strengthening Detailed Calculations-Midas Design Plus 2021)

Case 8: Strengthening the Beam Cross section with U-Wraps (3Sides), with Compression Rebars.

For more details check case 8 in **Appendix C**

General Information

Design Code	Reference Code	Code Unit
ACI318M-14	ACI 440.2R-08	N, mm

Material

Concrete / Rebar

f_{ck}	E_c	f_y	f_{ys}	E_s	λ
70.50MPa	39,463MPa	460MPa	420MPa	200,000MPa	-

FRP / Carbon (Table 14)

Name	f^*_{fu}	E^*_{fs}	t_f	ε^*_{fu}	Fiber Type
MasterBrace FIB 600/50 CFS	3,500MPa	230,000MPa	0.337mm	0.021000	Carbon

Section

Beam

Section	Slab Thickness	Effective Width	Cover	Compression	Splicing Limit
150 x 200mm	0.0mm	0.0mm	23.00 / 40.00mm	**Considered**	50%

FRP / Carbon

POS.	Apply	Size(mm)	Pieces	Description
(1)	**Yes**	**150**	**1**	**Bottom of Beam**
(2)	**Yes**	**200**	**1**	**Side of Beam (Shear)**
(3)	No	120	1	Side of Beam (Bottom)
(4)	No	120	1	Side of Beam (Top)
(5)	No	100	1	Bottom of Slab
(6)	No	150	1	Top of Beam

FRP / Carbon (Shear)

Wrapping Schemes	w_f	s_f
U-Wraps (3 Sides Bonded)	500mm	400mm

Rebar

Top Bar	Bot Bar	Stirrup	Skin Bar
2-P12(Considered)	3-P12	2-P10@300	-

Case 8 Results:

Check Item	Value	Criteria	Ratio
Negative Moment (Before)			
Strength (kN.m)	-	-	-
Rebar Ratio (Min)	-	-	-
Rebar Ratio (Max)	-	-	-
Rebar Space (mm)	-	-	-
Positive Moment (Before)			
Strength (kN.m)	37.88	19.58	NG(1.934)
Rebar Ratio (Min)	0.01570	0.00456	OK(0.291)
Rebar Ratio (Max)	0.01570	0.04341	OK(0.362)
Rebar Space (mm)	19.00	222	OK(0.086)
Shear Force (Before)			
Strength (kN)	63.14	46.64	NG(1.354)
Max. Strength (kN)	63.14	112	OK(0.565)
Rebar Space (mm)	300	72.05	NG(4.164)
Skin Rebar			
Rebar Space (mm)	-	-	-
Negative Moment (After)			
Limit (kN.m)	-	-	-
Strength (kN.m)	-	-	-
Stress (MPa)	-	-	-
Creep (MPa)	-	-	-
Positive Moment (After)			
Limit (kN.m)	0.000	19.58	OK(0.000)
Strength (kN.m)	37.88	36.99	NG(1.024)
Stress (MPa)	0.000	368	OK(0.000)
Creep (MPa)	0.000	1636	OK(0.000)
Shear Force (After)			
Strength (kN)	63.14	112	OK(0.565)

Figure 102(Case 8 Results-Midas Design Plus)

Detailed Calculations Report in Appendix C (Case 8- FRP Strengthening Detailed Calculations-Midas Design Plus 2021)

6.3 Results Summarization

6.3.1 Analytical Summarization Results

6.3.1.1 Section 1- (ANSYS Workbench 2021) Results Summarization

The following comparison matrix summarizes sections 6.2.1.3.1, 6.2.1.3.2, 6.2.1.3.3 and 6.2.1.3.4.

ANSYS Workbench Analytical Values Before and After Strengthening of (NWA, RCA, RCA-5D$_{Fibers}$) Samples															
Sample Type	Experimental Loads		Compression Rebars	Analysis Types							Shear Load (KN)	Ductility Index (Δ max/Δ y)		CFPR Improvement %	
				Non-Linear Static Analysis (NLA)				Explicate Dynamic (EX.DY)							
				Before Strengthening		After Strengthening CFRP Laminates		Before Strengthening	After Strengthening CFRP Laminates	Failure Type					
				Deflection (Δ y)	Strain	Deflection (Δ y)	Strain	Deflection (Δ max)	Deflection (Δ max)						
	NLA(KN)	EX.DY(MPa)		(mm)	--	(mm)	--	(mm)	(mm)			Before Strengthening	After Strengthening	NLA	EX.DY
NWA-1 70.5MPa	120.1	4.00	Considered	2.547	0.00027	2.52	0.00084	19.644	17.847	Shear	60.05	7.71	7.08	1.07	10.1
			Not Considered	3.082	0.00034	3.050	0.0010	24.777	23.459	Shear		8.04	7.69	1.05	5.61
NWA-2 70.5MPa	126.27	4.209	Considered	2.701	0.00029	2.67	0.00094	21.448	18.747	Shear	63.135	7.94	7.02	1.16	14.4
			Not Considered	3.27	0.00036	3.238	0.0011	27.122	25.699	Shear		8.30	7.94	0.98	5.53
RCA 64.5MPa	81.7	2.723	Considered	1.631	0.00022	1.617	0.00050	10.348	9.457	Shear	40.85	6.34	5.85	0.87	9.42
			Not Considered	2.008	0.00023	1.95	0.00060	12.303	12.174	Shear		6.13	6.24	2.97	1.06
RCA-5D$_{fibers}$ 77.0MPa	130.09	4.336	Considered	2.738	0.00029	2.703	0.00095	19.88	19.736	Shear-Moment	65.045	7.26	7.30	1.29	0.73
			Not Considered	4.436	0.00036	4.409	0.00106	23.262	22.727	Shear-Moment		5.24	5.15	0.61	2.35

Table 29(ANSYS Workbench Analytical Values Before and After Strengthening of (NWA, RCA, RCA-5D$_{Fibers}$) Samples)

6.3.1.2 Section 2- (Midas Gen & Midas Design Plus 2021) Results Summarization

The following comparison matrix summarizes stage 1 and stage 2 data from sections 6.3.2.1 and 6.3.2.2.

Midas Gen and Midas Design Plus Analytical Values Before and After Strengthening of (NWA, RCA, RCA-5D$_{Fibers}$) Samples													
Sample Type	(Midas Gen)		Compression Rebars	(Midas Design Plus)						% Improvement		Deflection (mm)- (Midas Gen)
	Analytical Values			Before Strengthening		After Strengthening		CFRP Contribution Value				
	Moment KN.m`	Shear KN		Moment KN.m`	Shear KN	Moment KN.m`	Shear KN	Moment KN.m`	Shear KN			
	Main Values			Criteria		Criteria		Criteria		Moment	Shear	
NWA-1 70.5MPa	36.03	60.05	Considered	19.58	46.64	36.99	112	17.41	65.36	89	140	2.586
			Not Considered	19.02				17.97	65.36	94	140	
NWA-2 70.5MPa	37.88	63.13	Considered	19.58	46.64	36.99	112	17.41	65.36	89	140	2.719
			Not Considered	19.02				17.97	65.36	94	140	
RCA 64.5MPa	24.51	40.85	Considered	19.30	45.90	40.12	108	20.82	62.1	107	135	1.811
			Not Considered	18.91				21.21	62.1	112	135	
RCA-5D$_{fibers}$ 77.0MPa	39.03	65.05	Considered	19.86	46.64	38.17	112	18.31	65.36	92	140	2.686
			Not Considered	19.13				19.04	65.36	99	140	

Table 30(Midas Gen and Midas Design Plus Analytical Values Before and After Strengthening of (NWA, RCA, RCA-5D$_{Fibers}$) Samples)

6.3.2 Experimental Results

The following table shows experimental shear forces and deflection results for several types of samples before and after strengthening.

Experimental Results								
Sample Type	Before Strengthening			After Strengthening		% Improvement	Ductility Index $\Delta max/\Delta y$	References
	Shear	Deflection		Shear	Deflection			
		Δy	Δmax		Δmax			
	KN	mm		KN	mm			
NWA-1 70.5MPa	60.05	6.58	11.79	--	--	--	1.79	(Mohamed Ghoneim, 2020)
NWA-2 70.5MPa	--	--	--	63.14	14.93	76	--	(Abdalla Ghoneim, 2019)
RCA 64.5MPa	40.85	7.08	9.22	--	--	--	1.3	(Mohamed Ghoneim, 2020)
RCA-5D$_{fibers}$ 77.0MPa	65.05	4.96	14.43	--	--	--	2.91	(Mohamed Ghoneim, 2020)

Table 31(Experimental Values of (NWA, RCA, RCA-5D$_{Fibers}$) Samples, Before and After Strengthening)

6.3.3 Results Comparison of (Experimental and Analytical)

The following table shows experimental and analytical shear forces and deflection results for several types of samples before and after strengthening.

Shear and Deflection Comparison (Experimental and Analytical) (Δy)																	
		Deflection					Shear					Differences and Changes					
												Deflection ($\Delta y_{EX.}$) $\neq$ ($\Delta y_{AN.}$)				Shear	
		mm					KN					%				%	
		Experimental		Analytical			Experimental	Analytical				Ansys (NLA)		Midas Gen			
				Ansys ($\Delta y_{AN.}$)		Midas			Midas								
		($\Delta y_{EX.}$)		(NLA)						Midas Design Plus Shear Capacity							
Sample Types	Compression Rebars	Before Strengthening	After Strengthening	Before Strengthening	After Strengthening	Midas Gen	Experimental	Ansys (NLA)	Midas Gen	Before Strengthening	After Strengthening	Before Strengthening (Difference)	Before Strengthening Changes (Decrease)	Differences	Decrease	Ansys	Midas
NWA-1 70.5MPa	Considered			2.547	2.520	2.586	60.05	60.05	60.05	46.64	112			87.15	60.70	0	0
	Not Considered	6.58		3.082	3.050							72.40	53.16				
NWA-2 70.5MPa	Considered			2.701	2.670	2.719	63.14	63.135	63.13	46.64	112					0	0
	Not Considered			3.27	3.238												
RCA 64.5MPa	Considered			1.631	1.617	1.811	40.85	40.85	40.85	45.90	108			118.52	74.42	0	0
	Not Considered	7.08		2.008	1.950							111.6	71.64				
RCA-5D$_{fibers}$ 77.0MPa	Considered			2.738	2.703	2.686	65.05	65.045	65.05	46.64	112			59.48	45.85	0	0
	Not Considered	4.96		4.436	4.409							11.15	10.56				

Table 32(Shear and Deflection Comparison (Experimental and Analytical)- (Δ y))

Shear and Deflection Comparison (Experimental and Analytical) ($\Delta\, max$)																	
		Deflection					Shear					Differences and Changes					
												Deflection ($\Delta\, max_{EX.}$) ≠ ($\Delta\, max.$)				Shear	
		mm					KN					%				%	
		Experimental		Analytical			Experimental	Analytical				Ansys (EX.DY)		Midas Gen			
				Ansys ($\Delta\, max_{EX.}$)		Midas			Midas								
Sample Types	Compression Rebars	($\Delta\, max_{EX.}$)		(EX.DY)		Midas Gen		Ansys (EX.DY)	Midas Gen	Midas Design Plus Shear Capacity							
		Before Strengthening	After Strengthening	Before Strengthening	After Strengthening					Before Strengthening	After Strengthening	Before Strengthening (Difference)	Before Strengthening Changes (Increase)	Differences	Decrease	Ansys	Midas
NWA-1 70.5MPa	Considered			19.644	17.847	2.586	60.05	60.05	60.05	46.64	112			128.05	78.06	0	0
	Not Considered	11.79		24.777	23.459							71.0	110.15				
NWA-2 70.5MPa	Considered			21.448	18.747	2.719	63.14	63.135	63.13	46.64	112			138.38	81.80	0	0
	Not Considered		14.93	27.122	25.699							53.01	72.13				
RCA 64.5MPa	Considered			10.348	9.457	1.811	40.85	40.85	40.85	45.90	108			134.33	80.36	0	0
	Not Considered	9.22		12.303	12.174							28.6	33.44				
RCA-5D$_{fibers}$ 77.0MPa	Considered			19.88	19.736	2.686	65.05	65.045	65.05	46.64	112			137.23	81.39	0	0
	Not Considered	14.43		23.262	22.727							46.86	61.20				

Table 33(Shear and Deflection Comparison (Experimental and Analytical)-(Δ max))

Comparison of Ductility Index Results (Experimental and Analytical)						
Sample Type	Experimental (Before Strengthening & Without compression Rebars)	Compression Rebars	Ductility Index ($\Delta\ max/\Delta\ y$)		Differences and Changes %	
			Before Strengthening	After Strengthening	Before Strengthening (Difference)	Before Strengthening (Increase)
NWA-1 70.5MPa	1.79	Considered	7.71	7.08	124.63	330.7
		Not Considered	8.04	7.69	127.16	349.16
NWA-2 70.5MPa	---	Considered	7.94	7.02		
		Not Considered	8.30	7.93		
RCA 64.5MPa	1.30	Considered	6.34	5.85	131.93	387.7
		Not Considered	6.13	6.24	130.01	371.5
RCA-5D$_{fibers}$ 77.0MPa	2.91	Considered	7.26	7.30	85.54	149.5
		Not Considered	5.24	5.15	57.18	80.07

Table 34(Comparison of Ductility Index Results (Experimental and Analytical))

CHAPTER 7

7. DISCUSSION OF RESULTS

7.1 Introduction

This section discusses the outcomes presented in CHAPTER 6 of this research. The discussion focuses on the behaviour of the research finite element model of various types of pre-damaged beams with different characteristics (NWA, RCA, $RCA_{5d\ Fibers}$), before and after strengthening in terms of shear capacity forces and deflections under various types of loading, including four-point loading test simulation, compared to those of previous experiments done by (Mohamed Ghoneim, 2020, Abdalla Ghoneim, 2019) .

7.2 Results Related to Deflection

7.2.1 The Deflections Resulted from Nonlinear Static Loading ($\Delta\ y$)

The values behaviour of deflection has been examined in this section by applied the specified load for each sample using [Ansys workbench] and [Midas Gen] softwares and applied non-linear static analysis using (Menetrey-Willam Base with softening) as (Geo-Mechanical Properties). The results have been displayed related to strengthening with CFRP laminates and compression rebars. The results illustrated, that samples deflection values without strengthening and compression rebars decreased by 53.16% ,71.64%, 10.56% and differed by 72.40% ,111.6%, 11.15% for NWA-1, RCA, $RCA_{5D\ Fibers}$ samples respectively when used [ANSYS workbench] software. On the other side, the deflection values decreased by 60.70%,74.42%, 45.85% and differed by 87.15%, 118.52, 59.48% when used [Midas Gen] software compared to experimental results as shown in Table 32 & Figure 103 . On the contrary, when compression rebars are considered in the analysis model, we notice that deflection values have been decreased, because compression rebars from analysis process shown an effectiveness resisting and decreasing the deflection values as shown in Table 32 . In addition, when CFRP laminates employed in the analysis model as strengthening techniques, it also decreases the deflection values with small changes, as cleared in Table 32. On the other hand, near values of deflection have been resulted between [ANSYS Workbench] and [Midas gen] softwares, when compression rebars are considered and before-after strengthening.

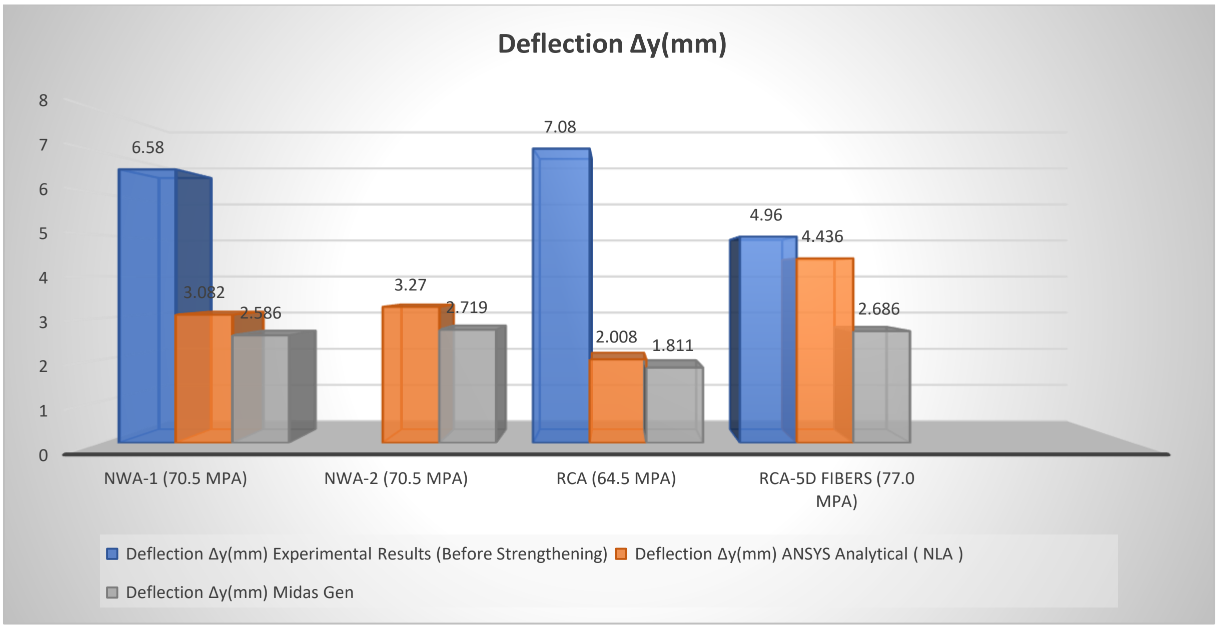

Figure 103(Deflection Comparison (Experimental and Analytical)- (Δ y) graph)

7.2.2 The Deflections Resulted from Explicit Dynamic Loading ($\Delta\ max$)

The behaviour of deflection has been examined in this section by applied the specified equivalent pressure load for each sample using [Ansys workbench] software and applied explicit dynamic analysis using (RHT Concrete Strength Properties-Brittle/Granular) with three types of failures technique which are (Plastic Strain Failure, Tensile Pressure Failure and Crack Softening Failure) properties as (Geo-Mechanical Properties). The results have been displayed related to strengthening with CFRP laminates and compression rebars. The results illustrated, that samples deflection values without strengthening and compression rebars increased by 110.15% ,33.44%, 61.20% and differed by 71.0%, 28.6%, 46.86 % for NWA-1, RCA, RCA $_{5D}$

Fibers samples respectively when used [ANSYS workbench] software. On the other hand, the deflection values decreased by 78.06%, 80.36%, 81.39% and differed by 128.05%, 134.33%, 137.23 when used [Midas Gen] software compared to experimental results as shown in

Table 33, Figure 104 .On the other hand, deflection values with strengthening and without compression rebars increased by 72.13% and differed by 53.01% for NWA-2 sample when used [ANSYS workbench] software; while, the deflection values decreased by 81.80% and differed by 138.38% when used [Midas Gen] software compared to experimental results as shown in Table 33 .

On the other side, when compression rebars are considered in the analysis model, we notice that deflection values have been decreased, because compression rebars from analysis process shown an effectiveness resisting and decreasing the deflection values as shown in Table 33. In addition, when CFRP laminates employed in the analysis model as strengthening techniques, it also decreases the deflection values with small changes, as cleared in Table 33.

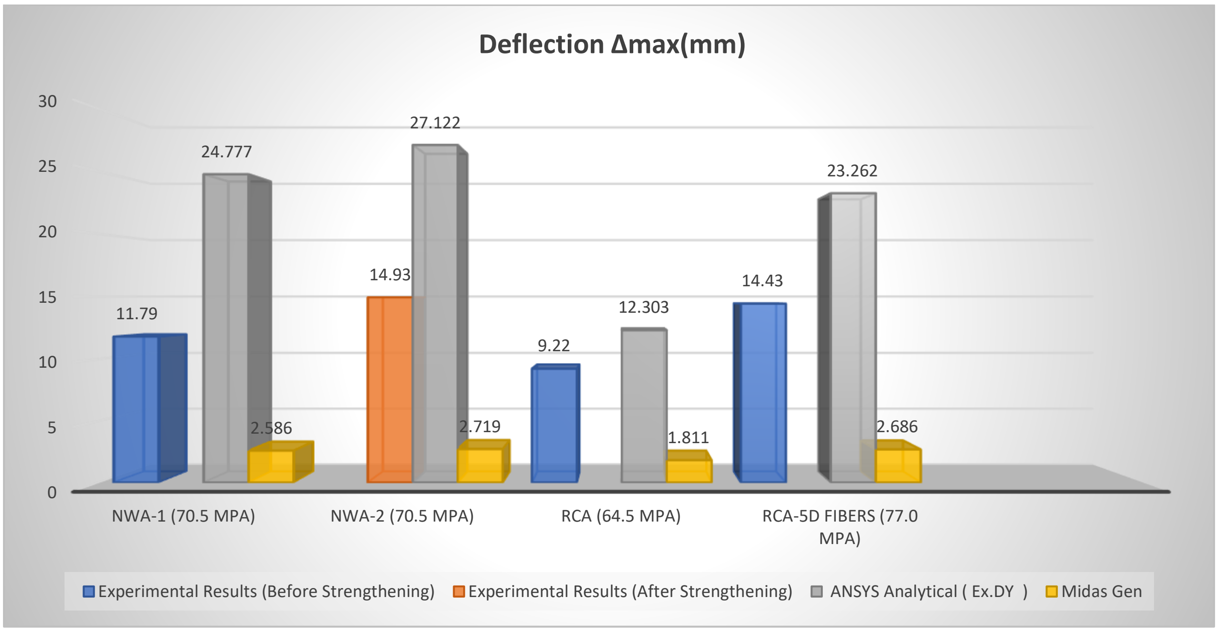

Figure 104(Deflection Comparison (Experimental and Analytical)- (Δ max) graph)

7.3 Results Related to Shear

7.3.1 Shear Loads resulted from Nonlinear Static and Explicit Dynamic Analysis (ANSYS Workbench)

The shear values from both analysis types non-linear static loading and explicit dynamic in terms of CFRP strengthening (with or without) and compression rebars, resulted as follow 60.05KN, 63.13KN, 40.85KN, 65.05 KN for NWA-1, NWA-2, RCA, RCA $_{5D\ Fibers}$ samples respectively when used [ANSYS workbench] software. On the hand, the shear values from both analysis types illustrated identical values with the experimental results as shown in Table 32 & Table 33.

7.3.3 Shear Capacity Resulted From (Midas Gen & Midas Design Plus) with Linear Analysis

The shear values from linear analysis, resulted as follow 60.05KN, 63.13KN, 40.85KN, 65.05 KN for NWA-1, NWA-2, RCA, RCA $_{5D\ Fibers}$ samples respectively when used [Midas Gen] software, so the shear values illustrated identical values with the experimental results as shown in Table 32 & Table 33. On the other side, shear rebars are not used in this analysis, so the shear capacity has failed as shown in section 6.2.2.2 Stage 2 - ACI440.2R-17 Code Check Using (Midas Design Plus 2021)The used of [Midas design plus] software, shear capacity values varied before CFRP laminates as strengthening used with section capacity values of 46.64 KN for NWA-1, NWA-2, RCA $_{5D\ Fibers}$ & 45.90KN for RCA, on the contrary, when used CFRP laminates as strengthening, the section capacity values will increased by 140% for NWA-1, NWA-2, RCA $_{5D\ Fibers}$ & 135% for RCA so, the values will be 112 KN for NWA-1, NWA-2, RCA $_{5D\ Fibers}$ & 108KN for RCA as shown in Table 30, which fulfilled the required shear values see. Figure 105. In addition, the CFRP contribution values has been resulted by 65.36 KN for NWA-1, NWA-2, RCA $_{5D\ Fibers}$ & 62.1 KN for RCA, which illustrate the importance of using CFRP if shear reinforcement no exists.

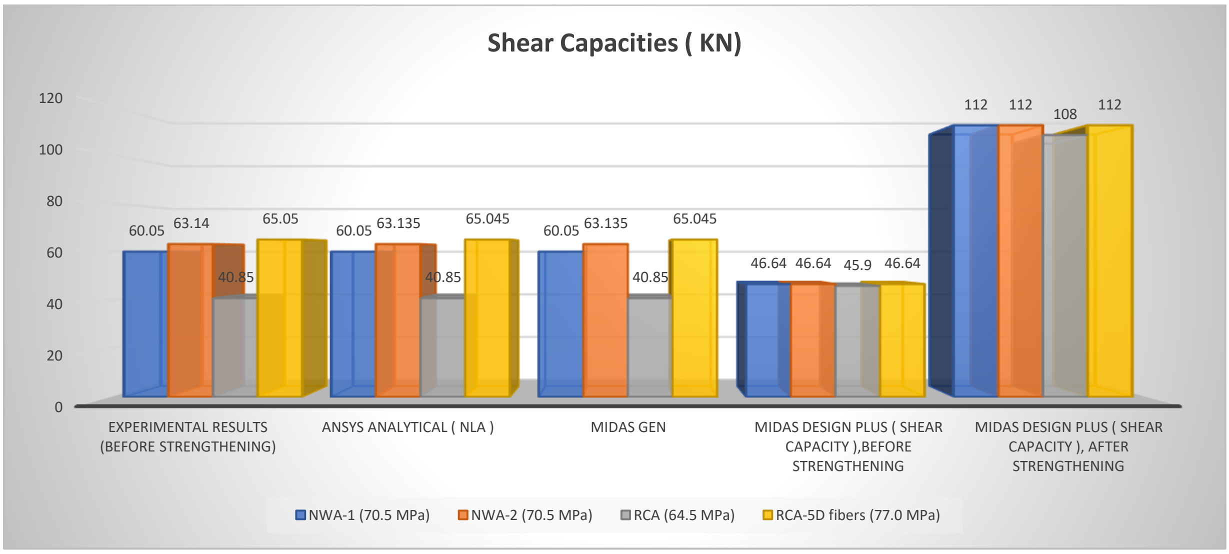

Figure 105(Shear Capacities (KN) Comparison (Experimental and Analytical))

7.4 Results Related to Ductility Index

The non-linear static loading and explicit dynamic analysis has conducted a results of yielding load ($\Delta\ y$) and ultimate load (Δ max) deflections respectively. Therefore, the ratio between two types of deflection based on two types of analysis has been defined as [the ductility index], ($\Delta\max/\Delta\ y$). As per analytical solution with [ANSYS Workbench] considered no strengthening and compression rebars, the ductility index increased by 349.16 %, 371.5%, 80.07% and differed by 127.16%, 130.01%, 57.18% for NWA-1, RCA, $RCA_{5DFibers}$ samples compared to experimental results as shown in Table 34 .

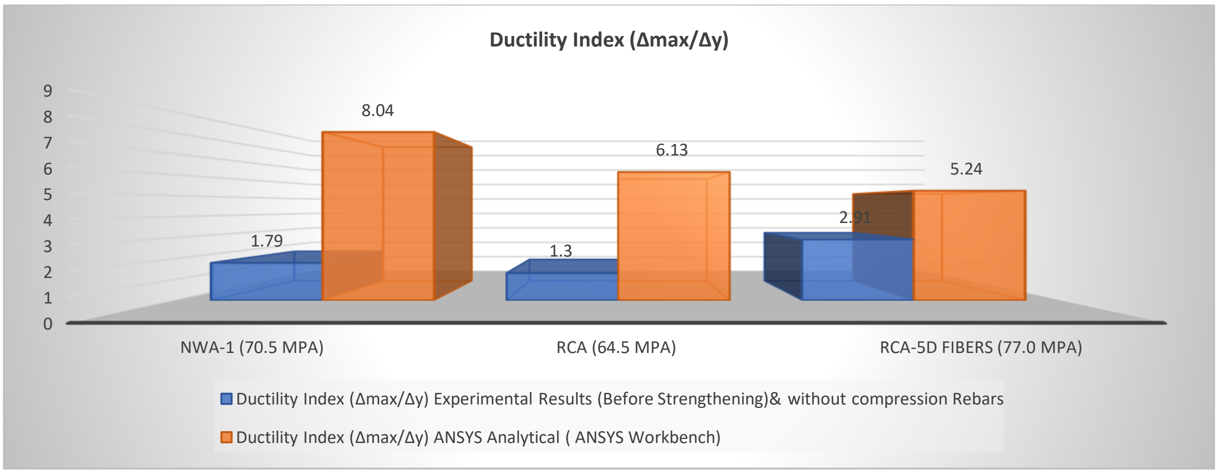

*Figure 106(*Ductility Index (Δmax/Δy) *Comparison (Experimental and Analytical)*

CHAPTER 8

8. CONCLUSIONS AND RECOMMENDATION

8.1 Conclusions

The research presents a numerical evaluations using [ANSYS workbench, Midas Gen and Midas Design Plus] software of pre-damaged recycled concrete beam with self-consolidating concrete matrix for un-strengthened and strengthened in shear samples using CFRP-U wrapping laminates including normal weight aggregate sample as control specimen. All samples have been compared to experimental results conducted by(Mohamed Ghoneim, 2020, Abdalla Ghoneim, 2019) as clarified in section 6.3 Results Summarization, the conclusions can be summarised as follows:

1- The analytical models using [ANSYS Workbench] and [Midas gen] software with different types of analysis (Linear, Non-linear and Explicit Dynamic) has proved good matching with experimental results of samples in terms of shear capacity values as discussed in section 7.3.1 Shear Loads resulted from Nonlinear Static and Explicit Dynamic Analysis (ANSYS Workbench).

The [Midas Design Plus] has been used to calculating shear capacities before and after CFRP strengthening as per (ACI-440, 2017) recommendations and the results shown variety in shear capacities after and before strengthening as per section 7.3.3 Shear Capacity Resulted From (Midas Gen & Midas Design Plus) with Linear Analysis. The experimental results have recorded shear load values from 40.85 to 65.05 KN of samples due to different applied loads see. Table 7 , therefore when CFRP used the shear capacity increased by 135% to 140 % to let the section to carry shear loads until 108 to 112 KN which proves the effectiveness of strengthening technique system to shear loads see. Table 30 .

2-The non-linear static loading analysis by [ANSYS Workbench] for deflections, have experienced decrease values by 53.16% ,71.64%, 10.56% , while the explicit dynamic loading analysis by [ANSYS Workbench] has recorded an increase values by 110.15% ,33.44%, 61.20% for NWA-1, RCA, RCA $_{5D\ Fibers}$ samples respectively,

3- Compression rebars have influenced deflection when used, which reduce the deflection values. The non-linear static loading and explicit dynamic loading analysis when employed by [ANSYS Workbench] for NWA-1, RCA, RCA $_{5D\ Fibers}$ samples with compression rebars and simulated as finite element models, the outcomes show that models deflections with compression rebars are less than models without compression rebars see.Table 29. On the other hand, CFRP strengthening laminates have has a slight effect that hardly effects on deflection values when applied (Non-linear Static Loading Analysis & Explicit Dynamic Loading Analysis), by [ANSYS Workbench] see.Table 29.

4- The ratio between two types of deflections (Ductility Index) based numerical analysis (Non-linear Static Loading & Explicit Dynamic Loading) by [ANSYS Workbench] has experienced significantly rise values by 349.16 %, 371.5%, 80.07% for NWA-1, RCA, RCA$_{5DFibers}$ samples compared to experimental results as shown in Table 34 .

5- The failure modes simulated by [ANSYS workbench] under explicit dynamic analysis, has predicted failure modes for different types of samples under different types of loadings see Appendix A.

8.2 Recommendation

According to the results of the analytical evaluation, there are significant discrepancies in the deflection values between the numerical analysis and the experimental results. As a result, I would suggest conducting additional and extensive numerical analysis in order to investigate the differences in the deflection values. In addition, I would suggest using a variety of software programs that utilized the finite element method (FEM) or the distinct element method (DEM) in conjunction with a variety of strengthening techniques in order to predict the shear behaviour and capacity, failure modes and locations, and deflections.

9. REFERENCES

A. MOFIDI, O. C., B. BENMOKRANE, K. NEALE 2012. Performance of end-anchorage systems for RC beams strengthened in shear with epoxy-bonded FRP. *Composite Construction ASCE,* 16**,** 322-331.

A. S. GEORGIADIS, K. K. S., AND N. S. ANAGNOSTOPOULOS 2010. Properties of scc produced with limestone filler or viscosity modifying admixture. *Materials in Civil Engineering,* 22**,** 352-360.

A.G.RAZAQPUR, M. L., F.ASCIONE 2020. Debonding evolution in nonlinear FRP-retrofitted RC beams with cohesive interface. *Composite Structures,* 236**,** 111-858.

ABDALLA GHONEIM, M. G., SHERIF YEHIA AND RAMI HAWILEH 2019. Shear Capacity of Precracked Beams Externally Bonded With FRP Sheets.

ABERA, S. A. 2022. Analytical study on properties of concrete materials incorporating recycled aggregates from construction and demolition waste. *Materials Today: Proceedings,* 52**,** 2172-2183.

ACI-318, A. C. 2019. ACI 318-19M-Building Code Requirements for Structural Concrete *One-way shear strength.*

ACI-440, A. C. 2017. ACI 440.2R.17 -Structures, Guide for the Design and Construction of Externally Bonded FRP Systems for Strengthening Concrete *Shear Strengthening*

ACI Committee 44.

ACI-AC, A. C. I.-. 2007. Aggregates for concrete. *Recycled Aggregate.*

ADEL YOUNIS, U. E., KSHITIJ C.SHRESTHA 2017. Different FRCM systems for shear-strengthening of reinforced concrete beams. *Construction and Building Materials,* 153**,** 514-526.

ANNA M. GRABIEC , O., DANIEL ZAWAL AND WAHEED ADEWALE RASAQ 2020. The Effect of Curing Conditions on Selected Properties of Recycled Aggregate Concrete. *Institute of Construction and Geoengineering,Appl. Sci.* , 10.

AOHAN ZHENG, S., DENGFENG ZHANG, YUHONG YAN 2021. Shear strengthening of RC beams with corrosion-damaged stirrups using FRP grid-reinforced ECC matrix composites. *Composite Structures,* 272**,** 114-229.

ASHRAF A.BAHRAQ, J., MOHAMMEDSHAMEEM, MOHAMMEDMASLEHUDDIN 2022. A review on treatment techniques to improve the durability of recycled aggregate concrete: Enhancement mechanisms, performance and cost analysis. *Building Engineering,* 55**,** 104-713.

ASHRAF M. WAGIH, H. Z. E.-K., MAGDA EBID, SAMIR H. OKBA 2019. Recycled construction and demolition concrete waste as aggregate for structural concrete. *HBRC,* 9**,** 193-200.

ASIFUZ ZAMAN, S. A. G., MAHMOUD A WAFA 2013. A review on FRP composites applications and durability concerns in the construction sector. *Reinforced Plastics and Composites,* 32.

ATSUSHI SUMIDA, H. M. 2008. Mechanical Properties of Newly Developed Heat-Resistant FRP Bars. *Advanced Concrete Technology,* 61**,** 157-170.

AYESHA SIDDIKA, M. A. A., WAHID FERDOUS, RAYED ALYOUSEFD 2020. Performances, challenges and opportunities in strengthening reinforced concrete structures by using FRPs – A state-of-the-art review. *ELSEVIER,* 111**,** 104-480.

AZZAM AHMED, S. G., ZUHUAZHANG, DEJUZHU 2020. A review on durability of fiber reinforced polymer (FRP) bars reinforced seawater sea sand concrete. *Construction and Building Materials,* 256**,** 119-484.

B.ABDOLLAHI, M. B., Z.MIRZAEE, M.SHEKARCHI, M.MOTAVALLI 2012. SIFCON strengthening of concrete cylinders in comparison with conventional GFRP confinement method. *Construction and Building Materials,* 36**,** 765-778.

BAGHI, H. 2015. *The effectiveness of SHCC-FRP panels of the shear resistance of RC beams.* Ph.D, University of Minho.

BAKRI, A. M. M. A. 2011. Effects of HDPE C&D waste aggregate on the properties of concrete. *Asian Sci. Res,* 17**,** 340-345.

BANIBAYAT, P. 2011. Experimental Investigation of the Mechanical and Creep Rupture Properties of Basalt Fiber Reinforced Polymer (BFRP) Bars. *2011,* Doctor of Philosophy, University of Akron.

BOUSSELHAM A, C. O. 2008. Mechanisms of shear resistance of concrete beams strengthened in shear with externally bonded FRP. *Journal of Composites for Construction(ASCE),* 12**,** 499-512.

BRAHIM BENMOKRANE, A. H. A., HAMDY M. MOHAMED, ADEL ELSAFTY, ALLAN MANALO 2017. Laboratory assessment and durability performance of vinyl-ester,polyester, and epoxy glass-FRP bars for concrete structures. *Composites Part B: Engineering,* 114**,** 163-174.

C. S. POON, S. C. K. 2007. Influence of recycled aggregate on slump and bleeding of fresh concrete. *Materials and Structures volume,* 40**,** 981-988.

C.A. ISSA, P. D. 2007. Experimental study of epoxy repairing of cracks in concrete. *Construction and Building Materials,* 2007**,** 157-163.

C.FAELLA, E. M., E.NIGRO 2008. Formulation and validation of a theoretical model for intermediate debonding in FRP-strengthened RC beams. *Composites Part B: Engineering,* 39**,** 645-655.

CAO, S. Y., CHEN, J. F., TENG, J. G. & HAO, Z. 2005. Debonding in RC Beams Shear Strengthened with Complete FRP Wraps.

CHAALLAL O, M. A., BENMOKRANE B, NEALE K. 2011. Embedded through-section FRP rod method for shear strengthening of RC beams: Performance and comparison with existing techniques. *Journal of Composites for Construction(ASCE),* 15**,** 374-83.

CHENG CHEN, X. W., LIJUAN CHENG 2019. Modelling NSM FRP strengthened RC beams under fatigue due to IC-debonding. *International Journal of Fatigue,* 126**,** 174-187.

CLAYTON A. BURNINGHAM, C. P. P., LAWRENCE D. REAVELEY 2015. Repair of reinforced concrete deep beams using post-tensioned CFRP Rods. *Composite Structures.* ELSEVIER.

CONSTRUCTION, H. *Application of CFRP in strengthening RC Beams* [Online]. Available: https://www.horseen.com/solution/application-cfrp-strengthening-rc-beams?page=67 [Accessed].

DARBY, A. P., IBELL, T. J. , VALERIO, P 2009. Deep embedment of FRP for concrete shear strengthening. *Proceedings of the ICE - Structures and Buildings,* 162.

DRITSOS, K. G. V. A. S. E. 2008. Concrete jacket construction detail effectiveness when strengthening RC columns. *Construction and Building Materials,* 22**,** 264-276.

E. TZOURA, T. C. T. 2016. Shear strengthening of reinforced concrete T-beams under cyclic loading with TRM or FRP jackets. *Materials and Structures* 49**,** 17-28.

E. U. CHOWDHURY, R. E., L. A. BISBY, M. F. GREEN, N. BENICHOU 2009. Mechanical Characterization of Fibre Reinforced Polymers Materials at High Temperature. *Fire Technology,* 47**,** 1063-1080.

E. U. CHOWDHURY, R. E., L. A. BISBY, M. F. GREEN, N. BENICHOU 2011. Mechanical Characterization of Fibre Reinforced Polymers Materials at High Temperature. *Fire Technology,* 47**,** 1063-1080.

EUGENIJUS GUDONIS, E. T., VIKTOR GRIBNIAK, VIKTOR GRIBNIAK, ALEKSANDR K. ARNAUTOV, VYTAUTAS TAMULĖNAS 2014. FRP Reinforcement For Concrete Structures: State-Of-The-Art Review Of Application And Design. *Engineering Structures & Technologies,* 5**,** 147-158.

FATIHÖZALP, H. D., MUSTAFAKARA, ÖMERKAYA, AYLINŞAHIN 2016. Effects of recycled aggregates from construction and demolition wastes on mechanical and permeability properties of paving stone, kerb and concrete pipes. *Construction and Building Materials,* 110**,** 17-23.

FRIEDERIKE FLEISCHHAKER, A. P. H., ANDREA M. MISSKE, MATHIEU BLANCHOT, SYLKE HAREMZA, CHRISTOPHER BARNER-KOWOLLIK 2014. Glass-Transition-, Melting-, and Decomposition Temperatures of Tailored Polyacrylates and Polymethacrylates: General Trends and Structure–Property Relationships. *Macromol Chemistry and Physics,* 215**,** 1192-1200.

G C MAYS, A. C. H. 1992. *Adhesives in Civil Engineering.* Cambridge University Press.

G. E. THERMOU, S. J. P., AND A. S. ELNASHAI 2007. lexural behavior of brittle RC members rehabilitated with concrete jacketing. *Structural Engineering,* 133**,** 1373-1384.

G.L. VIEIRA, J. Z. S., P.M. BORGES, S.R. DA SILVA, J.J. DE OLIVEIRA ANDRADE 2020. Influence of recycled aggregate replacement and fly ash content in performance of pervious concrete mixtures. *Cleaner Production* 271.

GAO, D., ZHANG, L. & NOKKEN, M. 2017. Compressive Behavior of Steel Fiber Reinforced Recycled Coarse Aggregate Concrete Designed with Equivalent Cubic Compressive Strength. *Construction and Building Materials.* ELSEVIER.

GODAT, A., L'HADY, A., CHAALLAL 2012. Bond behavior of the ETS FRP bar shear-strengthening method. Journal of Composites for Construction. *Journal of Composites for Construction(ASCE),* 16**,** 529-539.

H. M. ELSANADEDY, H. A., Y. A. AL-SALLOUM, T. H. ALMUSALLAM 2014. Prediction of Intermediate Crack Debonding Strain of Externally Bonded FRP Laminates in RC Beams and One-Way Slabs. *Composite Construction ASCE,* 18**,** 1-16.

H.C. SHIN, H. M., K. TANAKA 2011. An experimental study of fatigue resistance in epoxy injection for cracked mortar and concrete considering the temperature effect. *Construction and Building Materials,* 25**,** 1316-1324.

HADI BAGHI , J. A. O. B., MOHAMMAD ALI REZAZADEH 2017. Shear strengthening of damaged reinforced concrete beams with Hybrid Composite Plates. *Composite Structures,* 178**,** 353-371.

HAITHAM AL AJMANI , F. S., ISMAIL ABUZAYED AND ADIL TAMIMI 2019. Evaluation of Concrete Strength Made with Recycled Aggregate. *Buildings,* 9.

HONG K, L. S., YEON Y, JUNG K. 2018. Flexural Response of Reinforced Concrete Beams Strengthened with Near-Surface-Mounted Fe-Based Shape-Memory Alloy Strips. *International Journal of Concrete Structures and Materials,* 45.

HONGJUN LIANG, S. L., YIYAN LU, 2018. Reliability Study on FRP Composites Exposed to Wet-Dry Cycles. *Applied Sciences,* 8**,** 892.

HUAN ZHANG, Y. W., DAWN E.LEHMAN, YUE GENG, KATHERINEKUDER 2020. Time-dependent drying shrinkage model for concrete with coarse and fine recycled aggregate. *Cement and Concrete Composites,* 105**,** 103-426.

IMAD SHAKIR ABBOOD, S. A. O., KAMALALDIN F. HASAN, MOHAMMED A. JASIM 2021. Properties evaluation of fiber reinforced polymers and their constituent materials used in structures – A review. *Materials Today: Proceedings,* 43**,** 1003-1008.

IZAT, M. 2004. *Fiber Reinforced Ploymer(FRP) in Construction, Types and Uses* [Online]. Available: https://theconstructor.org/concrete/fibre-reinforced-polymer/1583/ [Accessed].

J.F. CHEN , S. Q. L., L.A. BISBY, J. AI. 2011. FRP Rupture Strains in The Split-Disk Test. *Composites:Part B* [Online].

JEONGHYUN KIM, N. K., SUNGCHUL YANG 2015. The Effect of the Residual Mortar of Recycled Concrete Aggregate on Alkali Silica Reaction. *International Journal of Highway Engineering,* 17.

JIA-XIANG LIN, P.-Y. H., YONG-CHANG GUO, XIN-YAN GUO, JUN-JIE ZENG, CHEN ZHAO, ZHAN-BIAO CHEN 2020. Fatigue behaviour of RC beams strengthened with CFRP laminate under hot-wet environments and vehicle random loads coupling. *International Journal of Fatigue,* 131**,** 105-329.

JUN WANG, H. G. R., RUIFENG LIANG, WEIQING LIU 2015. Durability and prediction models of fiber-reinforced polymer composites under various environmental conditions: A critical review. *REinforced Plastics and Composites,* 33**,** 1-33.

JUN ZHAO , G. C., LU CUI ,AMIR SI LARBI , KONSTANTINOS DANIEL 2017. Deterioration of Basic Properties of the Materials in FRP-Strengthening RC Structures under Ultraviolet Exposure. *Polymers***,** 402.

KADER LAOUBI, E. E.-S., BRAHIM BENMOKRANE 2006. Creep and durability of sand-coated glass FRP bars in concrete elements under freeze/thaw cycling and sustained loads. *Cement and Concrete Composites,* 28**,** 869-878.

KAM YOKE M. LOO, S. J. F. A. S. T. S. 2012. FE Modelling of CFRP-Repaired RC Beams Subjected to Fatigue Loading. *Composites for Construction(ASCE),* 16**,** 80-572.

KIM, J. 2021. Construction and demolition waste management in Korea: recycled aggregate and its application. *Clean Technologies and Environmental Policy,* 23**,** 2223-2234.

LEONIDAS ALEXANDROS S.KOURIS, T. C. T. 2018. State-of-the-art on strengthening of masonry structures with textile reinforced mortar (TRM). *Construction and Building Materials,* 188**,** 1221-1233.

LI YAO, Y.-P., CHENWEN-JIE 2019. Seismic behaviour of corrosion-damaged RC columns strengthened with TRC under a chloride environment. *Construction and Building Materials,* 201**,** 736-745.

LIANHENG CAI , Q. L., RUI GUO 2021. Study on the shear behaviour of RC beams strengthened by CFRP grid with epoxy mortar. *Composite Structures.* ELSEVIER.

LINDUNG ZALBUIN MASEA, SUCHED LIKITLERSUANG,TETSUO TOBITA, SUSIT CHAIPRAKAIKEOW, SUTTISAK SORALUMP 2020. Local Site Investigation of Liquefied Soils Caused by Earthquake in Northern Thailand. *Earthquake Engineering,* 24**,** 1181-1204.

LIYING GUO, M. D., HUI CHEN, RUIZHE LI, XIANGKUN MA, YANGXI ZHANG 2022. Experimental study on pre-damaged RC beams shear-strengthened with textile-reinforced mortar (TRM). *Engineering Structures,* 256**,** 113-956.

M. EKENEL, J. J. M. 2007. Durability performance of RC beams strengthened with epoxy injection and CFRP fabrics. *Construction and Building Materials,* 21**,** 1182-1190.

M. S. ABDEL-JABER, P. R. W. A. R. H. 2003. Shear strengthening of reinforced concrete beams using different configurations of externally bonded carbon fibre reinforced plates. *Materials and Structures.* Springer.
M.ETXEBERRIA, E. V., A.MARÍ M.BARRA 2007. Influence of amount of recycled coarse aggregates and production process on properties of recycled aggregate concrete. *Cement and Concrete Research,* 37**,** 735-742.
M.L.BENNEGADI, K. H., Z.SEREIR, S.AMZIANE, B.EL MAHI 2016. General cohesive zone model for prediction of interfacial stresses induced by intermediate flexural crack of FRP-plated RC beams. *Engineering Structures,* 126**,** 147-157.
MAHESHWARAN BHANUGOBAN, H. D. Y., SAMIR DIRAR 2021. Efficient shear retrofitting of reinforced concrete beams using prestressed deep embedded bars. *Engineering Structures,* 246.
MANJOLA CARO, S. D., ANDREW QUINN 2021. Shear strengthening of existing reinforced concrete beams with embedded bars–an overview. *Structures and Buildings (ICE)***,** 1-14.
MARWA SAADAH, A. A., YASMIN MURAD 2021. Shear strengthening of RC beams using side near surface mounted CFRP ropes and strips. *Structures.* ELSEVIER.
MATHEUS PIMENTEL TINOCO , F. A. D. A. S. 2021. Repair of pre-damaged RC beams using hybrid fiber reinforced strain hardening cementitious composites. *Engineering Structures*, 235.
MD ASHRAFUL ALAM, A. S. A., KAMAL NASHARUDDIN MUSTAPHA 2016. An Experimental Study on the Debonding of Steel and CFRP Strips Externally Bonded to Concrete in the Presence of Embedded Shear Connectors. *Kamal Nasharuddin Mustapha* 41**,** 4171-4186.
MD ASHRAFUL ALAM, S. A. O., KAMAL NASHARUDDIN BIN MUSTAPHA 2020. Crack based bond strength model of externally bonded steel plate and CFRP laminate to predict debonding failure of shear strengthened RC beams. *Journal of Building Engineering,* 27**,** 100-943.
MEDDAH, M. S. B., M. 2009. Properties of Concrete Reinforced with Different Kinds of Industrial Waste Fibre Materials. *Construction and Building Materials.* ELSEVIER.
MIAO LU, Q. S. 2007. The Bend Stiffness of Crane beam Strengthened with CFRP under Monotonic and Fatigue Load Condition. *International Journal of Nonlinear Science,* 4**,** 44-51.
MILAD BAZLI, M. A. 2020a. Mechanical Properties of Fibre Reinforced Polymers under Elevated Temperatures: An Overview. *Polymers,* 12**,** 1-31.
MILAD BAZLI, X. Z., ARMIN JAFARI, HAMED ASHRAFI, Y. BAI, R.K. SINGH RAMAN, HAMED KHEZRZADEH 2020b. Mechanical properties of pultruded GFRP profiles under seawater sea sand concrete environment coupled with UV radiation and moisture. *Construction and Building Materials,* 258**,** 120-369.
MOHAMED GHONEIM, A. Y., SHERIF YEHIA , AND WAEL ABUZAID 2020. Shear Strength of Fiber Reinforced Recycled Aggregate Concrete.
MSAI KRISHNA, G. A. V. S. K., ACYRIL THOMAS 2021. Behaviour of reinforced concrete beams bonded with side bonded FRP sheets. *Materialstoday: Proceedings,* 43**,** 2104-2410.
MUKHTAR FM, F. R. 2018. A review of test methods for studying the FRP-concrete interfacial bond behavior. *Construction and Building Materials.*
MULUKEN YEHEYIS, K. H., M. SHAHRIA ALAM, CIGDEM ESKICIOGLU & REHAN SADIQ 2013. An overview of construction and demolition waste management in

Canada: a lifecycle analysis approach to sustainability. *Clean Technologies and Environmental Policy,* 15**,** 81-91.

NAWAL K. BANJARA, K. R. 2017. Experimental and numerical investigations on the performance evaluation of shear deficient and GFRP strengthened reinforced concrete beams. *Construction and Building Materials.* ELSEVIER.

NAWAL KISHORBANJARA, K. R. 2019. Investigations on behaviour of flexural deficient and CFRP strengthened reinforced concrete beams under static and fatigue loading. *Construction and Building Materials*, 201**,** 746-762.

NEVEN KRSTULOVIC, O., MOHAMMAD JAMAL AL-SHANNAG 1999. Slurry Infiltrated Mat Concrete (SIMCON)-Based Shear Retrofit of Reinforced Concrete Members. *ACI Structural Journal*, 96**,** 105-114.

OBAIDAT YT, A. A., OBAIDAT AT, ALFARIS SF 2020. A new technique for repairing reinforced concrete columns. *Journal of Building Engineering*.

P. VALERIO, T. J. I., A. P. DARBY 2003. Shear strengthening of existing concrete bridges. *Proceedings of the Institution of Civil Engineers - Structures and Buildings,* 156**,** 75-84.

P. VALERIO, T. J. I., A. P. DARBY 2009. Deep embedment of FRP for concrete shear strengthening. *Proceedings of the Institution of Civil Engineers - Structures and Buildings,* 162.

P.SARAVANAKUMAR, K. A., B.MANOJ 2016. Properties of treated recycled aggregates and its influence on concrete strength characteristics. *Construction and Building Materials,* 111**,** 611-617.

PAPAKONSTANTINOU CG, B. N., PETROU MF 2002. Analysis of reinforced concrete beams strengthened with composites subjected to fatigue loading. *ACI special publication SP206,* 3**,** 41-60.

PARK, T. W. 2012. Inspection of collapse cause of Sampoong Department Store. *Forensic Science International,* 217**,** 119-126.

PAWEŁ GRZEGORZ KOSSAKOWSKI, W. W. S. 2022. Fiber-Reinforced Polymer Composites in the Construction of Bridges: Opportunities, Problems and Challenges. *Fibers,* 10.

PIYA CHOTICKAI, P. T., SATJA JANTHARAKSA 2021. Performance of corroded rectangular RC columns strengthened with CFRP composite under eccentric loading. *Construction and Building Materials.* ELSEVIER.

POURZITIDIS, C. E. C. A. C. N. 2012. Rehabilitation of Shear-Damaged Reinforced Concrete Beams Using Self-Compacting Concrete Jacketing. *International Scholarly Research Network***,** 12.

R. SONNENSCHEIN, J. B., K. GAJDOSOVA 2016. Crack Width Control in Concrete Structures with FRP Reinforcement. *Presented at Engineering Mechanics.* Svratka, Czech Republic.

R.A.BARNES, P. S. B., G.C.MAYS, N.K.SUBEDI 2001. External steel plate systems for the shear strengthening of reinforced concrete beams. *Engineering Structures,* 23**,** 1162-1176.

R.V.SILVA, J. D. B., R.K.DHIR 2015. Comparative analysis of existing prediction models on the creep behaviour of recycled aggregate concrete. *Engineering Structures,* 100**,** 31-42.

RAICIC V, I. T., DARBY A, EVERNDEN M 2017. Effectiveness of the Deep Embedment (DE) Technique for Shear Strengthening of Reinforced Concrete Continuous T-beams.

ACIC 2017-Proceedings of the 8th Biennial Conference on Advanced Composites in Construction.
RAJAI Z. AL-ROUSAN, M. J. S. 2018. Shear Repairing and Strengthening of Reinforced Concrete Beams Using SIFCON. *Structures,* 14**,** 389-399.
RAMI J.A.HAMAD, M. A. M. J., RAMI H.HADDAD 2017. Mechanical properties and bond characteristics of different fiber reinforced polymer rebars at elevated temperatures. *Construction and Building Materials,* 142**,** 521-535.
RAWAN AL-SHAMAYLEH, H. A.-S., MU'TASIM ABDEL-JABER, MAHA ALQAM 2022. Shear and flexural strengthening of reinforced concrete beams with variable compressive strength values using externally bonded carbon fiber plates. *Results in Engineering,* 14**,** 100-427.
RICARDO P., R. P. 2010. A unified approach for the static and dynamic analyses of intermediate debonding in FRP-strengthened reinforced concrete beams. *Composite Structures,* 92**,** 2728-2737.
RICHARD ANDREW BARNES, G. C. M. 2006a. Strengthening of reinforced concrete beams in shear by the use of externally bonded steel plates: Part 1 – Experimental programme. *Construction and Building Materials,* 20**,** 396-402.
RICHARD ANDREW BARNES, G. C. M. 2006b. Strengthening of reinforced concrete beams in shear by the use of externally bonded steel plates: Part 1 – Experimental programme. *Construction and Building Materials,* 20**,** 396-402.
RICHARD ANDREW BARNES, G. C. M. 2006c. Strengthening of reinforced concrete beams in shear by the use of externally bonded steel plates: Part 2 – Design guidelines. *Construction and Building Materials,* 20**,** 403-411.
RONGWEI LIN, P. H., CHEN ZHAO, XINYAN GUO, XIAOHONG ZHENG 2008. Prediction of fatigue lives of RC beams strengthened with CFL under random loading. *Acta Mechanica Solida Sinica,* 21**,** 359-363.
RUI GUO, L. C., SHINICHI HINO, BO WANG 2019. Experimental Study on Shear Strengthening of RC Beams with an FRP Grid-PCM Reinforcement Layer. *Applied Sciences,* 9(15)**,** 26-118.
SALEH ALSAYED, Y. A.-S., TAREK ALMUSALLAM, TAREK ALMUSALLAM 2012. Performance of glass fiber reinforced polymer bars under elevated temperatures. *Composites Part B Engineering,* 43**,** 2265-2271.
SALLAL R. ABID, K. A.-L. 2018. Critical review of strength and durability of concrete beams externally bonded with FRP. *CIVIL & ENVIRONMENTAL ENGINEERING,* 5.
SARDASHT S WELI, I. S. A., KAMALALDIN F HASAN, MOHAMMED A JASIM 2020. Effect of Steel Fibers on the Concrete Strength Grade: A Review. *IOP Conference Series: Materials Science and Engineering.*
SHENGHU CAO, Z. W., XIN WANG 2009. Tensile properties of CFRP and hybrid FRP composites at elevated temperatures. *Composite Materials,* 43**,** 315-330.
SHERIF EL-TAWIL, C. O., AYMAN M OKEIL, MOHSEN SHAHAWY 2001. Static and Fatigue Analyses of RC Beams Strengthened with CFRP Laminates. *Composites for Construction(ASCE),* 5**,** 67-258.
SIKA. *Structural Strengthening* [Online]. Available: https://www.sika.com/en/construction/structural-strengthening.html [Accessed].
SILVA, R. V. D. B., J.DHIR, R.K. 2018. Fresh-state Performance of Recycled Aggregate Concrete. *Construction and Building Materials.*
SINAN ALTIN, Ö. A., M. EMIN KARA 2005. Improving shear capacity of existing RC beams using external bonding of steel plates. *Engineering Structures,* 27**,** 781-791.

SOFFIAN NOOR MAT SALIAH , N. M. N., NOORHAZLINDA ABD RAHMAN 2021. Evaluation of severely damaged reinforced concrete beam repaired with epoxy injection using acoustic emission technique. *Theoretical and Applied Fracture Mechanics.* ELSEVIER.

TENG, J. G. 2009. Behavior of RC Beams Shear Strengthened with Bonded or Unbonded FRP Wraps. *Composites for Construction-ASCE,* 13**,** 12.

TIDARUT JIRAWATTANASOMKUL, S. L., NATTAMET WUTTIWANNASAK, TAMONUEDA, DAWEI ZHANG, DAWEIZHANG 2020. Structural behaviour of pre-damaged reinforced concrete beams strengthened with natural fibre reinforced polymer composites. 244**,** 112-309.

TRIANTAFILLOU 1998. Shear strengthening of reinforced concrete beams using epoxybonded FRP composites. *ACI Structures***,** 15-107.

TSONOS, A. D. G. 2010. Performance enhancement of R/C building columns and beam-column joints through shotcrete jacketing. *Engineering Structures,* 32**,** 726-740.

V. MECHTCHERINE, O. M., M. BUTLER & K. THOMA 2012. Mechanical Behavior of SHCC under Impact Loading. *High Performance Fiber Reinforced Cement Composites 6.* Springer.

VIET QUOC DANG, Y. O., PHUONG TRINH BUI, KENJIKAWAI 2021. Effects of chloride ions on the durability and mechanical properties of sea sand concrete incorporating supplementary cementitious materials under an accelerated carbonation condition. *Construction and Building Materials,* 274**,** 122.

WANG WW, Z. Y. 2015. Experimental research on shear capacity of concrete beams strengthened with BFRP Grid reinforced ECC Proceedings of the 9th national FRP applied academic exchange conference on construction projects. *Chongqing.* China.

WANG YC, W. P., KODUR 2007. An experimental study of the mechanical properties of fibre reinforced polymer (FRP) and steel reinforcing bars at elevated temperatures. *Composite Structures,* 80**,** 131-140.

WASSIMBEN CHAABENE, M. L. N. 2021. Genetic programming based symbolic regression for shear capacity prediction of SFRC beams. *Construction and Building Materials,* 280**,** 122-523.

XIAODAN TENG, Y. X. Z. 2015. Nonlinear Finite Element Analyses of FRP-Strengthened Concrete Slabs under Fixed-Point Cyclic Loading. *Composites for Construction(ASCE),* 19**,** 0401-4057.

XIAOLONG HU, J. X., KAIJIAN ZHANG, QINGTIAN ZHANG 2022. The state-of-the-art study on durability of FRP reinforced concrete with seawater and sea sand. *Journal of Building Engineering,* 51**,** 104-294.

XINYAN GUO, Y. W., PEIYAN HUANG, SHENYUNHAO SHU 2021. Fatigue behaviour of RC beams strengthened with FRP considering the influence of FRP-concrete interface. *International Journal of Fatigue,* 143.

XINYAN GUO, Y. W., PEIYAN HUANG, ZHANBIAO CHEN 2019. Finite element modelling for fatigue life prediction of RC beam strengthened with prestressed CFRP based on failure modes. *Composite Structures,* 226**,** 111-289.

XUYANG, X., JIAN-GUODAI, ZHOU-DAOLU 2020. Shear strengthening of RC beams with FRP grid-reinforced ECC matrix. *Zhou-DaoLu,* 241**,** 112-120.

Y.C.WANG, V. K. 2005. Variation of strength and stiffness of fibre reinforced polymer reinforcing bars with temperature. *Cement and Concrete Composites,* 27**,** 864-874.

Y.H.MUGAHED AMRAN, R., RAIZAL S.M.RASHID, HISHAMALABDULJABBAR, CHUNG-CHAN 2018. Properties and applications of FRP in strengthening RC structures: A review. *Structures,* 16**,** 208-238.

YANHUI LIU, A. D., SHICHUN ZHAO 2021. The effect of CFRP-shear strengthening on existing circular RC columns under impact loads. *Construction and Building Materials.* ELSEVIER.

YEHIA, S. A., A. MANSOUR, D. Crystals 2020. Effect of Aggregate Type and Specimen Configuration on Concrete.

YEONHO PARK, K. Y., SWOO-HEON LEE 2014. Long-term flexural behaviors of GFRP reinforced concrete beams exposed to accelerated aging exposure conditions. *Polymers,* 6**,** 1773-1793.

YOUSEF A. AL-SALLOUM, S. E.-G., TAREK H. ALMUSALLAM, SALEH H. ALSAYED,MOHAMMED AQEL 2013. Effect of harsh environmental conditions on the tensile properties of GFRP bars. *Composites Part B: Engineering,* 45**,** 835-844.

YU-ZHOU ZHENG , W.-W. W., JOHN C. BRIGHAM 2016. Flexural behaviour of reinforced concrete beams strengthened with a composite reinforcement layer: BFRP grid and ECC. *Construction and Building Materials.* ELSEVIER.

ZHIFANG DONG, M. D., YANGXI ZHANG, PINGMA, CONG ZHANG 2020. Out-of-plane strengthening of unreinforced masonry walls using textile reinforced mortar added short polyvinyl alcohol fibers. *Construction and Building Materials,* 260**,** 119-910.

ZHONGYU LU, L. S., GUIJUN XIAN, BAIHANG LU, JIANHE XIE 2020. Durability study of concrete-covered basalt fiber-reinforced polymer (BFRP) bars in marine environment. *Composite Structures*, 234**,** 111-650.

ZOI C.TETTA, L. N. K., DIONYSIOS A.BOURNAS 2015. Textile-reinforced mortar (TRM) versus fiber-reinforced polymers (FRP) in shear strengthening of concrete beams. *Composites Part B: Engineering,* 77**,** 338-348.

ZOI C.TETTA, L. N. K., DIONYSIOS A.BOURNAS 2016. Shear strengthening of full-scale RC T-beams using textile-reinforced mortar and textile-based anchors. *Composites Part B: Engineering,* 95**,** 225-239.

ZOI C.TETTA, L. N. K., DIONYSIOS A.BOURNAS 2018. Shear strengthening of concrete members with TRM jackets: Effect of shear span-to-depth ratio, material and amount of external reinforcement. *Composites Part B: Engineering,* 137**,** 184-201.

APPENDICES

List of Appendices Figures

Appendix A

1-Static Non-Linear Analysis - Without Strengthening and with Top Rebars

Geometry and loads

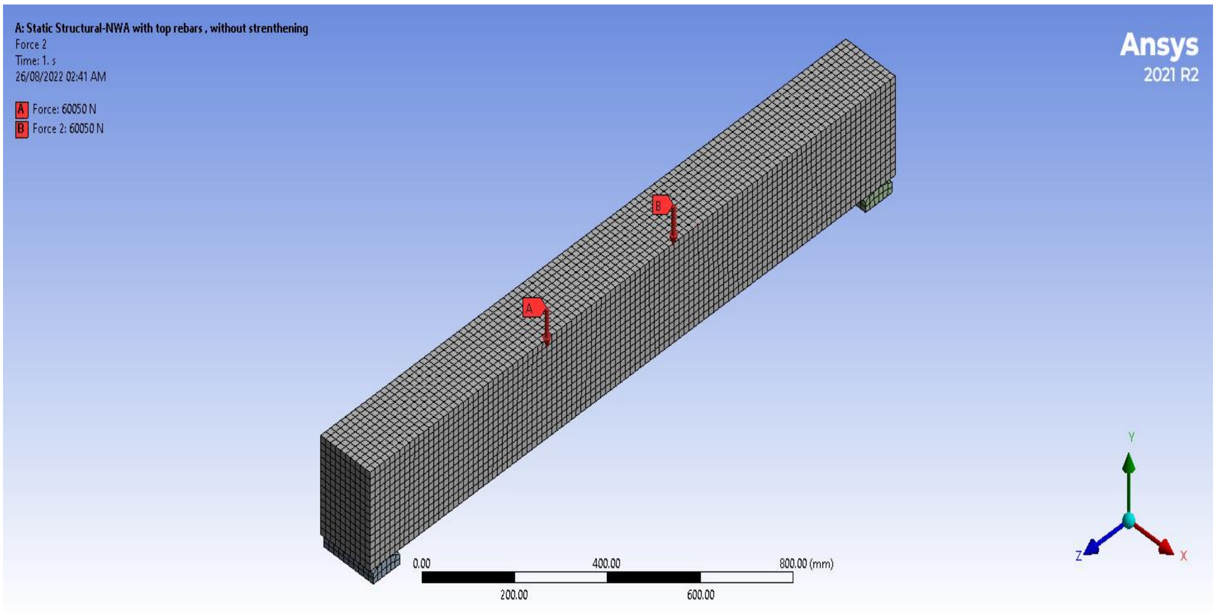

Figure 107(NWA-1/70.5MPa - Geometry and loads without strengthening and with top rebars - Static Nonlinear Analysis)

The ultimate load has been divided in to loads which is 120.1/2 =60.05KN.

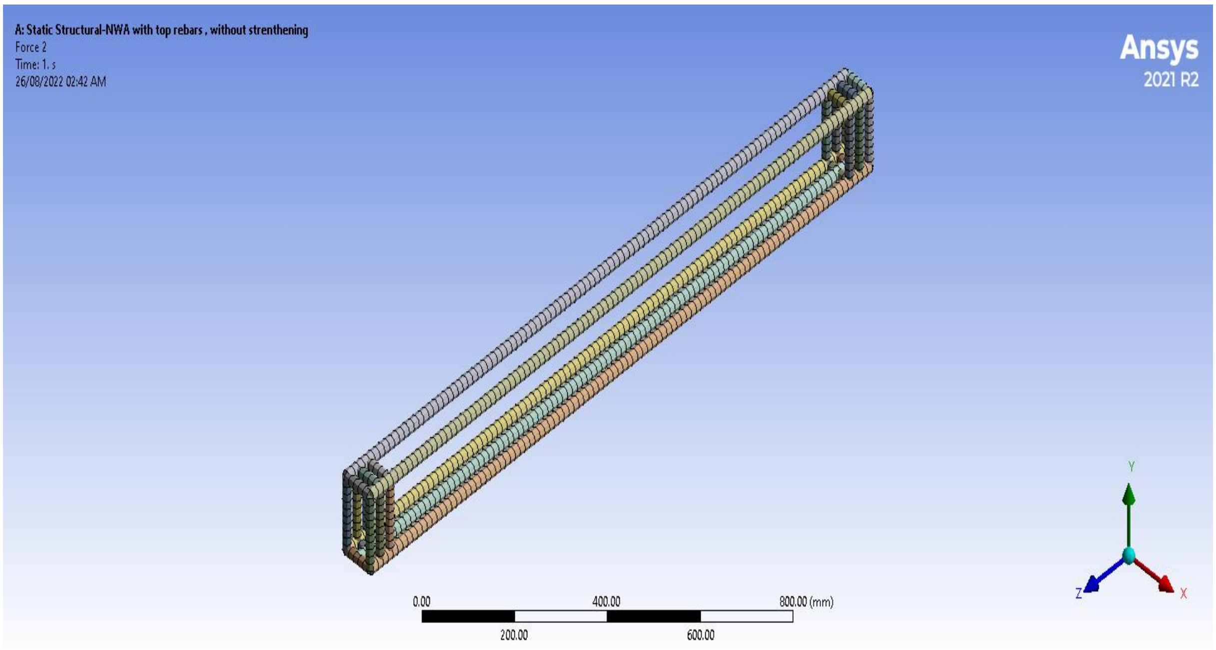

Figure 108(NWA-1/70.5MPa - Rebars view without strengthening - Static Nonlinear Analysis)

Deformations

-Total Deformations

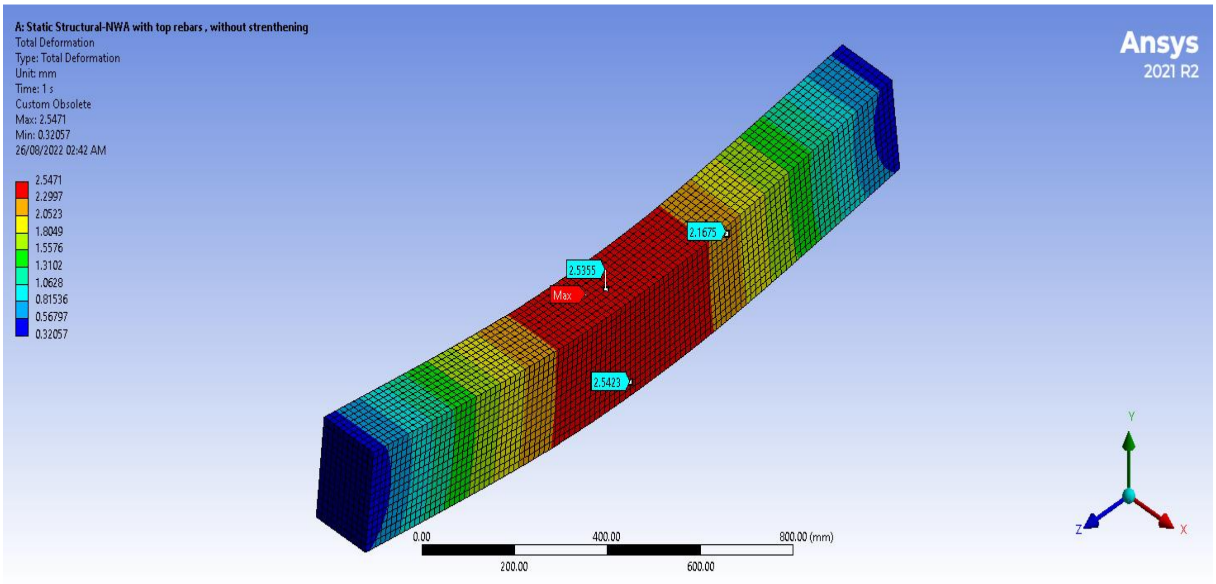

Figure 109(NWA-1/70.5MPa - Total deflections of beam sample without strengthening and with top rebars- Static Nonlinear Analysis)

The value is 2.5471 mm.

Directional Deformation (Y-Direction)

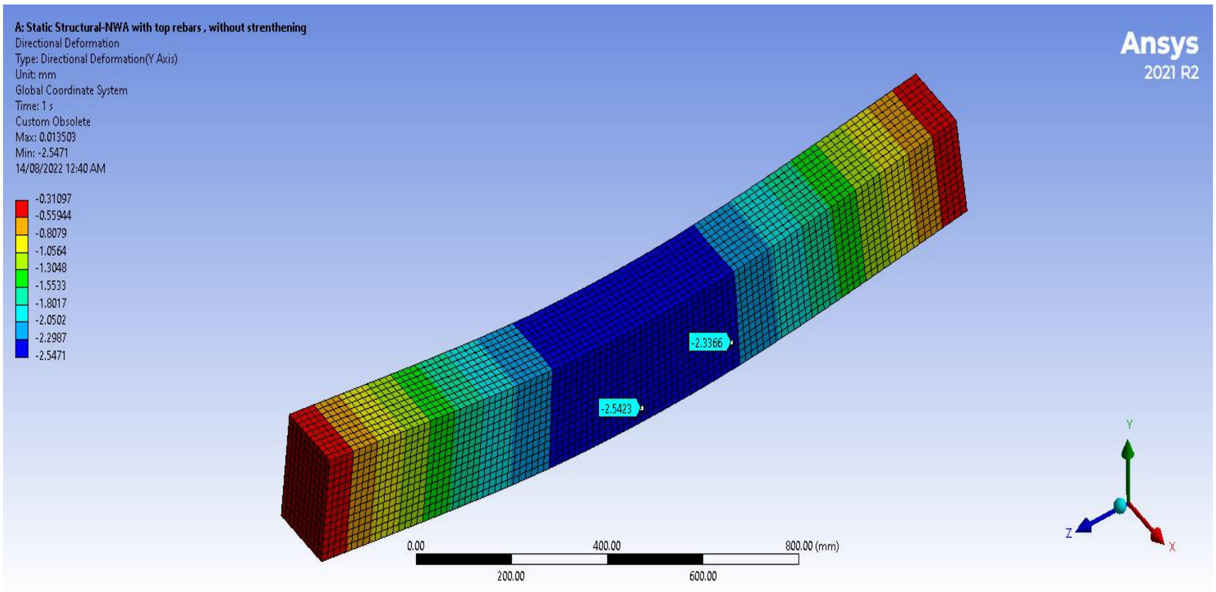

Figure 110(NWA-1/70.5MPa - Directional deflections (Y-Dir.) of beam sample without strengthening and with top rebars - Static Nonlinear Analysis)

The value is 2.5471 mm.

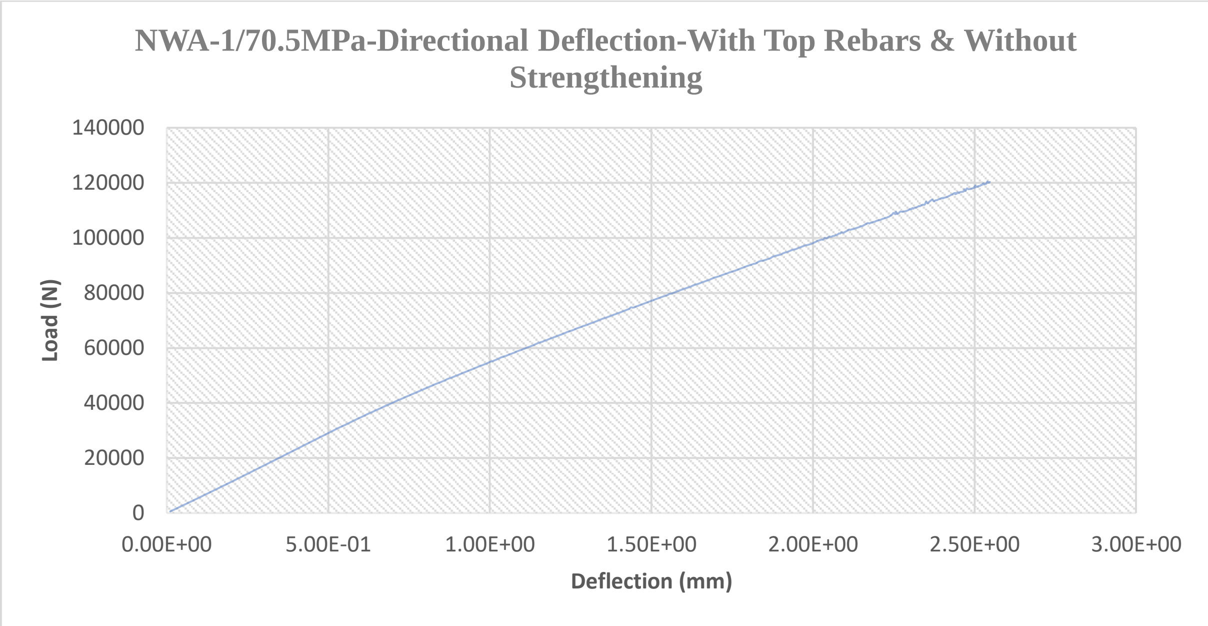

Figure 111(NWA-1/70.5MPa - Directional deflections graph of beam sample without strengthening and with top rebars - Static Nonlinear Analysis)

Normal Stress (Concrete)

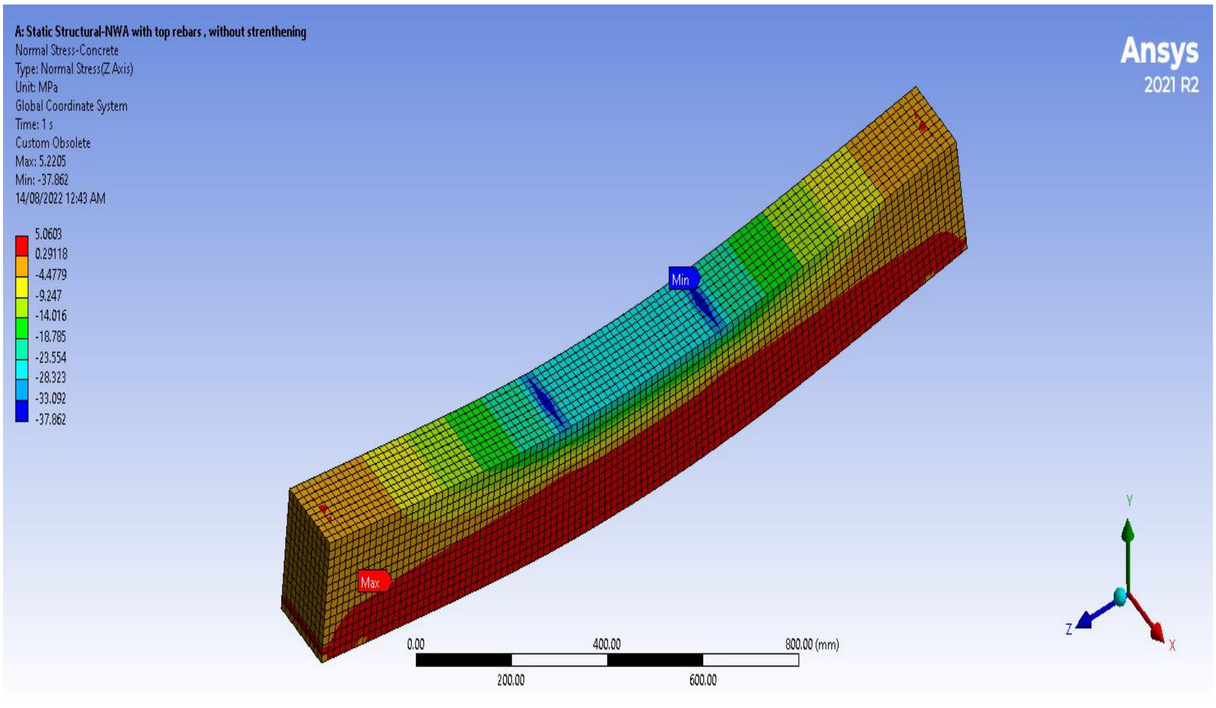

Figure 112(NWA-1/70.5MPa – Normal Stress (Concrete) of beam sample without strengthening and with top rebars - Static Nonlinear Analysis)

The blue zones show the crushing from loading machine and the maximum value is 37.862 MPa, whereas the red zones indicate to tension.

Normal Stress (Rebars)

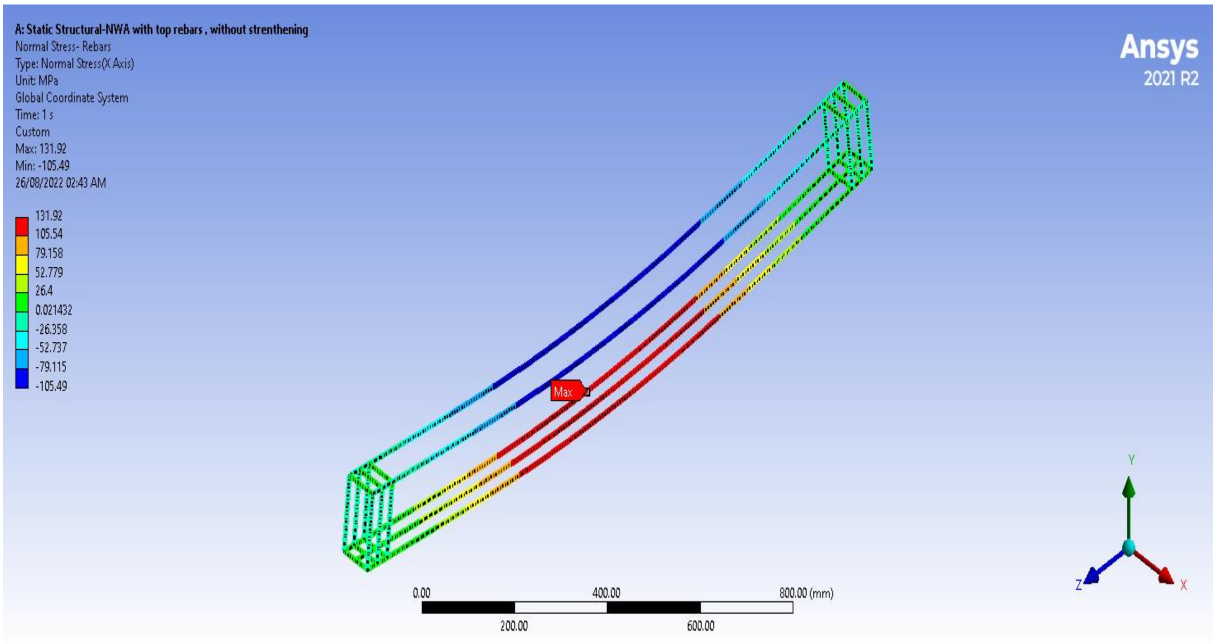

Figure 113(NWA-1/70.5MPa – Normal Stress (Rebars) of beam sample without strengthening and with top rebars - Static Nonlinear Analysis)

The red zones show that the rebars is yielding by 131.92 MPa, in the middle span due to tension.

Shear Stress

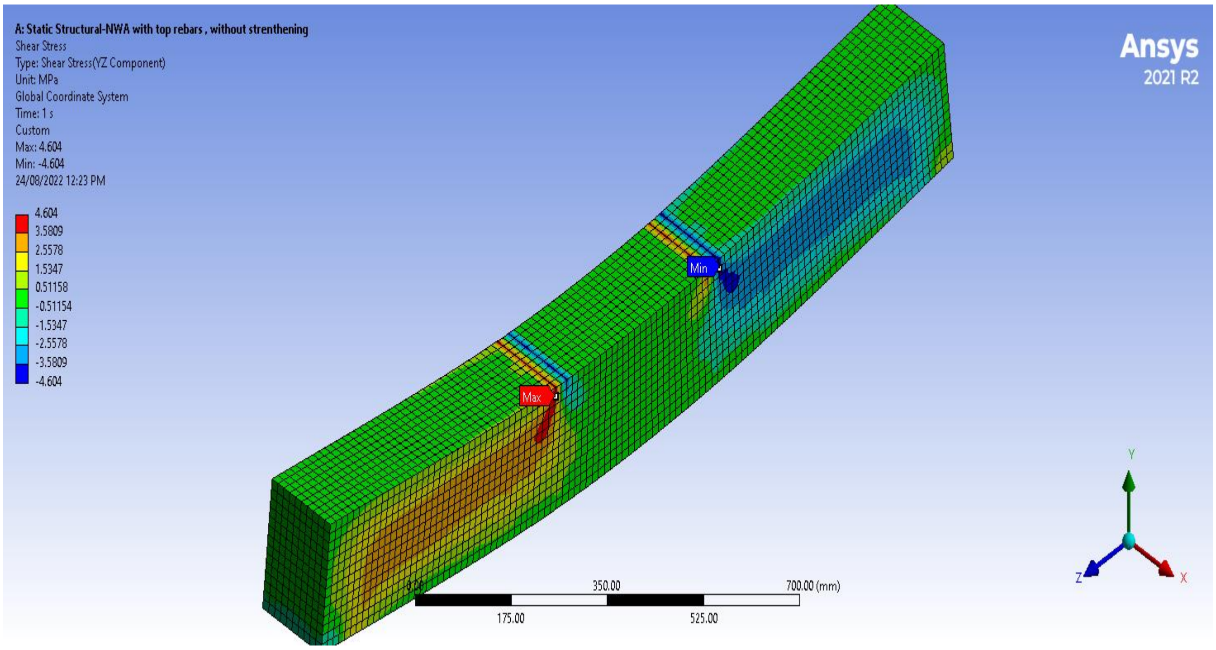

Figure 114(NWA-1/70.5MPa – Shear Stress of beam sample without strengthening and with top rebars - Static Nonlinear Analysis)

Elastic Strain

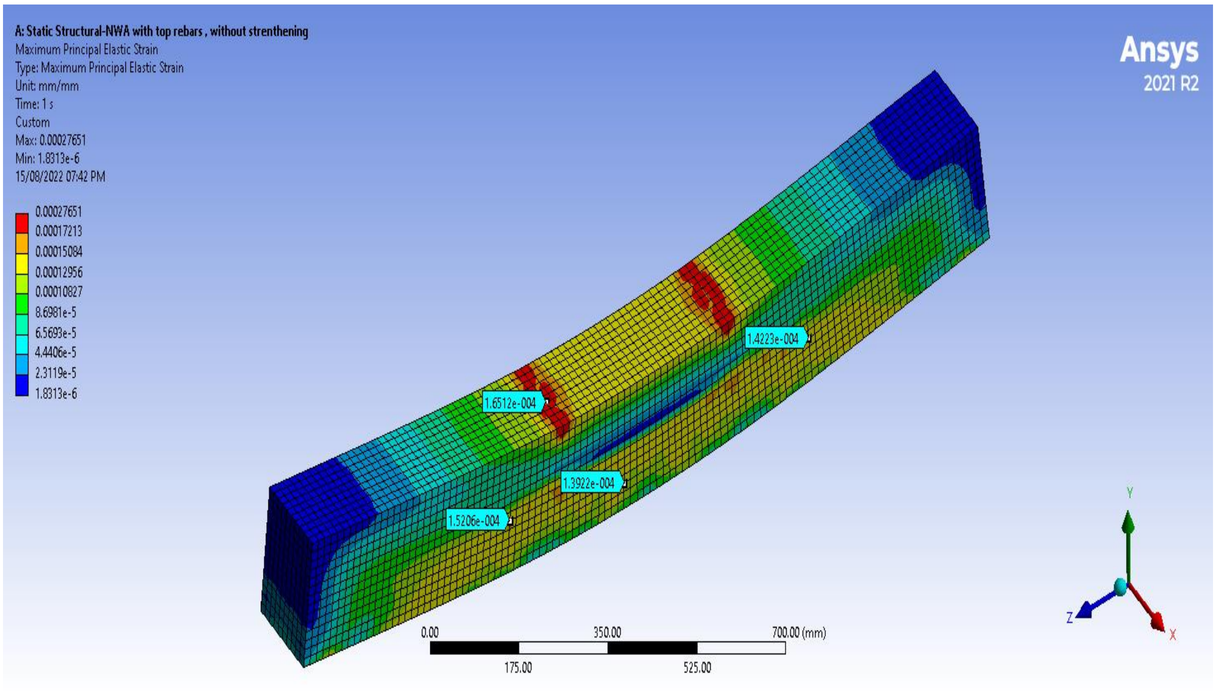

Figure 115(NWA-1/70.5MPa – Elastic Strain of beam sample without strengthening and with top rebars - Static Nonlinear Analysis)

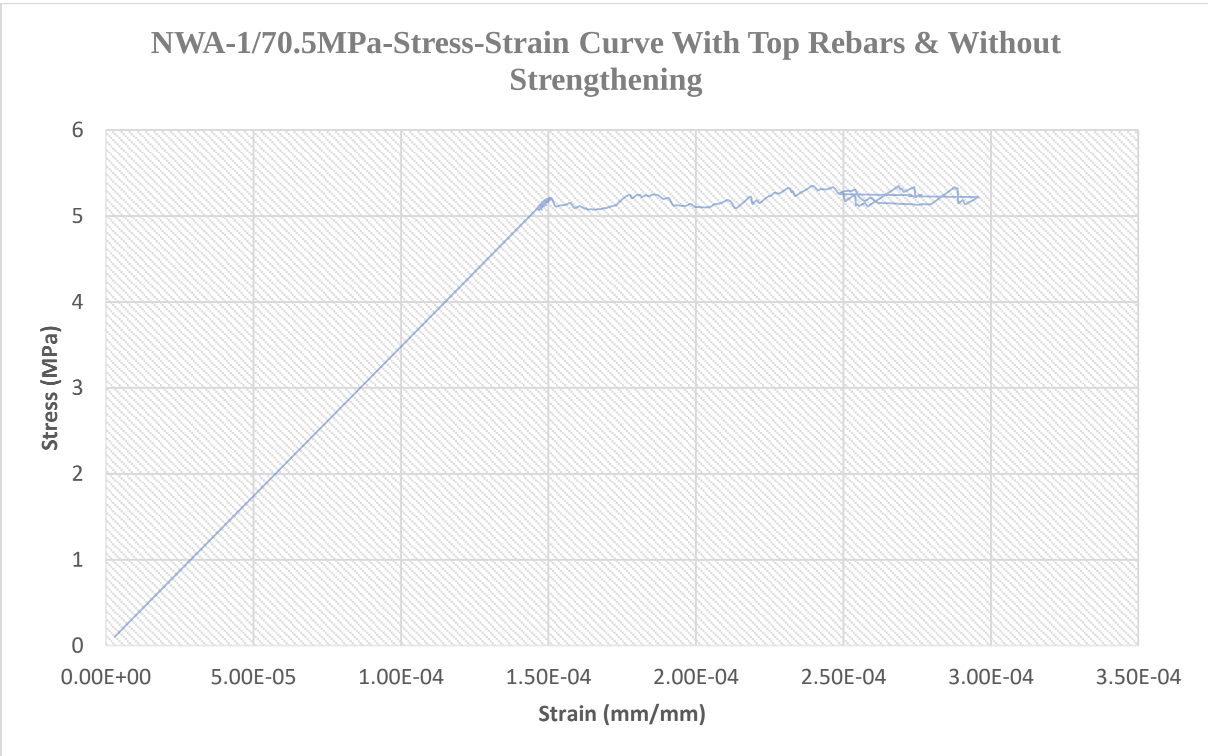

Figure 116(NWA-1/70.5MPa – Stress and Strain graph of beam sample without strengthening and with top rebars - Static Nonlinear Analysis)

2-Explicit Dynamics-With Top Rebars & Without Strengthening

Geometry and loads

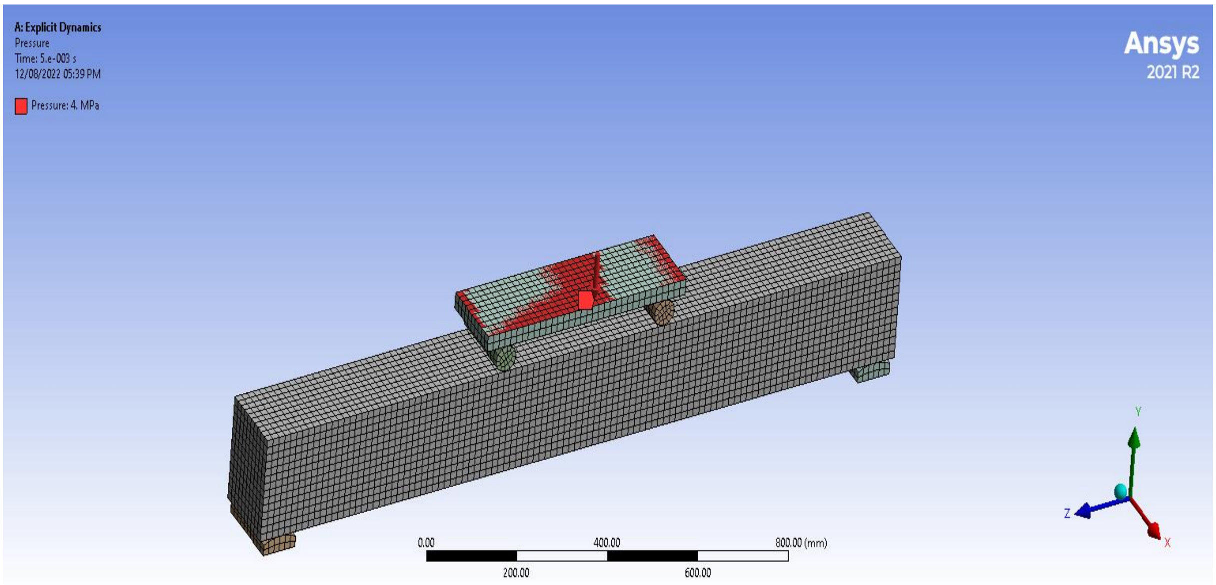

Figure 117(NWA-1/70.5MPa – Geometry & Loads of beam sample without strengthening and with top rebars- Explicit Dynamic Analysis)

The ultimate load has been transferred to be as a pressure load which is 4.0 MPa as shown above with rate loading 0.6mm/min.

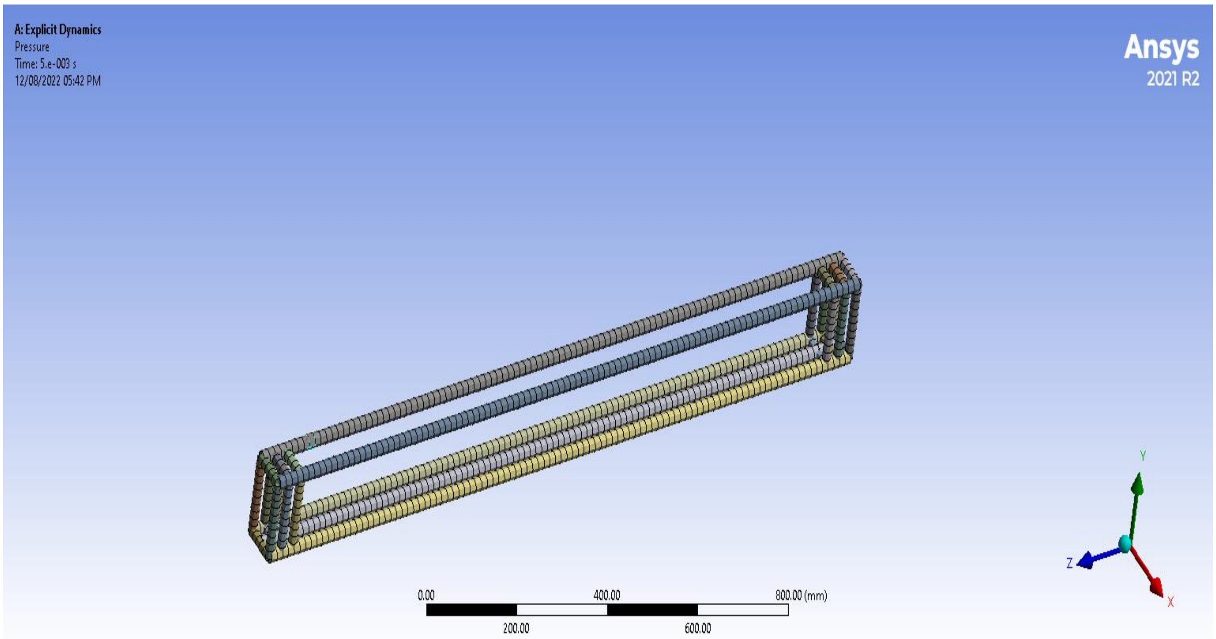

Figure 118(NWA-1/70.5MPa – Rebars of beam sample without strengthening - Explicit Dynamic Analysis)

Deformations

Total Deformations

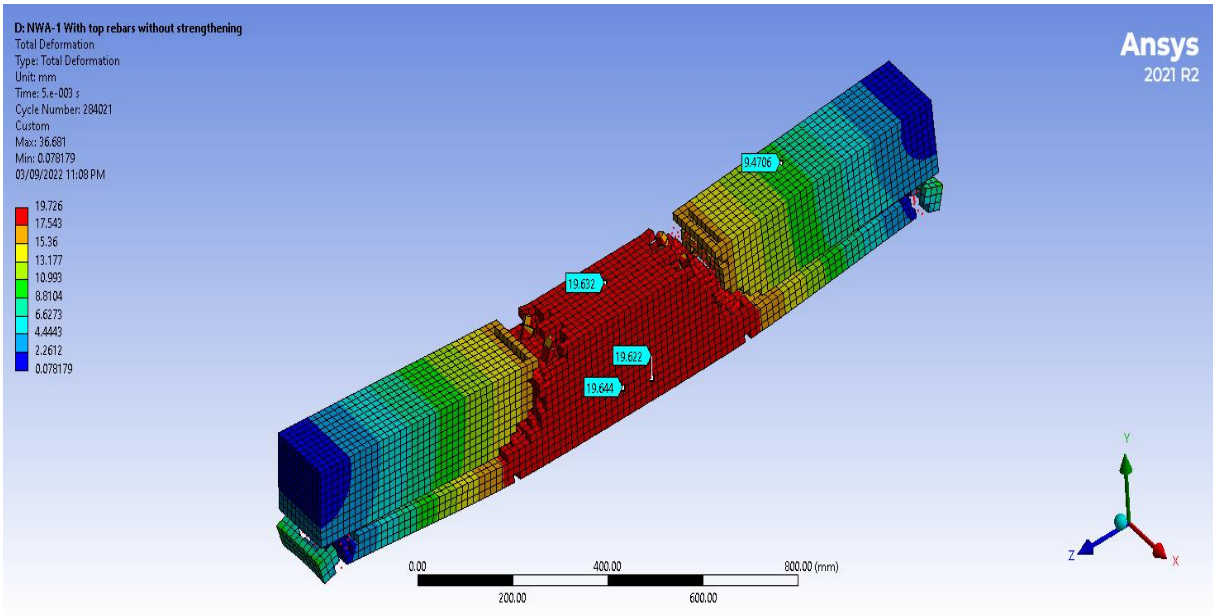

Figure 119(NWA-1/70.5MPa – Total deflections of beam sample without strengthening and with top rebars- Explicit Dynamic Analysis)

The value is 19.644 mm.

Directional Deformation (Y-Direction)-Concrete

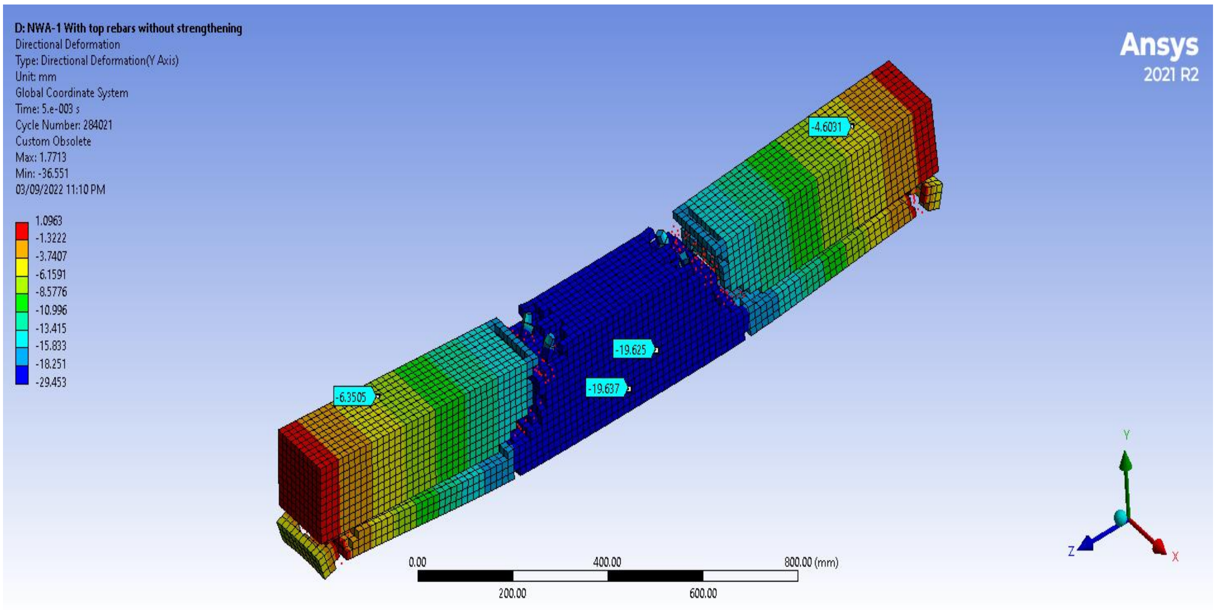

Figure 120(NWA-1/70.5MPa – Directional deflections (Y-Dir.) of beam sample without strengthening and with top rebars-Explicit Dynamic Analysis)

The value is 19.644 mm.

Directional Deformation (Y-Direction)- Rebars

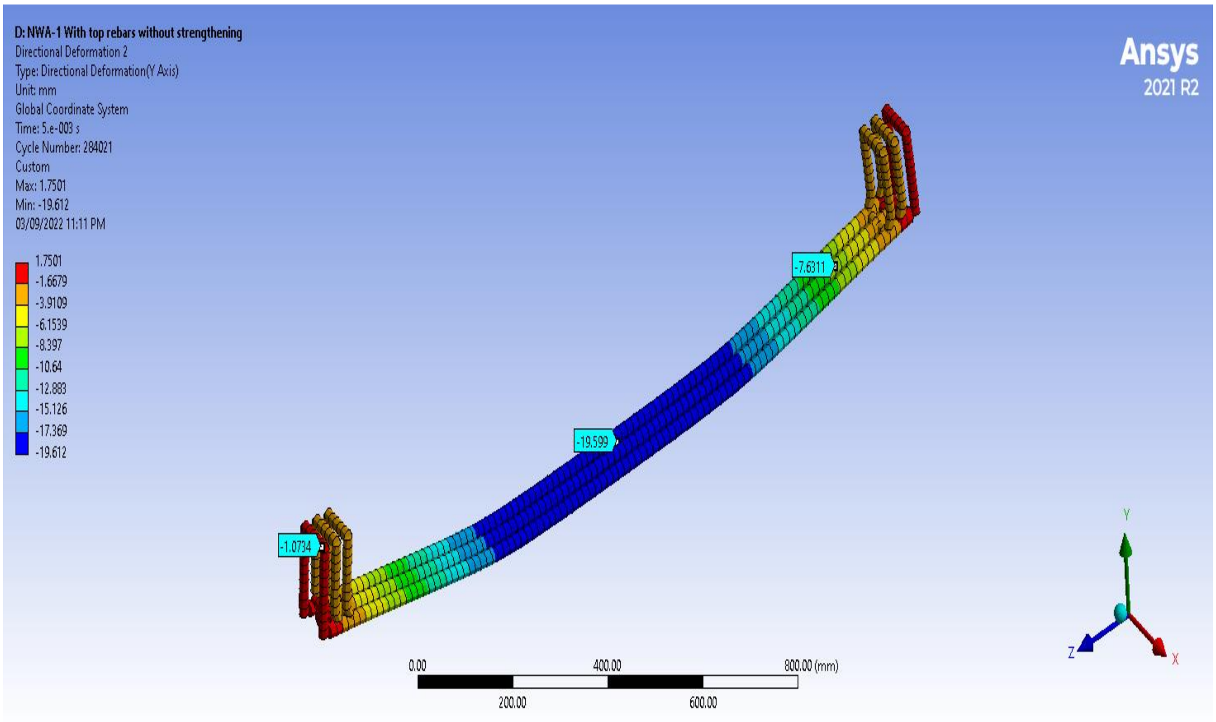

Figure 121(NWA-1/70.5MPa – Directional deflections (Y-Dir.) of beam rebars without strengthening- Explicit Dynamic Analysis)

Normal strain

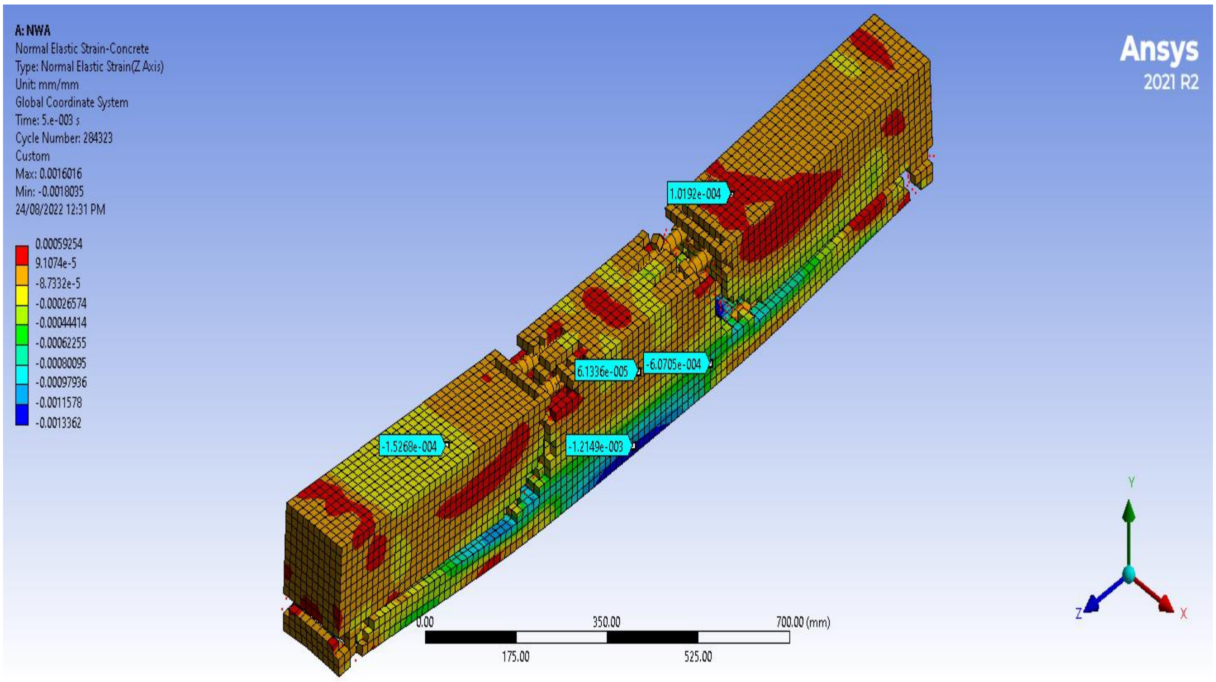

Figure 122(NWA-1/70.5MPa – Normal strain of beam sample without strengthening and with top rebars- Explicit Dynamic Analysis)

Shear Stress

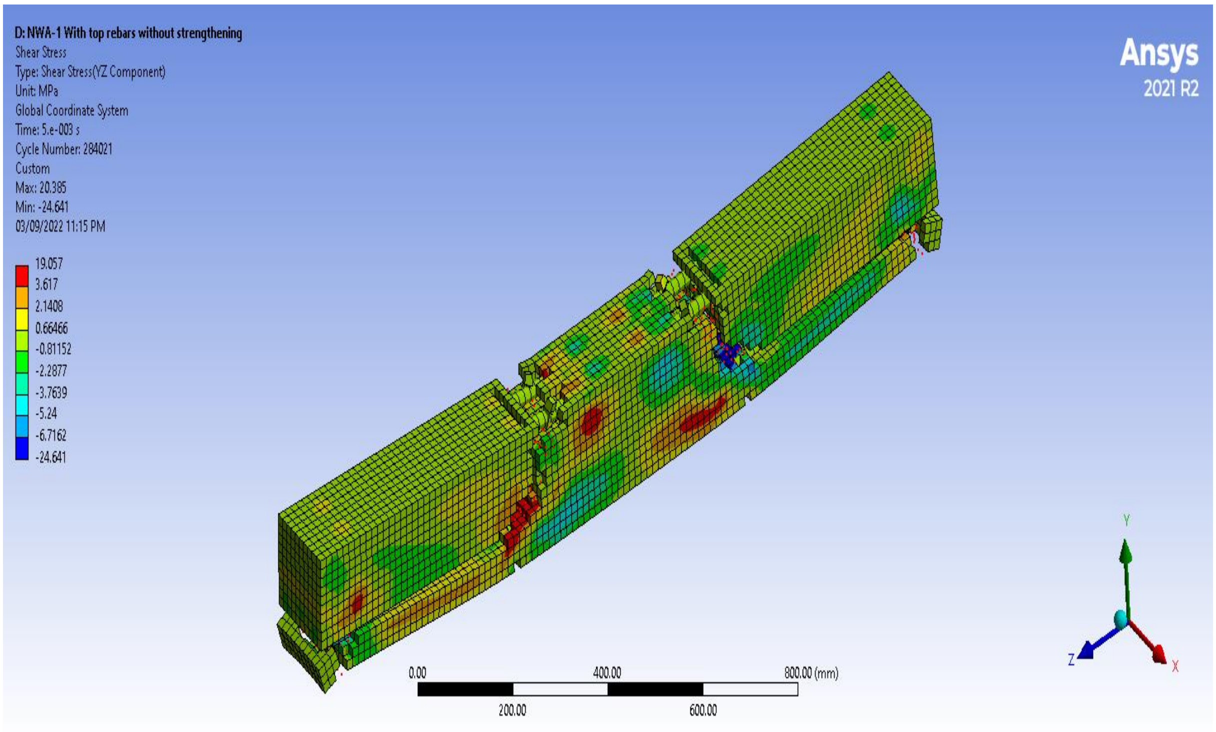

Figure 123(NWA-1/70.5MPa – Shear stress of beam sample without strengthening and with top rebars- Explicit Dynamic Analysis)

Total shape strain

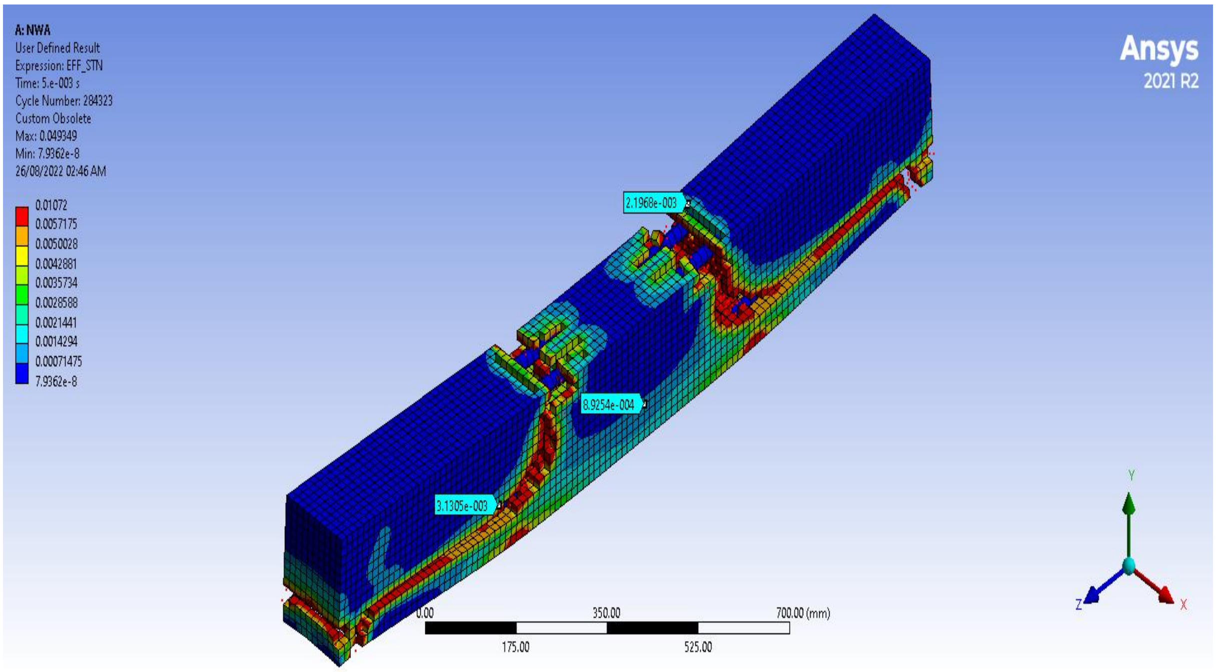

Figure 124(NWA-1/70.5MPa – Total strain of beam sample without strengthening and with top rebars- Explicit Dynamic Analysis)

Maximum Stress

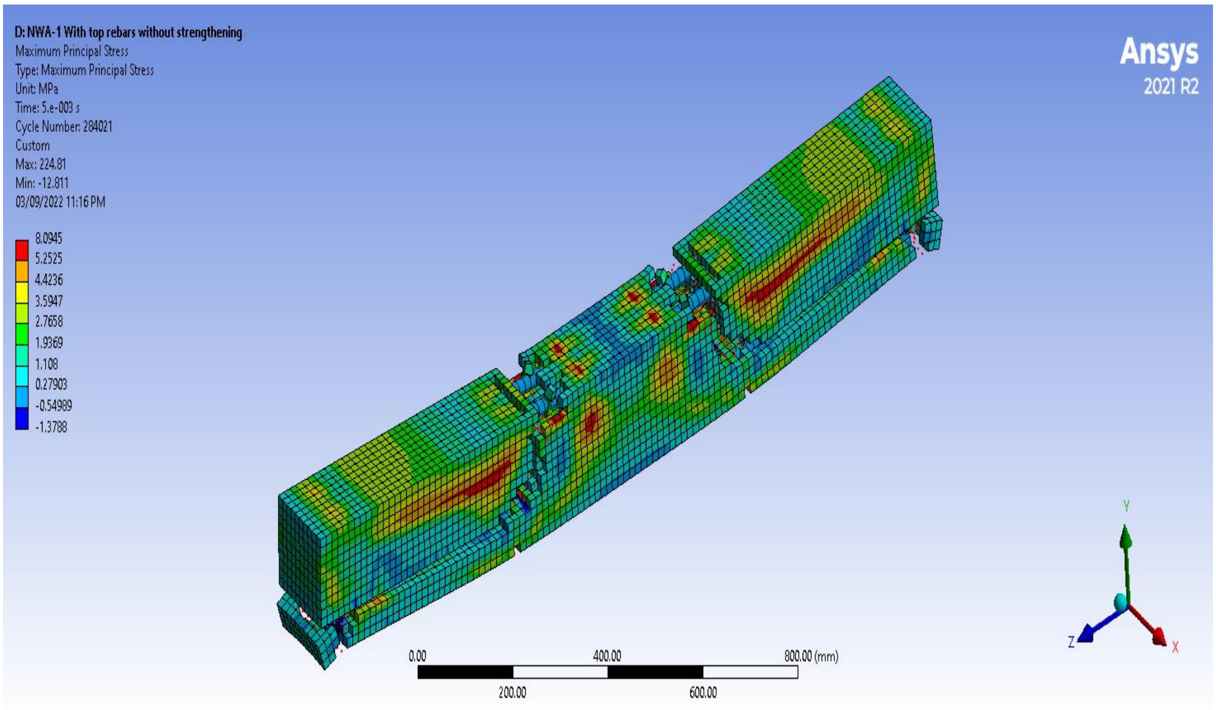

Figure 125(NWA-1/70.5MPa – Maximum stress of beam sample without strengthening and with top rebars- Explicit Dynamic Analysis)

The Damage Pattern

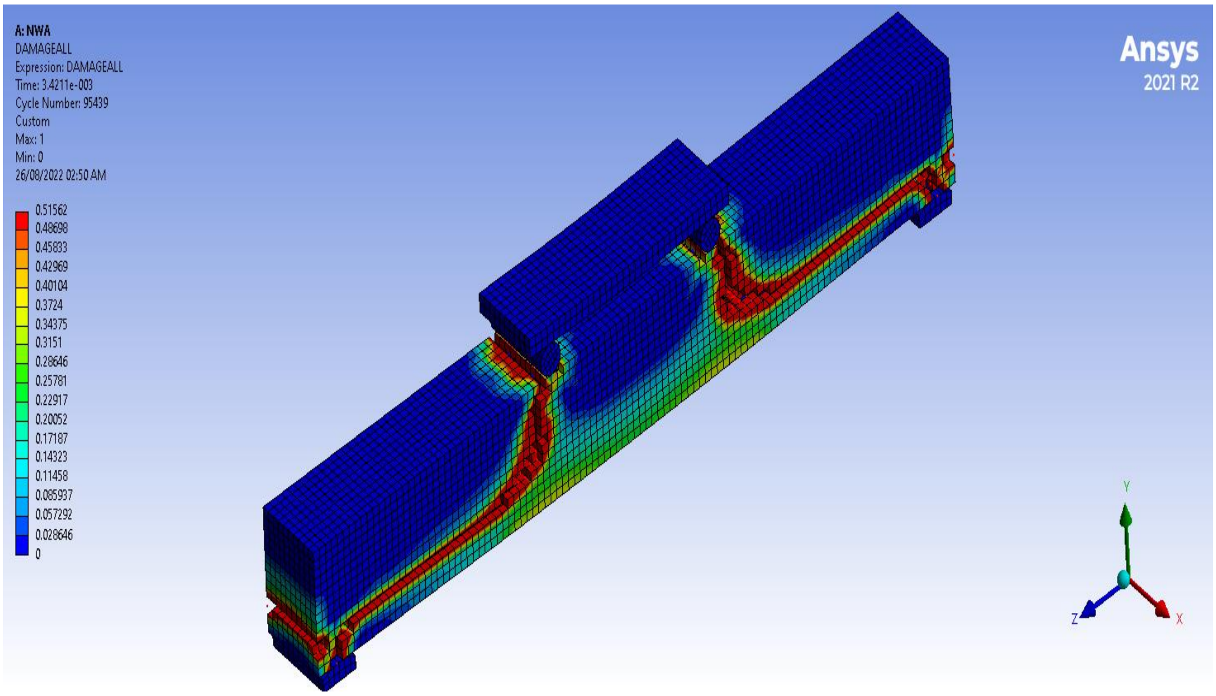

Figure 126(NWA-1/70.5MPa – Damage pattern of beam sample without strengthening and with top rebars- Explicit Dynamic Analysis)

As we can see the shear damage cracks and concrete failures.

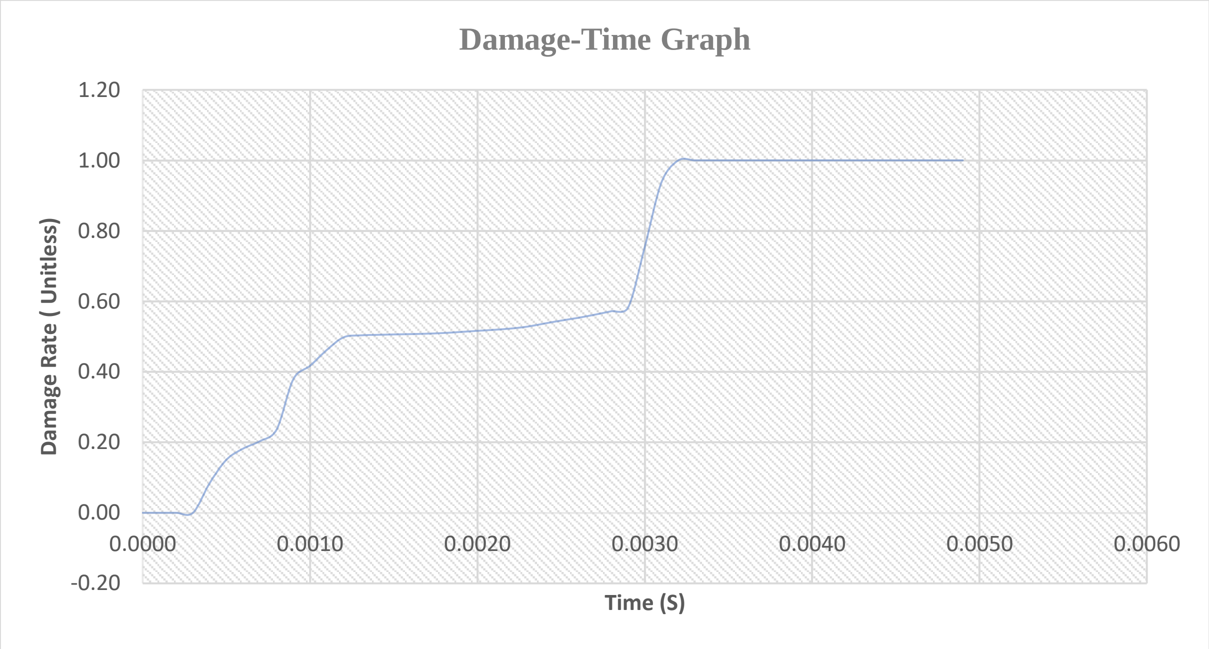

Figure 127(NWA-1/70.5MPa – Damage pattern graph of beam sample without strengthening and with top rebars- Explicit Dynamic Analysis)

3-Static Non-Linear Analysis – Without Top Rebars and Strengthening

Geometry and loads

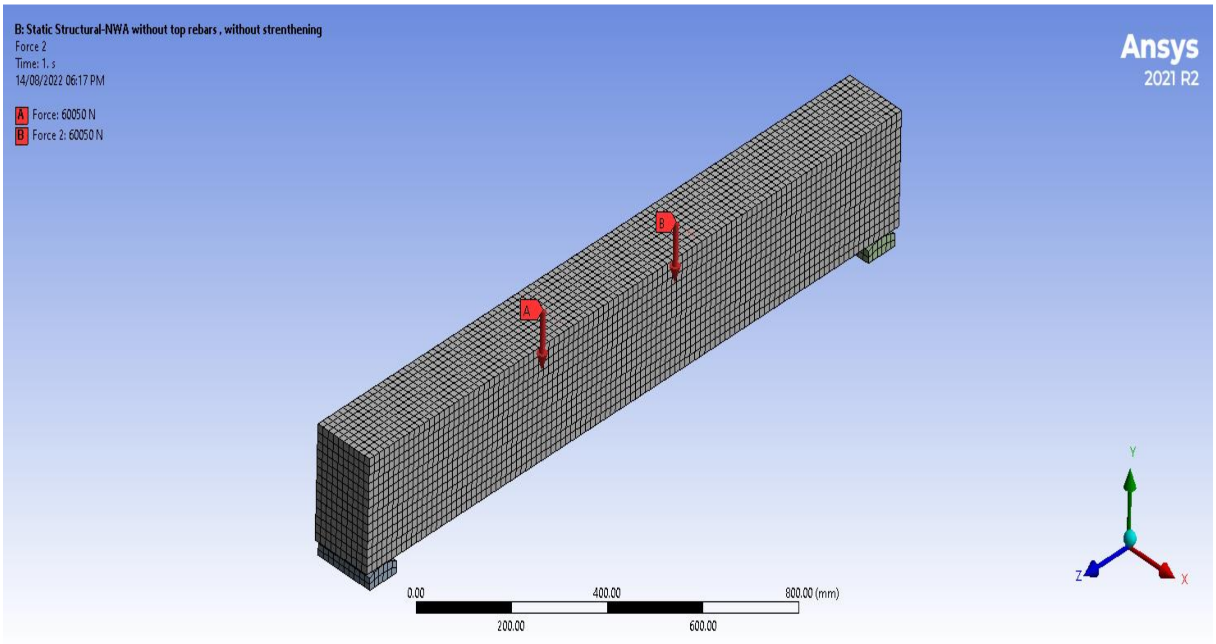

Figure 128(NWA-1/70.5MPa – Geometry & loads of beam sample without strengthening and top rebars- Static Nonlinear Analysis)

The ultimate load has been divided in to loads which is 120.1/2 =60.05KN.

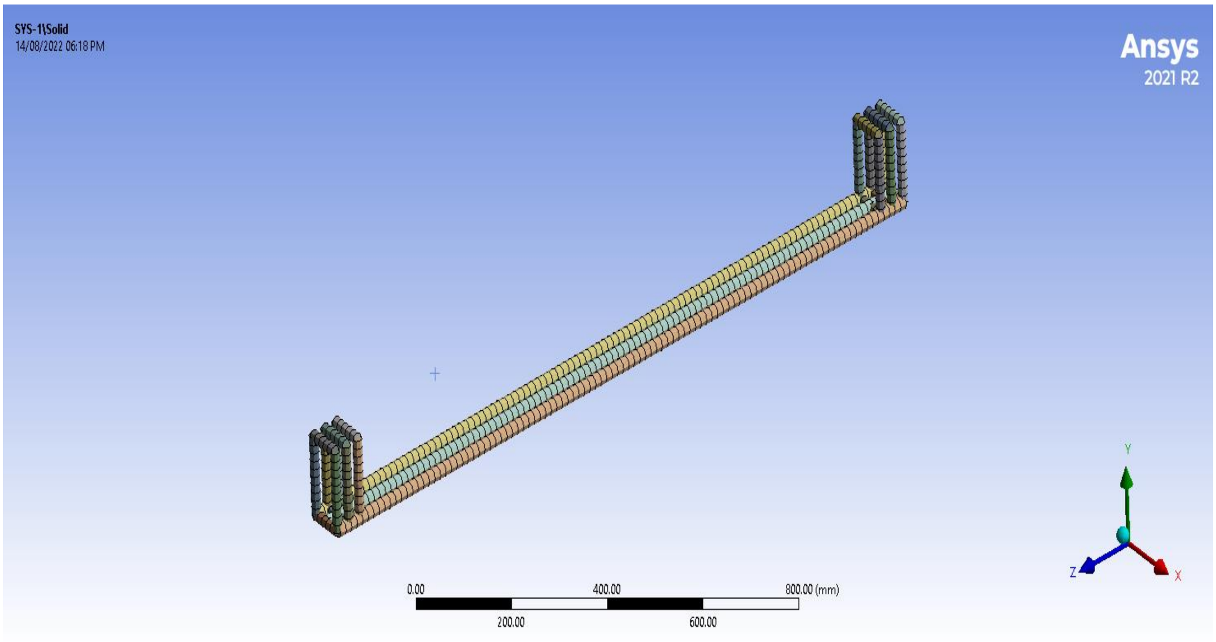

Figure 129(NWA-1/70.5MPa – Rebars of beam sample without strengthening - Static Nonlinear Analysis)

Deformations

Total Deformations

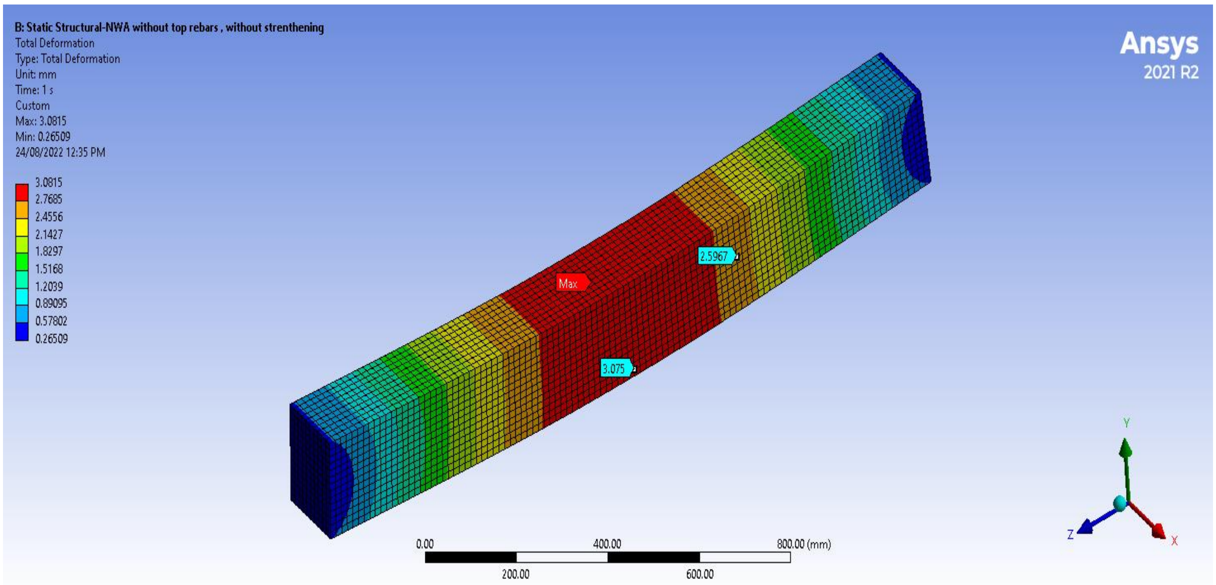

Figure 130((NWA-1/70.5MPa – Total deflections of beam sample without strengthening and top rebars- Static Nonlinear Analysis)

The value is 3.0815 mm.

Directional Deformation (Y-Direction)

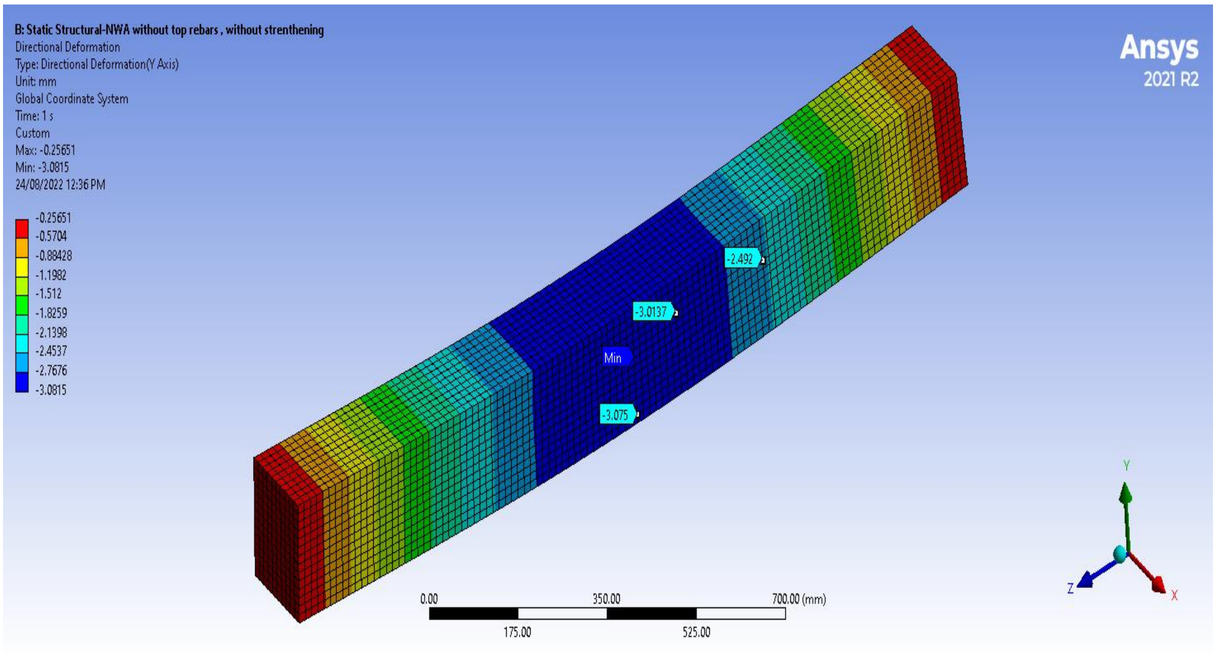

Figure 131(NWA-1/70.5MPa – Directional deflections (Y-Dir.) of beam sample without strengthening and top rebars- Static Nonlinear Analysis)

The value is 3.0815 mm.

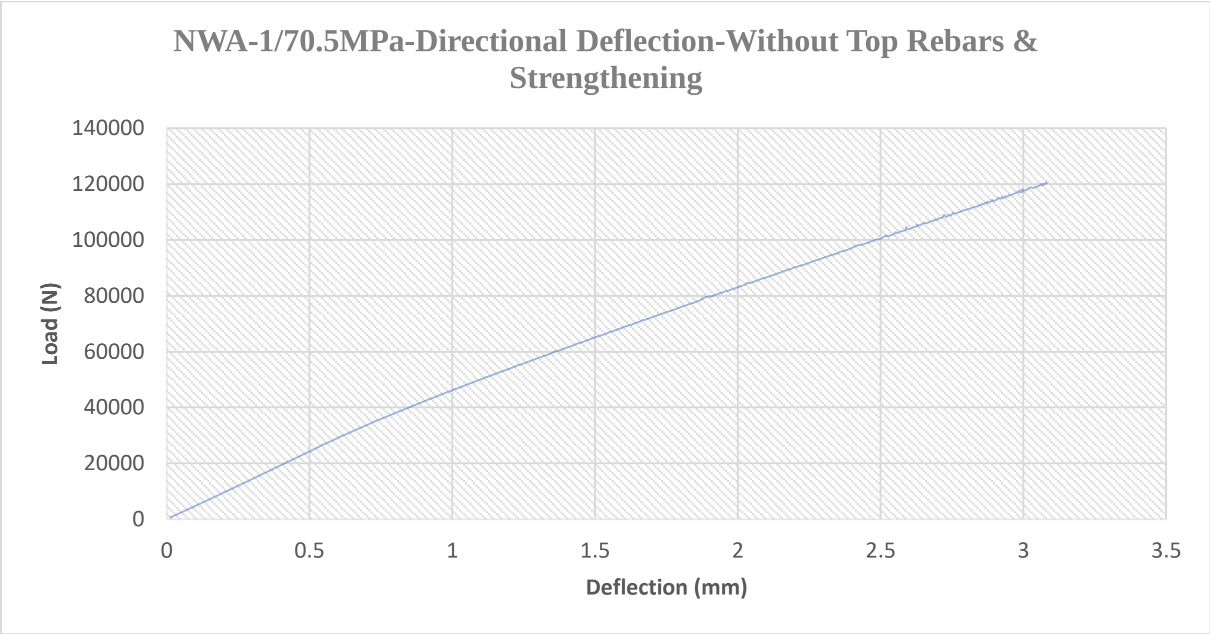

Figure 132(NWA-1/70.5MPa – Directional deflections (Y-Dir.) graph of beam sample without strengthening and top rebars- Static Nonlinear Analysis)

Normal Stress (Concrete)

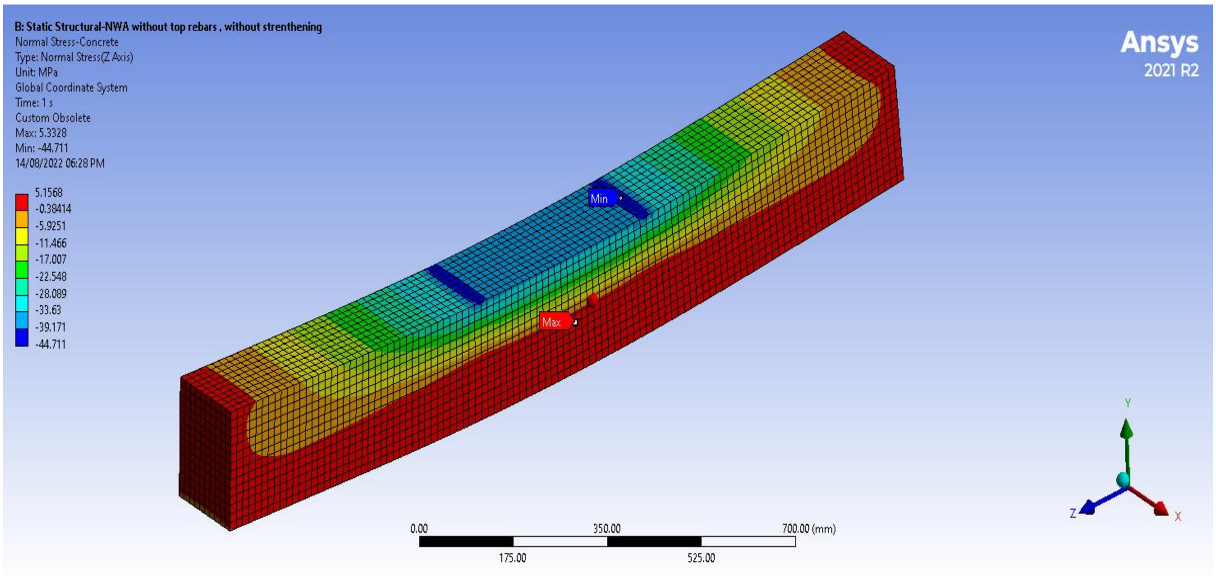

Figure 133(NWA-1/70.5MPa – Normal stress (concrete) of beam sample without strengthening and top rebars- Static Nonlinear Analysis)

The blue zones show the crushing from loading machine and the maximum value is 44.71 MPa, whereas the red zones indicate to tension.

Normal Stress (Rebars)

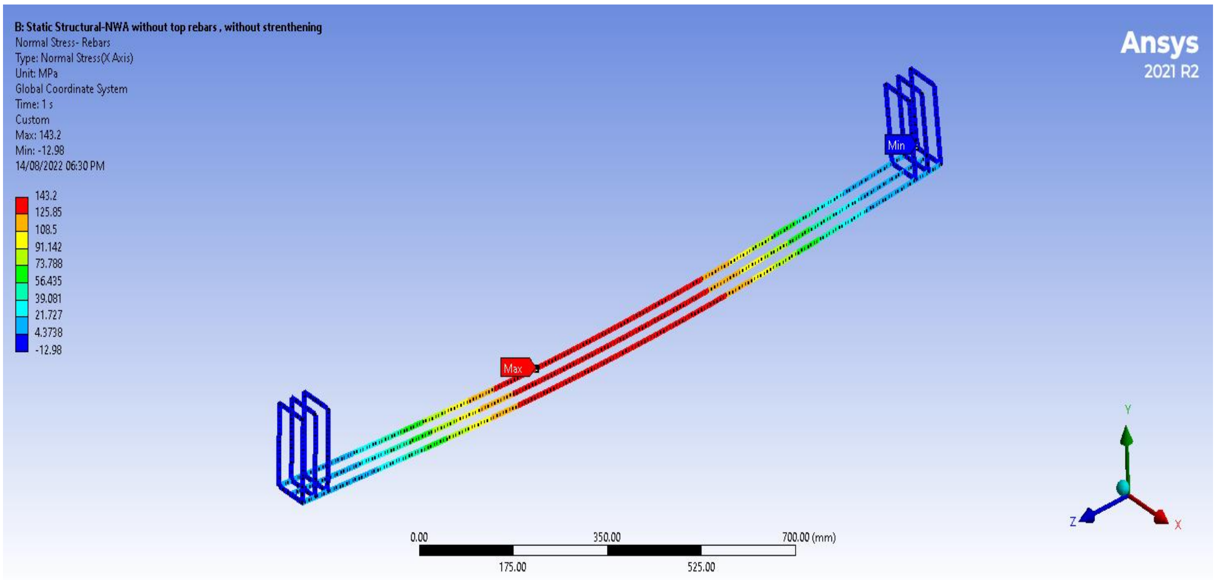

Figure 134(NWA-1/70.5MPa – Normal stress (Rebars) of beam sample without strengthening and top rebars- Static Nonlinear Analysis)

The red zones show that the rebars is yielding by 143.2MPa, in the middle span due to tension.

Shear Stress

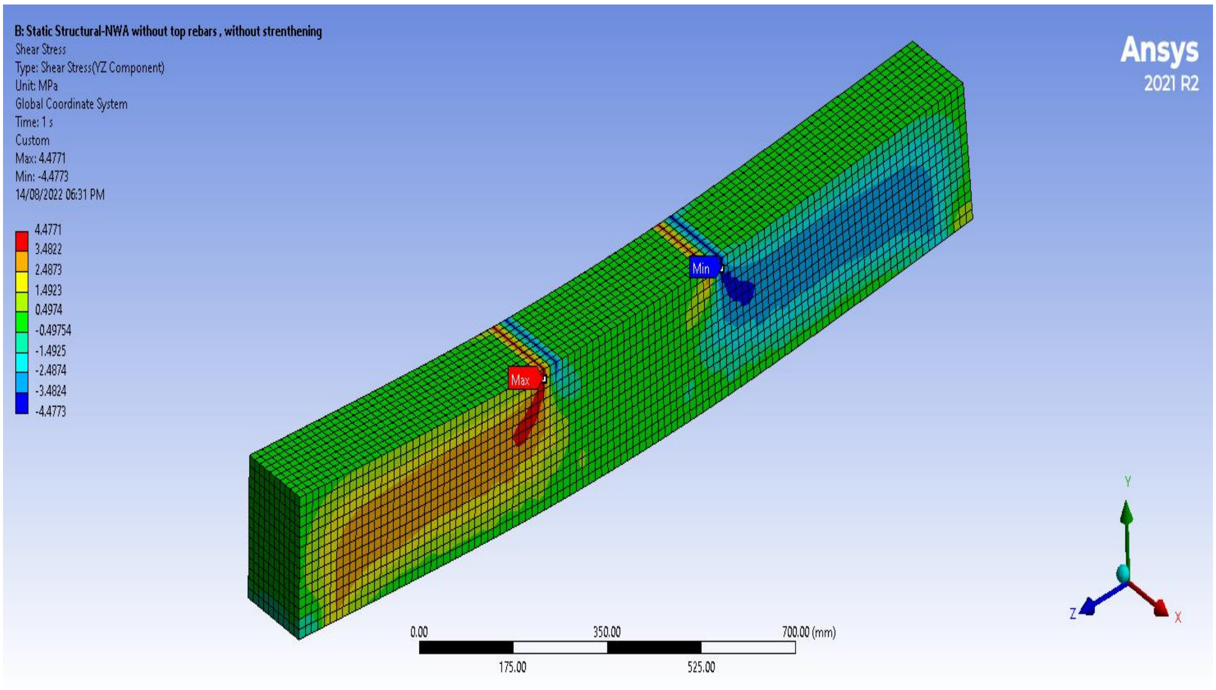

Figure 135(NWA-1/70.5MPa – Shear stress of beam sample without strengthening and top rebars- Static Nonlinear Analysis)

Elastic Strain

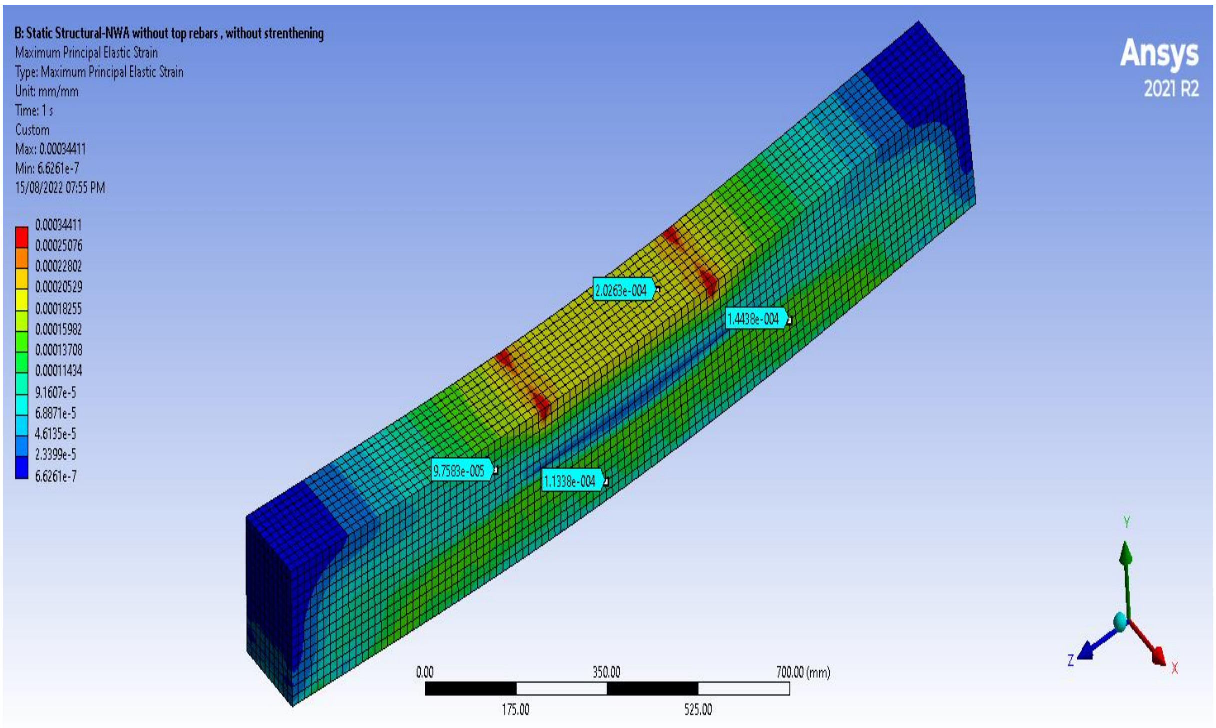

Figure 136(NWA-1/70.5MPa – Elastic strain of beam sample without strengthening and top rebars- Static Nonlinear Analysis)

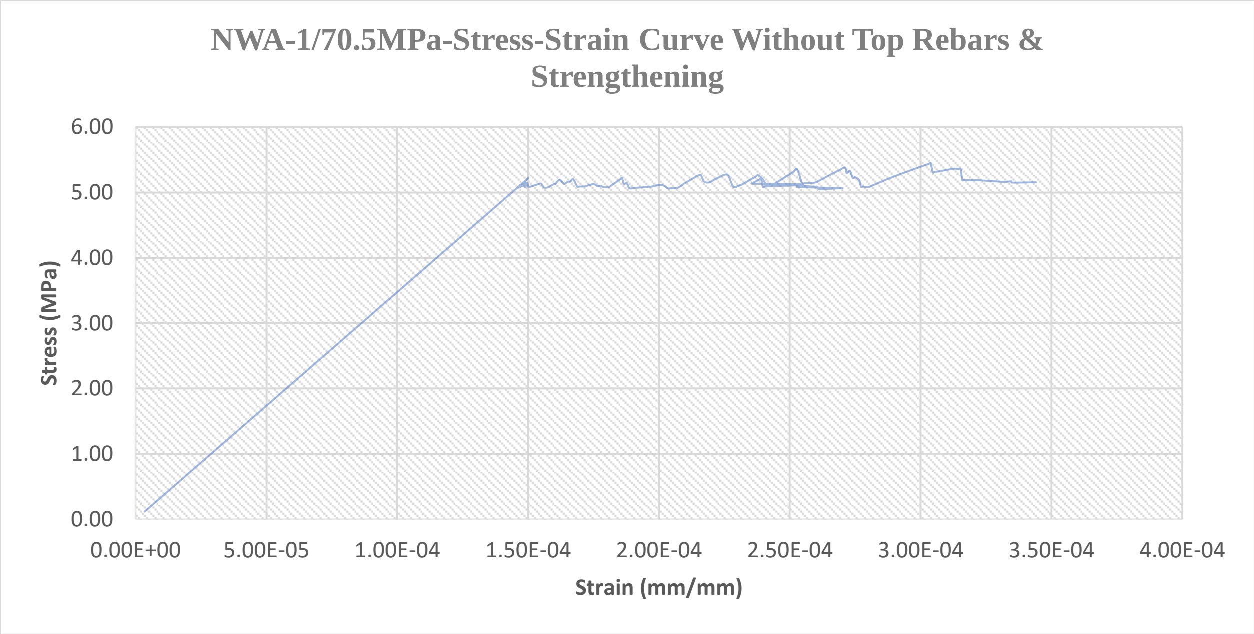

Figure 137(NWA-1/70.5MPa – Stress & Strain graph of beam sample without strengthening and top rebars- Static Nonlinear Analysis)

4-Explicit Dynamic-Without Top Rebars & Strengthening

Geometry and loads

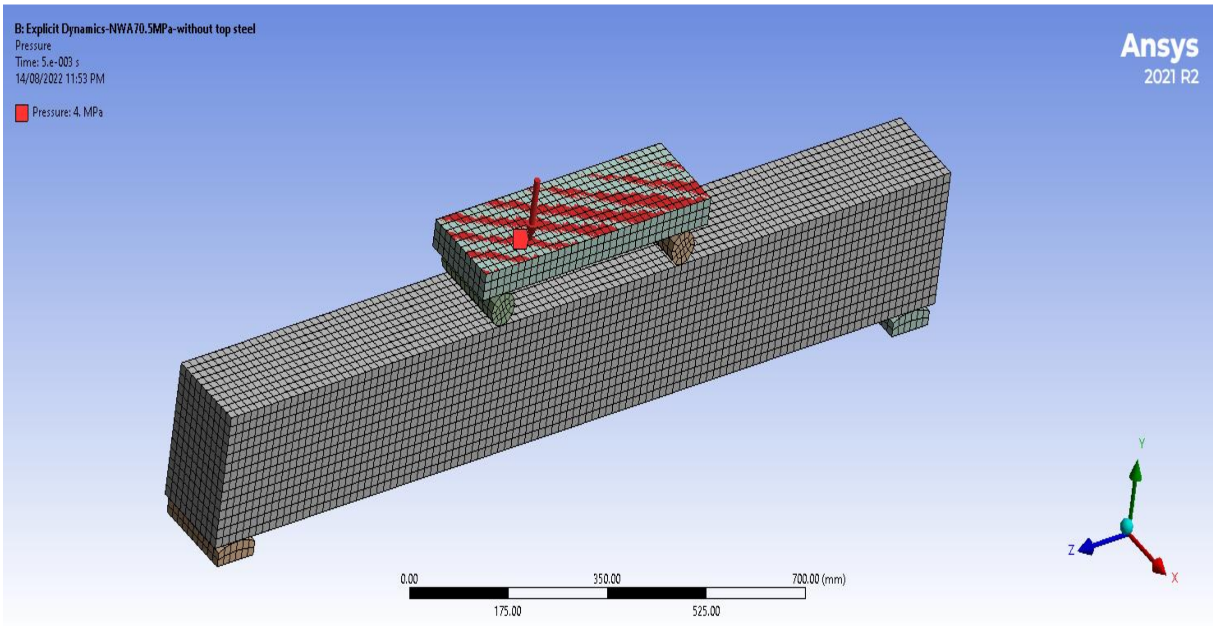

Figure 138(NWA-1/70.5MPa – Geometry & loads of beam sample without strengthening and top rebars- Explicit Dynamic Analysis)

The ultimate load has been transferred to be as a pressure load which is 4.0 MPa as shown above with rate loading 0.6mm/min

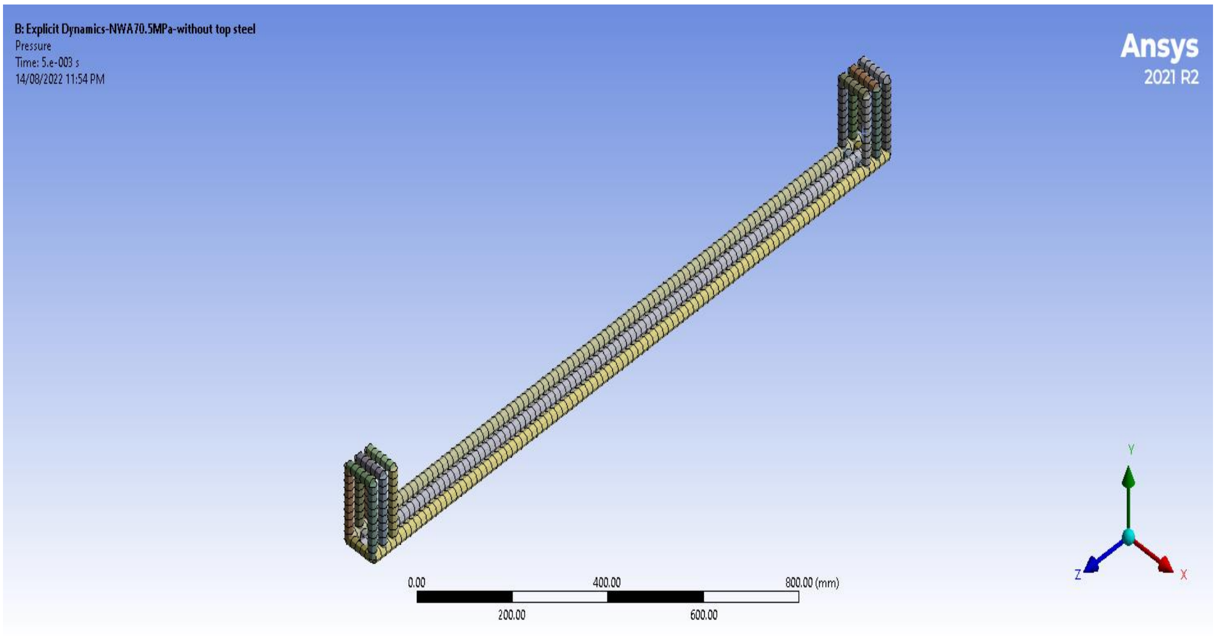

Figure 139(NWA-1/70.5MPa – Rebars of beam sample without strengthening- Explicit Dynamic Analysis)

Deformations

Total Deformations

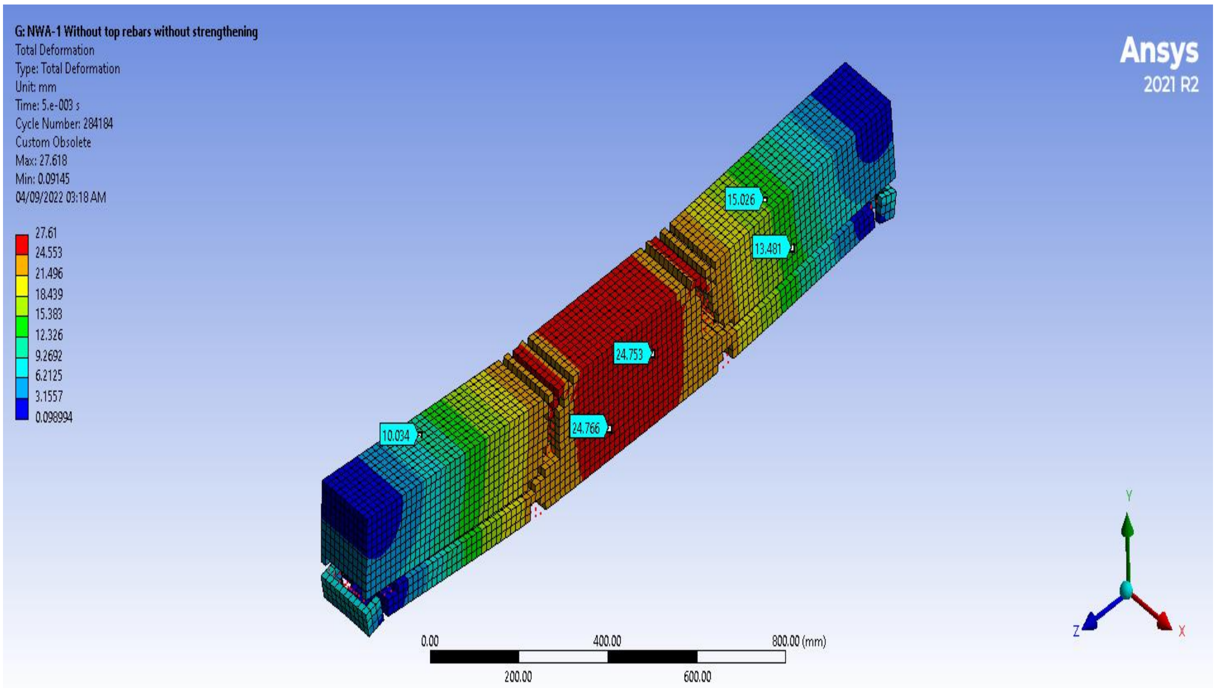

Figure 140(NWA-1/70.5MPa – Total deflections of beam sample without strengthening and top rebars- Explicit Dynamic Analysis)

The value is 24.766 mm.

Directional Deformation (Y-Direction)-Concrete

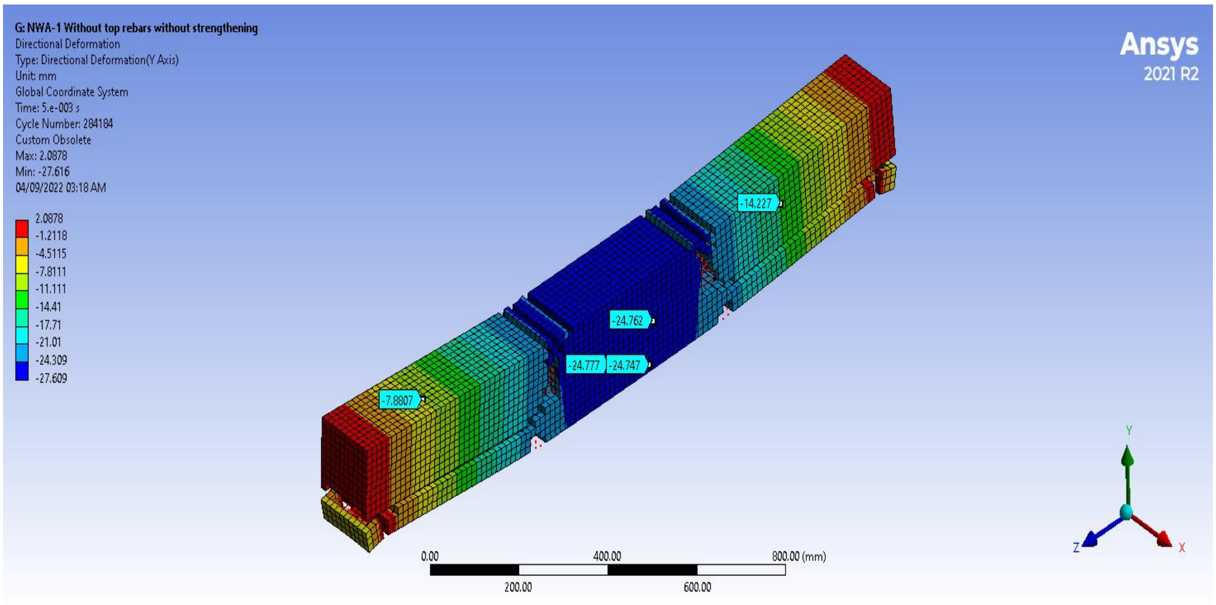

Figure 141(NWA-1/70.5MPa – Directional deflections (Y-Dim.) of beam sample without strengthening and top rebars- Explicit Dynamic Analysis)

The value is 21.063 mm.

Directional Deformation (Y-Direction)- Rebars

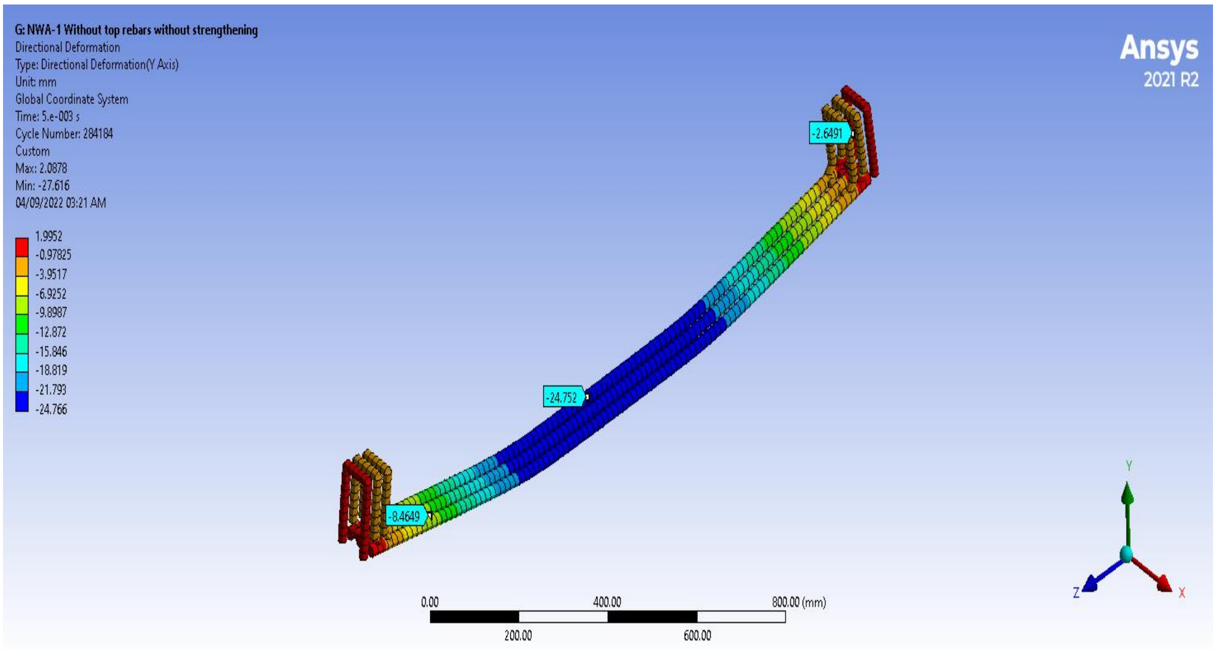

Figure 142(NWA-1/70.5MPa – Directional deflections (Rebars) of beam sample without strengthening- Explicit Dynamic Analysis)

Normal strain

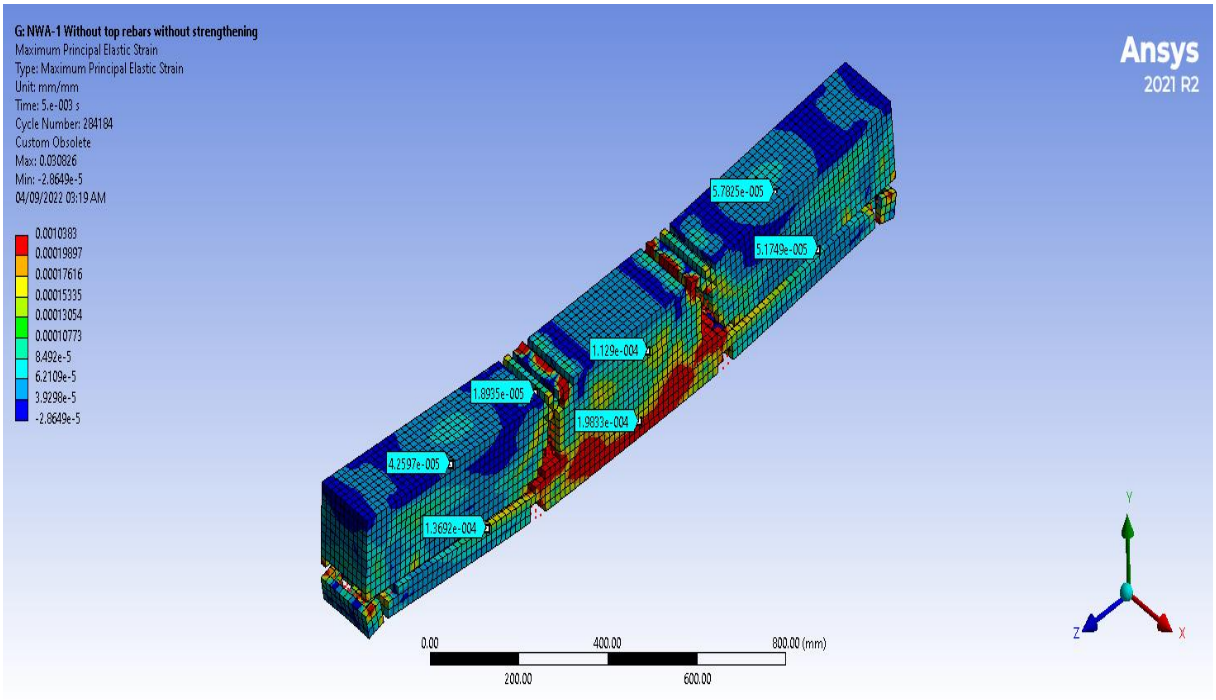

Figure 143(NWA-1/70.5MPa – Normal strain of beam sample without strengthening and top rebars- Explicit Dynamic Analysis)

Shear Stress

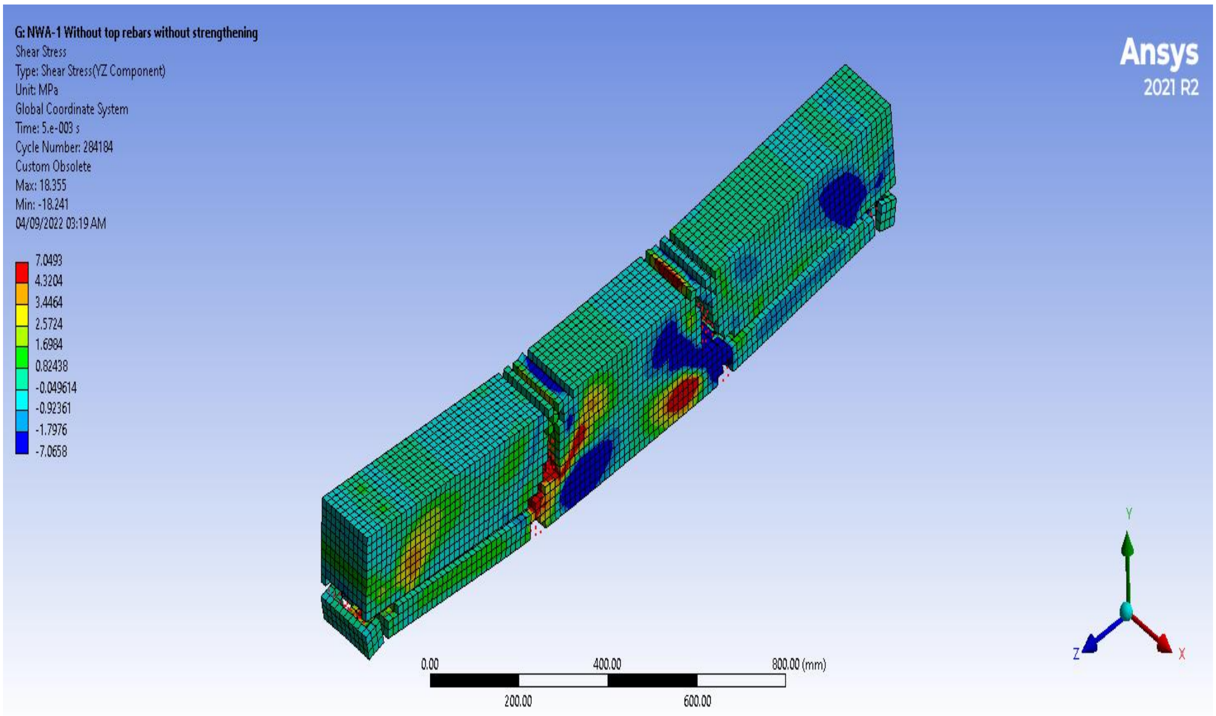

Figure 144(NWA-1/70.5MPa – Shear Stress of beam sample without strengthening and top rebars- Explicit Dynamic Analysis)

Total shape strain

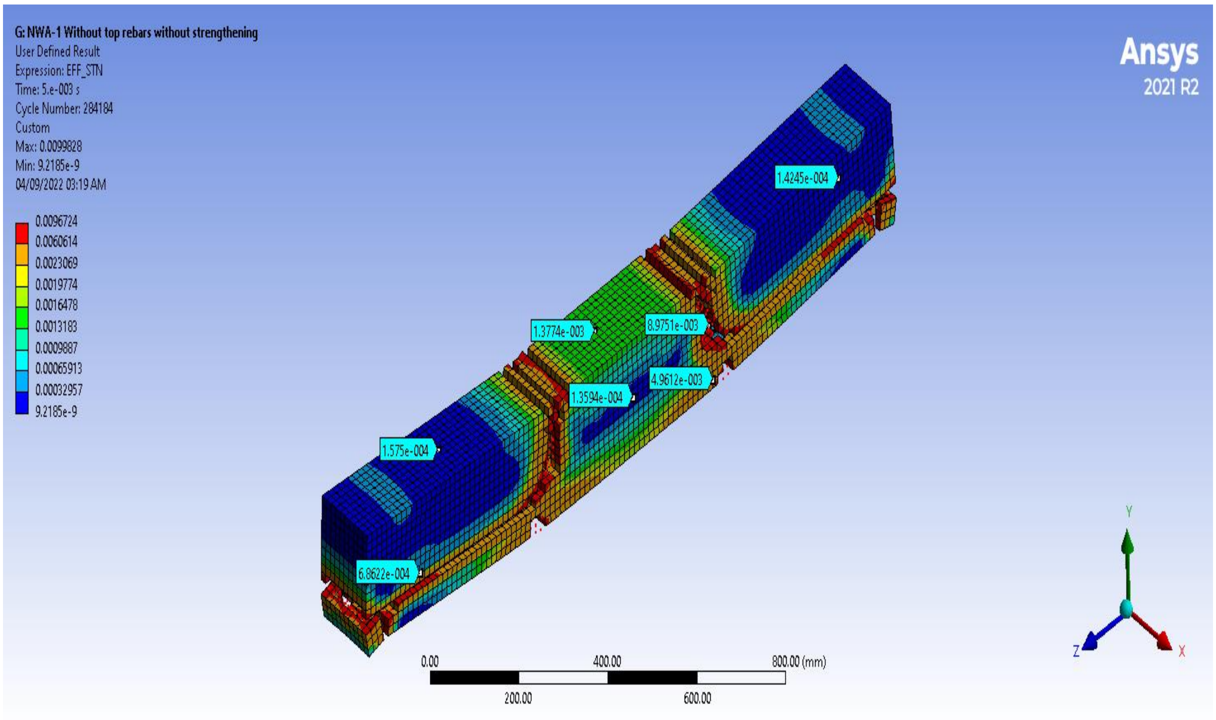

Figure 145(NWA-1/70.5MPa – Total strain of beam sample without strengthening and top rebars- Explicit Dynamic Analysis)

Maximum Stress

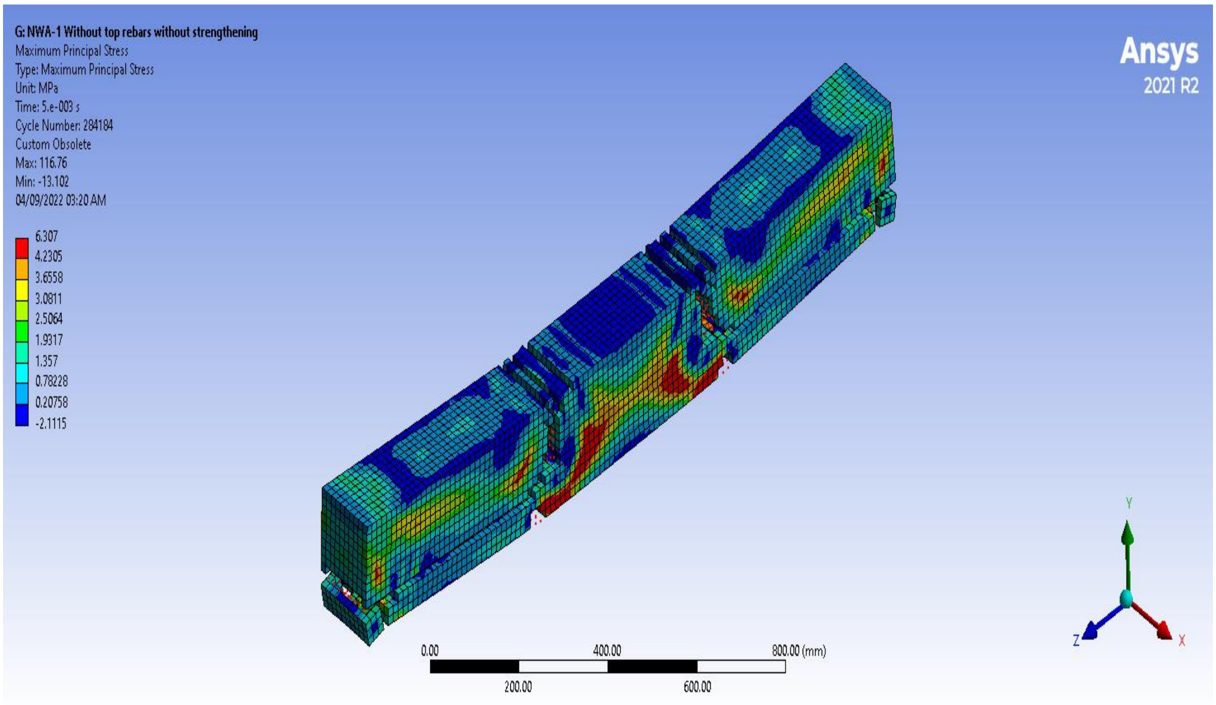

Figure 146(NWA-1/70.5MPa –Maximum Stress of beam sample without strengthening and top rebars- Explicit Dynamic Analysis)

The Damage Pattern

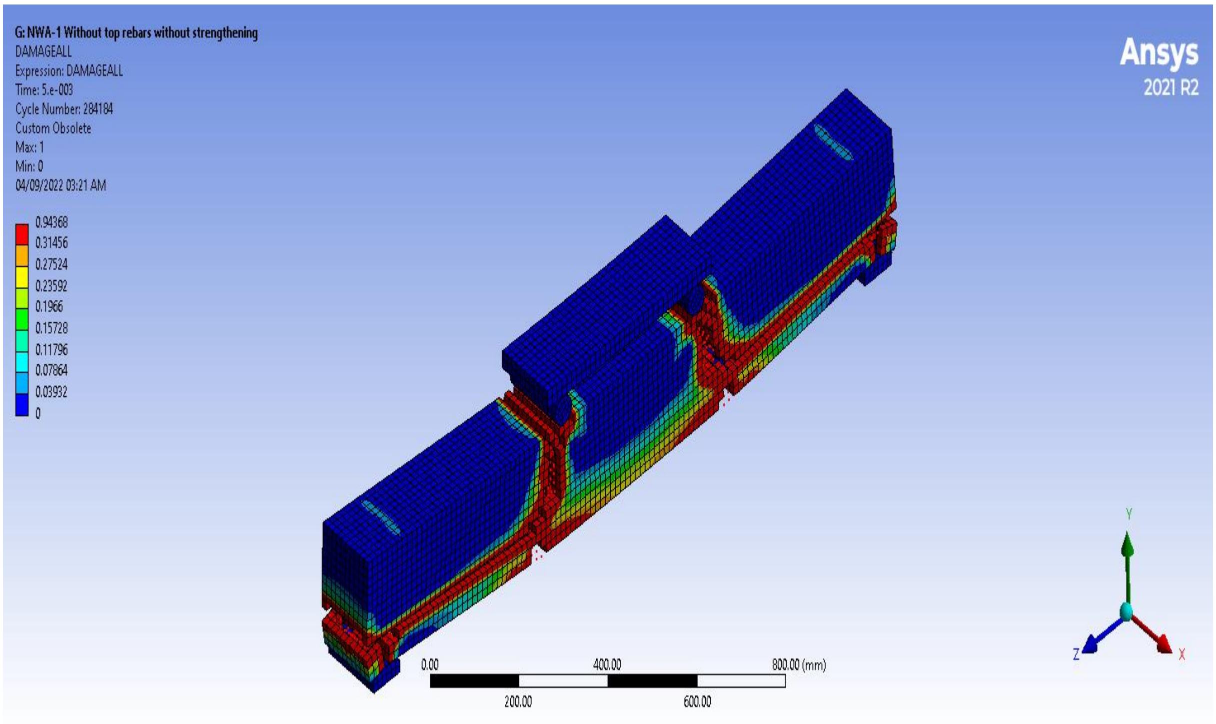

Figure 147(NWA-1/70.5MPa – Damage Pattern of beam sample without strengthening and top rebars- Explicit Dynamic Analysis)

As we can see the shear damage cracks and concrete failures.

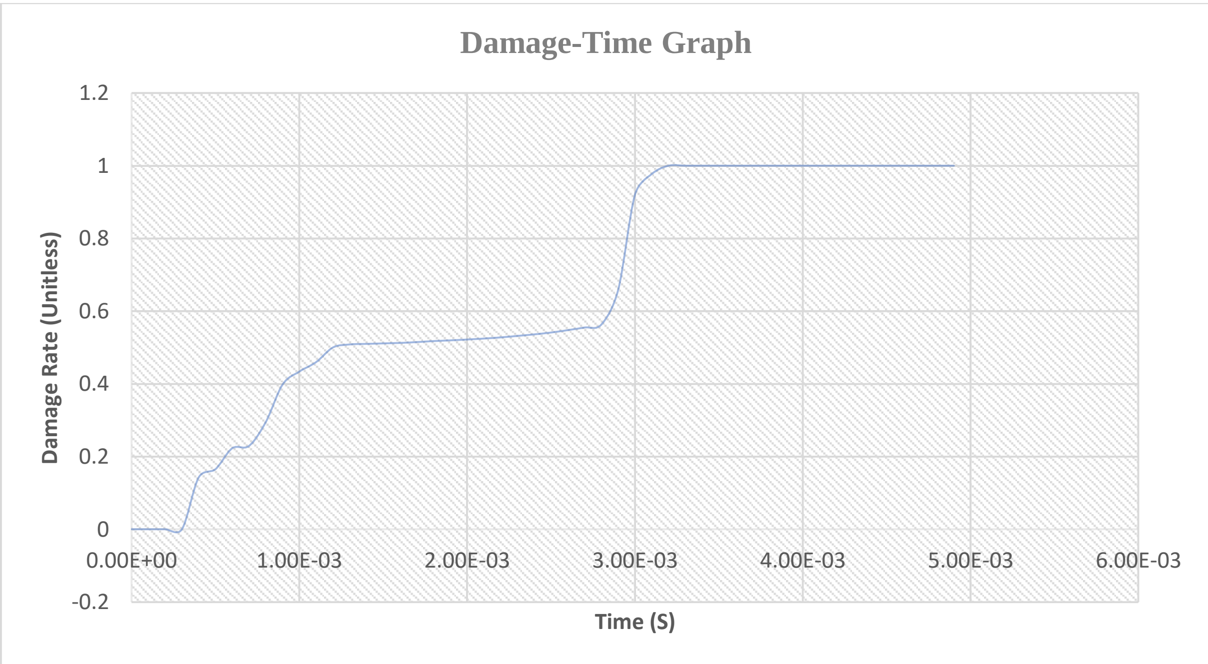

Figure 148(NWA-1/70.5MPa – Damage pattern graph of beam sample without strengthening and top rebars- Explicit Dynamic Analysis)

5-Static Non-Linear Analysis – With Top Rebars and Strengthening

Geometry and loads

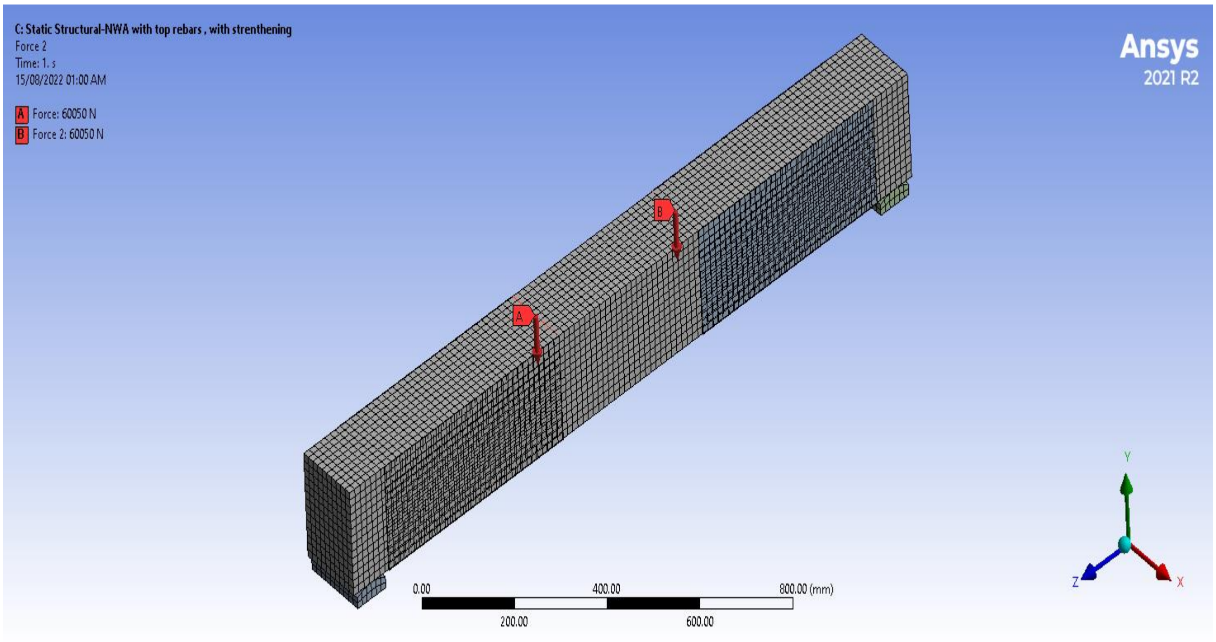

Figure 149(NWA-1/70.5MPa – Geometry & loads of beam sample with strengthening and top rebars- Static Nonlinear Analysis)

The ultimate load has been divided in to loads which is 120.1/2 =60.05KN.

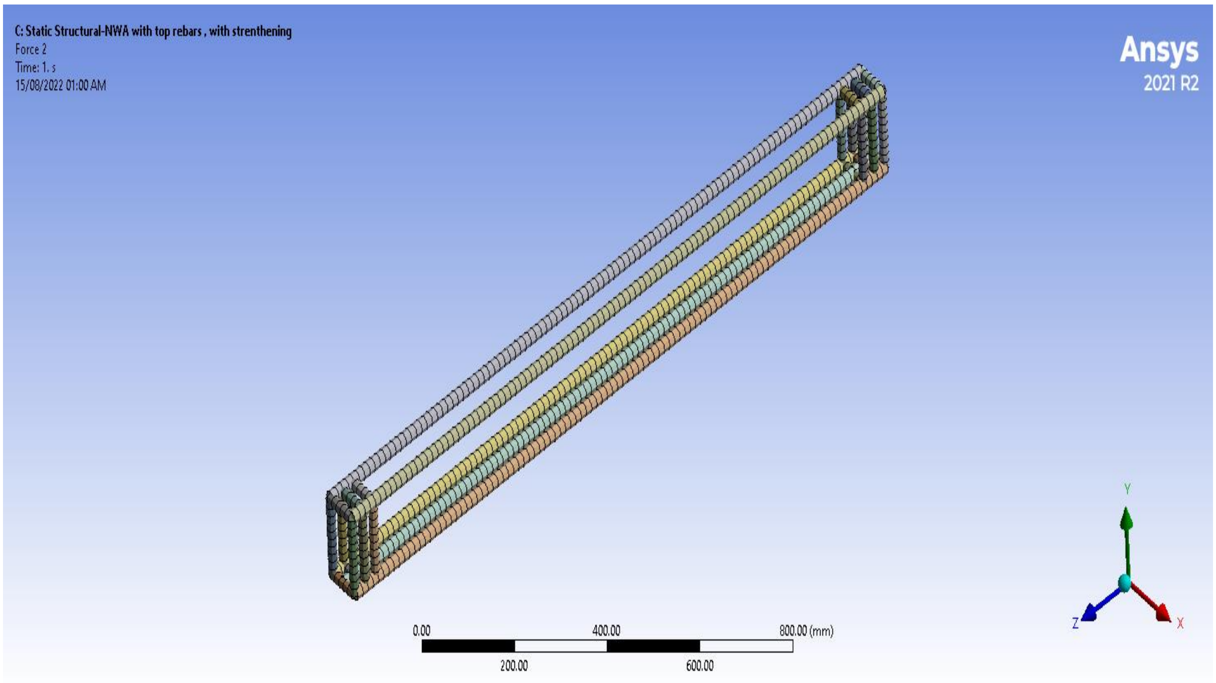

Figure 150(NWA-1/70.5MPa –Rebars of beam sample with strengthening- Static Nonlinear Analysis)

Deformations

Total Deformations

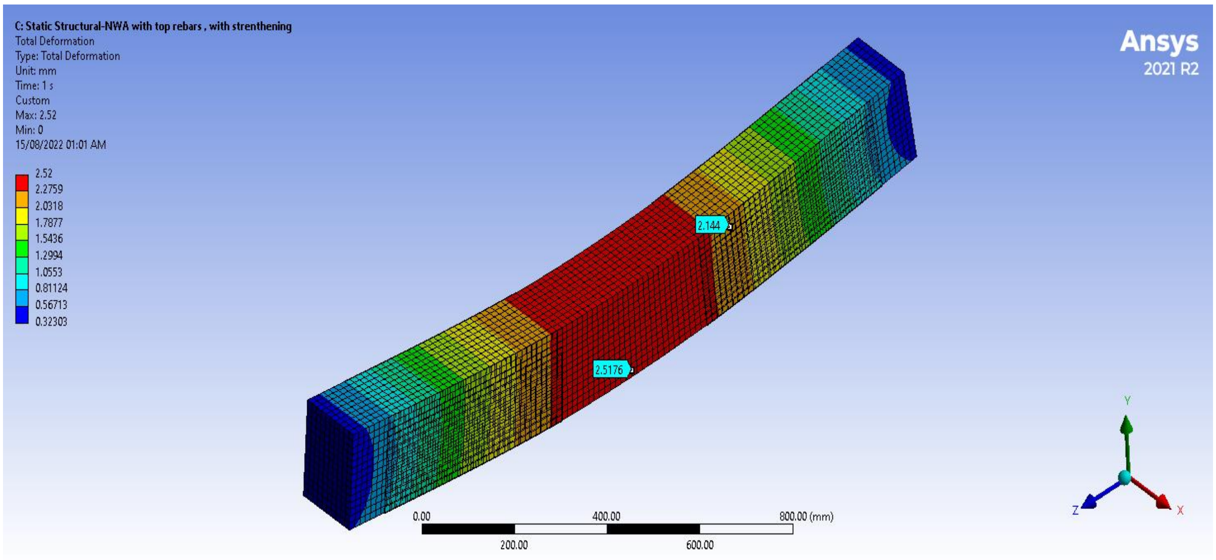

Figure 151(NWA-1/70.5MPa – Total deflections of beam sample with strengthening and top rebars- Static Nonlinear Analysis)

The value is 2.52 mm.

Directional Deformation (Y-Direction)

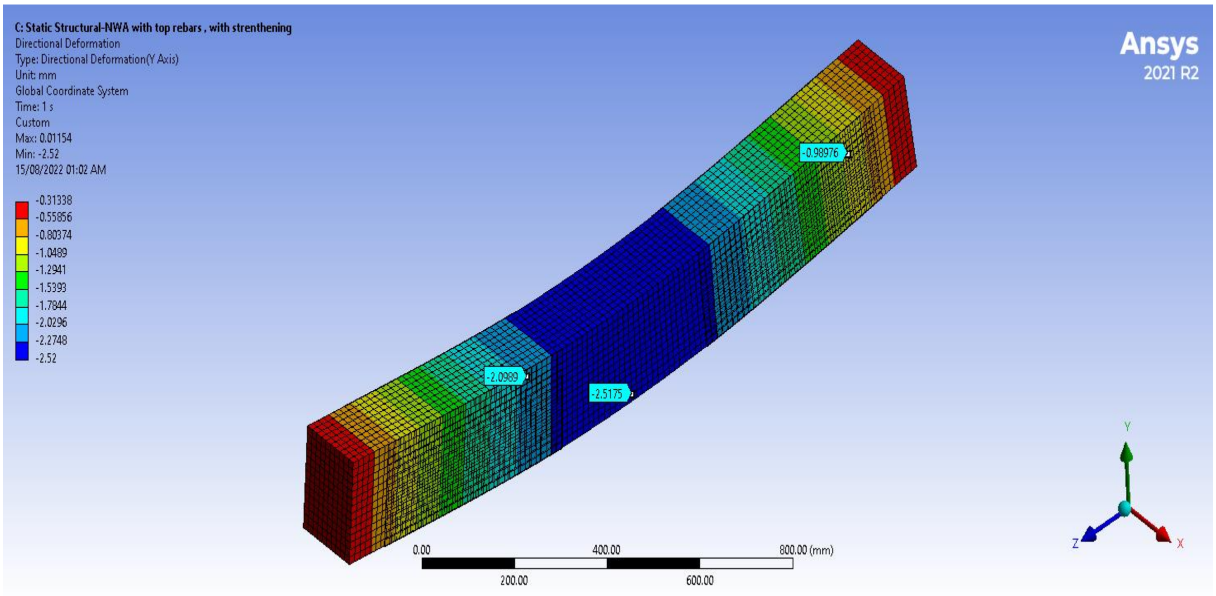

Figure 152(NWA-1/70.5MPa – Directional deflections (Y-Dim.) of beam sample with strengthening and top rebars- Static Nonlinear Analysis)

The value is 2.52 mm.

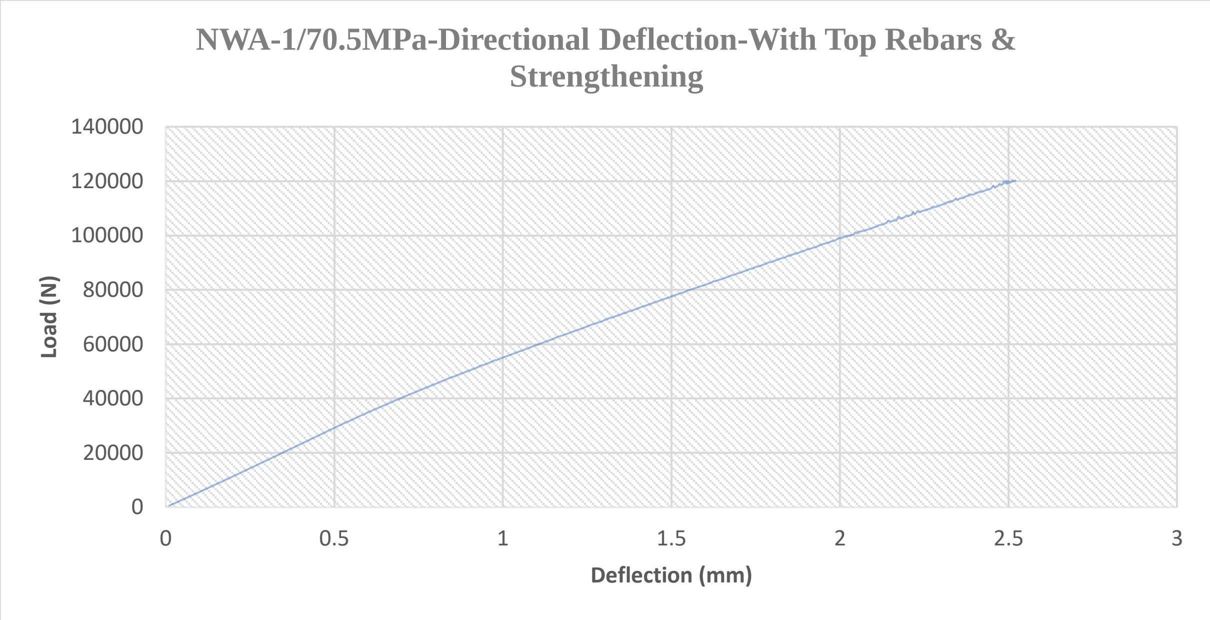

Figure 153(NWA-1/70.5MPa – Directional deflections (Y-Dim.) graph of beam sample with strengthening and top rebars- Static Nonlinear Analysis)

Normal Stress (Concrete)

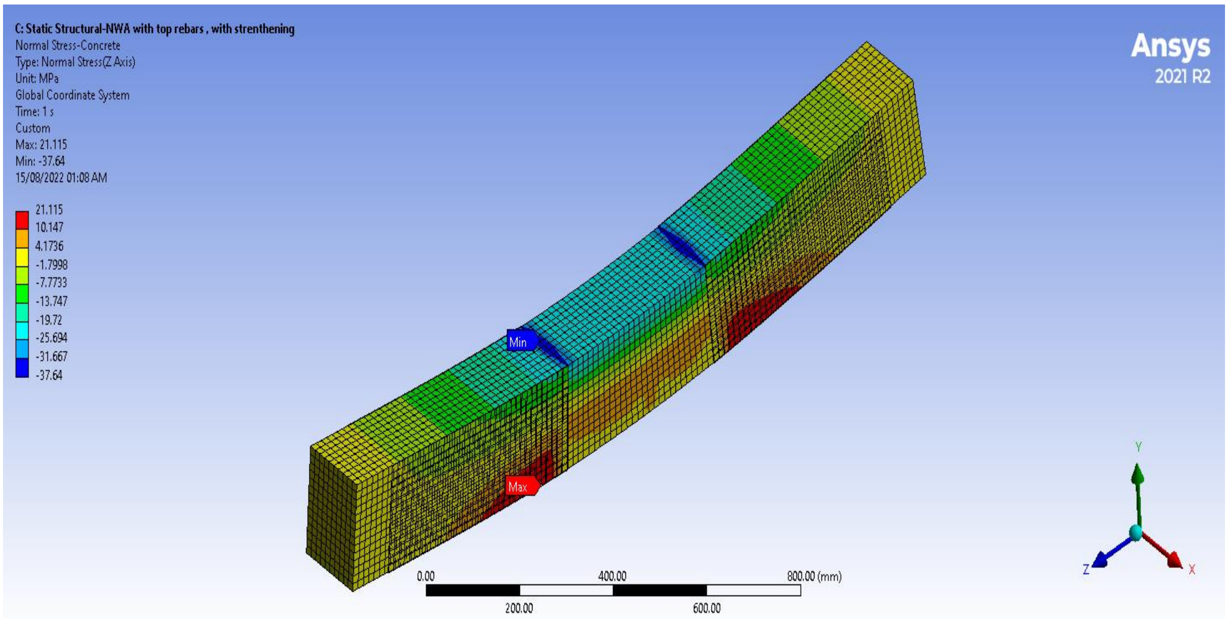

Figure 154(NWA-1/70.5MPa – Normal Stress (Concrete) of beam sample with strengthening and top rebars- Static Nonlinear Analysis)

The blue zones show the crushing from loading machine and the maximum value is 37.64 MPa, whereas the red zones indicate to tension.

Normal Stress (Rebars)

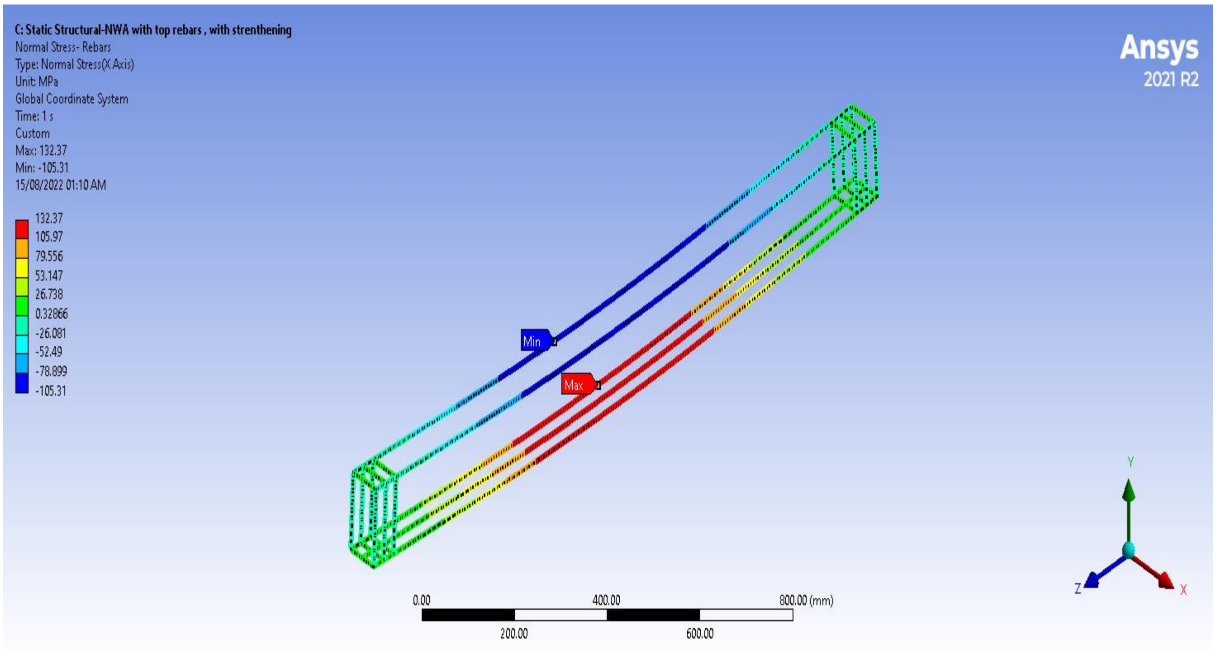

Figure 155(NWA-1/70.5MPa – Normal Stress (Rebars) of beam sample with strengthening and top rebars- Static Nonlinear Analysis)

The red zones show that the rebars is yielding by 132.37MPa, in the middle span due to tension.

Shear Stress

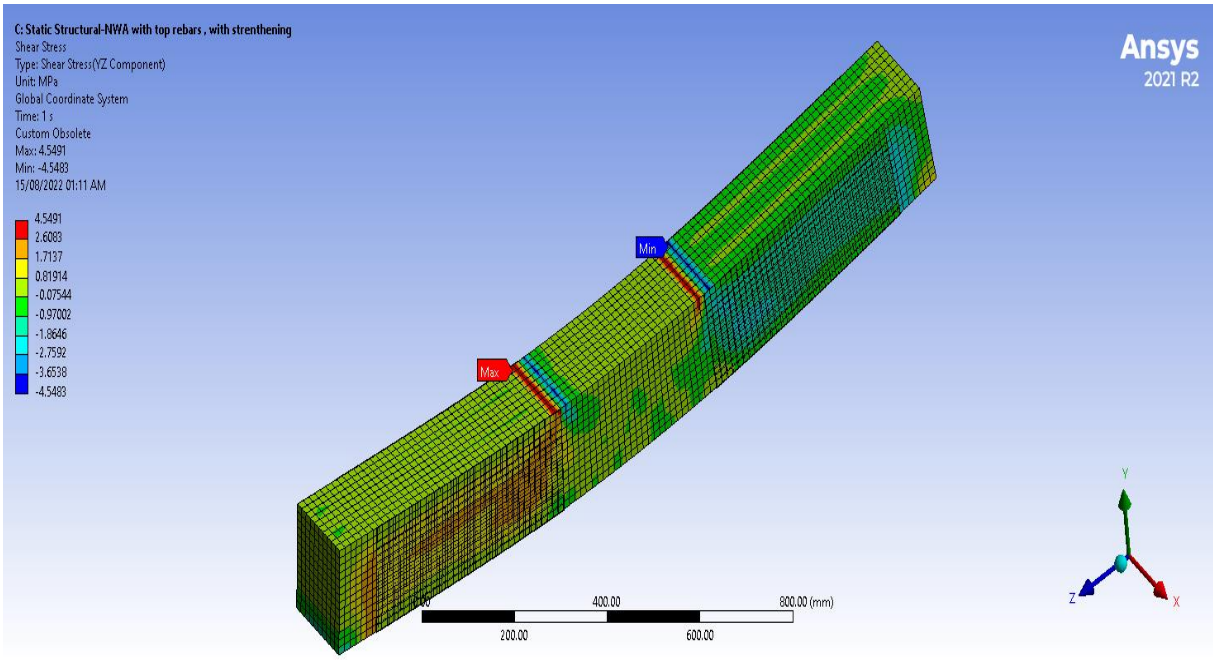

Figure 156(NWA-1/70.5MPa – Shear Stress of beam sample with strengthening and top rebars- Static Nonlinear Analysis)

Elastic Strain

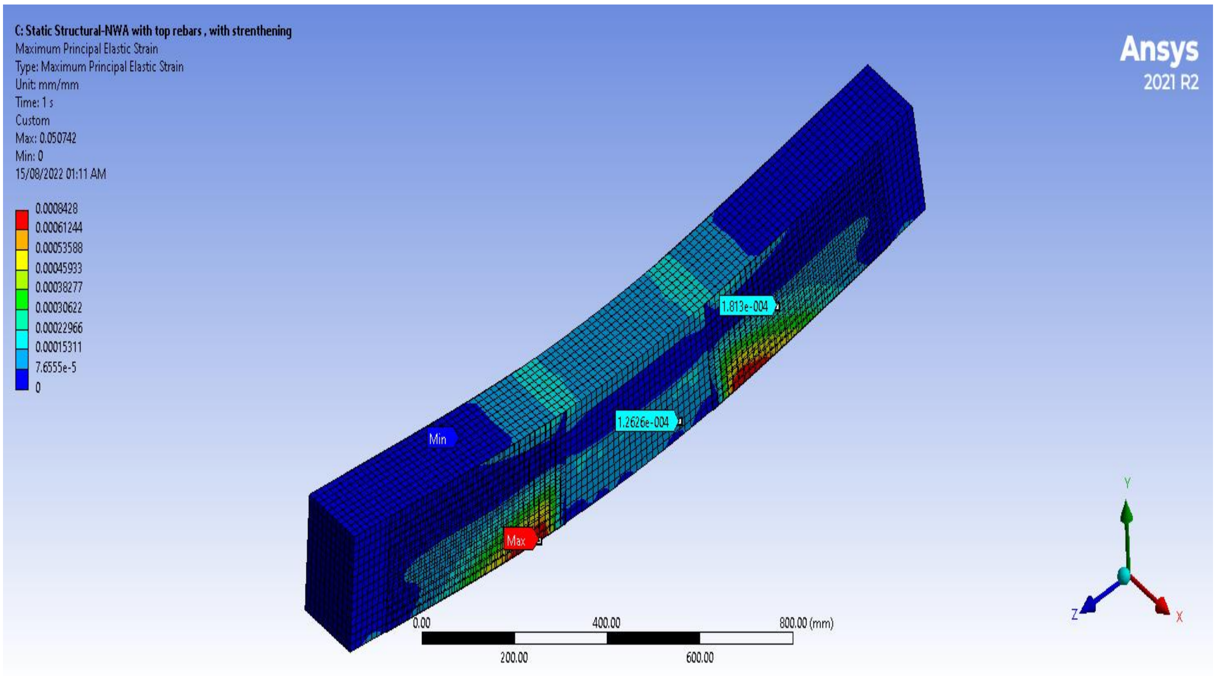

Figure 157(NWA-1/70.5MPa – Elastic strain of beam sample with strengthening and top rebars- Static Nonlinear Analysis)

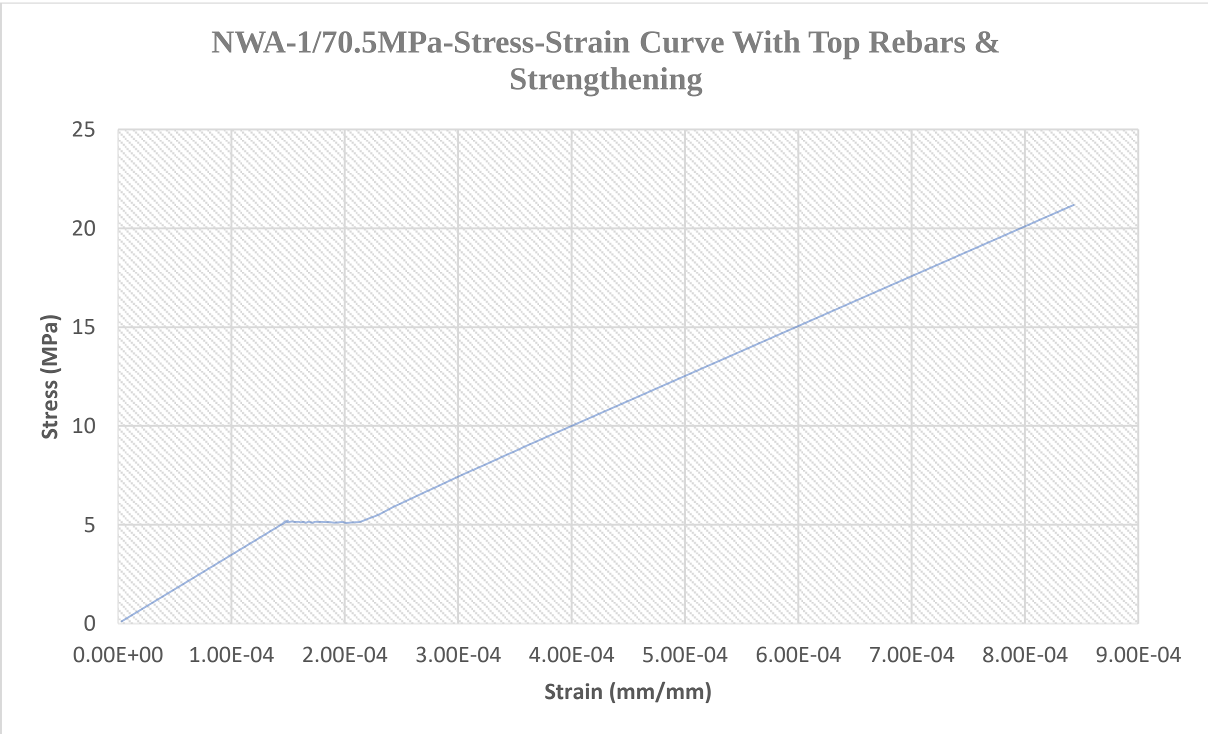

Figure 158(NWA-1/70.5MPa – Stress & Strain graph of beam sample with strengthening and top rebars- Static Nonlinear Analysis)

6-Explicit Dynamic-With Top Rebars & Strengthening

Geometry and loads

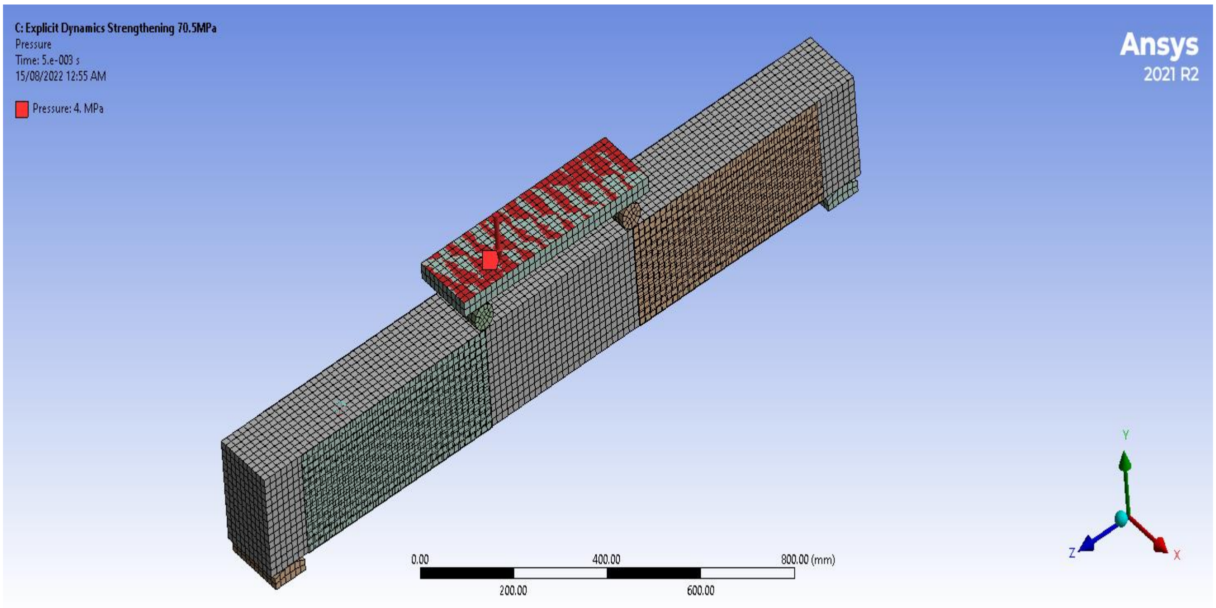

Figure 159(NWA-1/70.5MPa – Geometry & loads of beam sample with strengthening and top rebars- Explicit Dynamic Analysis)

The ultimate load has been transferred to be as a pressure load which is 4.0 MPa as shown above with rate loading 0.6mm/min

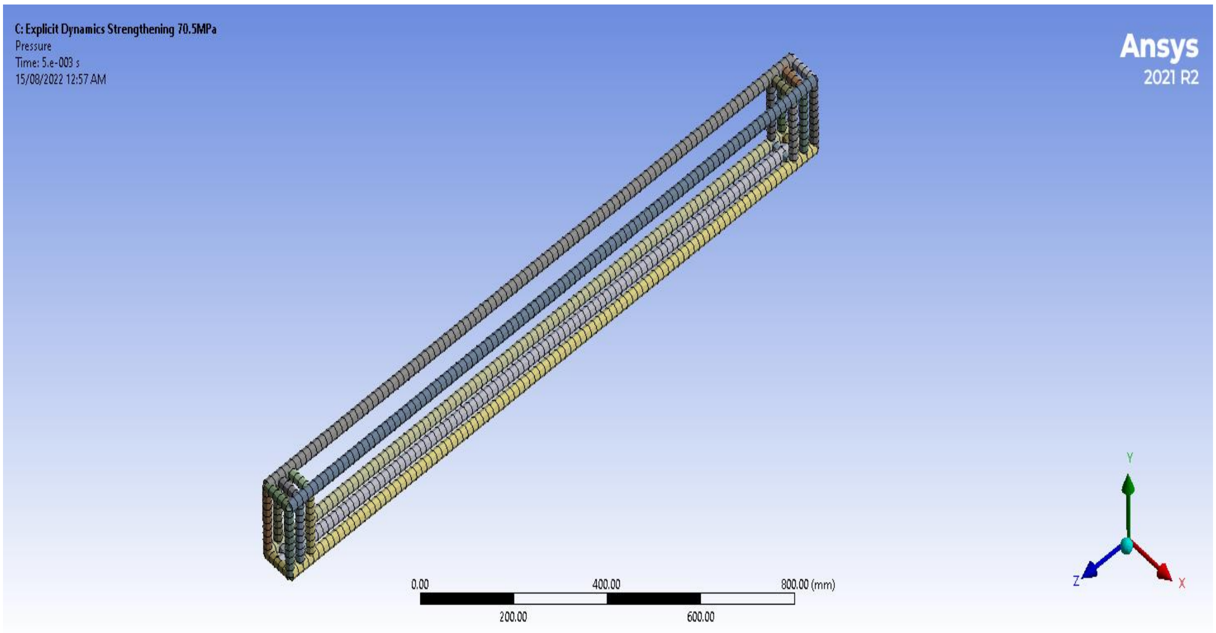

Figure 160(NWA-1/70.5MPa – Rebars of beam sample with strengthening – Explicit Dynamic Analysis)

Deformations

Total Deformations

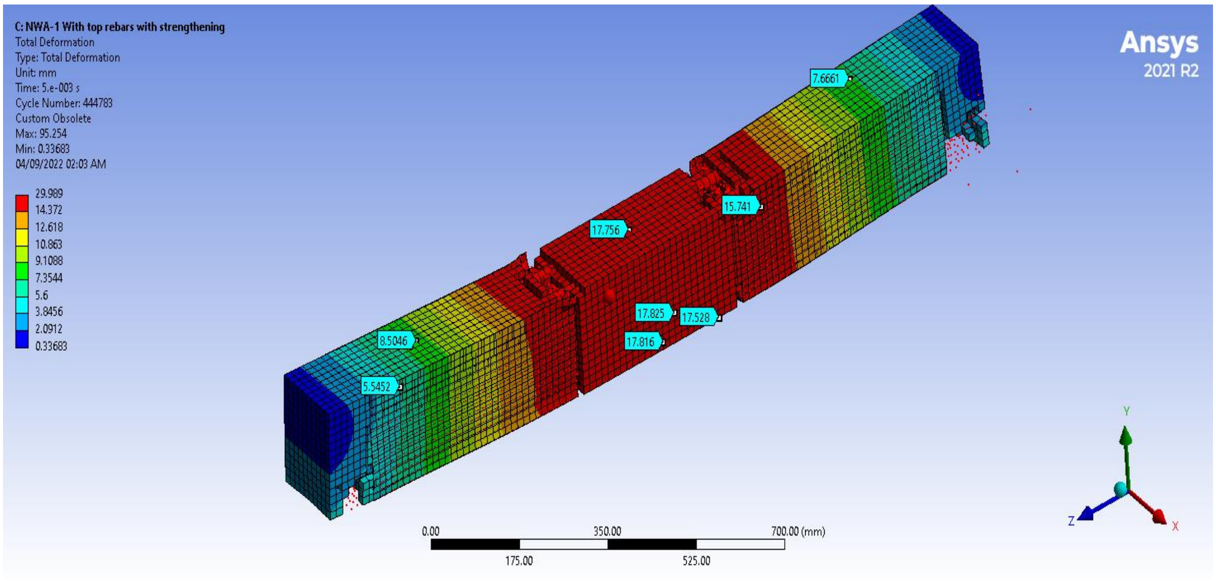

Figure 161(NWA-1/70.5MPa – Total deflections of beam sample with strengthening and top rebars- Explicit Dynamic Analysis)

The value is 17.825 mm.

Directional Deformation (Y-Direction)-Concrete

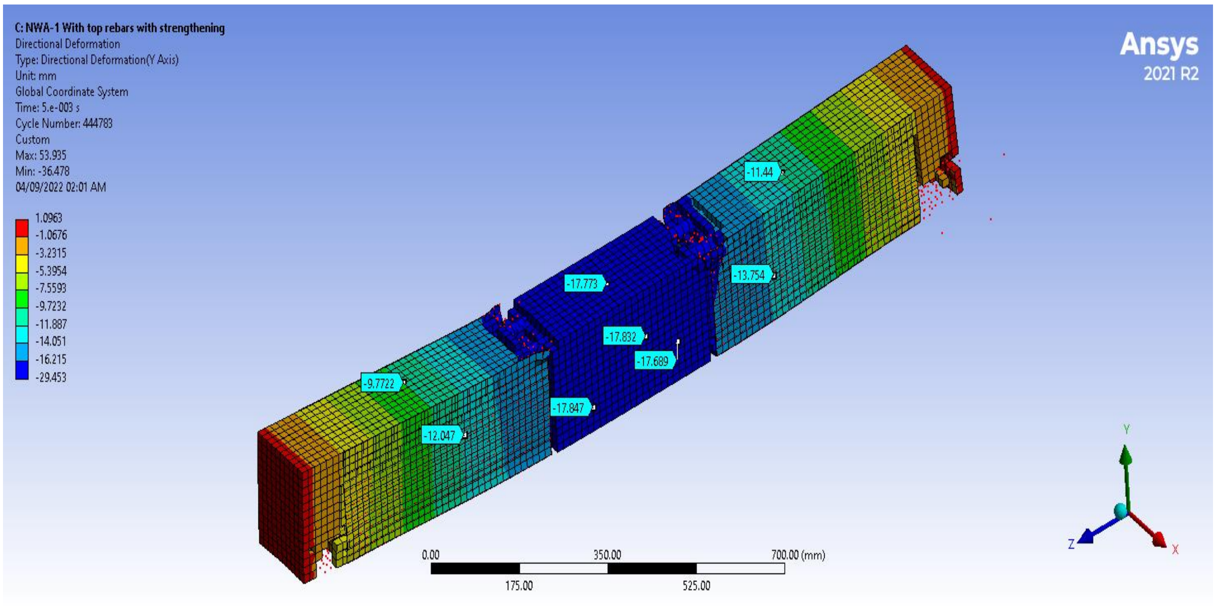

Figure 162(NWA-1/70.5MPa – Directional deflection (Y-Dim.) of beam sample with strengthening and top rebars- Explicit Dynamic Analysis)

The value is 17.847 mm

Directional Deformation (Y-Direction)- Rebars

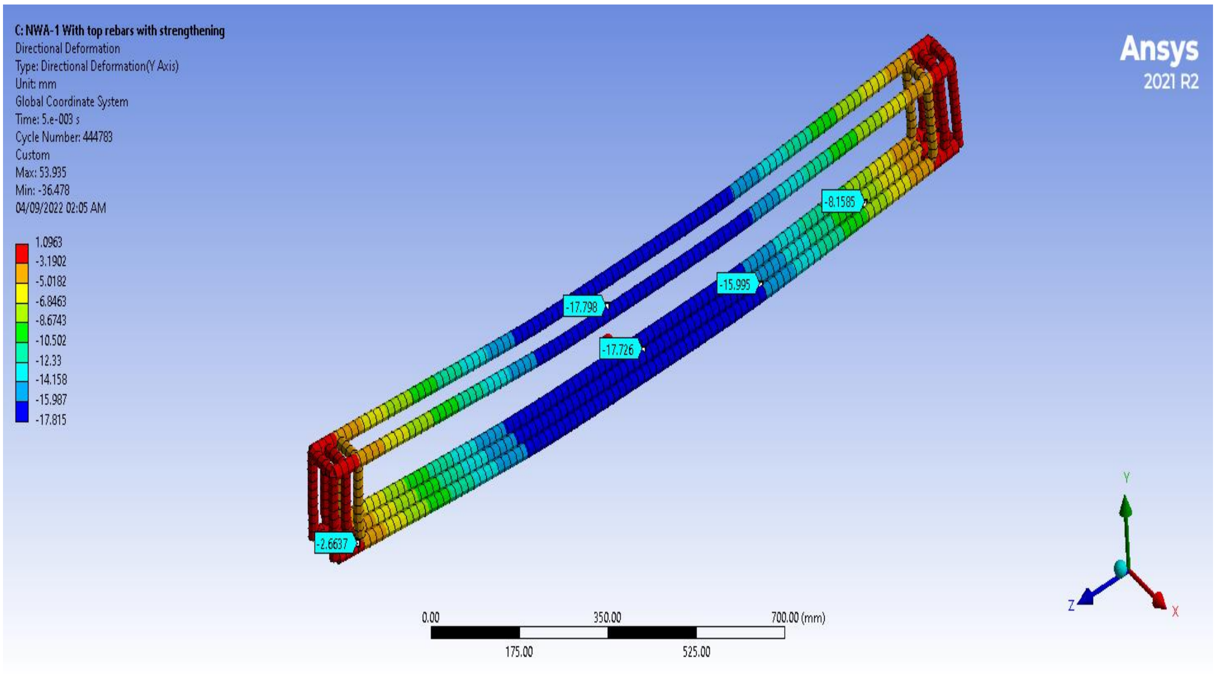

Figure 163(NWA-1/70.5MPa –Directional deflection (Y-Dim.) Rebars of beam sample with strengthening - Explicit Dynamic Analysis)

Normal strain

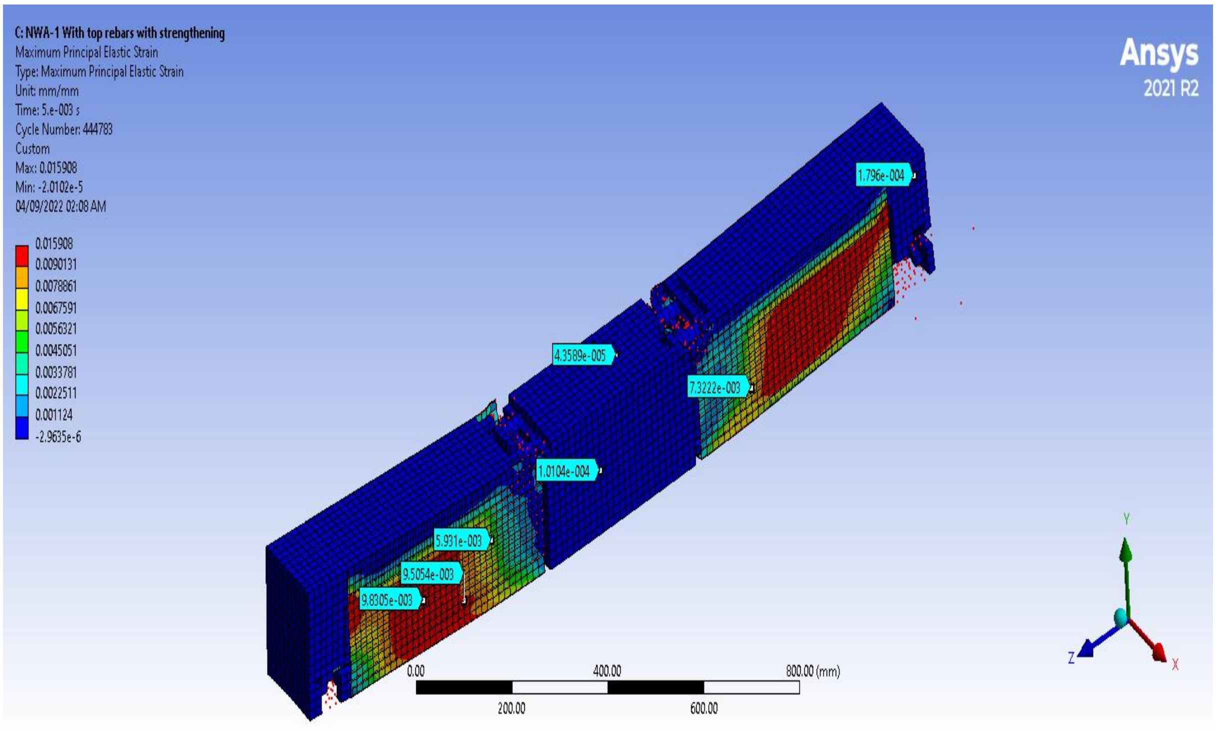

Figure 164(NWA-1/70.5MPa –Normal strain of beam sample with strengthening and top rebars- Explicit Dynamic Analysis)

Shear Stress

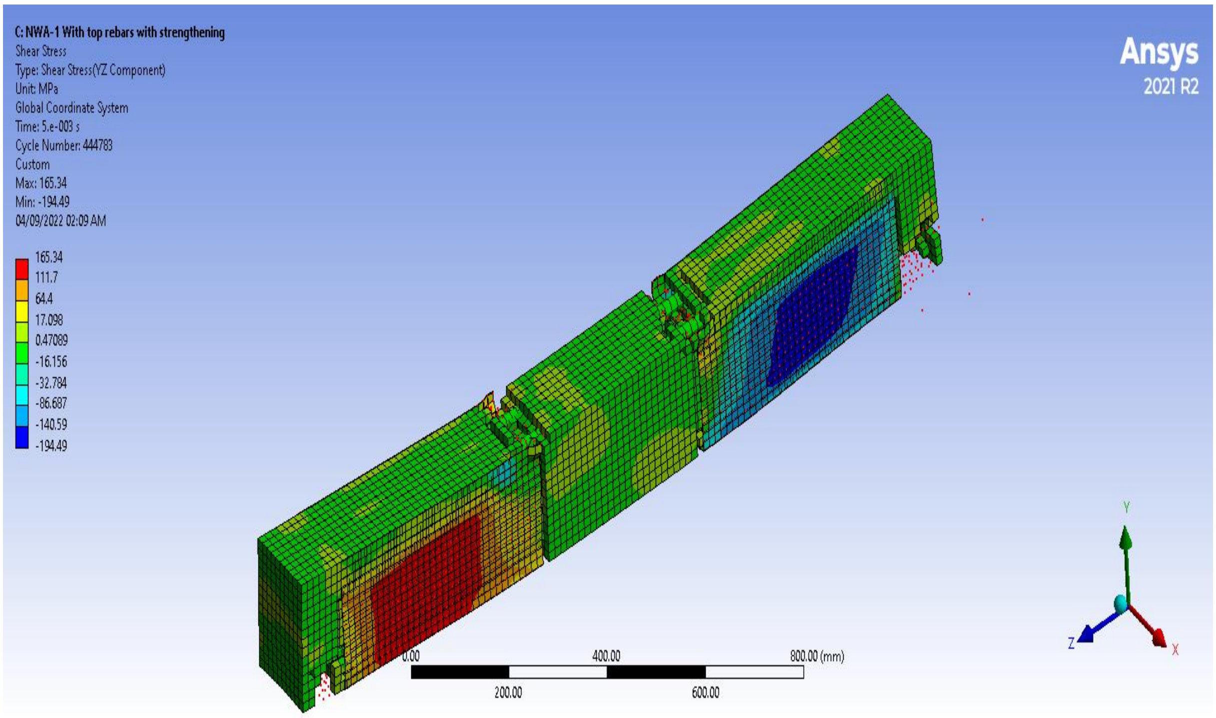

Figure 165(NWA-1/70.5MPa – Shear stress of beam sample with strengthening and top rebars- Explicit Dynamic Analysis)

Total shape strain

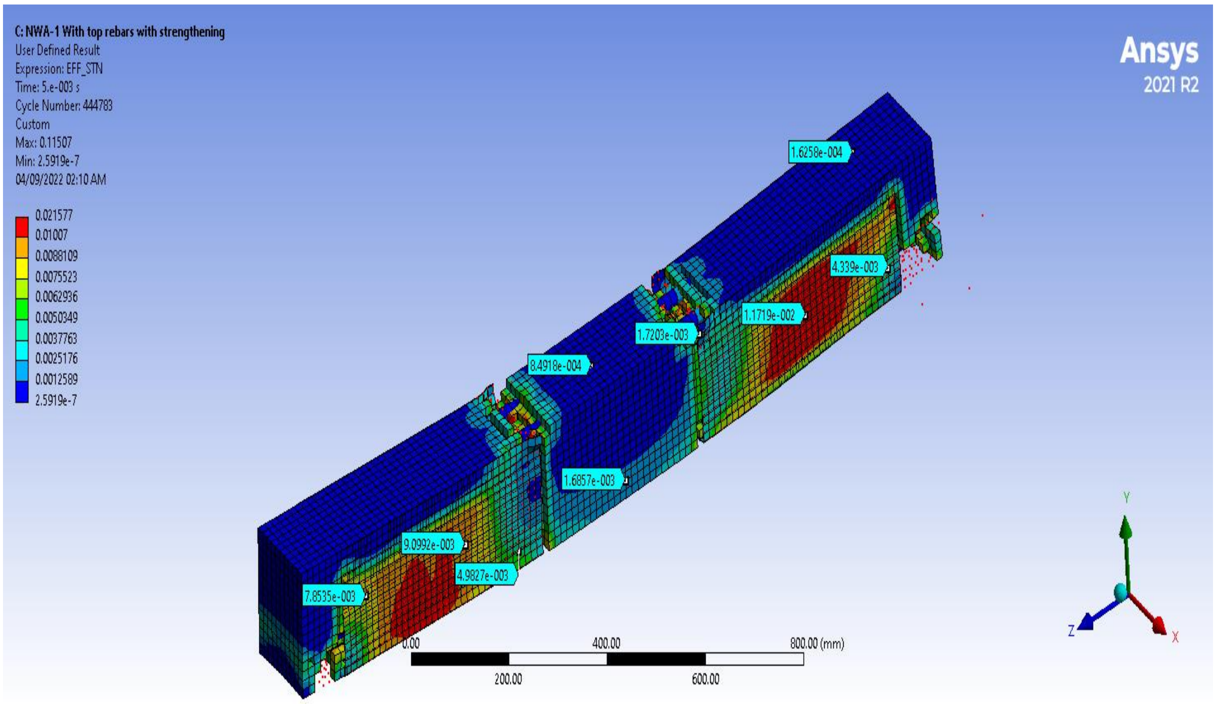

Figure 166(NWA-1/70.5MPa – Total strain of beam sample with strengthening and top rebars- Explicit Dynamic Analysis)

Maximum Stress

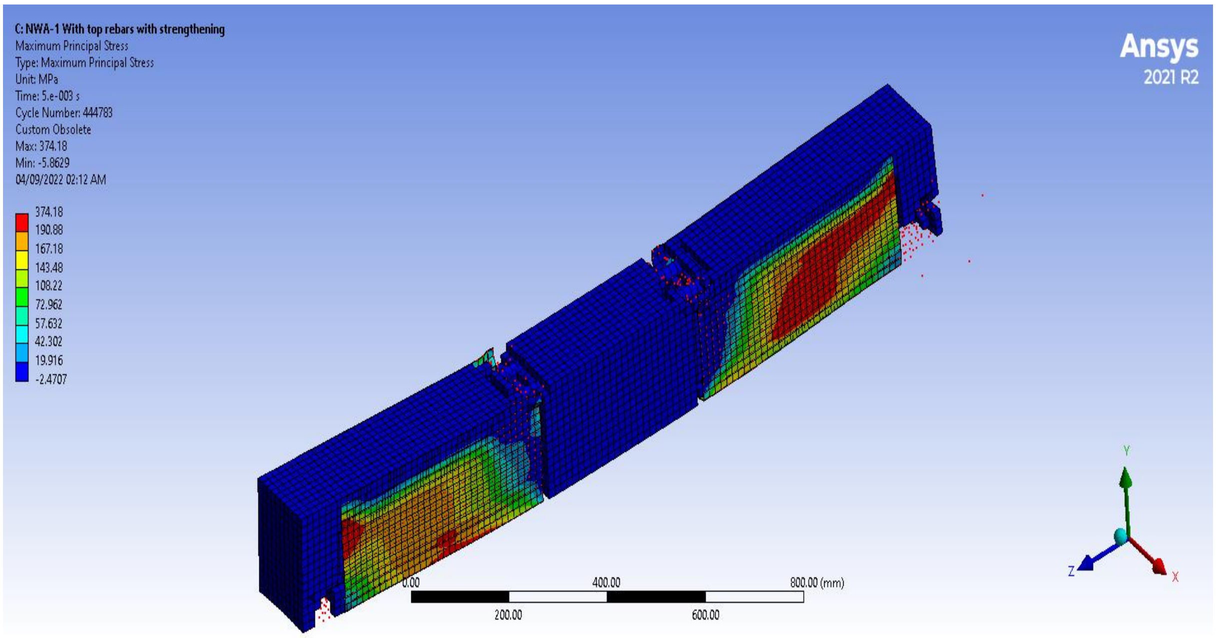

Figure 167(NWA-1/70.5MPa – Maximum stress of beam sample with strengthening and top rebars- Explicit Dynamic Analysis)

The Damage Pattern

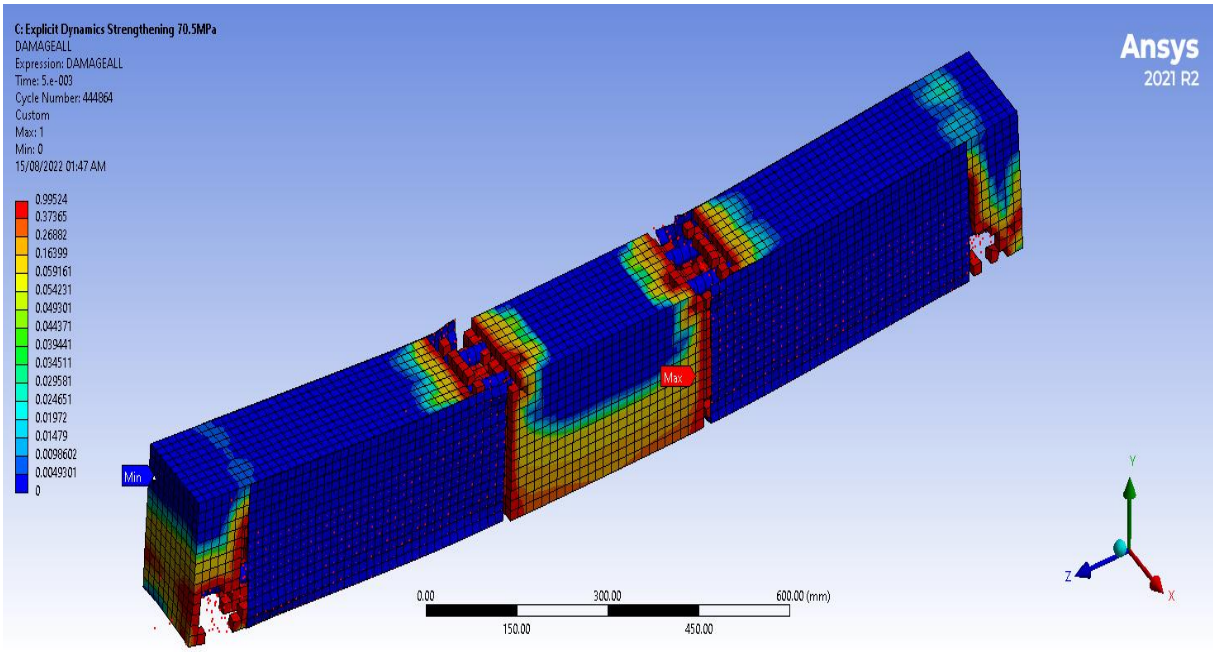

Figure 168(NWA-1/70.5MPa – Damage pattern-1 of beam sample with strengthening and top rebars- Explicit Dynamic Analysis)

As we can see the shear damage cracks in red and CFRP debonding on edges of concrete failure.

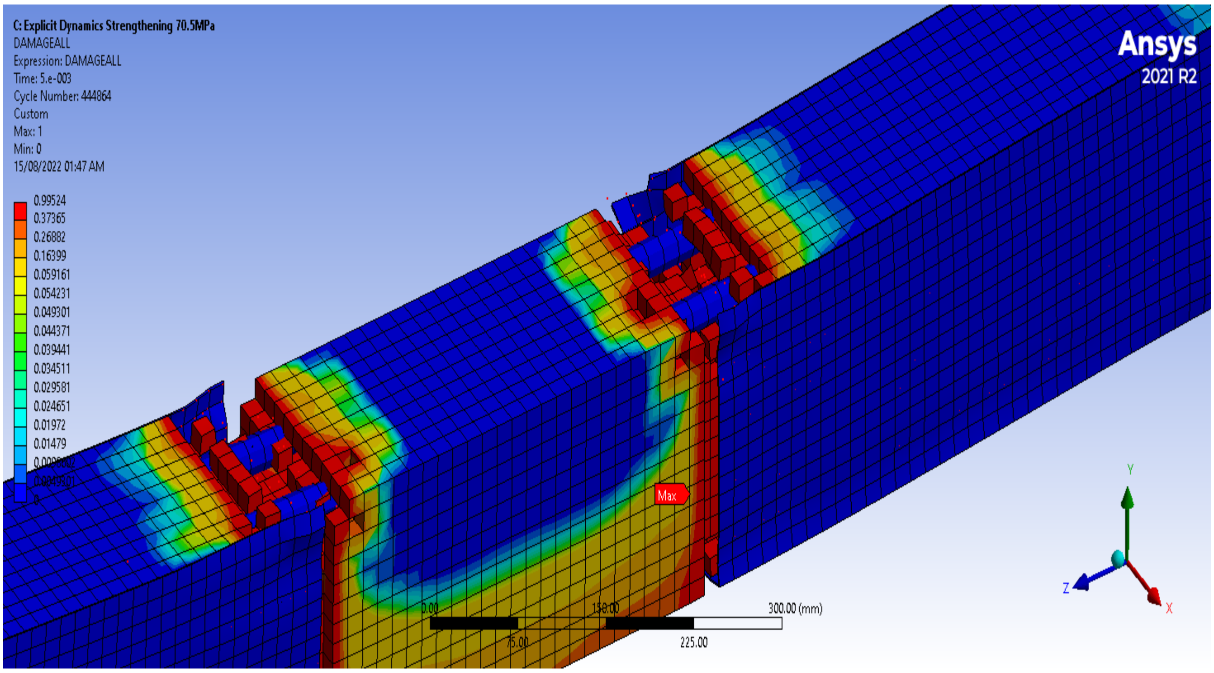

Figure 169(NWA-1/70.5MPa – Damage pattern-2 of beam sample with strengthening and top rebars- Explicit Dynamic Analysis)

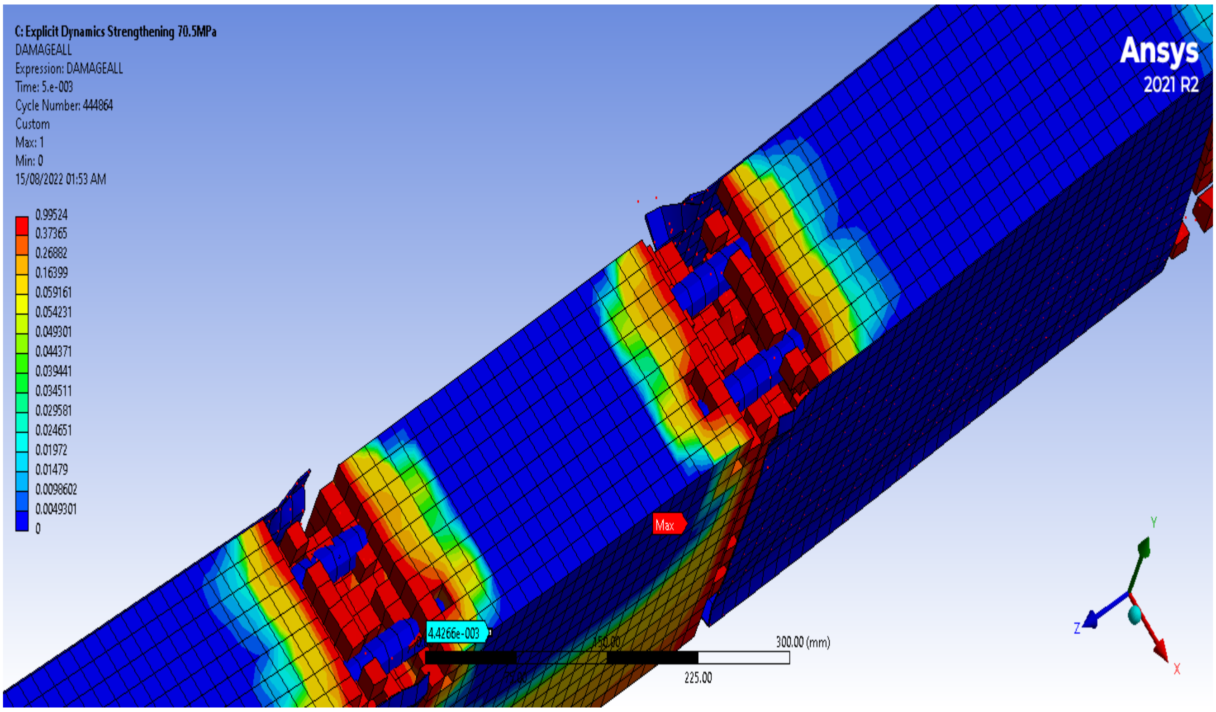

Figure 170(NWA-1/70.5MPa – Damage pattern-3 of beam sample with strengthening and top rebars- Explicit Dynamic Analysis)

CFRP laminates due to ultimate load has been debonding as shown in images above

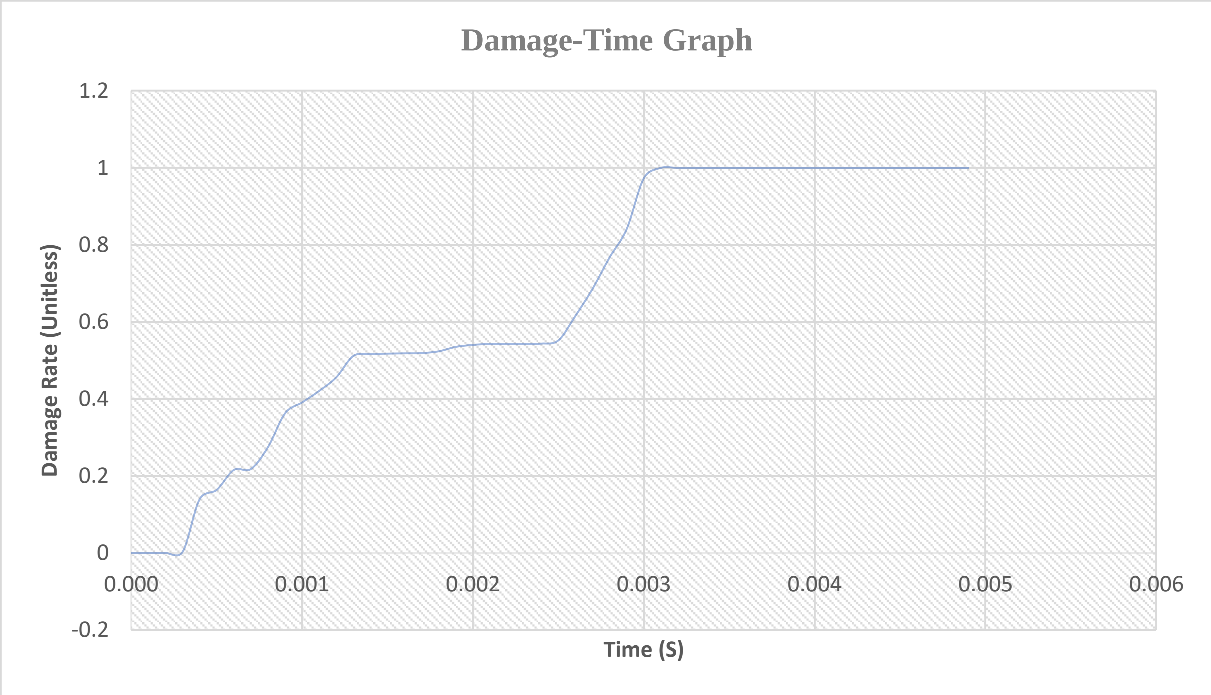

Figure 171(NWA-1/70.5MPa – Damage pattern graph of beam sample with strengthening and top rebars- Explicit Dynamic Analysis)

7-Static Non-Linear Analysis – Without Top Rebars and With Strengthening

Geometry and loads

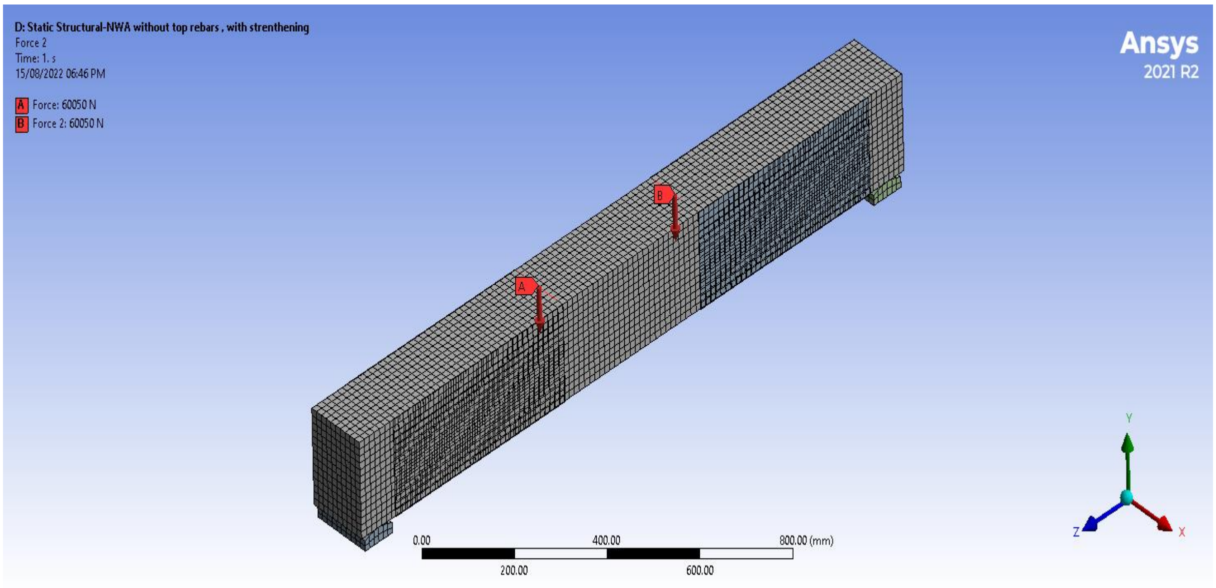

Figure 172(NWA-1/70.5MPa – Geometry & Loads of beam sample with strengthening and without top rebars- Static Nonlinear Analysis)

The ultimate load has been divided in to loads which is 120.1/2 =60.05KN.

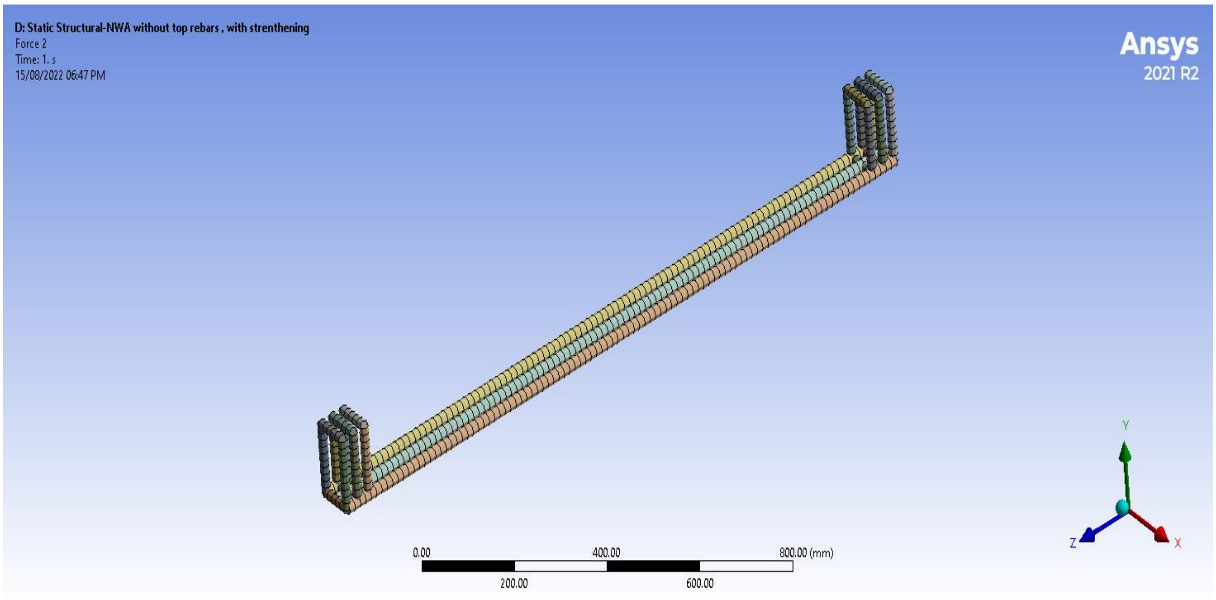

Figure 173(NWA-1/70.5MPa – Rebars of beam sample without strengthening - Static Nonlinear Analysis)

Deformations

Total Deformations

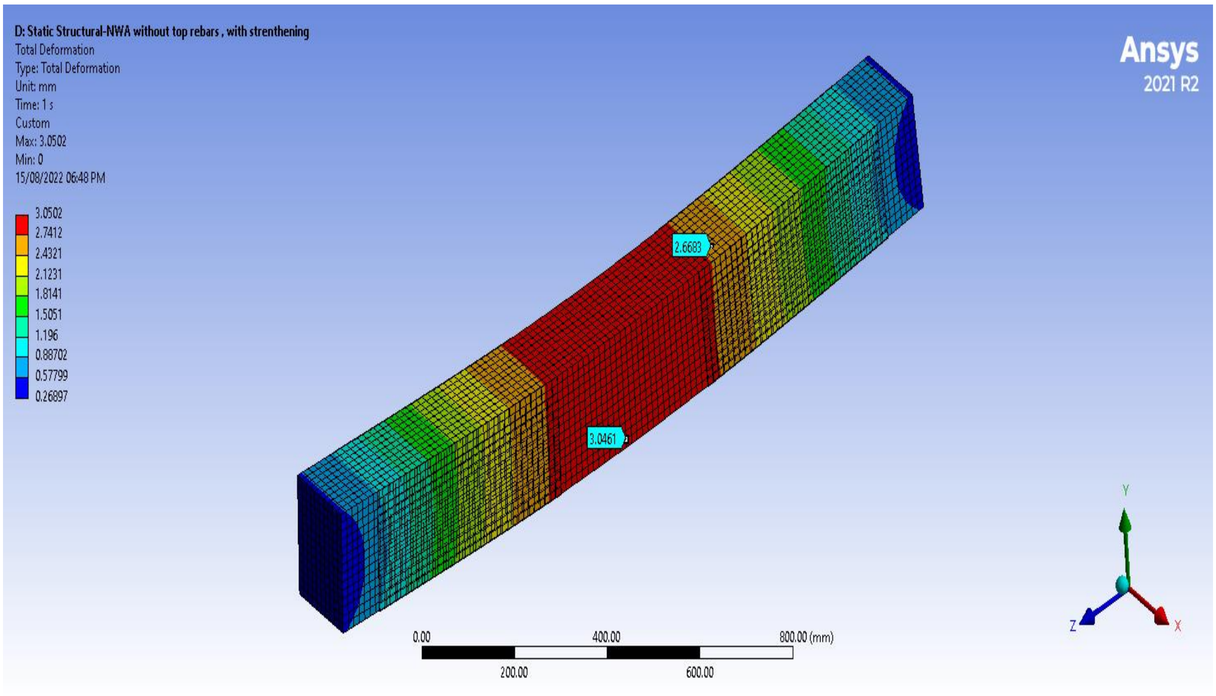

Figure 174(NWA-1/70.5MPa – Total deflections of beam sample with strengthening and without top rebars- Static Nonlinear Analysis)

The value is 3.050 mm.

Directional Deformation (Y-Direction)

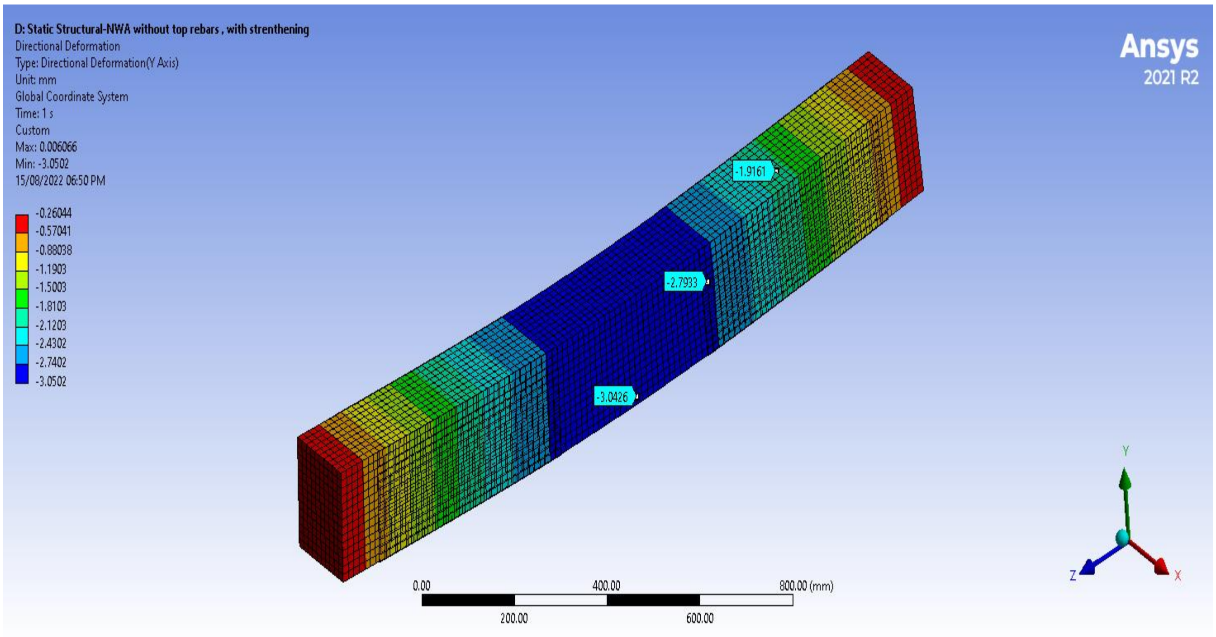

Figure 175(NWA-1/70.5MPa – Directional deflections (Y-Dim.) of beam sample with strengthening and without top rebars-Static Nonlinear Analysis)

The value is 3.050 mm.

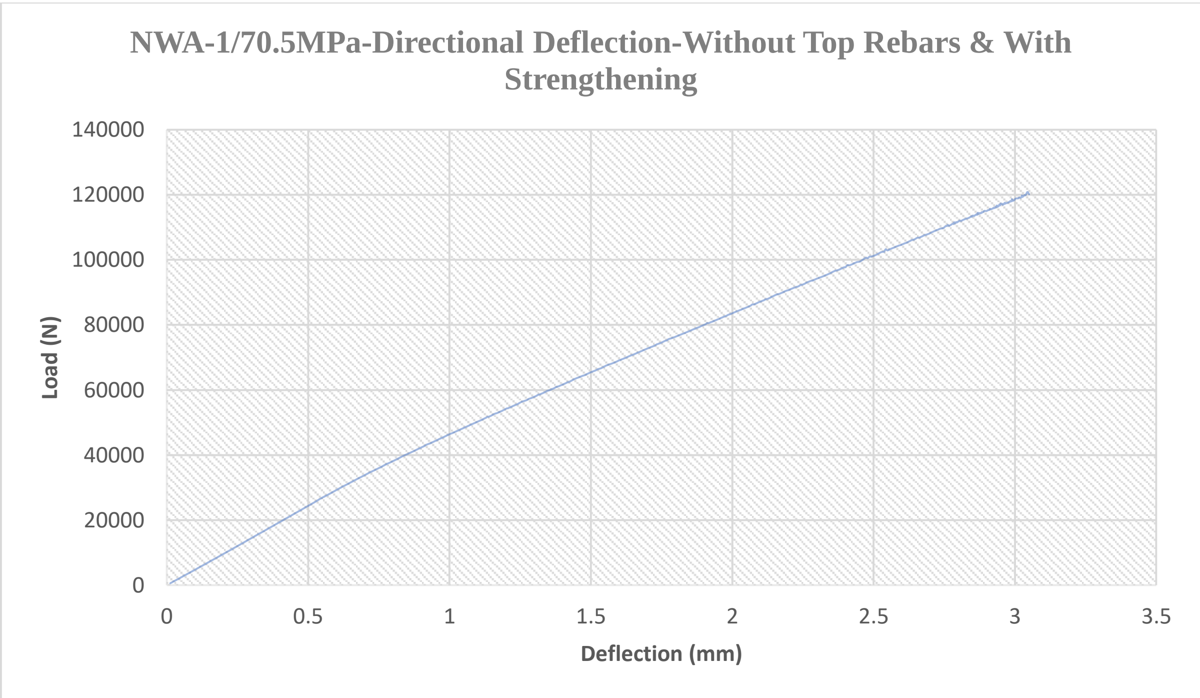

Figure 176(NWA-1/70.5MPa – Directional deflections (Y-Dim.) of beam sample with strengthening and without top rebars-Static Nonlinear Analysis)

Normal Stress (Concrete)

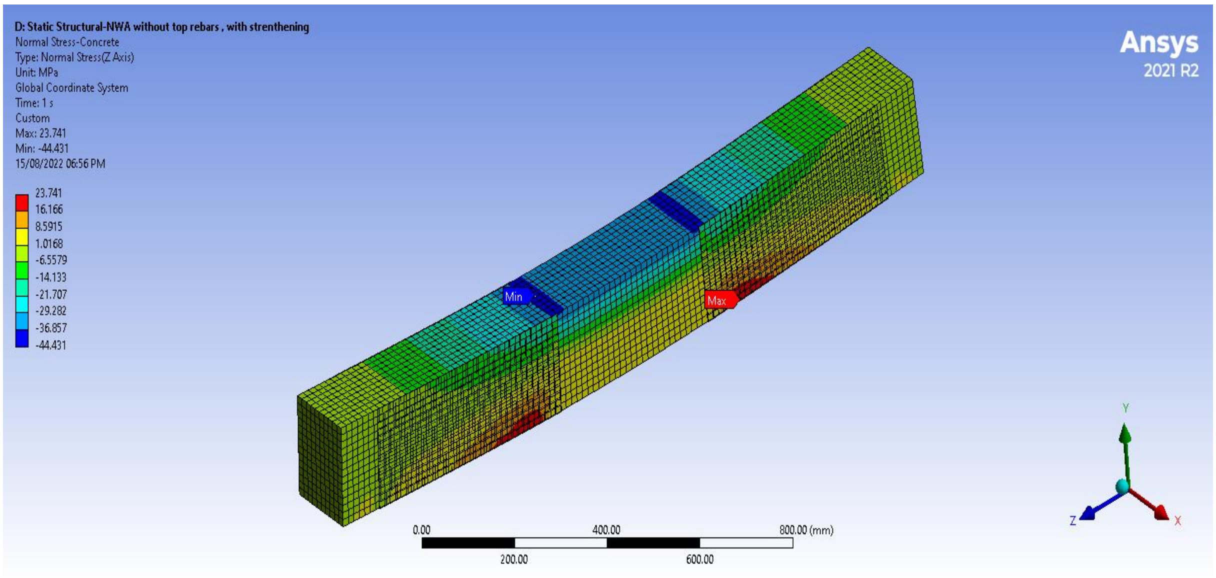

Figure 177(NWA-1/70.5MPa – Normal stress (Concrete) of beam sample with strengthening and without top rebars- Static Nonlinear Analysis)

The blue zones show the crushing from loading machine and the maximum value is 44.431 MPa, whereas the red zones indicate to tension.

Normal Stress (Rebars)

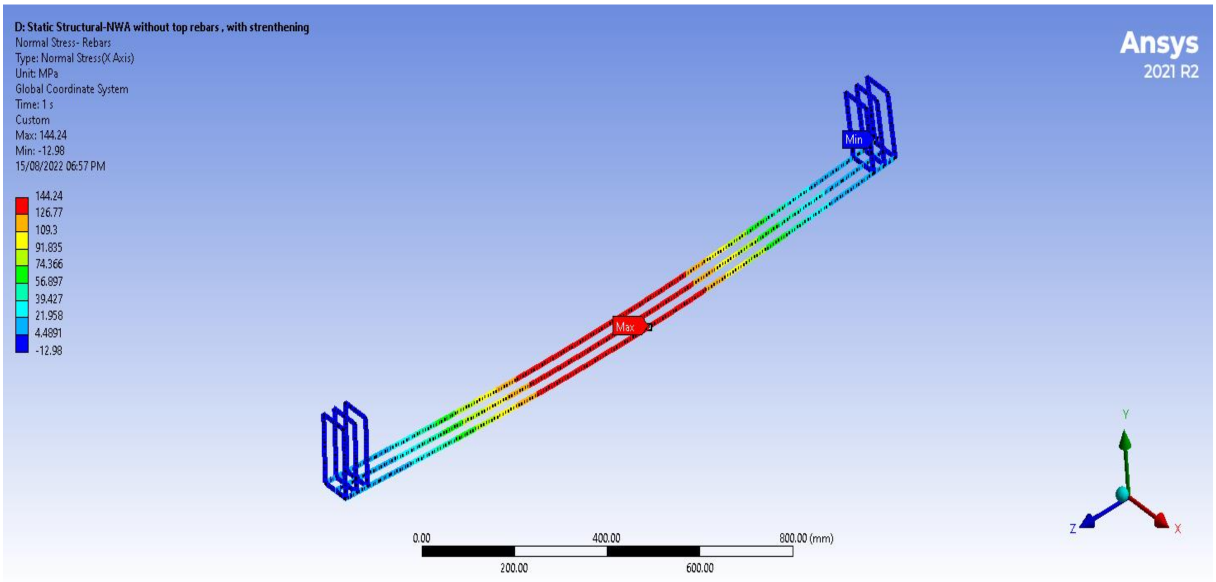

Figure 178(NWA-1/70.5MPa – Normal stress (Rebars) of beam sample with strengthening and without top rebars- Static Nonlinear Analysis)

The red zones show that the rebars is yielding by 144.24MPa, in the middle span due to tension.

Shear Stress

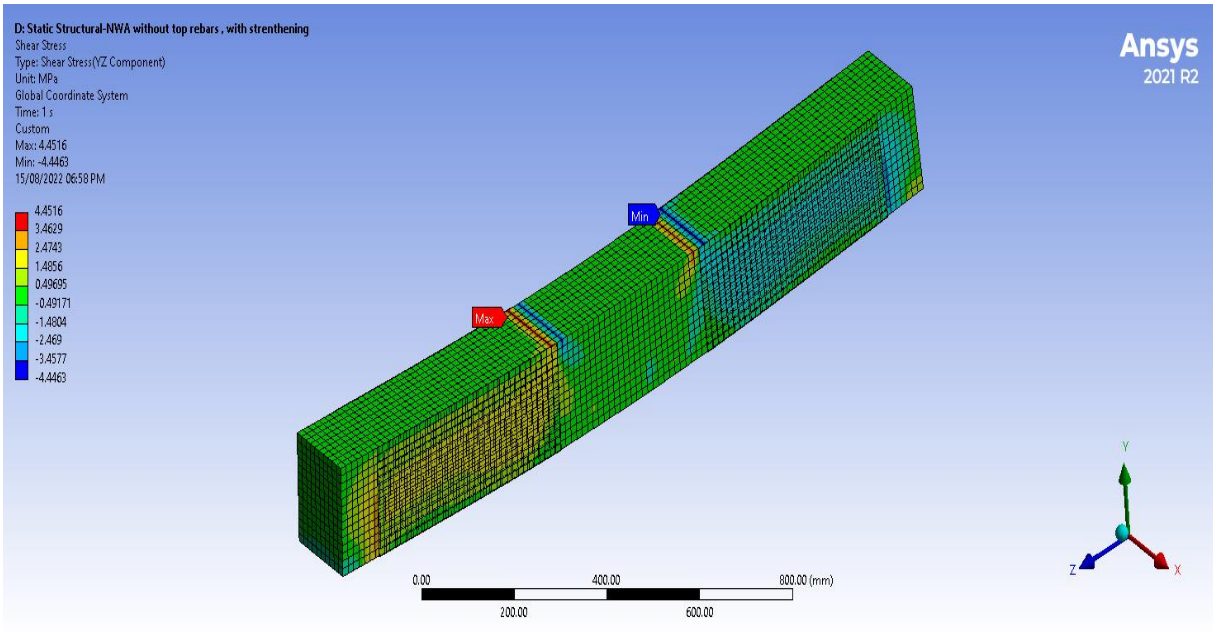

Figure 179(NWA-1/70.5MPa – Shear stress of beam sample with strengthening and without top rebars- Static Nonlinear Analysis)

Elastic Strain

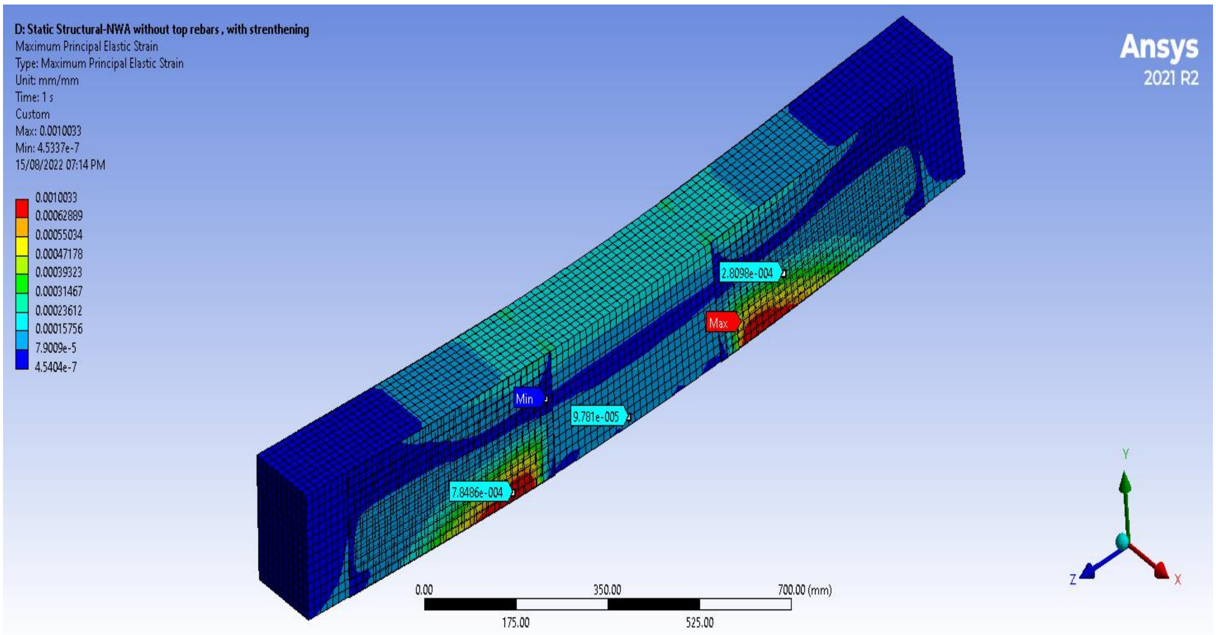

Figure 180(NWA-1/70.5MPa – Elastic strain of beam sample with strengthening and without top rebars- Static Nonlinear Analysis)

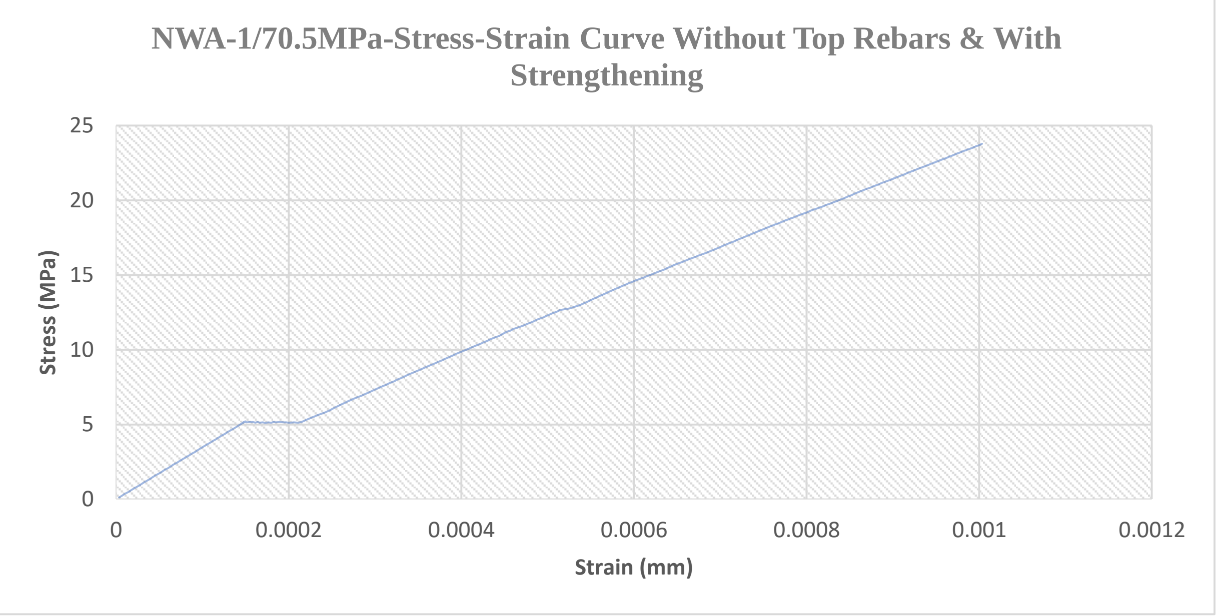

Figure 181(NWA-1/70.5MPa – Stress & Strain graph of beam sample with strengthening and without top rebars- Static Nonlinear Analysis)

8-Explicit Dynamic-Without Top Rebars & With Strengthening

Geometry and loads

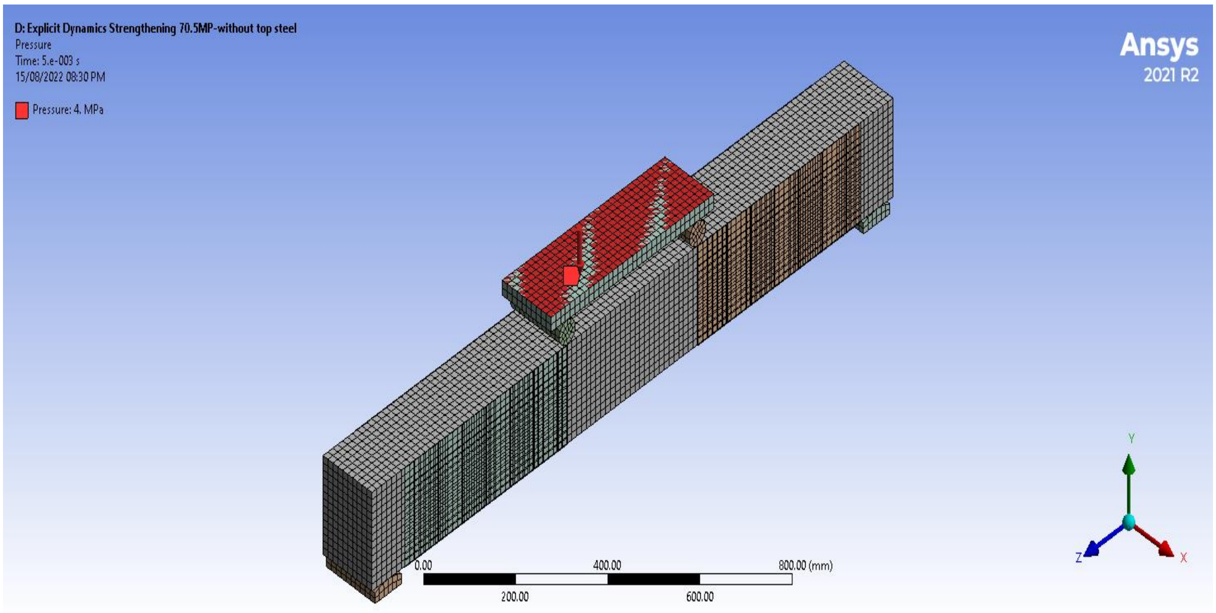

Figure 182(NWA-1/70.5MPa – Geometry & Loads of beam sample with strengthening and without top rebars- Explicit Dynamic Analysis)

The ultimate load has been transferred to be as a pressure load which is 4.0 MPa as shown above with rate loading 0.6mm/min

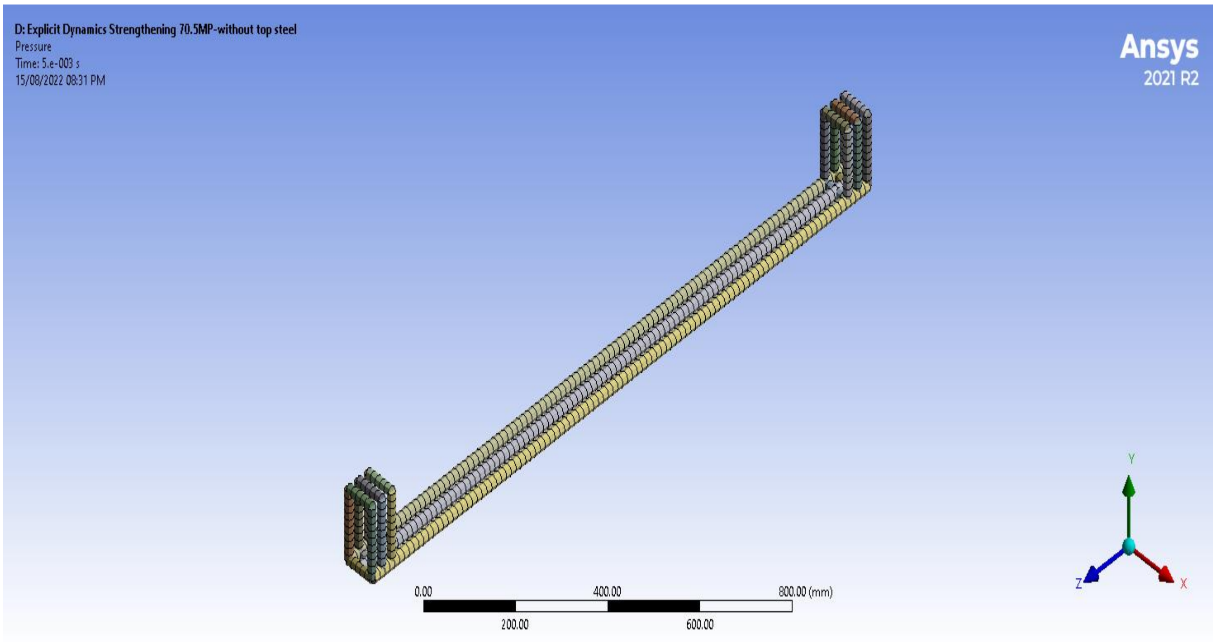

Figure 183(NWA-1/70.5MPa – Rebars of beam sample with strengthening - Explicit Dynamic Analysis)

Deformations

Total Deformations

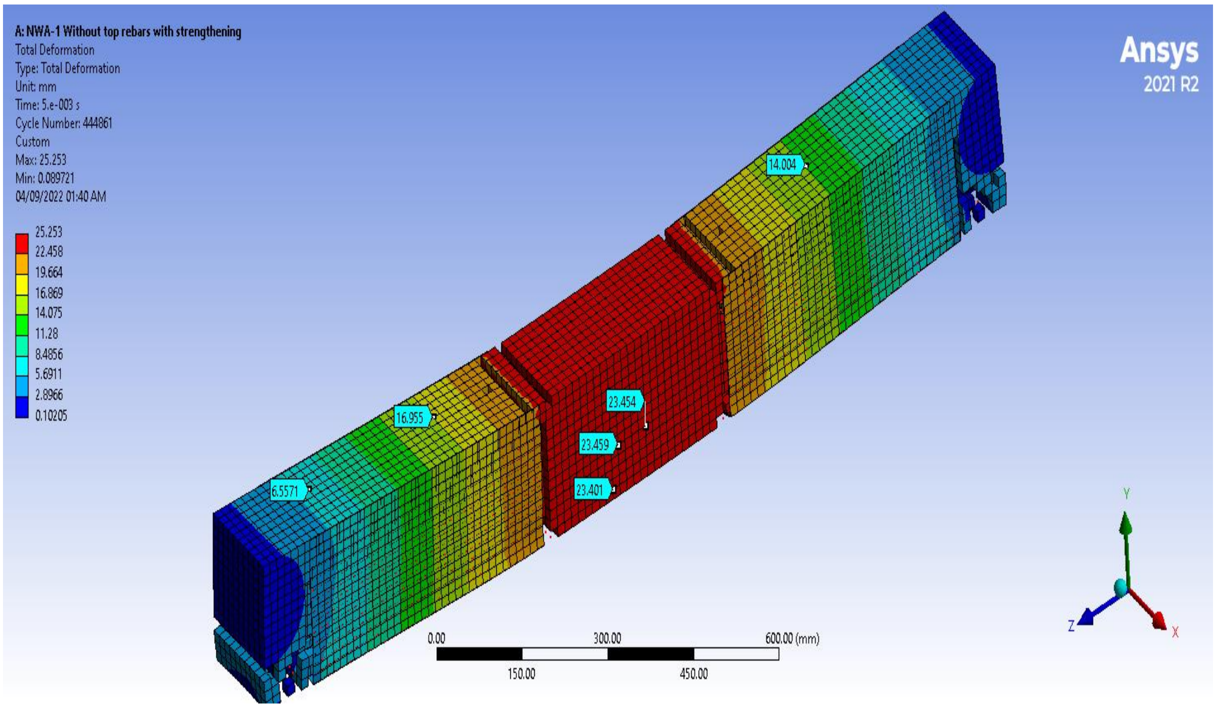

Figure 184(NWA-1/70.5MPa – Total deflections of beam sample with strengthening and without top rebars- Explicit Dynamic Analysis)

The value is 23.459 mm.

Directional Deformation (Y-Direction)-Concrete

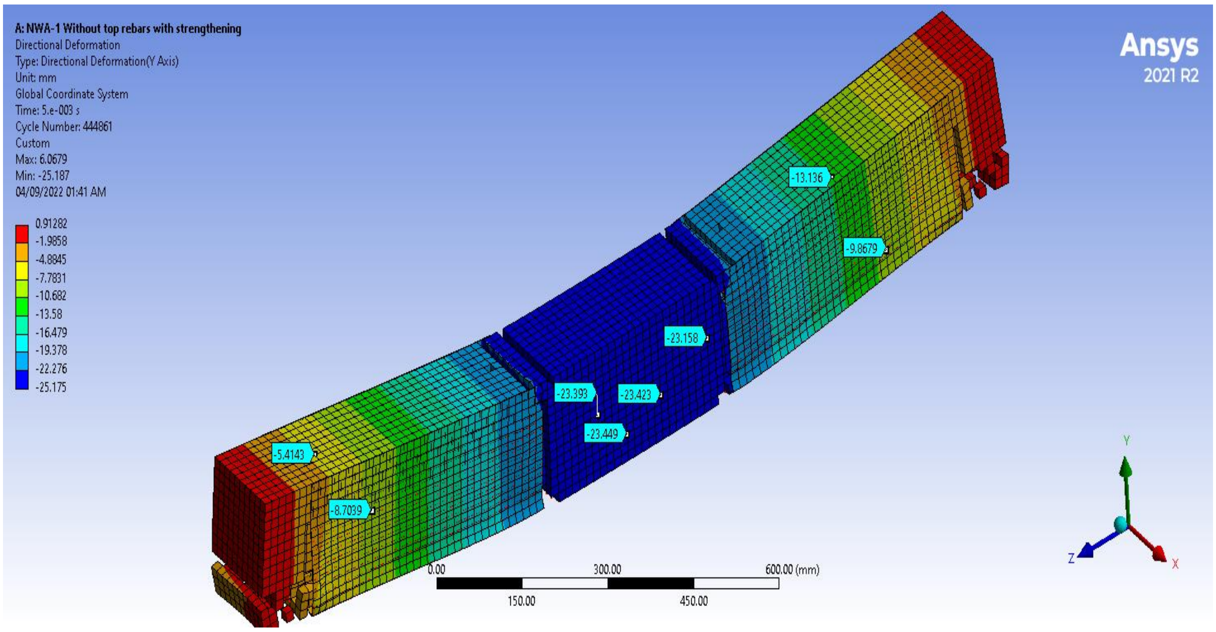

Figure 185(NWA-1/70.5MPa – Directional deflections (Y-Dim.) of beam sample with strengthening and without top rebars- Explicit Dynamic Analysis)

The value is 23.449 mm

Directional Deformation (Y-Direction)- Rebars

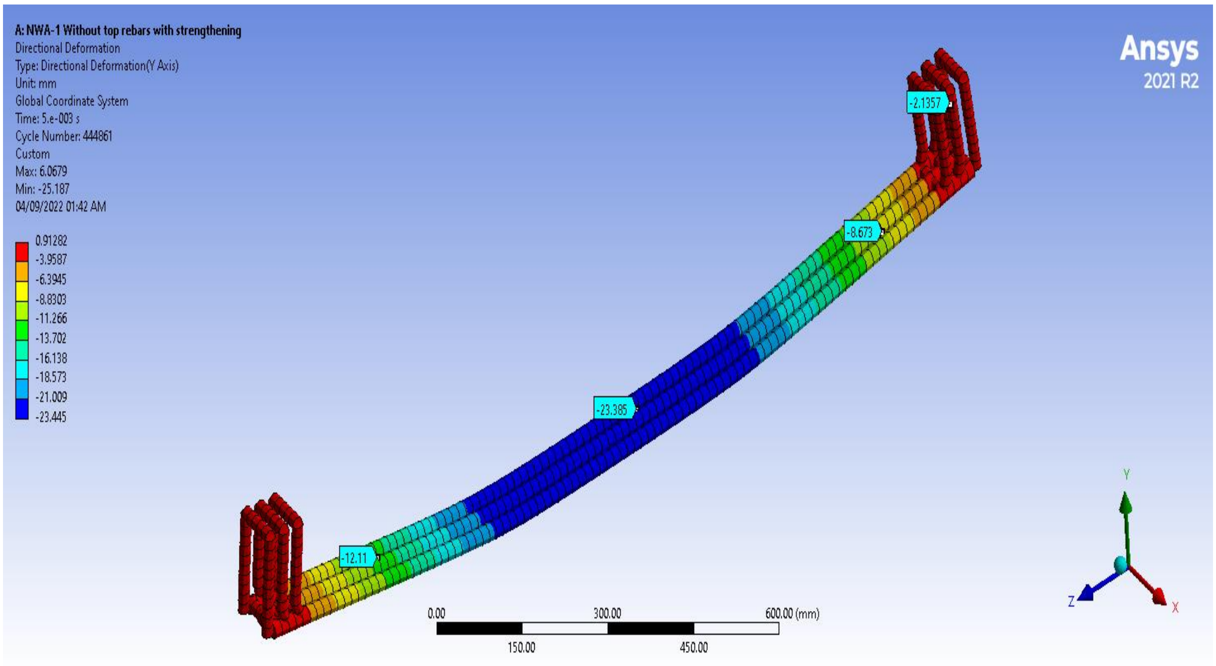

Figure 186(NWA-1/70.5MPa – Directional deflections (Y-Dim.) Rebars of beam sample with strengthening and without top rebars- Explicit Dynamic Analysis)

Normal strain

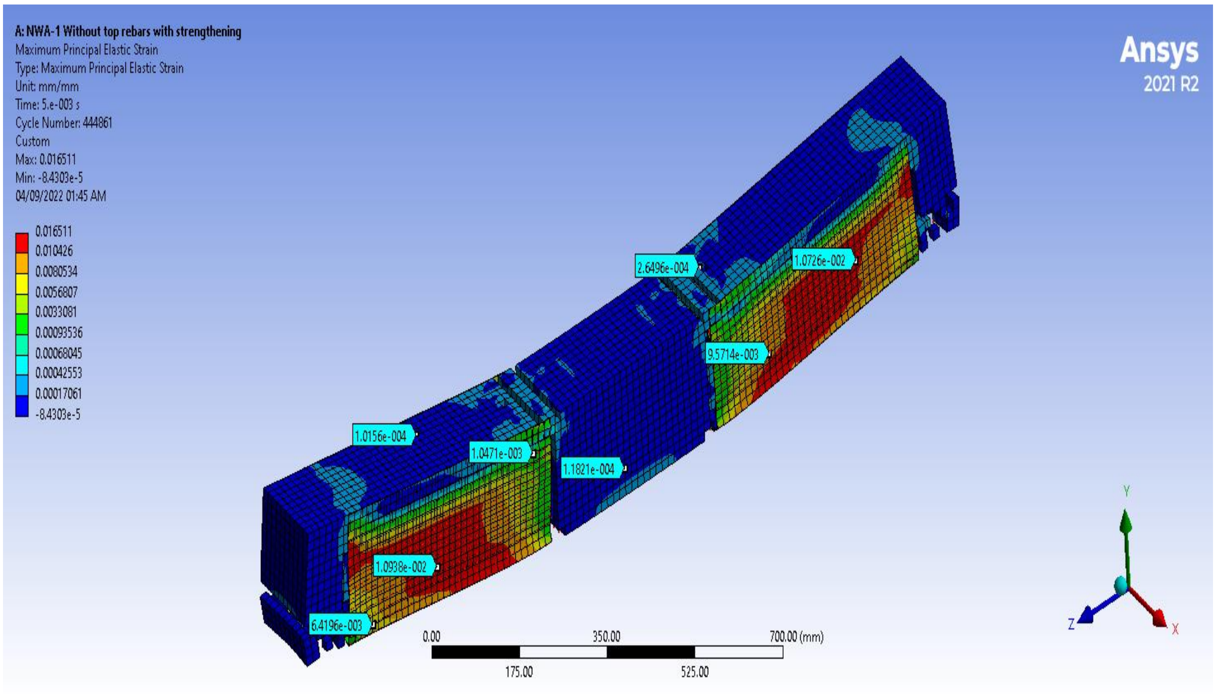

Figure 187(NWA-1/70.5MPa – Normal strain of beam sample with strengthening and without top rebars- Explicit Dynamic Analysis)

Shear Stress

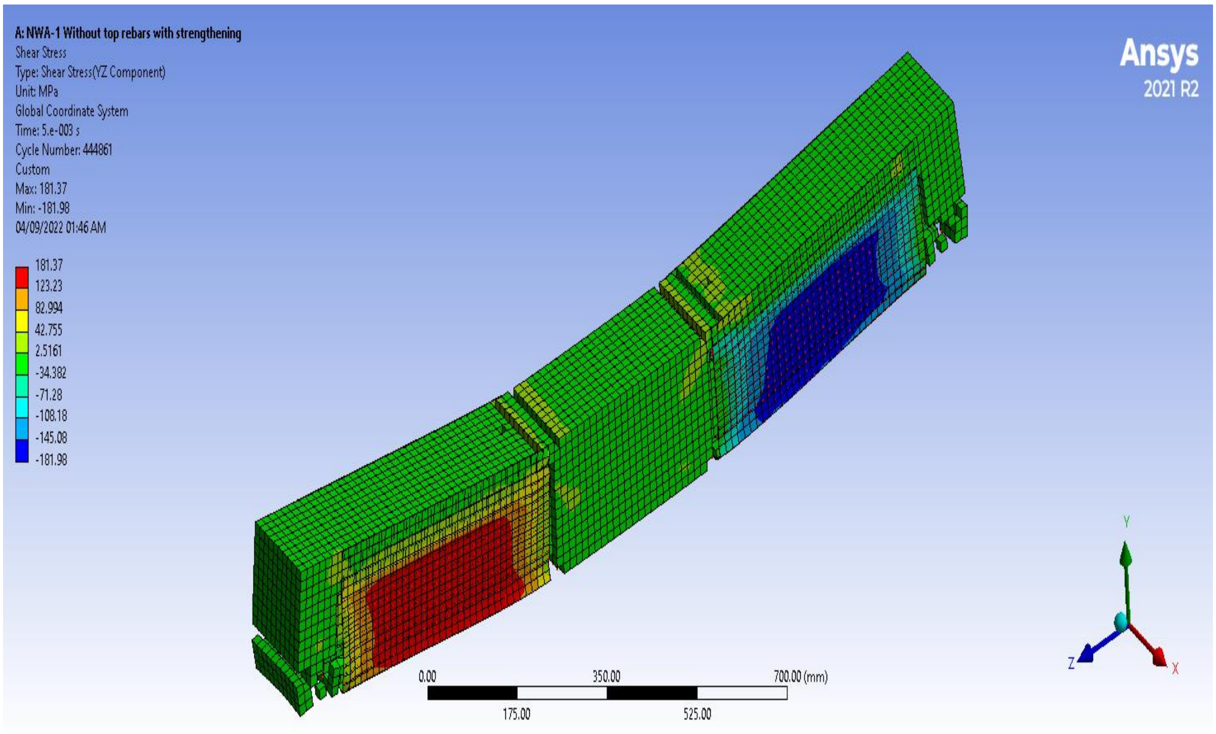

Figure 188(NWA-1/70.5MPa – Shear stress of beam sample with strengthening and without top rebars- Explicit Dynamic Analysis)

Total shape strain

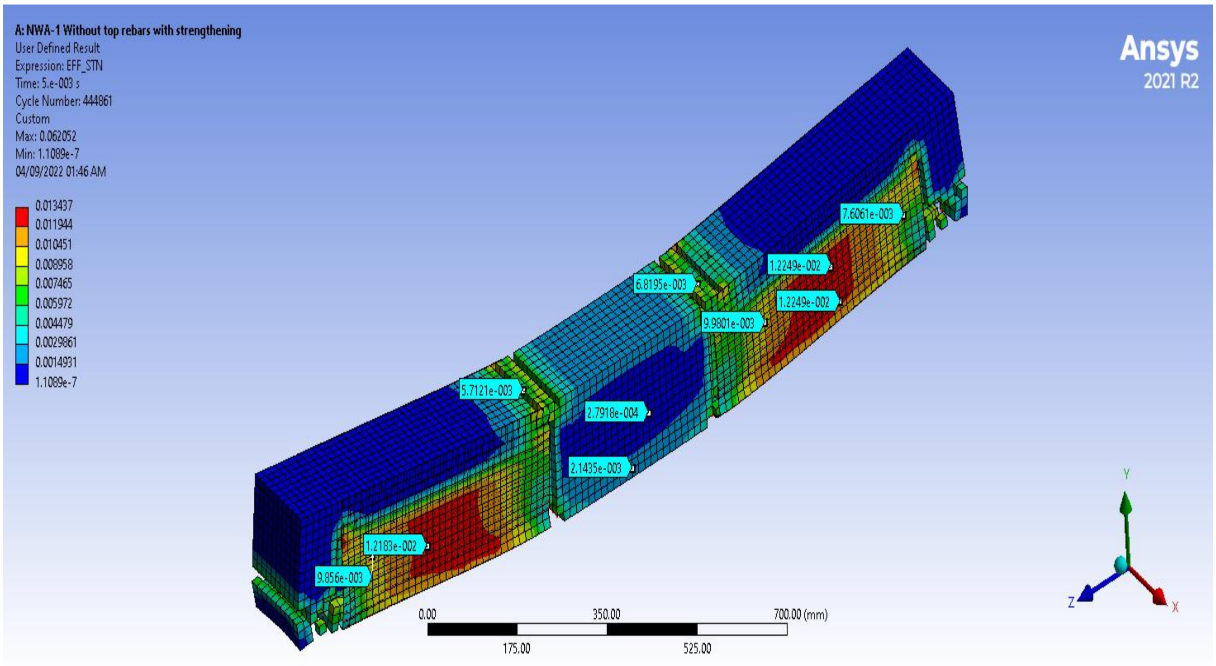

Figure 189(NWA-1/70.5MPa – Total strain of beam sample with strengthening and without top rebars- Explicit Dynamic Analysis)

Maximum Stress

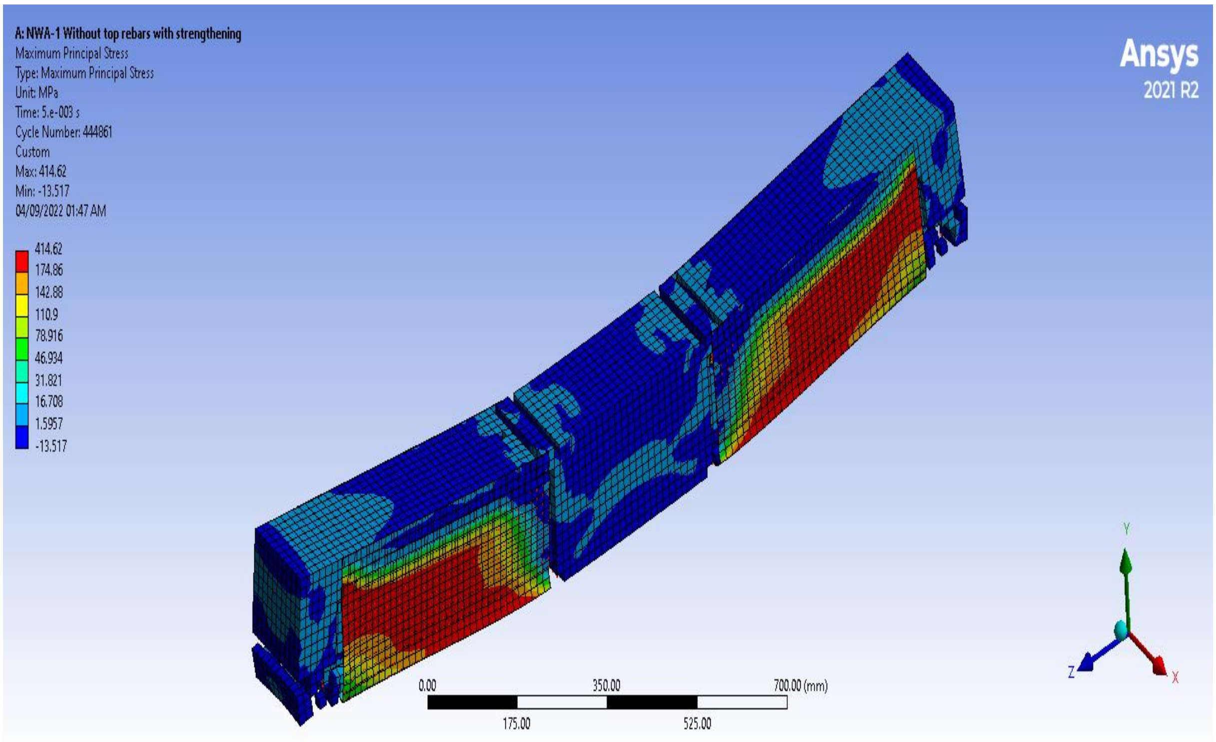

Figure 190(NWA-1/70.5MPa – Maximum stress of beam sample with strengthening and without top rebars- Explicit Dynamic Analysis)

The Damage Pattern

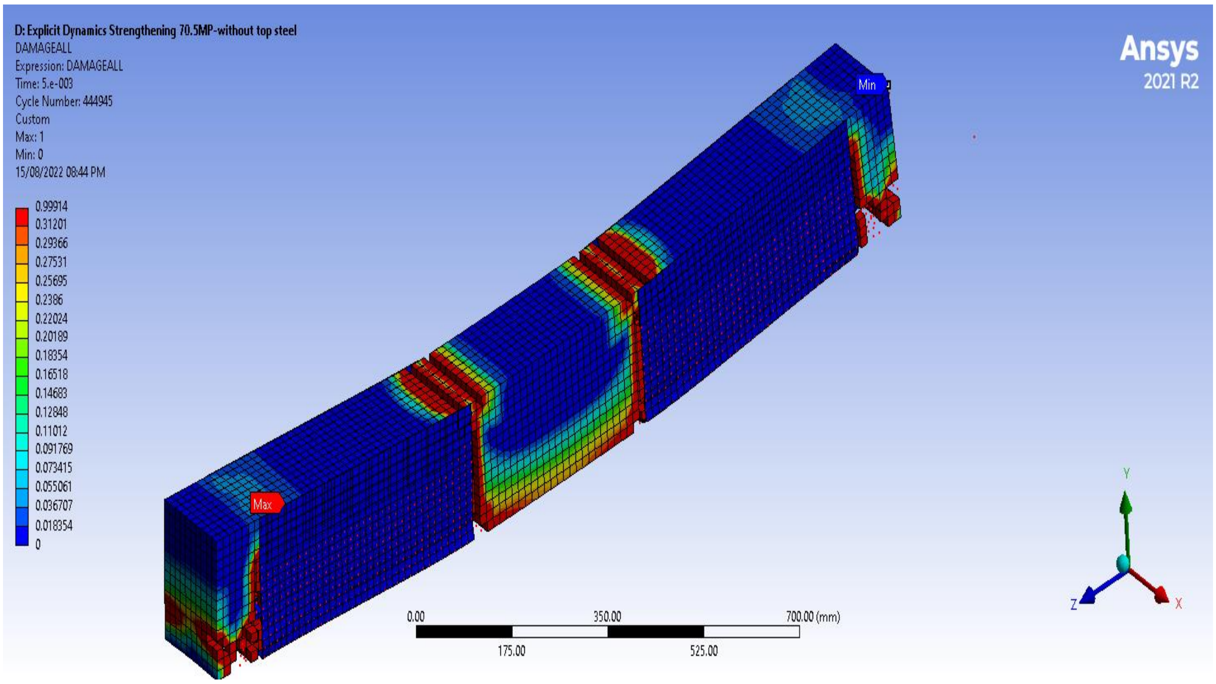

Figure 191(NWA-1/70.5MPa – Damage pattern-1 of beam sample with strengthening and without top rebars- Explicit Dynamic Analysis)

As we can see the shear damage cracks in red and CFRP debonding on edges of concrete failure.

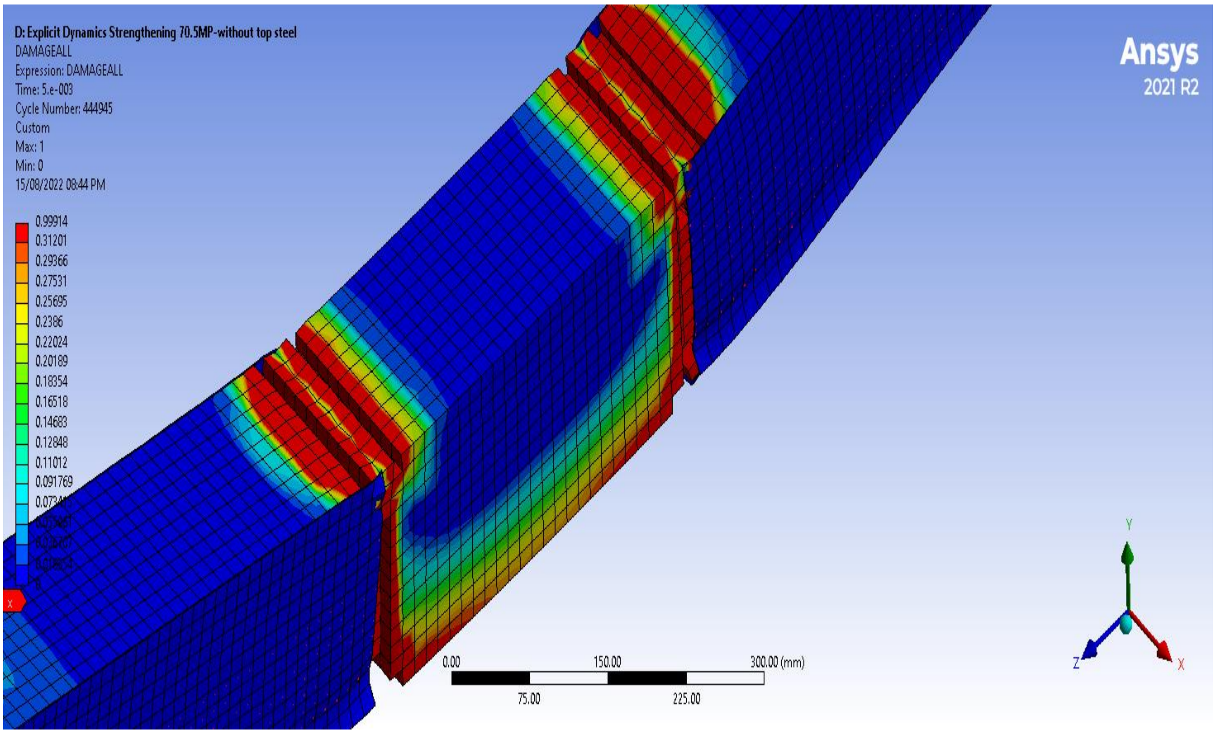

Figure 192(NWA-1/70.5MPa – Damage pattern-2 of beam sample with strengthening and without top rebars- Explicit Dynamic Analysis)

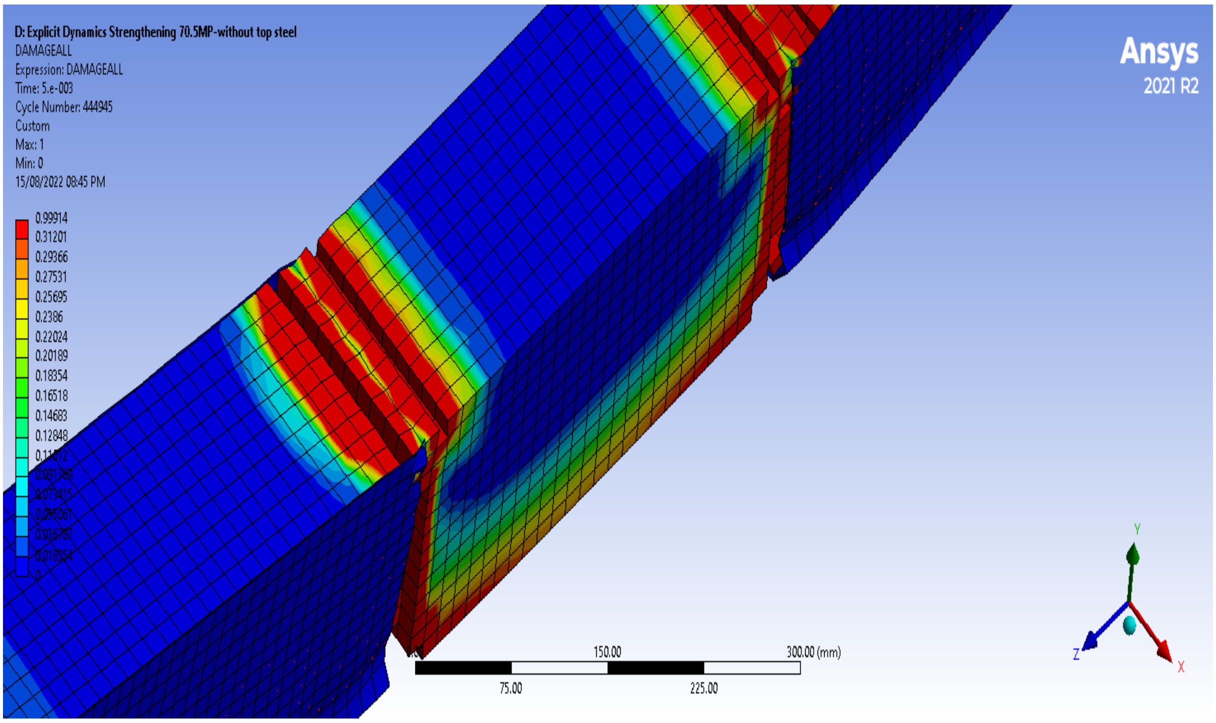

Figure 193(NWA-1/70.5MPa – Damage pattern-3 of beam sample with strengthening and without top rebars- Explicit Dynamic Analysis)

CFRP laminates due to ultimate load has been debonding as shown in images above

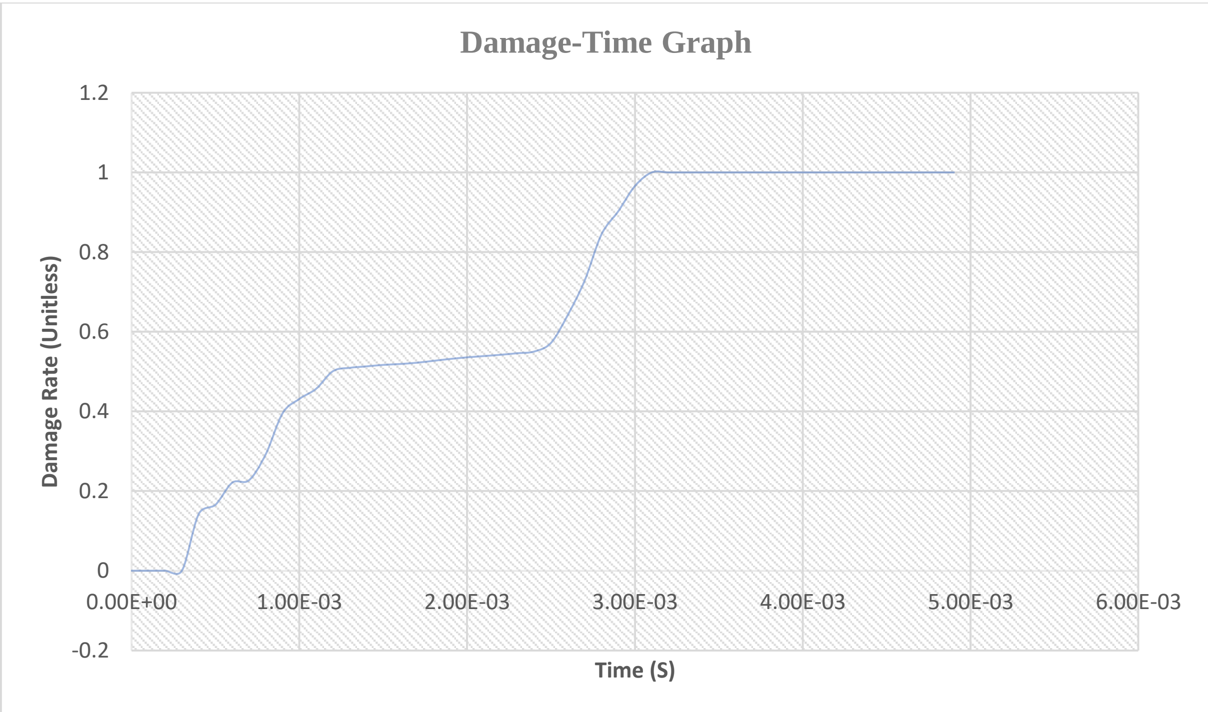

Figure 194(NWA-1/70.5MPa – Damage pattern graph of beam sample with strengthening and without top rebars- Explicit Dynamic Analysis)

9-Static Non-Linear Analysis - Without Strengthening and with Top Rebars

Geometry and loads

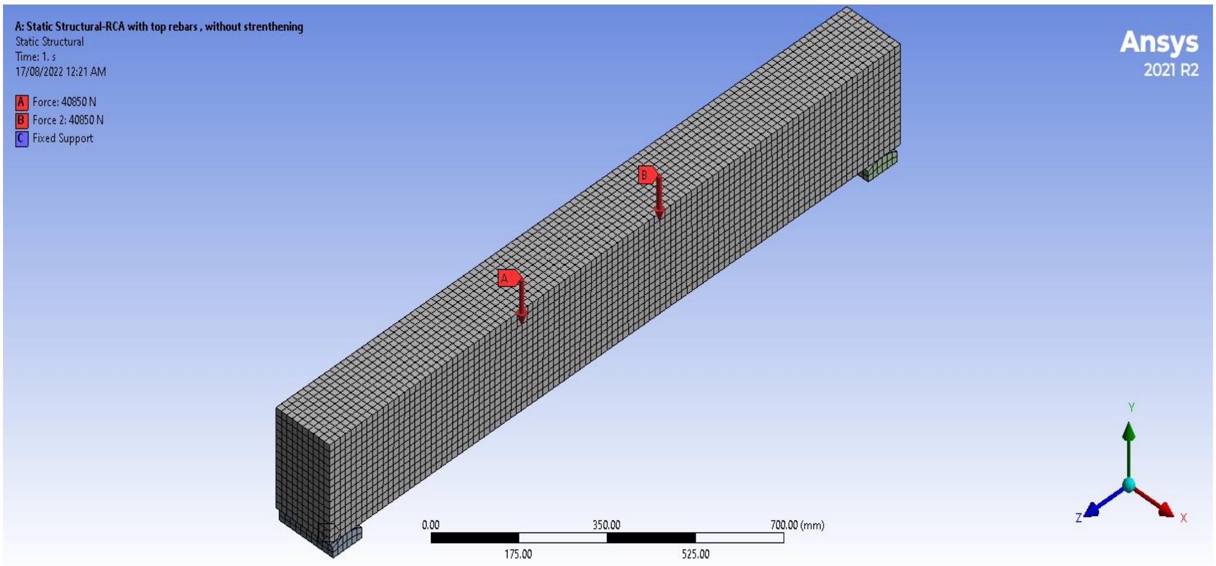

Figure 195(RCA-64.50MPa – Geometry & Loads of beam sample without strengthening and with top rebars- Static Nonlinear Analysis)

The ultimate load has been divided in to loads which is 81.7/2 =40.85KN.

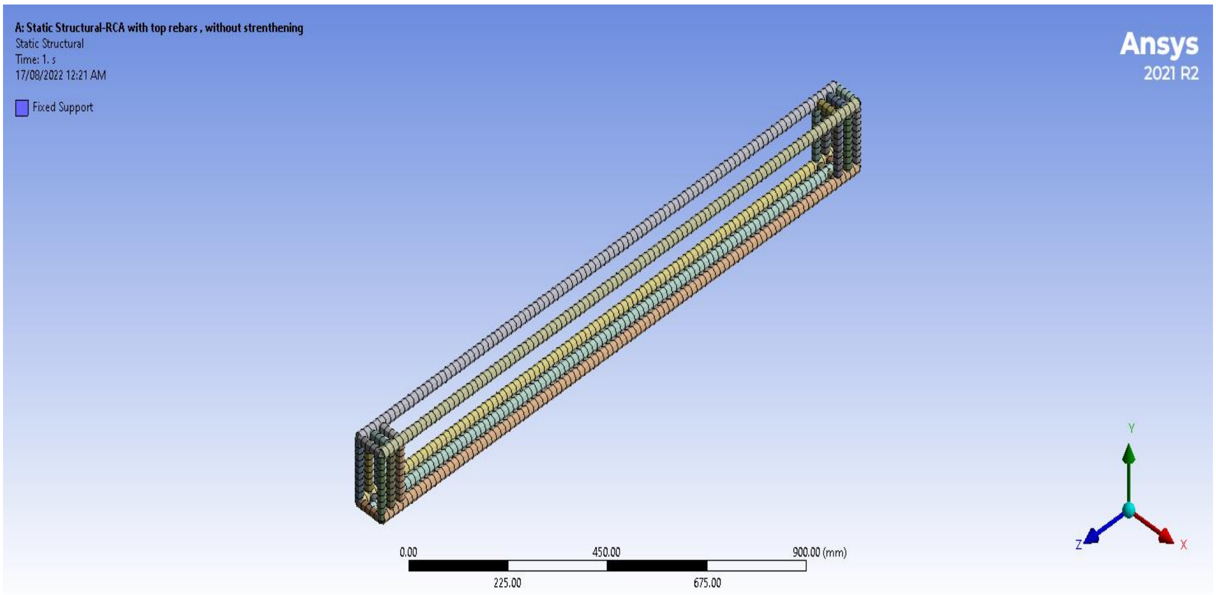

Figure 196(RCA-64.50MPa – Rebars of beam sample without strengthening - Static Nonlinear Analysis)

Deformations

Total Deformations

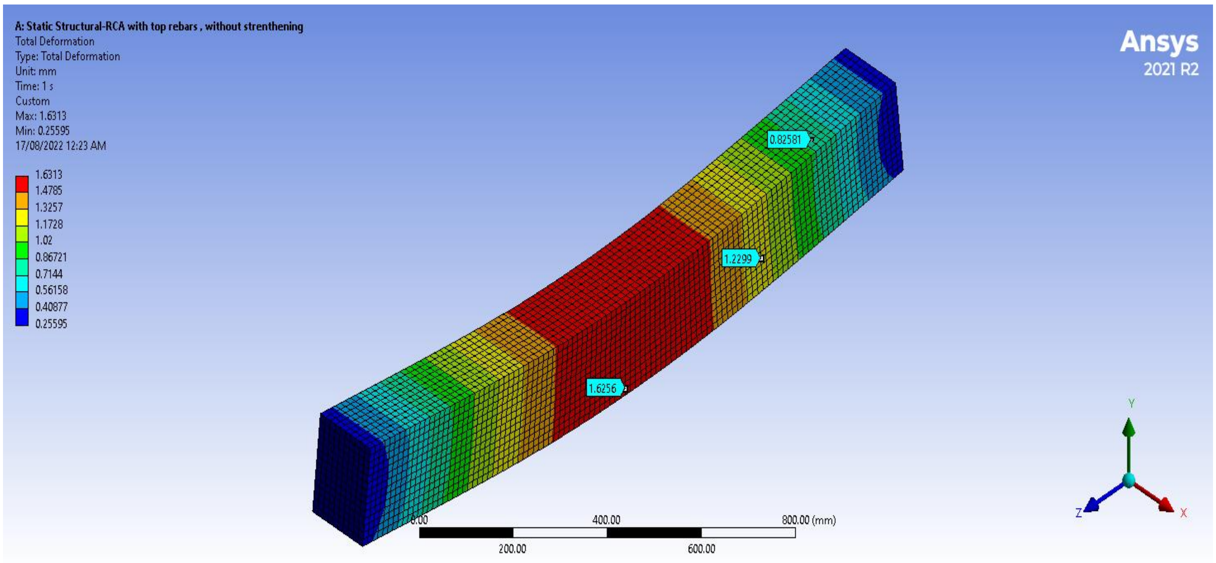

Figure 197(RCA-64.50MPa – Total deflections of beam sample without strengthening and with top rebars- Static Nonlinear Analysis)

The value is 1.6313 mm.

Directional Deformation (Y-Direction)

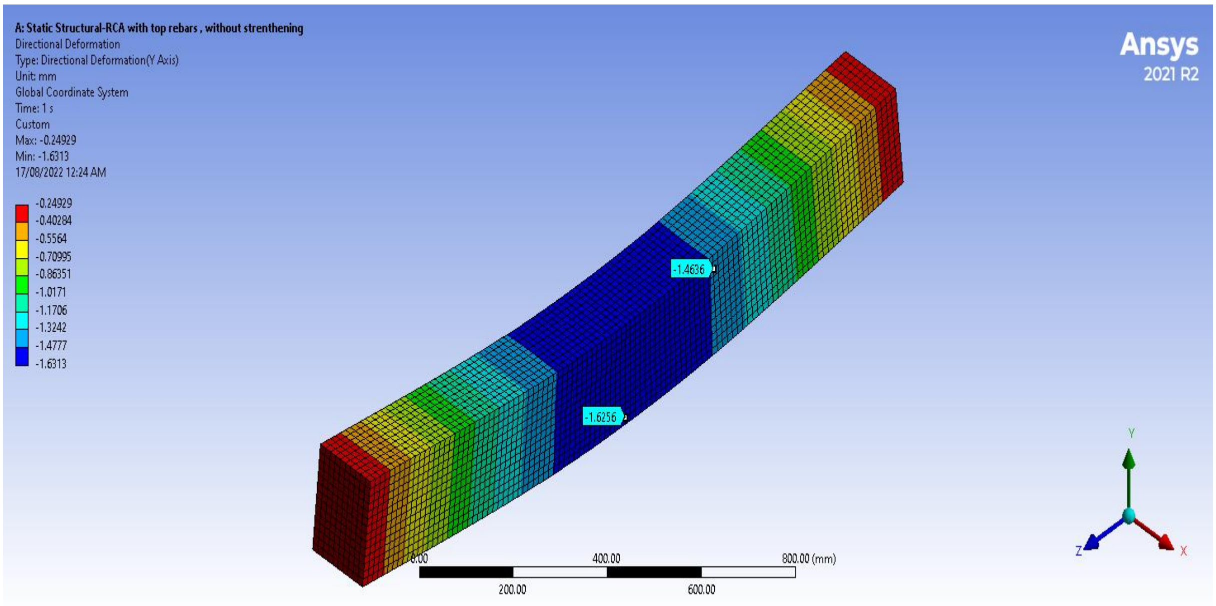

Figure 198(RCA-64.50MPa – Directional deflections (Y-Dim.) of beam sample without strengthening and without top rebars- Static Nonlinear Analysis)

The value is 1.6313 mm.

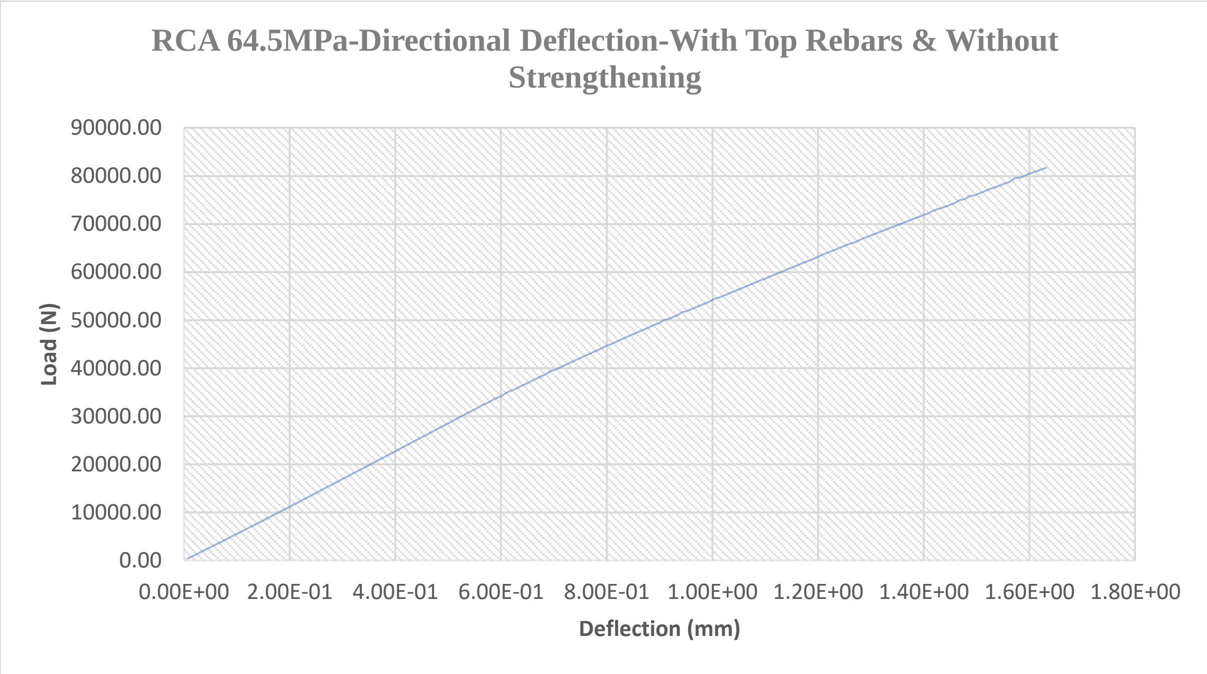

Figure 199(RCA-64.50MPa – Directional deflections (Y-Dim.) of beam sample without strengthening and with top rebars- Static Nonlinear Analysis)

Normal Stress (Concrete)

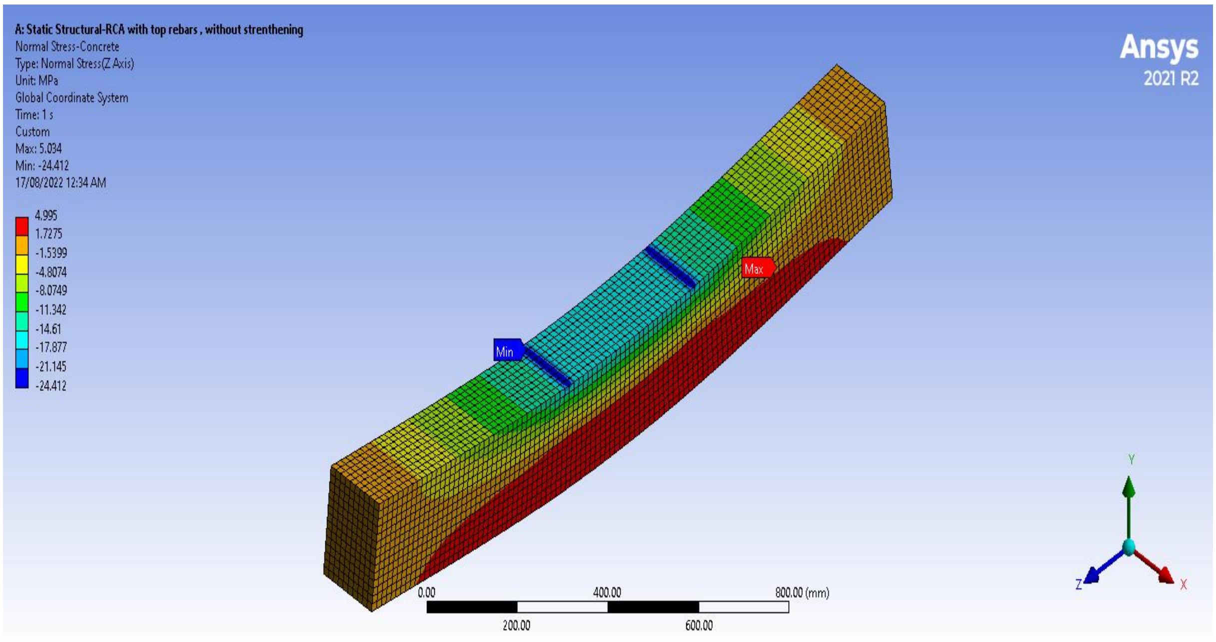

Figure 200(RCA-64.50MPa – Normal stress (Concrete) of beam sample without strengthening and with top rebars- Static Nonlinear Analysis)

The blue zones show the crushing from loading machine and the maximum value is 24.412 MPa, whereas the red zones indicate to tension.

Normal Stress (Rebars)

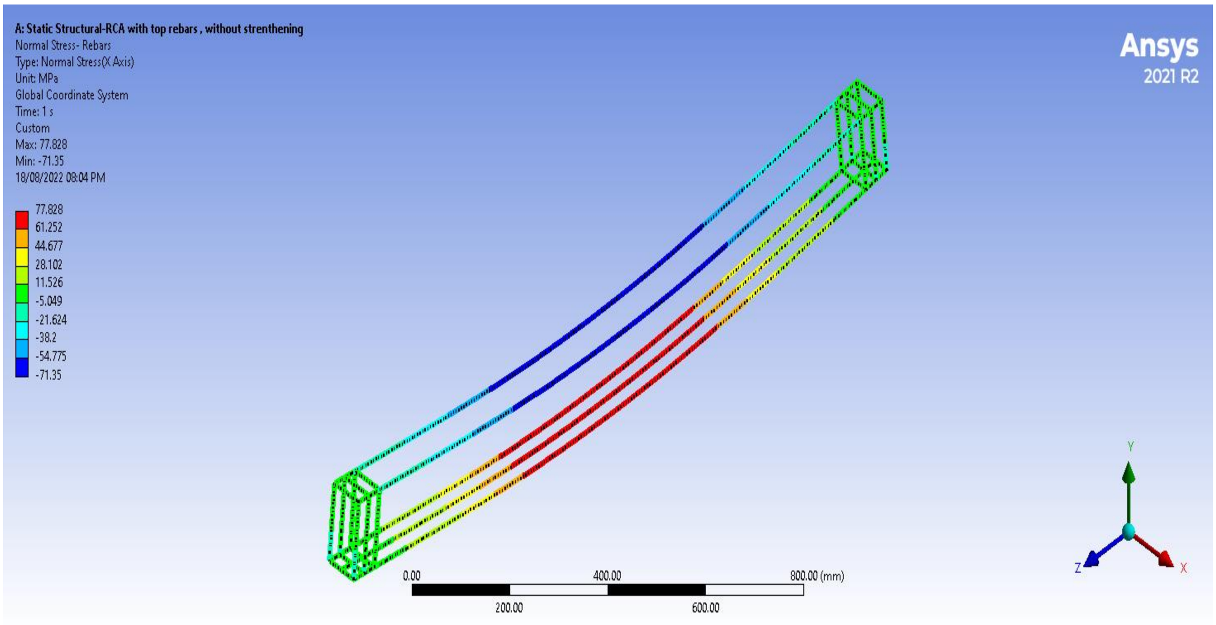

Figure 201(RCA-64.50MPa – Normal stress (Rebars) of beam sample without strengthening and with top rebars- Static Nonlinear Analysis)

The red zones show that the rebars is yielding by 77.828 MPa, in the middle span due to tension.

Shear Stress

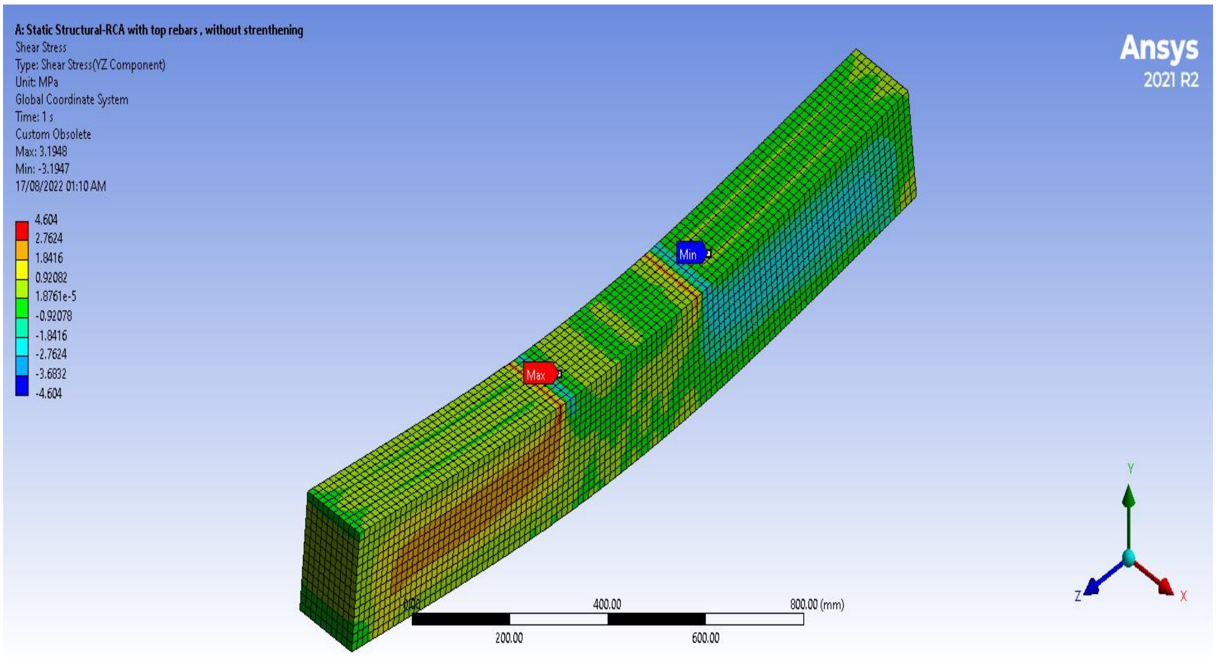

Figure 202(RCA-64.50MPa – Shear Stress of beam sample without strengthening and with top rebars - Static Nonlinear Analysis)

Elastic Strain

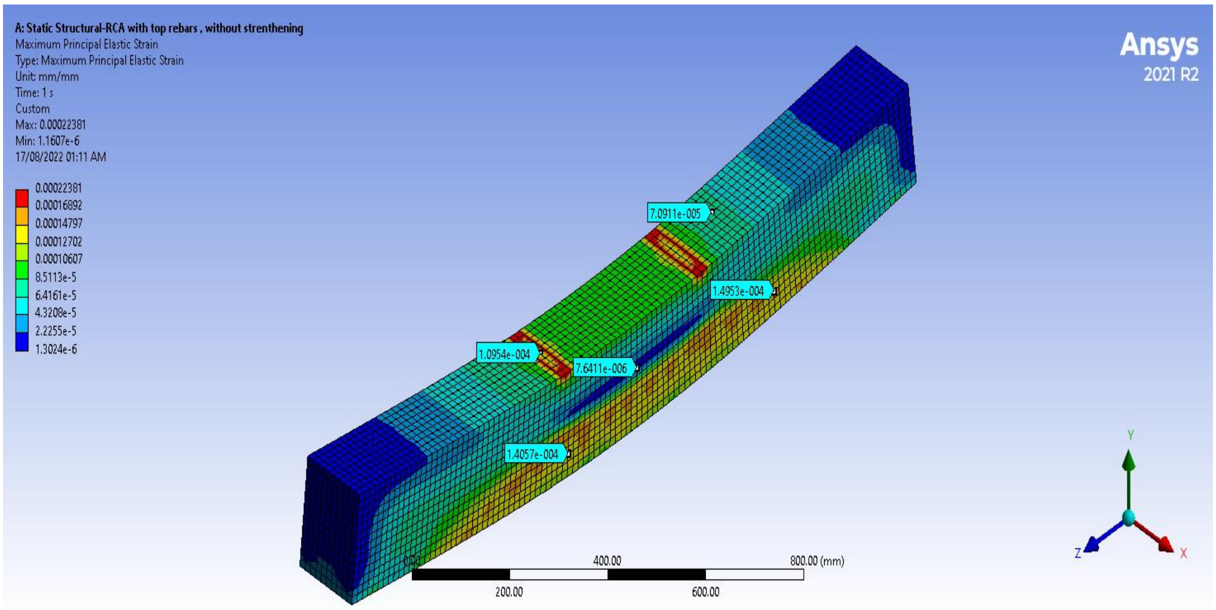

Figure 203(RCA-64.50MPa – Elastic Strain of beam sample without strengthening and with top rebars - Static Nonlinear Analysis)

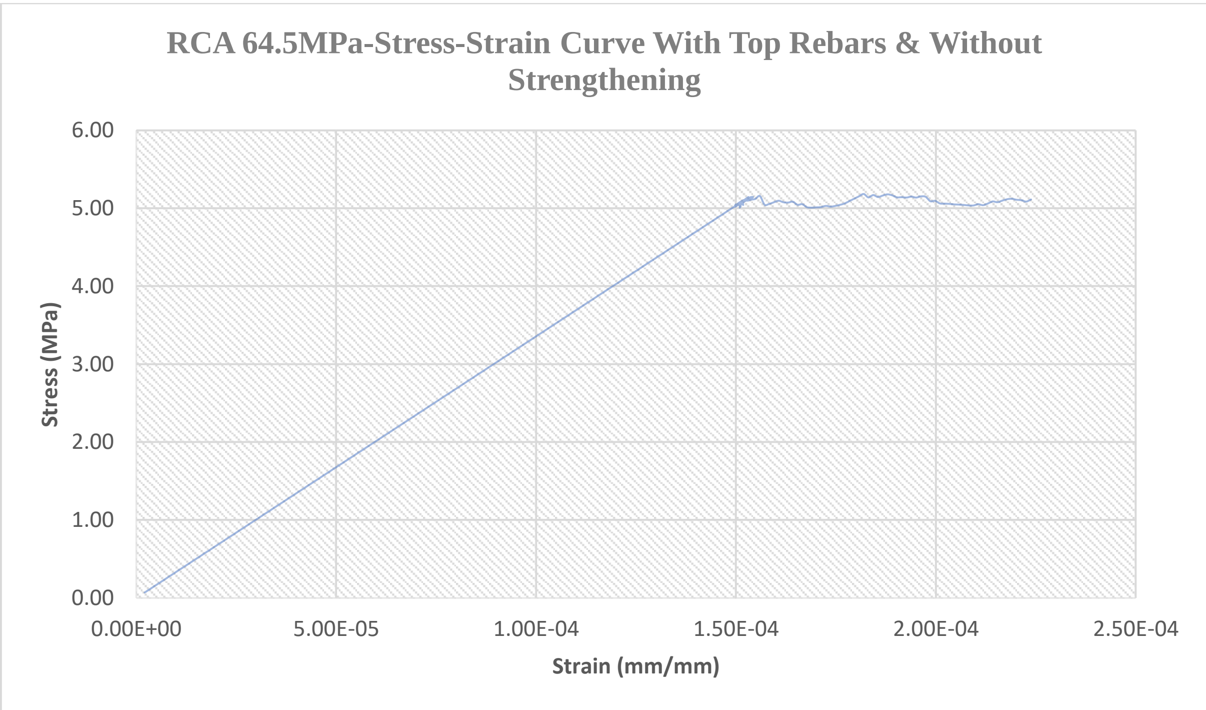

Figure 204(RCA-64.50MPa – Stress and Strain graph of beam sample without strengthening and with top rebars - Static Nonlinear Analysis)

10- Explicit Dynamic-With Top Rebars & Without Strengthening

Geometry and loads

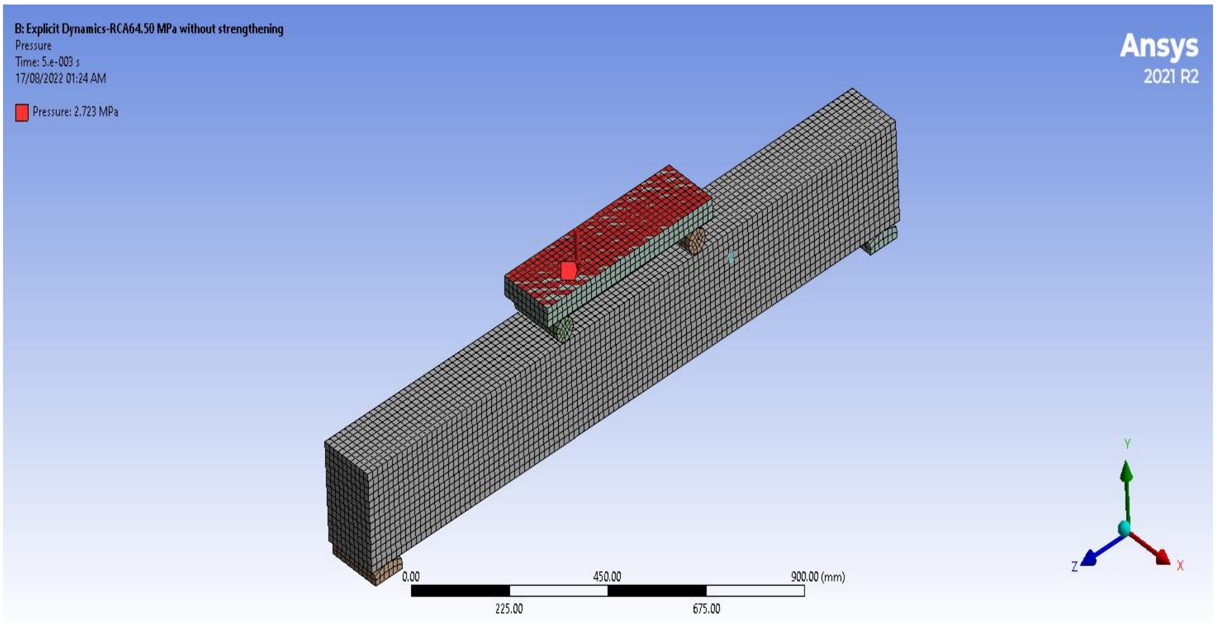

Figure 205(RCA-64.50MPa – Geometry & Loads of beam sample without strengthening and with top rebars- Explicit Dynamic Analysis)

The ultimate load has been transferred to be as a pressure load which is 2.723.0 MPa as shown above with rate loading 0.6mm/min.

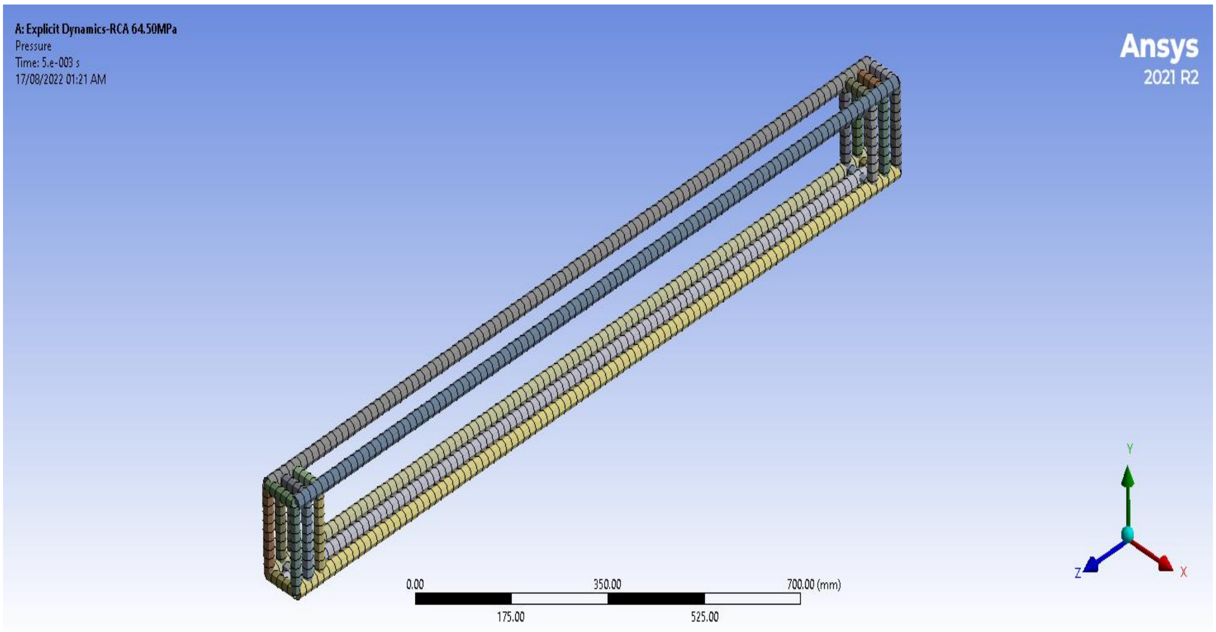

Figure 206(RCA-64.5MPa – Rebars of beam sample without strengthening - Explicit Dynamic Analysis)

Deformations

Total Deformations

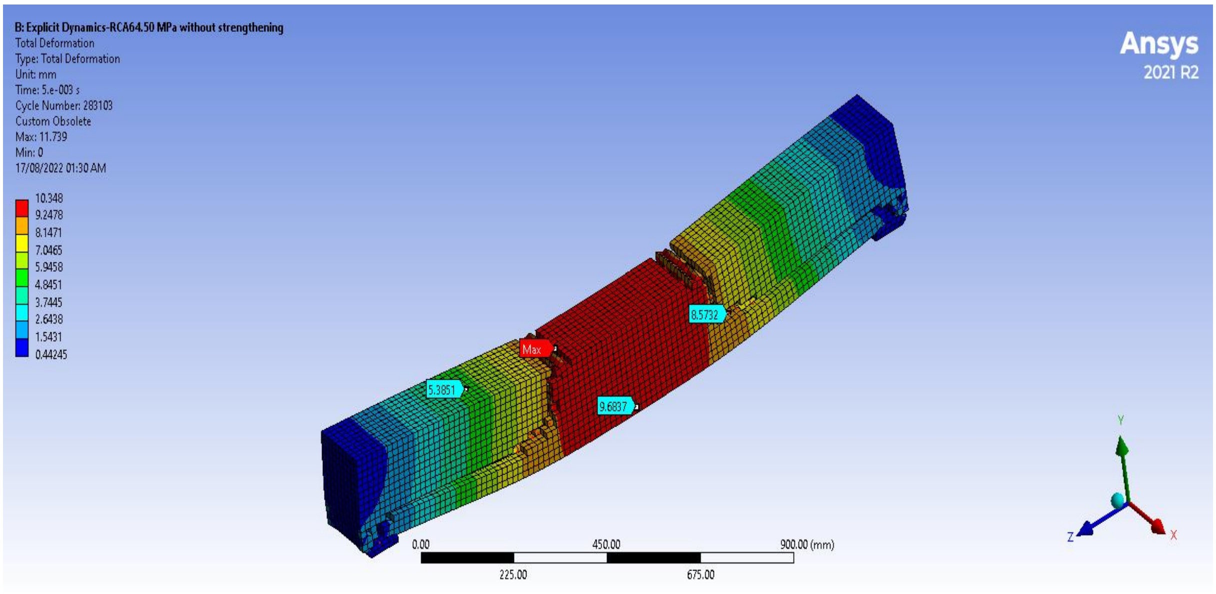

Figure 207(RCA-64.50MPa – Total deflections of beam sample without strengthening and with top rebars- Explicit Dynamic Analysis)

The value is 10.348 mm.

Directional Deformation (Y-Direction)-Concrete

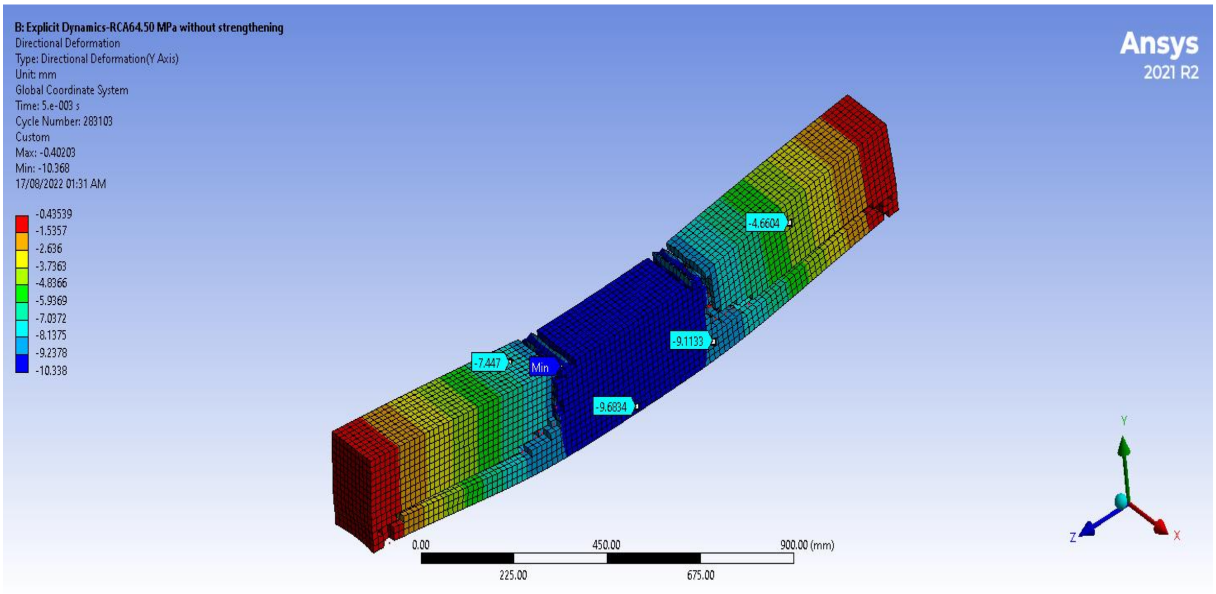

Figure 208(NWA-1/70.5MPa – Directional deflections (Y-Dir.) of beam sample without strengthening and with top rebars- Explicit Dynamic Analysis)

The value is 10.348 mm.

Directional Deformation (Y-Direction)- Rebars

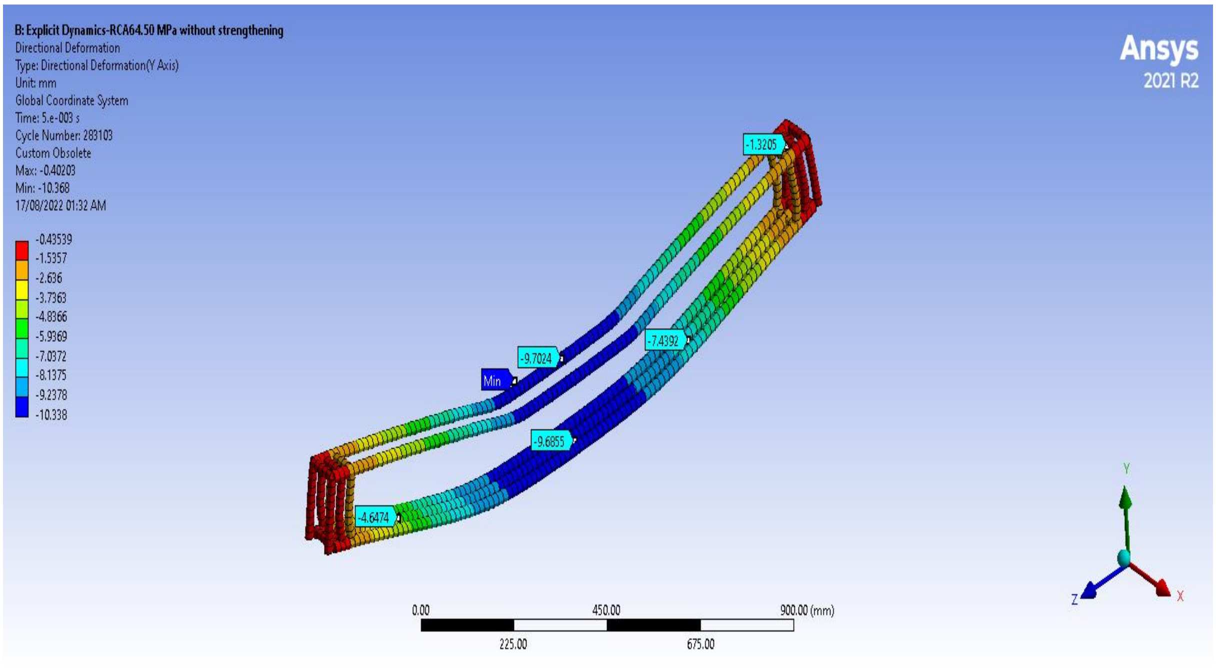

Figure 209(RCA-64.50MPa – Directional deflections (Y-Dir.) of beam rebars without strengthening- Explicit Dynamic Analysis)

Normal strain

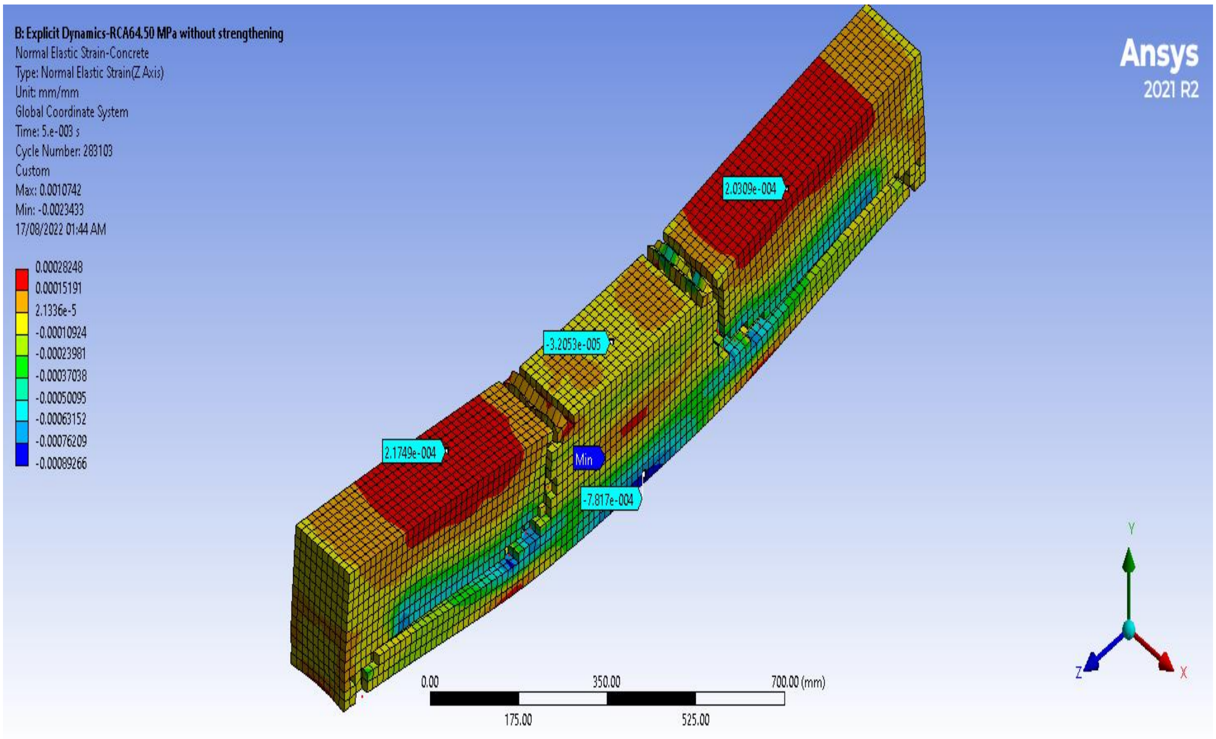

Figure 210(RCA-64.50MPa – Normal strain of beam sample without strengthening and with top rebars- Explicit Dynamic Analysis)

Shear Stress

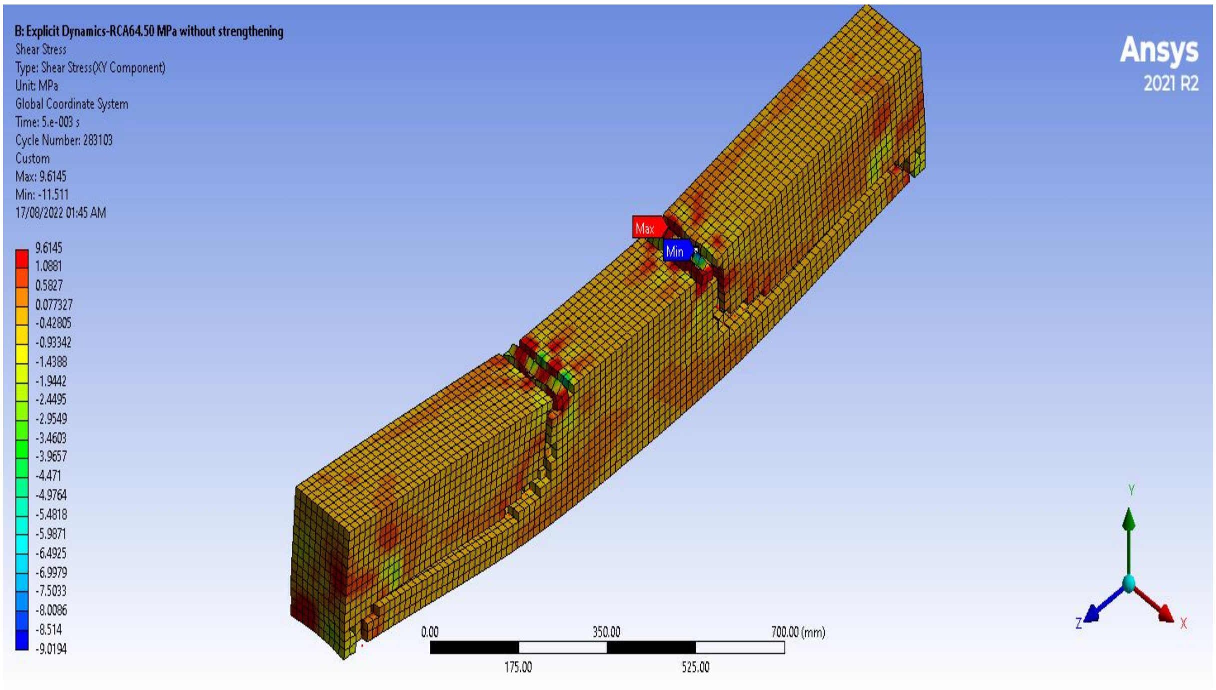

Figure 211(RCA-64.50MPa – Shear stress of beam sample without strengthening and with top rebars- Explicit Dynamic Analysis)

Total shape strain

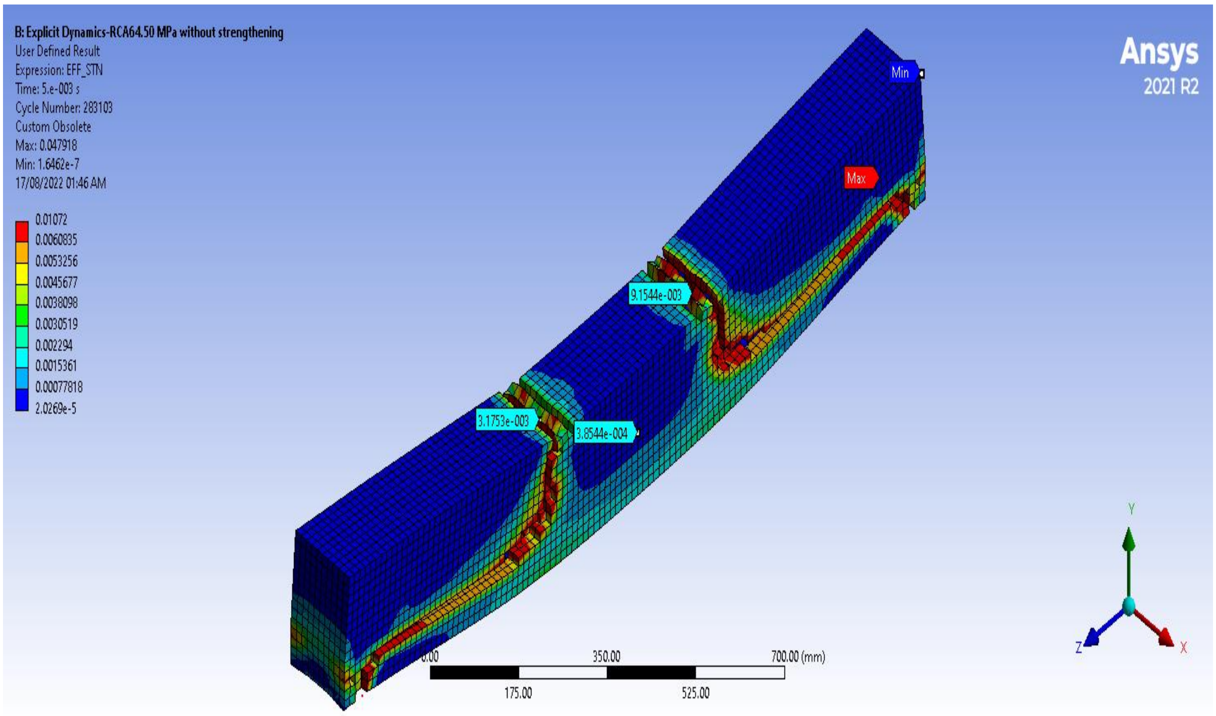

Figure 212(RCA-64.50MPa – Total strain of beam sample without strengthening and with top rebars- Explicit Dynamic Analysis)

Maximum Stress

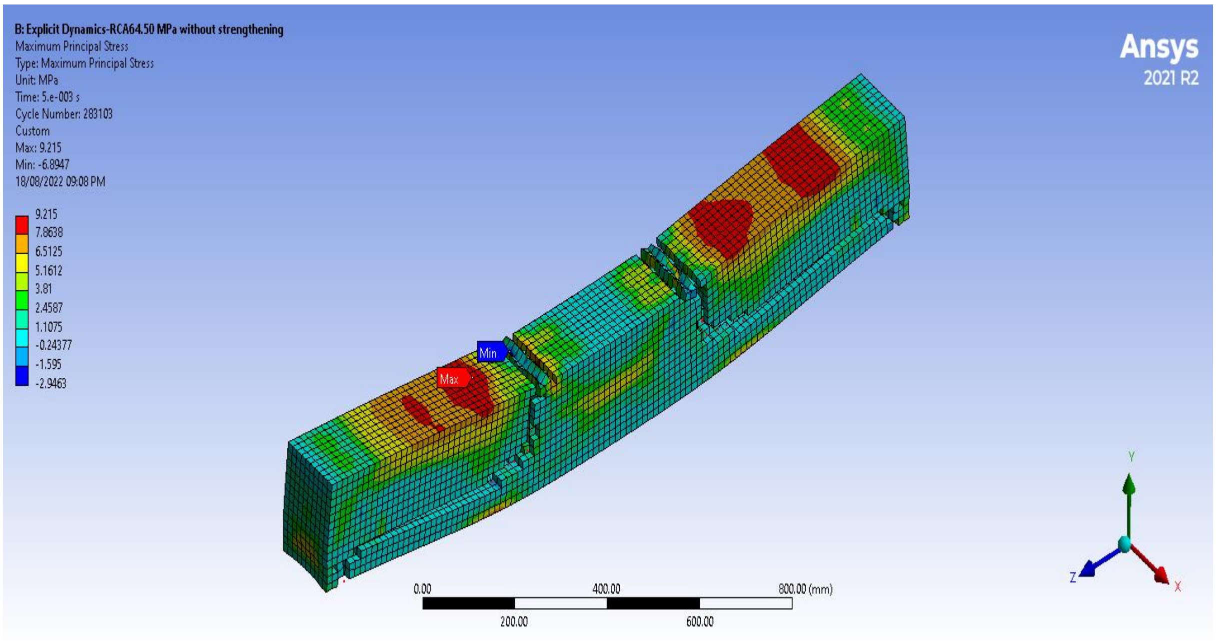

Figure 213(RCA-64.50MPa – Maximum stress of beam sample without strengthening and with top rebars- Explicit Dynamic Analysis)

The Damage Pattern

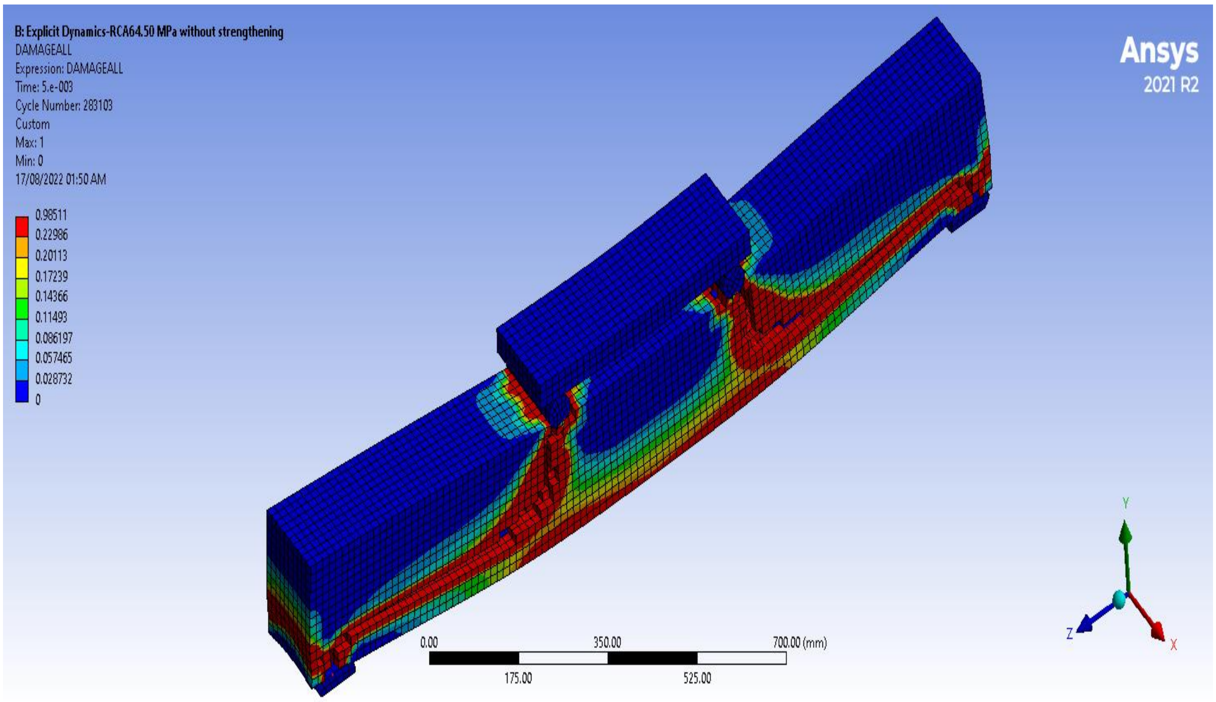

Figure 214(RCA-64.50MPa – Damage pattern-1 of beam sample without strengthening and with top rebars- Explicit Dynamic Analysis)

As we can see the shear damage cracks and concrete failures.

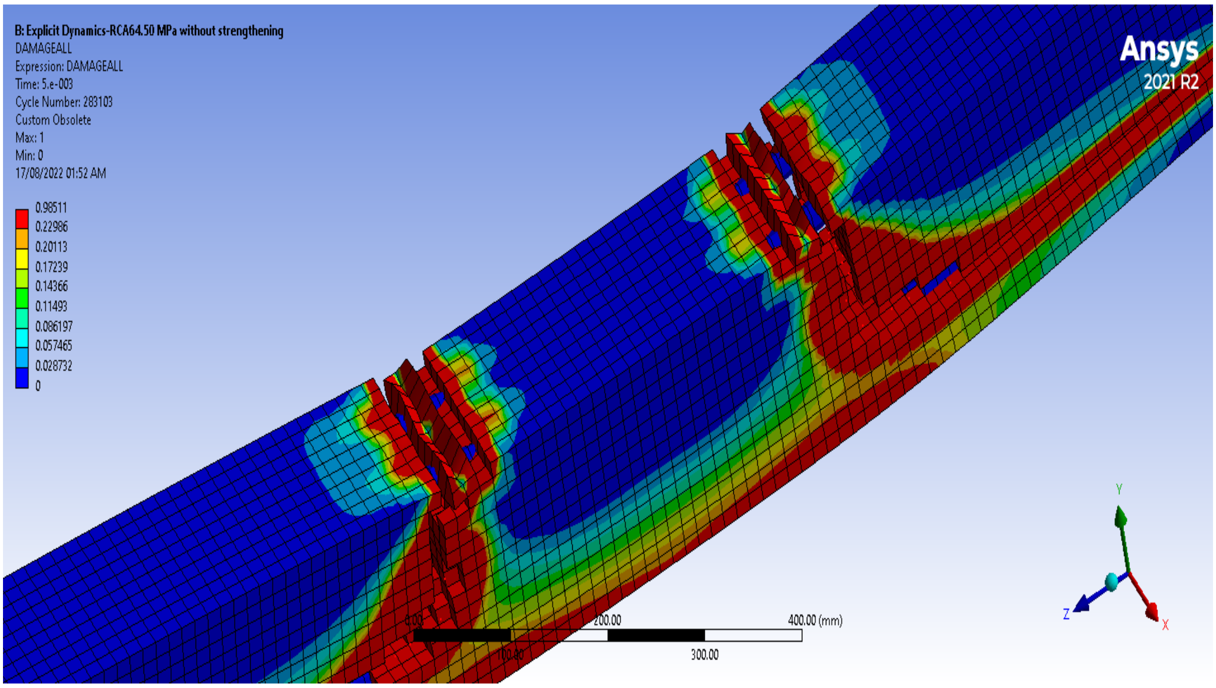

Figure 215(RCA-64.50MPa – Damage pattern-2 of beam sample without strengthening and with top rebars- Explicit Dynamic Analysis)

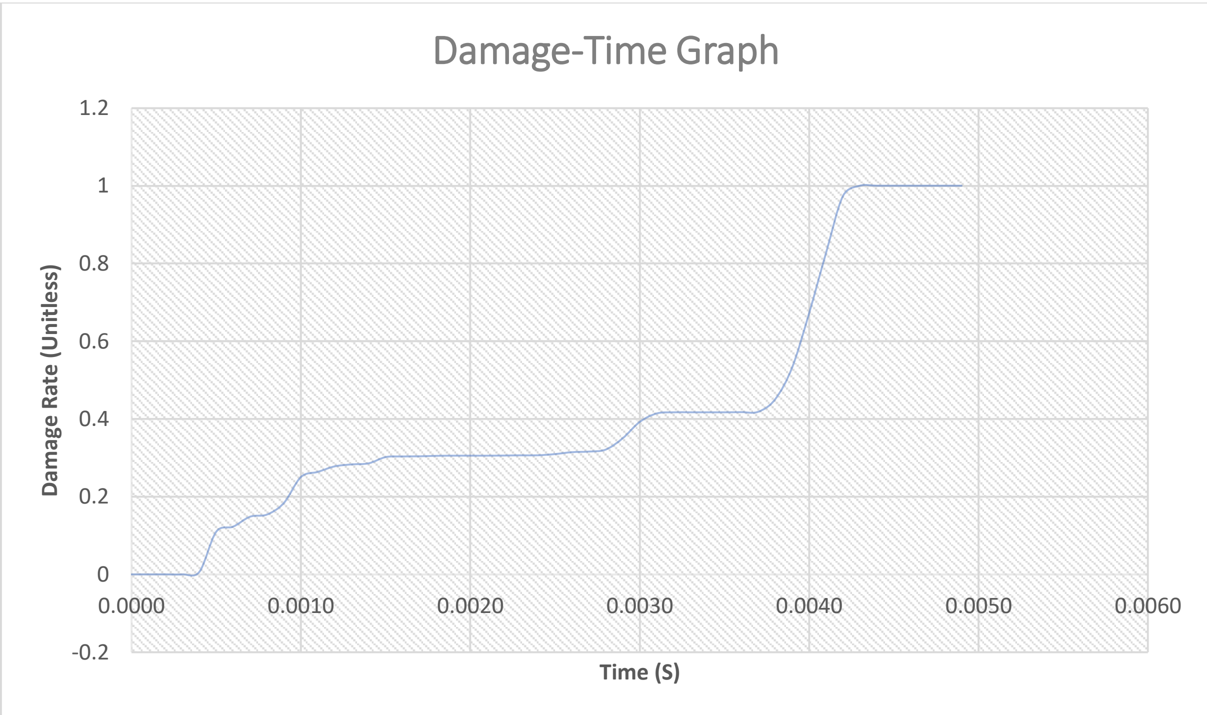

Figure 216(RCA-64.50MPa – Damage pattern graph of beam sample without strengthening and with top rebars- Explicit Dynamic Analysis)

11- Static Non-Linear Analysis - Without Strengthening and Top Rebars

Geometry and loads

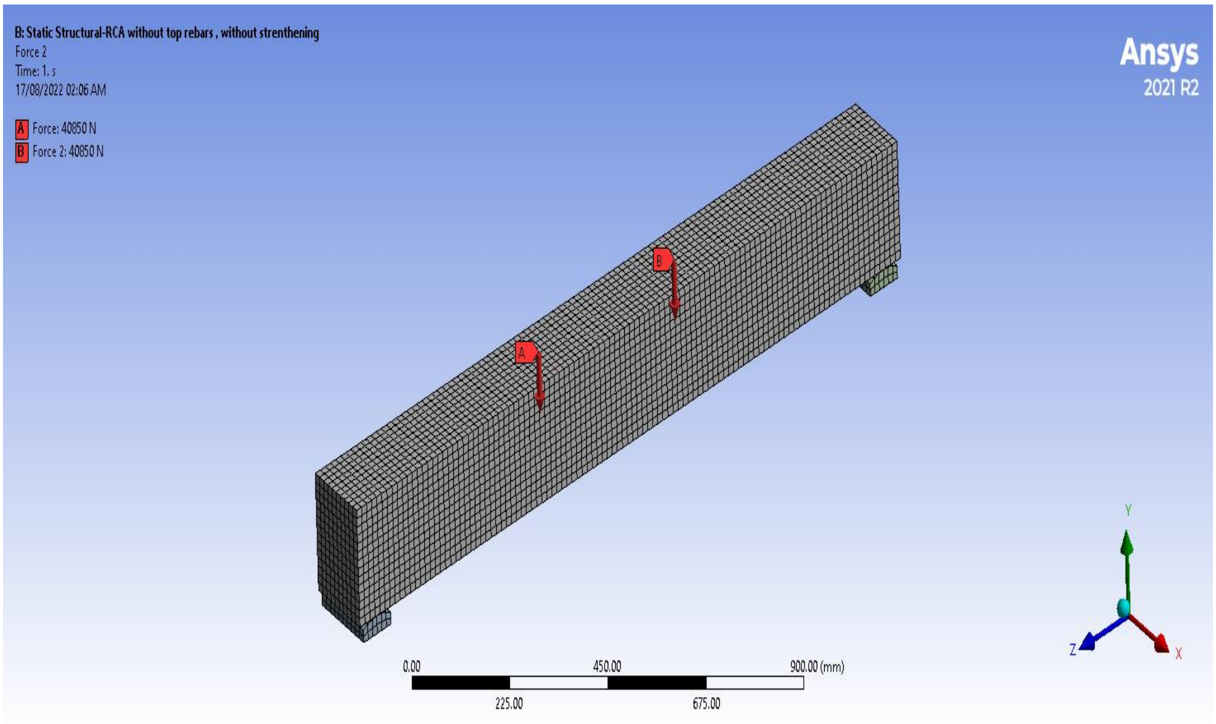

Figure 217(RCA-64.50MPa – Geometry & loads of beam sample without strengthening and top rebars- Static Nonlinear Analysis)

The ultimate load has been divided in to loads which is 81.7/2 =40.85KN.

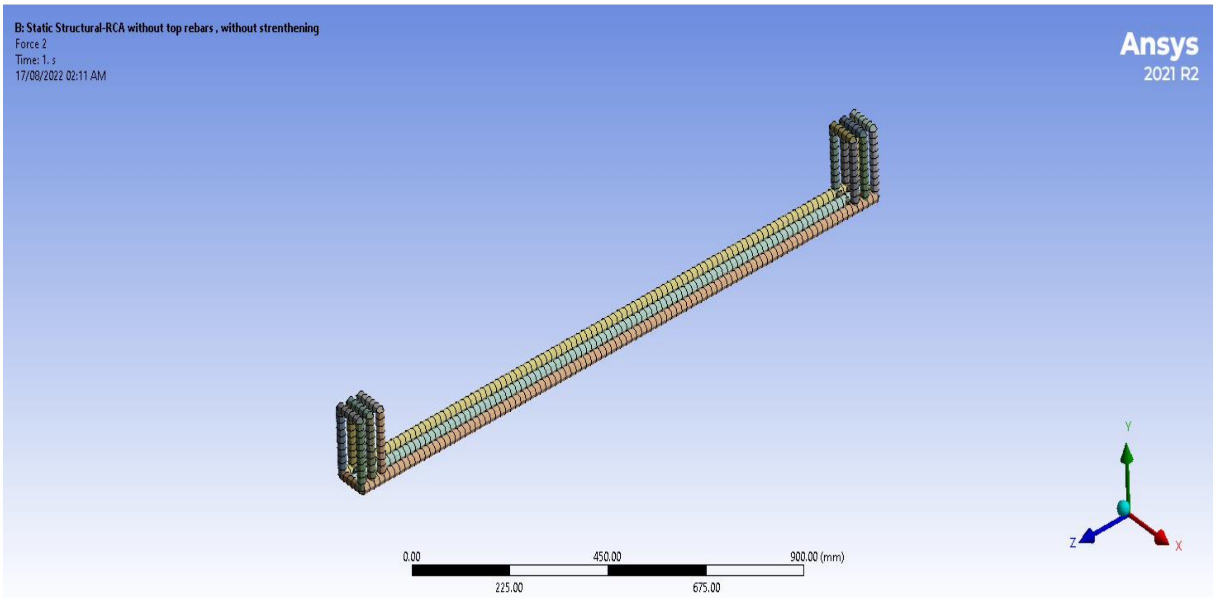

Figure 218(RCA-64.50MPa – Rebars of beam sample without strengthening - Static Nonlinear Analysis)

Deformations

Total Deformations

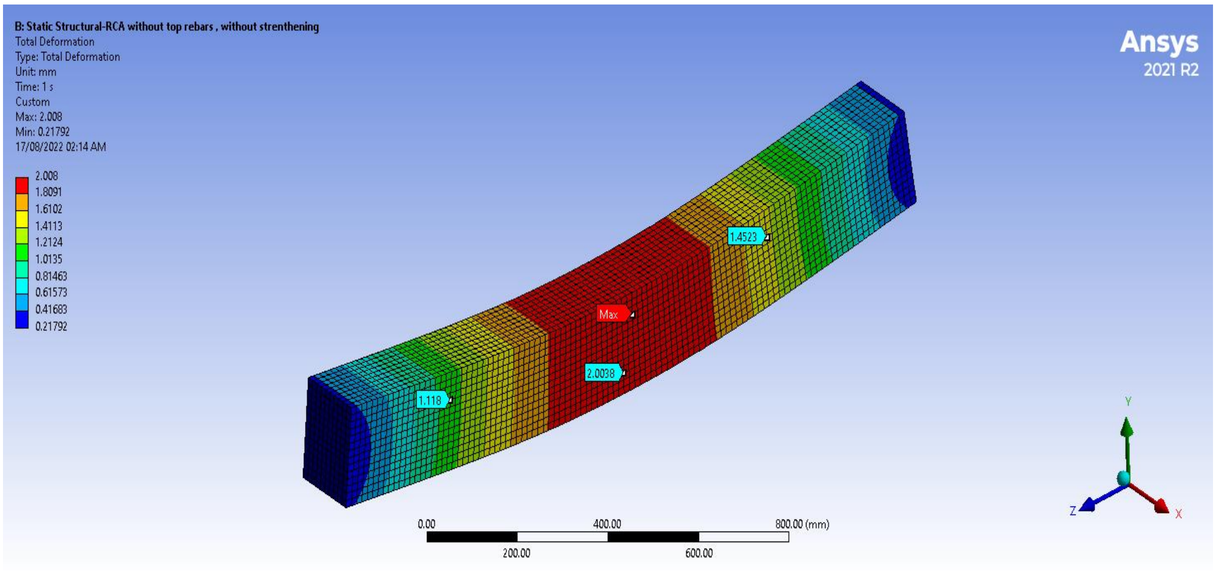

Figure 219(RCA-64.50MPa –Total deflections of beam sample without strengthening and top rebars- Static Nonlinear Analysis)

The value is 2.008 mm.

Directional Deformation (Y-Direction)

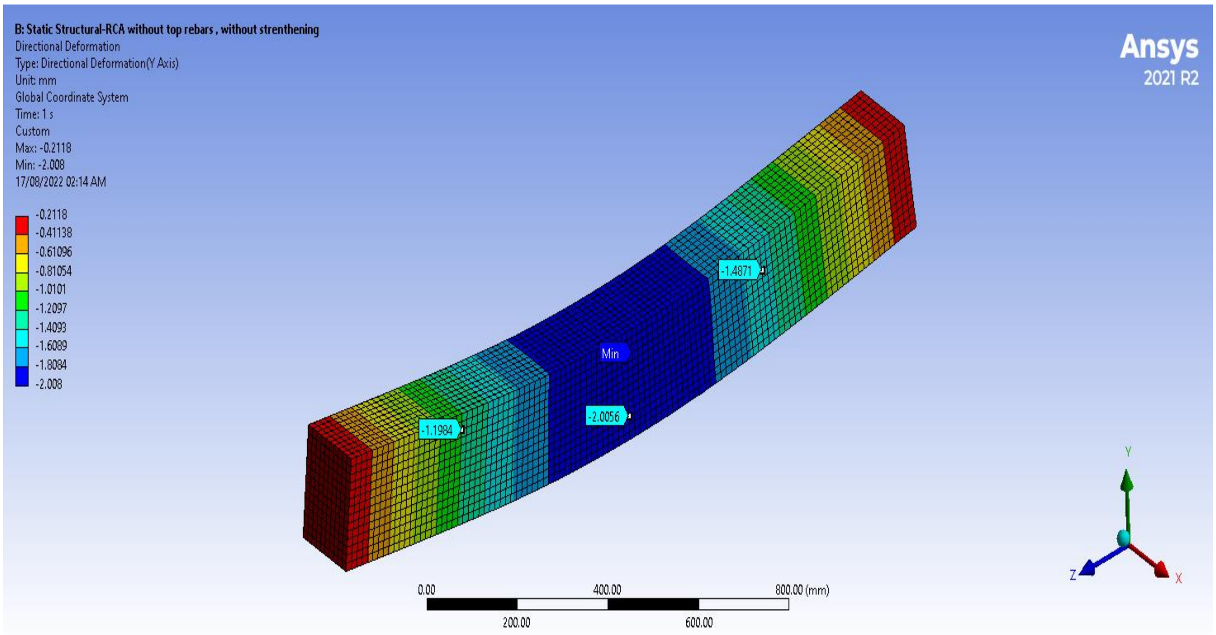

Figure 220(RCA-64.50MPa – Directional deflections (Y-Dir.) of beam sample without strengthening and top rebars- Static Nonlinear Analysis)

The value is 2.008 mm.

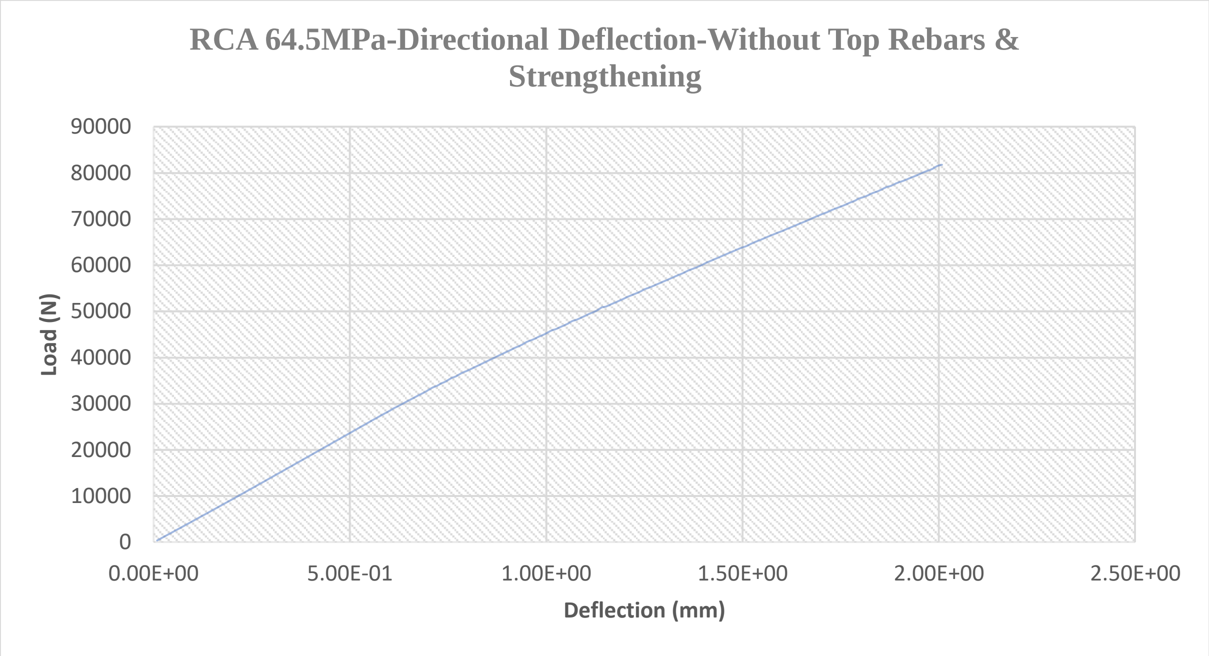

Figure 221(RCA-64.50MPa – Directional deflections (Y-Dir.) graph of beam sample without strengthening and top rebars- Static Nonlinear Analysis)

Normal Stress (Concrete)

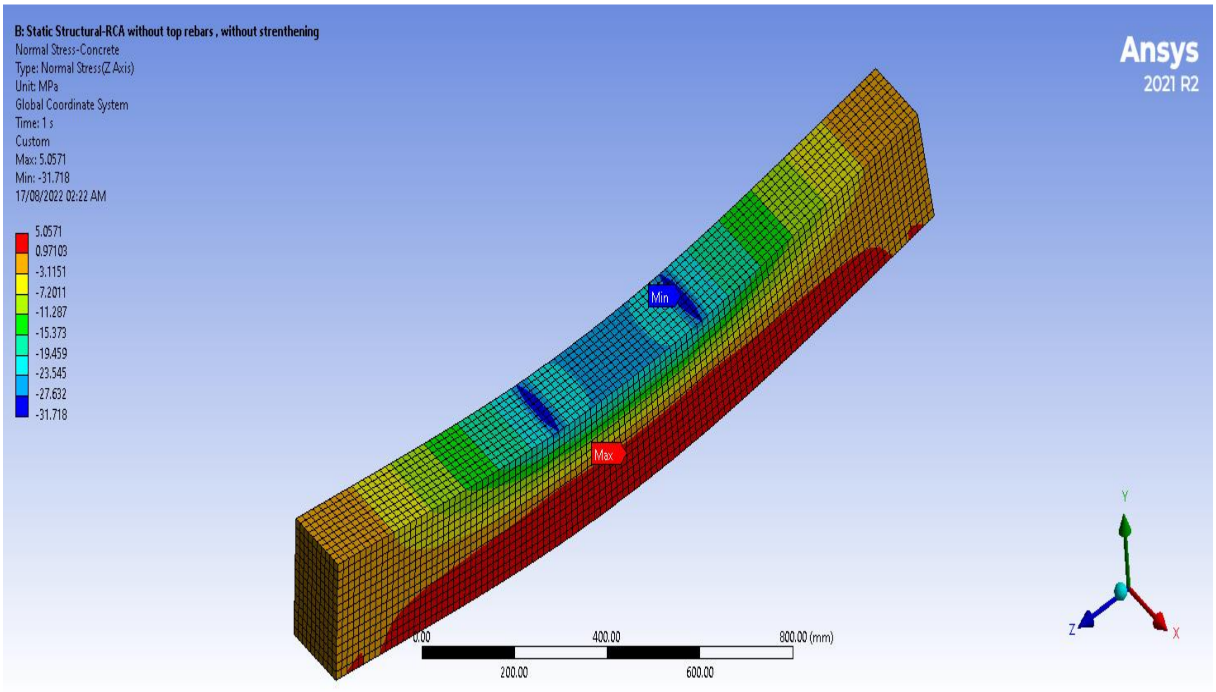

Figure 222(RCA-64.50MPa – Normal stress (concrete) of beam sample without strengthening and top rebars- Static Nonlinear Analysis)

The blue zones show the crushing from loading machine and the maximum value is 31.718 MPa, whereas the red zones indicate to tension.

Normal Stress (Rebars)

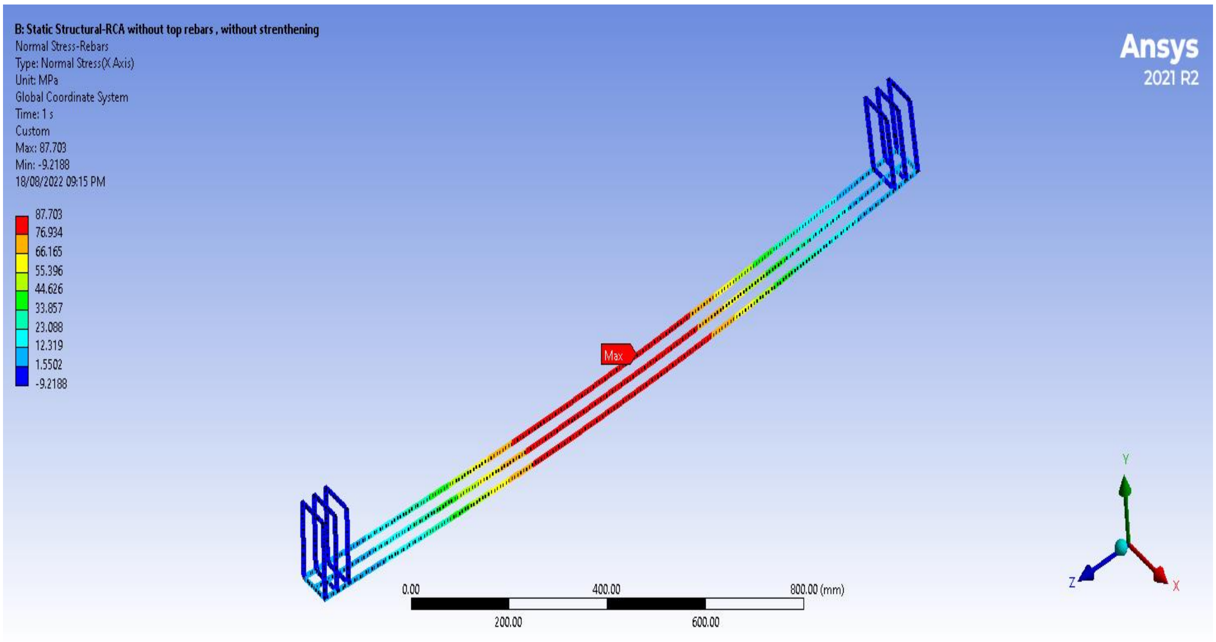

Figure 223(RCA-64.50MPa – Normal stress (Rebars) of beam sample without strengthening and top rebars- Static Nonlinear Analysis)

The red zones show that the rebars is yielding by 87.703 MPa, in the middle span due to tension.

Shear Stress

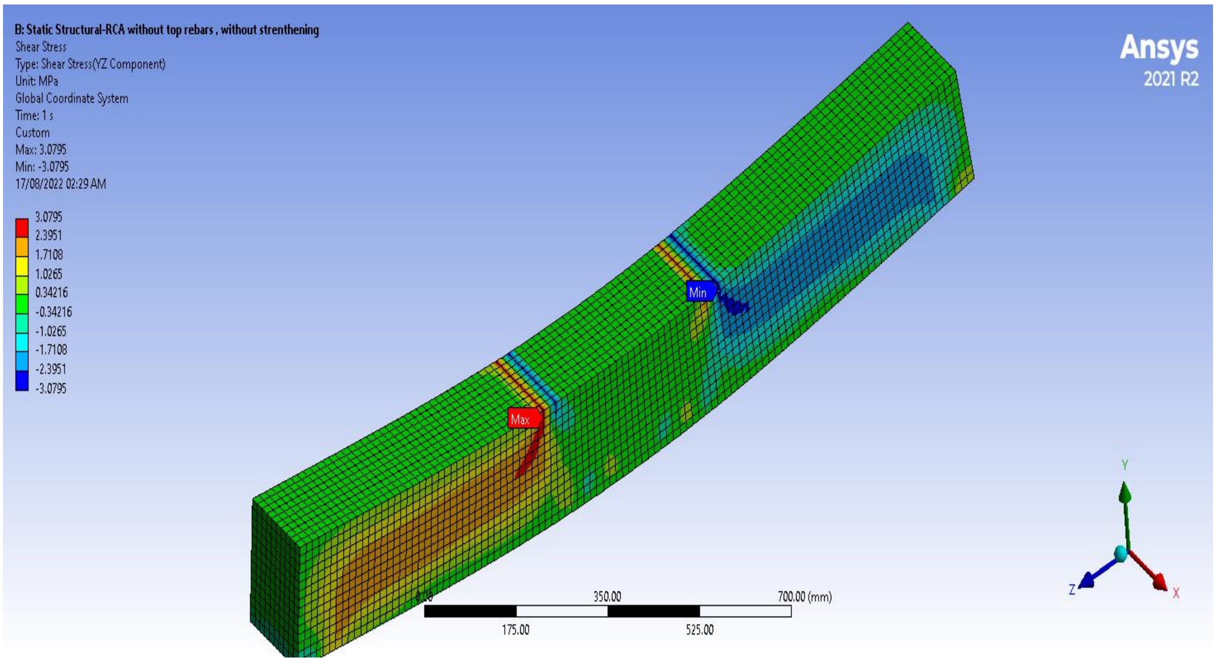

Figure 224(RCA-64.50MPa – Shear stress of beam sample without strengthening and top rebars- Static Nonlinear Analysis)

Elastic Strain

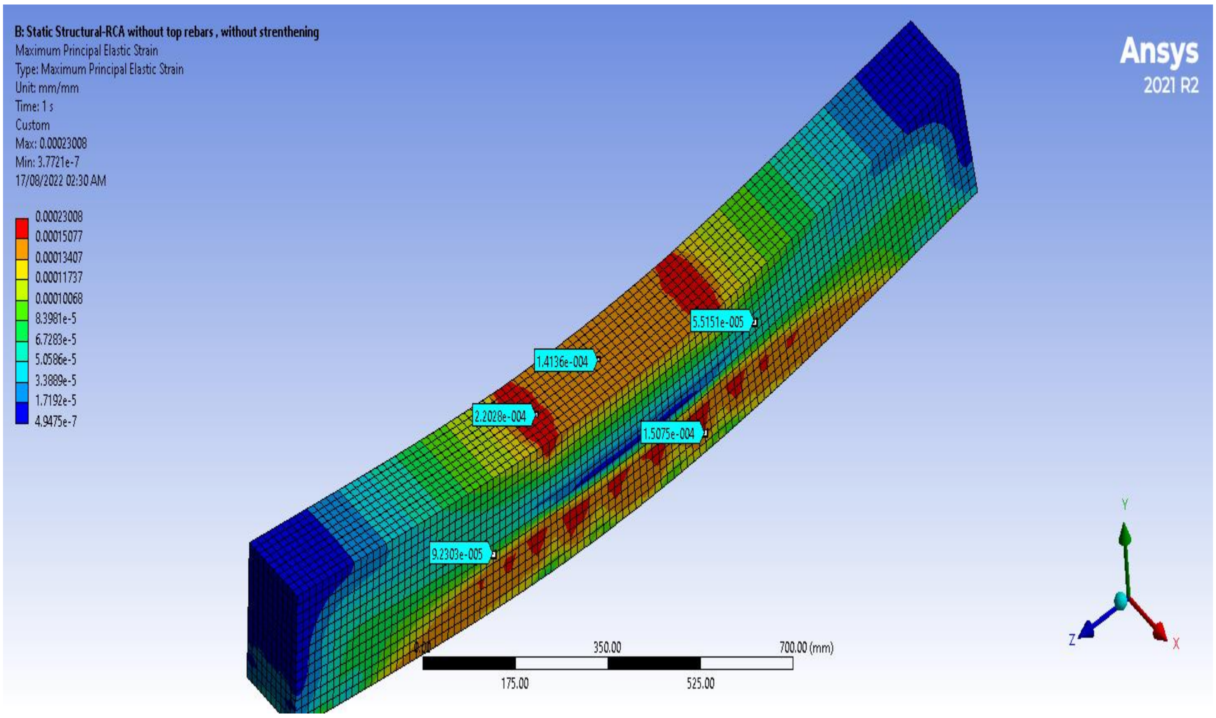

Figure 225(RCA-64.5MPa – Elastic strain of beam sample without strengthening and top rebars- Static Nonlinear Analysis)

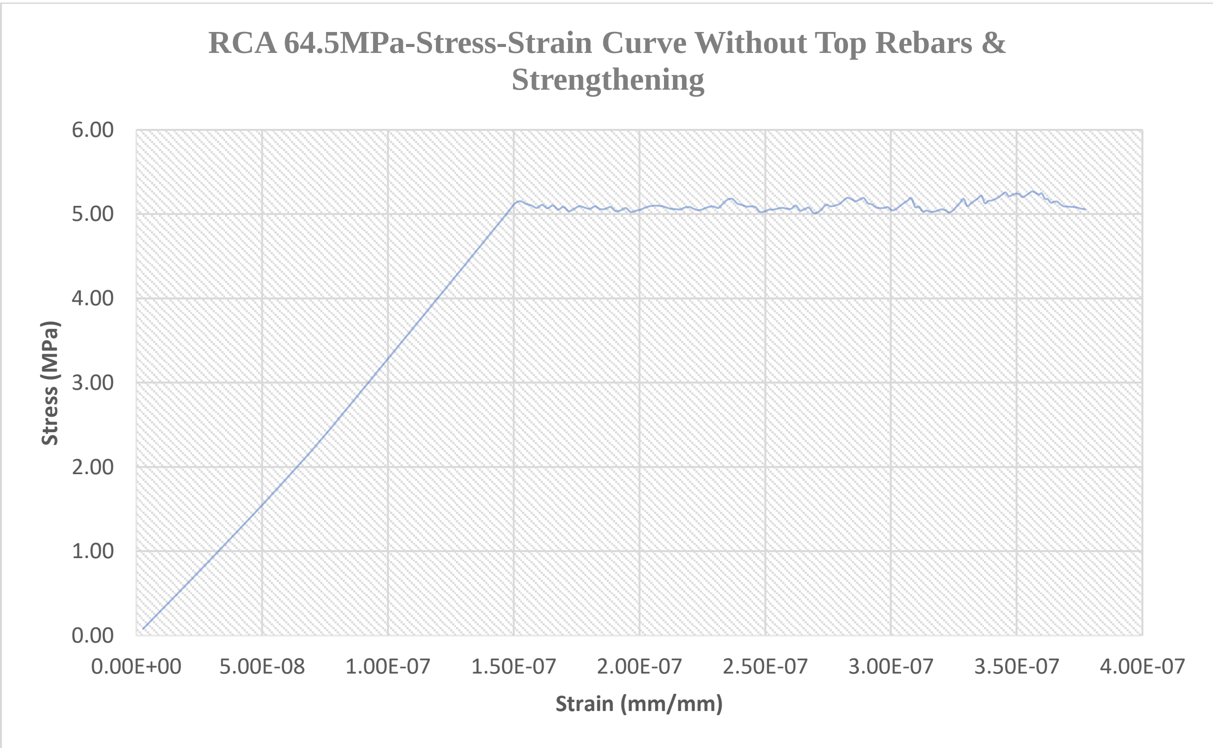

Figure 226(RCA-64.5MPa –Stress & Strain graph of beam sample without strengthening and top rebars- Static Nonlinear Analysis)

12- Explicit Dynamic-Without Top Rebars & Strengthening

Geometry and loads

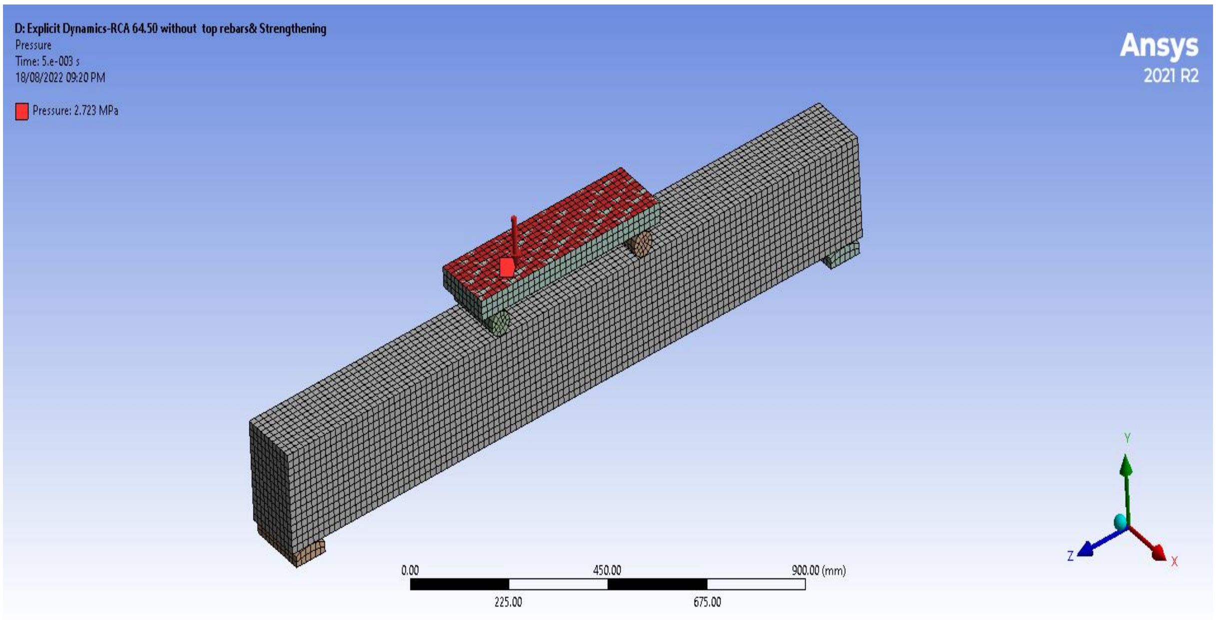

Figure 227(RCA-64.5MPa – Geometry & loads of beam sample without strengthening and top rebars- Explicit Dynamic Analysis)

The ultimate load has been transferred to be as a pressure load which is 2.723.0 MPa as shown above with rate loading 0.6mm/min.

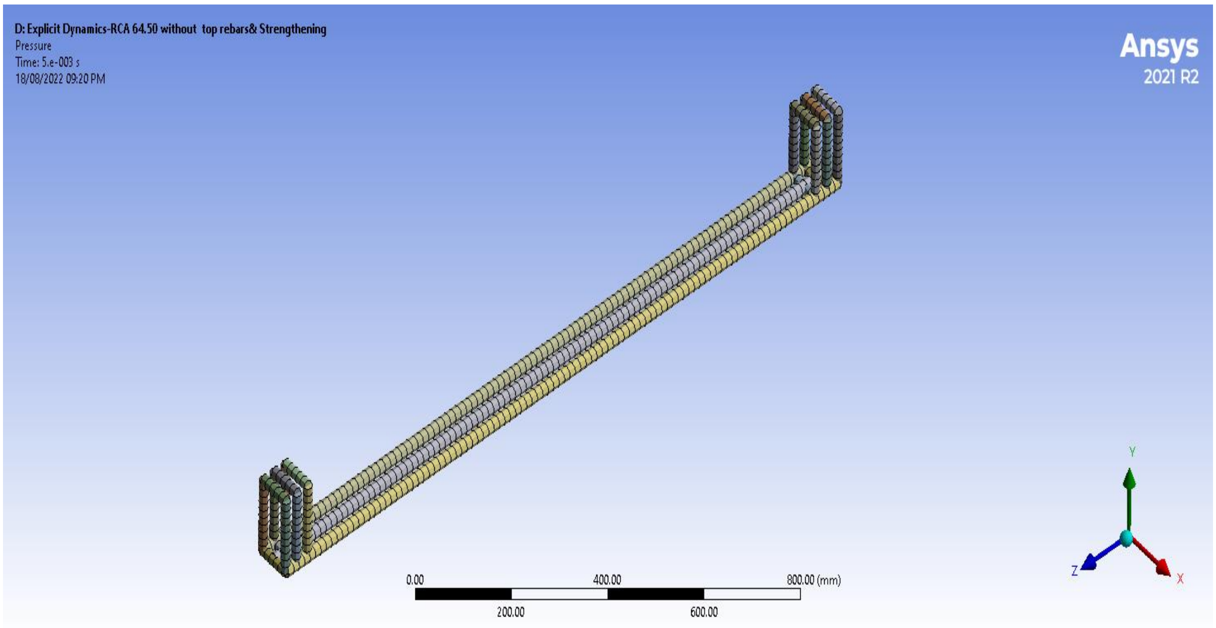

Figure 228(RCA-64.5MPa – Rebars of beam sample without strengthening- Explicit Dynamic Analysis)

Deformations

Total Deformations

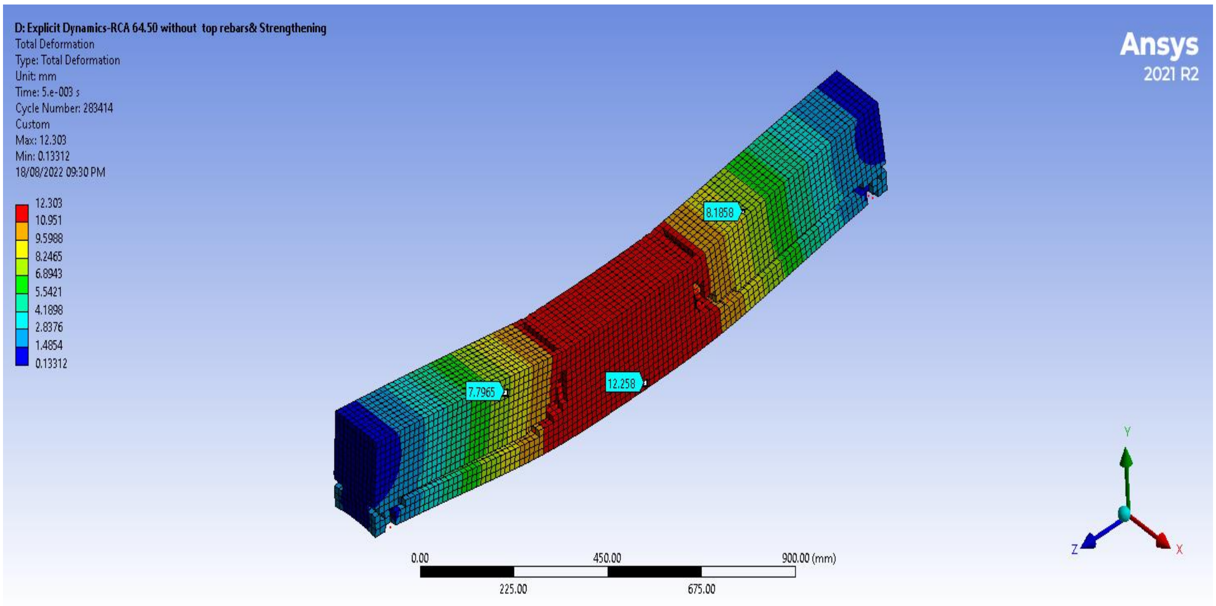

Figure 229(RCA-64.5MPa – Total deflections of beam sample without strengthening and top rebars- Explicit Dynamic Analysis)

The value is 12.303 mm.

Directional Deformation (Y-Direction)-Concrete

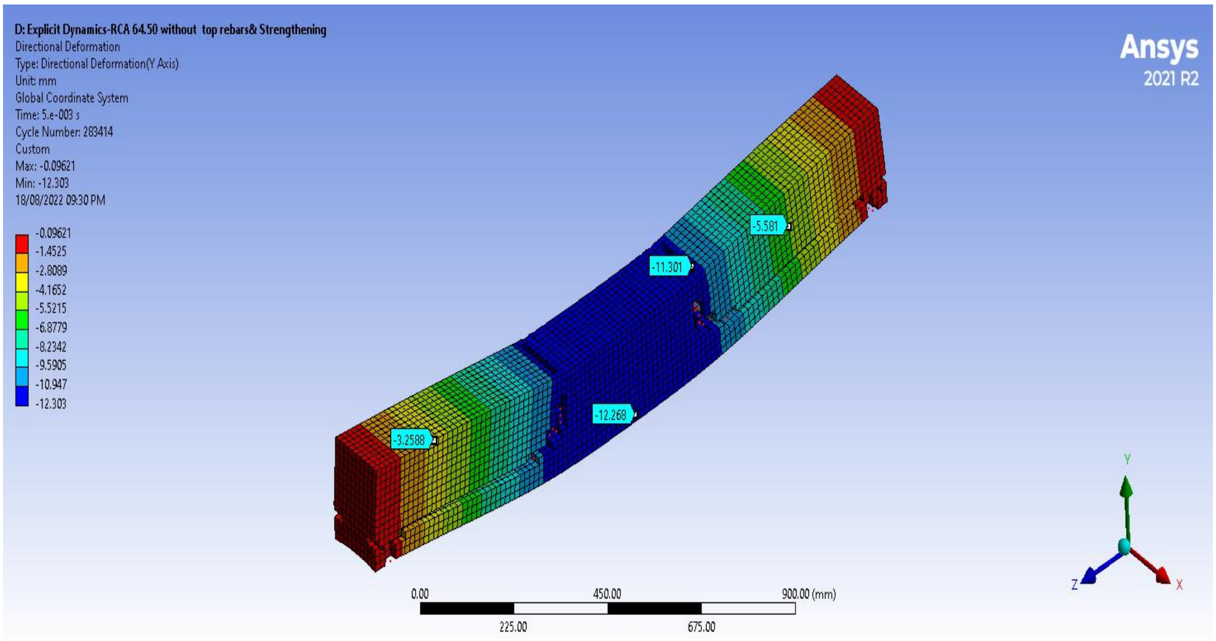

Figure 230(RCA-64.5MPa – Directional deflections (Y-Dim.) of beam sample without strengthening and top rebars- Explicit Dynamic Analysis)

The value is 12.303 mm.

Directional Deformation (Y-Direction)- Rebars

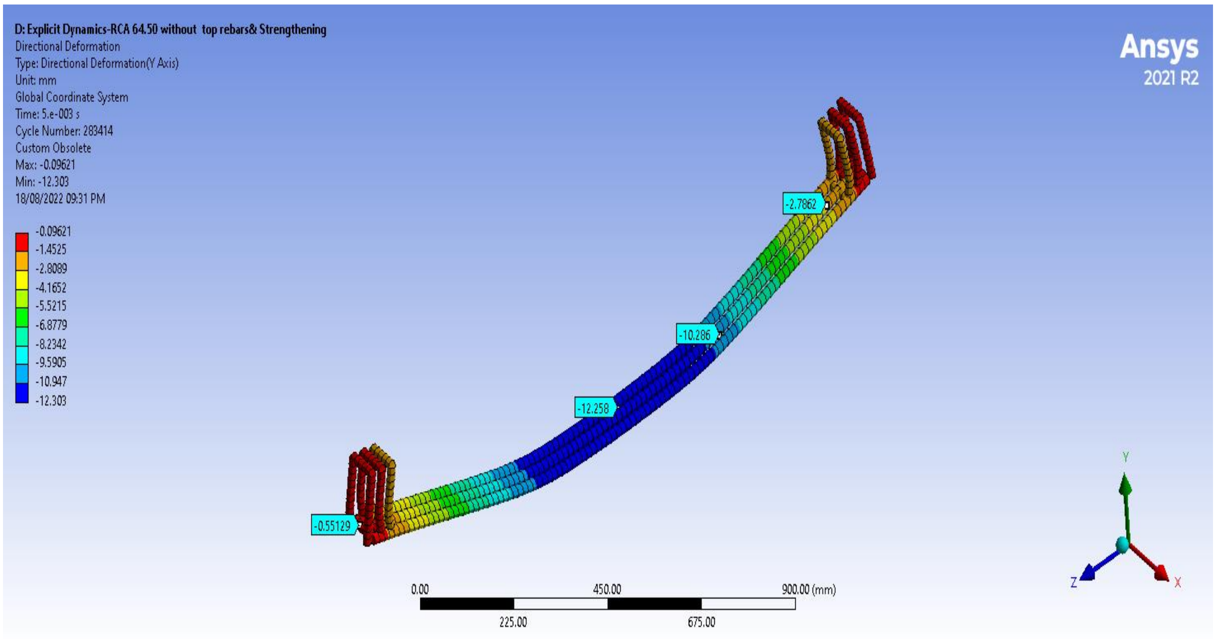

Figure 231(RCA-64.5MPa – Directional deflections (Rebars) of beam sample without strengthening- Explicit Dynamic Analysis)

Normal strain

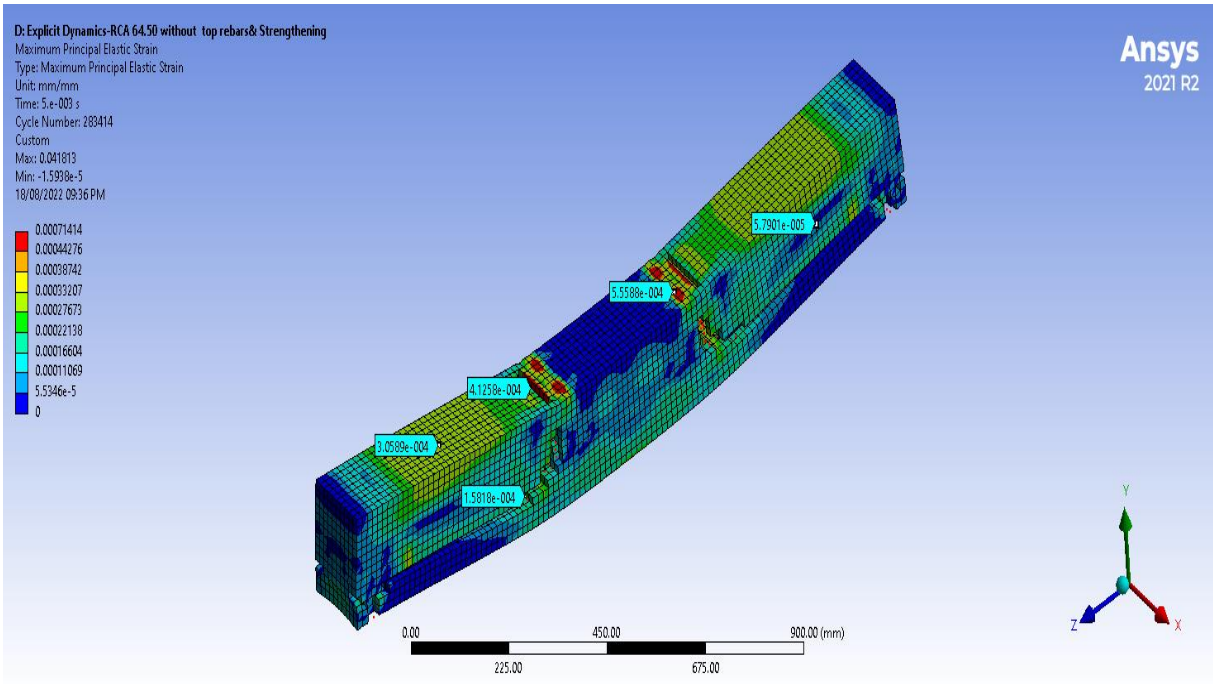

Figure 232(RCA-64.5MPa – Normal strain of beam sample without strengthening and top rebars- Explicit Dynamic Analysis)

Shear Stress

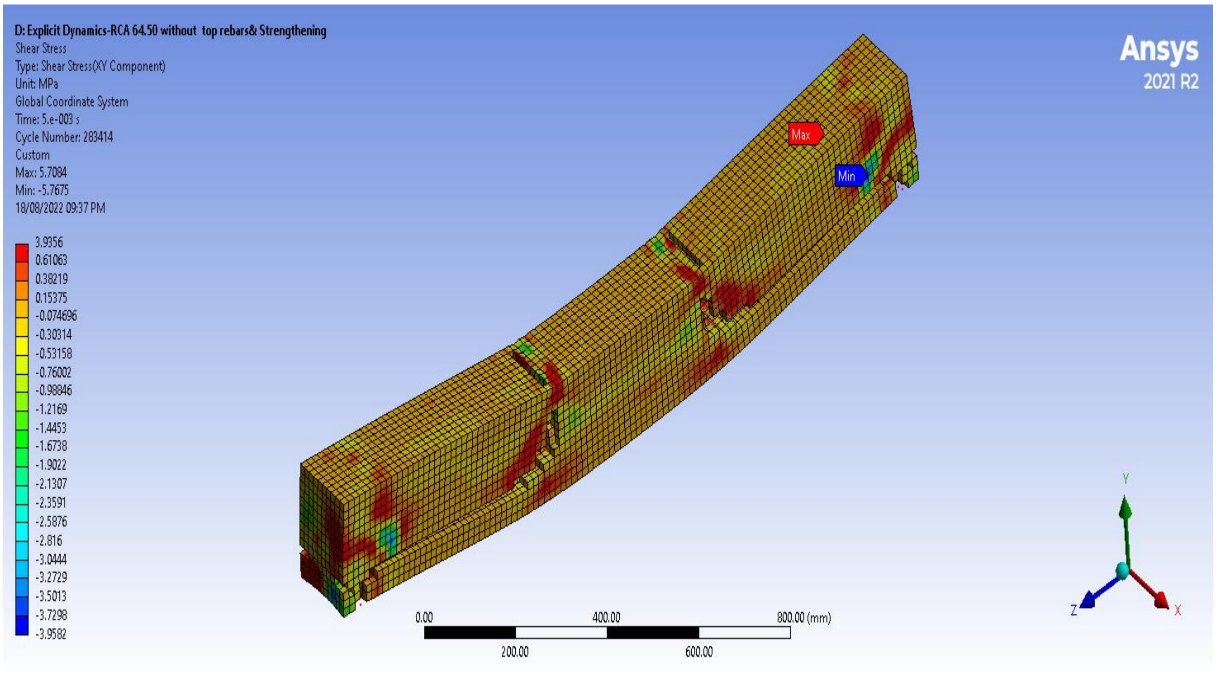

Figure 233(RCA-64.50MPa – Shear Stress of beam sample without strengthening and top rebars- Explicit Dynamic Analysis)

Total shape strain

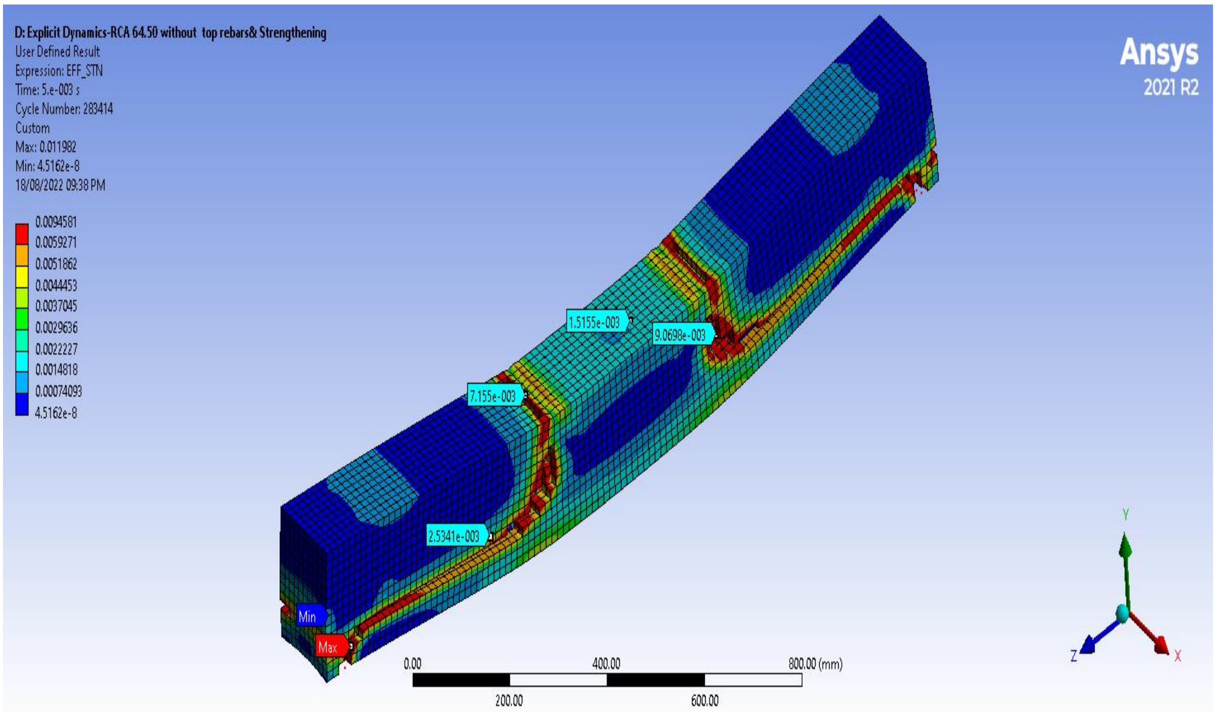

Figure 234(RCA-64.50MPa – Total strain of beam sample without strengthening and top rebars- Explicit Dynamic Analysis)

Maximum Stress

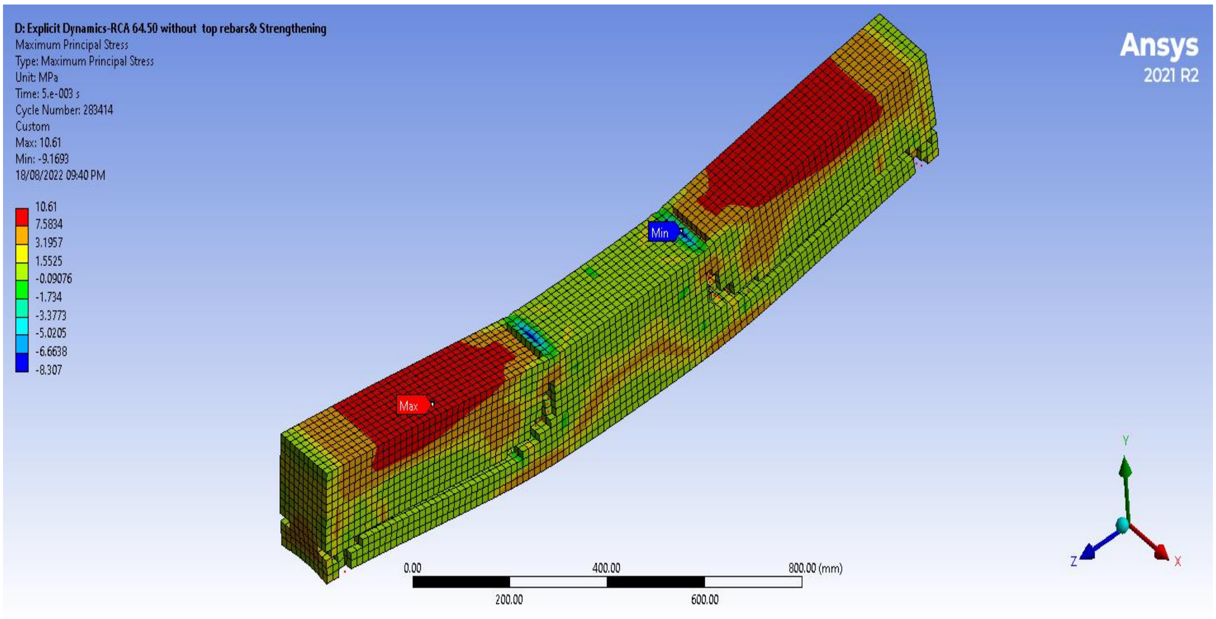

Figure 235(RCA-64.50MPa –Maximum Stress of beam sample without strengthening and top rebars- Explicit Dynamic Analysis)

The Damage Pattern

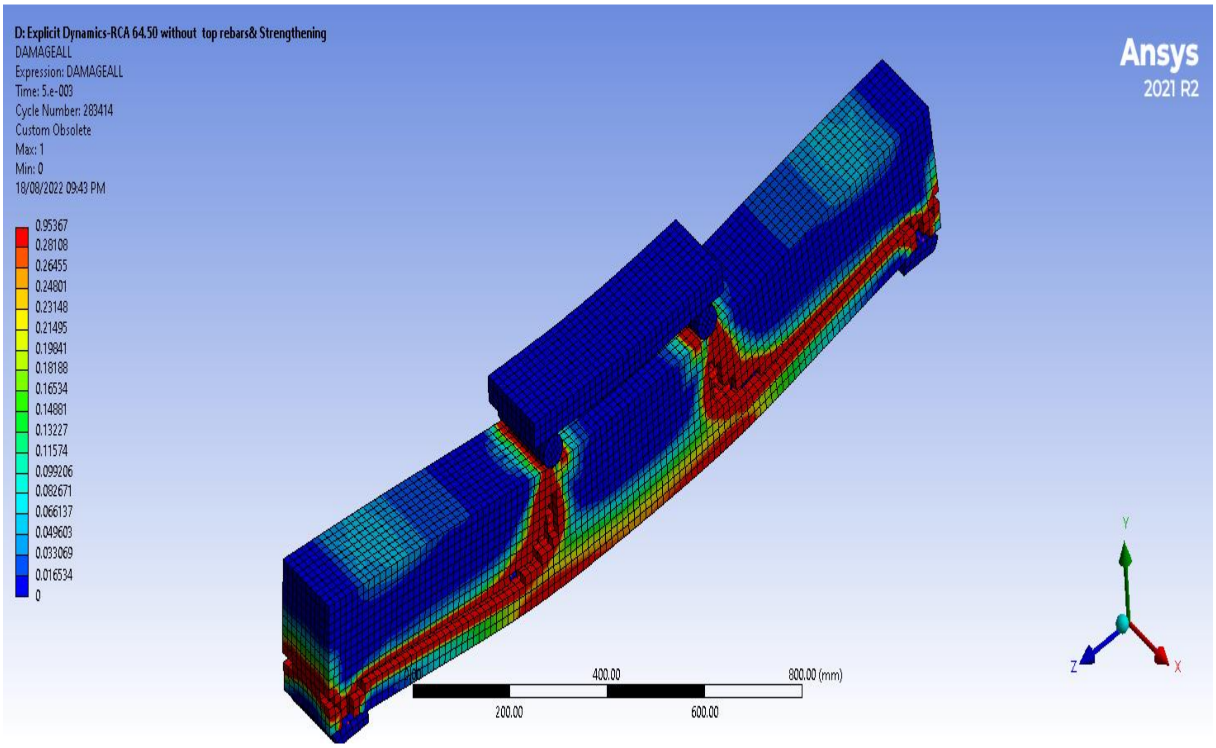

Figure 236(RCA-64.50MPa – Damage Pattern-1 of beam sample without strengthening and top rebars- Explicit Dynamic Analysis)

As we can see the shear damage cracks and concrete failures.

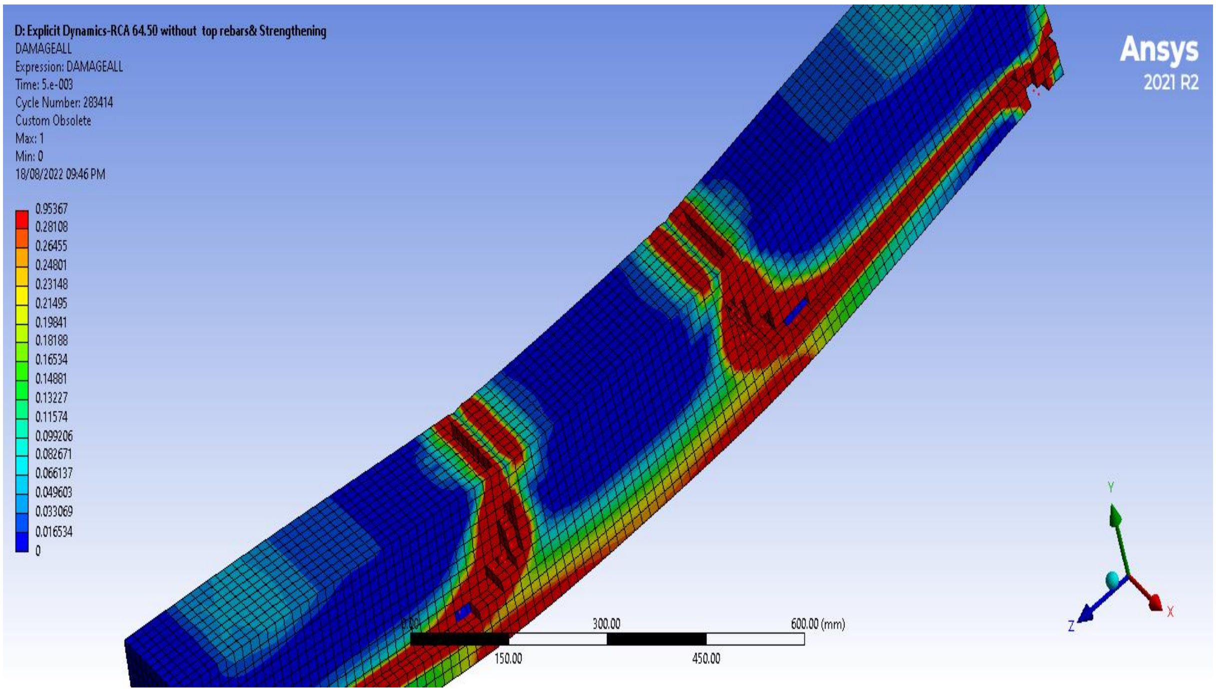

Figure 237(RCA-64.50MPa – Damage Pattern-2 of beam sample without strengthening and top rebars- Explicit Dynamic Analysis)

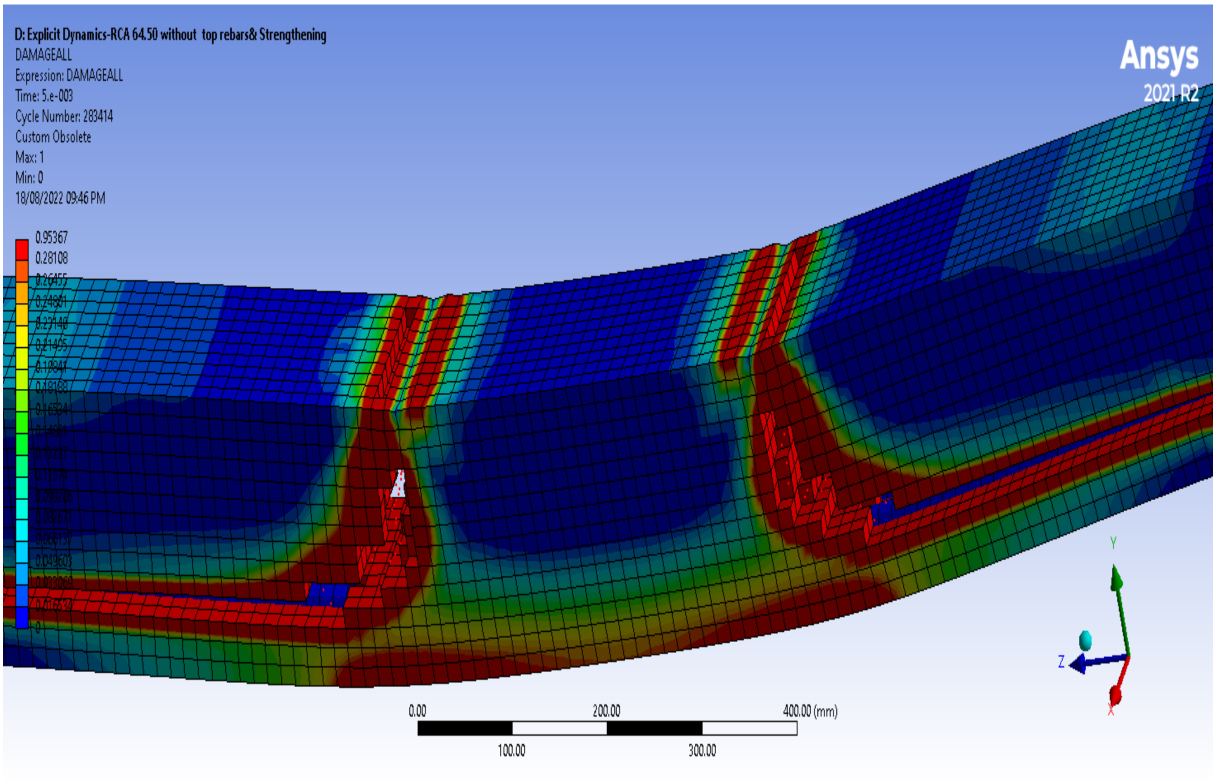

Figure 238(RCA-64.50MPa – Damage Pattern-3 of beam sample without strengthening and top rebars- Explicit Dynamic Analysis)

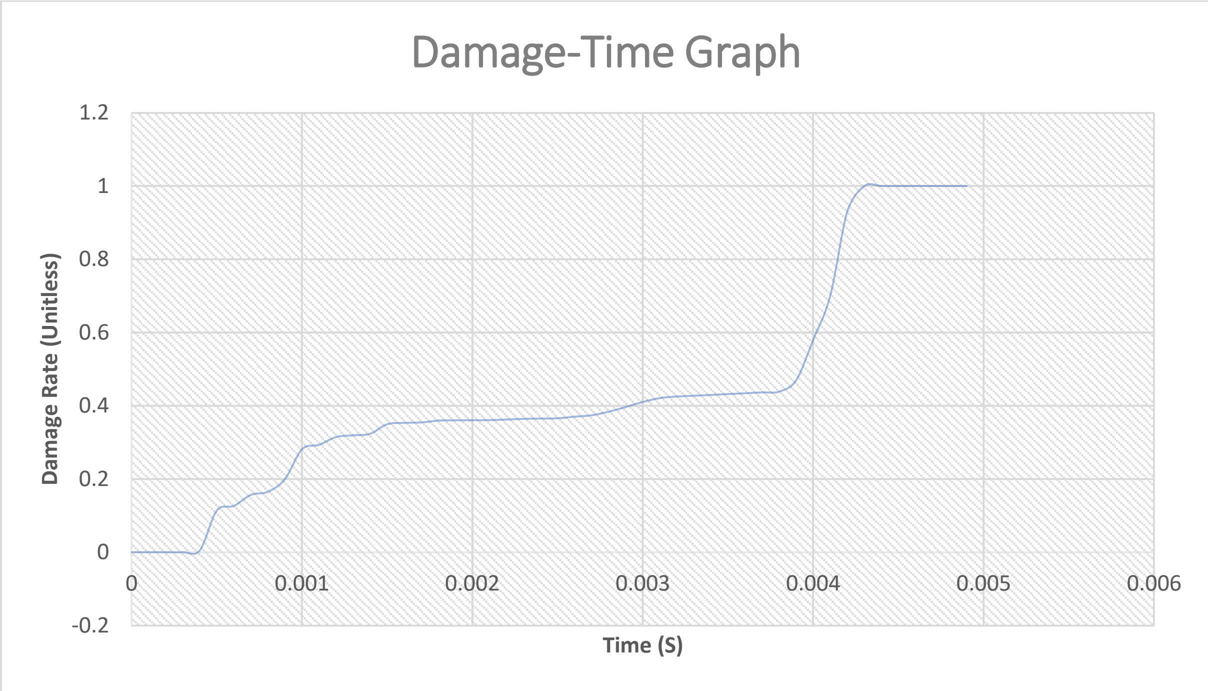

Figure 239(RCA-64.50MPa – Damage Pattern graph of beam sample without strengthening and top rebars- Explicit Dynamic Analysis)

13- Static Non-Linear Analysis - With Strengthening and Top Rebars

Geometry and loads

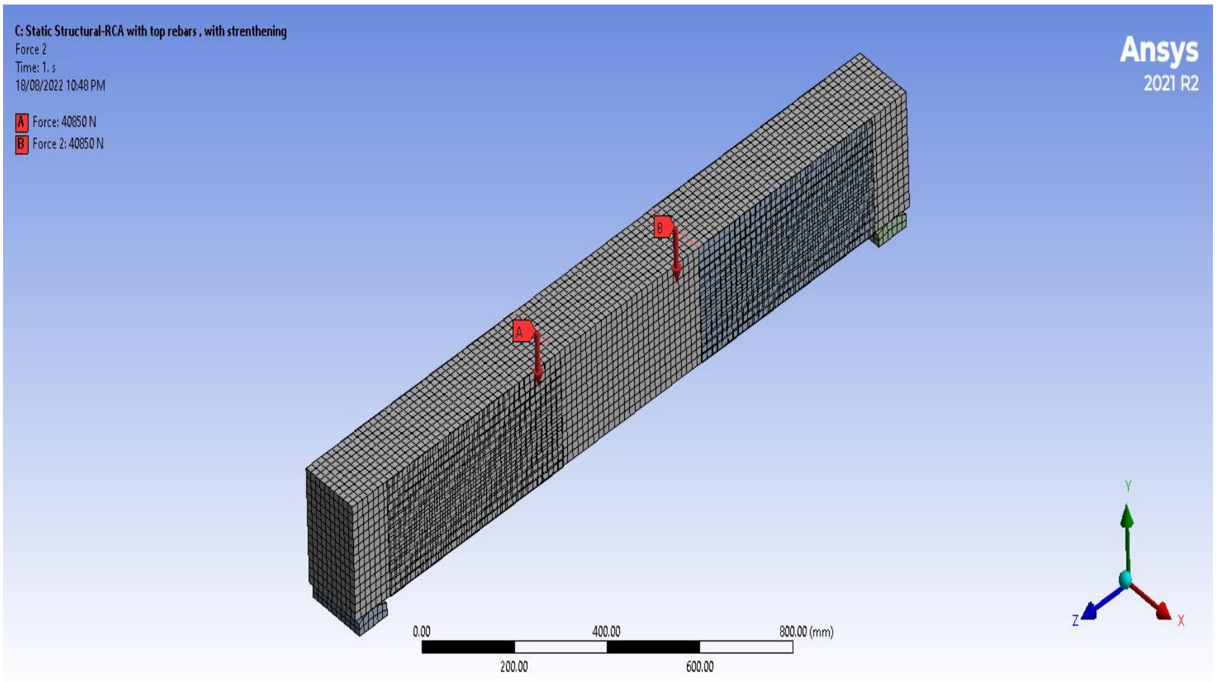

Figure 240(RCA-64.50MPa – Geometry & loads of beam sample with strengthening and top rebars- Static Nonlinear Analysis)

The ultimate load has been divided in to loads which is 81.7/2 =40.85KN.

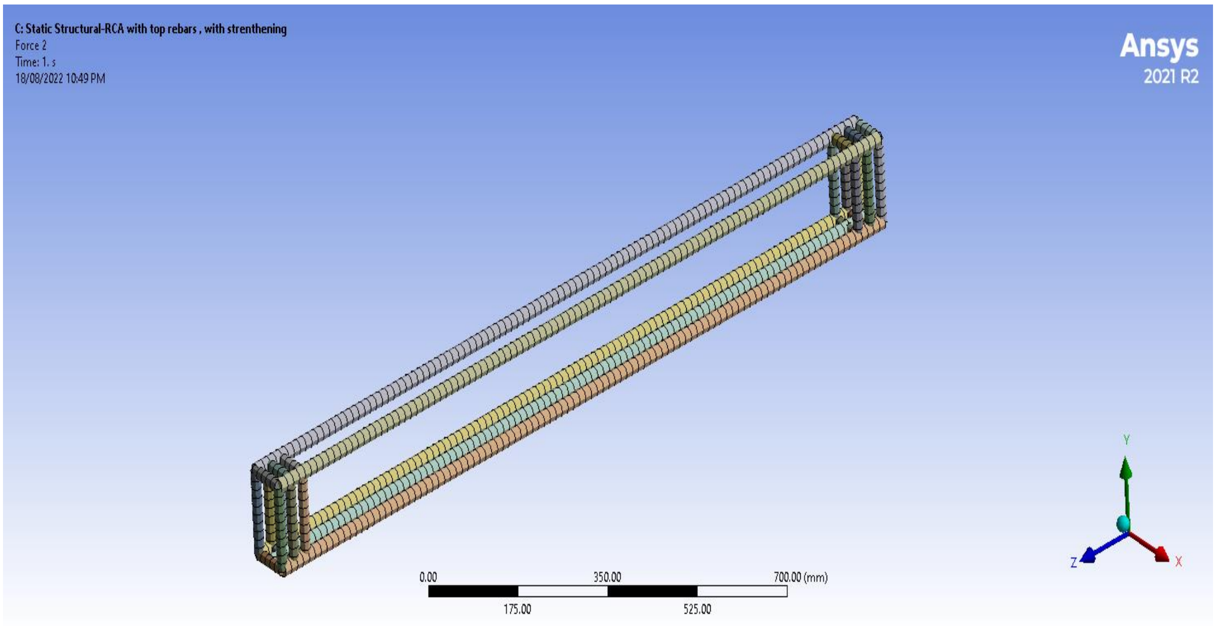

Figure 241(RCA-64.50MPa –Rebars of beam sample with strengthening- Static Nonlinear Analysis)

Deformations

Total Deformations

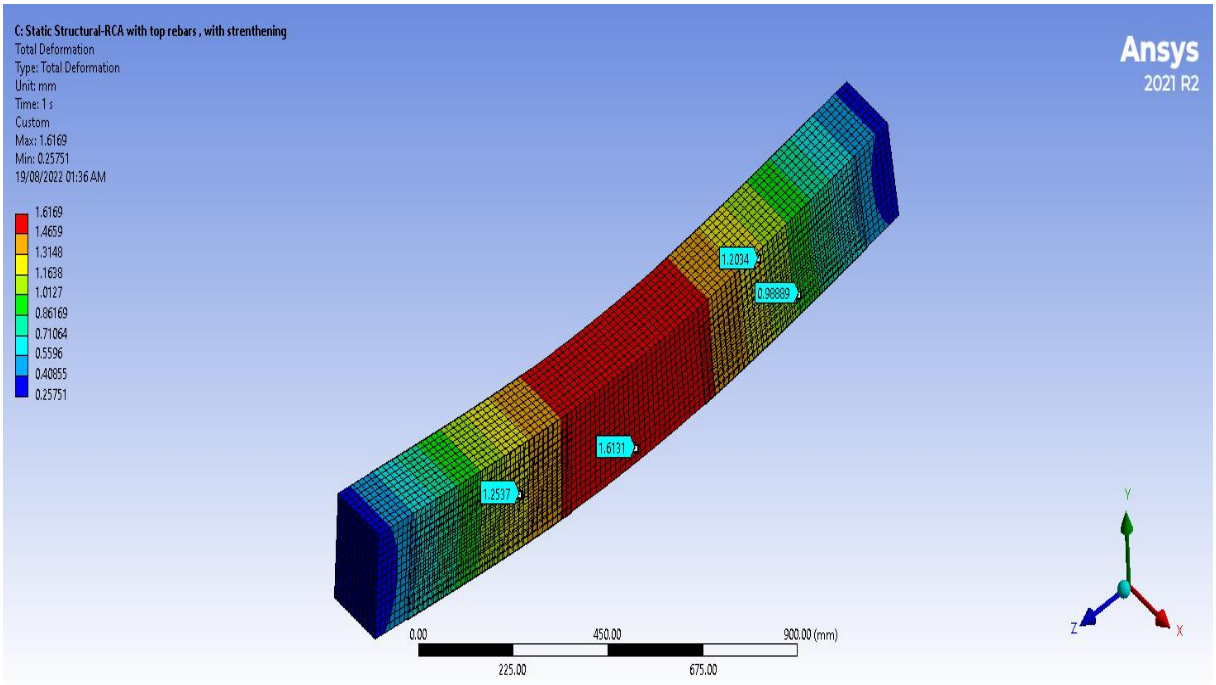

Figure 242(RCA-64.50MPa – Total deflections of beam sample with strengthening and top rebars- Static Nonlinear Analysis)

The value is 1.6169 mm.

Directional Deformation (Y-Direction)

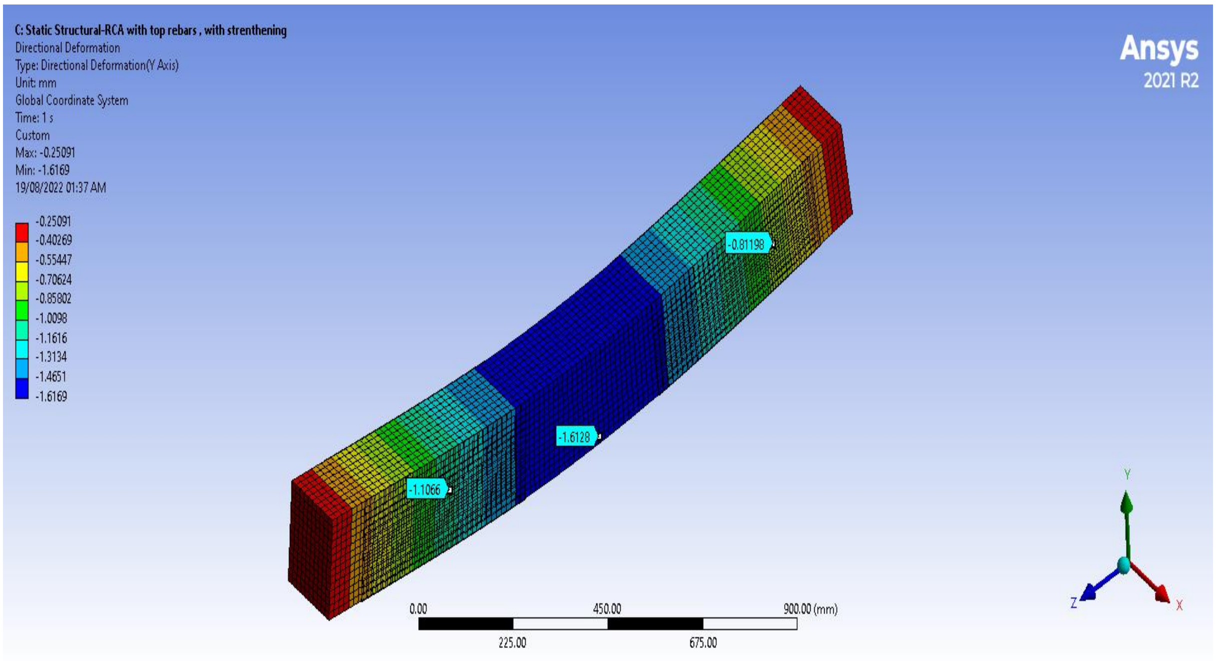

Figure 243(RCA-64.50MPa – Directional deflections (Y-Dim.) of beam sample with strengthening and top rebars- Static Nonlinear Analysis)

The value is 1.6169 mm.

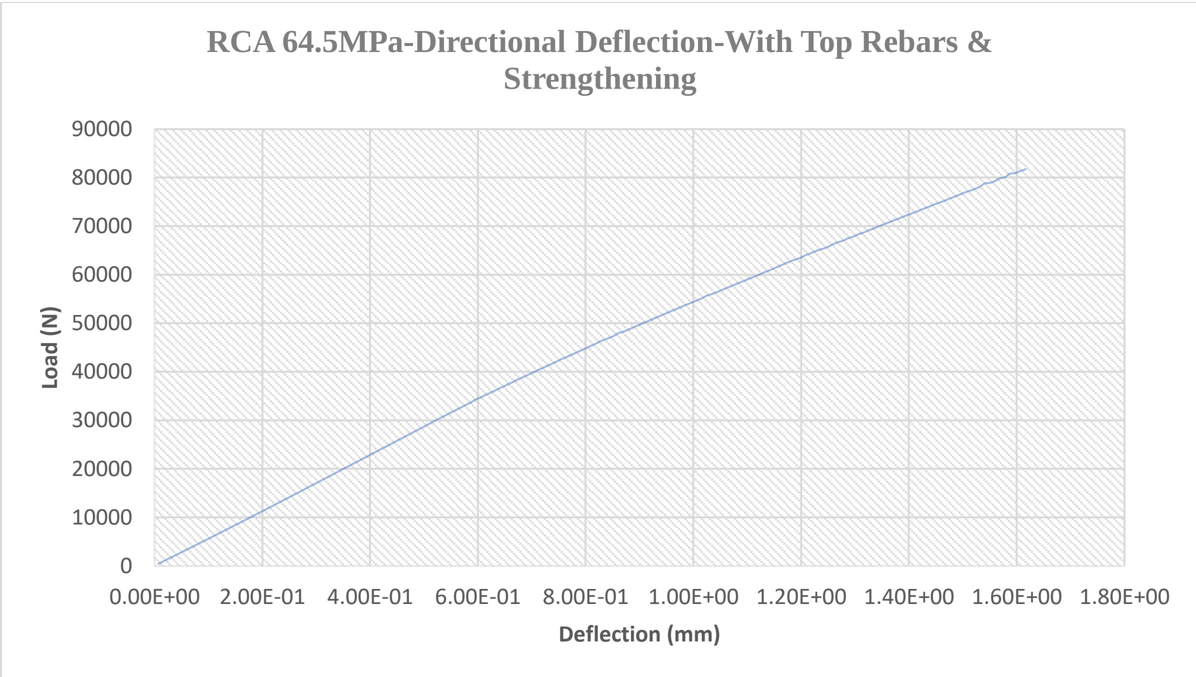

Figure 244(RCA-64.50MPa – Directional deflections (Y-Dim.) graph of beam sample with strengthening and top rebars- Static Nonlinear Analysis)

Normal Stress (Concrete)

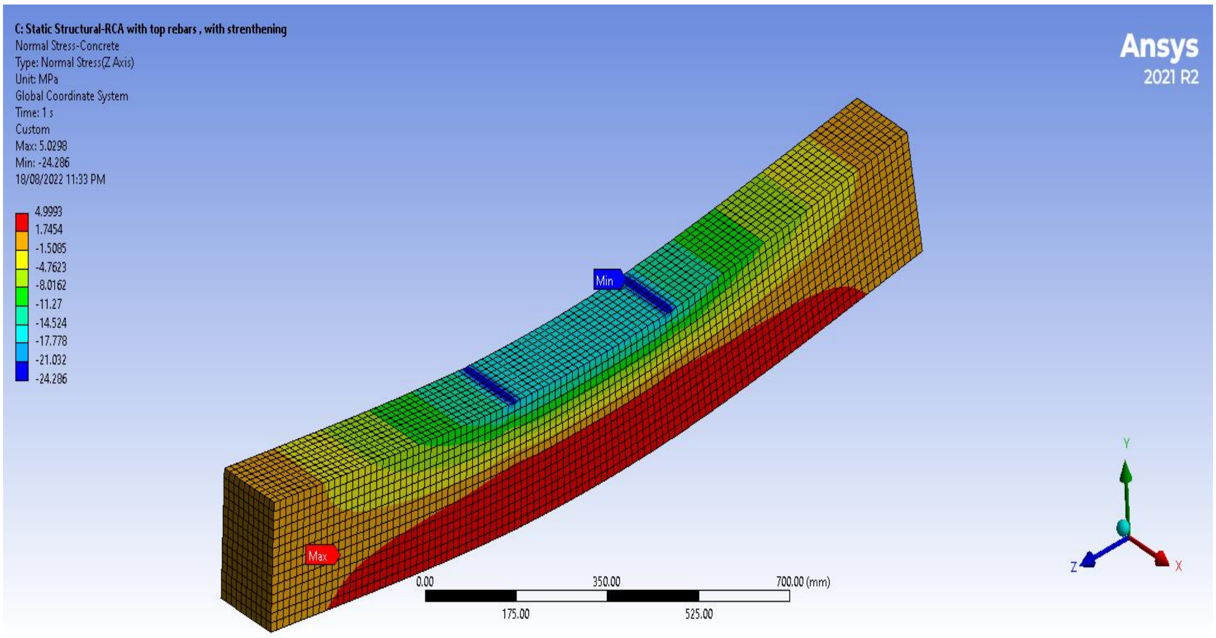

Figure 245(RCA-64.50MPa – Normal Stress (Concrete) of beam sample with strengthening and top rebars- Static Nonlinear Analysis)

The blue zones show the crushing from loading machine and the maximum value is 24.286 MPa, whereas the red zones indicate to tension.

Normal Stress (Rebars)

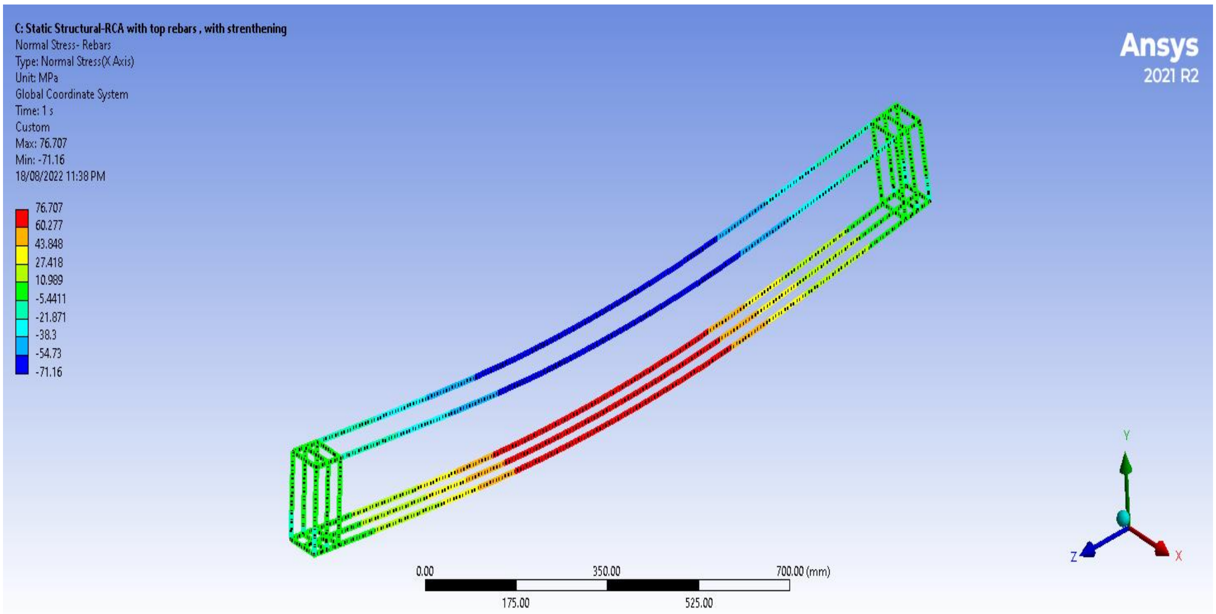

Figure 246(RCA-64.50MPa – Normal Stress (Rebars) of beam sample with strengthening and top rebars- Static Nonlinear Analysis)

The red zones show that the rebars is yielding by 76.707 MPa, in the middle span due to tension.

Shear Stress

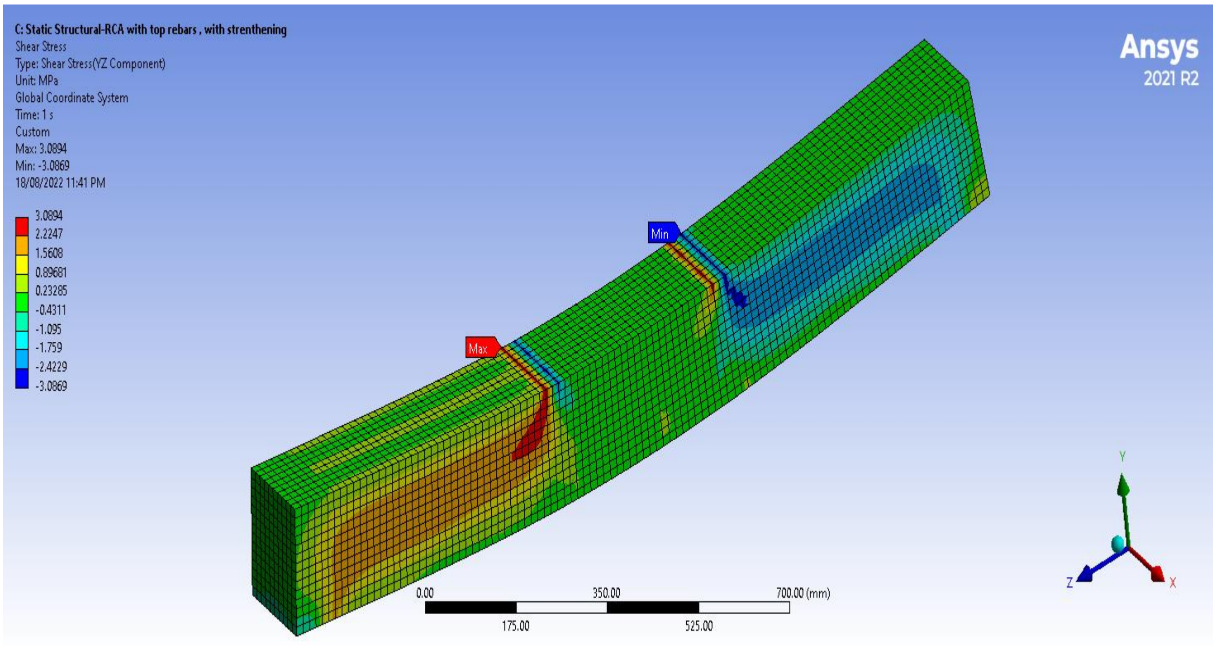

Figure 247(RCA-64.50MPa – Shear Stress of beam sample with strengthening and top rebars- Static Nonlinear Analysis)

Elastic Strain

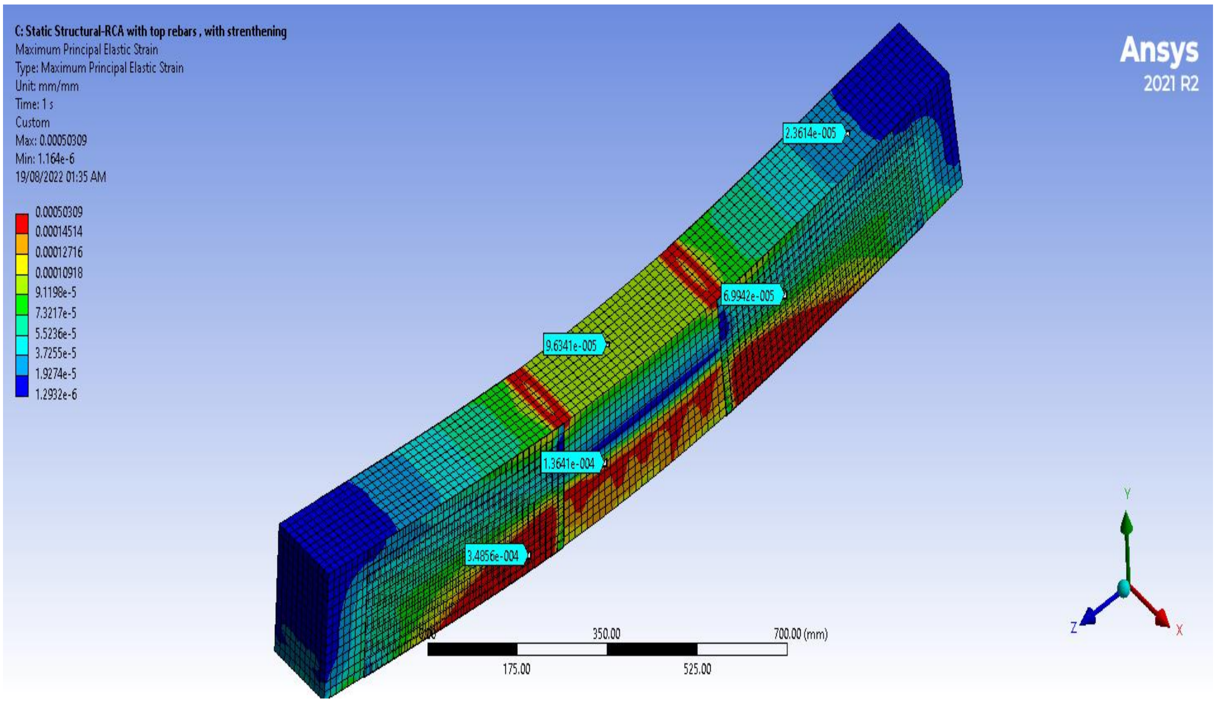

Figure 248(RCA-64.50MPa – Elastic strain of beam sample with strengthening and top rebars- Static Nonlinear Analysis)

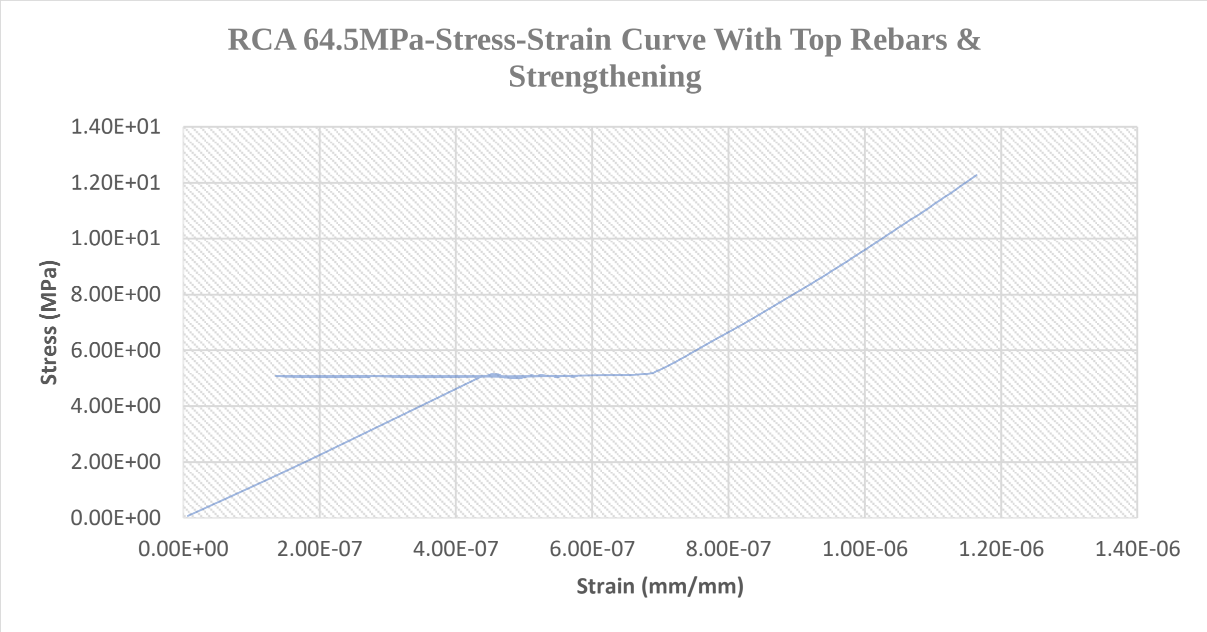

Figure 249(RCA-64.50MPa – Stress & Strain graph of beam sample with strengthening and top rebars- Static Nonlinear Analysis)

14- Explicit Dynamic-With Top Rebars & Strengthening

Geometry and loads

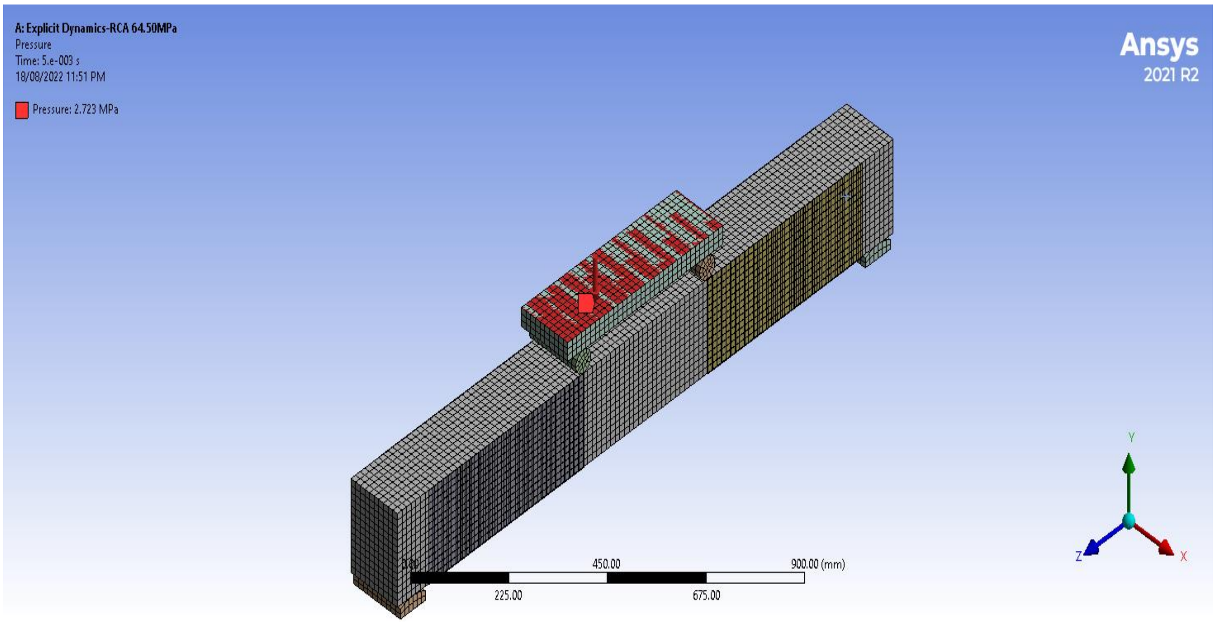

Figure 250(RCA-64.50MPa – Geometry & loads of beam sample with strengthening and top rebars- Explicit Dynamic Analysis)

The ultimate load has been transferred to be as a pressure load which is 2.723.0 MPa as shown above with rate loading 0.6mm/min.

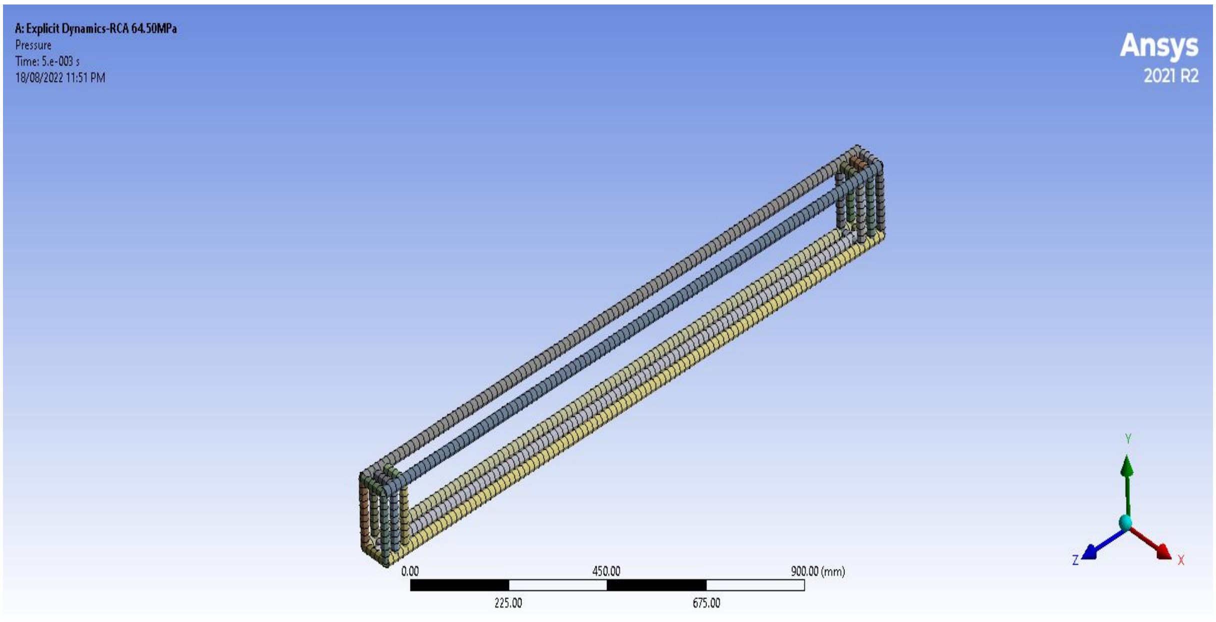

Figure 251(RCA-64.50MPa – Rebars of beam sample with strengthening – Explicit Dynamic Analysis)

Deformations

Total Deformations

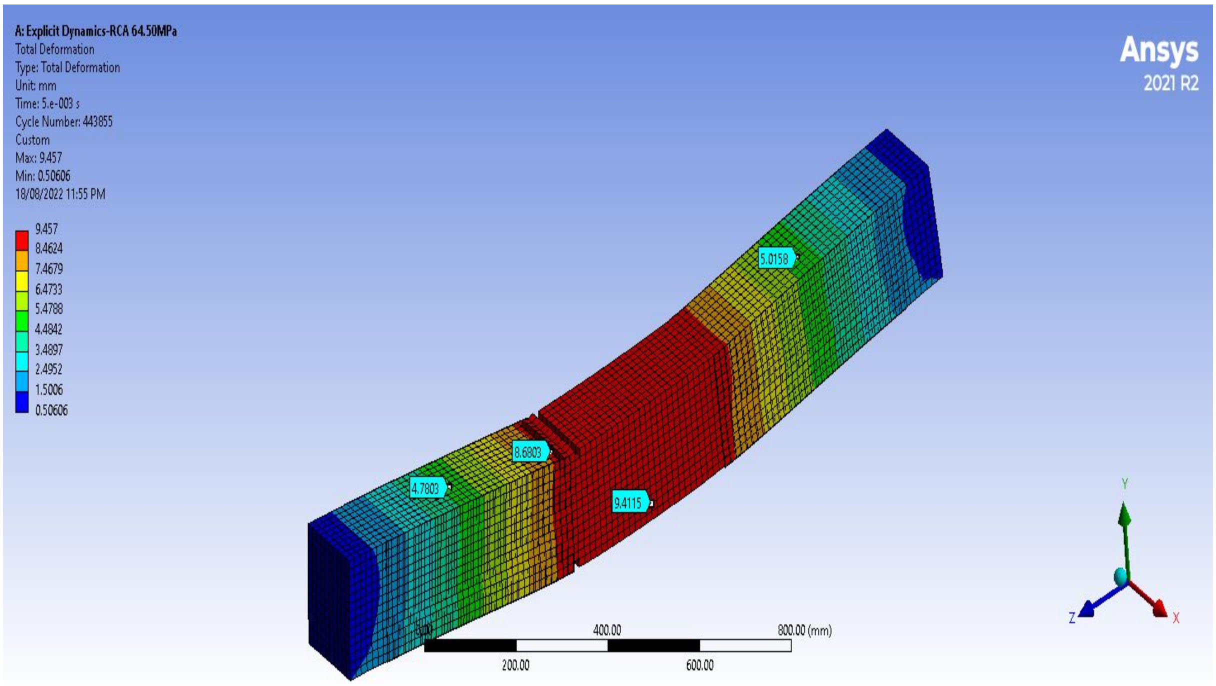

Figure 252(RCA-64.50MPa – Total deflections of beam sample with strengthening and top rebars- Explicit Dynamic Analysis)

The value is 9.457 mm.

Directional Deformation (Y-Direction)-Concrete

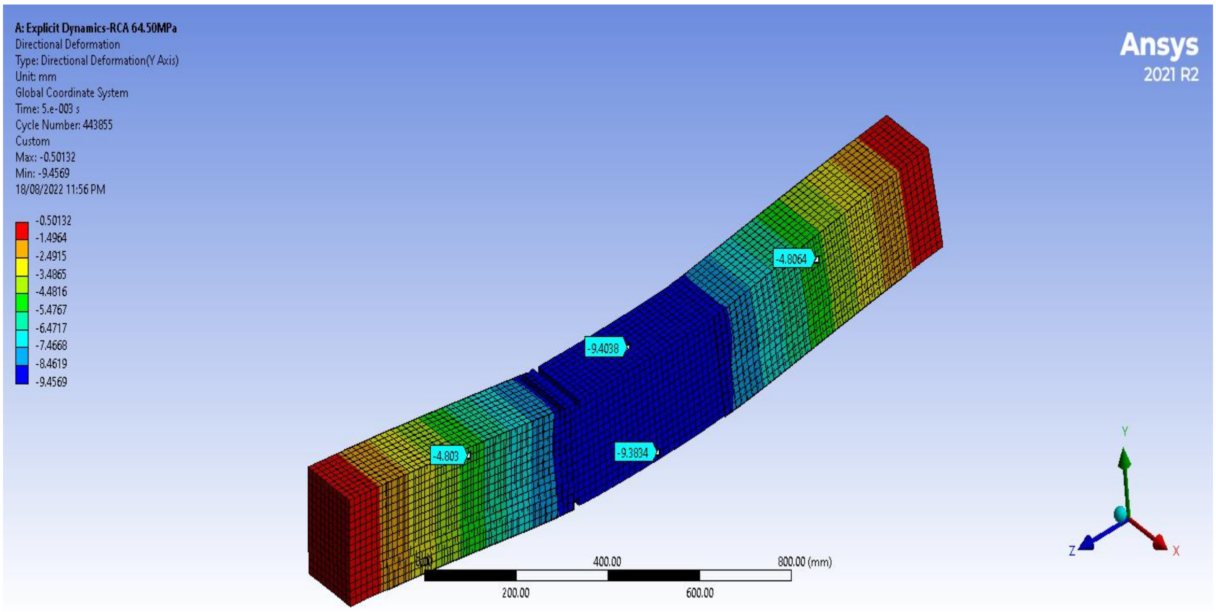

Figure 253(RCA-64.50MPa – Directional deflection (Y-Dim.) of beam sample with strengthening and top rebars- Explicit Dynamic Analysis)

The value is 9.457 mm.

Directional Deformation (Y-Direction)- Rebars

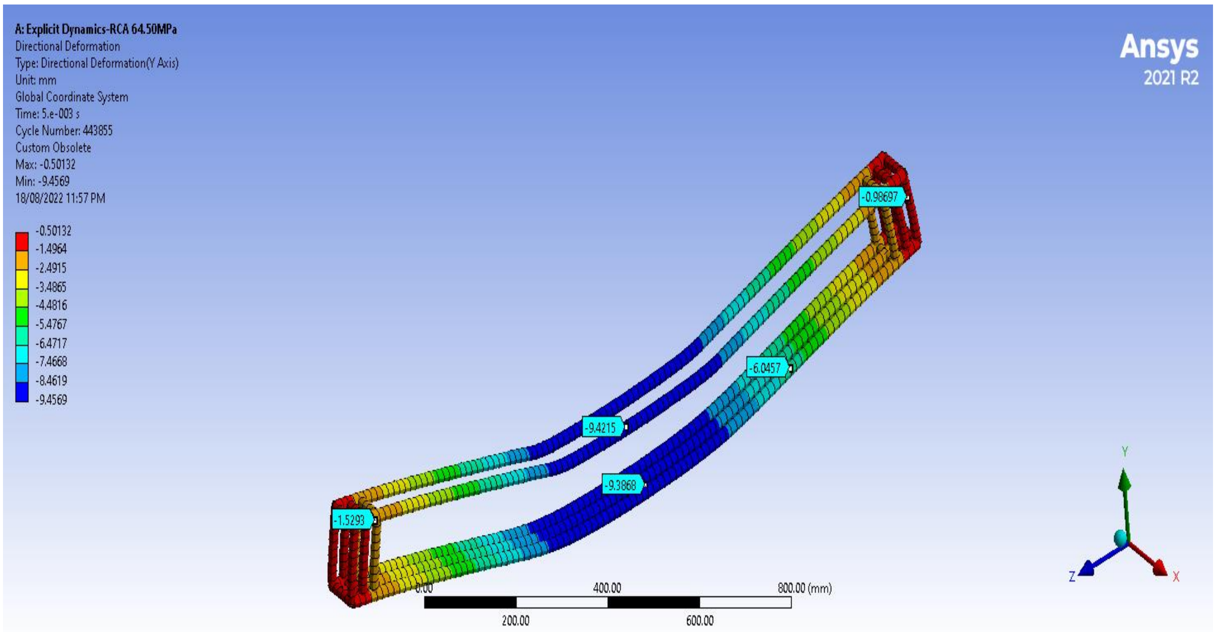

Figure 254(RCA-64.50MPa –Directional deflection (Y-Dim.) Rebars of beam sample with strengthening - Explicit Dynamic Analysis)

Normal strain

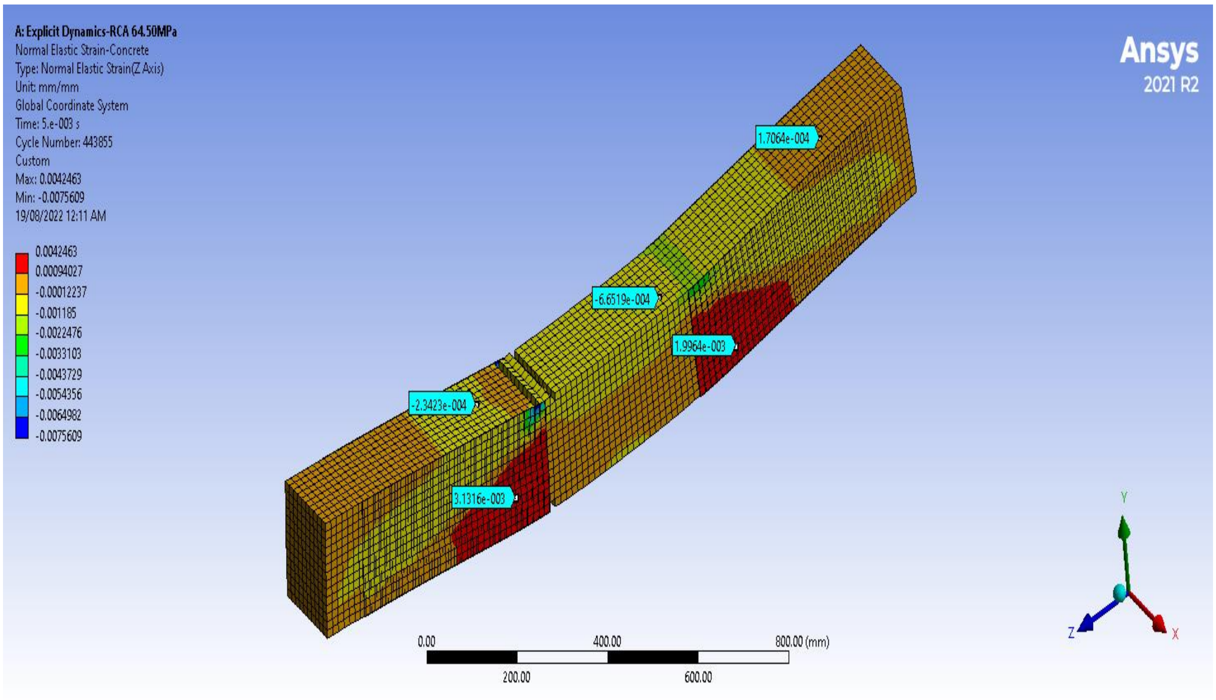

Figure 255(RCA-64.50MPa –Normal strain of beam sample with strengthening and top rebars- Explicit Dynamic Analysis)

Shear Stress

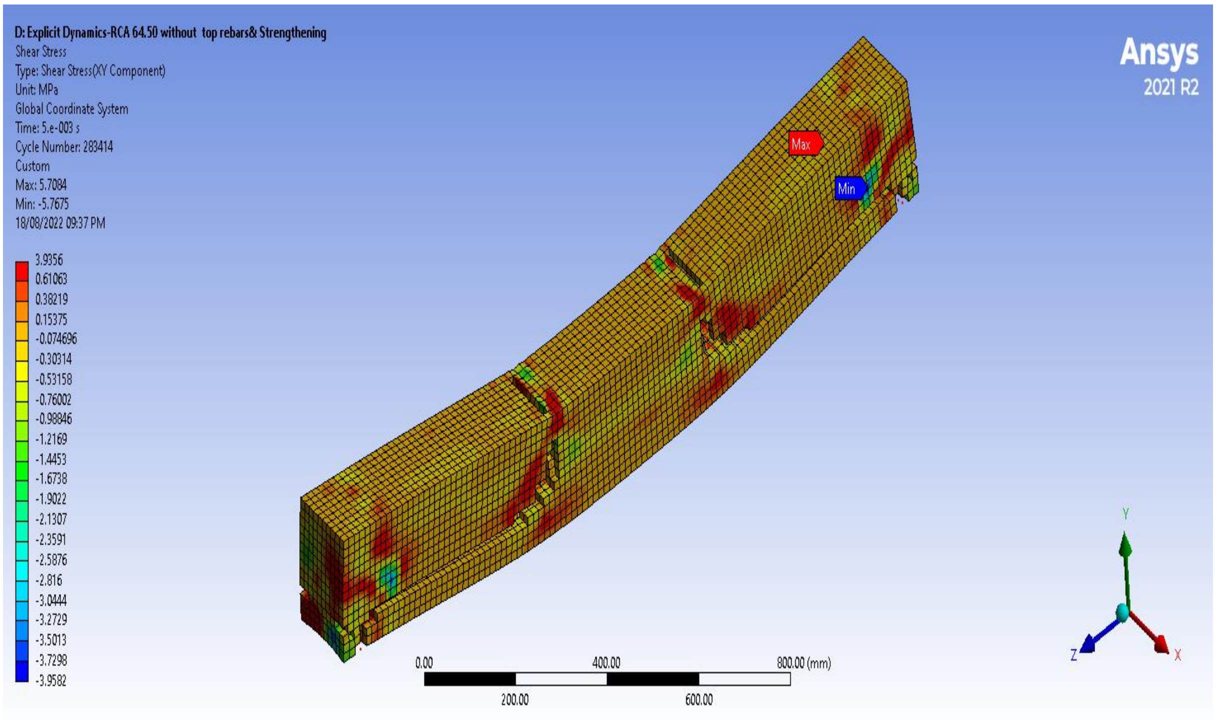

Figure 256(RCA-64.50MPa – Shear stress of beam sample with strengthening and top rebars- Explicit Dynamic Analysis)

Total shape strain

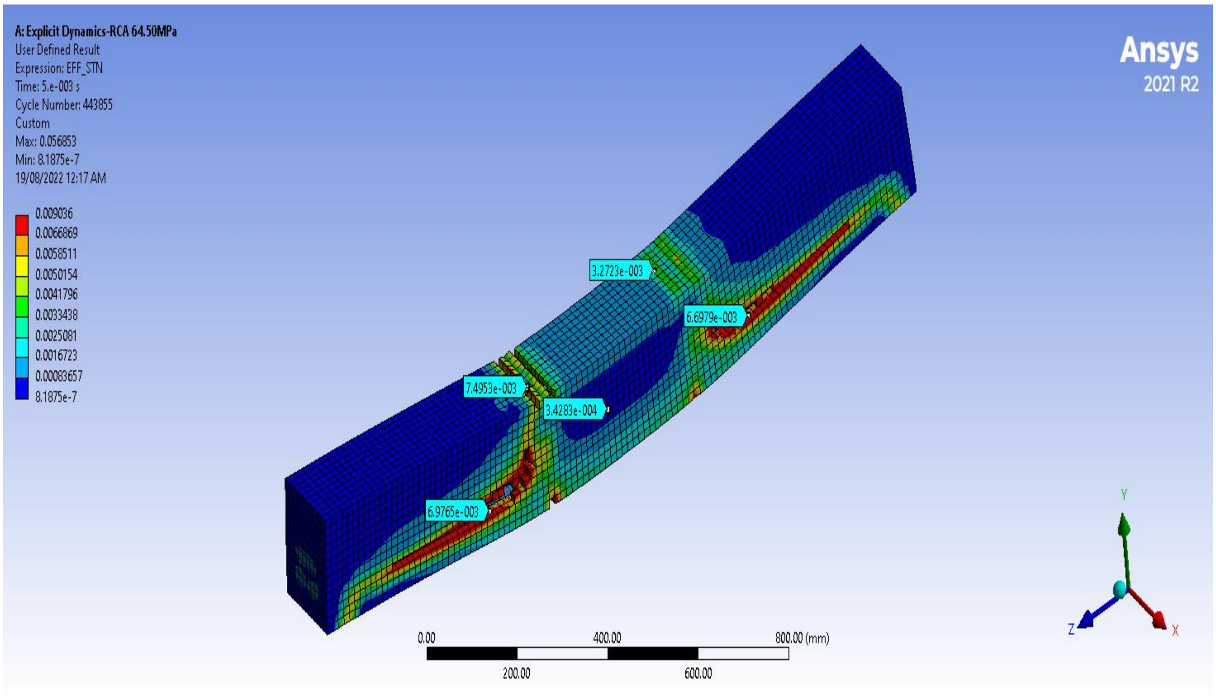

Figure 257(RCA-64.50MPa – Total strain of beam sample with strengthening and top rebars- Explicit Dynamic Analysis)

Maximum Stress

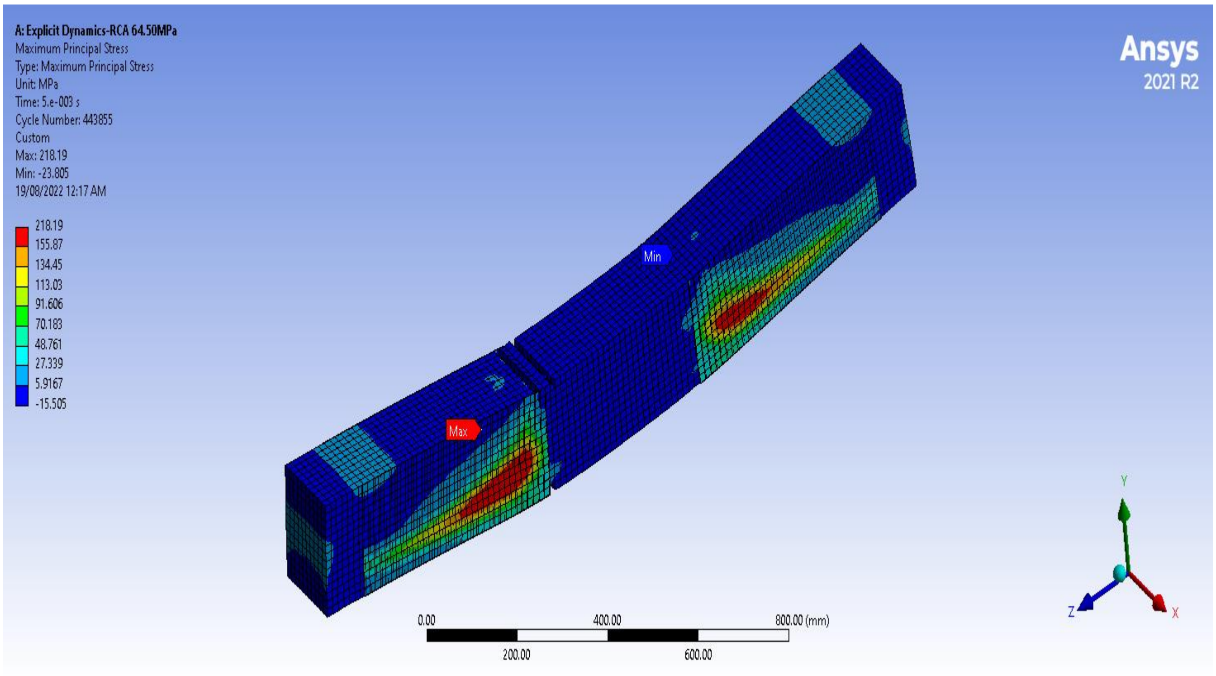

Figure 258(RCA-64.50MPa – Maximum stress of beam sample with strengthening and top rebars- Explicit Dynamic Analysis)

The Damage Pattern

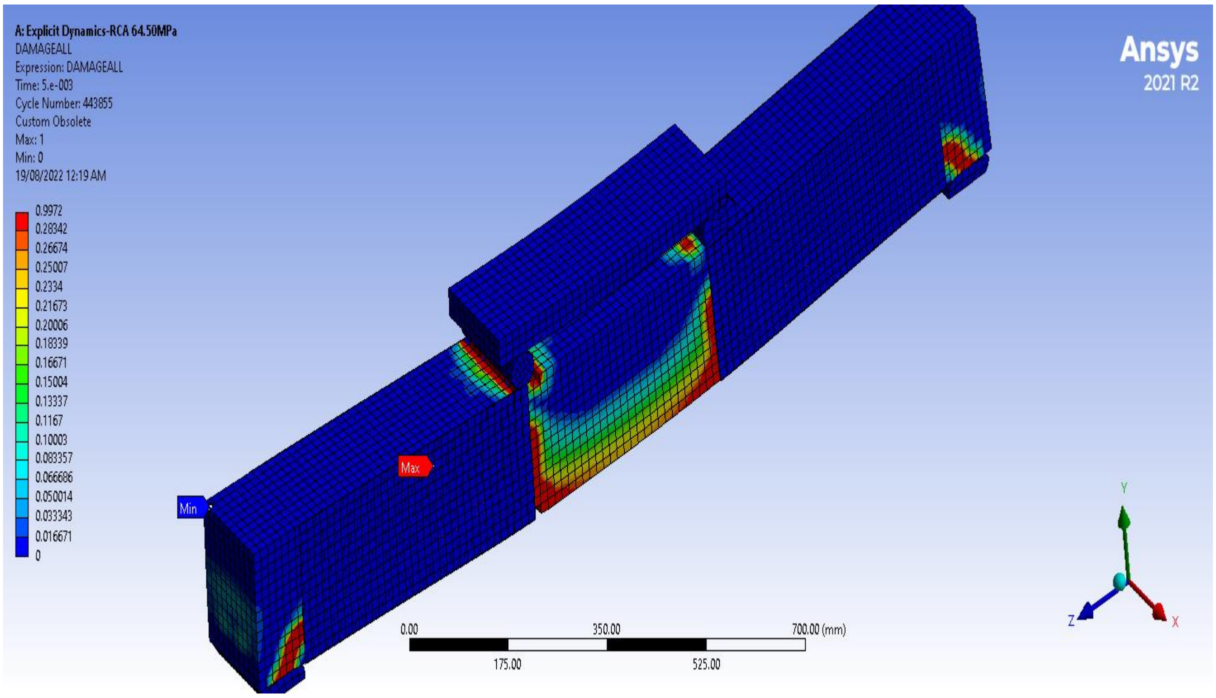

Figure 259(RCA-64.50MPa – Damage pattern-1 of beam sample with strengthening and top rebars- Explicit Dynamic Analysis)

As we can see the shear damage cracks in red and CFRP debonding on edges of concrete failure.

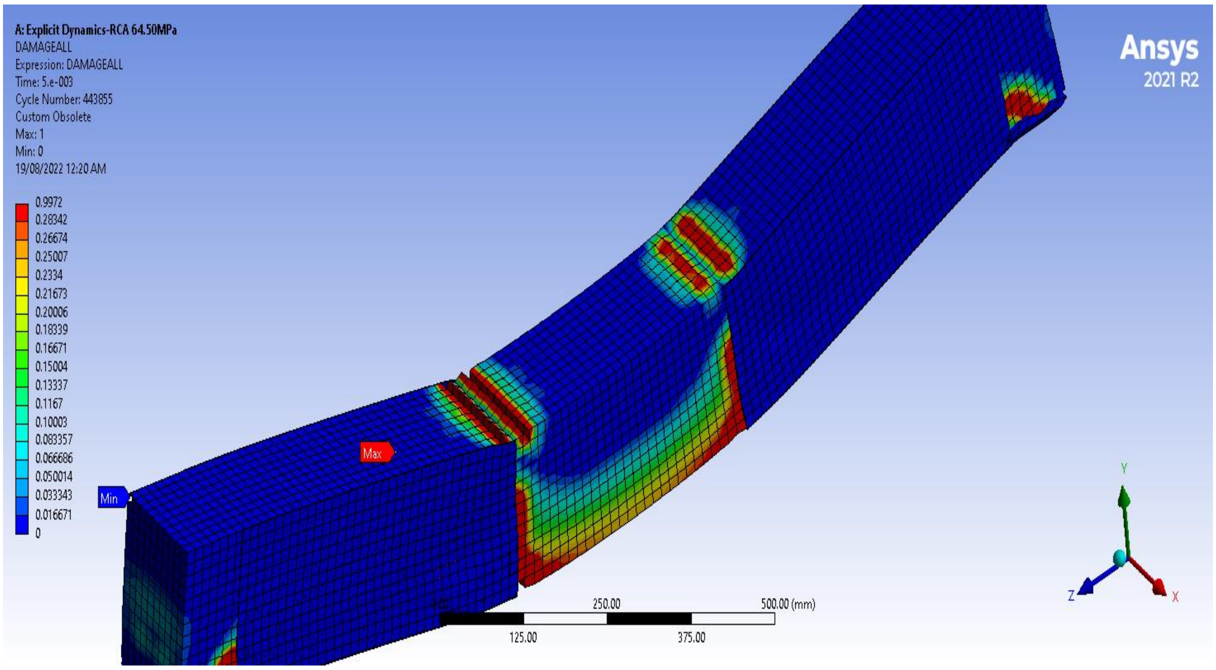

Figure 260(RCA-64.50MPa – Damage pattern-2 of beam sample with strengthening and top rebars- Explicit Dynamic Analysis)

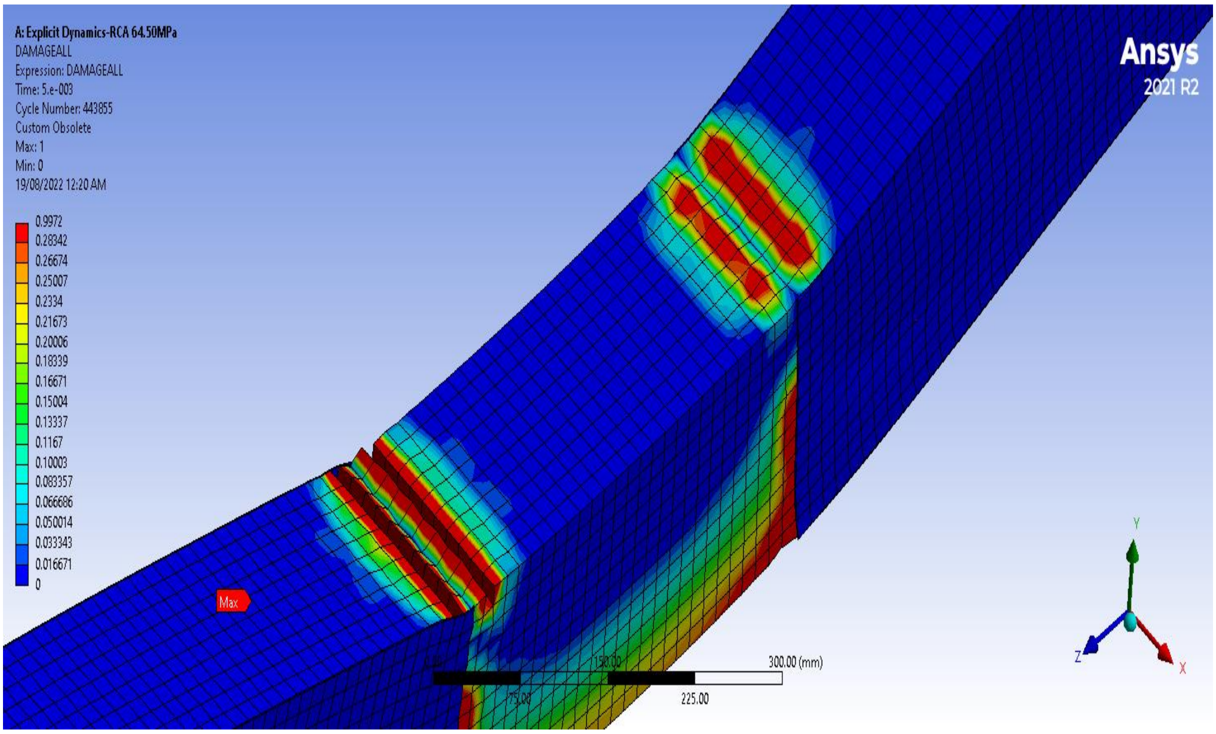

Figure 261(RCA-64.50MPa – Damage pattern-3 of beam sample with strengthening and top rebars- Explicit Dynamic Analysis)

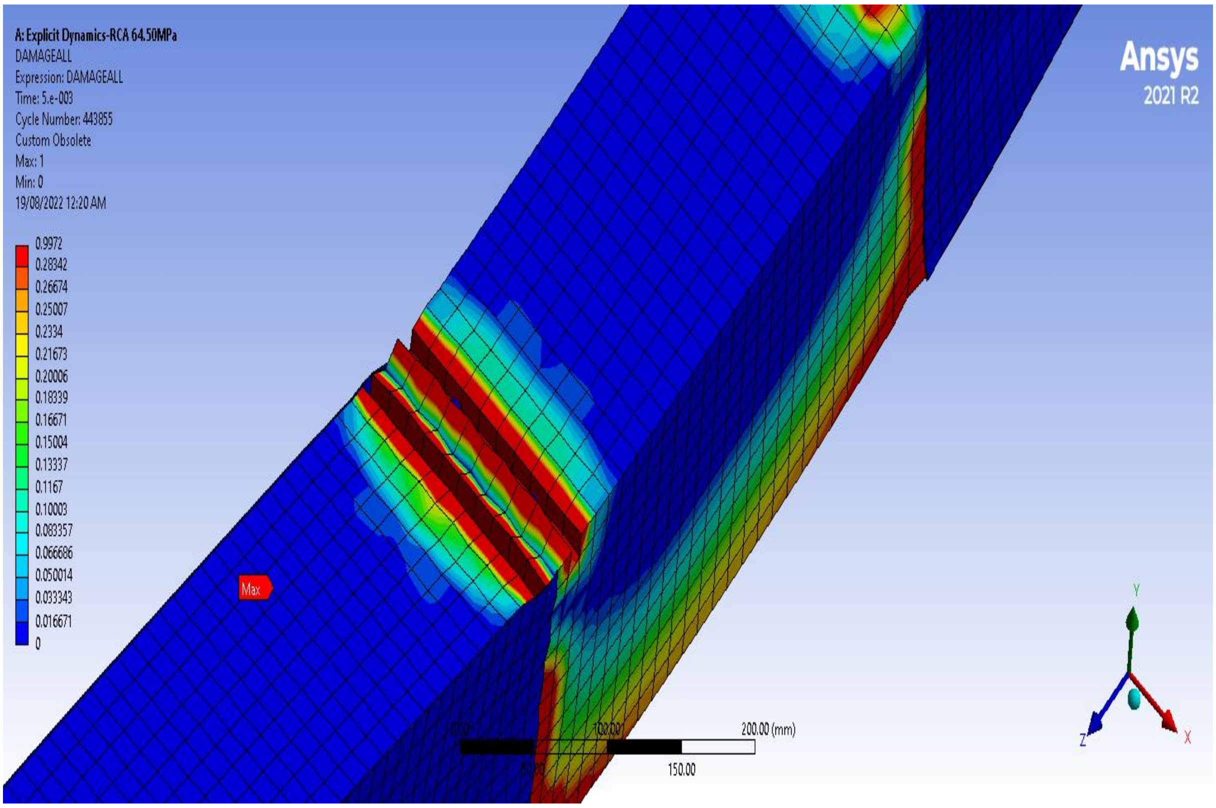

Figure 262(RCA-64.50MPa – Damage pattern-4 of beam sample with strengthening and top rebars- Explicit Dynamic Analysis)

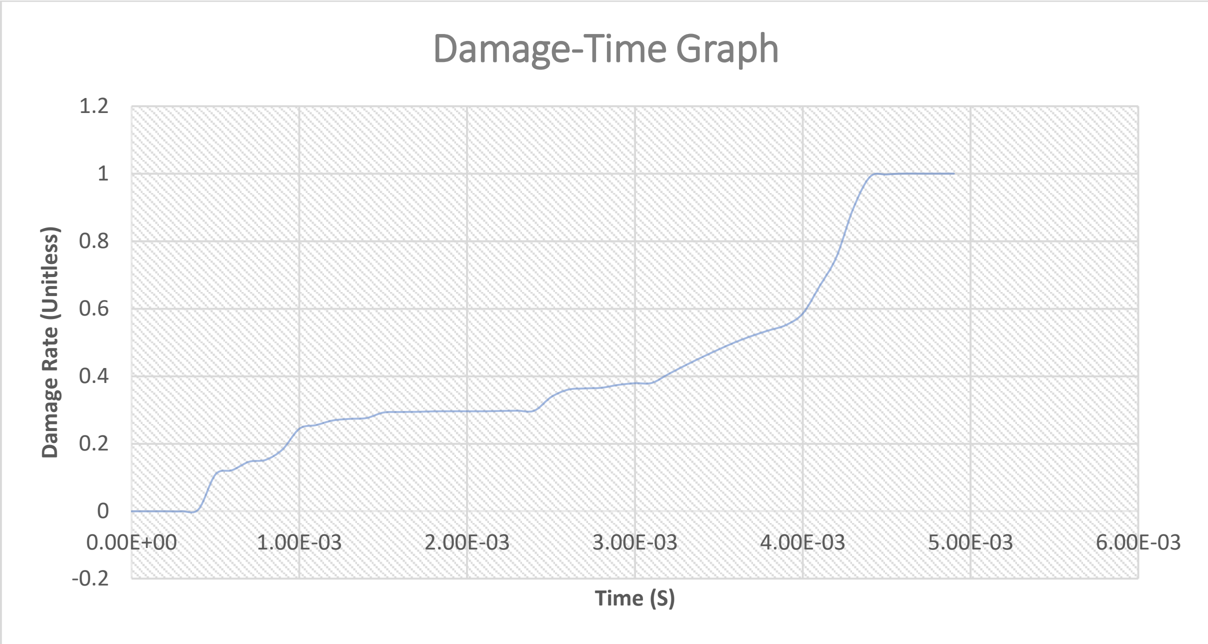

Figure 263(RCA-64.5MPa – Damage pattern graph of beam sample with strengthening and top rebars- Explicit Dynamic Analysis)

15- Static Non-Linear Analysis - With Strengthening and Without Top Rebars

Geometry and loads

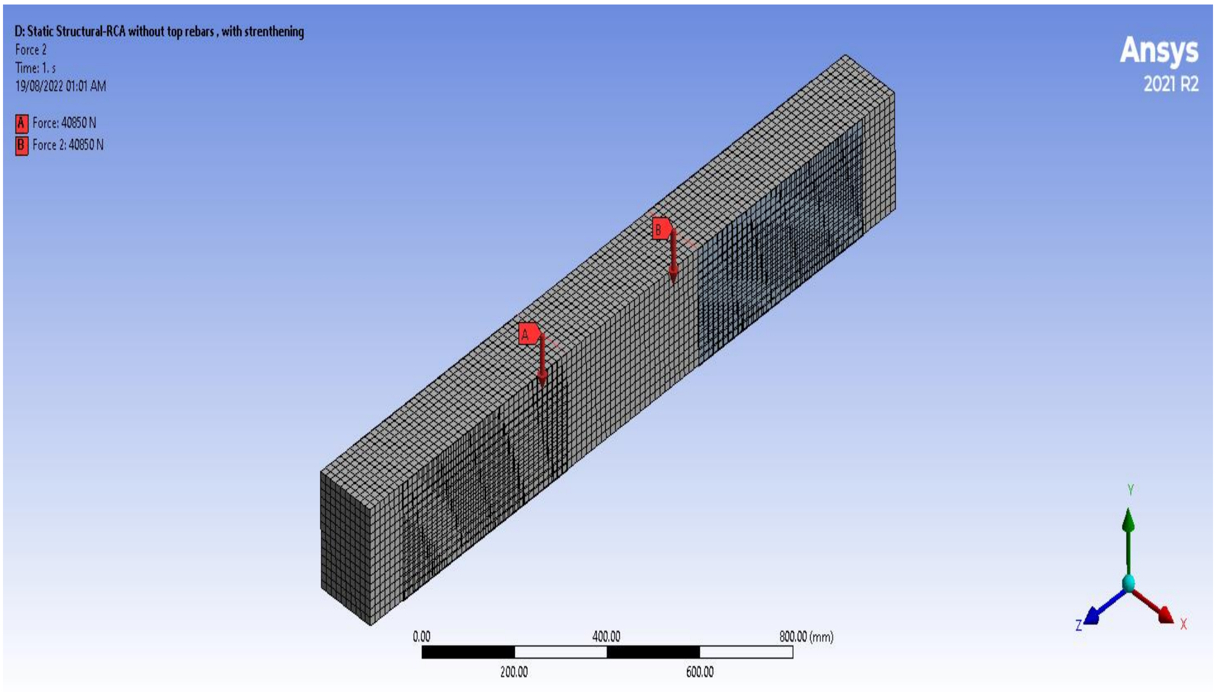

Figure 264(RCA-64.5MPa – Geometry & Loads of beam sample with strengthening and without top rebars- Static Nonlinear Analysis)

The ultimate load has been divided in to loads which is 81.7/2 =40.85KN.

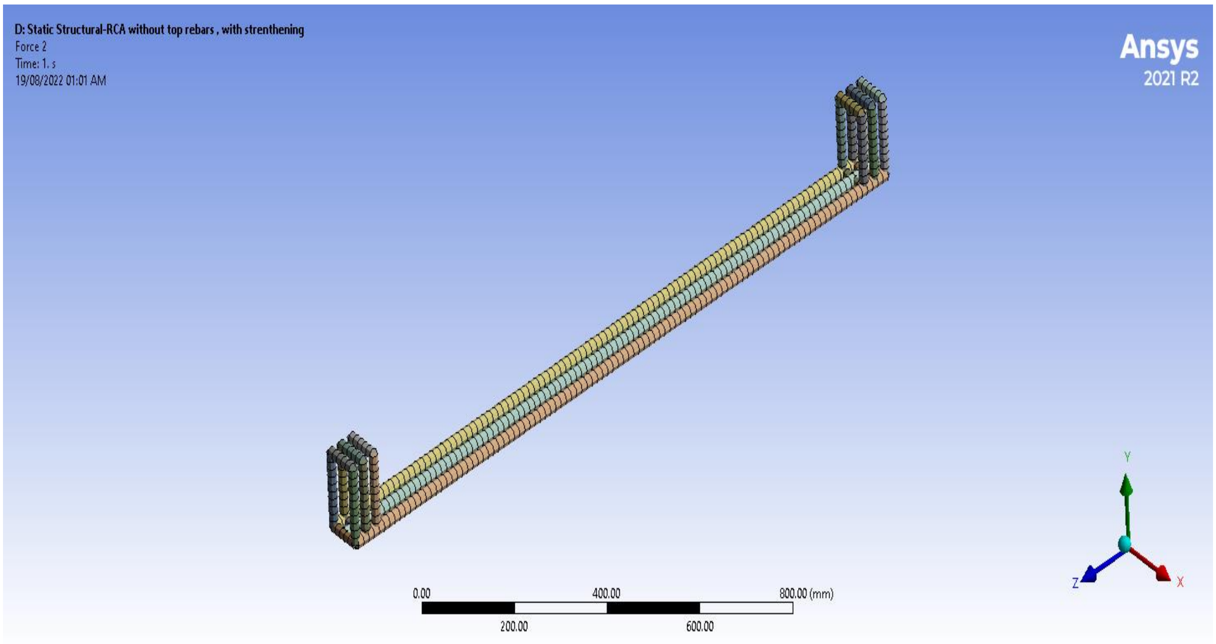

Figure 265(RCA-64.5MPa – Rebars of beam sample without strengthening - Static Nonlinear Analysis)

Deformations

Total Deformations

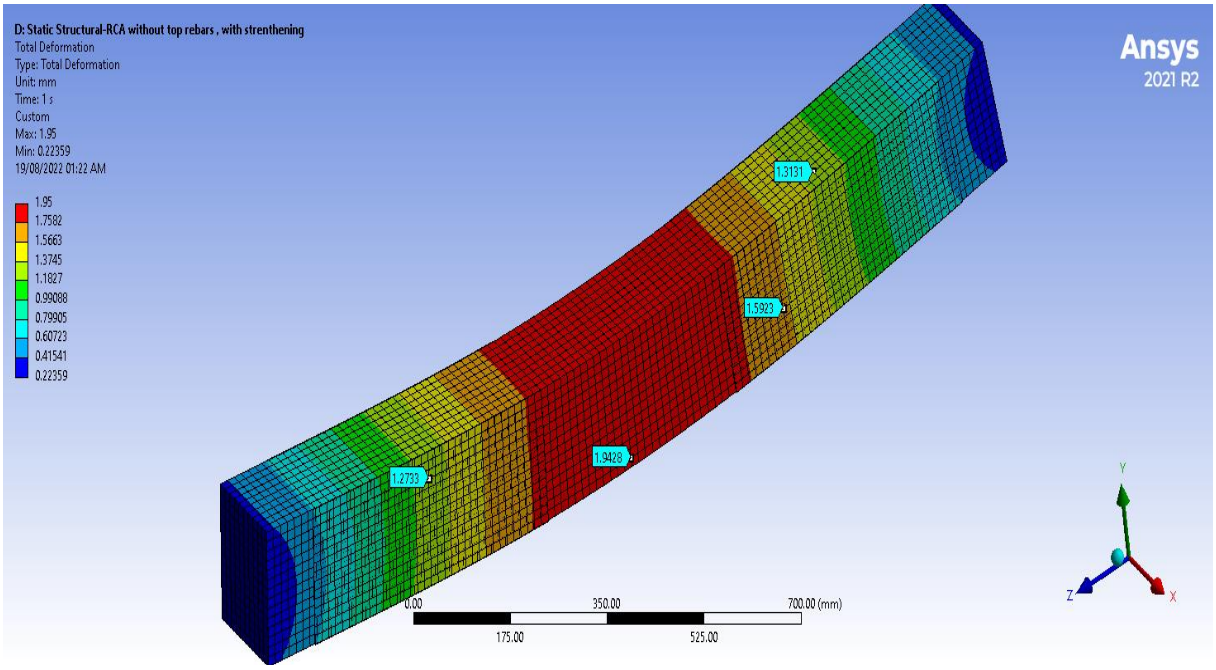

Figure 266(RCA-64.5MPa – Total deflections of beam sample with strengthening and without top rebars- Static Nonlinear Analysis)

The value is 1.95 mm.

Directional Deformation (Y-Direction)

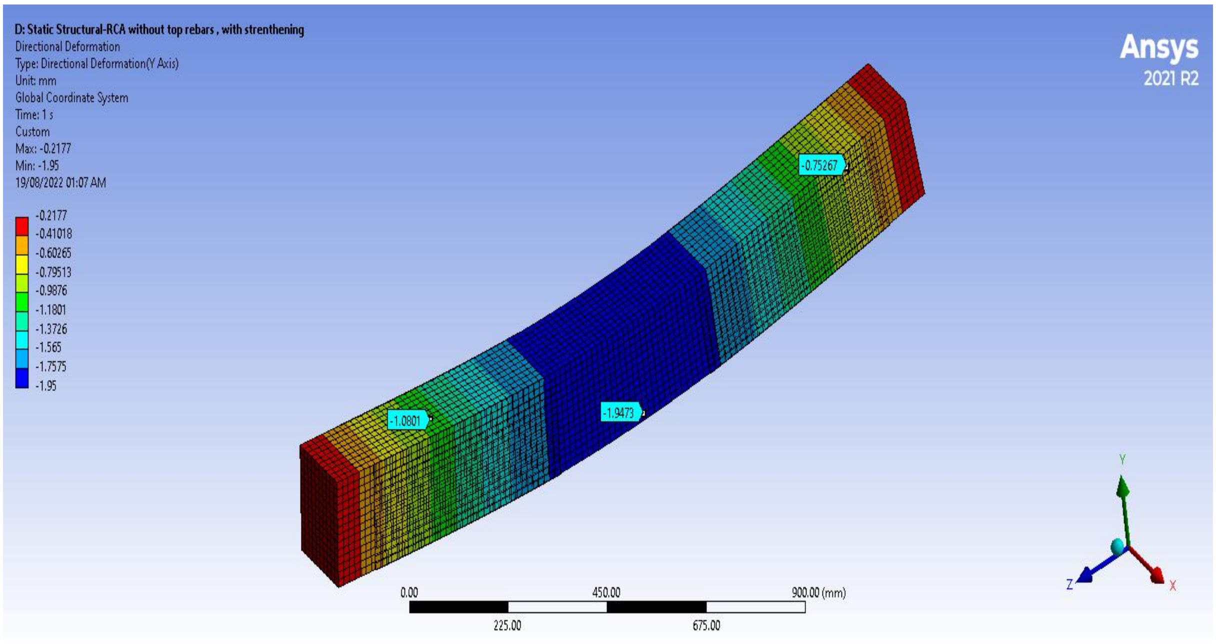

Figure 267(RCA-64.5MPa – Directional deflections (Y-Dim.) of beam sample with strengthening and without top rebars- Static Nonlinear Analysis)

The value is 1.95 mm.

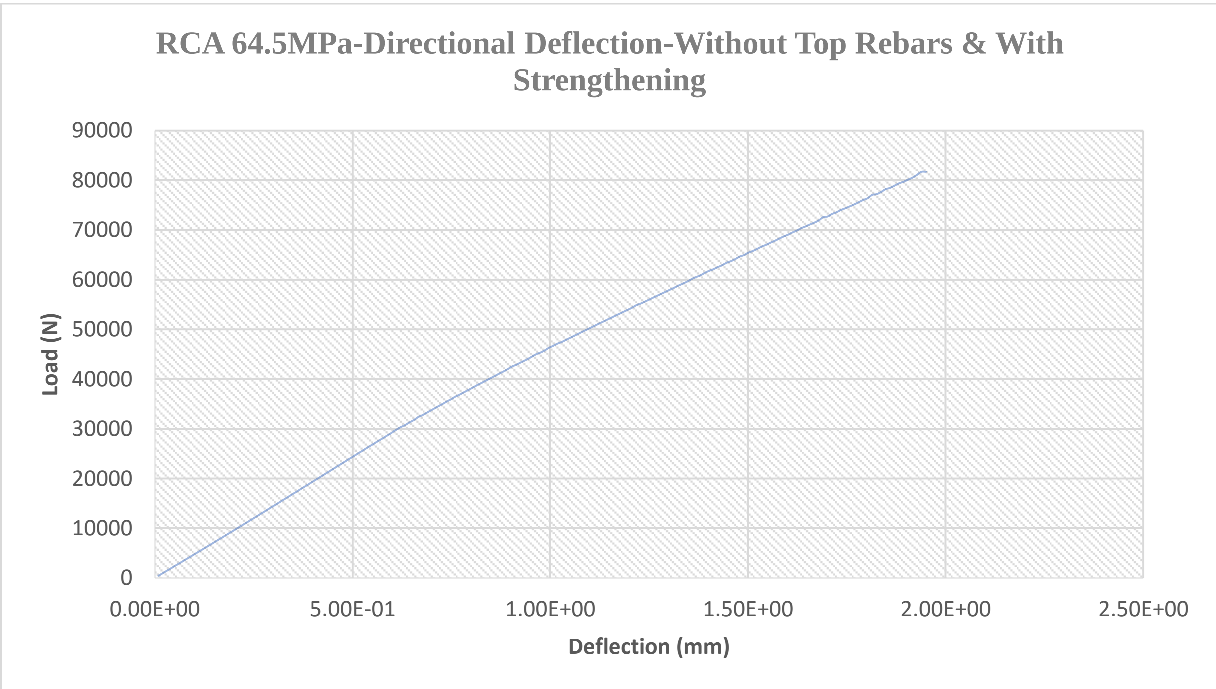

Figure 268(RCA-64.5MPa – Directional deflections (Y-Dim.) of beam sample with strengthening and without top rebars- Static Nonlinear Analysis)

Normal Stress (Concrete)

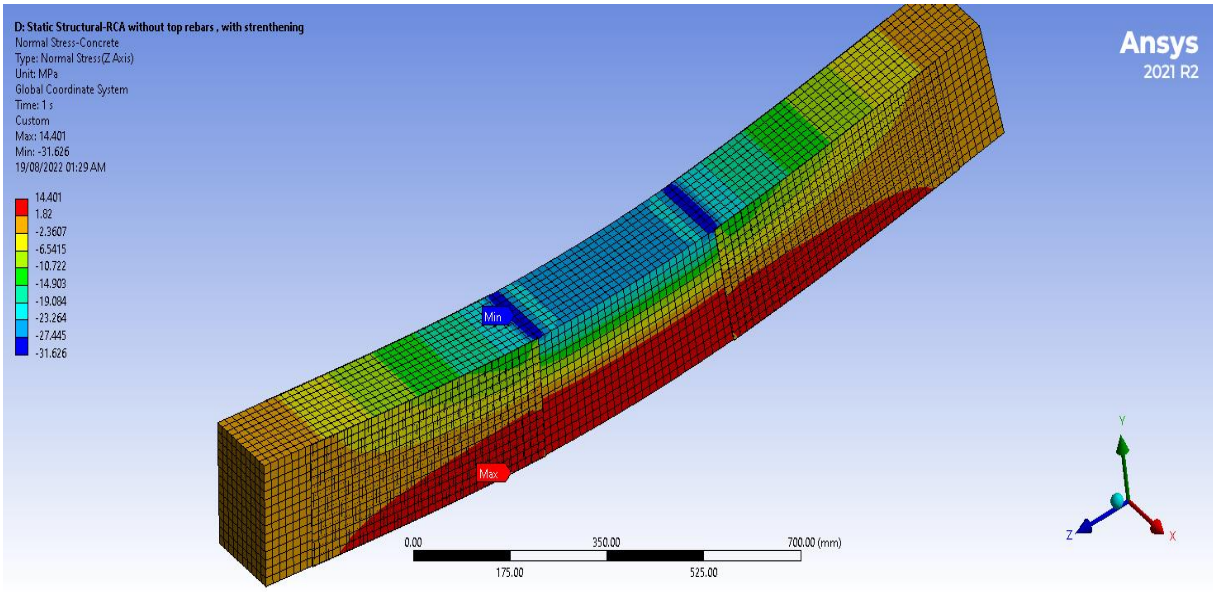

Figure 269(RCA-64.5MPa – Normal stress (Concrete) of beam sample with strengthening and without top rebars- Static Nonlinear Analysis)

The blue zones show the crushing from loading machine and the maximum value is 31.626 MPa, whereas the red zones indicate to tension.

Normal Stress (Rebars)

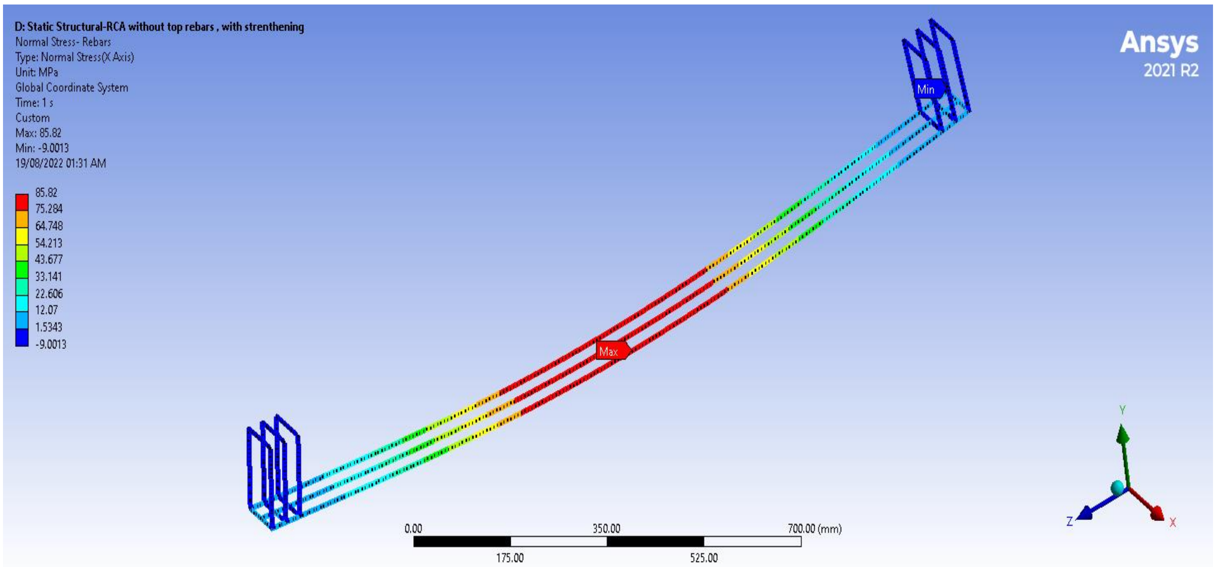

Figure 270(RCA-64.5MPa – Normal stress (Rebars) of beam sample with strengthening and without top rebars- Static Nonlinear Analysis)

The red zones show that the rebars is yielding by 85.82 MPa, in the middle span due to tension.

Shear Stress

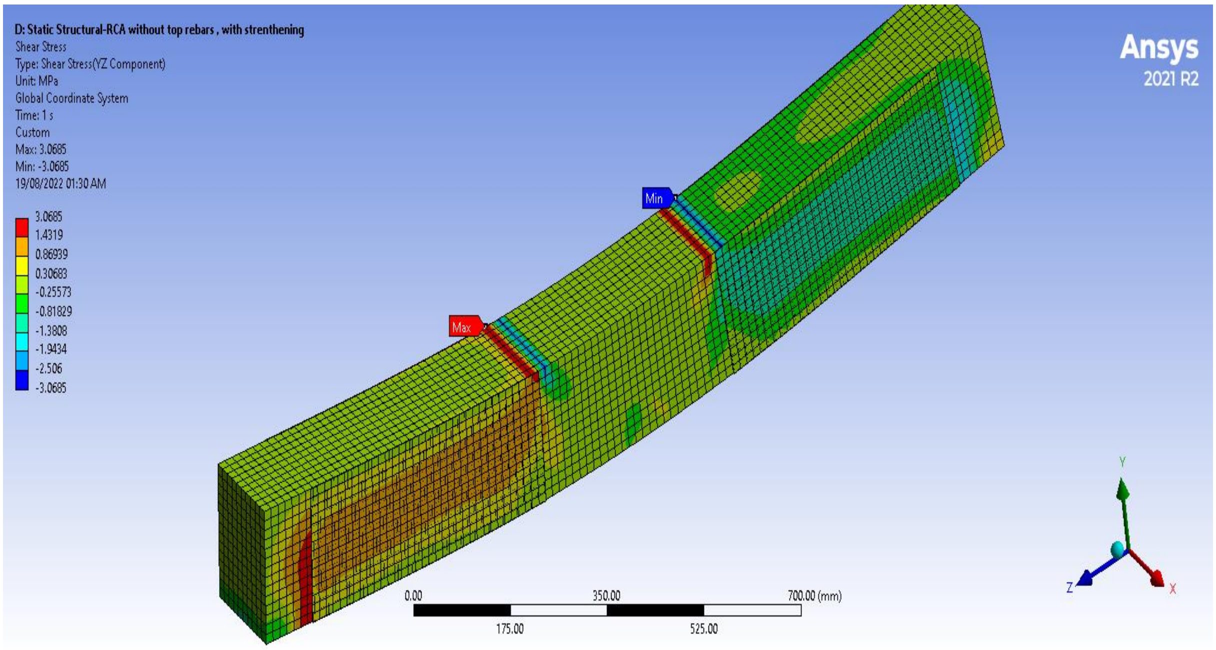

Figure 271(RCA-64.5MPa – Shear stress of beam sample with strengthening and without top rebars- Static Nonlinear Analysis)

Elastic Strain

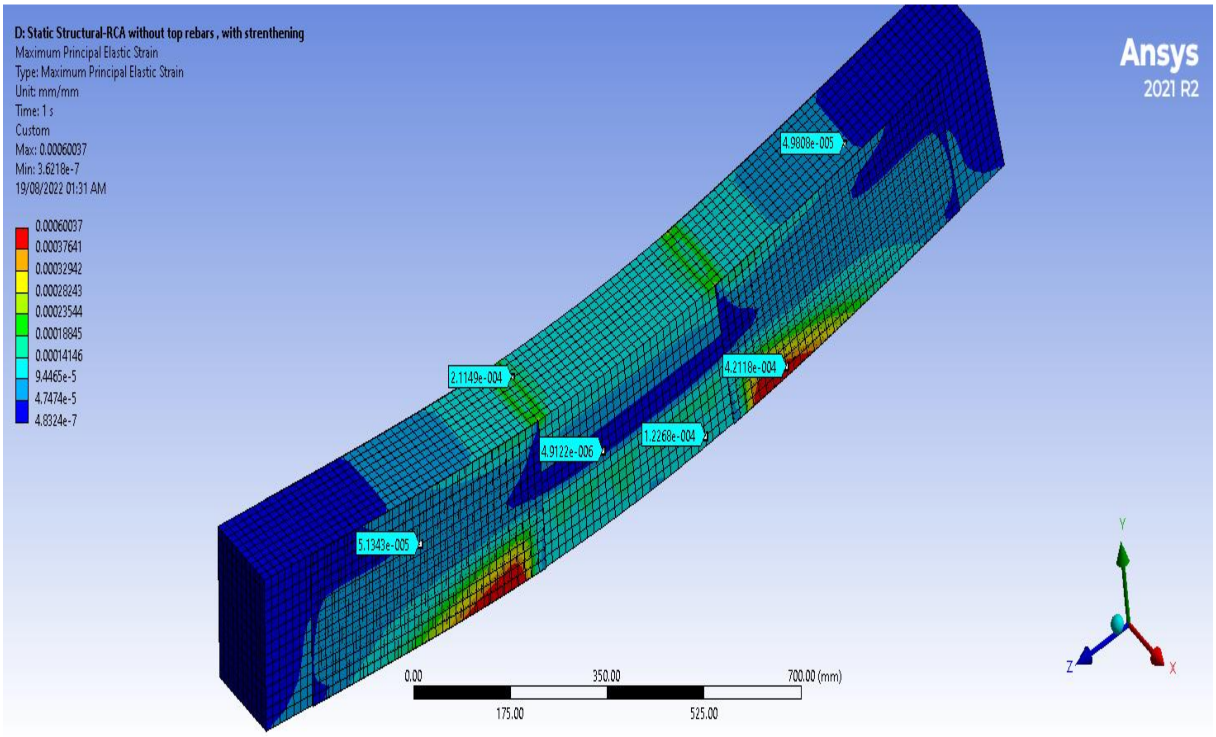

Figure 272(RCA-645MPa – Elastic strain of beam sample with strengthening and without top rebars- Static Nonlinear Analysis)

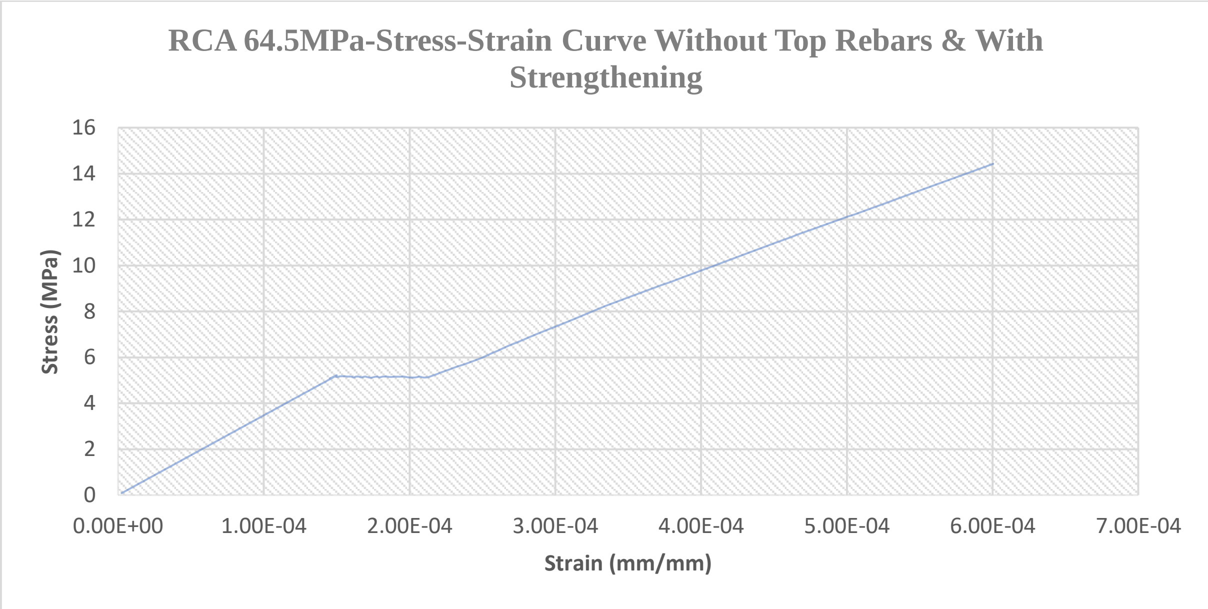

Figure 273(RCA-64.5MPa – Stress & Strain graph of beam sample with strengthening and without top rebars- Static Nonlinear Analysis)

16- Explicit Dynamic-Without Top Rebars & With Strengthening

Geometry and loads

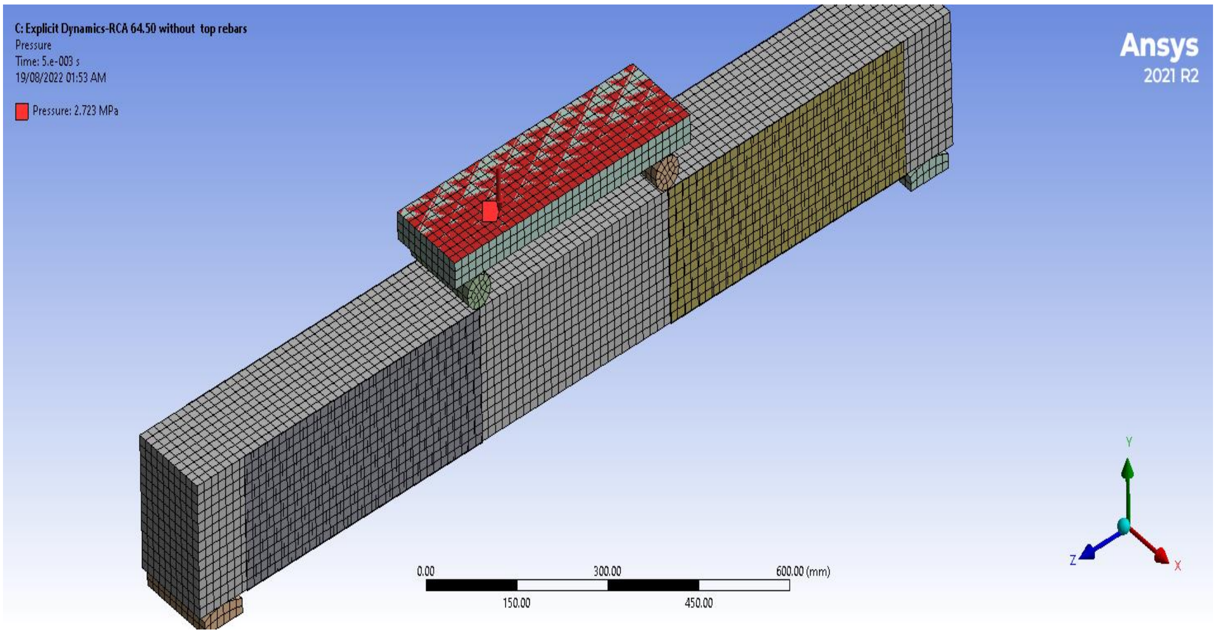

Figure 274(RCA-64.5MPa – Geometry & Loads of beam sample with strengthening and without top rebars- Explicit Dynamic Analysis)

The ultimate load has been transferred to be as a pressure load which is 2.723.0 MPa as shown above with rate loading 0.6mm/min.

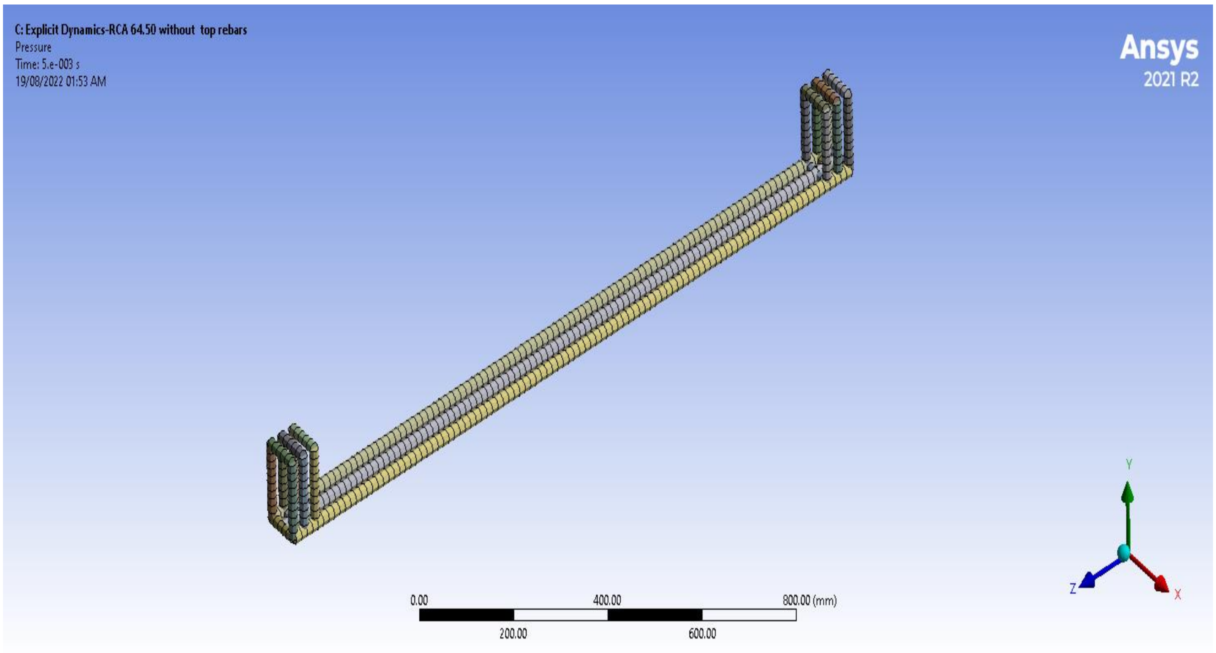

Figure 275(RCA-64.5MPa – Rebars of beam sample with strengthening - Explicit Dynamic Analysis)

Deformations

Total Deformations

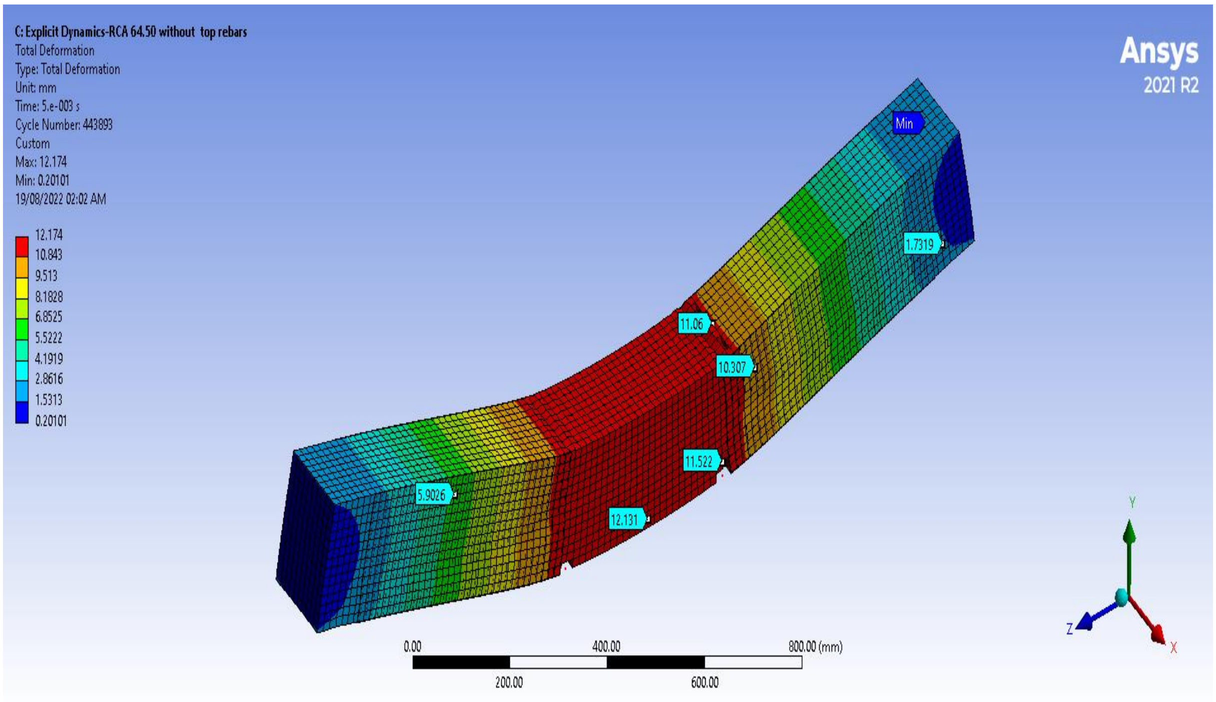

Figure 276(RCA-64.5MPa – Total deflections of beam sample with strengthening and without top rebars- Explicit Dynamic Analysis)

The value is 12.174 mm.

Directional Deformation (Y-Direction)-Concrete

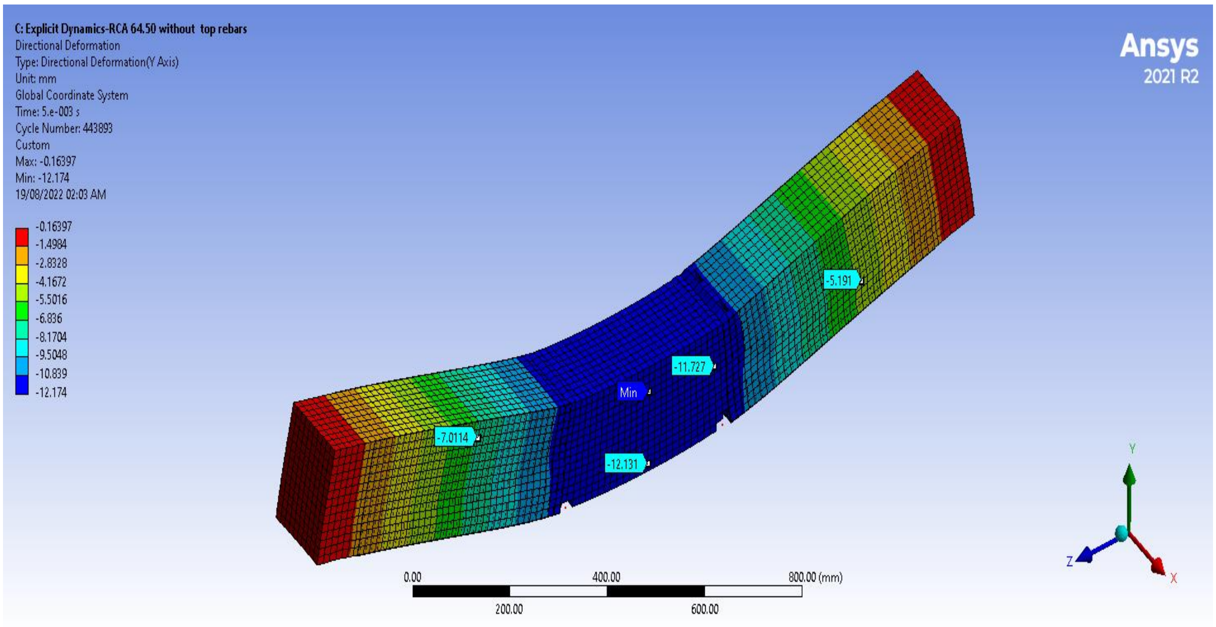

Figure 277(RCA-64.5MPa – Directional deflections (Y-Dim.) of beam sample with strengthening and without top rebars- Explicit Dynamic Analysis)

The value is 12.174 mm.

Directional Deformation (Y-Direction)- Rebars

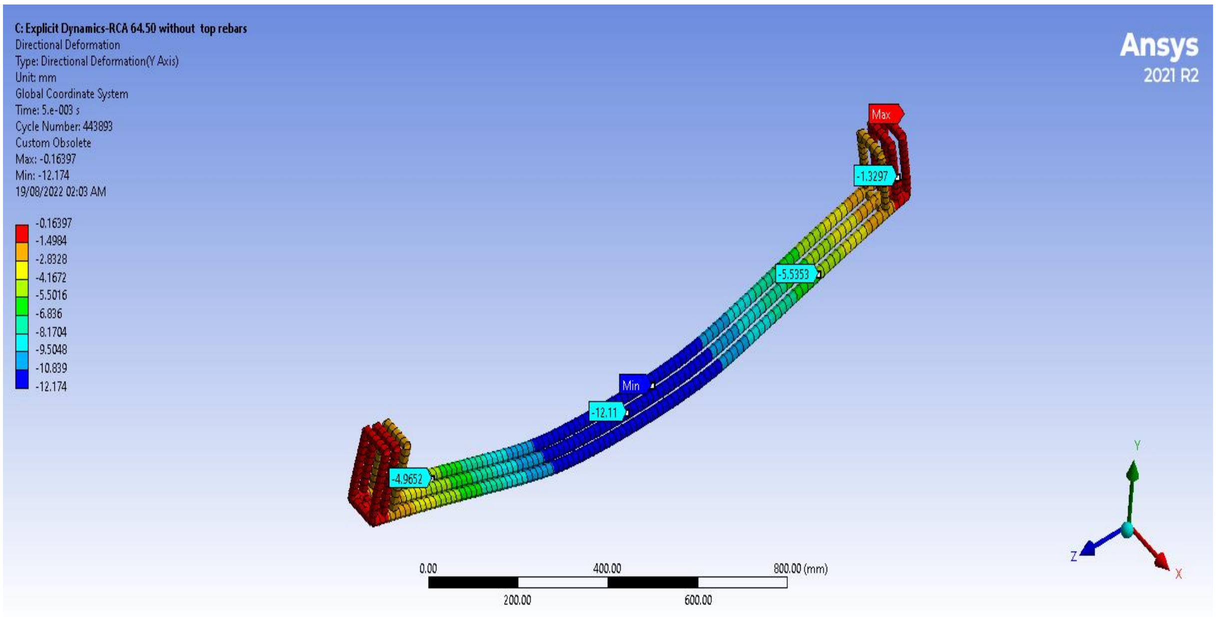

Figure 278(RCA-64.5MPa – Directional deflections (Y-Dim.) Rebars of beam sample with strengthening and without top rebars- Explicit Dynamic Analysis)

Normal strain

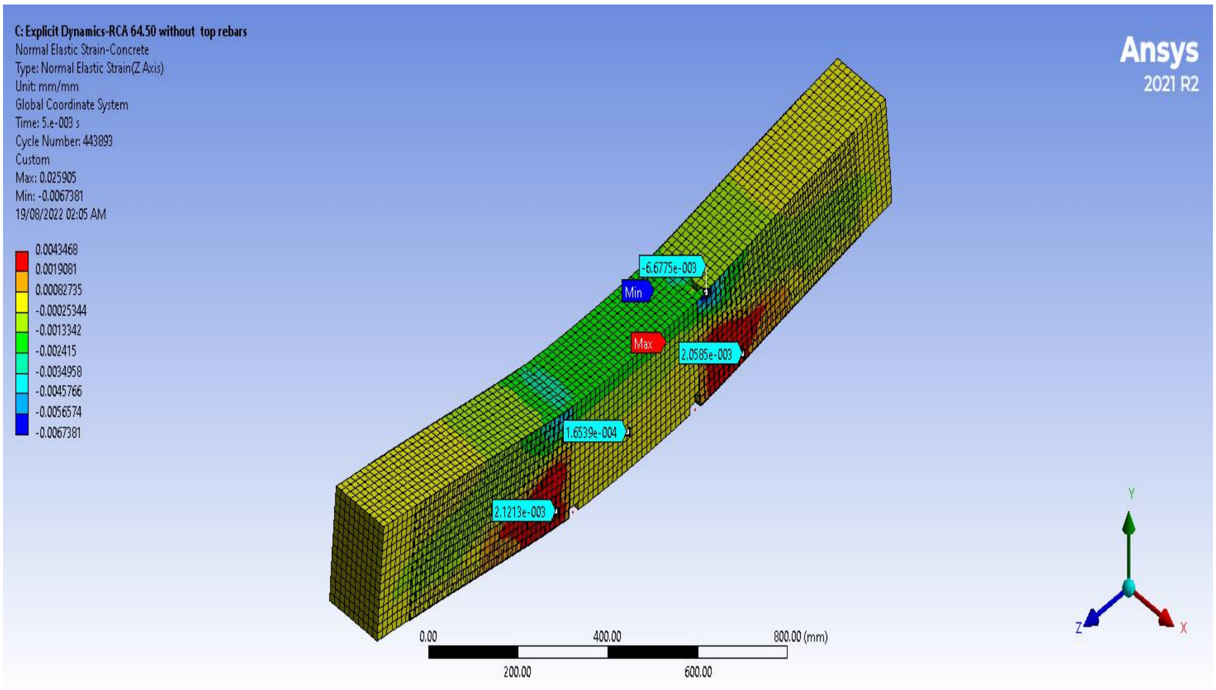

Figure 279(RCA-64.5MPa – Normal strain of beam sample with strengthening and without top rebars- Explicit Dynamic Analysis)

Shear Stress

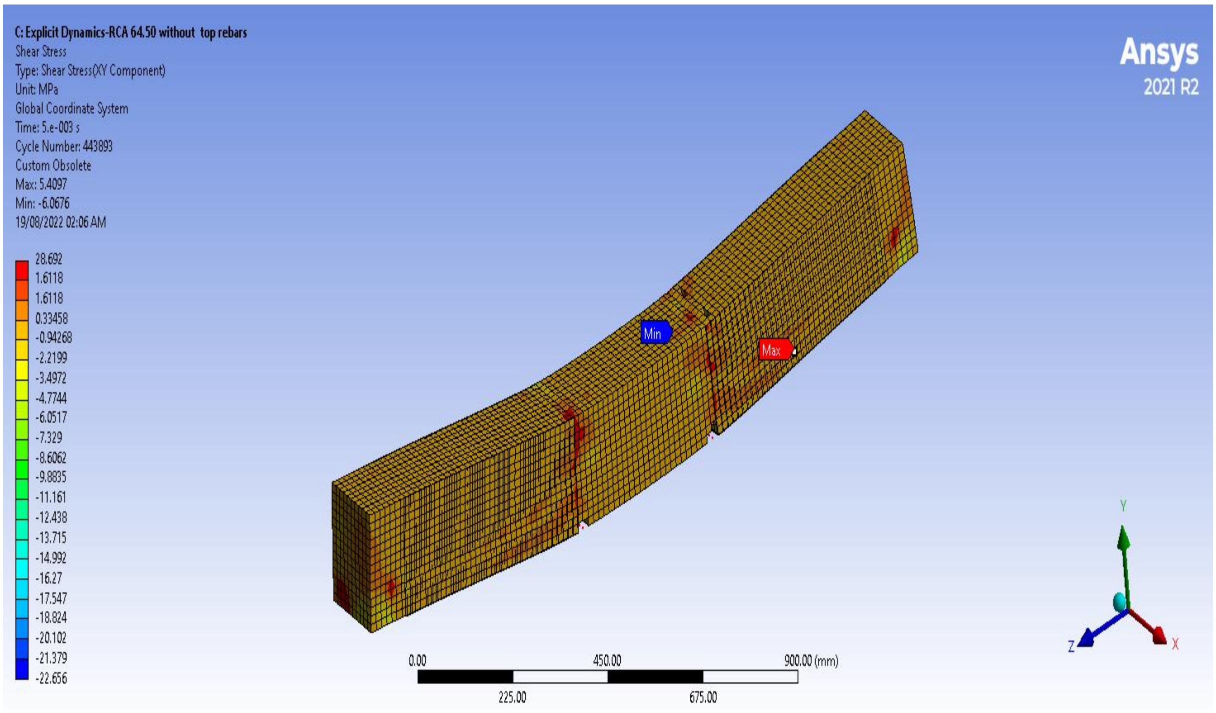

Figure 280(RCA-64.5MPa – Shear stress of beam sample with strengthening and without top rebars- Explicit Dynamic Analysis)

Total shape strain

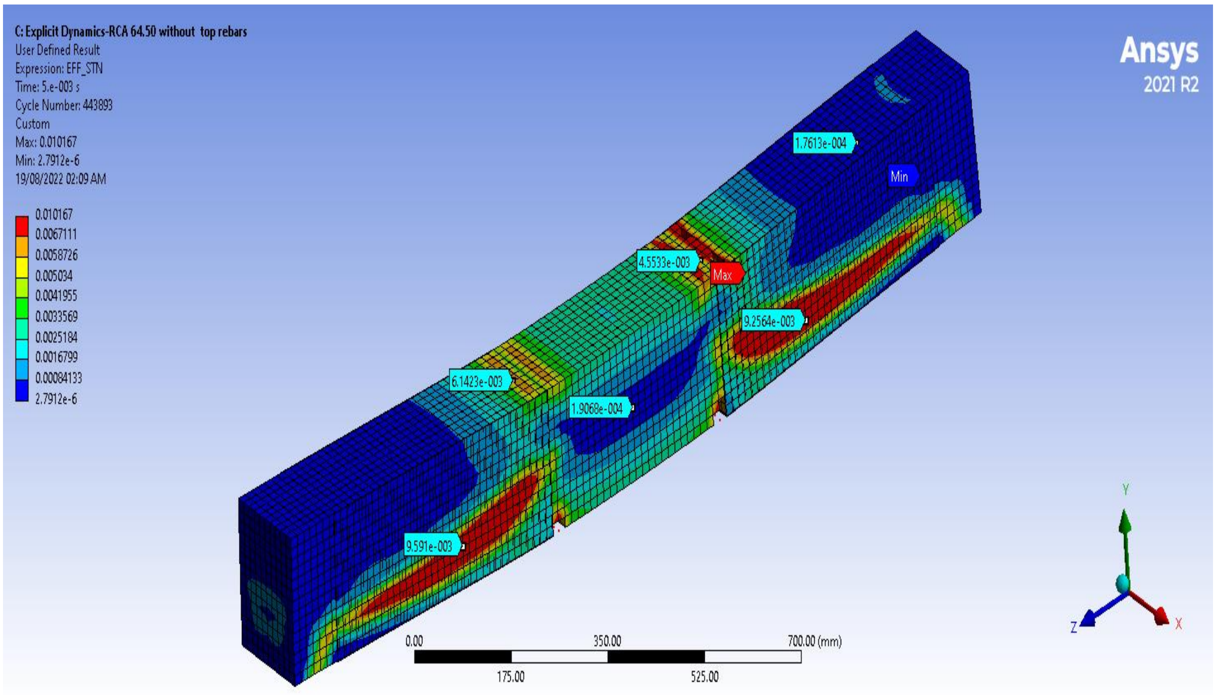

Figure 281(RCA-64.5MPa – Total strain of beam sample with strengthening and without top rebars- Explicit Dynamic Analysis)

Maximum Stress

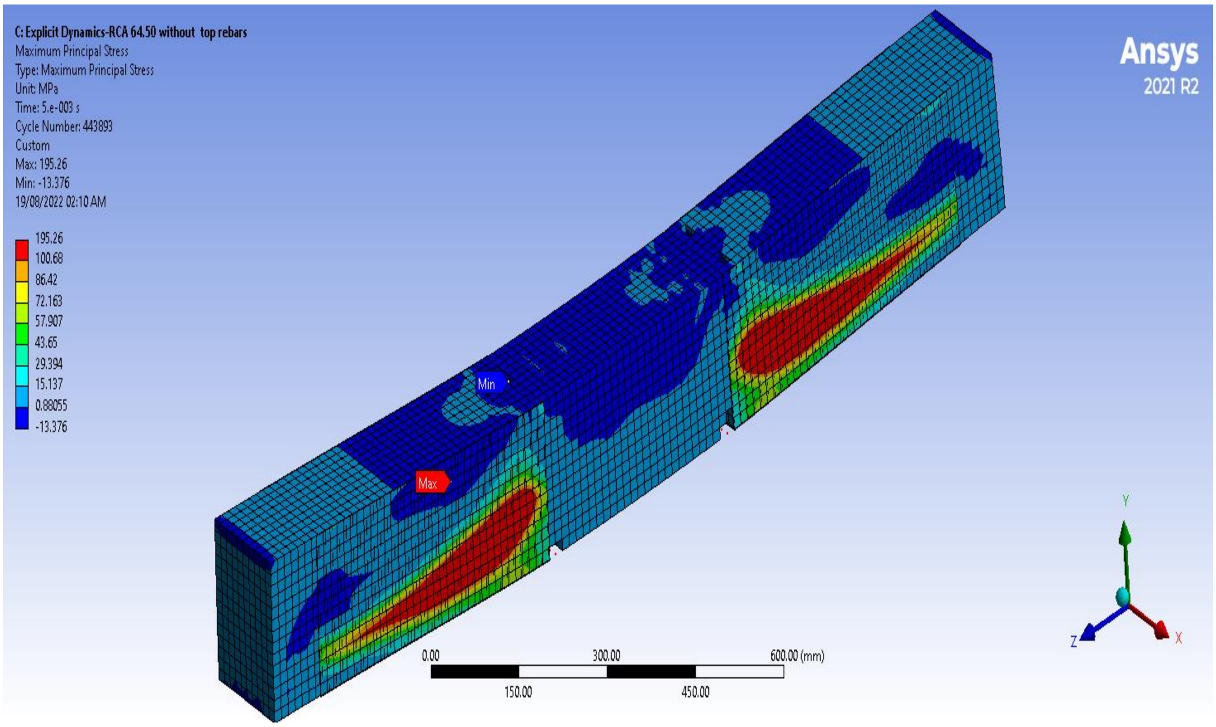

Figure 282(RCA-64.5MPa – Maximum stress of beam sample with strengthening and without top rebars- Explicit Dynamic Analysis)

The Damage Pattern

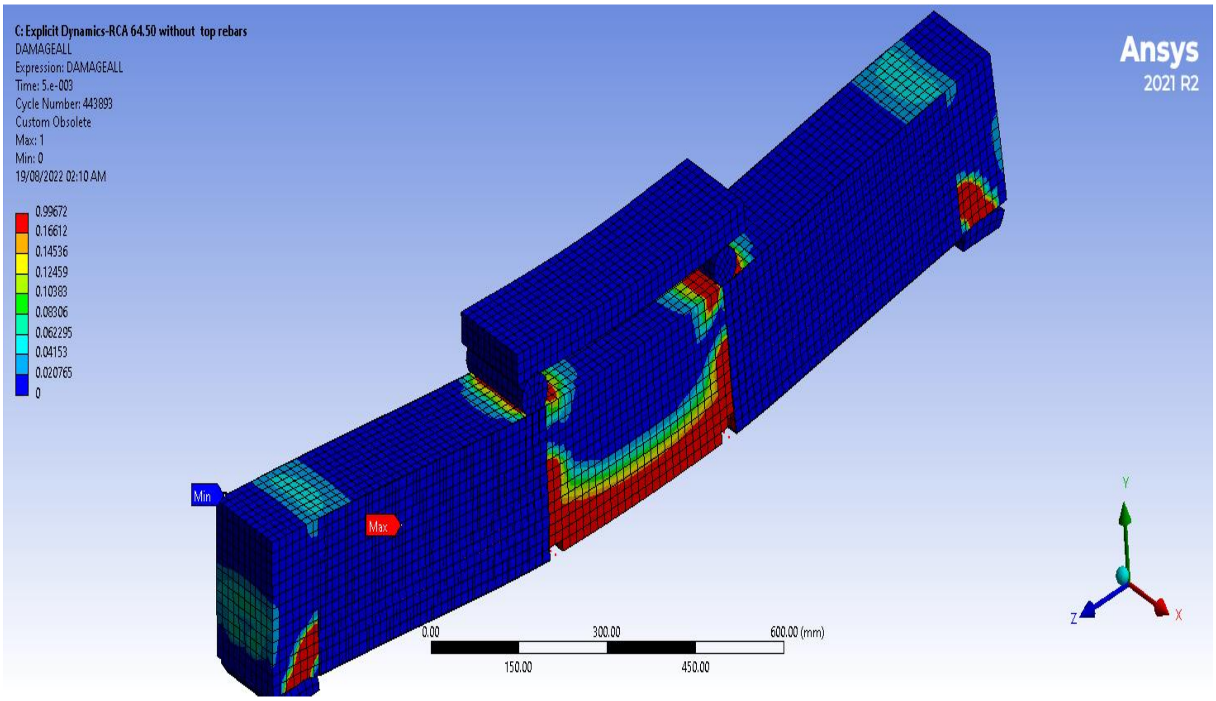

Figure 283(RCA-64.5MPa – Damage pattern-1 of beam sample with strengthening and without top rebars- Explicit Dynamic Analysis)

As we can see the shear damage cracks in red and CFRP debonding on edges of concrete failure.

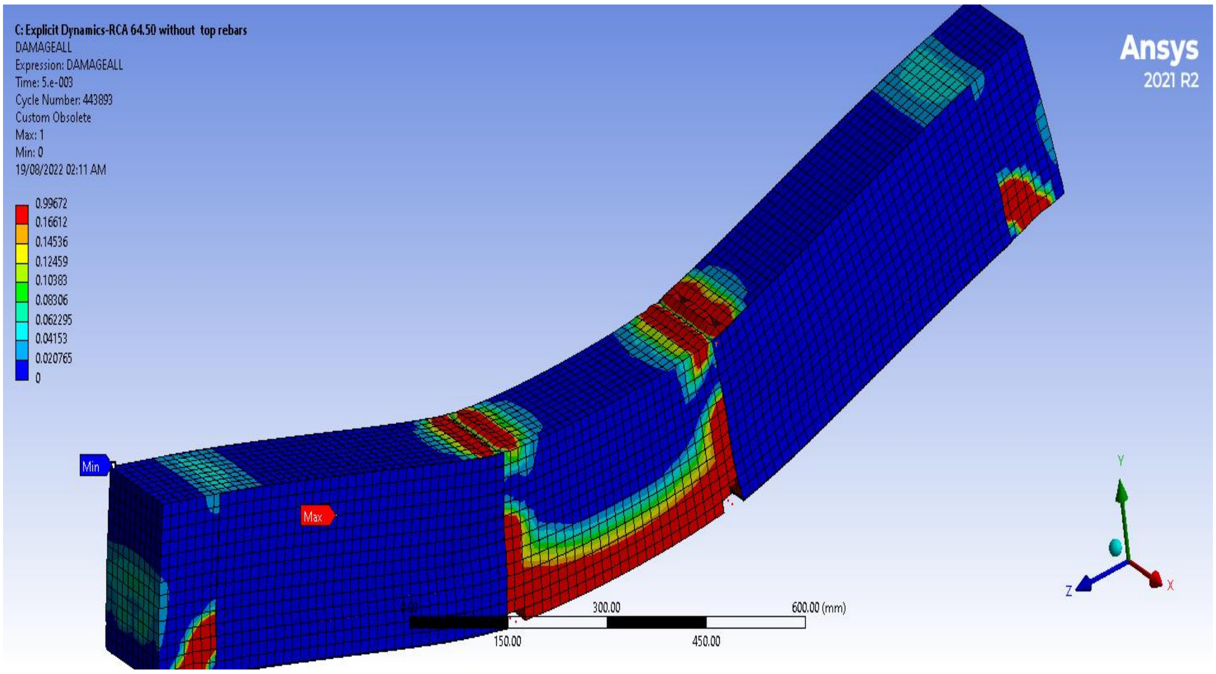

Figure 284(RCA-64.5MPa – Damage pattern-2 of beam sample with strengthening and without top rebars- Explicit Dynamic Analysis)

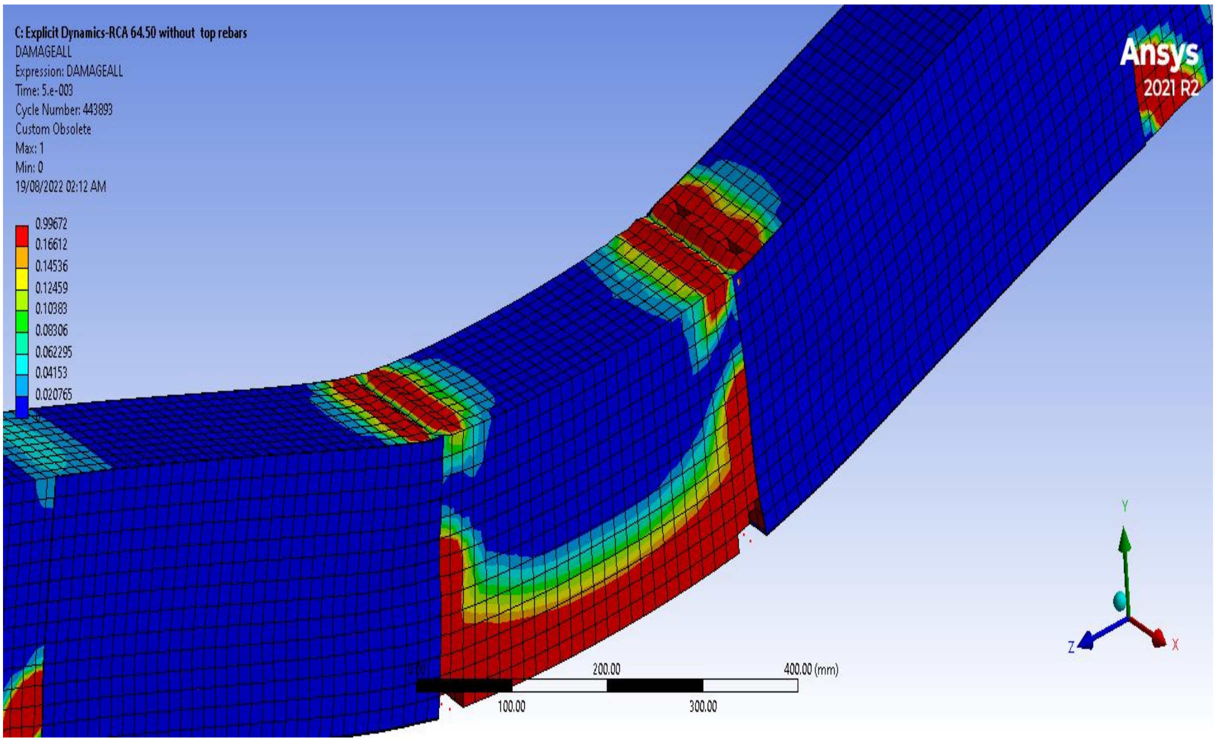

Figure 285(RCA-64.5MPa – Damage pattern-3 of beam sample with strengthening and without top rebars- Explicit Dynamic Analysis)

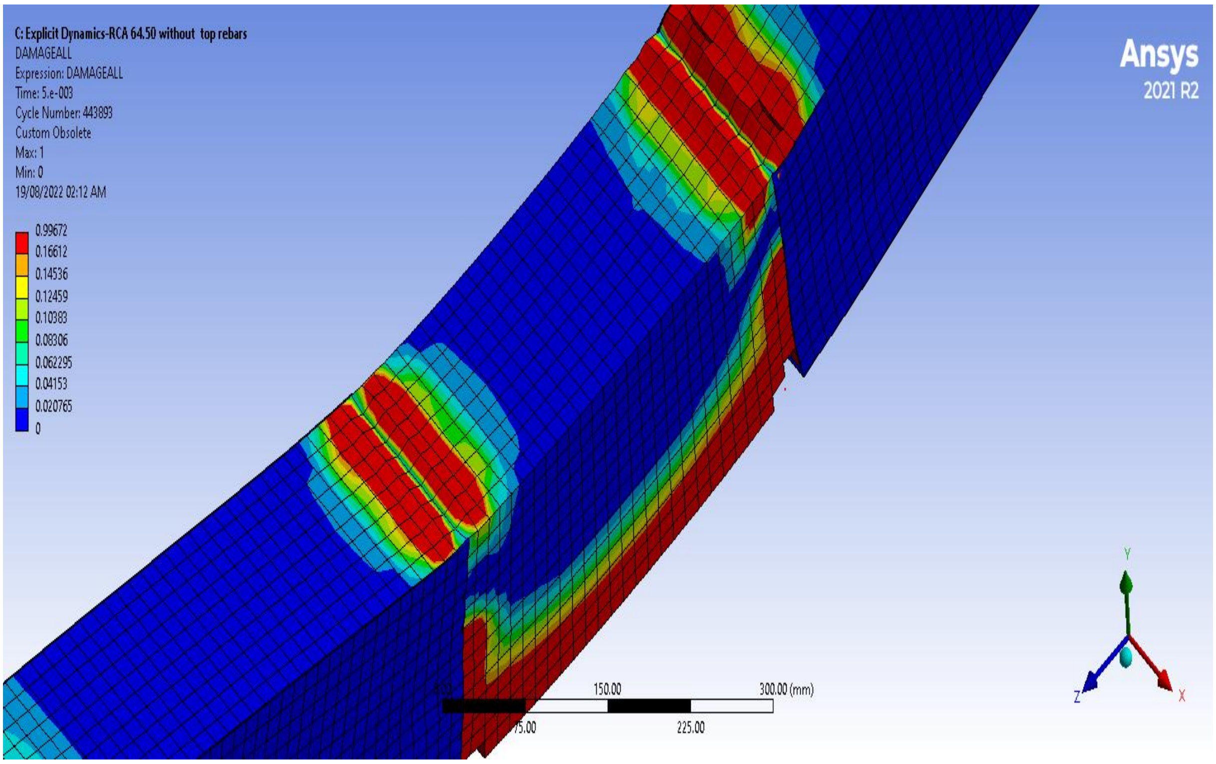

Figure 286(RCA-64.5MPa – Damage pattern-4 of beam sample with strengthening and without top rebars- Explicit Dynamic Analysis)

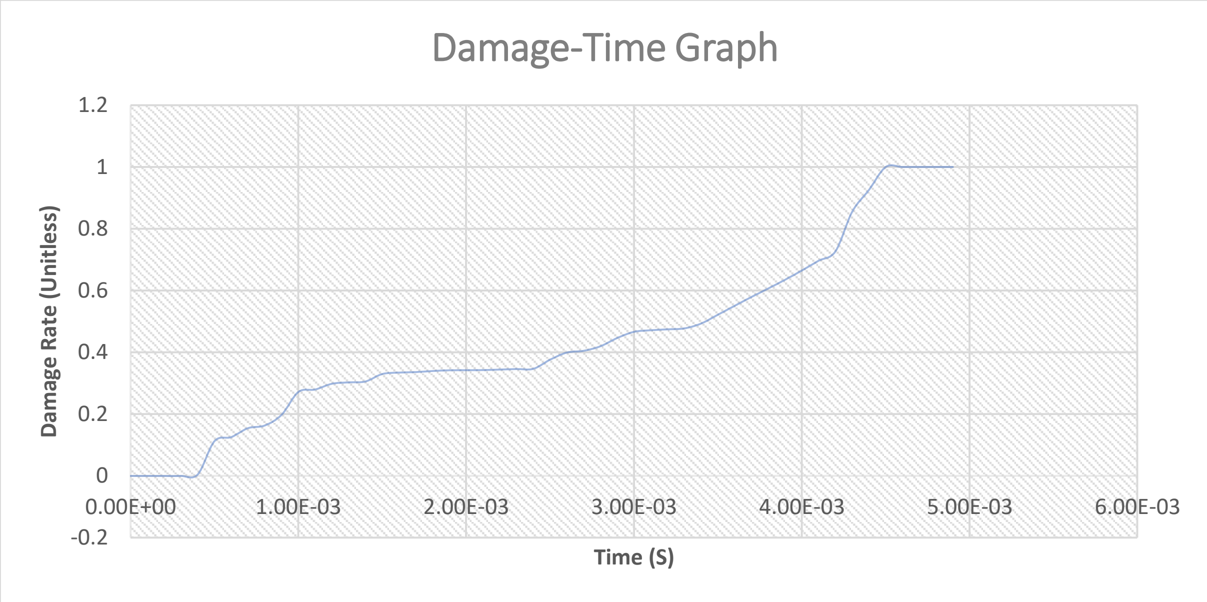

Figure 287(RCA-64.5MPa – Damage pattern graph of beam sample with strengthening and without top rebars- Explicit Dynamic Analysis)

17- Static Non-Linear Analysis - Without Strengthening and with Top Rebars

Geometry and loads

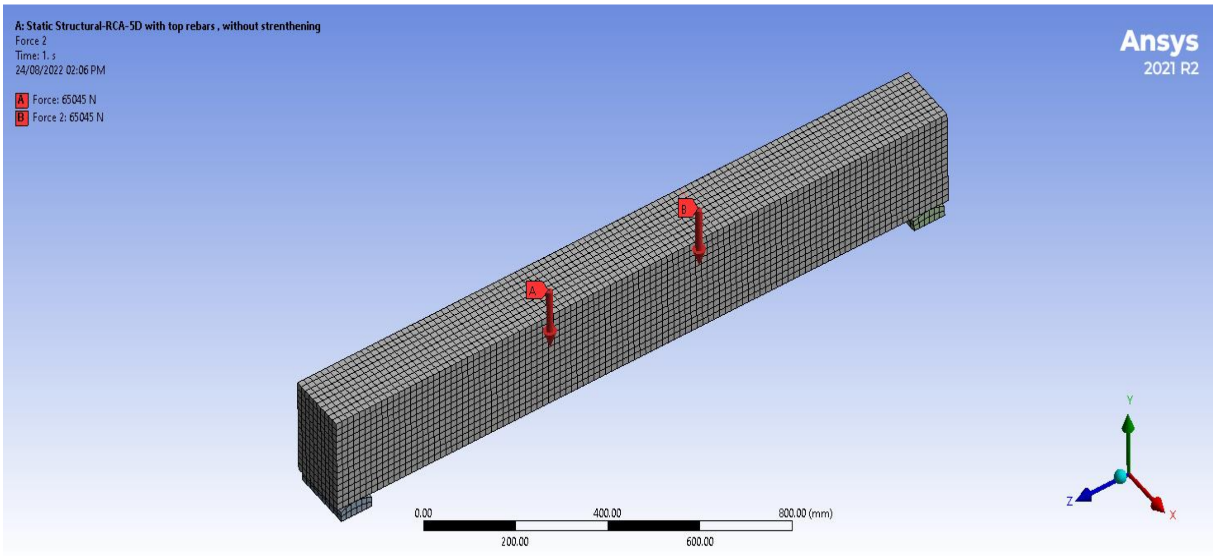

Figure 288(RCA-5D$_{Fibers}$-77.0MPa – Geometry & Loads of beam sample without strengthening and with top rebars- Static Nonlinear Analysis)

The ultimate load has been divided in to loads which is 130.09/2 =65.045KN.

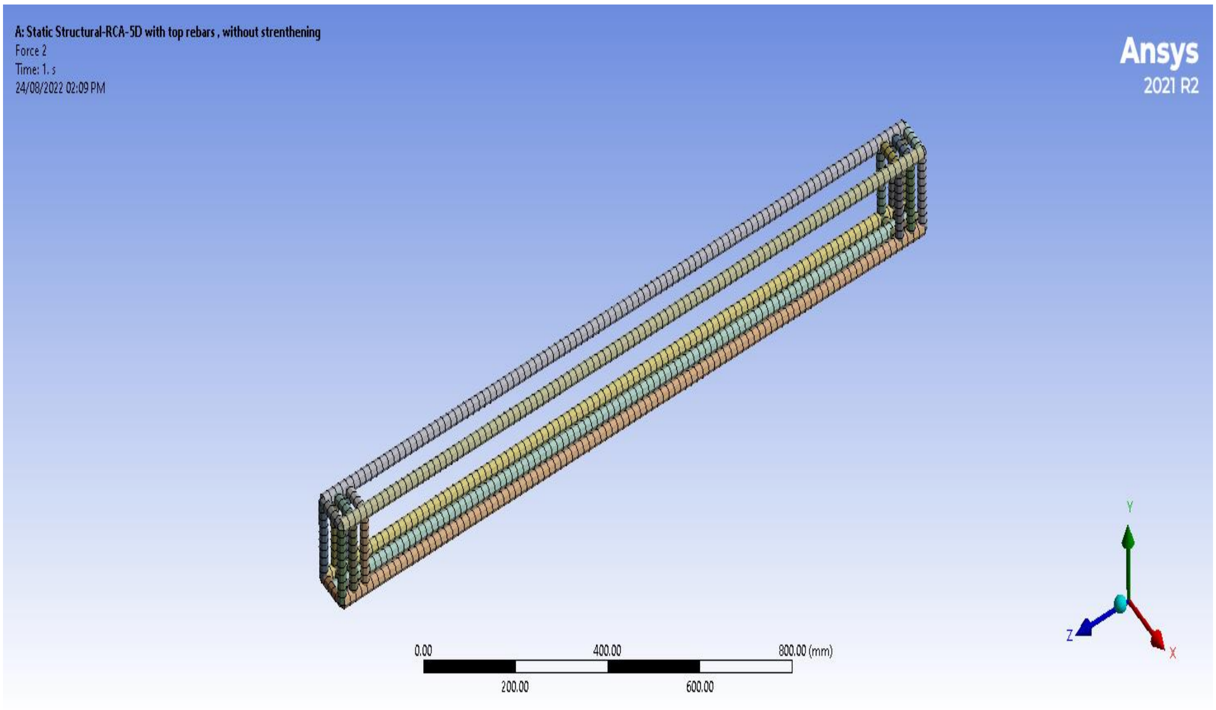

Figure 289(RCA-5D$_{Fibers}$-77.0MPa – Rebars of beam sample without strengthening - Static Nonlinear Analysis)

Deformations

Total Deformations

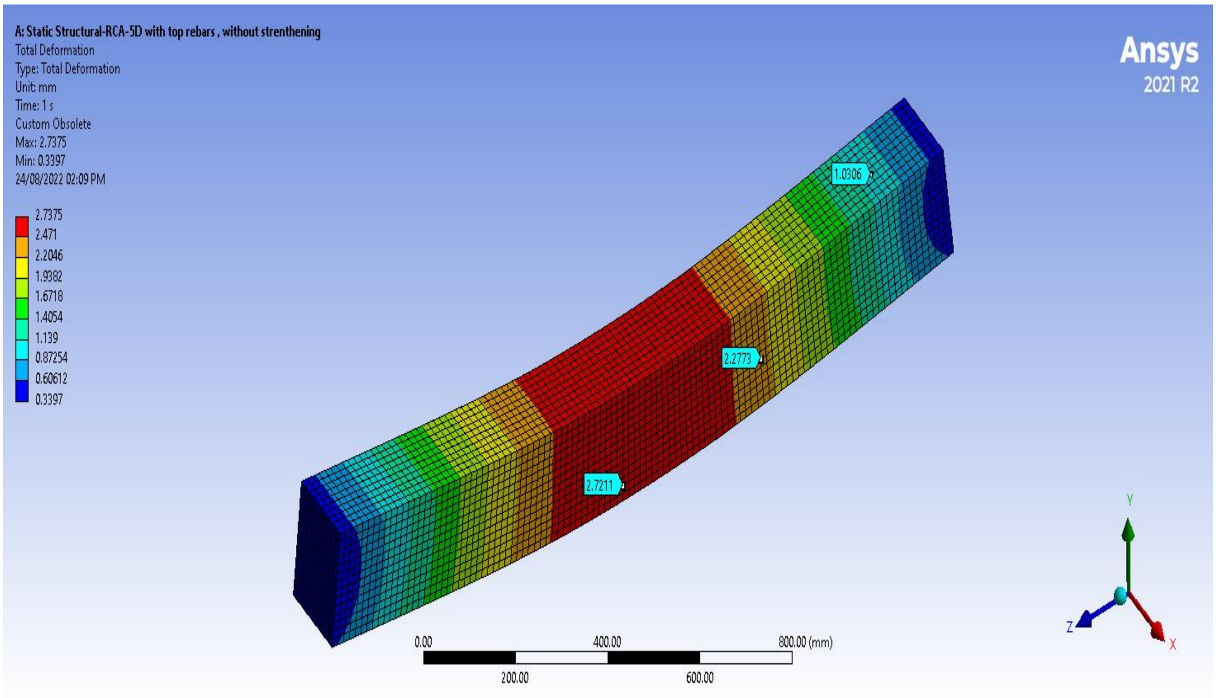

Figure 290(RCA-5D$_{Fibers}$-77.0MPa – Total deflections of beam sample without strengthening and with top rebars- Static Nonlinear Analysis)

The value is 2.7375 mm.

Directional Deformation (Y-Direction)

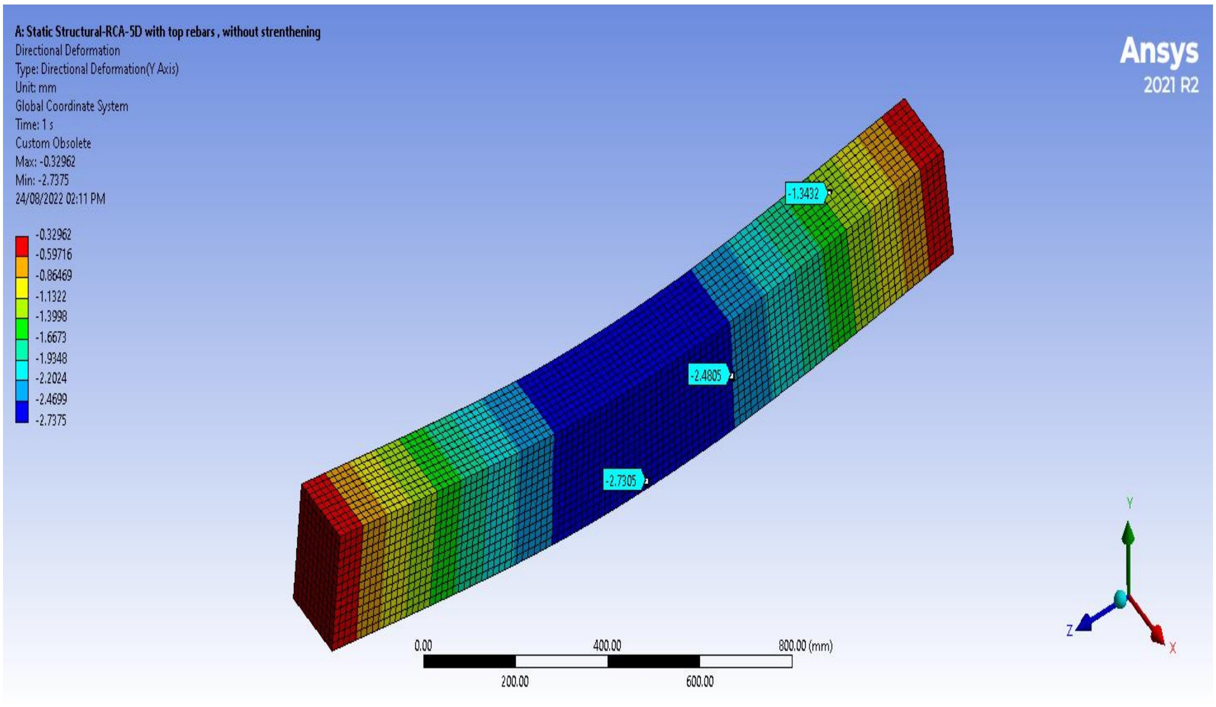

Figure 291(RCA-5D$_{Fibers}$-77.0MPa – Directional deflections (Y-Dim.) of beam sample without strengthening and without top rebars- Static Nonlinear Analysis)

The value is 2.7375 mm.

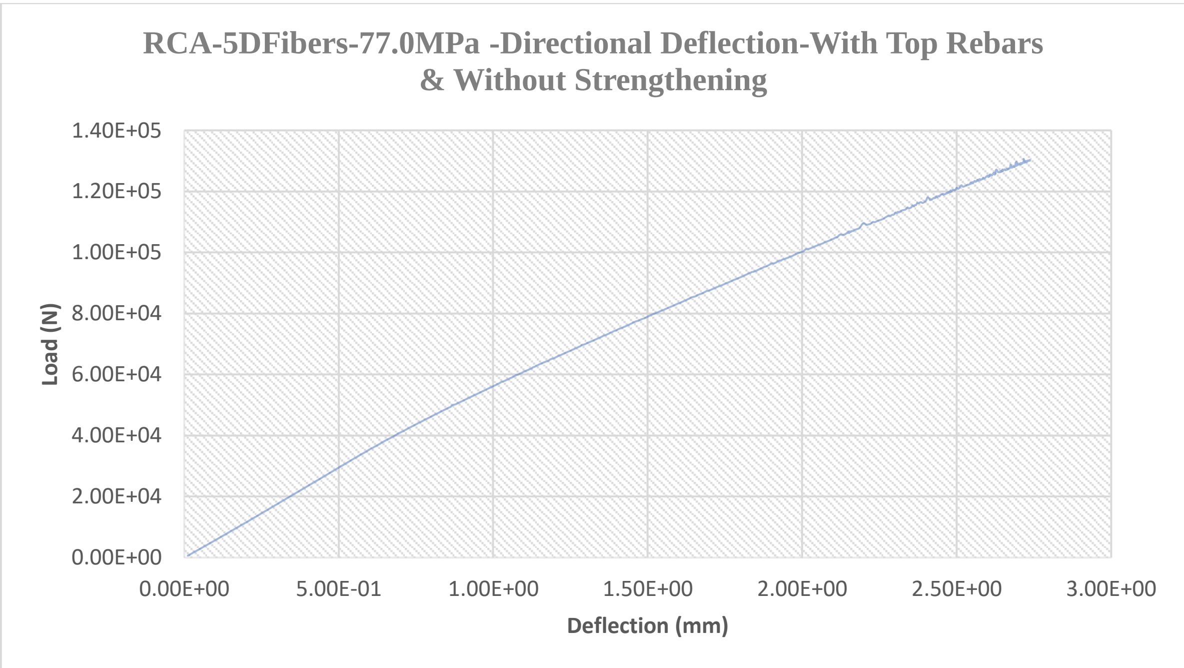

Figure 292(RCA-5D$_{Fibers}$-77.0MPa – Directional deflections (Y-Dim.) of beam sample without strengthening and with top rebars- Static Nonlinear Analysis)

Normal Stress (Concrete)

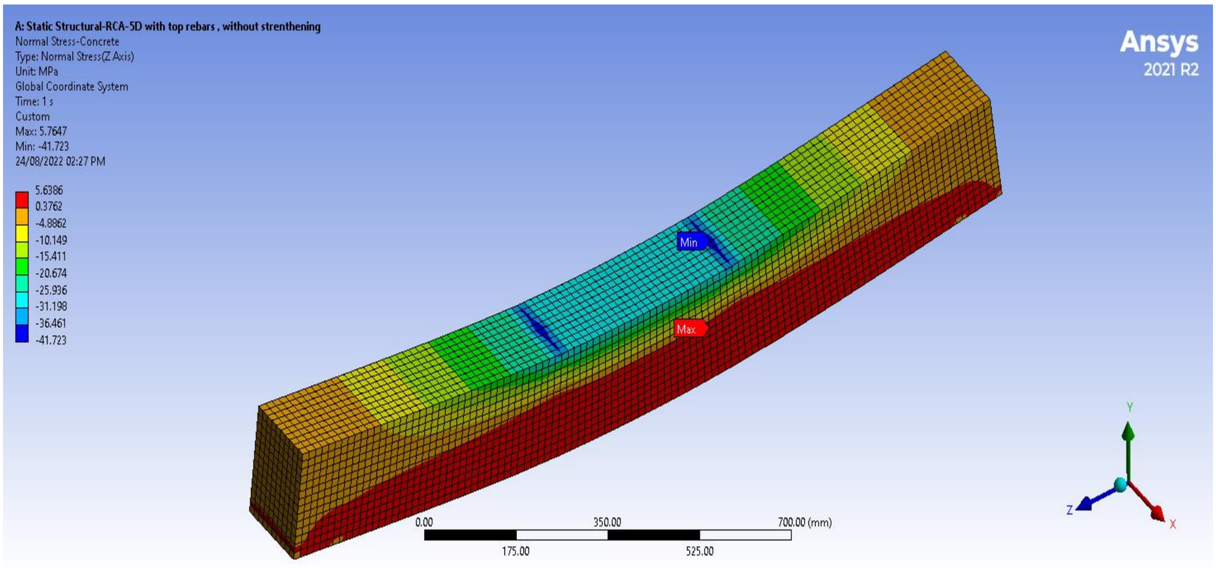

Figure 293(RCA-5D$_{Fibers}$-77.0MPa – Normal stress (Concrete) of beam sample without strengthening and with top rebars-Static Nonlinear Analysis)

The blue zones show the crushing from loading machine and the maximum value is 41.723 MPa, whereas the red zones indicate to tension.

Normal Stress (Rebars)

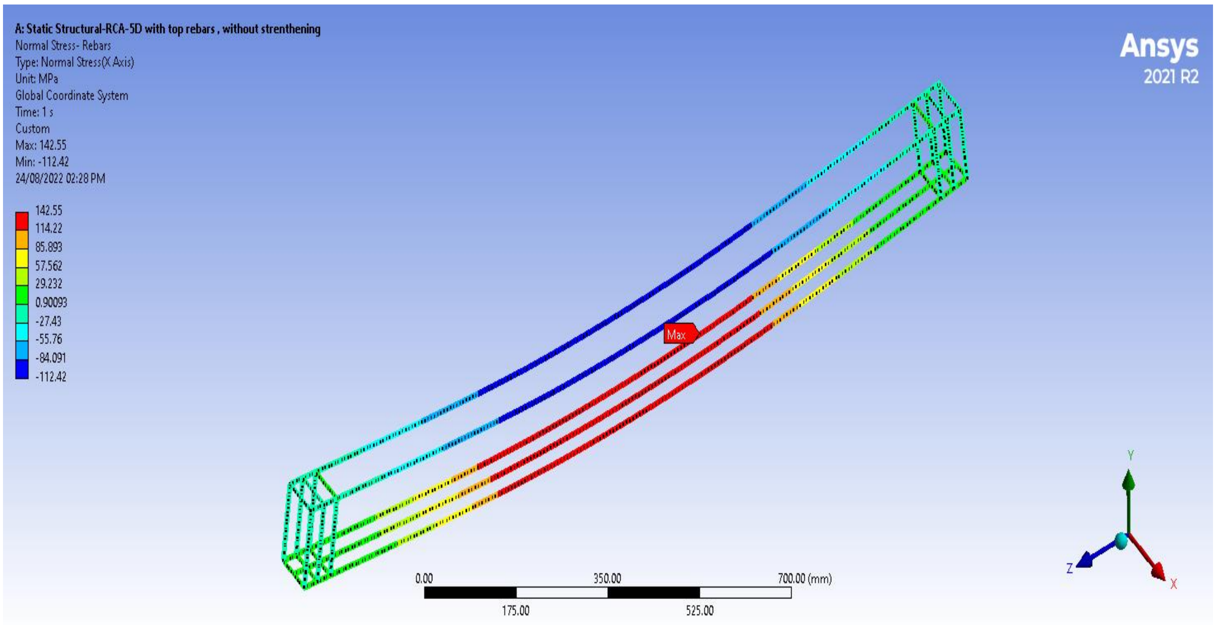

Figure 294(RCA-5D$_{Fibers}$-77.0MPa – Normal stress (Rebars) of beam sample without strengthening and with top rebars-Static Nonlinear Analysis)

The red zones show that the rebars is yielding by 142.55 MPa, in the middle span due to tension.

Shear Stress

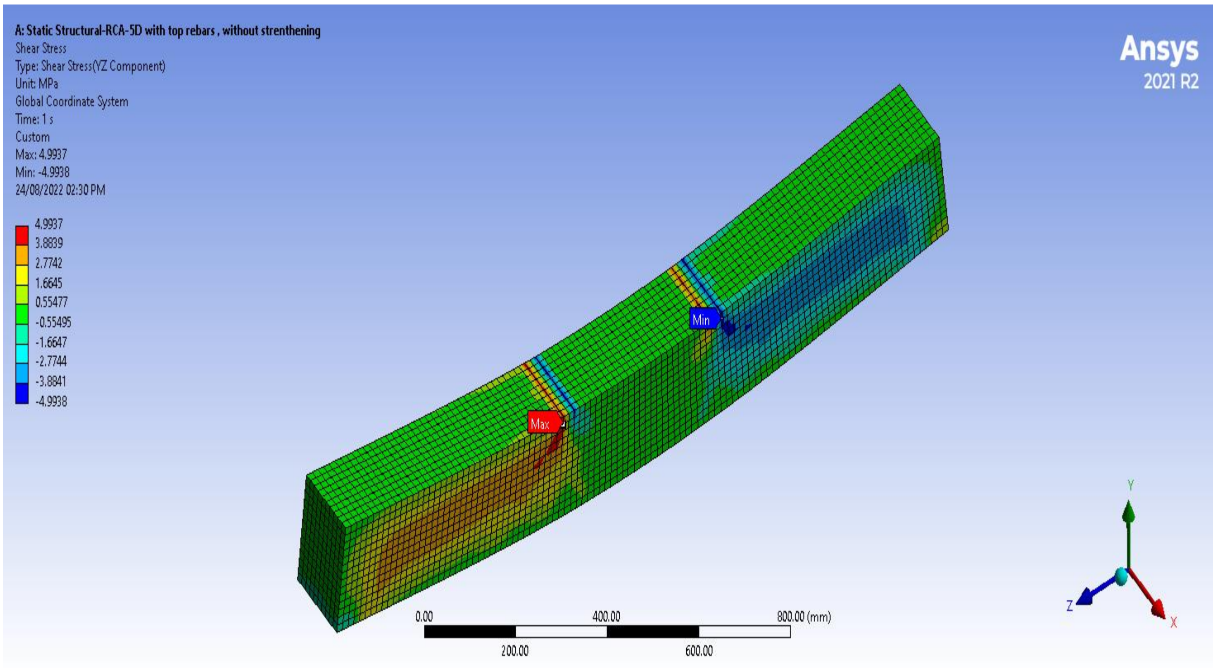

Figure 295(RCA-5D$_{Fibers}$-77.0MPa – Shear Stress of beam sample without strengthening and with top rebars - Static Nonlinear Analysis)

Elastic Strain

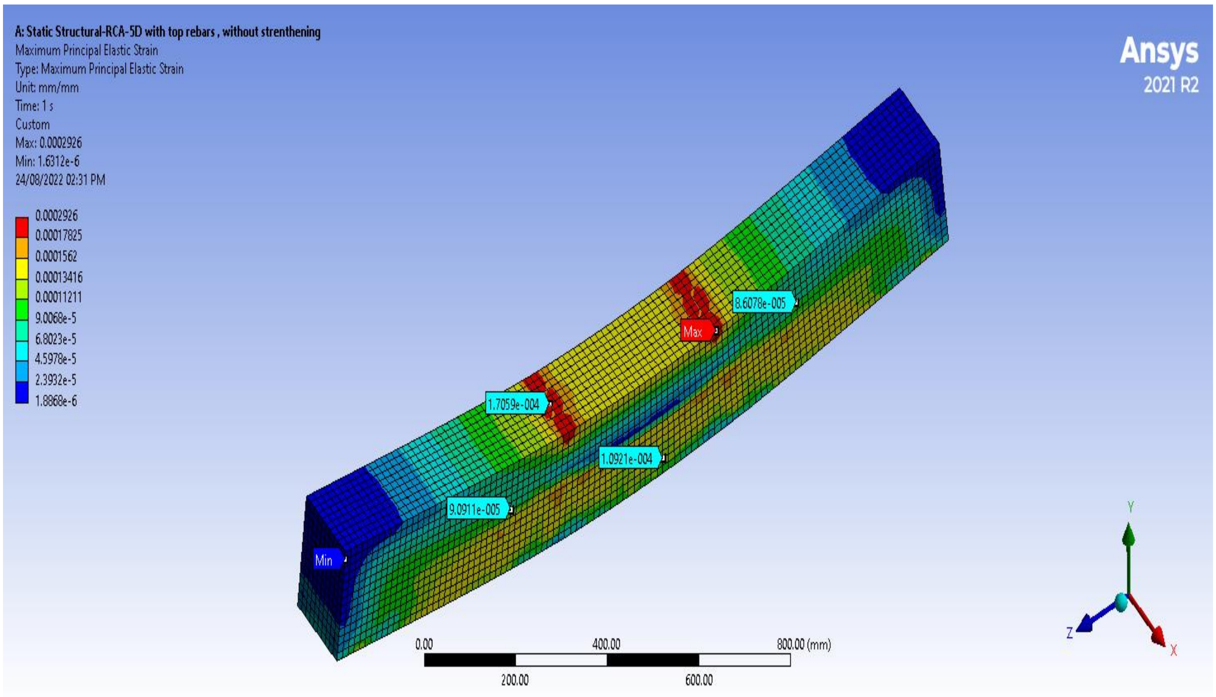

Figure 296(RCA-5D$_{Fibers}$-77.0MPa – Elastic Strain of beam sample without strengthening and with top rebars - Static Nonlinear Analysis)

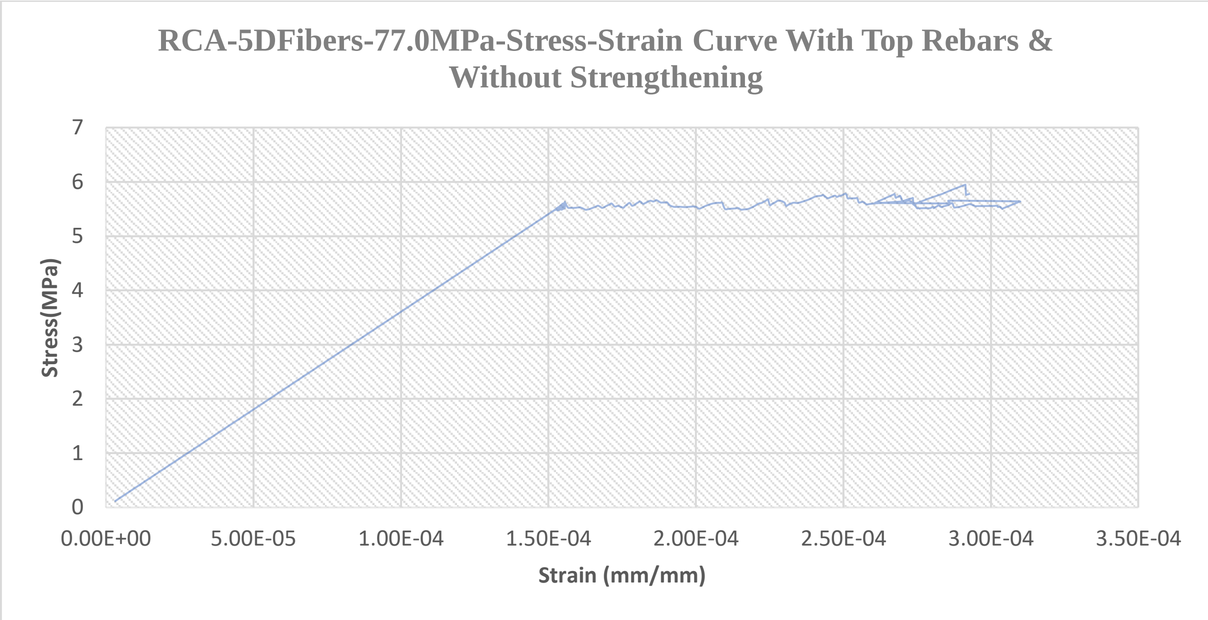

Figure 297(RCA-5D$_{Fibers}$-77.0MPa – Stress and Strain graph of beam sample without strengthening and with top rebars - Static Nonlinear Analysis)

18- Explicit Dynamics-With Top Rebars & Without Strengthening

Geometry and loads

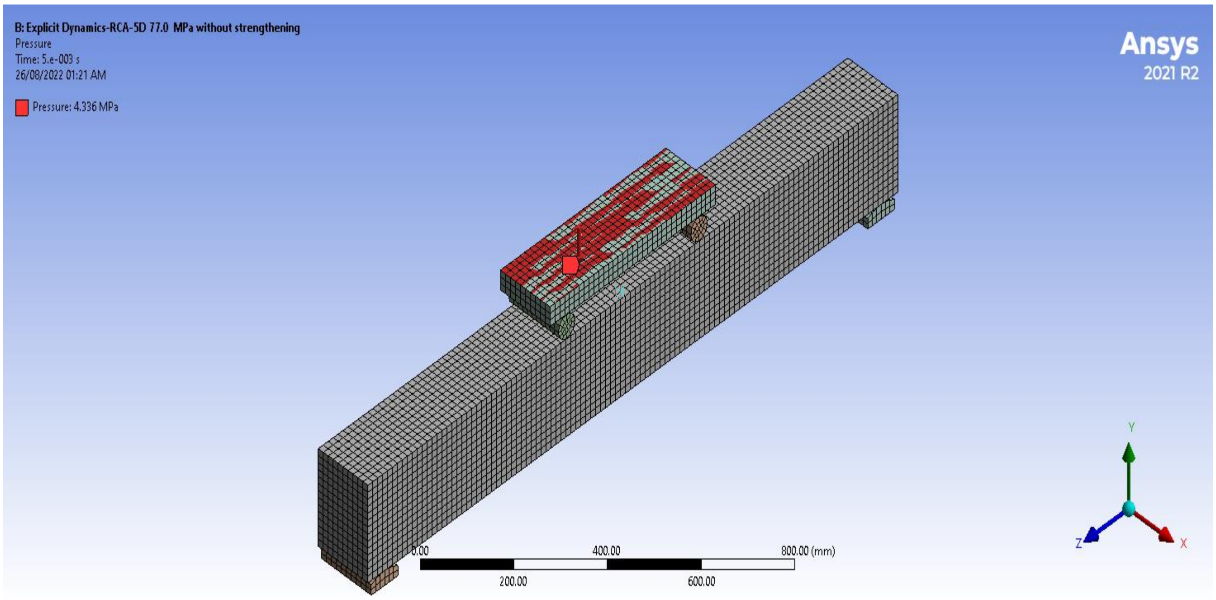

Figure 298(RCA-5D$_{Fibers}$-77.0MPa – Geometry & Loads of beam sample without strengthening and with top rebars- Explicit Dynamic Analysis)

The ultimate load has been transferred to be as a pressure load which is 4.336 MPa as shown above with rate loading 0.6mm/min.

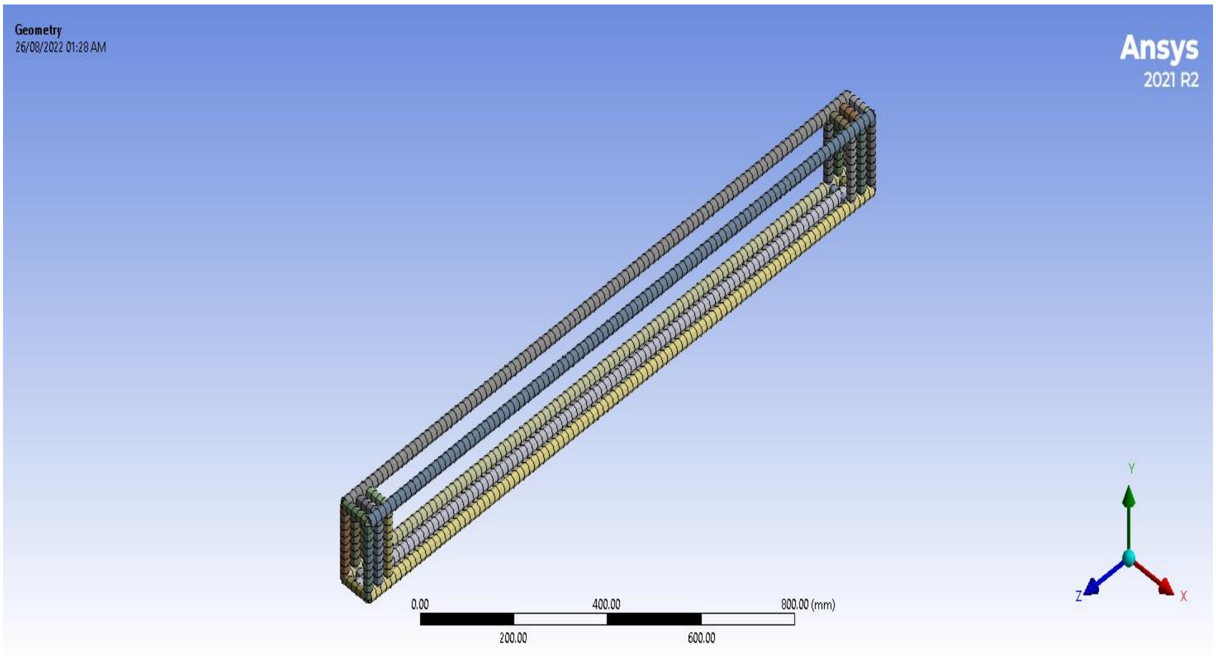

Figure 299(RCA-5D$_{Fibers}$-77.0MPa – Rebars of beam sample without strengthening - Explicit Dynamic Analysis)

Deformations

Total Deformations

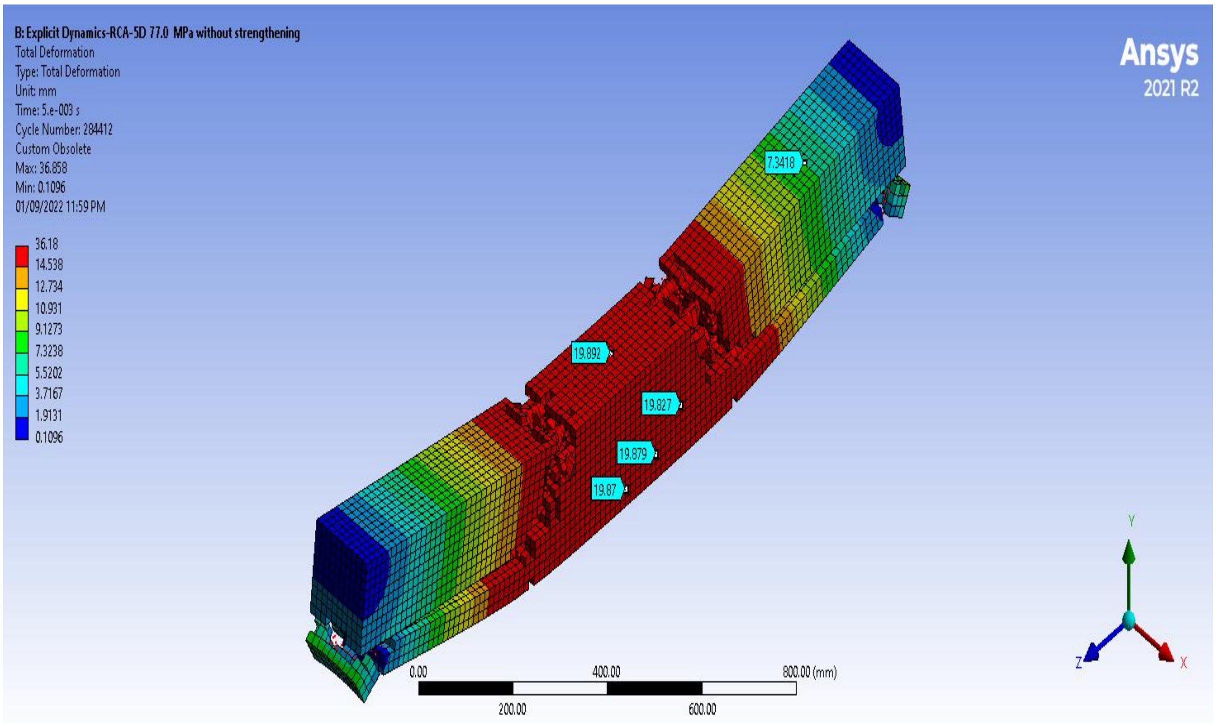

Figure 300(RCA-5D$_{Fibers}$-77.0MPa – Total deflections of beam sample without strengthening and with top rebars- Explicit Dynamic Analysis)

The value is 19.88 mm.

Directional Deformation (Y-Direction)-Concrete

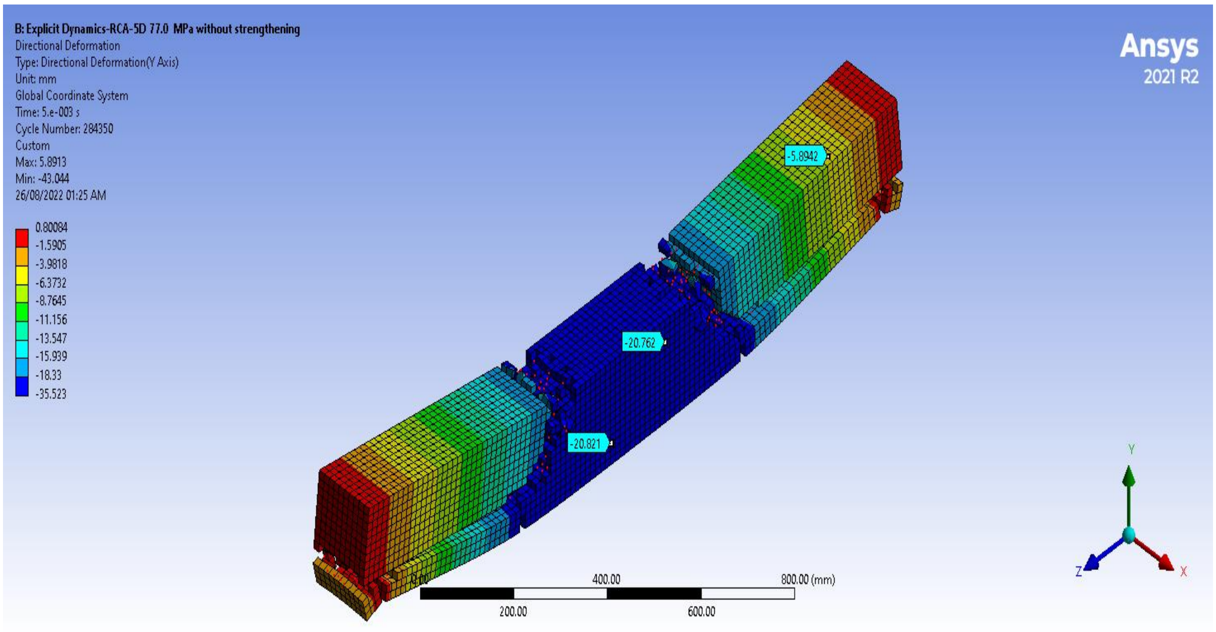

Figure 301(RCA-5D$_{Fibers}$-77.0MPa – Directional deflections (Y-Dir.) of beam sample without strengthening and with top rebars- Explicit Dynamic Analysis)

The value is 19.88 mm.

Directional Deformation (Y-Direction)- Rebars

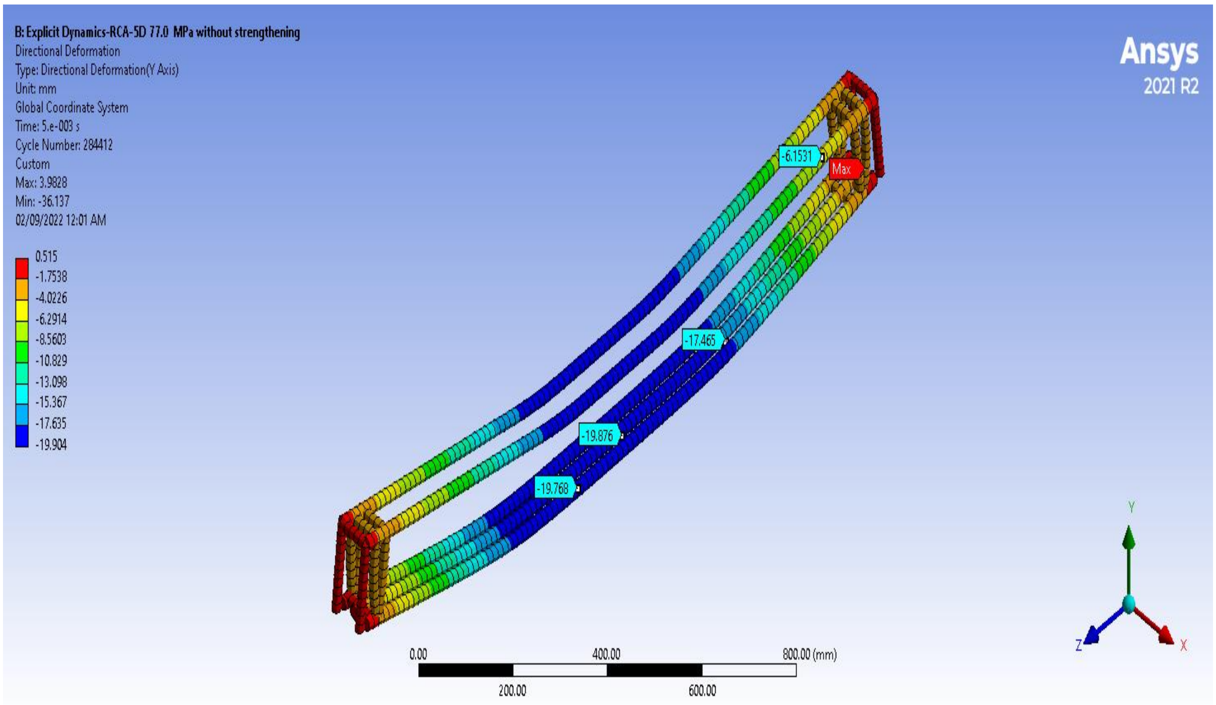

Figure 302(RCA-5D$_{Fibers}$-77.0MPa – Directional deflections (Y-Dir.) of beam rebars without strengthening- Explicit Dynamic Analysis)

Normal strain

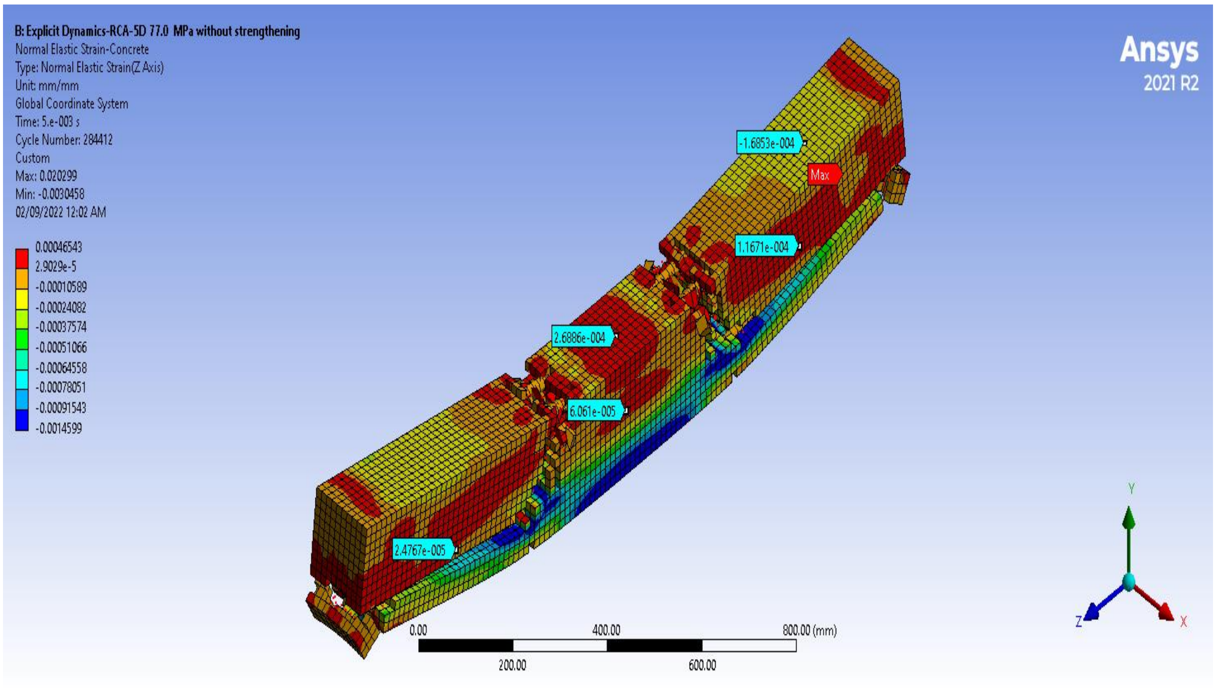

Figure 303(RCA-5DFibers-77.0MPa – Normal strain of beam sample without strengthening and with top rebars- Explicit Dynamic Analysis)

Shear Stress

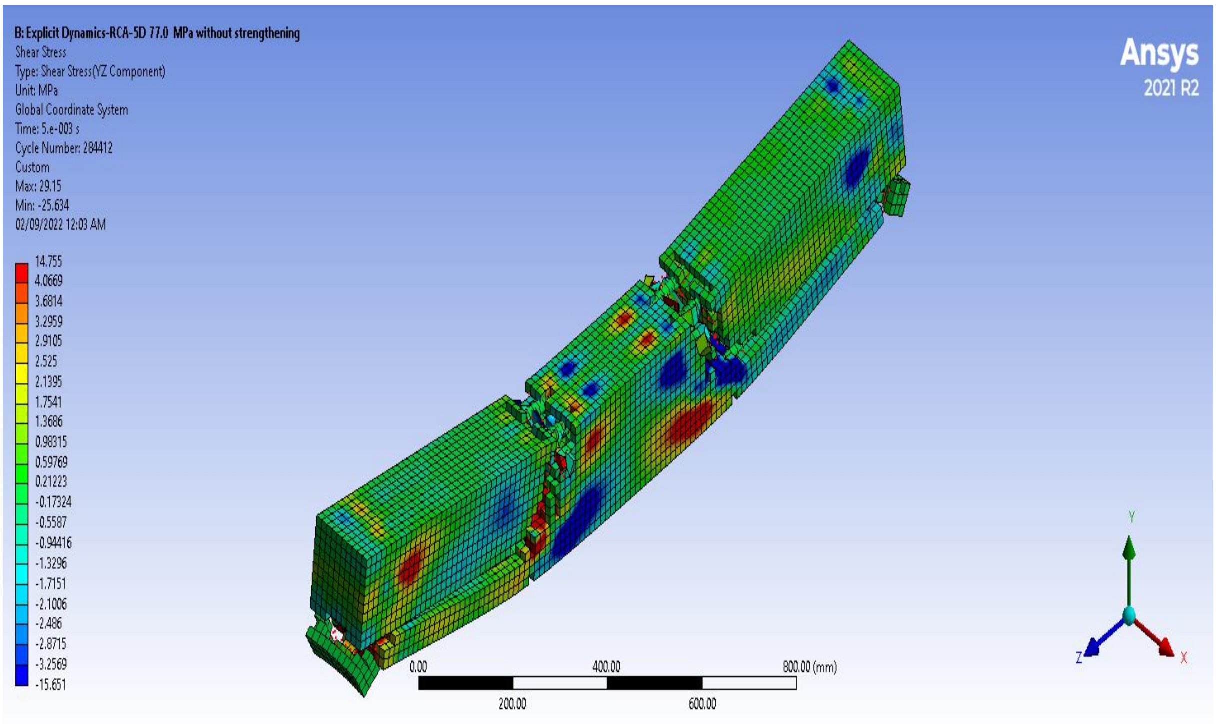

Figure 304(RCA-5DFibers-77.0MPa – Shear stress of beam sample without strengthening and with top rebars- Explicit Dynamic Analysis)

Total shape strain

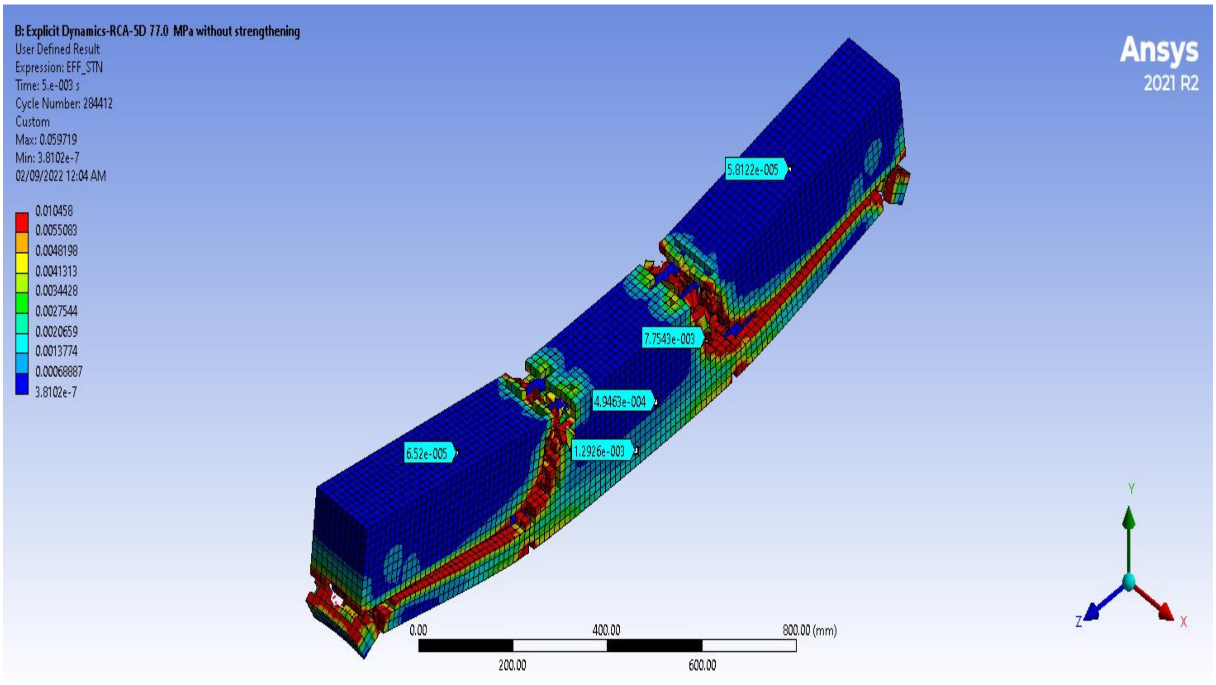

Figure 305(RCA-5D$_{Fibers}$-77.0MPa – Total strain of beam sample without strengthening and with top rebars- Explicit Dynamic Analysis)

Maximum Stress

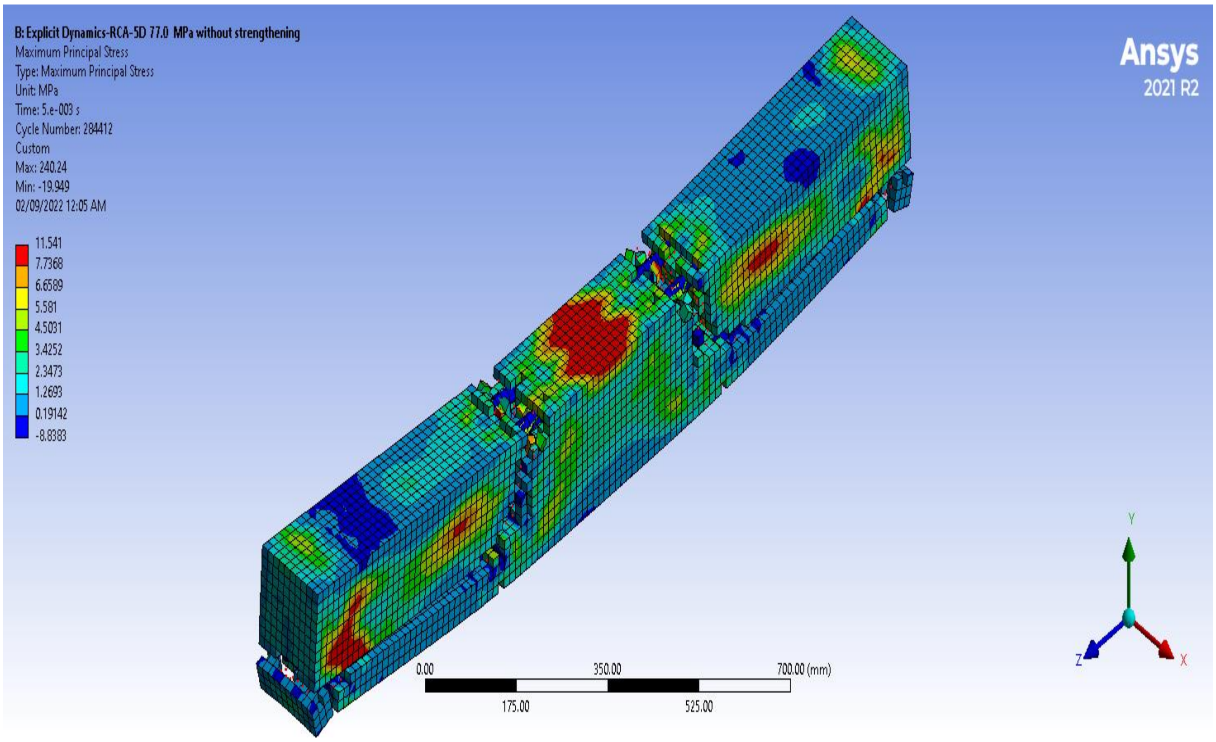

Figure 306(RCA-5D$_{Fibers}$-77.0MPa – Maximum stress of beam sample without strengthening and with top rebars- Explicit Dynamic Analysis)

The Damage Pattern

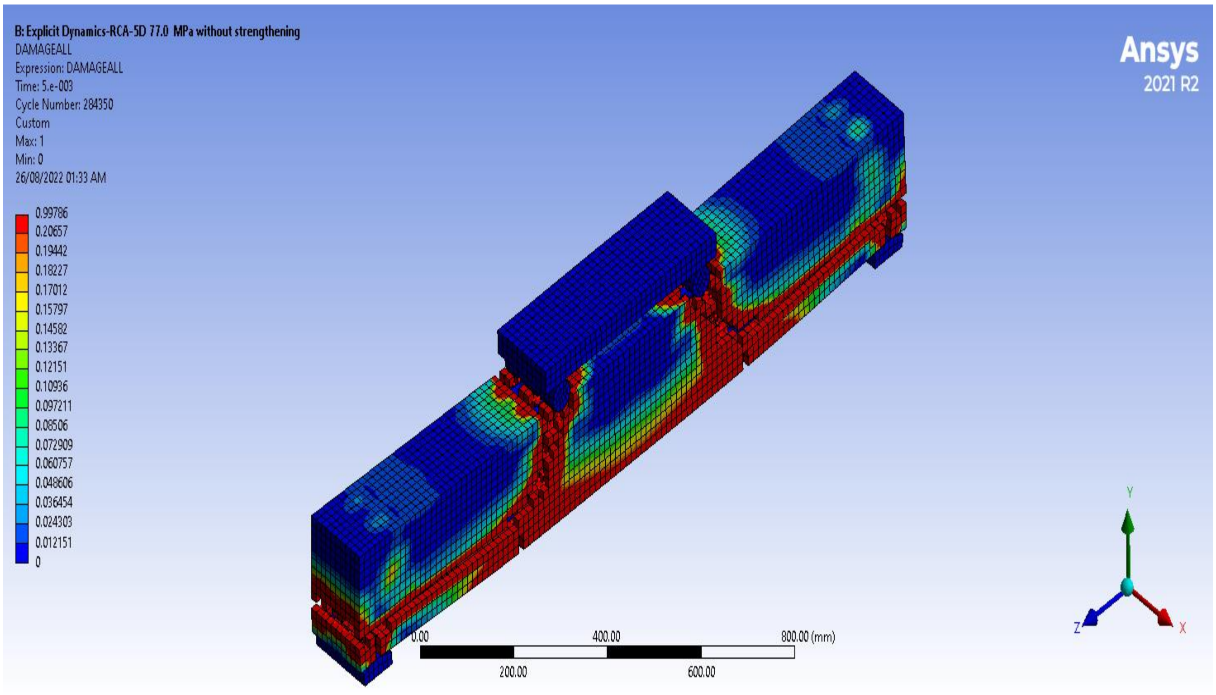

Figure 307(RCA-5DFibers-77.0MPa – Damage pattern-1 of beam sample without strengthening and with top rebars- Explicit Dynamic Analysis)

As we can see the shear damage cracks and concrete failures.

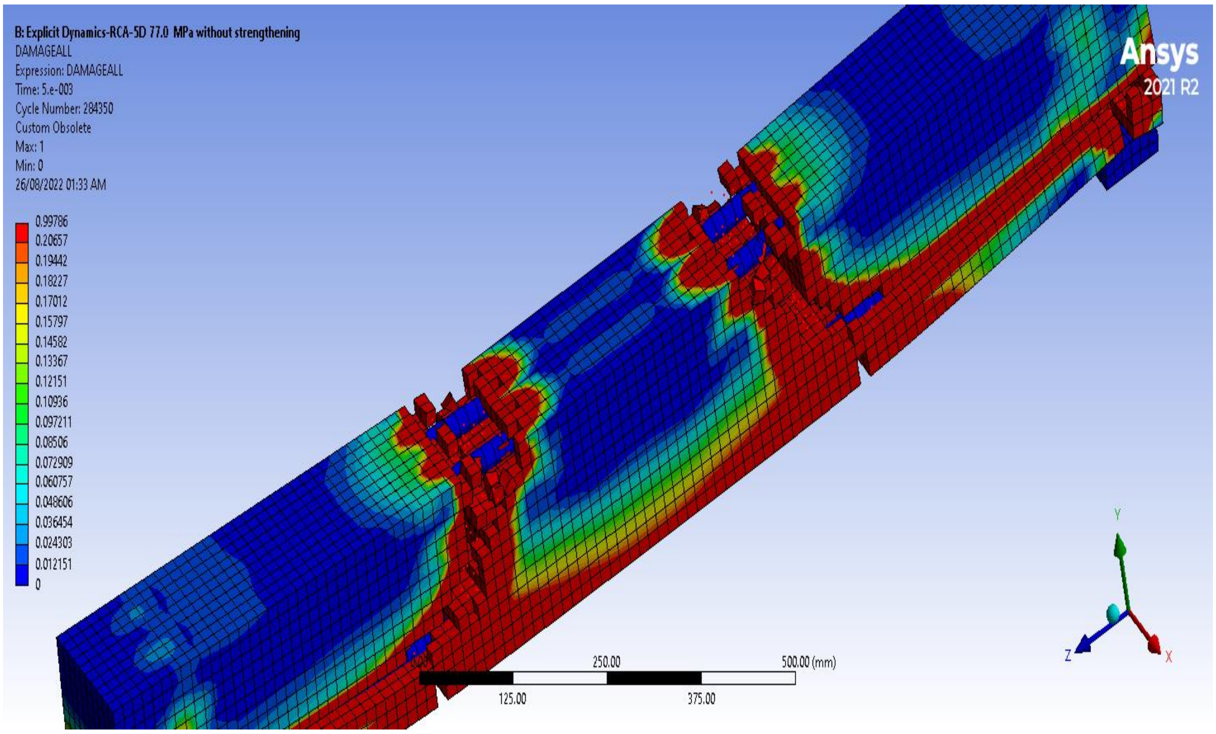

Figure 308(RCA-5DFibers-77.0MPa – Damage pattern-2 of beam sample without strengthening and with top rebars- Explicit Dynamic Analysis)

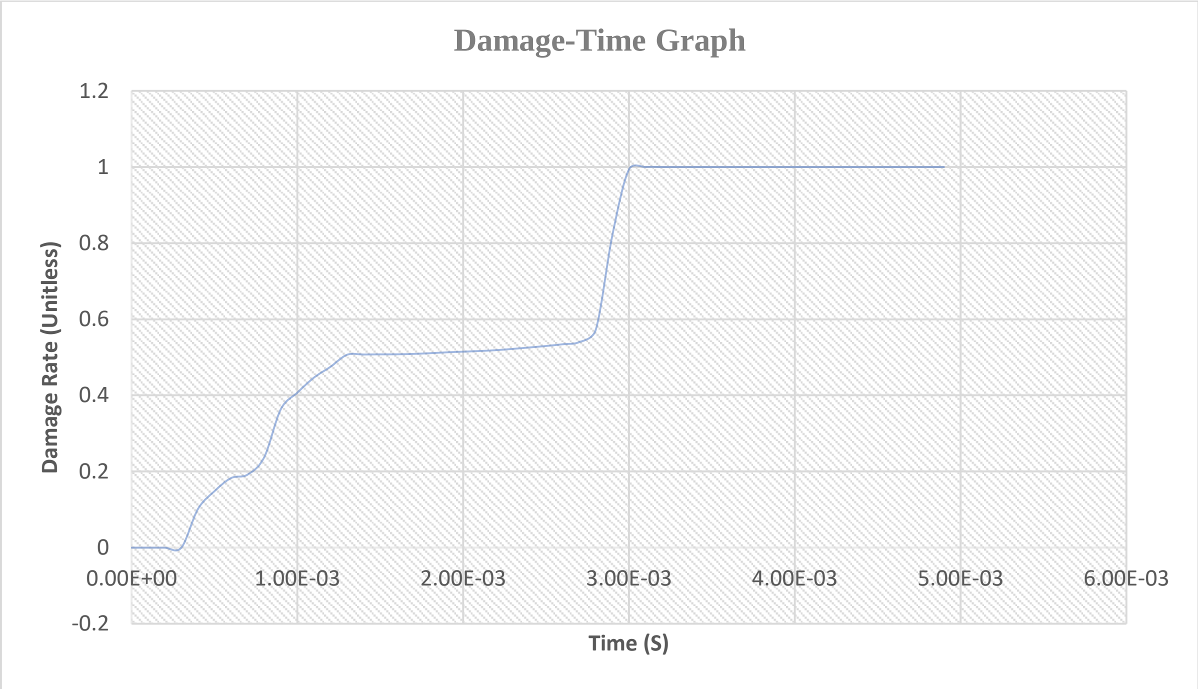

Figure 309(RCA-5D$_{Fibers}$-77.0MPa – Damage pattern graph of beam sample without strengthening and with top rebars-Explicit Dynamic Analysis)

20- Static Non-Linear Analysis – Without Top Rebars and Strengthening

Geometry and loads

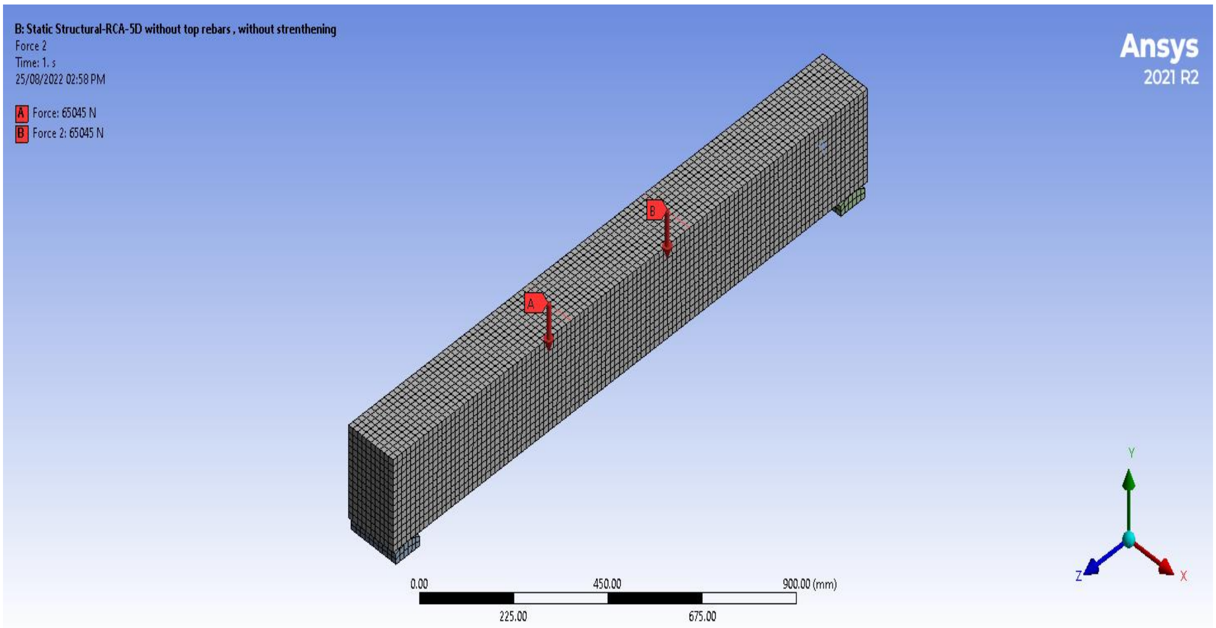

Figure 310(RCA-5D$_{Fibers}$-77.0MPa – Geometry & loads of beam sample without strengthening and top rebars- Static Nonlinear Analysis)

The ultimate load has been divided in to loads which is 130.09/2 =65.045KN.

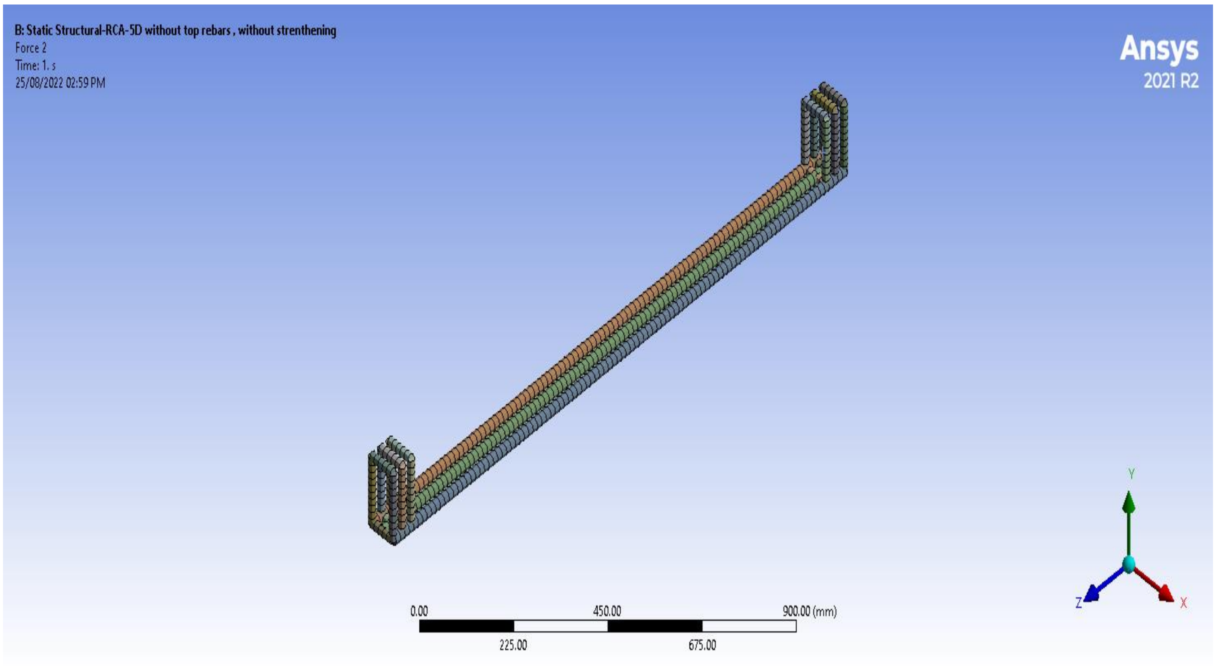

Figure 311(RCA-5DFibers-77.0MPa – Rebars of beam sample without strengthening - Static Nonlinear Analysis)

Deformations

Total Deformations

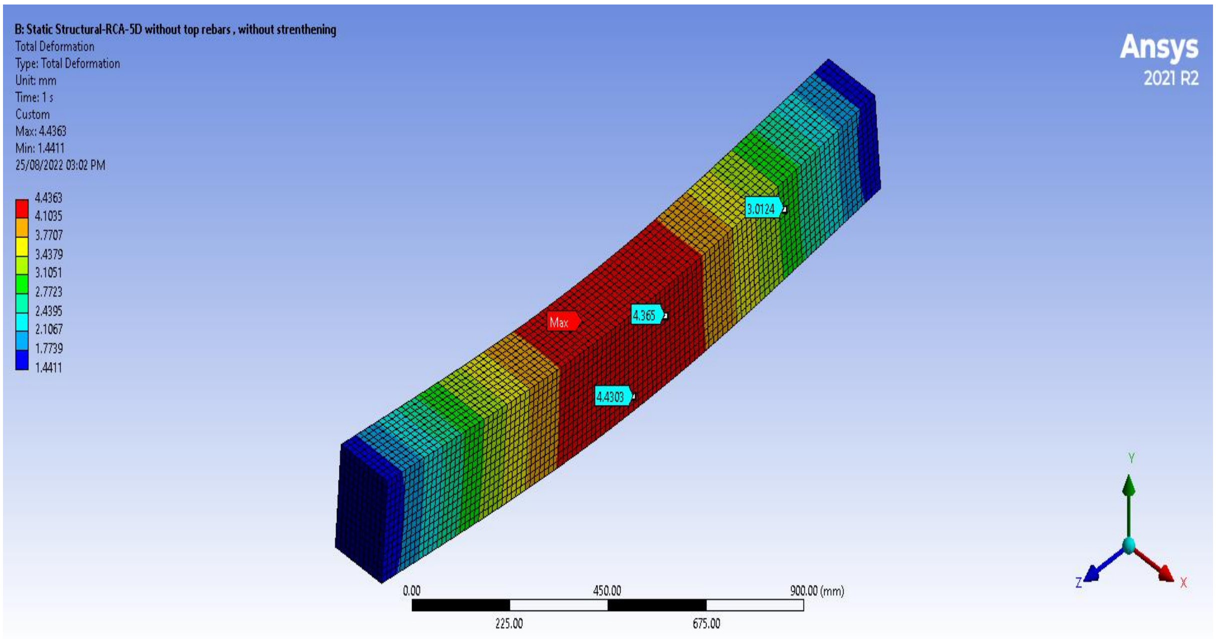

Figure 312(RCA-5DFibers-77.0MPa – Total deflections of beam sample without strengthening and top rebars- Static Nonlinear Analysis)

The value is 4.4363 mm.

Directional Deformation (Y-Direction)

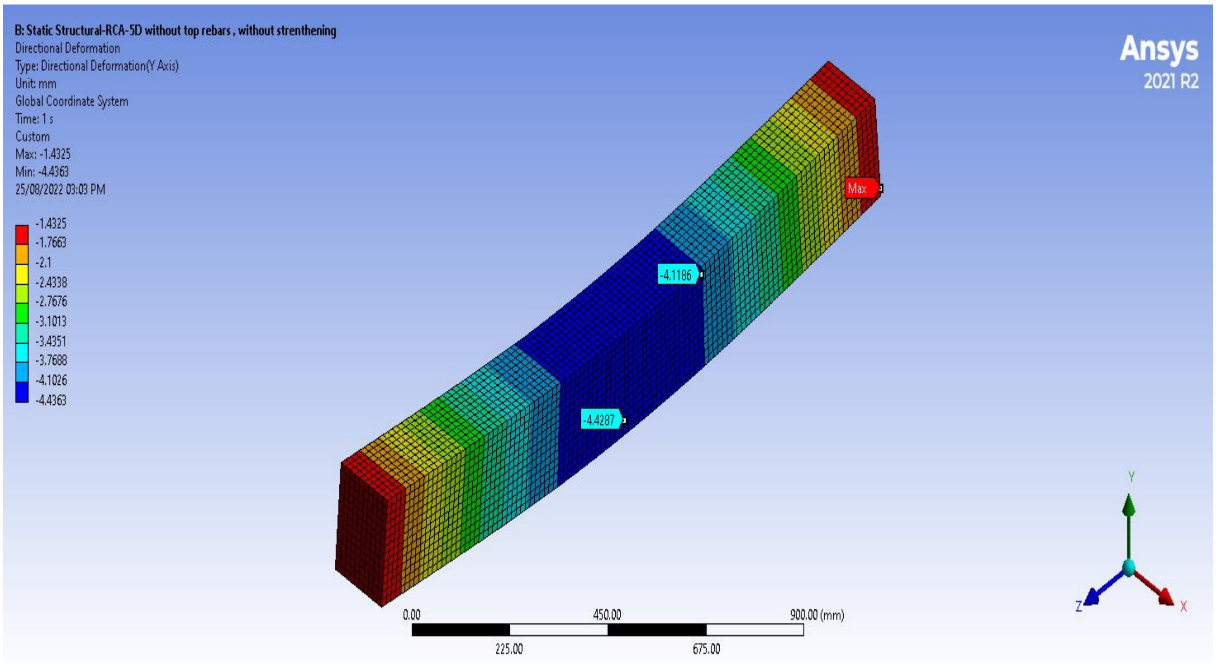

Figure 313(RCA-5D$_{Fibers}$-77.0MPa – Directional deflections (Y-Dir.) of beam sample without strengthening and top rebars- Static Nonlinear Analysis)

The value is 4.4363 mm.

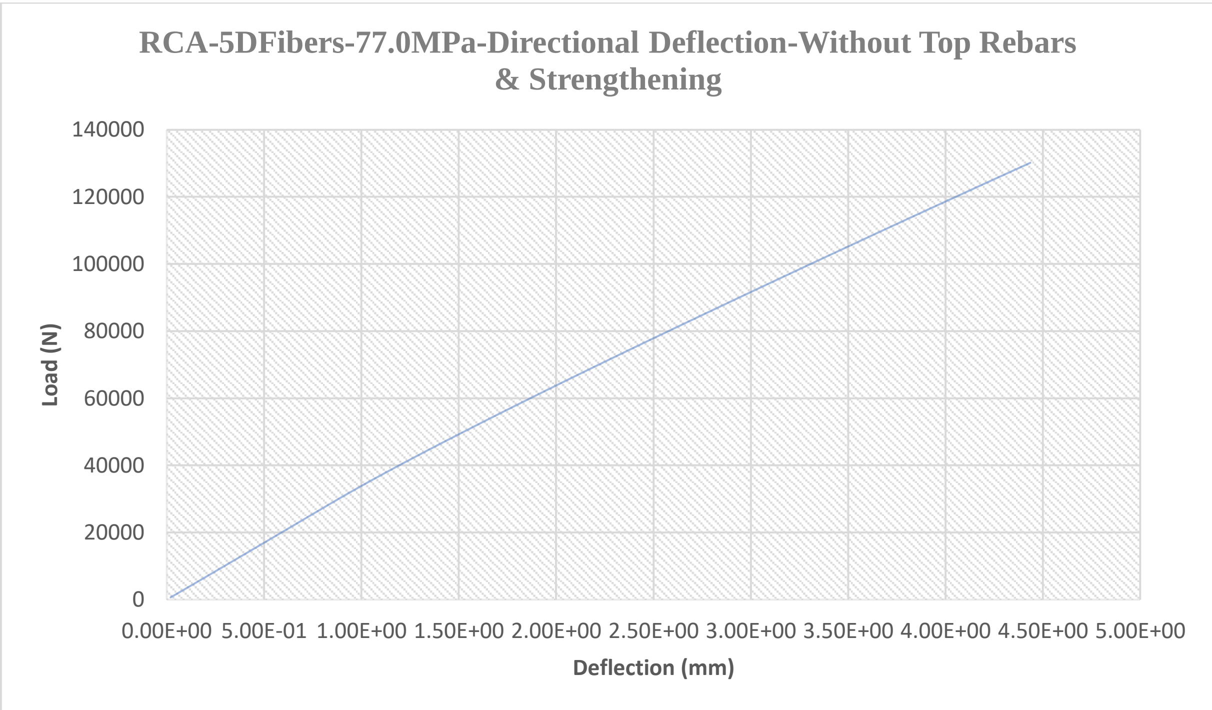

Figure 314(RCA-5D$_{Fibers}$-77.0MPa – Directional deflections (Y-Dir.) graph of beam sample without strengthening and top rebars- Static Nonlinear Analysis)

Normal Stress (Concrete)

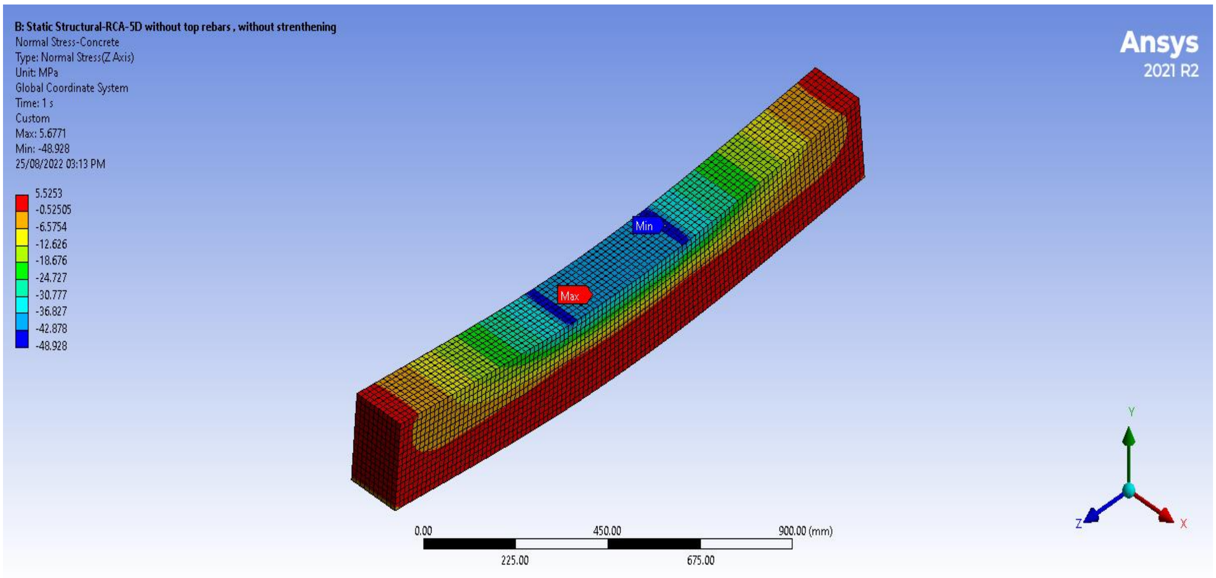

Figure 315(RCA-5DFibers-77.0MPa – Normal stress (concrete) of beam sample without strengthening and top rebars- Static Nonlinear Analysis)

The blue zones show the crushing from loading machine and the maximum value is 48.928MPa, whereas the red zones indicate to tension.

Normal Stress (Rebars)

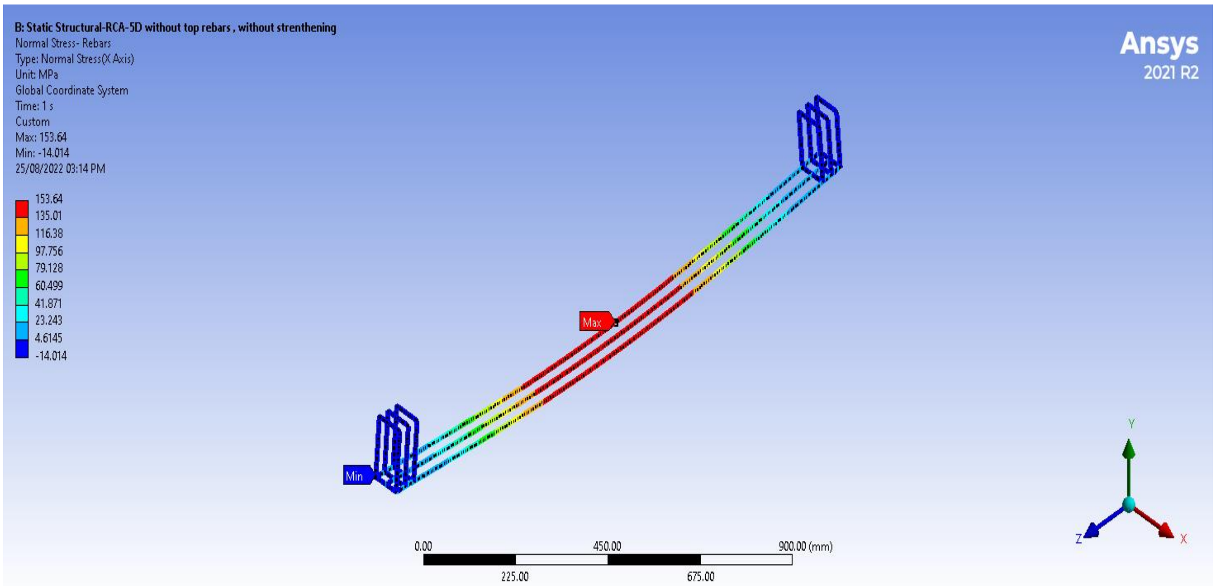

Figure 316(RCA-5DFibers-77.0MPa – Normal stress (Rebars) of beam sample without strengthening and top rebars- Static Nonlinear Analysis)

The red zones show that the rebars is yielding by 153.64MPa, in the middle span due to tension.

Shear Stress

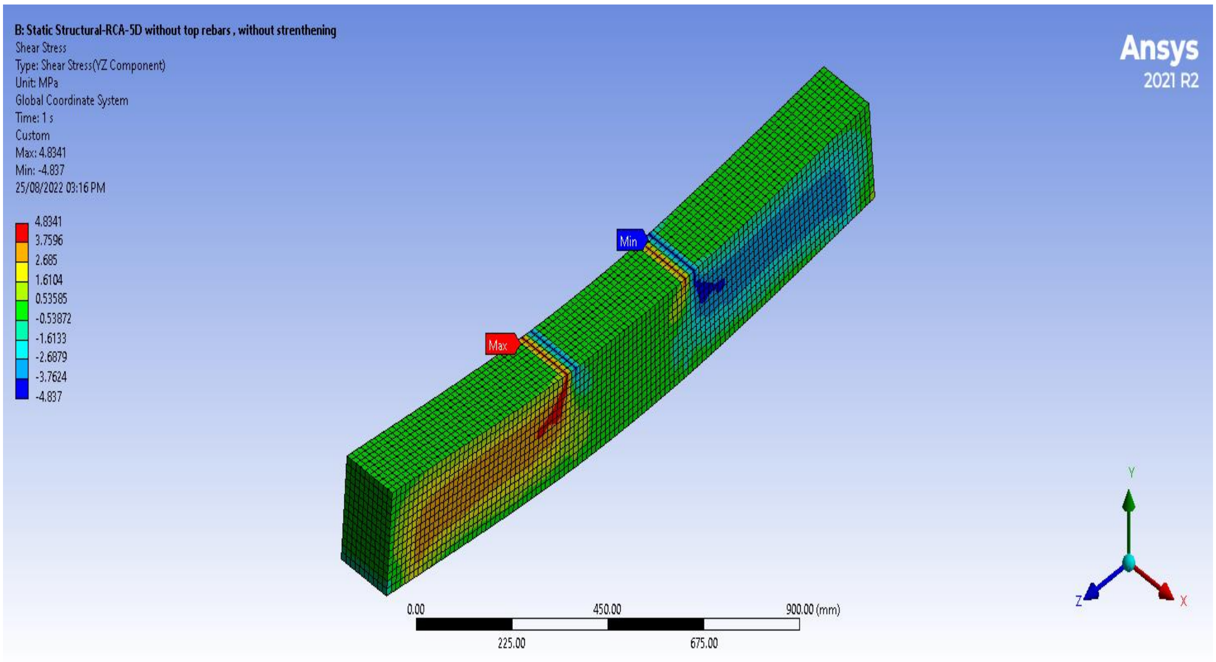

Figure 317(RCA-5D$_{Fibers}$-77.0MPa – Shear stress of beam sample without strengthening and top rebars- Static Nonlinear Analysis)

Elastic Strain

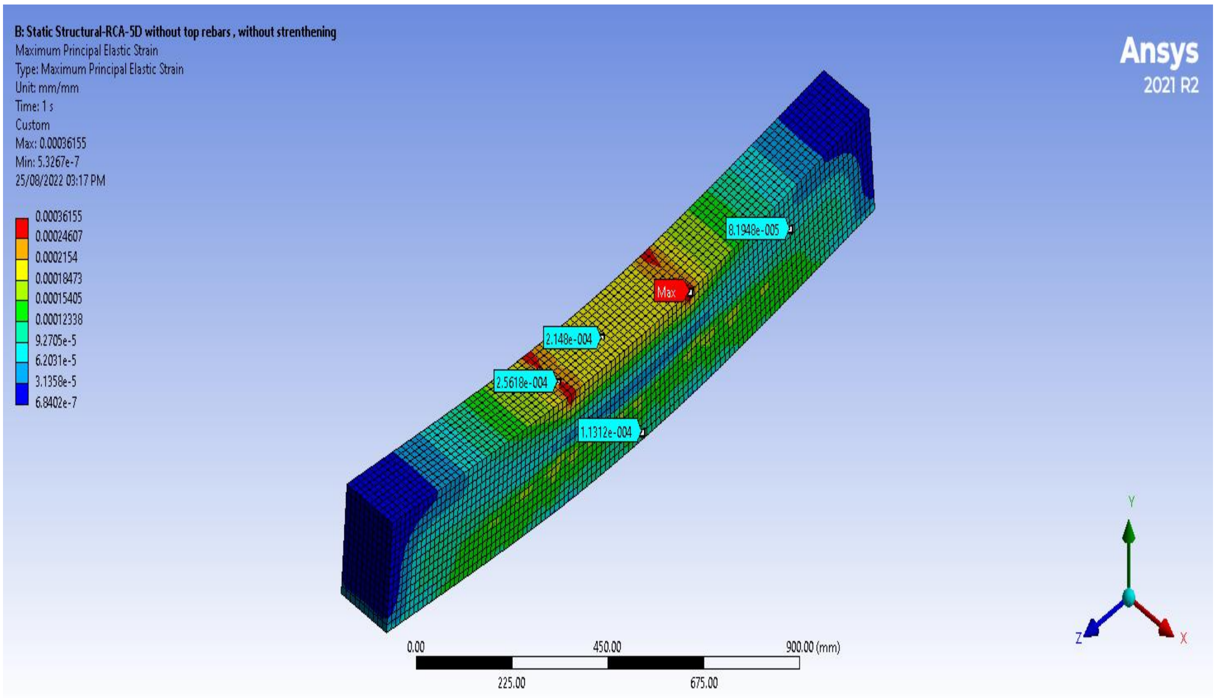

Figure 318(RCA-5D$_{Fibers}$-77.0MPa – Elastic strain of beam sample without strengthening and top rebars- Static Nonlinear Analysis)

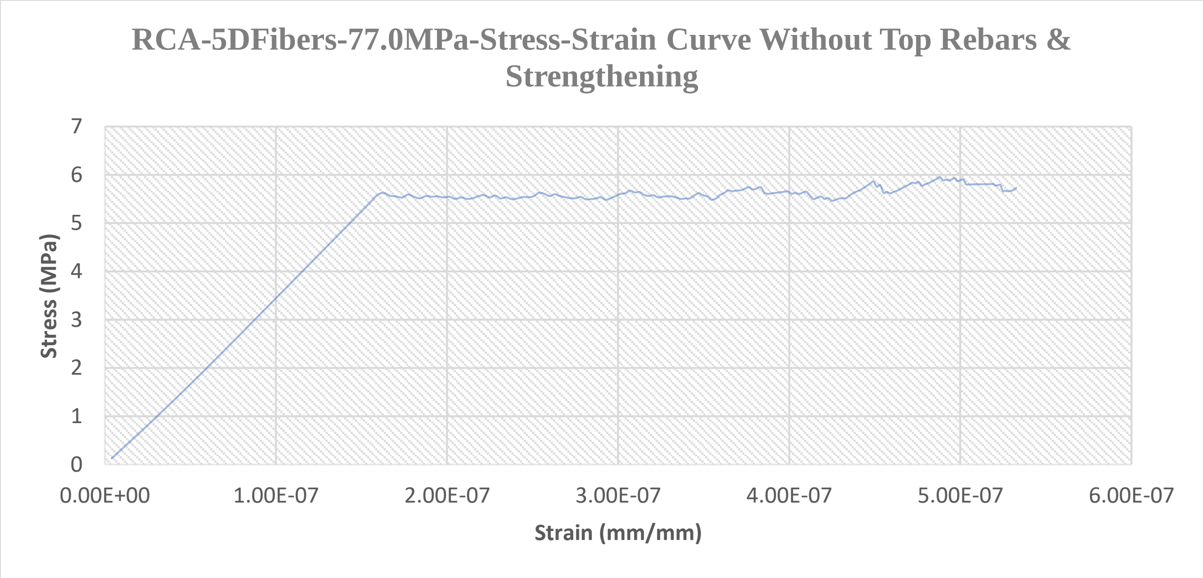

Figure 319(RCA-5D$_{Fibers}$-77.0MPa – Stress & Strain graph of beam sample without strengthening and top rebars- Static Nonlinear Analysis)

21- Explicit Dynamic-Without Top Rebars & Strengthening

Geometry and loads

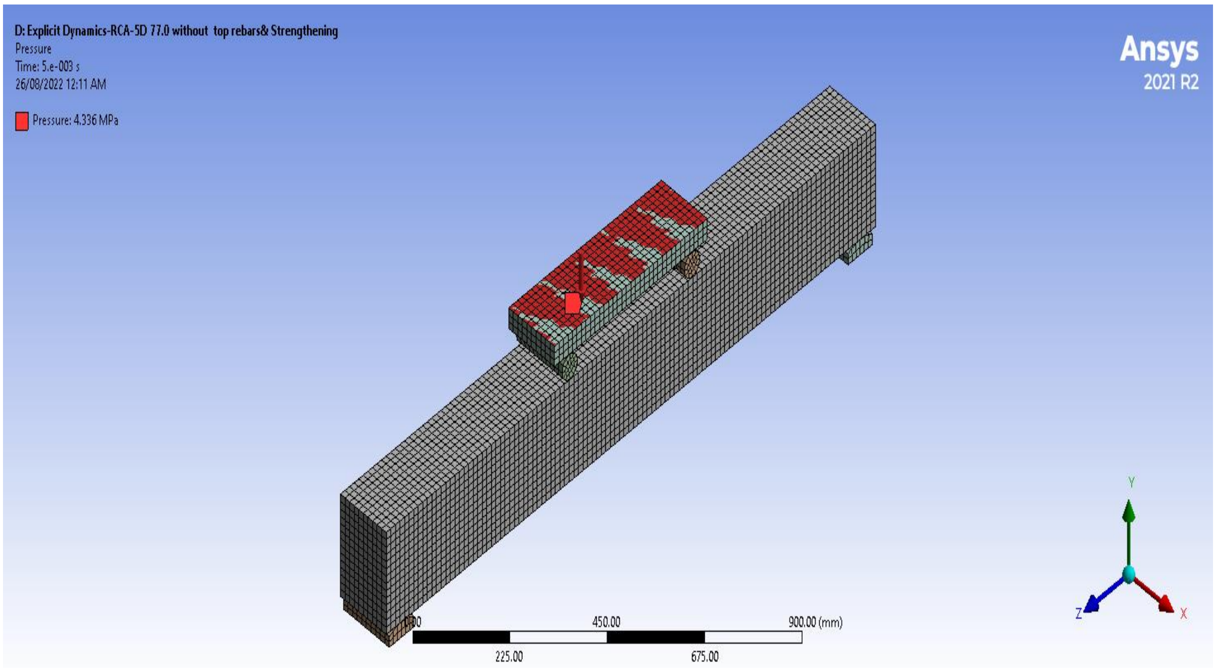

Figure 320(RCA-5D$_{Fibers}$-77.0MPa – Geometry & loads of beam sample without strengthening and top rebars- Explicit Dynamic Analysis)

The ultimate load has been transferred to be as a pressure load which is 4.336 MPa as shown above with rate loading 0.6mm/min

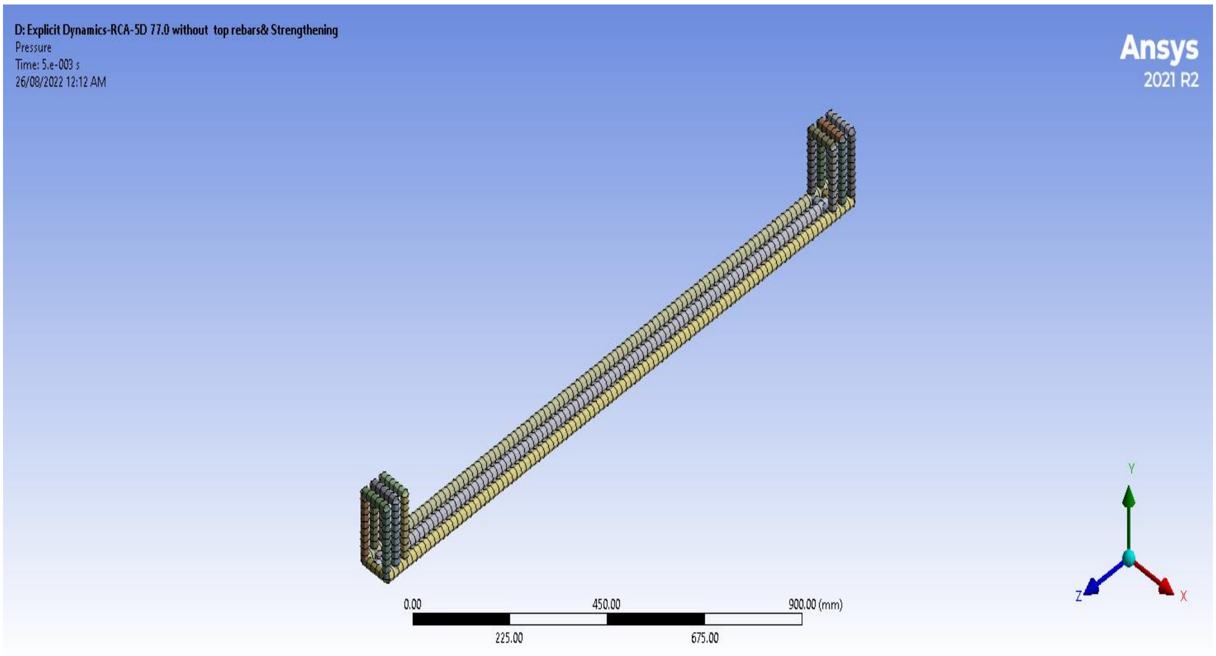

Figure 321(RCA-5D$_{Fibers}$-77.0MPa – Rebars of beam sample without strengthening- Explicit Dynamic Analysis)

Deformations

Total Deformations

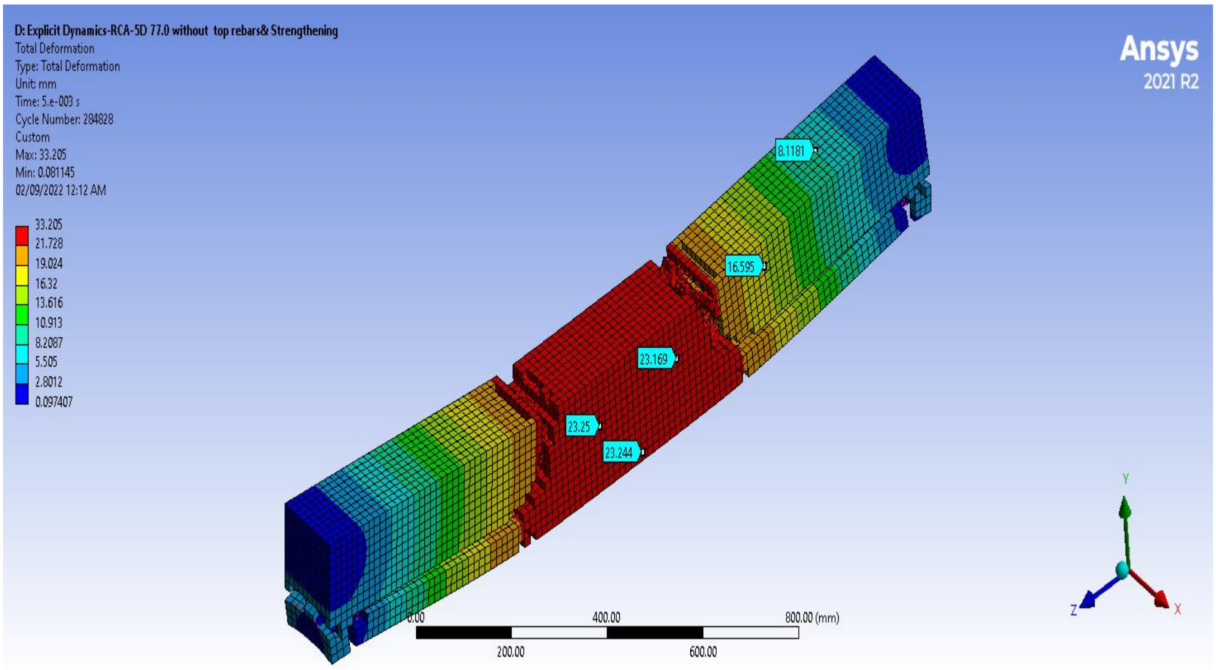

Figure 322(RCA-5D$_{Fibers}$-77.0MPa – Total deflections of beam sample without strengthening and top rebars- Explicit Dynamic Analysis)

The value is 23.25 mm.

Directional Deformation (Y-Direction)-Concrete

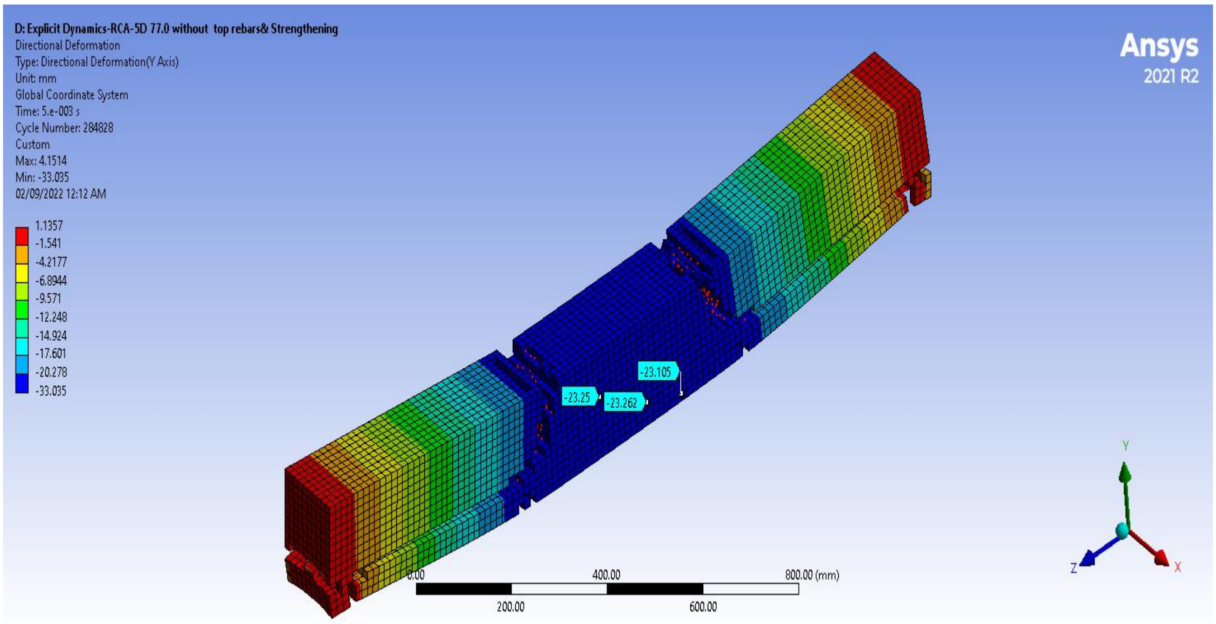

Figure 323(RCA-5D$_{Fibers}$-77.0MPa – Directional deflections (Y-Dim.) of beam sample without strengthening and top rebars- Explicit Dynamic Analysis)

The value is 23.262 mm.

Directional Deformation (Y-Direction)- Rebars

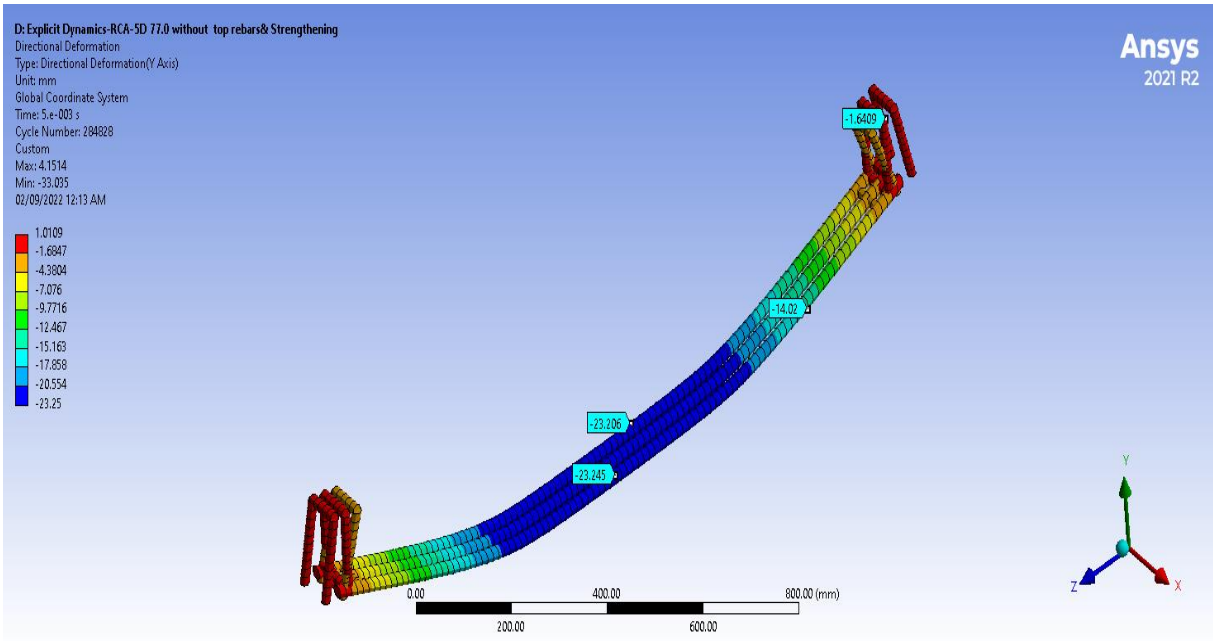

Figure 324(RCA-5D$_{Fibers}$-77.0MPa – Directional deflections (Rebars) of beam sample without strengthening- Explicit Dynamic Analysis)

Normal strain

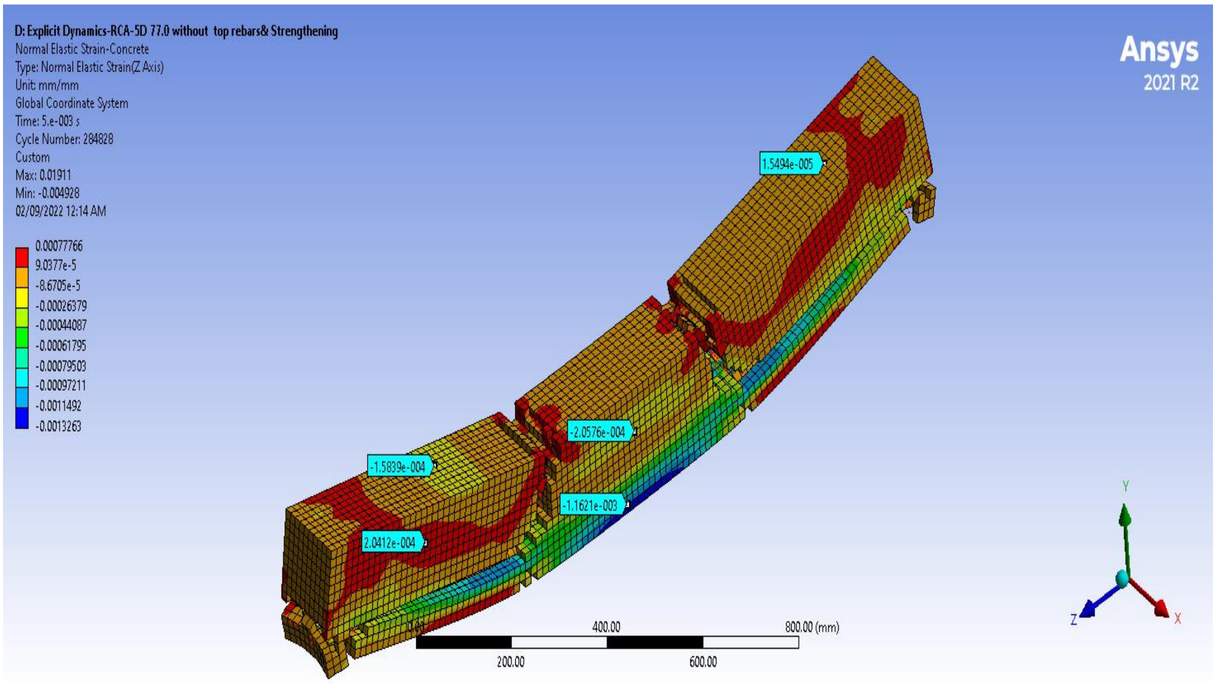

Figure 325(RCA-5D$_{Fibers}$-77.0MPa – Normal strain of beam sample without strengthening and top rebars- Explicit Dynamic Analysis)

Shear Stress

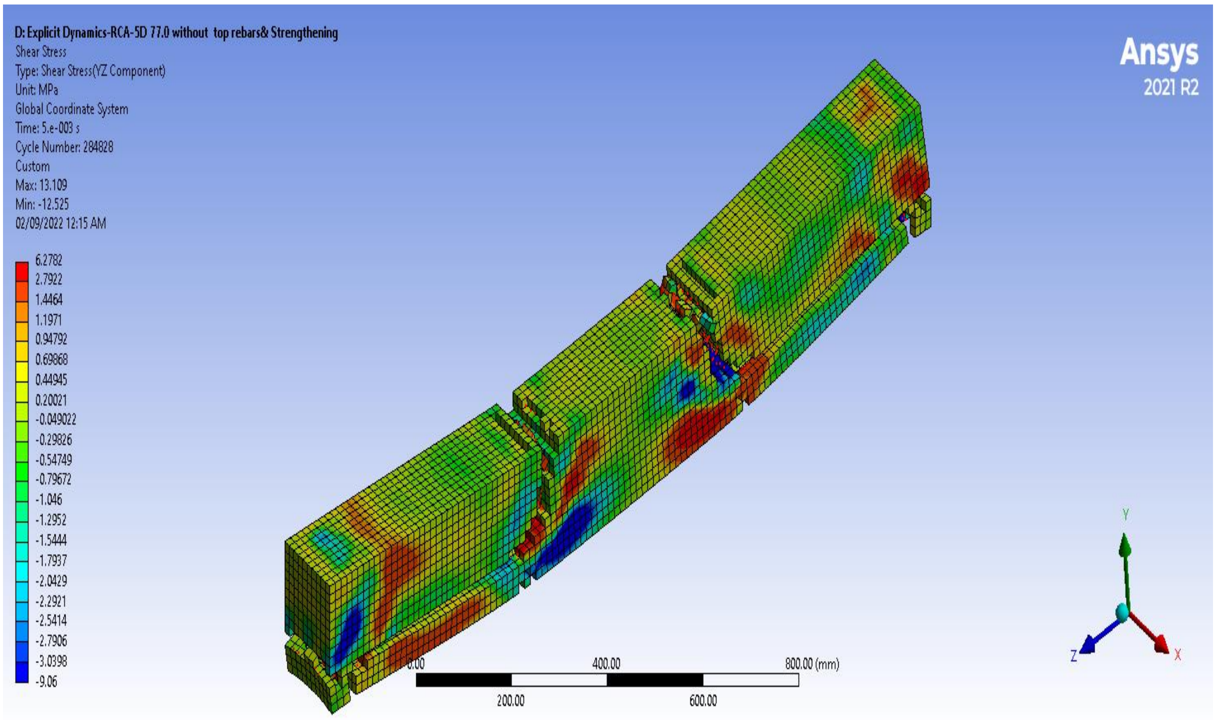

Figure 326(RCA-5D$_{Fibers}$-77.0MPa – Shear Stress of beam sample without strengthening and top rebars- Explicit Dynamic Analysis)

Total shape strain

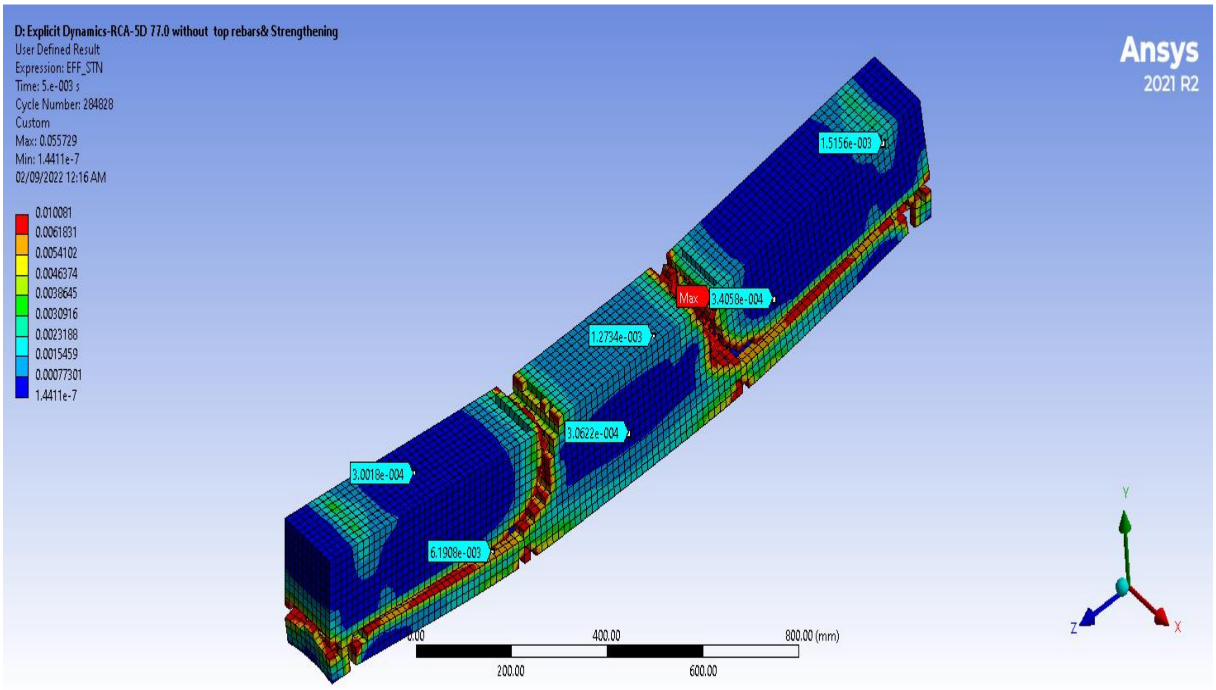

Figure 327(RCA-5D$_{Fibers}$-77.0MPa – Total strain of beam sample without strengthening and top rebars- Explicit Dynamic Analysis)

Maximum Stress

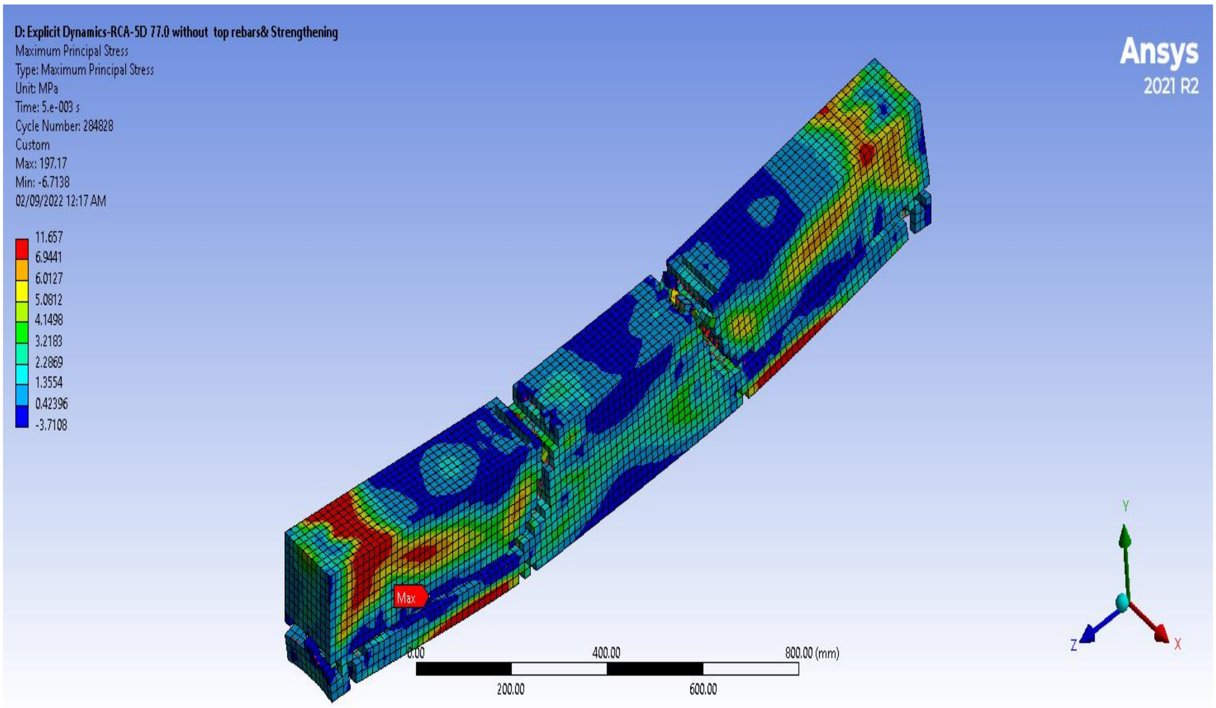

Figure 328(RCA-5D$_{Fibers}$-77.0MPa –Maximum Stress of beam sample without strengthening and top rebars- Explicit Dynamic Analysis)

The Damage Pattern

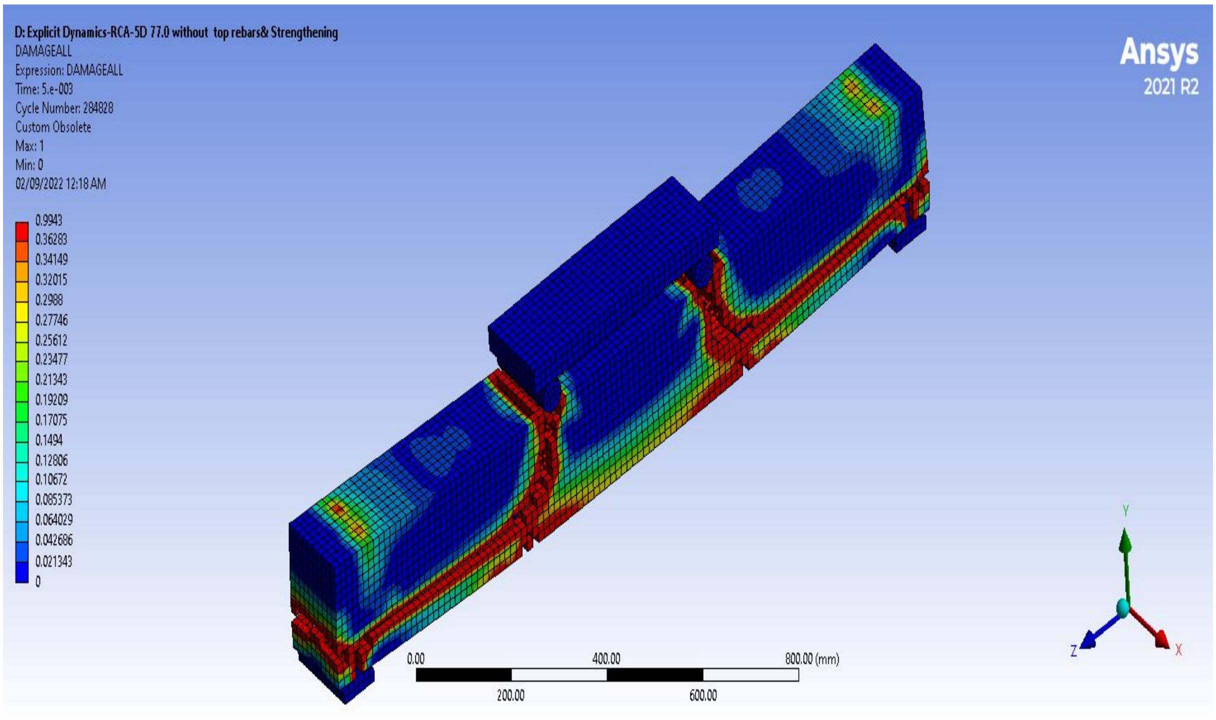

Figure 329(RCA-5DFibers-77.0MPa – Damage Pattern-1 of beam sample without strengthening and top rebars- Explicit Dynamic Analysis)

As we can see the shear damage cracks and concrete failures.

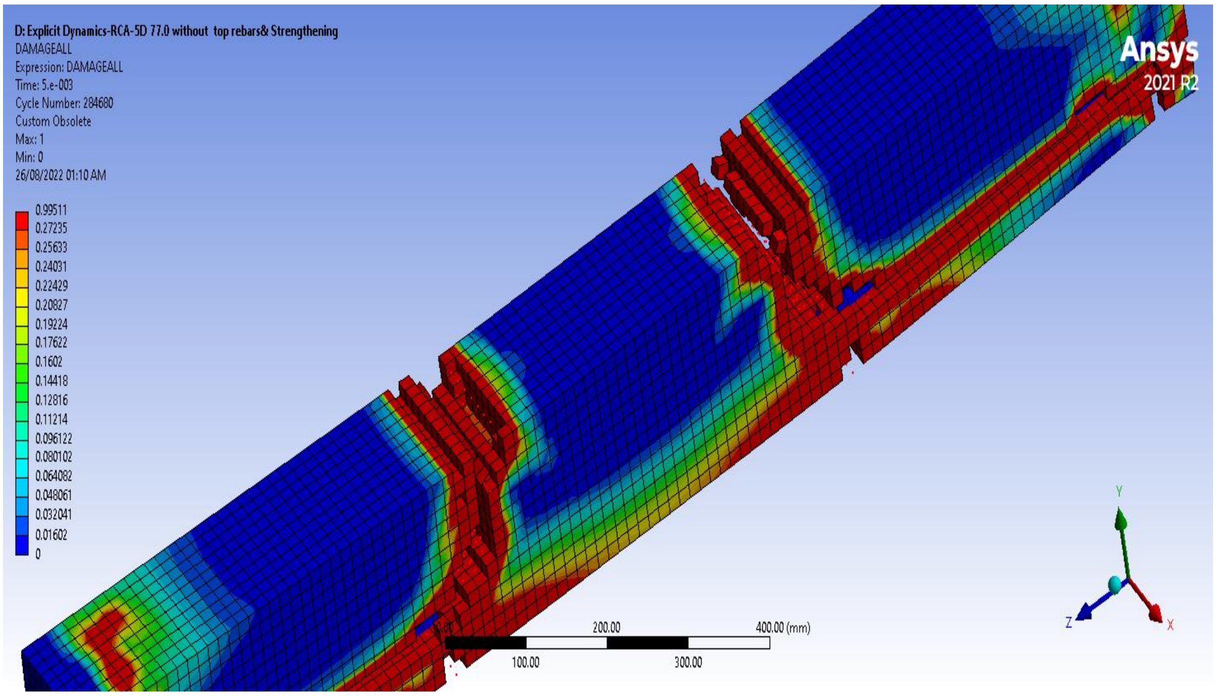

Figure 330(RCA-5DFibers-77.0MPa – Damage Pattern-2 of beam sample without strengthening and top rebars- Explicit Dynamic Analysis)

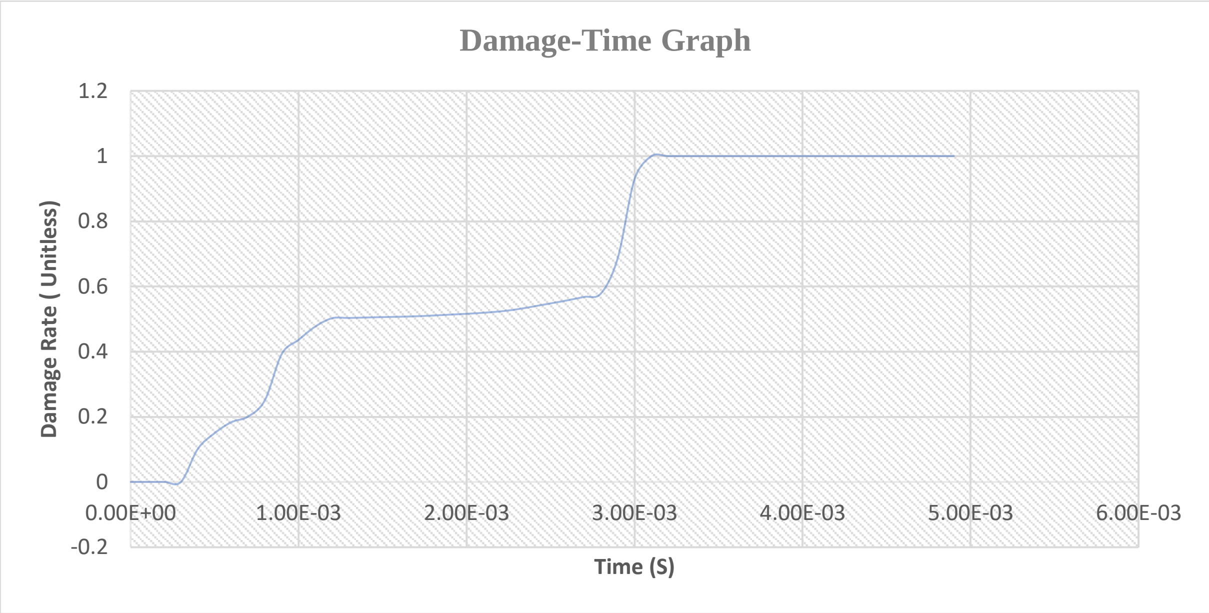

Figure 331(RCA-5D$_{Fibers}$-77.0MPa – Damage pattern graph of beam sample without strengthening and with top rebars-Explicit Dynamic Analysis)

22- Static Non-Linear Analysis – With Top Rebars and Strengthening

Geometry and loads

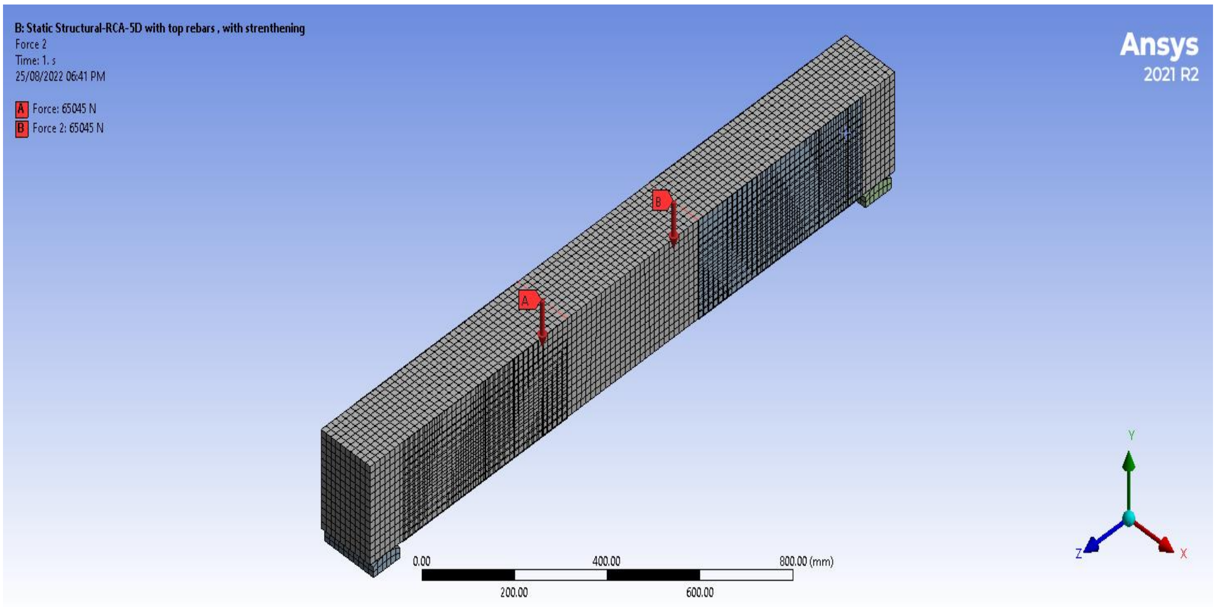

Figure 332(RCA-5D$_{Fibers}$-77.0MPa – Geometry & loads of beam sample with strengthening and top rebars- Static Nonlinear Analysis)

The ultimate load has been divided in to loads which is 130.09/2 =65.045KN.

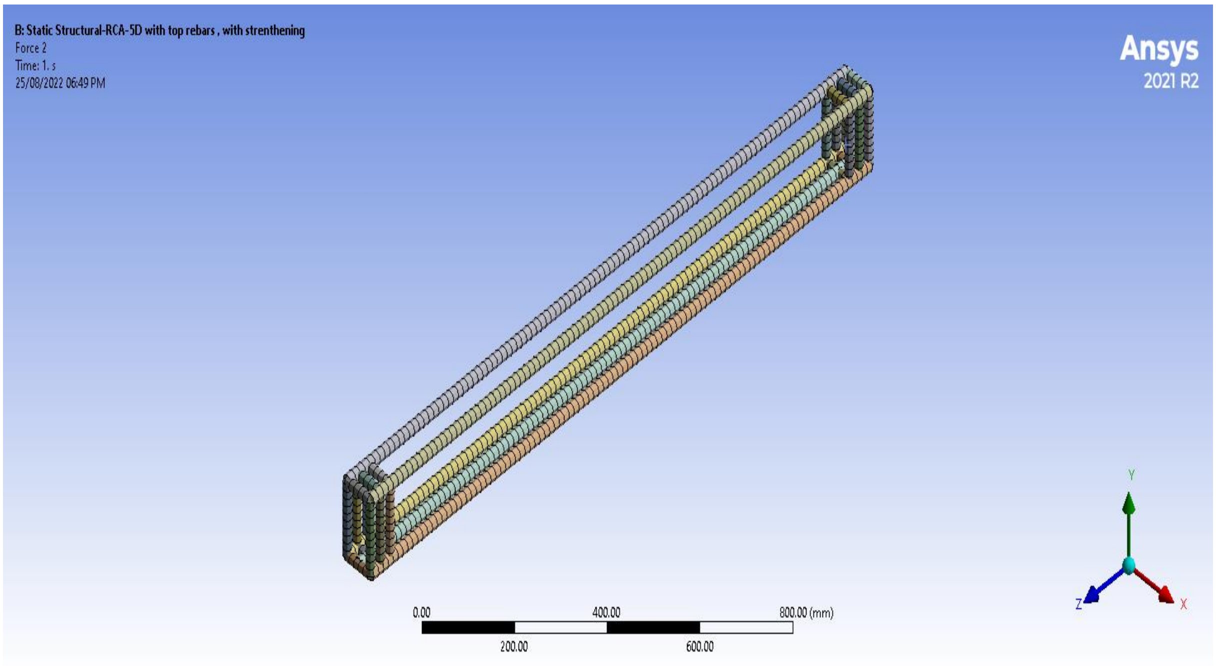

Figure 333(RCA-5D$_{Fibers}$-77.0MPa –Rebars of beam sample with strengthening- Static Nonlinear Analysis)

Deformations

Total Deformations

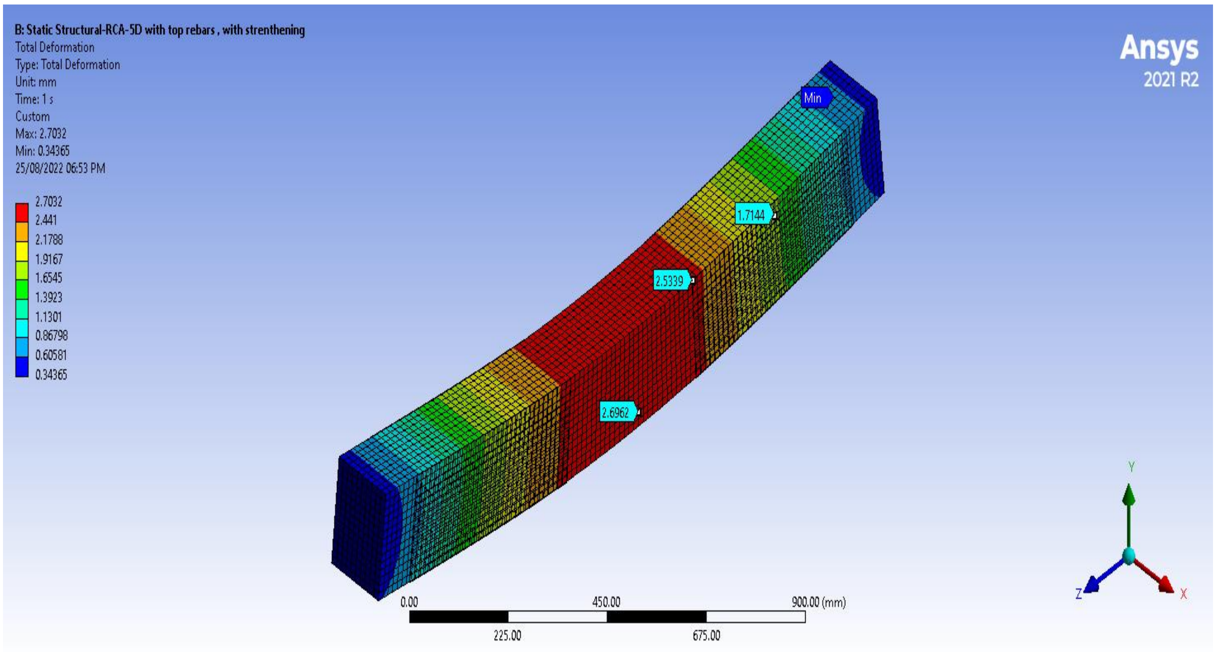

Figure 334(RCA-5D$_{Fibers}$-77.0MPa – Total deflections of beam sample with strengthening and top rebars- Static Nonlinear Analysis)

The value is 2.703 mm.

Directional Deformation (Y-Direction)

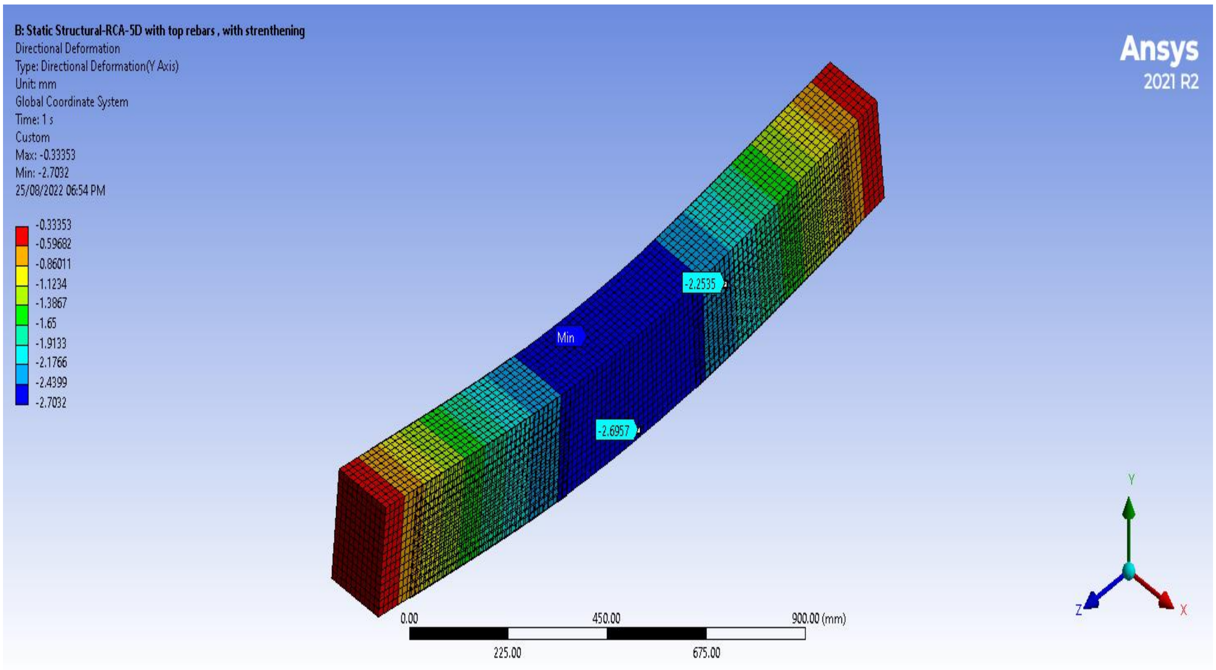

Figure 335(RCA-5DFibers-77.0MPa – Directional deflections (Y-Dim.) of beam sample with strengthening and top rebars- Static Nonlinear Analysis)

The value is 2.703 mm.

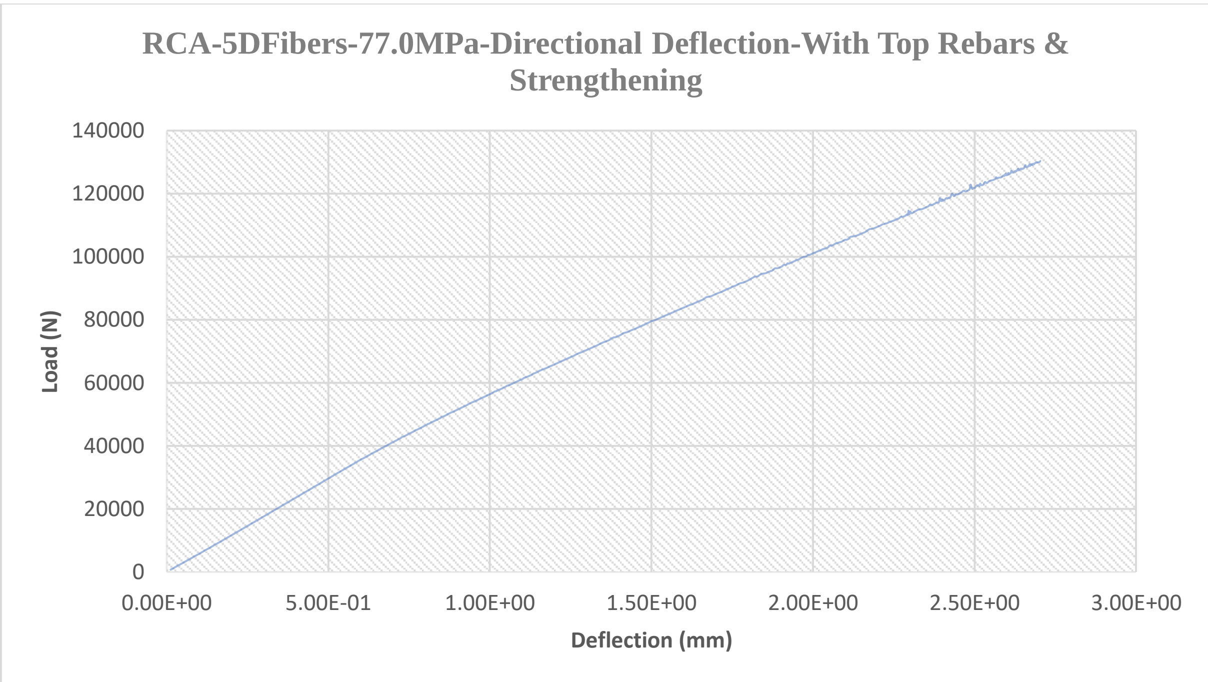

Figure 336(RCA-5D$_{Fibers}$-77.0MPa – Directional deflections (Y-Dim.) graph of beam sample with strengthening and top rebars- Static Nonlinear Analysis)

Normal Stress (Concrete)

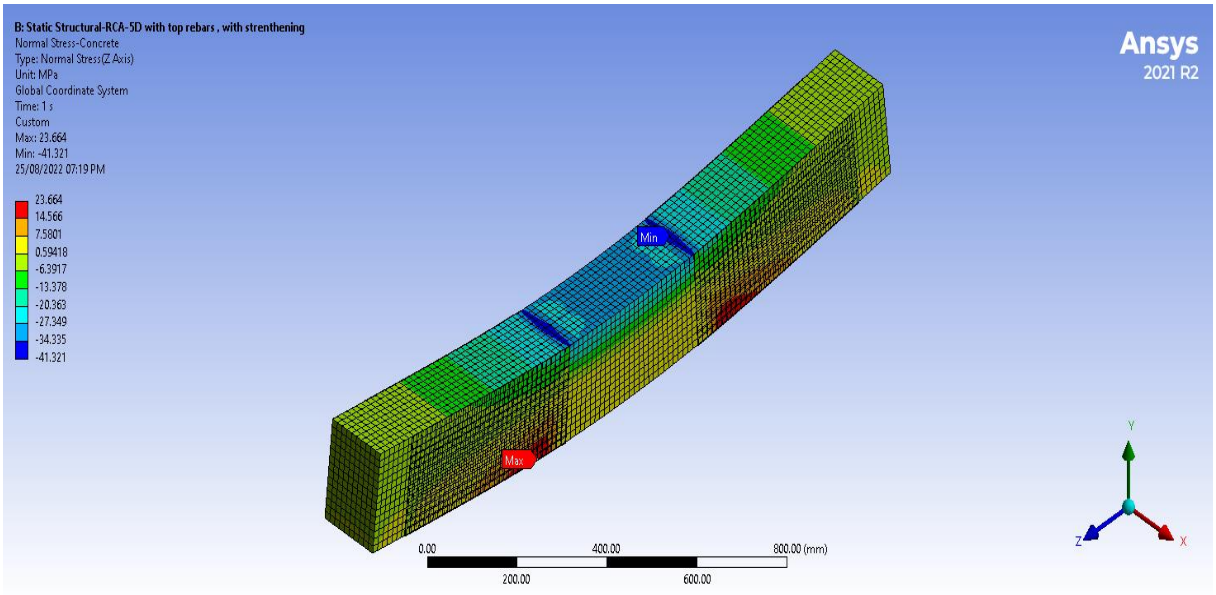

Figure 337(RCA-5D$_{Fibers}$-77.0MPa – Normal Stress (Concrete) of beam sample with strengthening and top rebars- Static Nonlinear Analysis)

The blue zones show the crushing from loading machine and the maximum value is 41.321 MPa, whereas the red zones indicate to tension.

Normal Stress (Rebars)

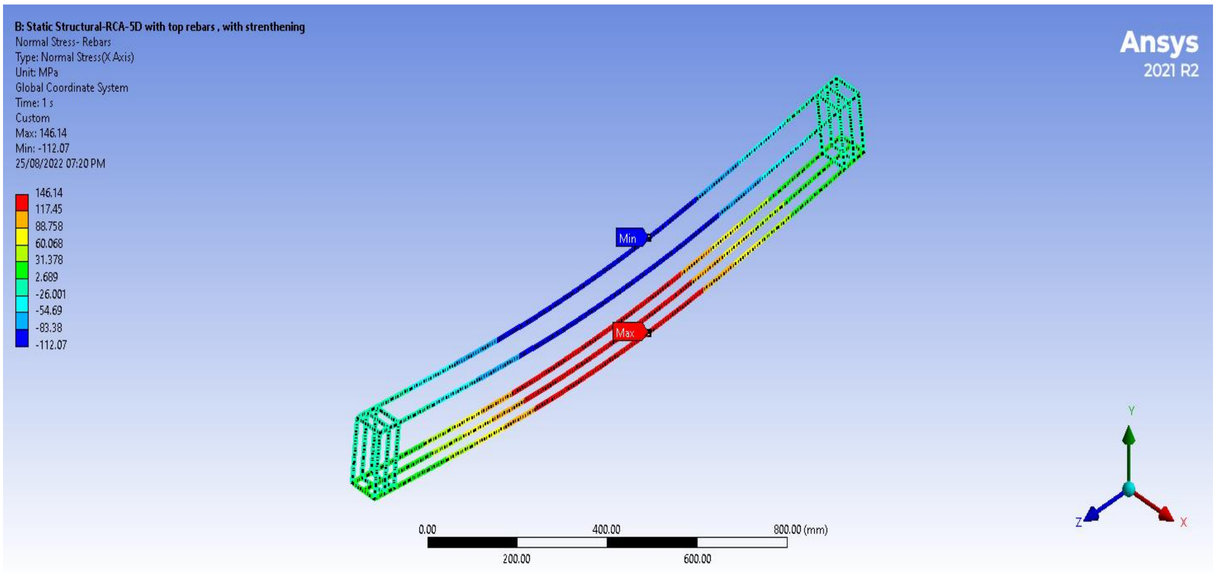

Figure 338(RCA-5D$_{Fibers}$-77.0MPa – Normal Stress (Rebars) of beam sample with strengthening and top rebars- Static Nonlinear Analysis)

The red zones show that the rebars is yielding by 146.14MPa, in the middle span due to tension.

Shear Stress

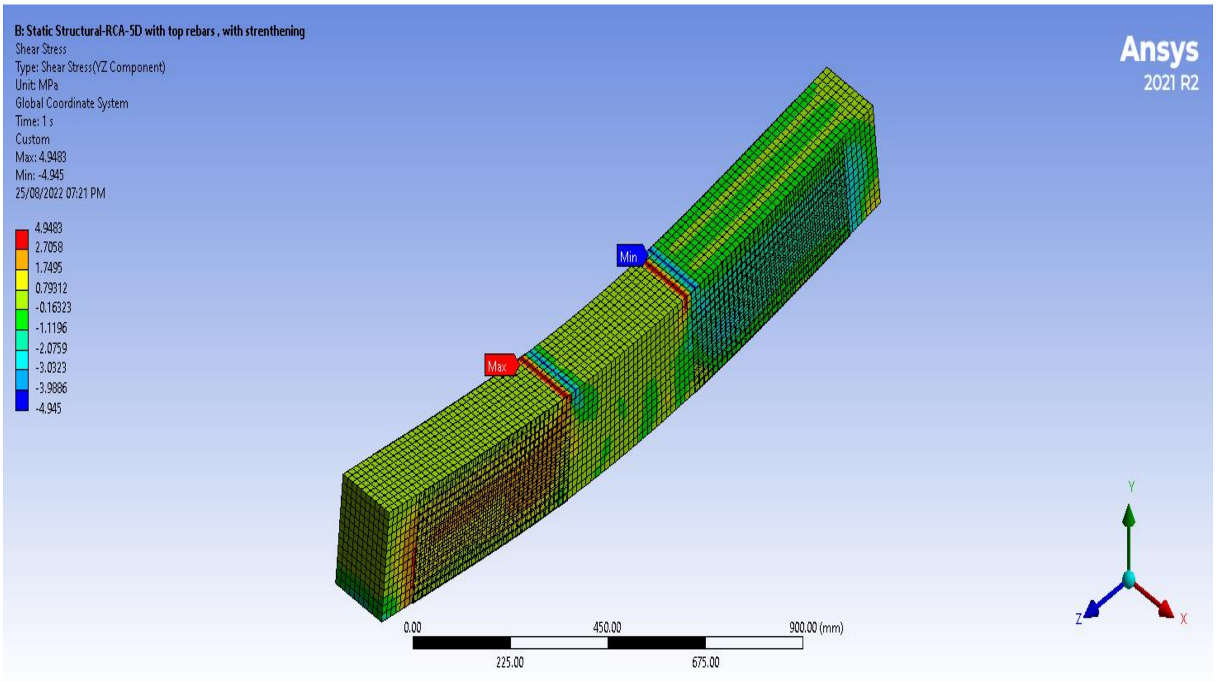

Figure 339(RCA-5D$_{Fibers}$-77.0MPa – Shear Stress of beam sample with strengthening and top rebars- Static Nonlinear Analysis)

Elastic Strain

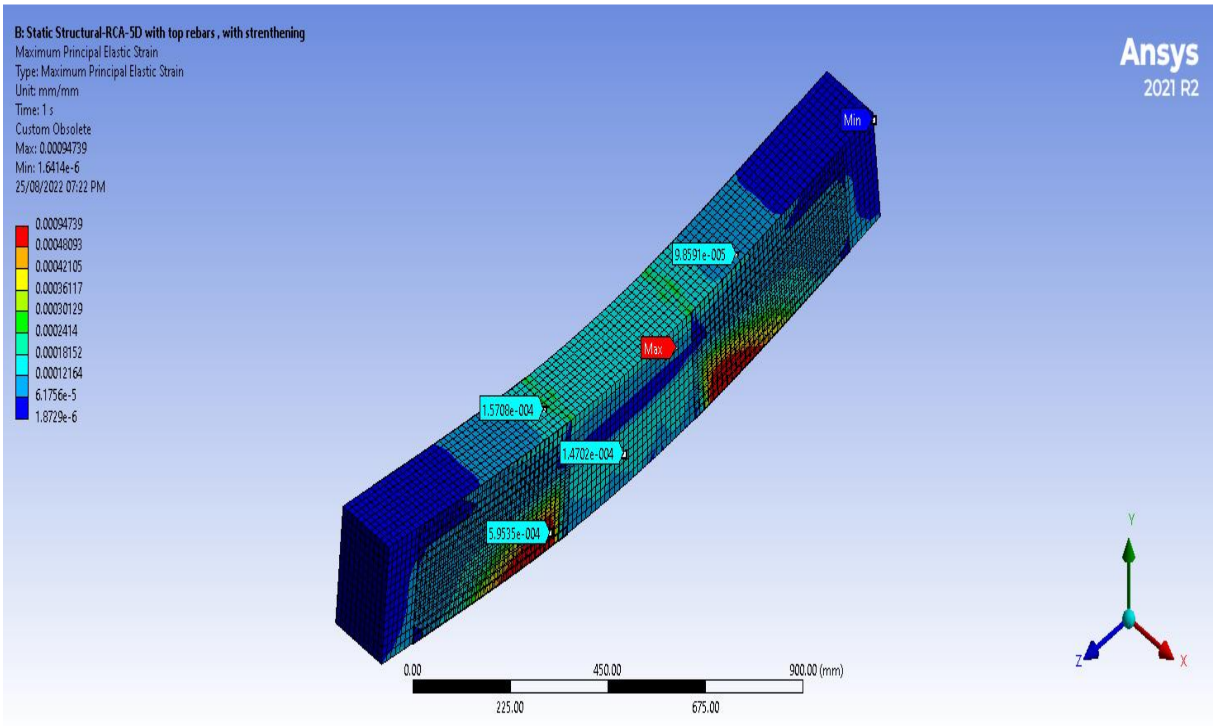

Figure 340(RCA-5D$_{Fibers}$-77.0MPa – Elastic strain of beam sample with strengthening and top rebars- Static Nonlinear Analysis)

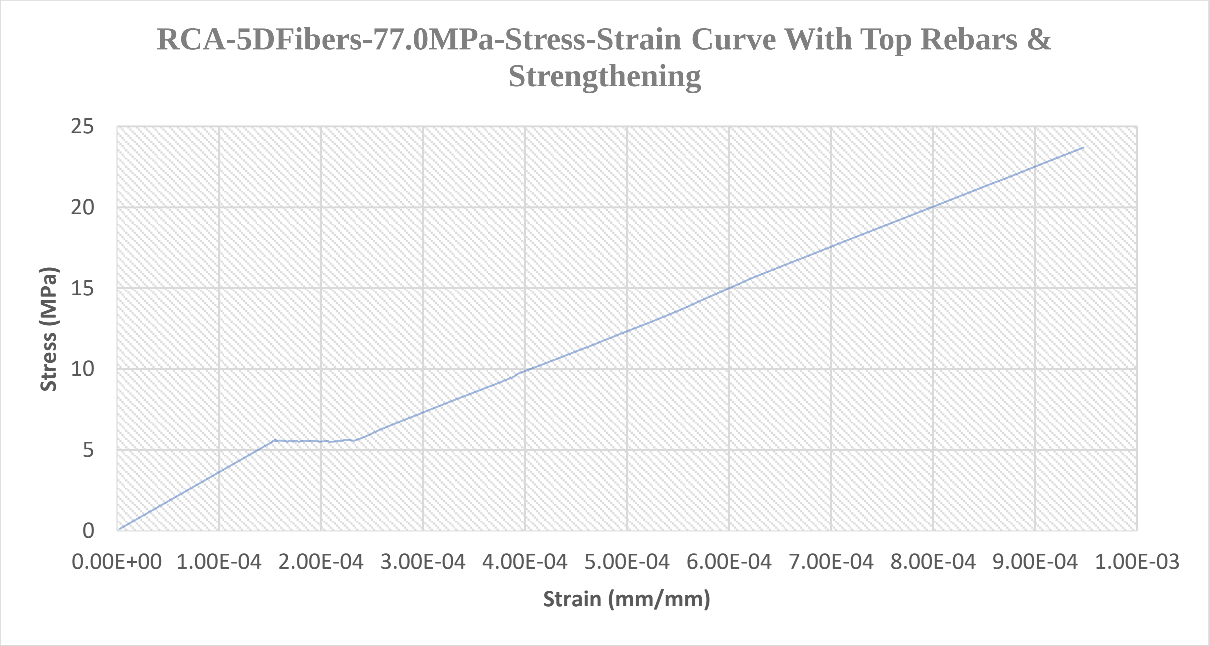

Figure 341(RCA-5D$_{Fibers}$-77.0MPa – Stress & Strain graph of beam sample with strengthening and top rebars- Static Nonlinear Analysis)

23- Explicit Dynamic-With Top Rebars & Strengthening

Geometry and loads

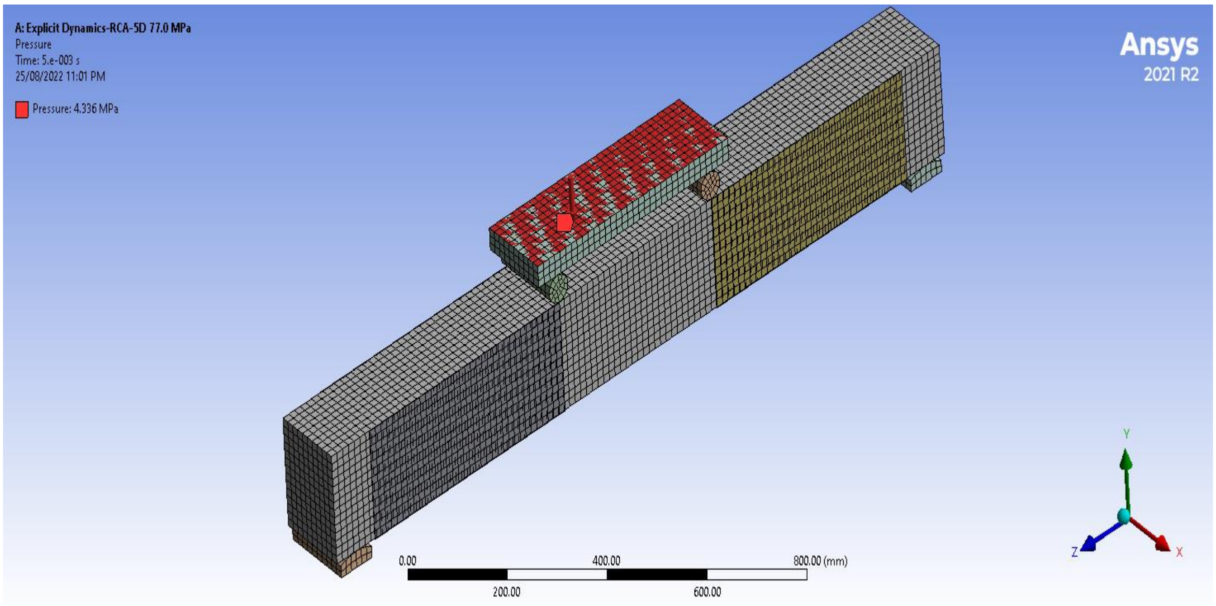

Figure 342(RCA-5D$_{Fibers}$-77.0MPa – Geometry & loads of beam sample with strengthening and top rebars- Explicit Dynamic Analysis)

The ultimate load has been transferred to be as a pressure load which is 4.336 MPa as shown above with rate loading 0.6mm/min

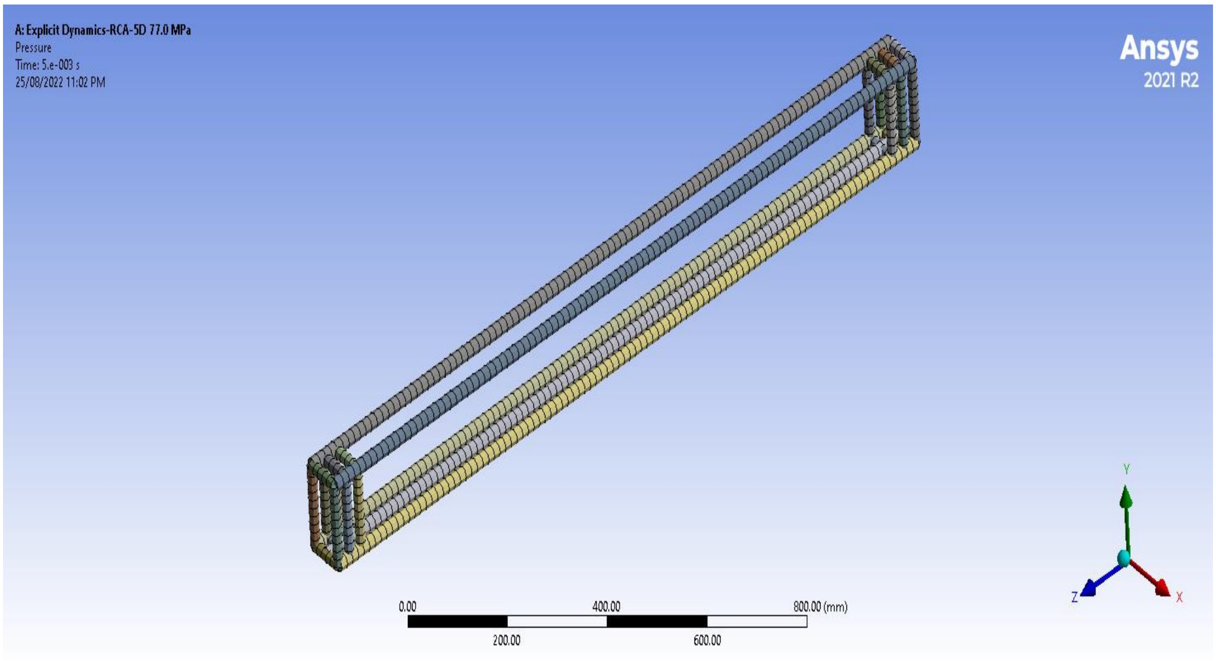

Figure 343(RCA-5D$_{Fibers}$-77.0MPa – Rebars of beam sample with strengthening – Explicit Dynamic Analysis)

Deformations

Total Deformations

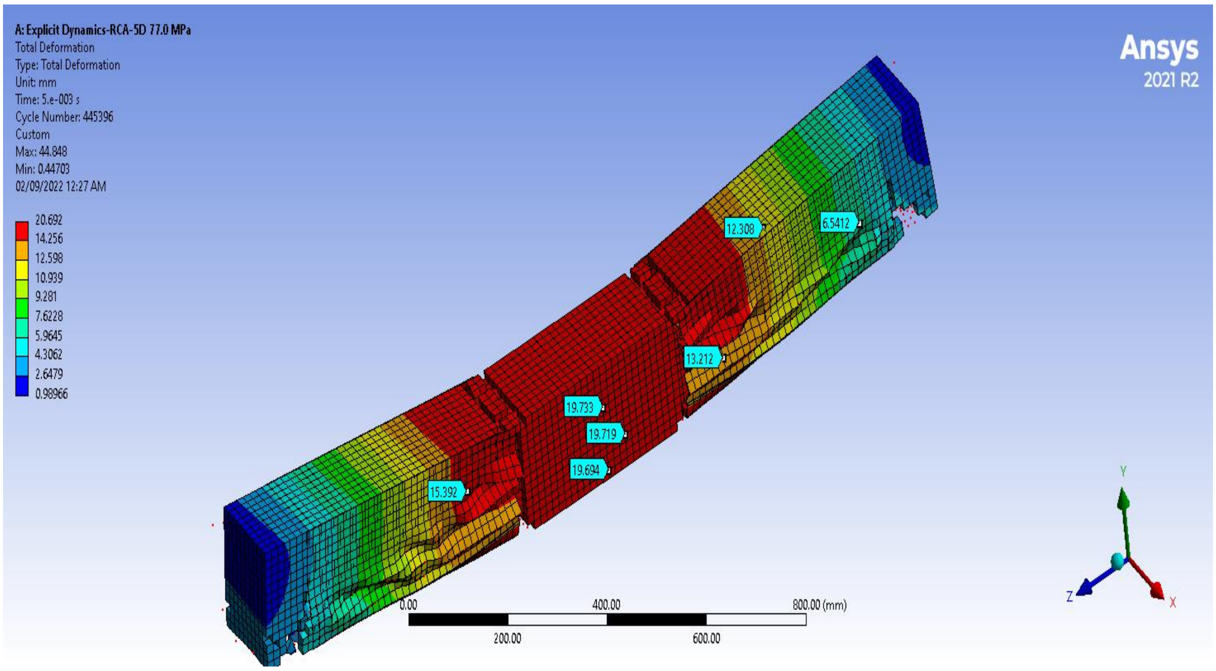

Figure 344(RCA-5D$_{Fibers}$-77.0MPa – Total deflections of beam sample with strengthening and top rebars- Explicit Dynamic Analysis)

The value is 19.733 mm.

Directional Deformation (Y-Direction)-Concrete

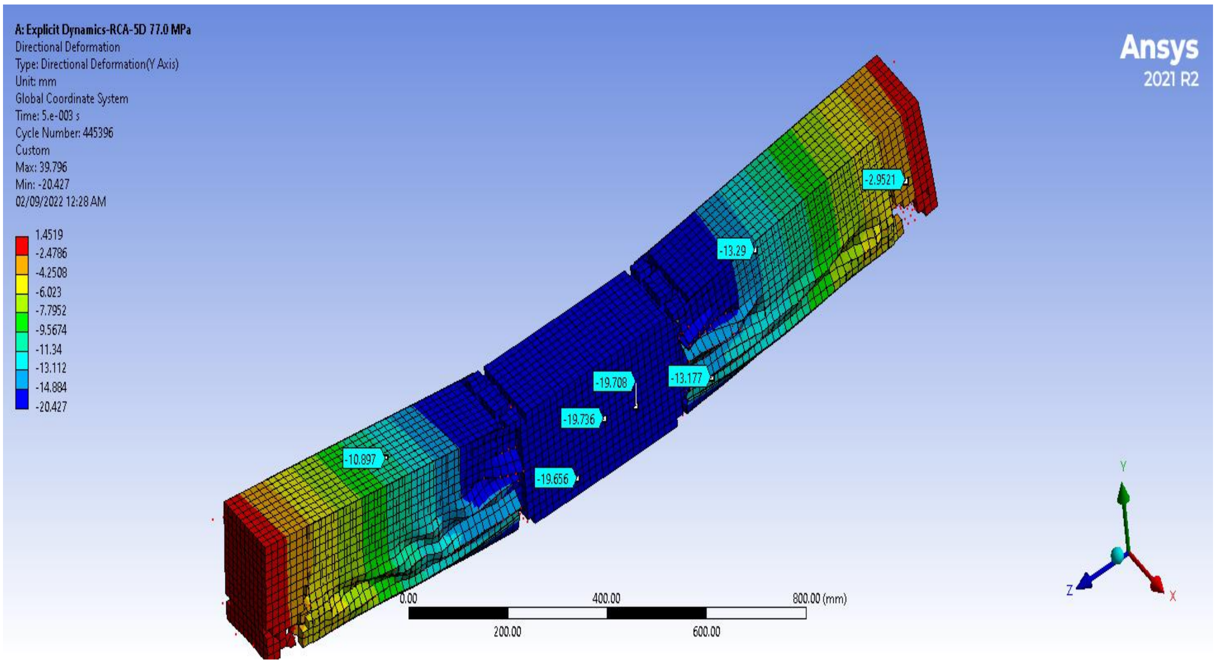

Figure 345(RCA-5D$_{Fibers}$-77.0MPa – Directional deflection (Y-Dim.) of beam sample with strengthening and top rebars- Explicit Dynamic Analysis)

The value is 19.736 mm

Directional Deformation (Y-Direction)- Rebars

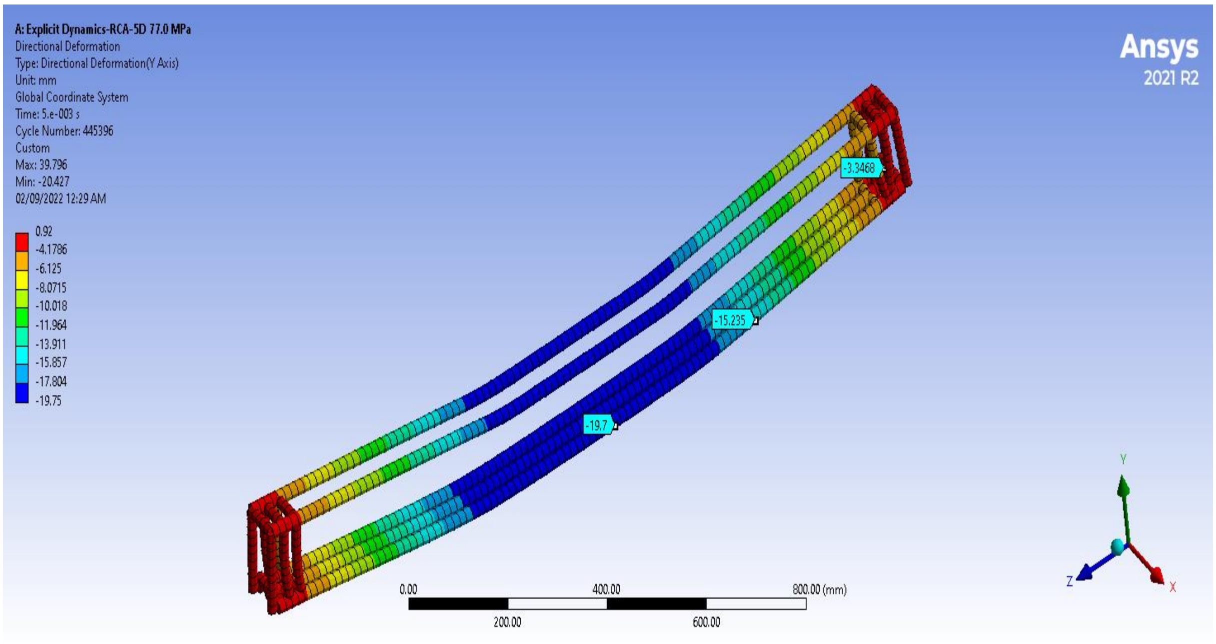

Figure 346(RCA-5D$_{Fibers}$-77.0MPa –Directional deflection (Y-Dim.) Rebars of beam sample with strengthening - Explicit Dynamic Analysis)

Normal strain

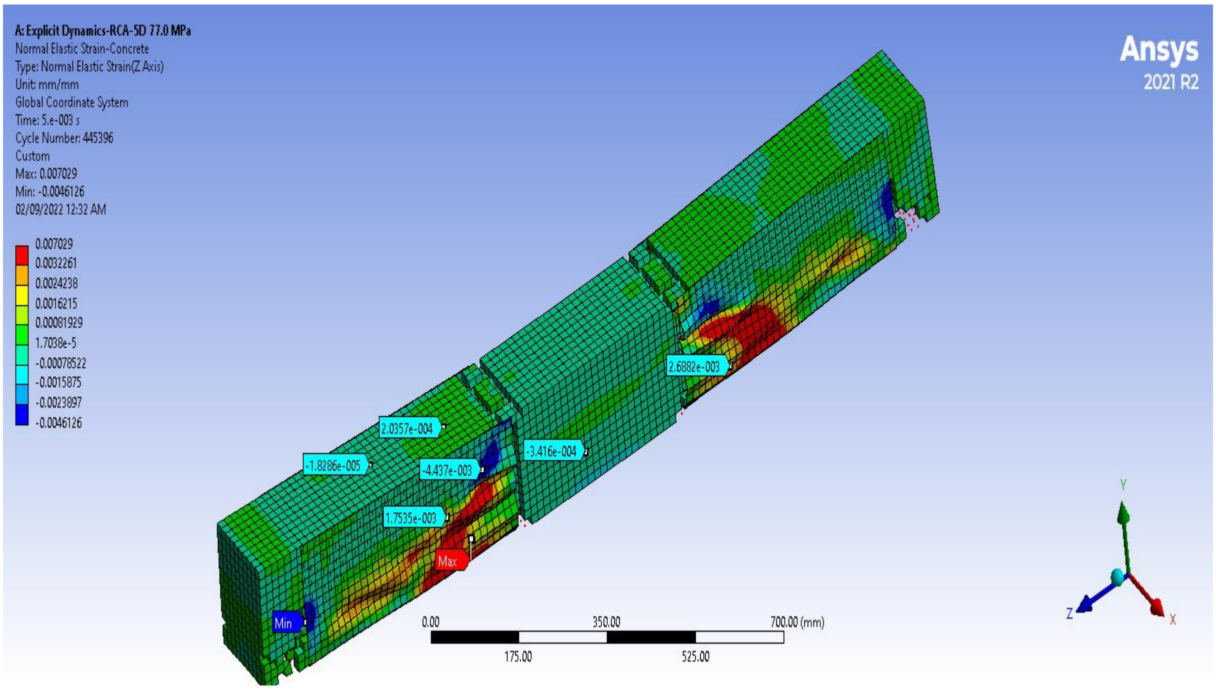

Figure 347(RCA-5D$_{Fibers}$-77.0MPa –Normal strain of beam sample with strengthening and top rebars- Explicit Dynamic Analysis)

Shear Stress

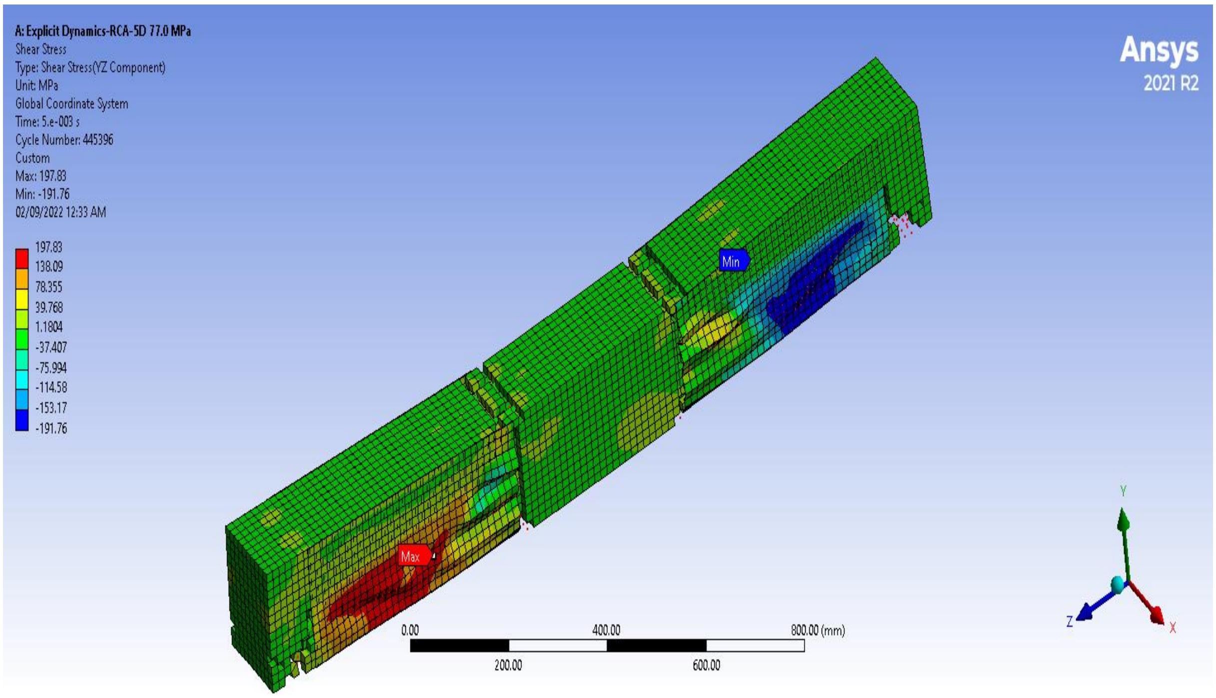

Figure 348(RCA-5D$_{Fibers}$-77.0MPa – Shear stress of beam sample with strengthening and top rebars- Explicit Dynamic Analysis)

Total shape strain

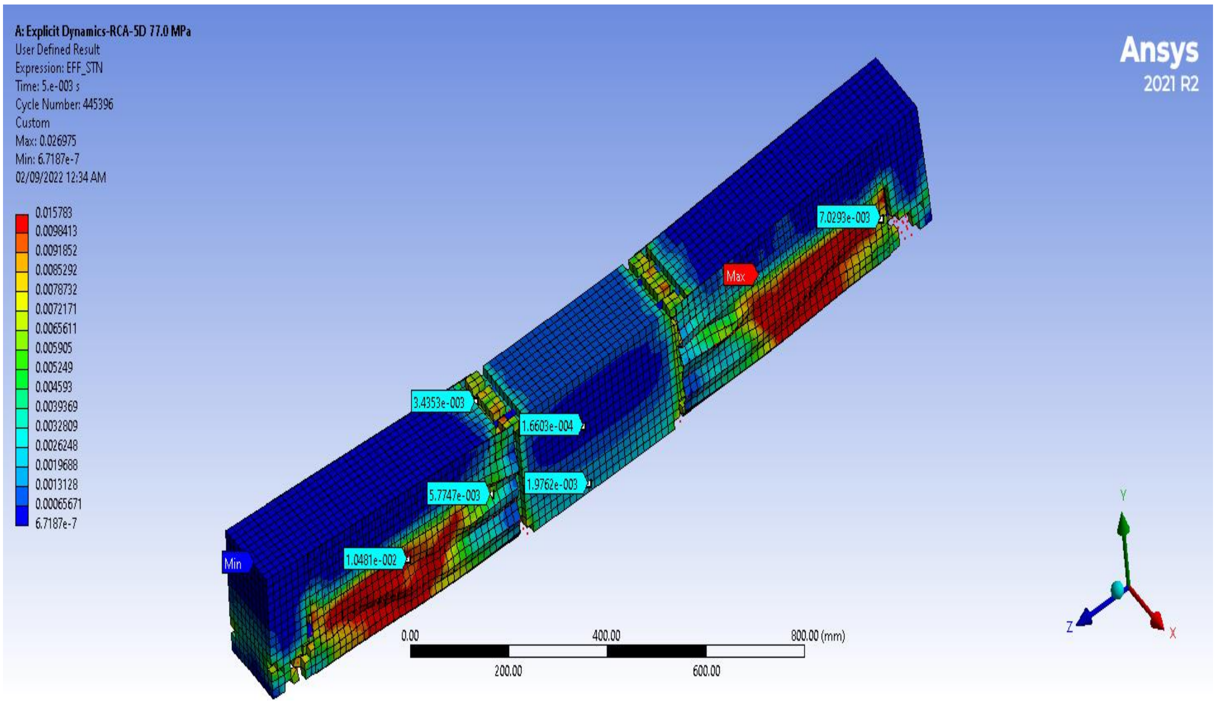

Figure 349(RCA-5DFibers-77.0MPa – Total strain of beam sample with strengthening and top rebars- Explicit Dynamic Analysis)

Maximum Stress

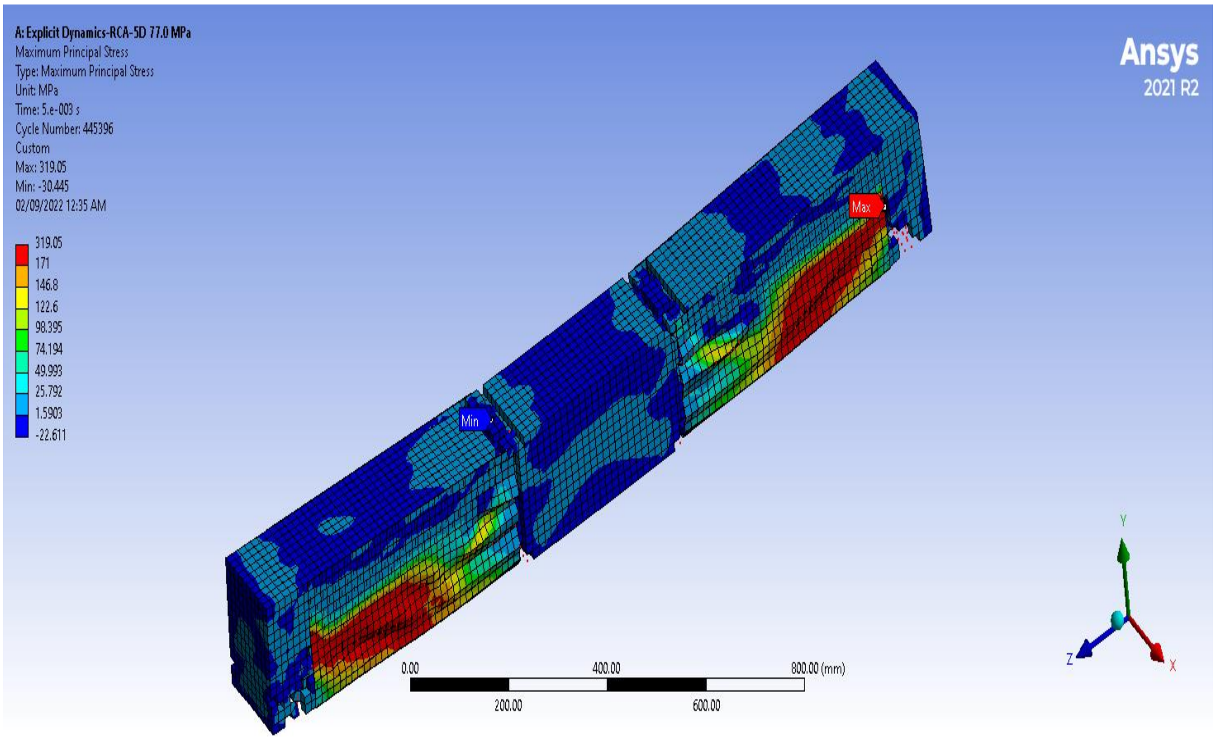

Figure 350(RCA-5DFibers-77.0MPa – Maximum stress of beam sample with strengthening and top rebars- Explicit Dynamic Analysis)

The Damage Pattern

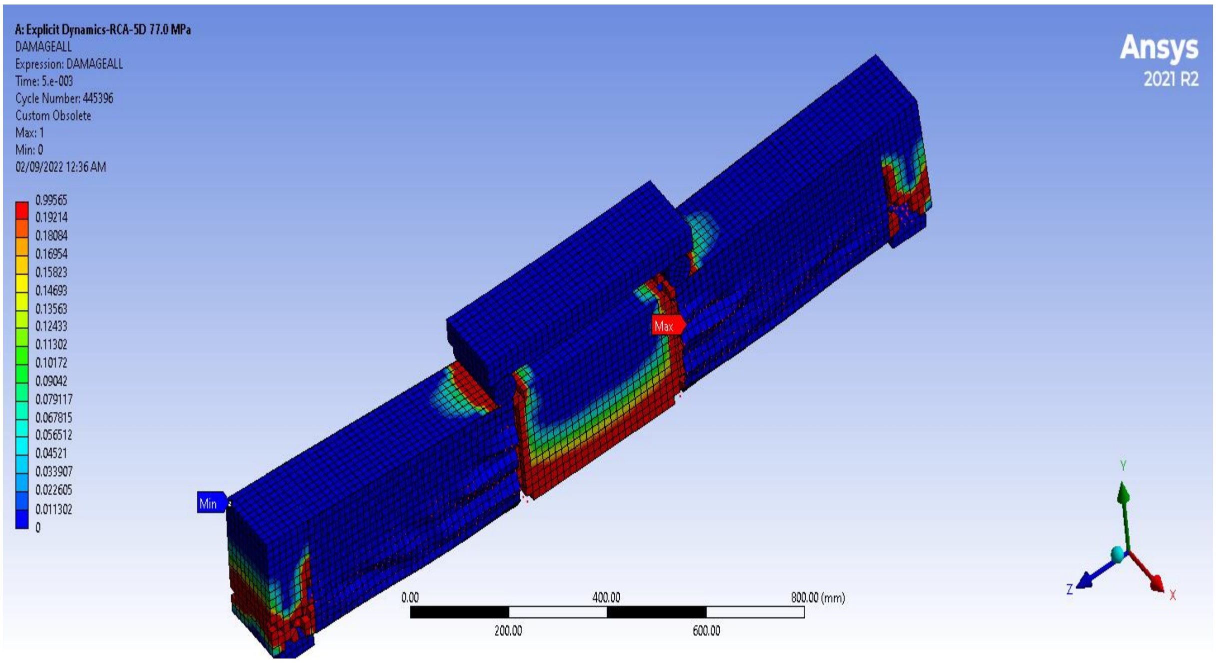

Figure 351(RCA-5D$_{Fibers}$-77.0MPa – Damage pattern-1 of beam sample with strengthening and top rebars- Explicit Dynamic Analysis)

As we can see the shear damage cracks in red and CFRP debonding on edges of concrete failure.

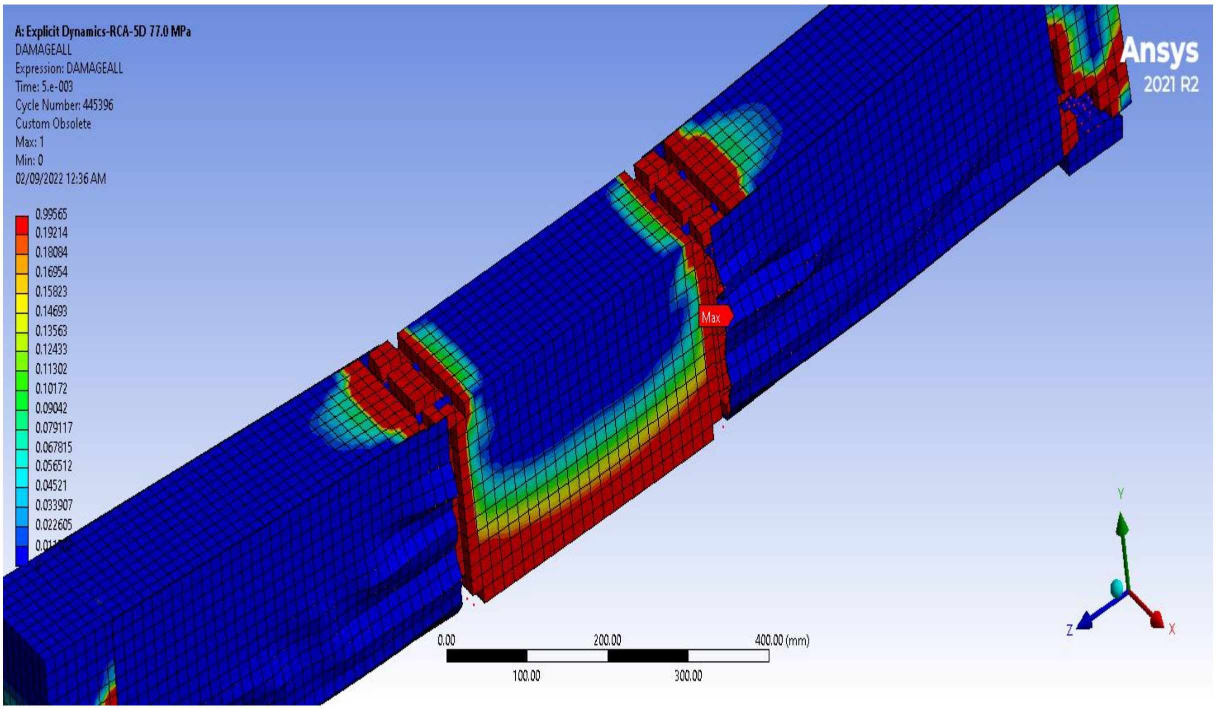

Figure 352(RCA-5D$_{Fibers}$-77.0MPa – Damage pattern-2 of beam sample with strengthening and top rebars- Explicit Dynamic Analysis)

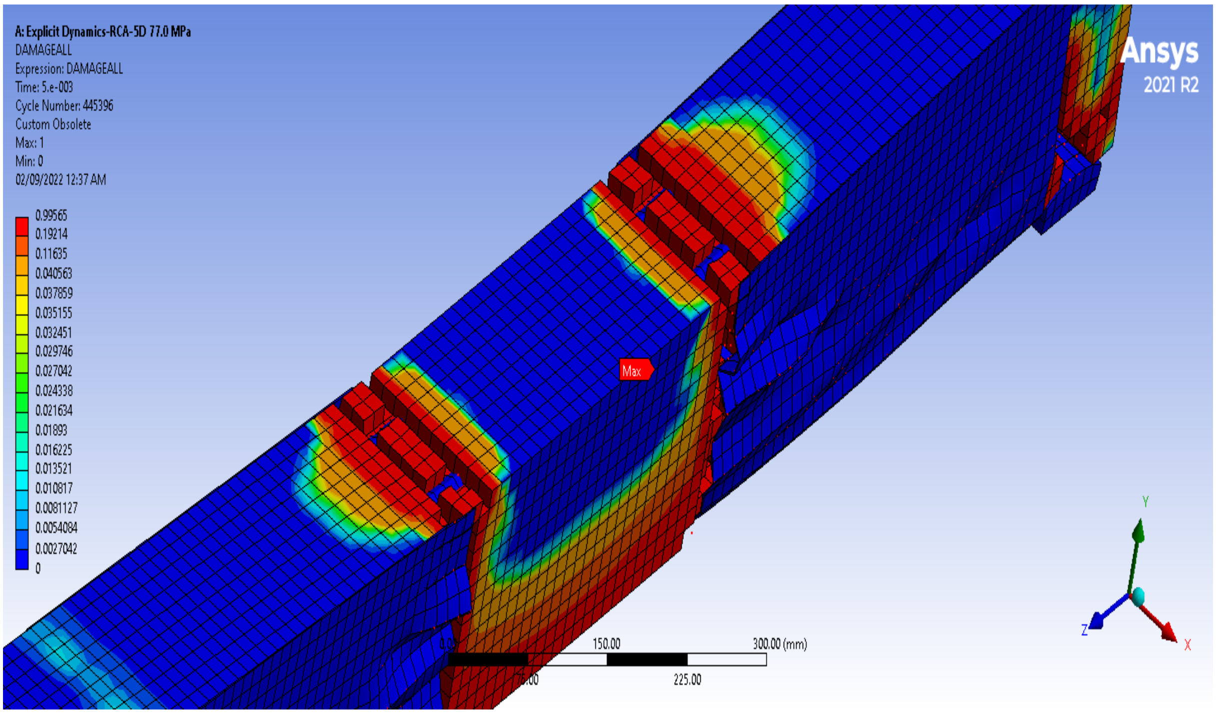

Figure 353(RCA-5D$_{Fibers}$-77.0MPa – Damage pattern-3 of beam sample with strengthening and top rebars- Explicit Dynamic Analysis)

CFRP laminates due to ultimate load has been debonding as shown in images above

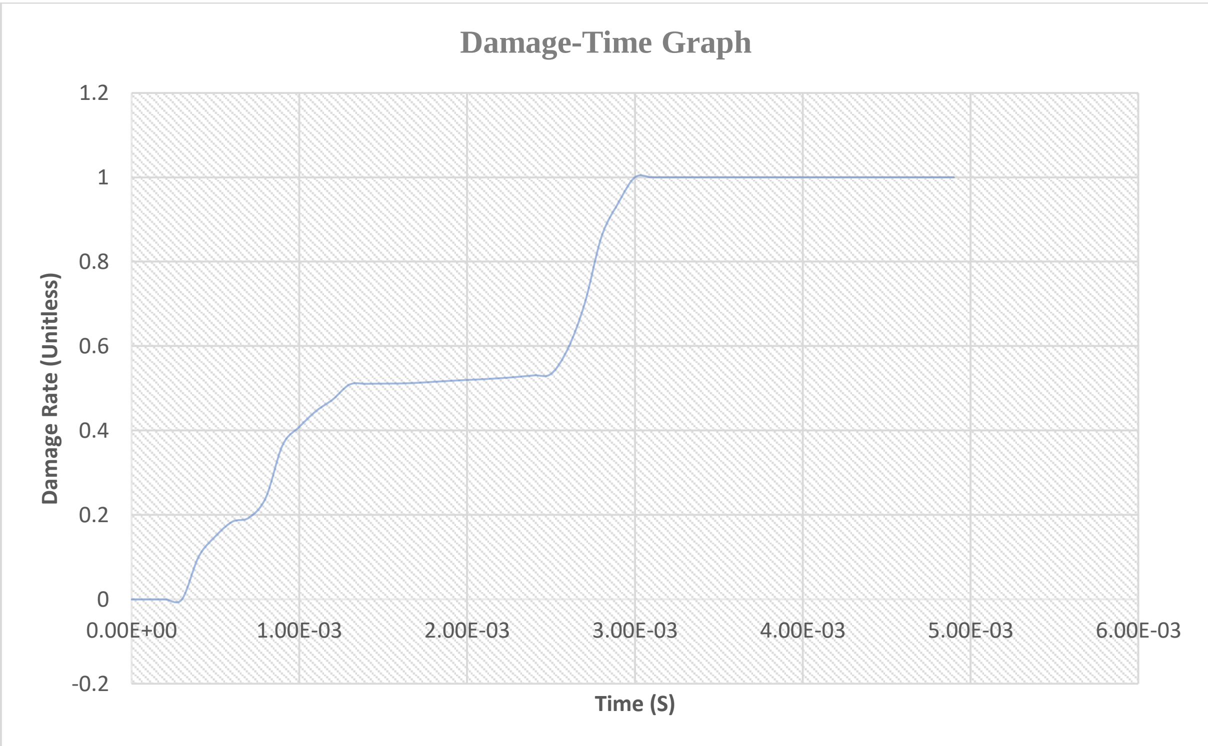

Figure 354(RCA-5D$_{Fibers}$-77.0MPa – Damage pattern graph of beam sample with strengthening and top rebars- Explicit Dynamic Analysis)

24- Static Non-Linear Analysis – Without Top Rebars and With Strengthening

Geometry and loads

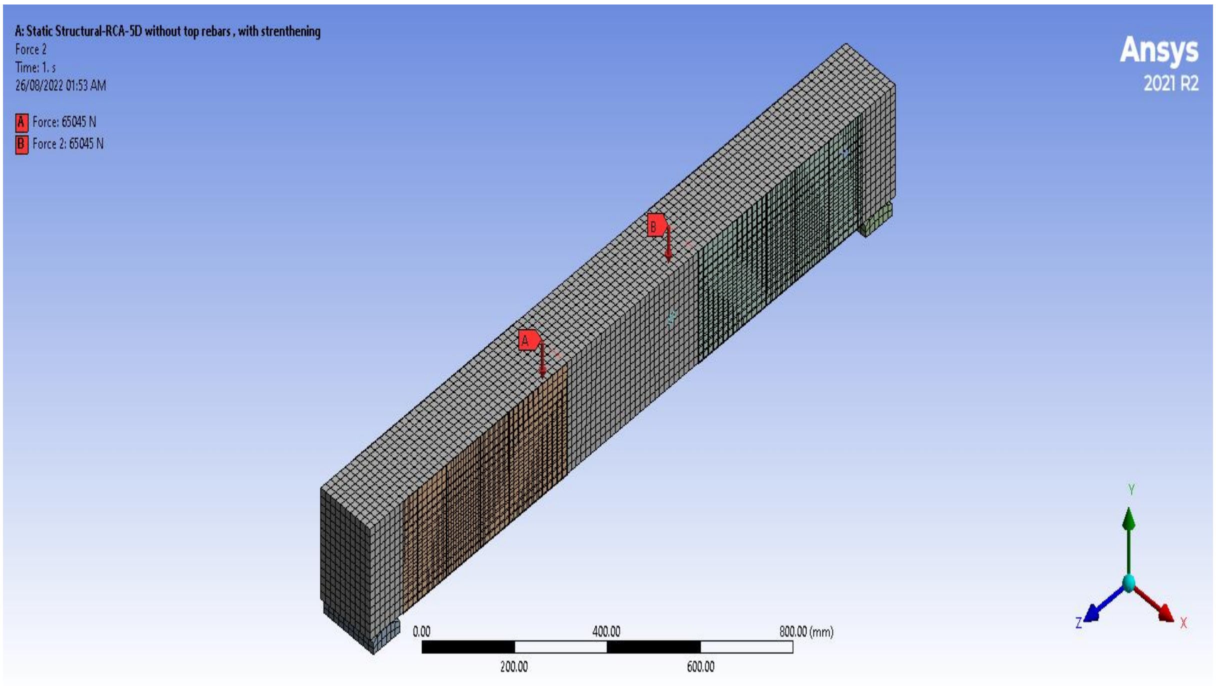

Figure 355(RCA-5D$_{Fibers}$-77.0MPa – Geometry & Loads of beam sample with strengthening and without top rebars- Static Nonlinear Analysis)

The ultimate load has been divided in to loads which is 130.09/2 =65.045KN.

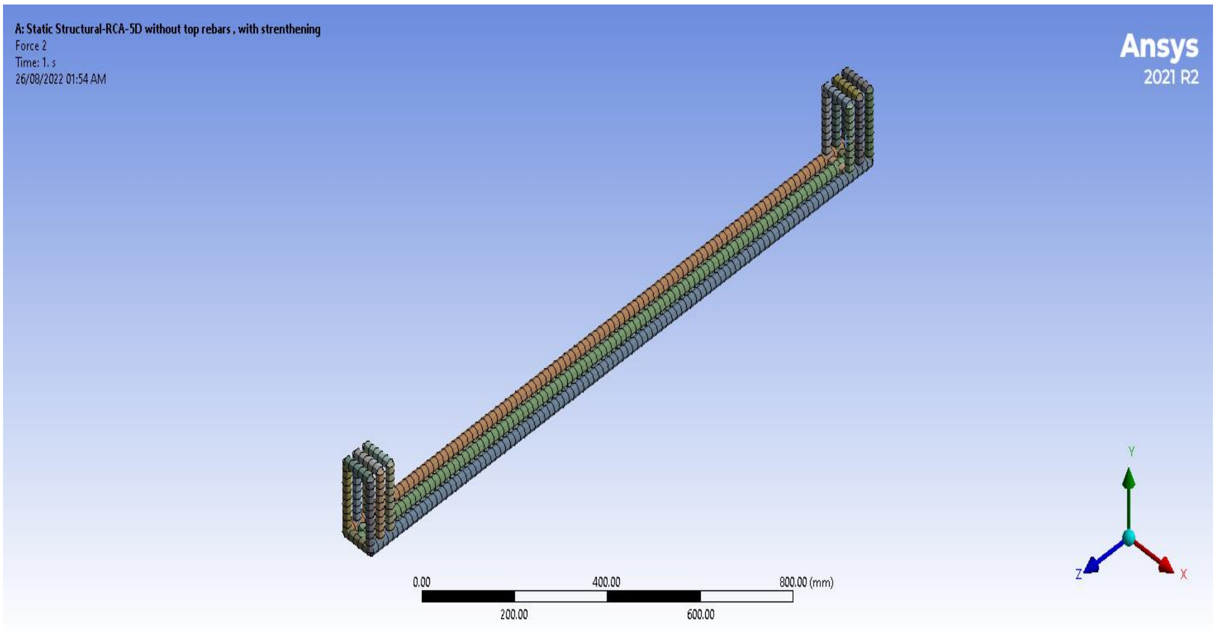

Figure 356(RCA-5D$_{Fibers}$-77.0MPa – Rebars of beam sample without strengthening - Static Nonlinear Analysis)

Deformations

Total Deformations

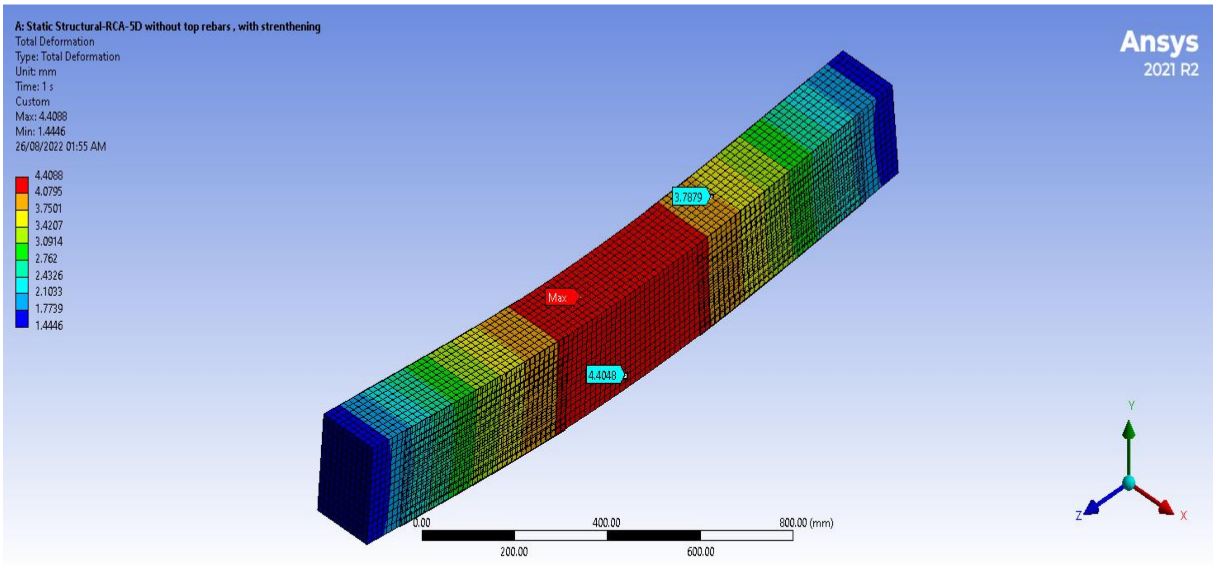

Figure 357(RCA-5D$_{Fibers}$-77.0MPa – Total deflections of beam sample with strengthening and without top rebars- Static Nonlinear Analysis)

The value is 4.4088 mm.

Directional Deformation (Y-Direction)

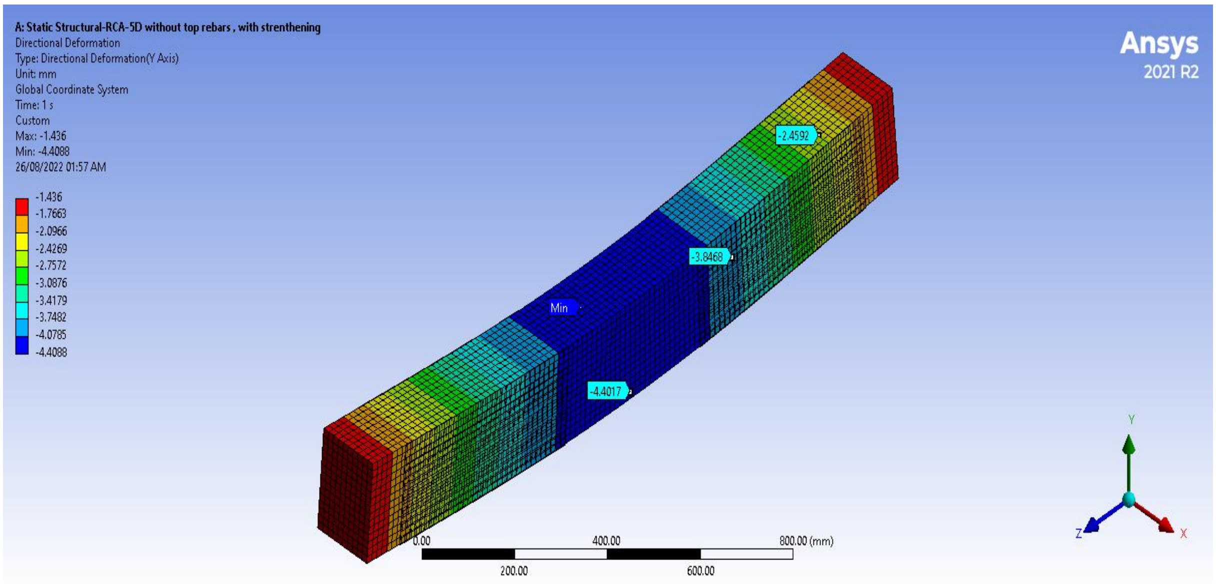

Figure 358(RCA-5D$_{Fibers}$-77.0MPa – Directional deflections (Y-Dim.) of beam sample with strengthening and without top rebars- Static Nonlinear Analysis)

The value is 4.4088 mm.

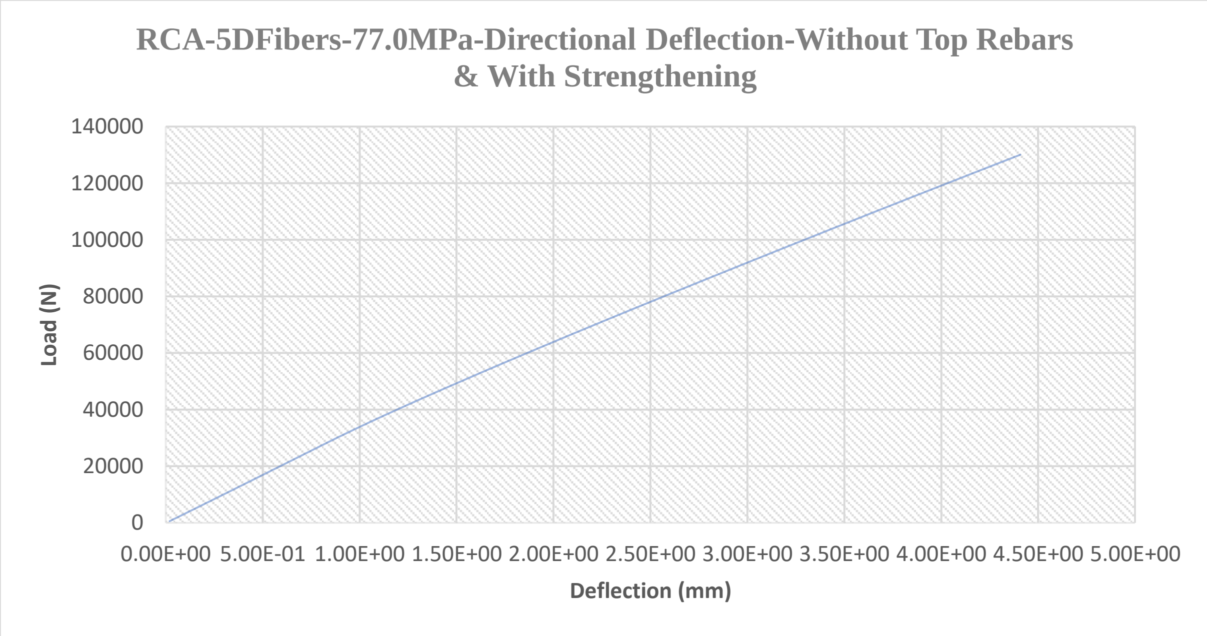

Figure 359(RCA-5D$_{Fibers}$-77.0MPa – Directional deflections (Y-Dim.) of beam sample with strengthening and without top rebars- Static Nonlinear Analysis)

Normal Stress (Concrete)

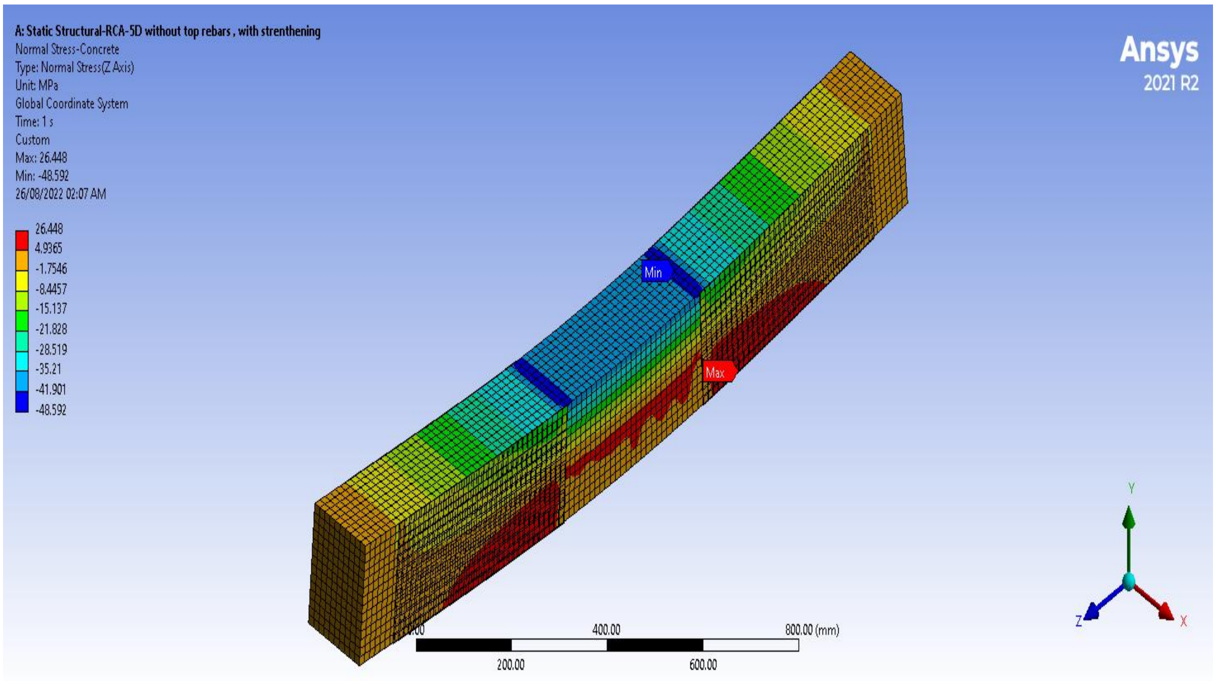

Figure 360(RCA-5D$_{Fibers}$-77.0MPa – Normal stress (Concrete) of beam sample with strengthening and without top rebars- Static Nonlinear Analysis)

The blue zones show the crushing from loading machine and the maximum value is 48.592 MPa, whereas the red zones indicate to tension.

Normal Stress (Rebars)

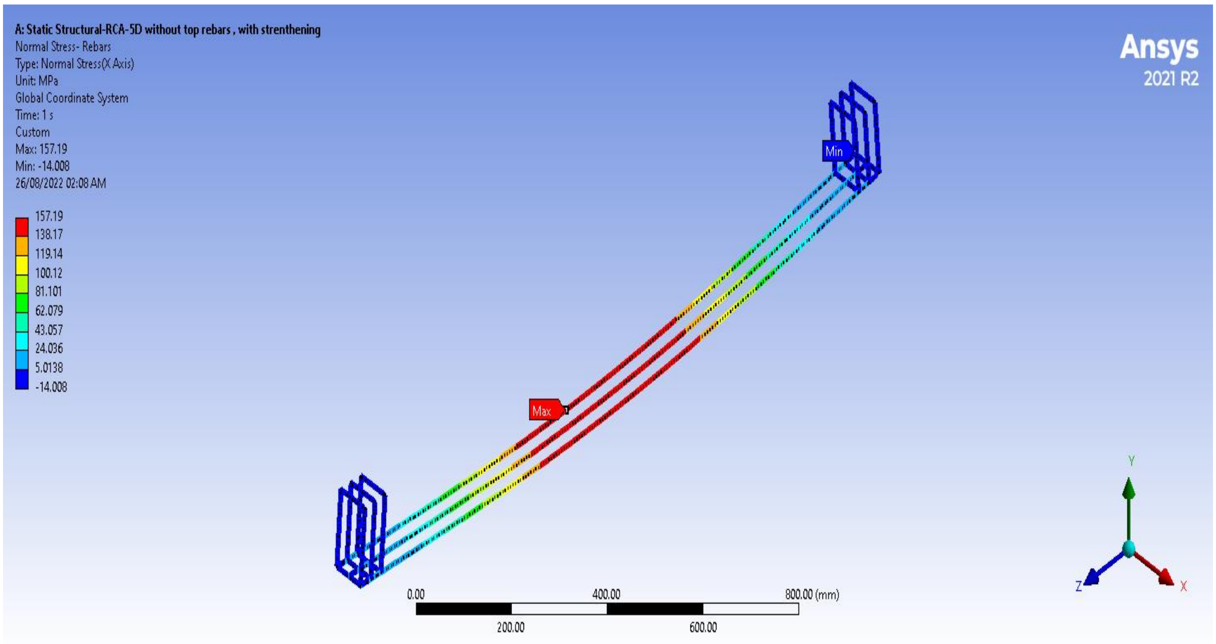

Figure 361(RCA-5D$_{Fibers}$-77.0MPa – Normal stress (Rebars) of beam sample with strengthening and without top rebars- Static Nonlinear Analysis)

The red zones show that the rebars is yielding by 157.19MPa, in the middle span due to tension.

Shear Stress

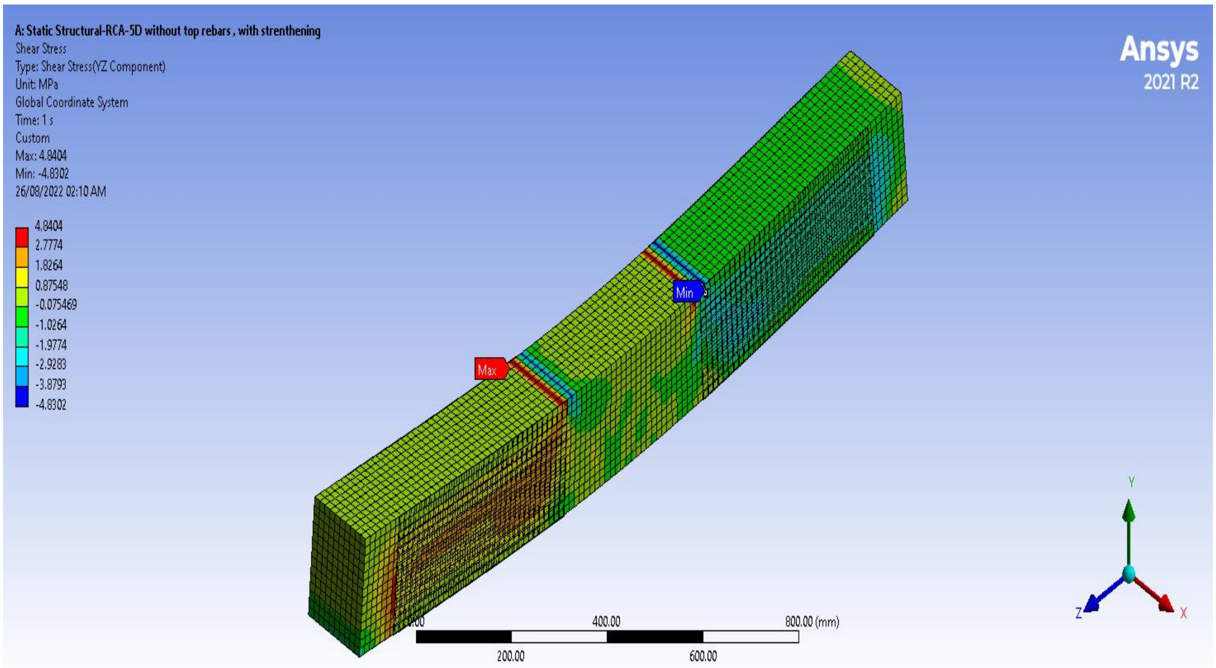

Figure 362(RCA-5D$_{Fibers}$-77.0MPa – Shear stress of beam sample with strengthening and without top rebars- Static Nonlinear Analysis)

Elastic Strain

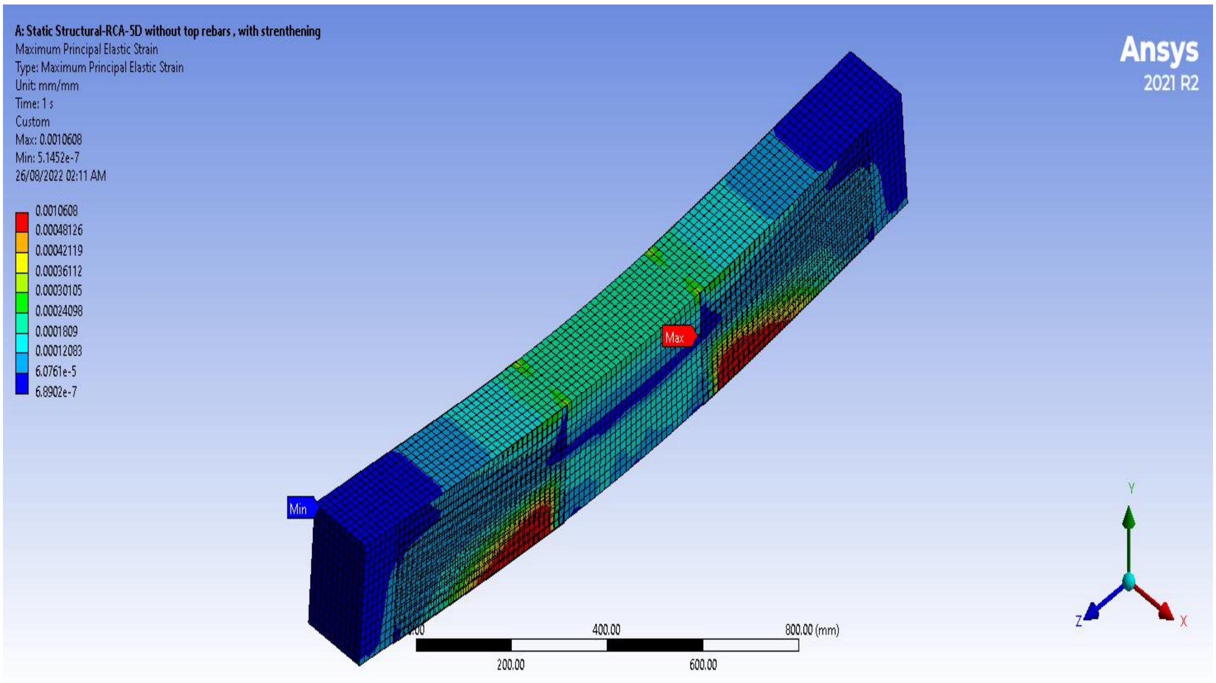

Figure 363(RCA-5D$_{Fibers}$-77.0MPa – Elastic strain of beam sample with strengthening and without top rebars- Static Nonlinear Analysis)

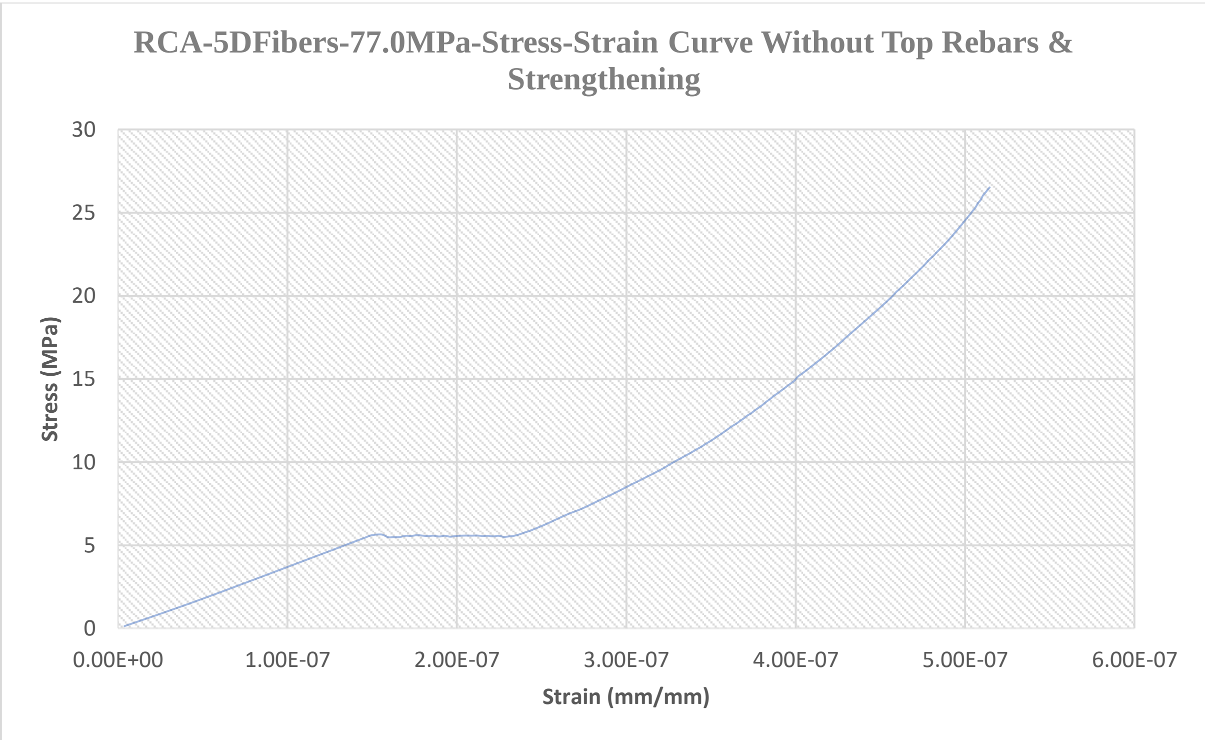

Figure 364(RCA-5D$_{Fibers}$-77.0MPa – Stress & Strain graph of beam sample with strengthening and without top rebars- Static Nonlinear Analysis)

25- Explicit Dynamic-Without Top Rebars & With Strengthening

Geometry and loads

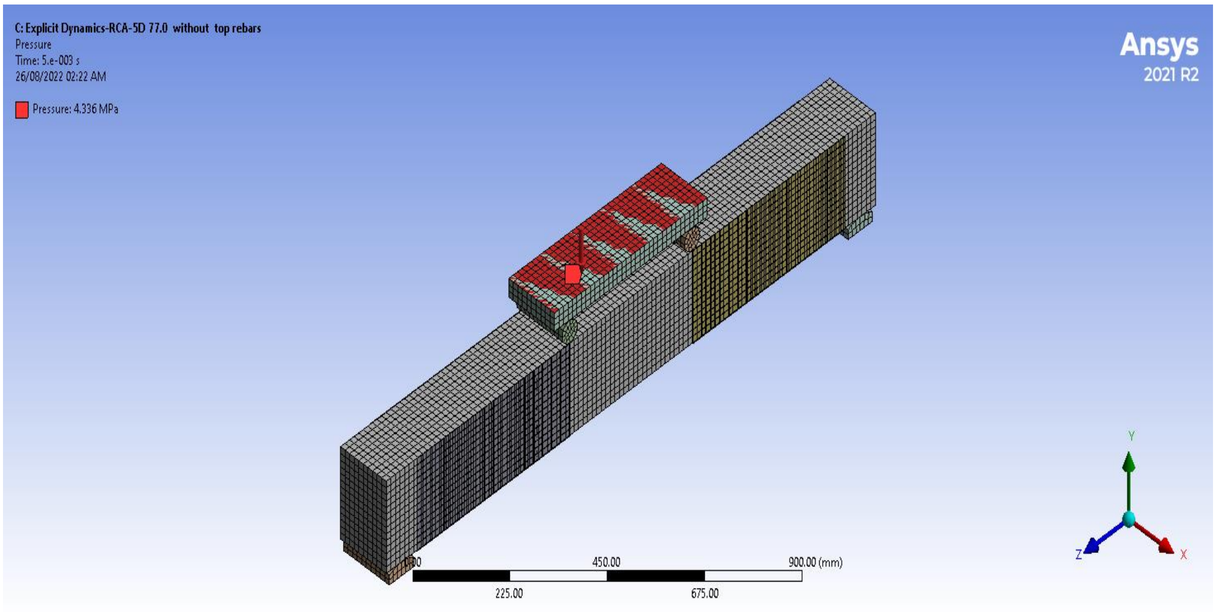

Figure 365(RCA-5D$_{Fibers}$-77.0MPa – Geometry & Loads of beam sample with strengthening and without top rebars- Explicit Dynamic Analysis)

The ultimate load has been transferred to be as a pressure load which is 4.336 MPa as shown above with rate loading 0.6mm/min

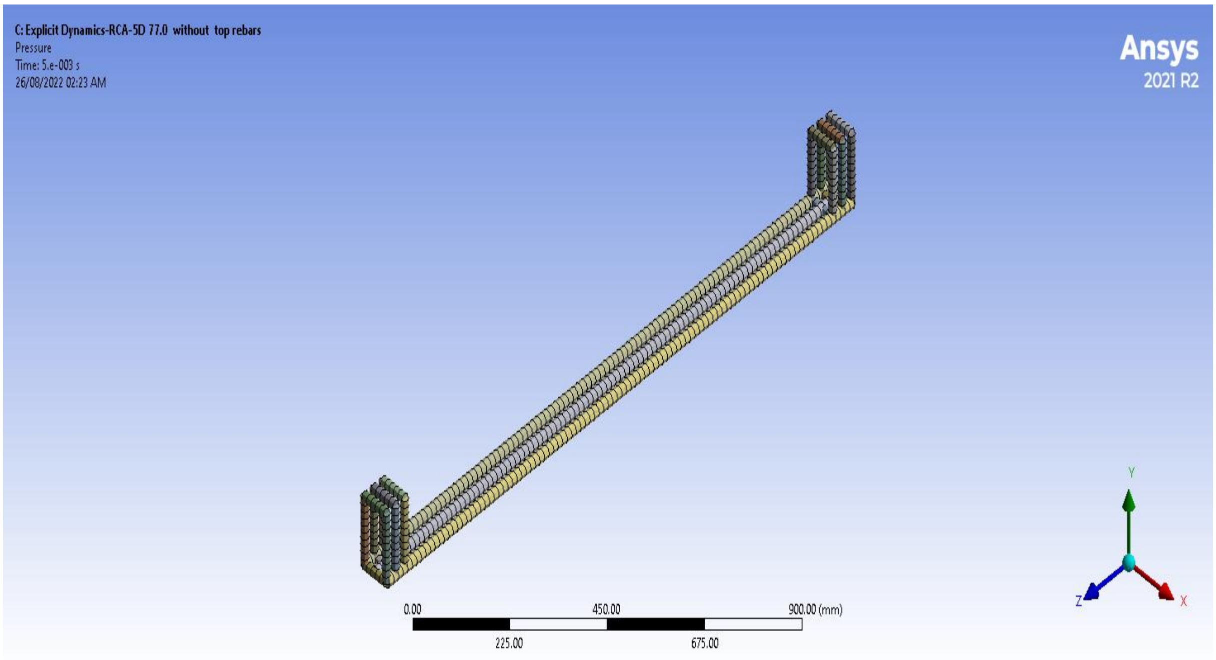

Figure 366(RCA-5D$_{Fibers}$-77.0MPa – Rebars of beam sample with strengthening - Explicit Dynamic Analysis)

Deformations

Total Deformations

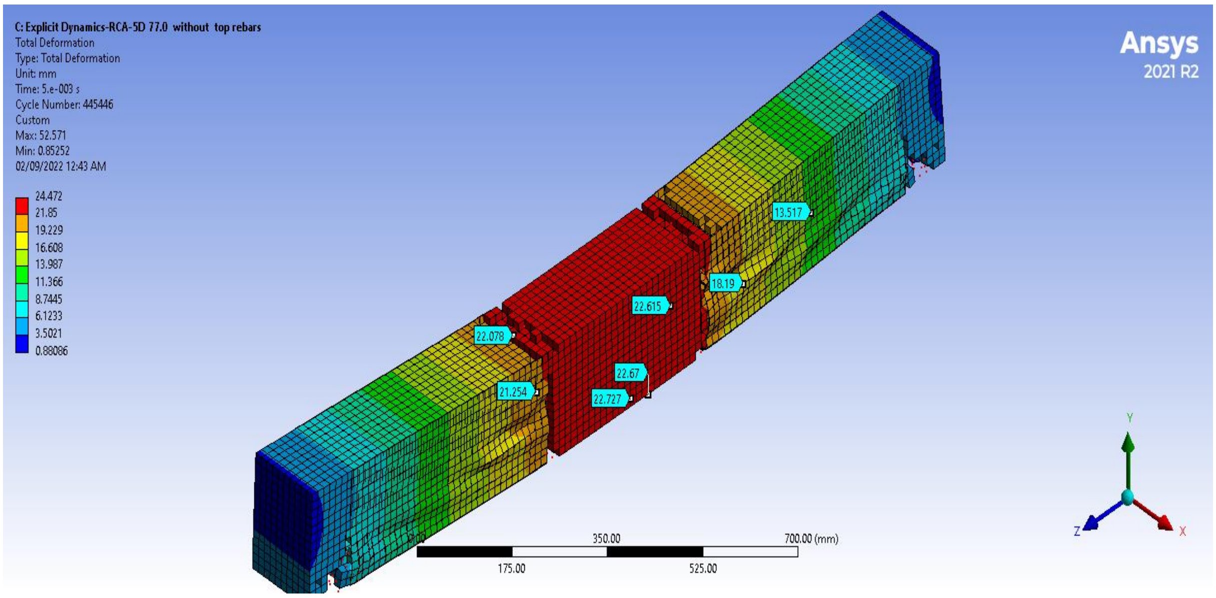

Figure 367(RCA-5D$_{Fibers}$-77.0MPa – Total deflections of beam sample with strengthening and without top rebars- Explicit Dynamic Analysis)

The value is 22.727 mm.

Directional Deformation (Y-Direction)-Concrete

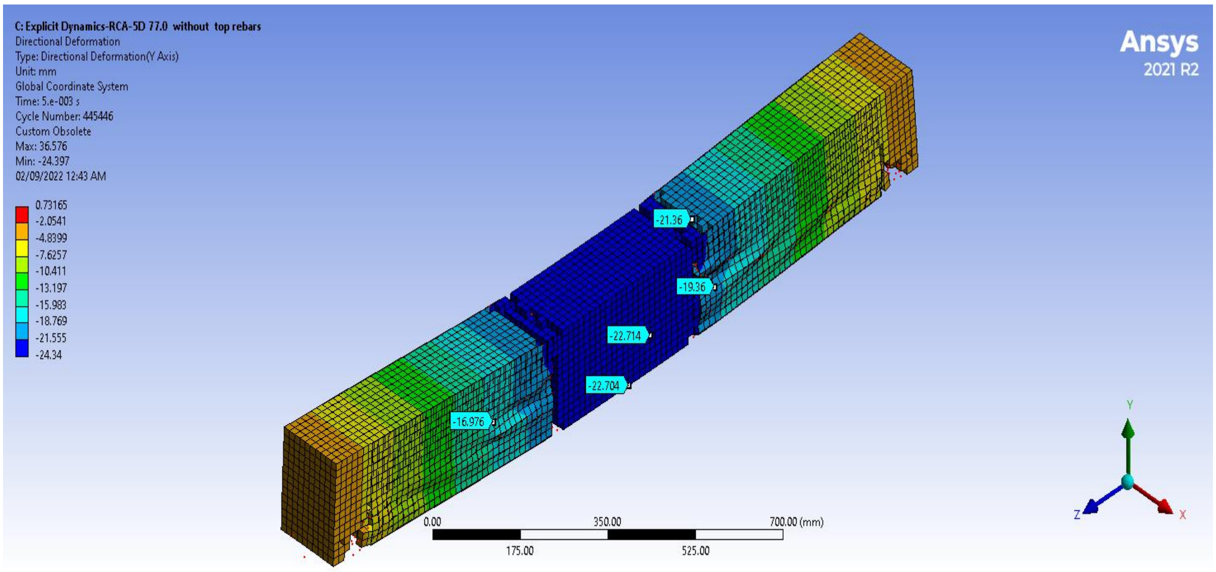

Figure 368(RCA-5D$_{Fibers}$-77.0MPa – Directional deflections (Y-Dim.) of beam sample with strengthening and without top rebars- Explicit Dynamic Analysis)

The value is 22.704 mm

Directional Deformation (Y-Direction)- Rebars

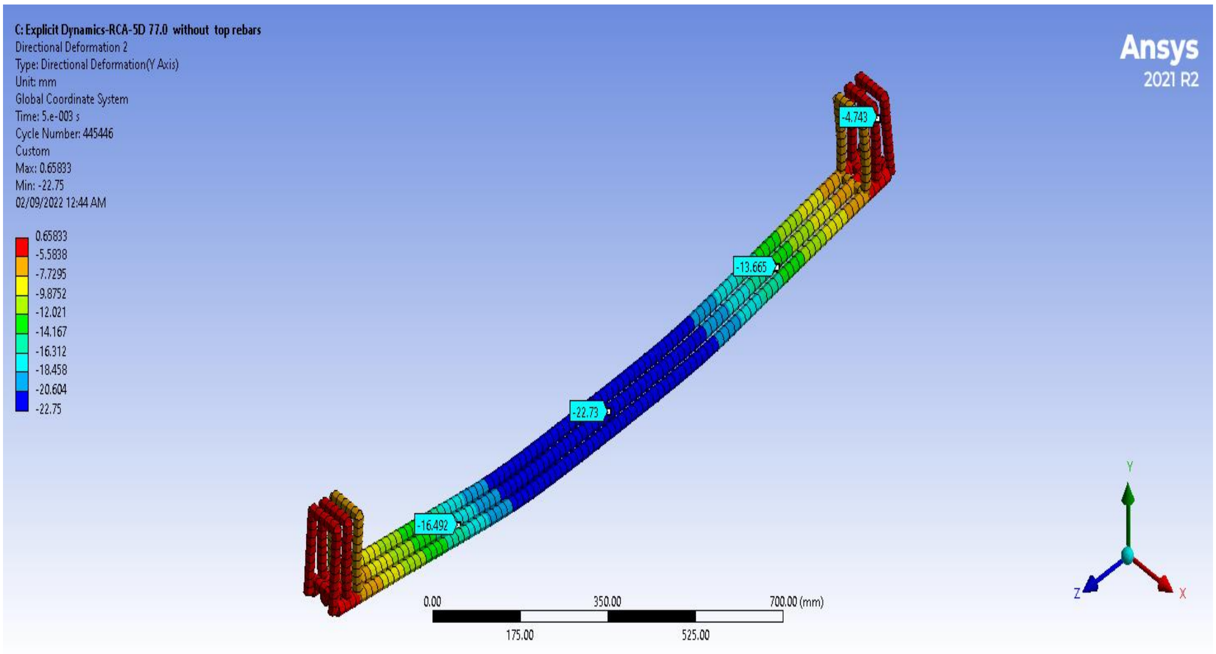

Figure 369(RCA-5D$_{Fibers}$-77.0MPa – Directional deflections (Y-Dim.) Rebars of beam sample with strengthening and without top rebars- Explicit Dynamic Analysis)

Normal strain

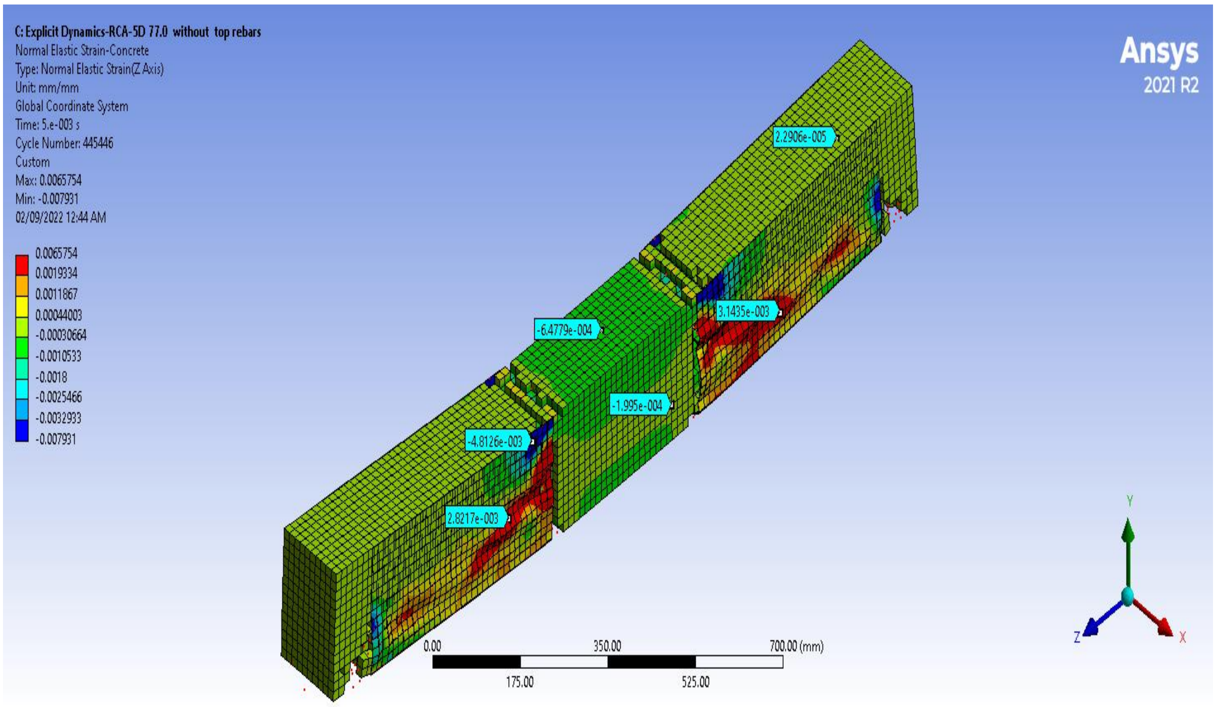

Figure 370(RCA-5D$_{Fibers}$-77.0MPa – Normal strain of beam sample with strengthening and without top rebars- Explicit Dynamic Analysis)

Shear Stress

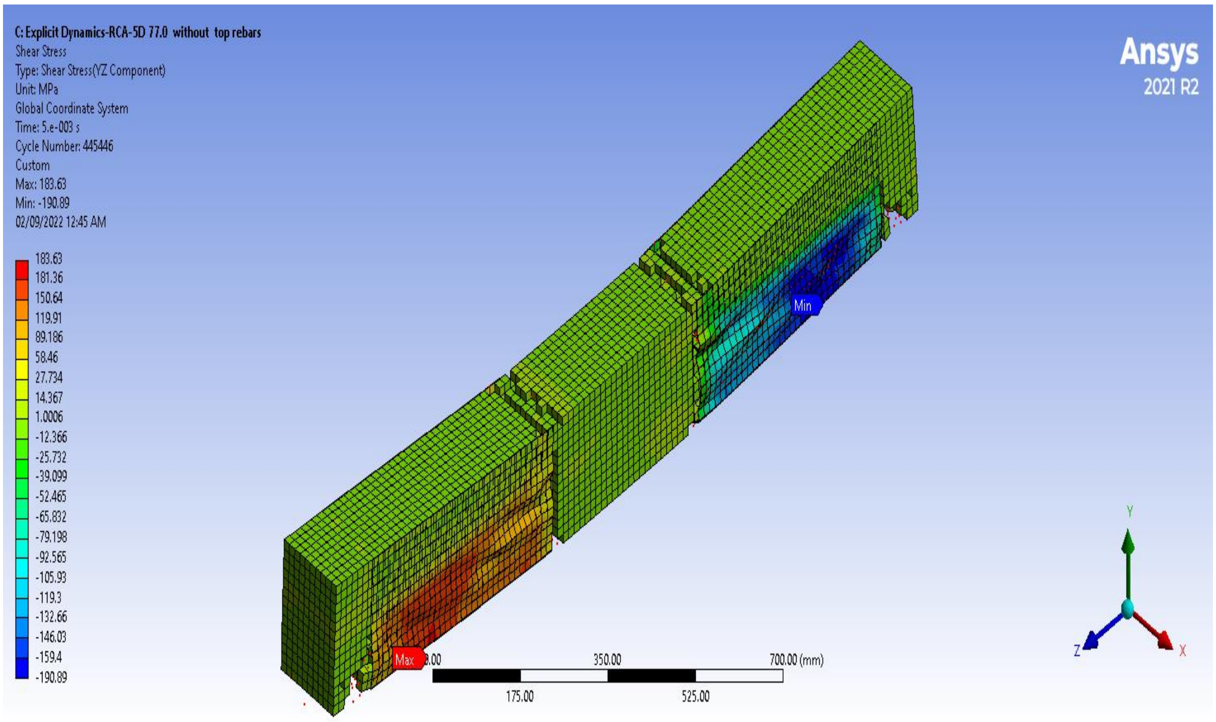

Figure 371(RCA-5D$_{Fibers}$-77.0MPa – Shear stress of beam sample with strengthening and without top rebars- Explicit Dynamic Analysis)

Total shape strain

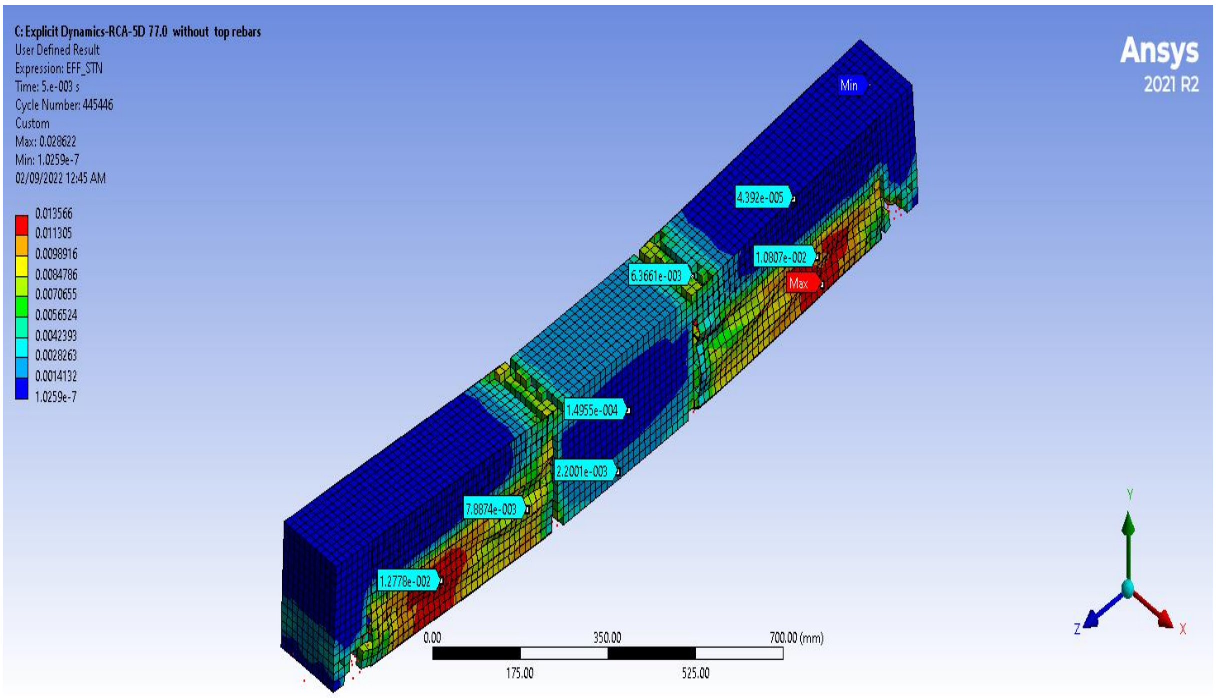

Figure 372(RCA-5D$_{Fibers}$-77.0MPa – Total strain of beam sample with strengthening and without top rebars- Explicit Dynamic Analysis)

Maximum Stress

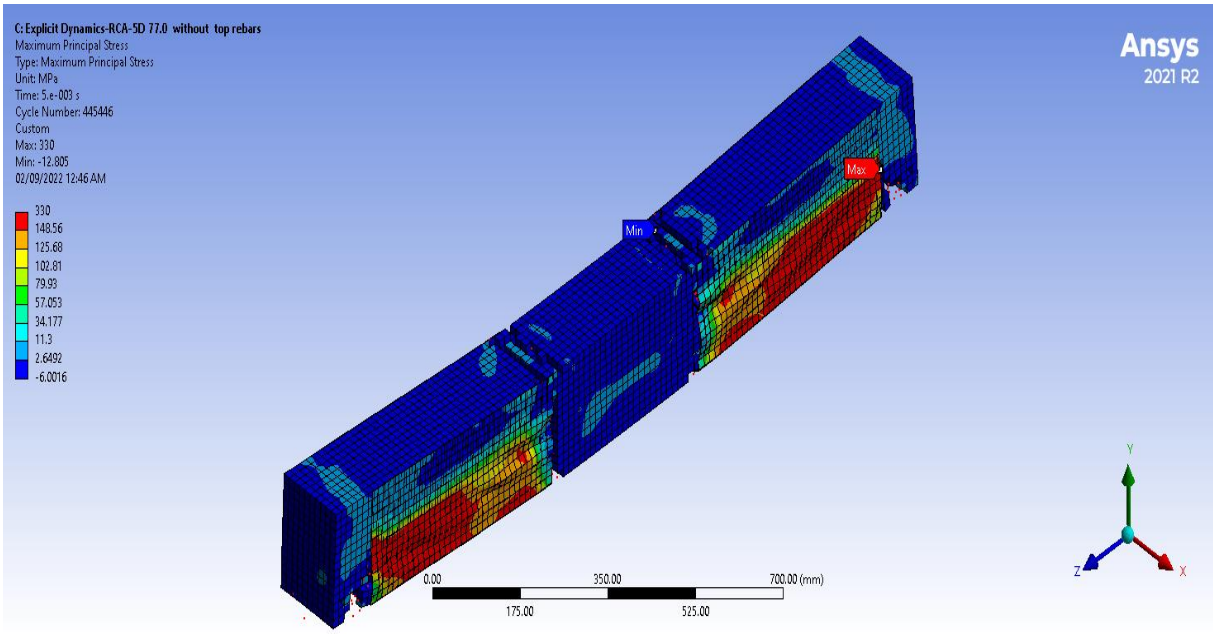

Figure 373(RCA-5D$_{Fibers}$-77.0MPa – Maximum stress of beam sample with strengthening and without top rebars- Explicit Dynamic Analysis)

The Damage Pattern

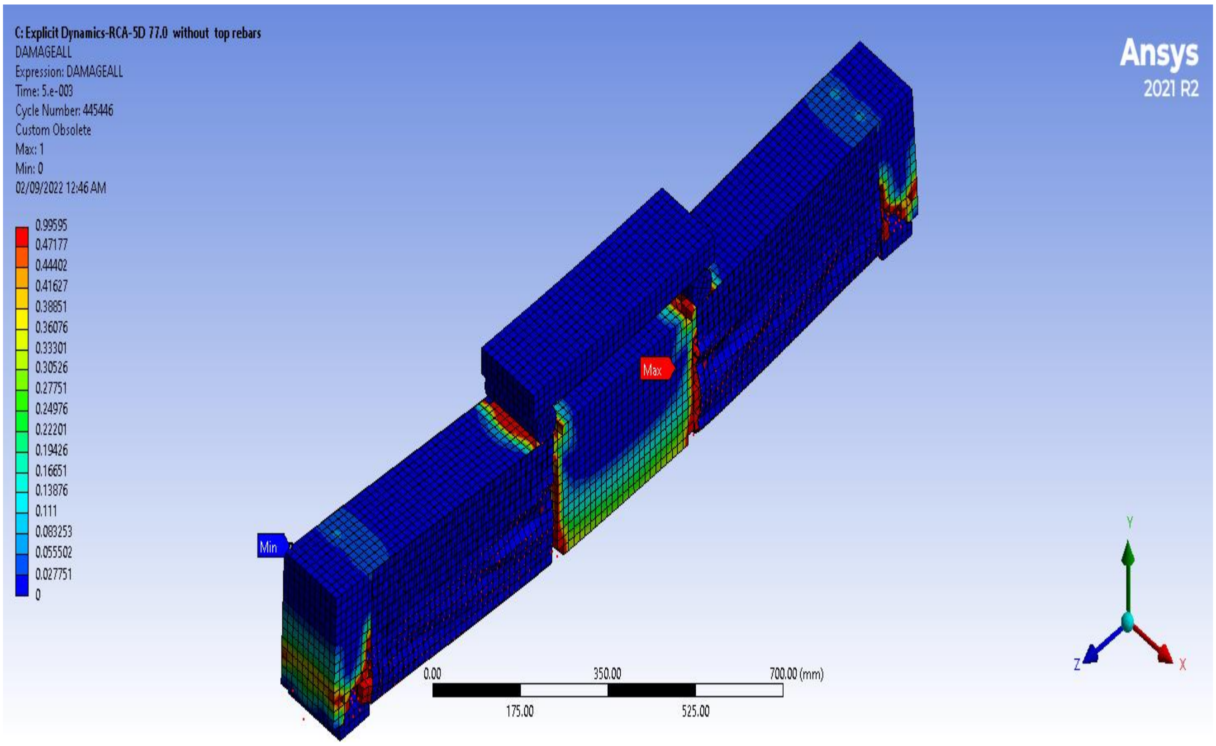

Figure 374(RCA-5D$_{Fibers}$-77.0MPa – Damage pattern-1 of beam sample with strengthening and without top rebars- Explicit Dynamic Analysis)

As we can see the shear damage cracks in red and CFRP debonding on edges of concrete failure.

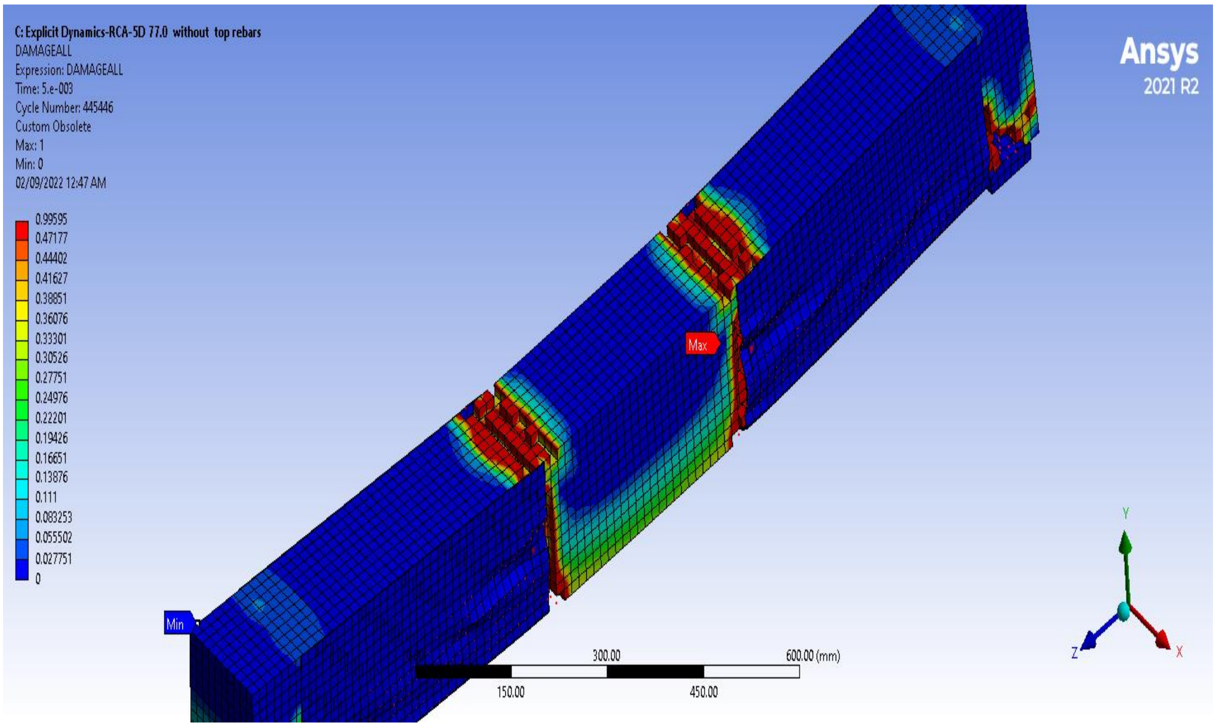

Figure 375(RCA-5D$_{Fibers}$-77.0MPa – Damage pattern-2 of beam sample with strengthening and without top rebars- Explicit Dynamic Analysis)

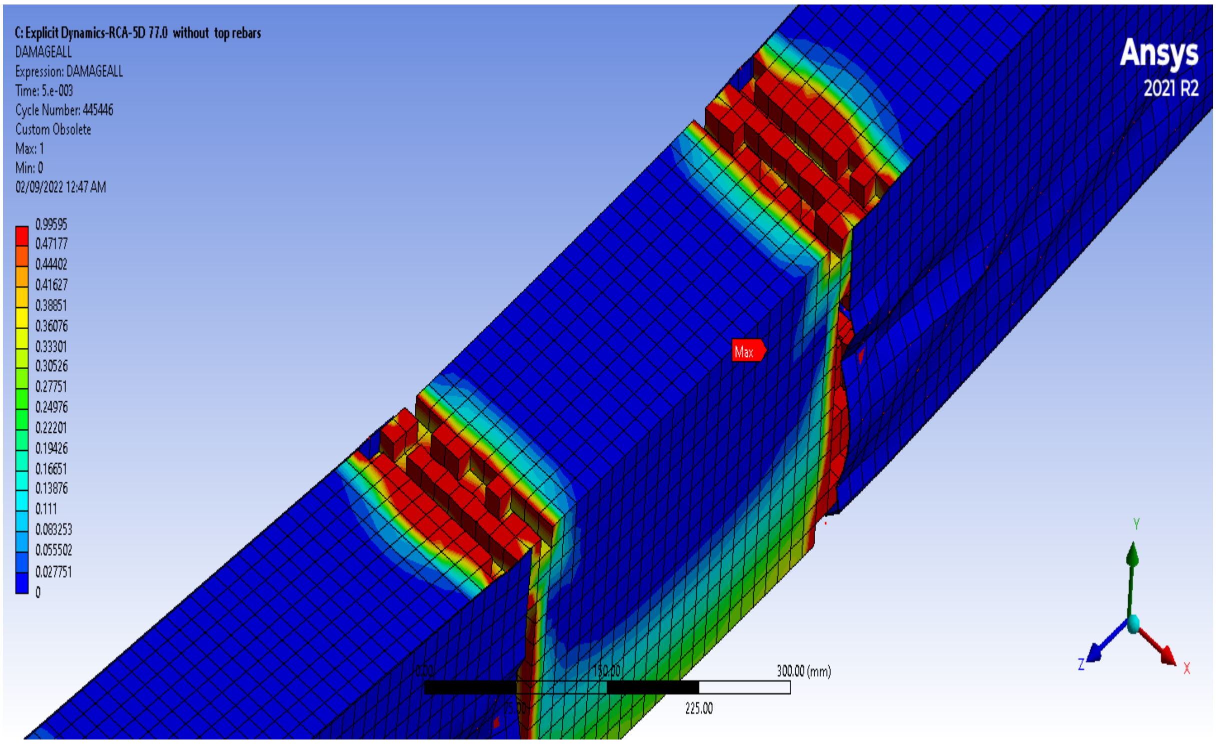

Figure 376(RCA-5D$_{Fibers}$-77.0MPa – Damage pattern-3 of beam sample with strengthening and without top rebars- Explicit Dynamic Analysis)

CFRP laminates due to ultimate load has been debonding as shown in images above

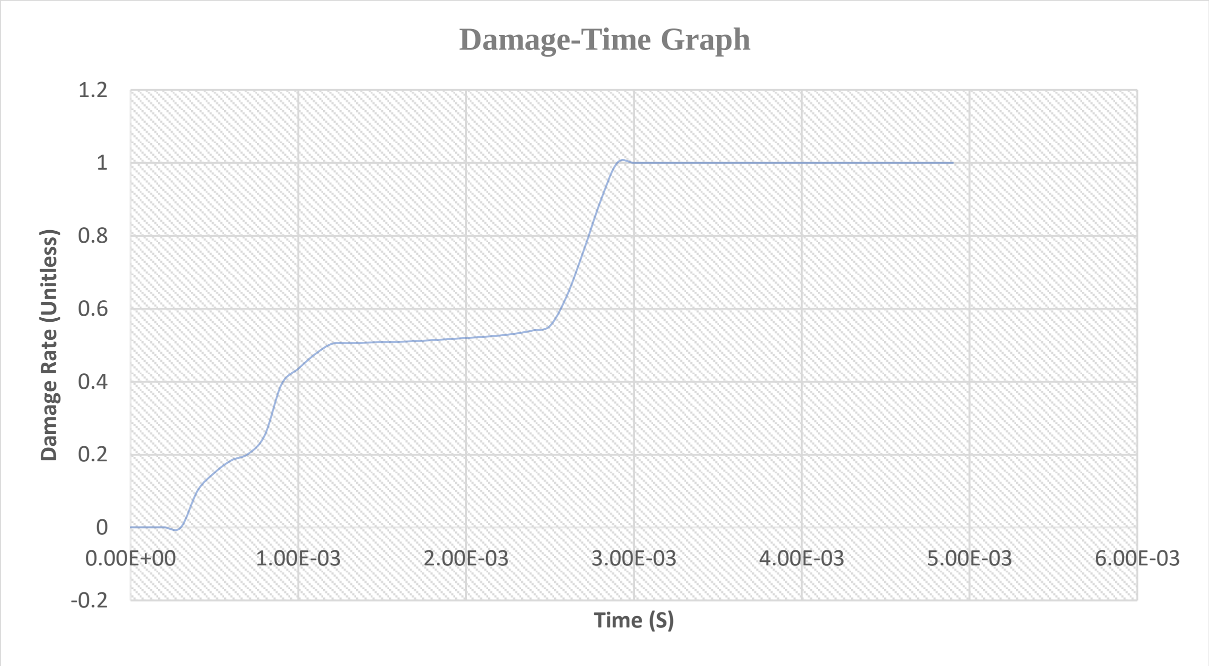

Figure 377(RCA-5D$_{Fibers}$-77.0MPa – Damage pattern graph of beam sample with strengthening and without top rebars- Explicit Dynamic Analysis)

26- Static Non-Linear Analysis - Without Strengthening and with Top Rebars

Geometry and loads

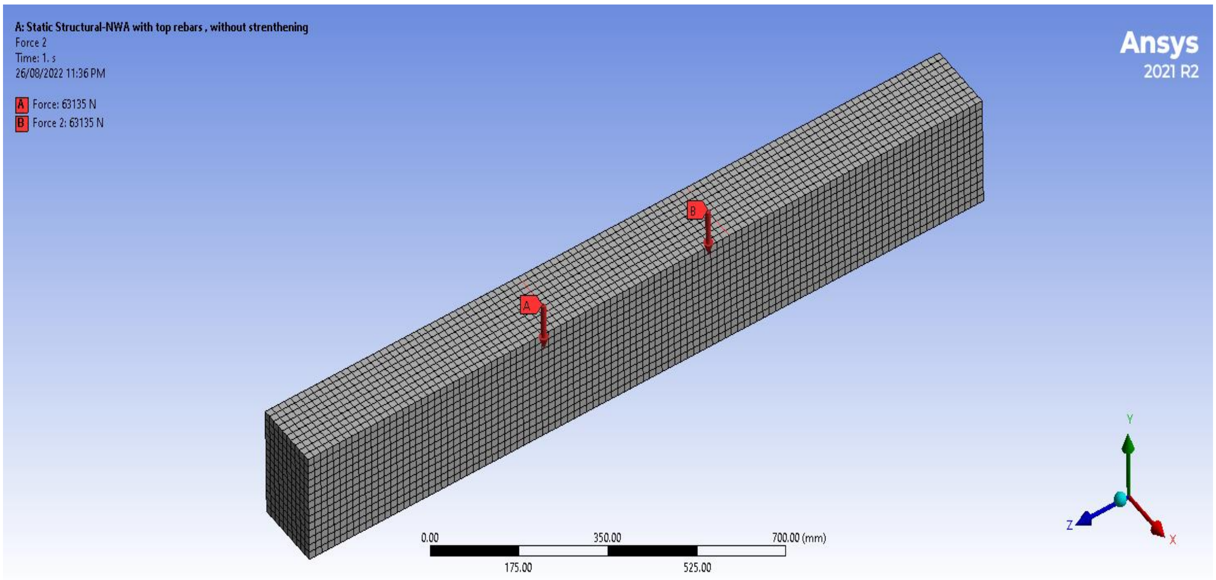

Figure 378(NWA-2/70.5MPa – Geometry & Loads of beam sample without strengthening and with top rebars- Static Nonlinear Analysis)

The ultimate load has been divided in to loads which is 126.27/2 =63.135KN.

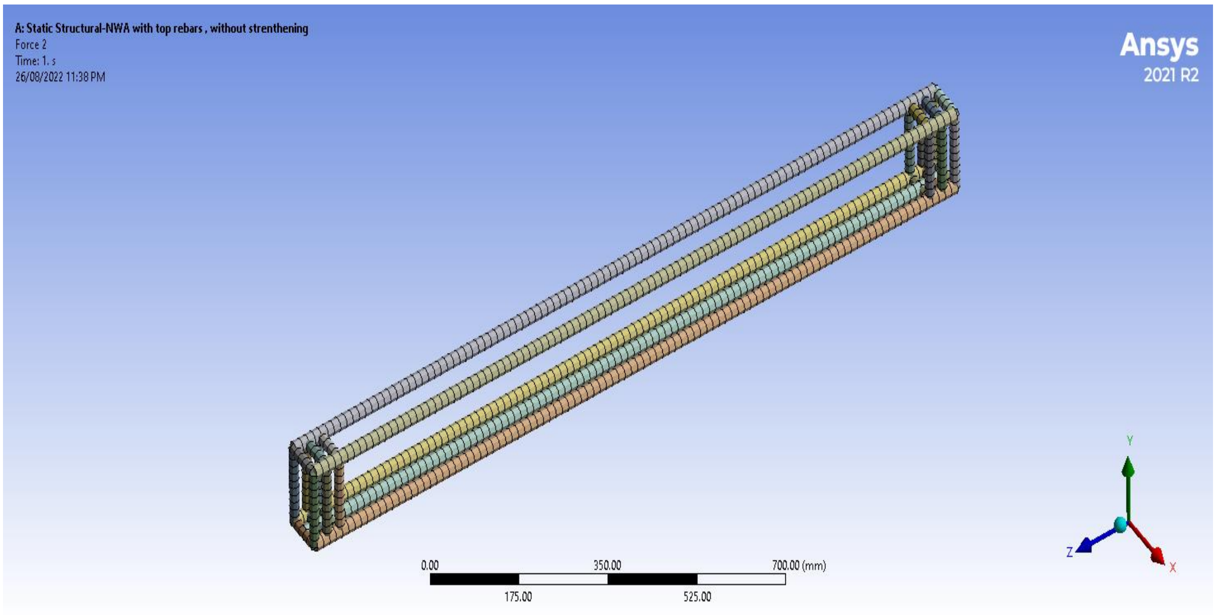

Figure 379(NWA-2/70.5MPa – Rebars of beam sample without strengthening - Static Nonlinear Analysis)

Deformations

Total Deformations

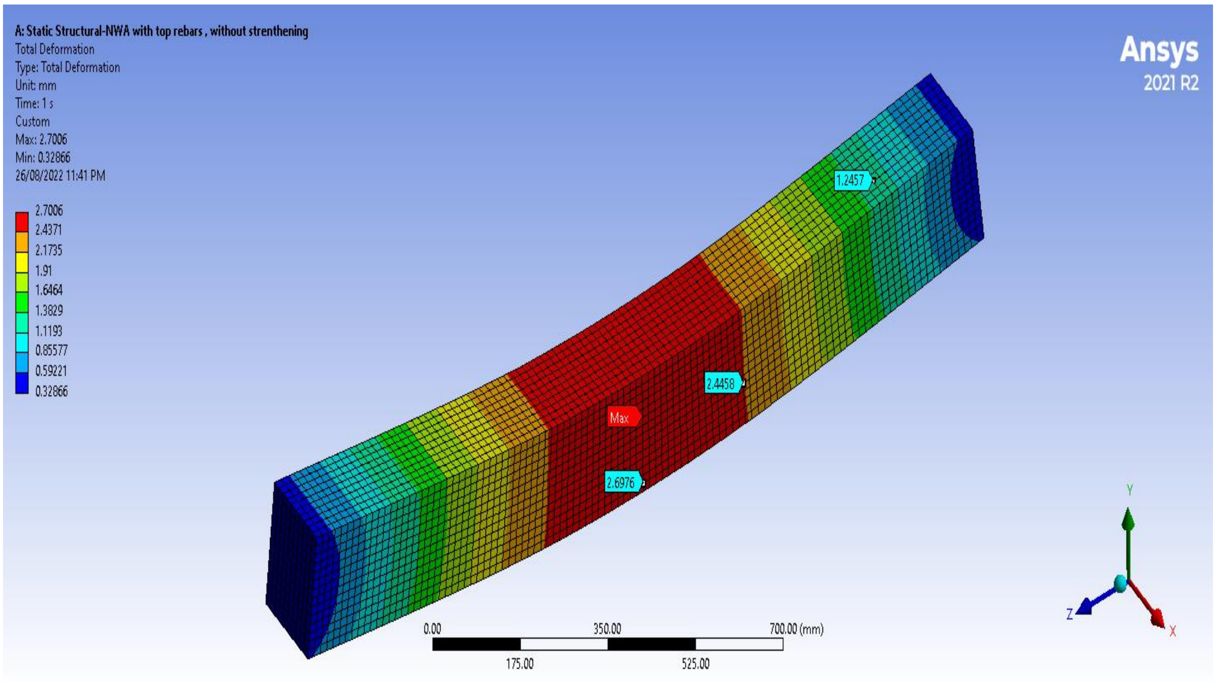

Figure 380(NWA-2/70.5MPa – Total deflections of beam sample without strengthening and with top rebars- Static Nonlinear Analysis)

The value is 2.7006 mm.

Directional Deformation (Y-Direction)

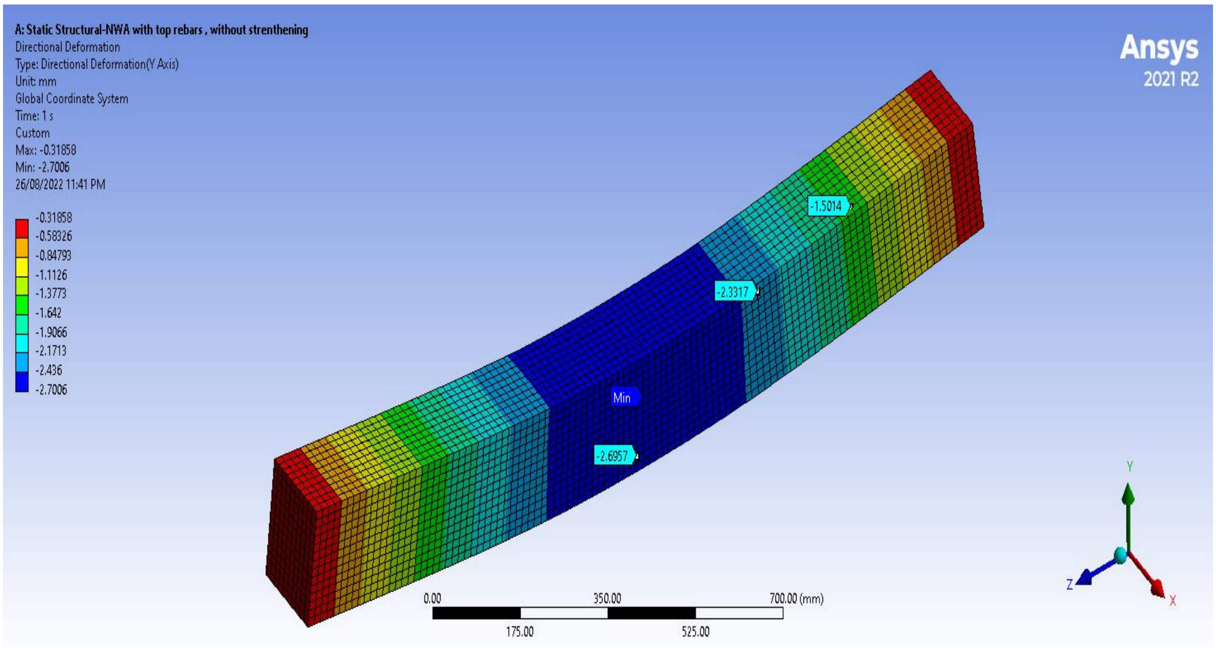

Figure 381(NWA-2/70.5MPa – Directional deflections (Y-Dim.) of beam sample without strengthening and without top rebars-Static Nonlinear Analysis)

The value is 2.7006 mm.

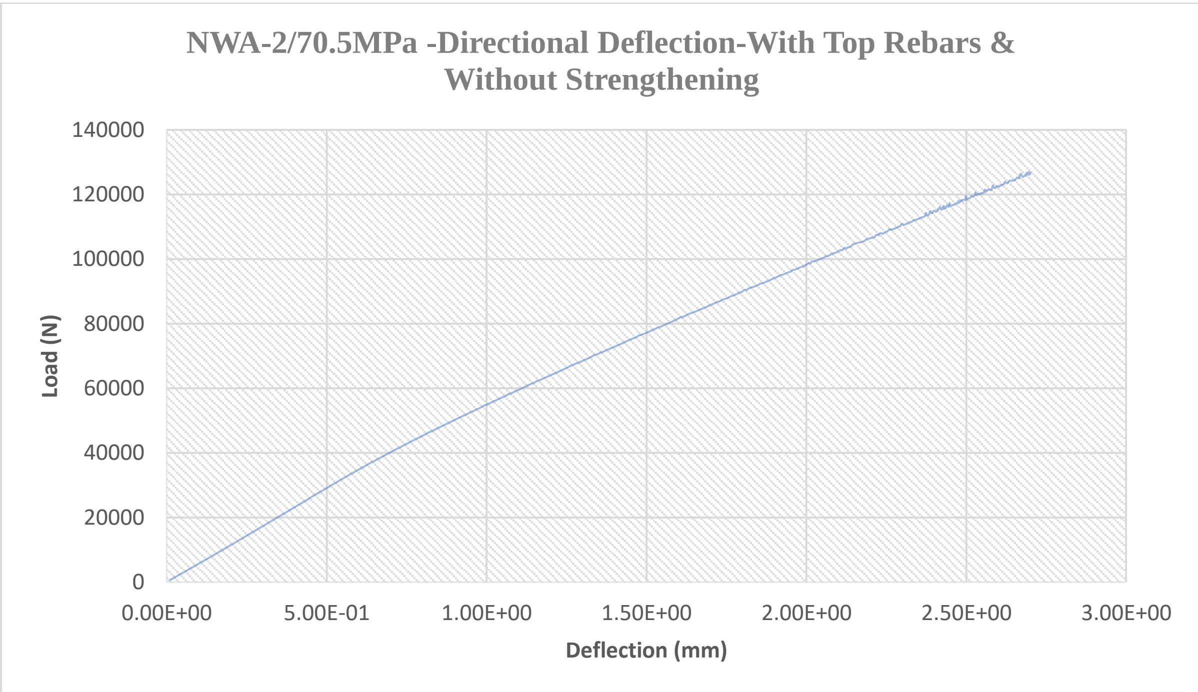

Figure 382(NWA-2/70.5MPa – Directional deflections (Y-Dim.) of beam sample without strengthening and with top rebars-Static Nonlinear Analysis)

Normal Stress (Concrete)

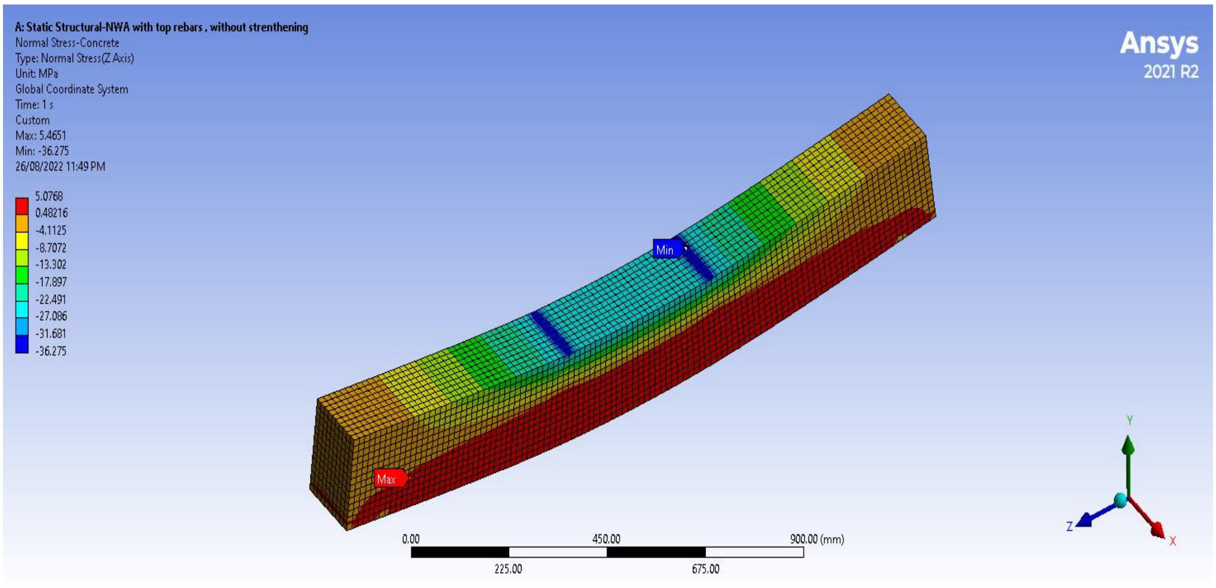

Figure 383(RC NWA-2/70.5MPa A-5D$_{Fibers}$-77.0MPa – Normal stress (Concrete) of beam sample without strengthening and with top rebars- Static Nonlinear Analysis)

The blue zones show the crushing from loading machine and the maximum value is 36.275MPa, whereas the red zones indicate to tension.

Normal Stress (Rebars)

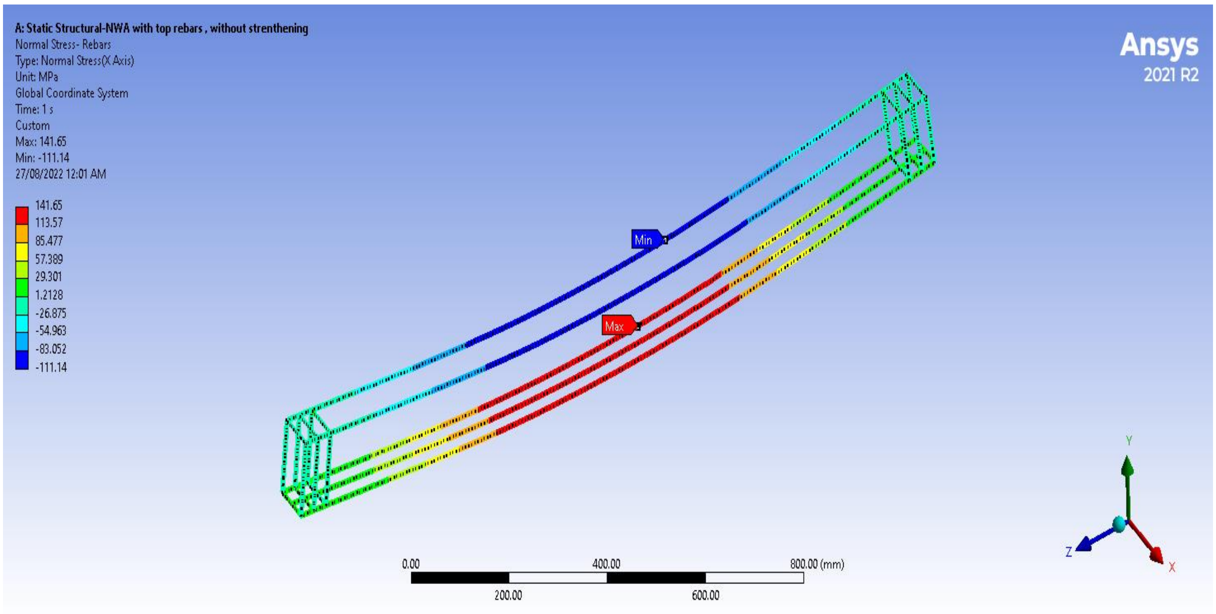

Figure 384(NWA-2/70.5MPa – Normal stress (Rebars) of beam sample without strengthening and with top rebars- Static Nonlinear Analysis)

The red zones show that the rebars is yielding by 141.65 MPa, in the middle span due to tension.

Shear Stress

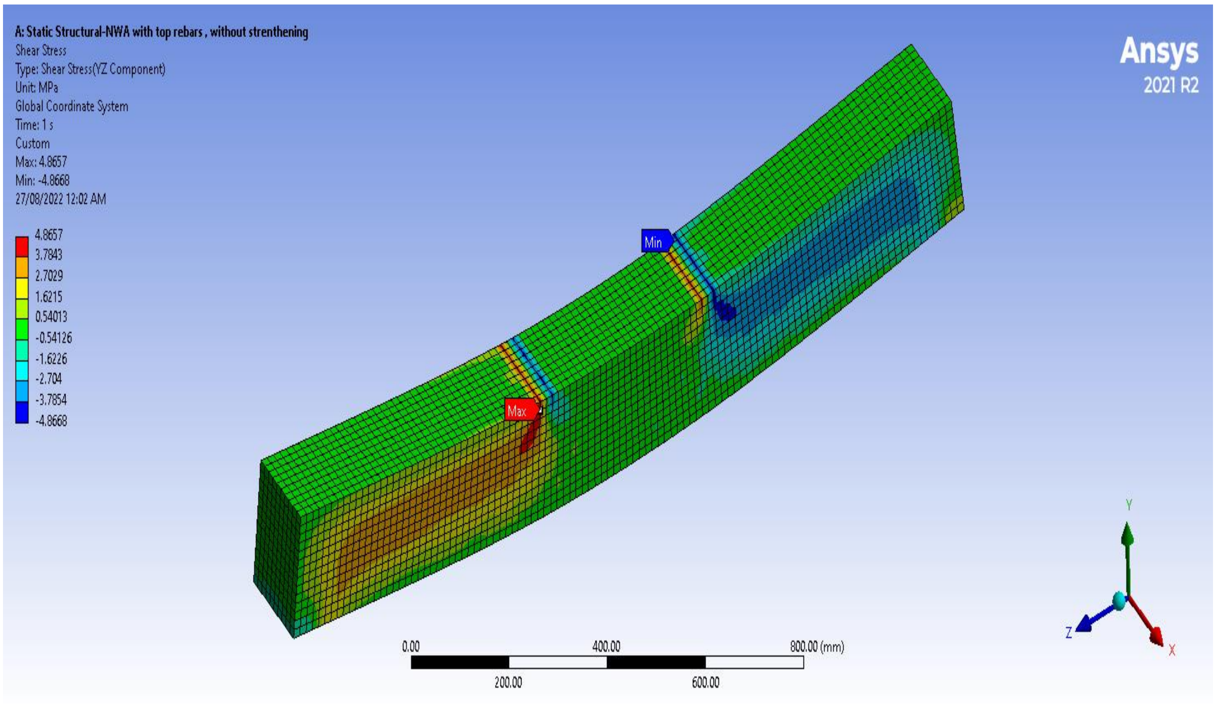

Figure 385(NWA-2/70.5MPa – Shear Stress of beam sample without strengthening and with top rebars - Static Nonlinear Analysis)

Elastic Strain

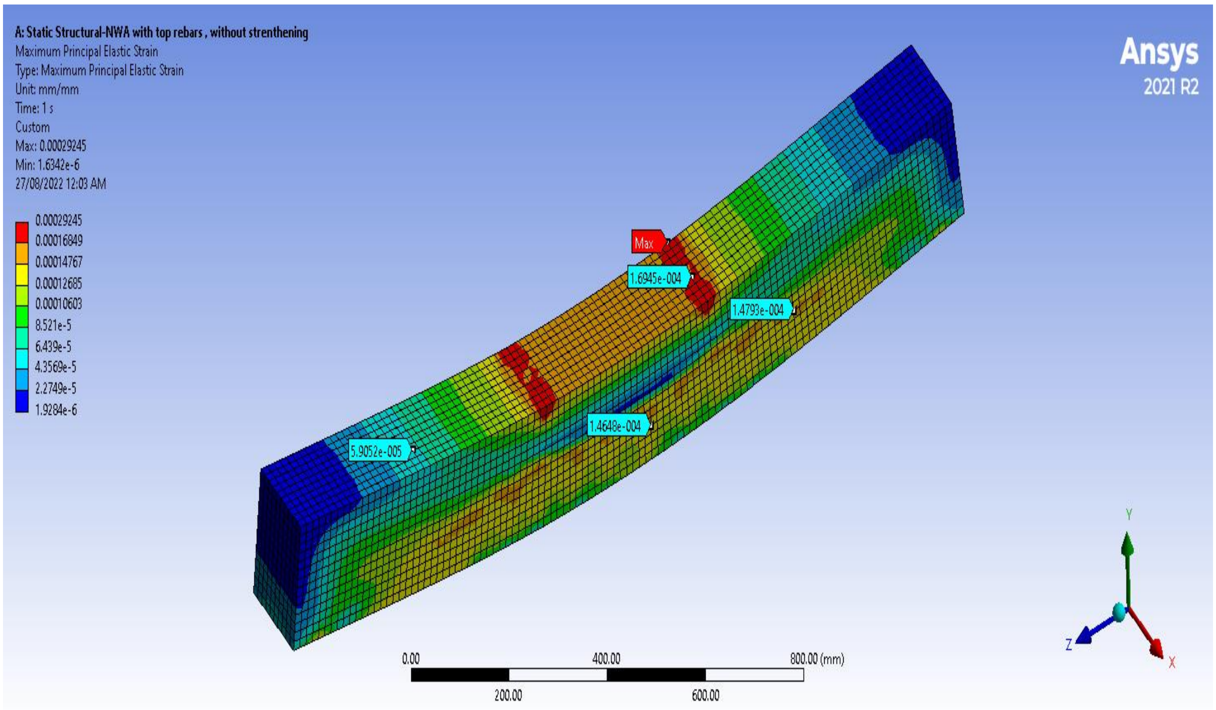

Figure 386(NWA-2/70.5MPa – Elastic Strain of beam sample without strengthening and with top rebars - Static Nonlinear Analysis)

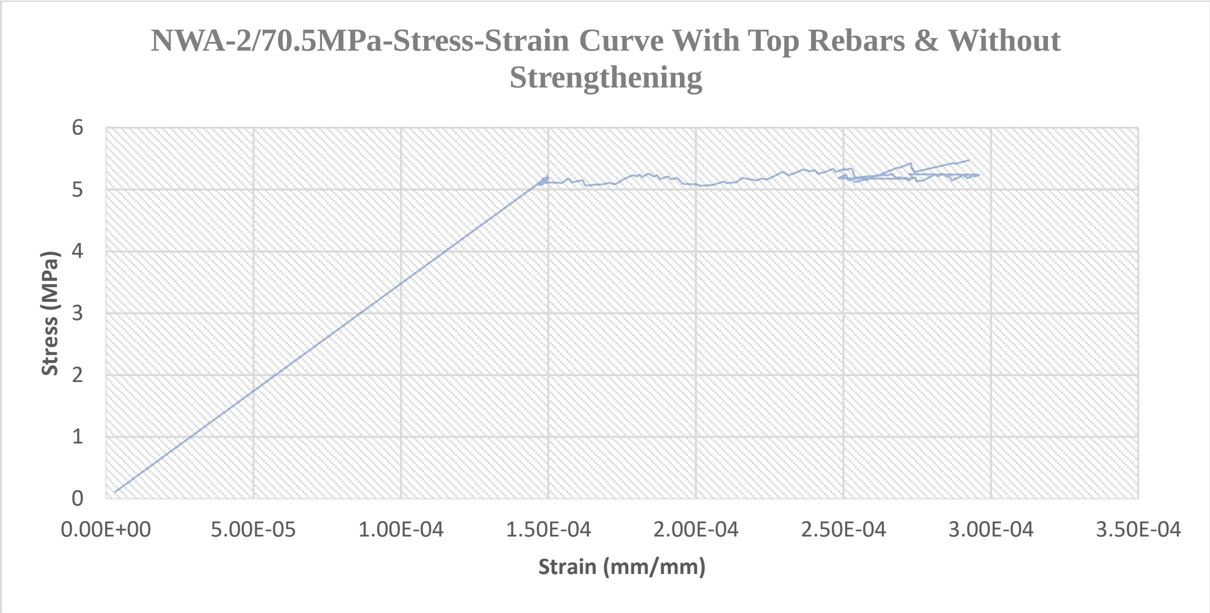

Figure 387(NWA-2/70.5MPa – Stress and Strain graph of beam sample without strengthening and with top rebars - Static Nonlinear Analysis)

27- Explicit Dynamics-With Top Rebars & Without Strengthening

Geometry and loads

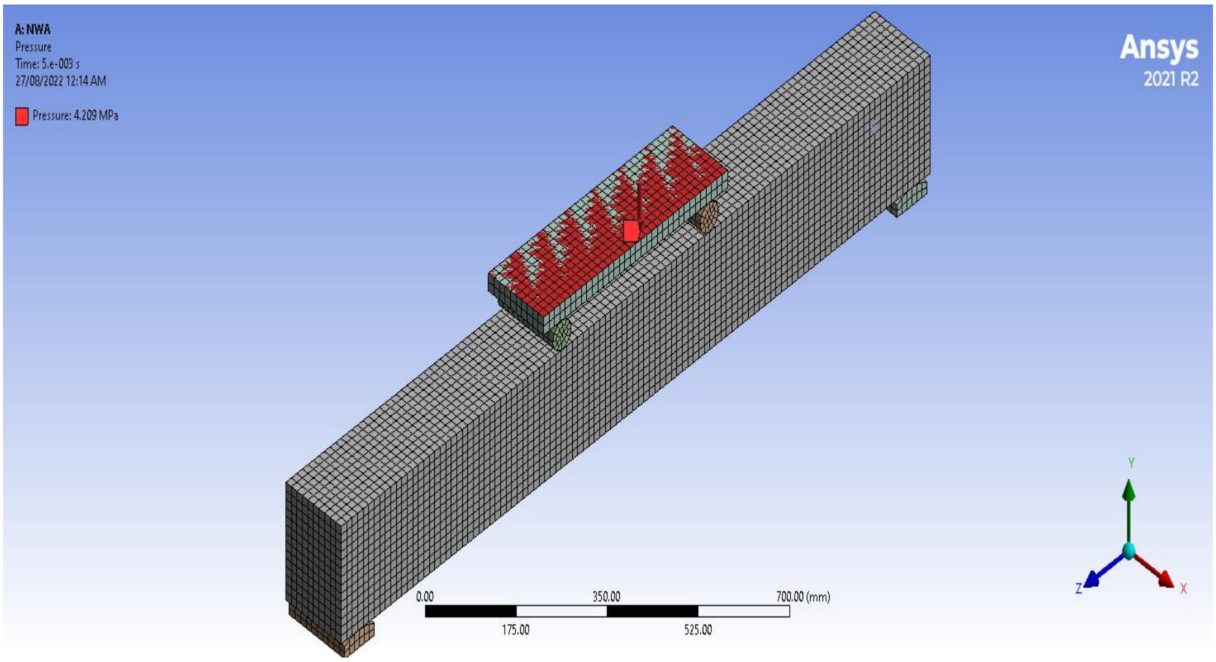

Figure 388(NWA-2/70.5MPa – Geometry & Loads of beam sample without strengthening and with top rebars- Explicit Dynamic Analysis)

The ultimate load has been transferred to be as a pressure load which is 4.209 MPa as shown above with rate loading 0.6mm/min.

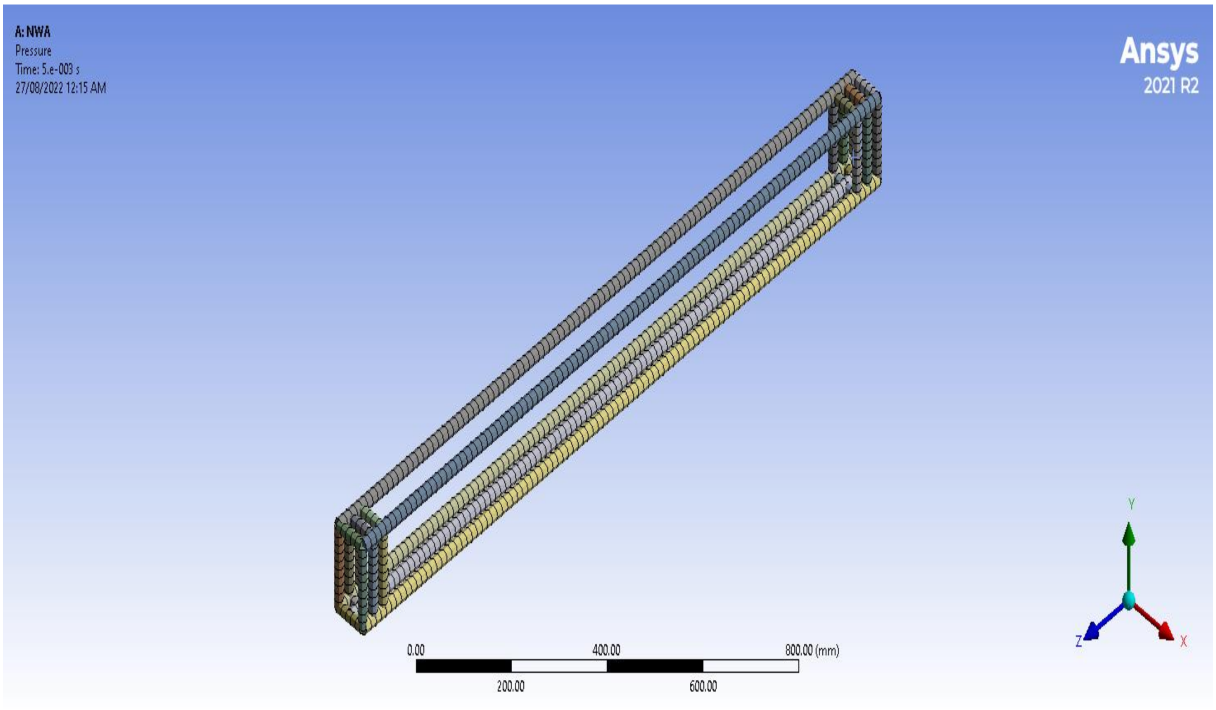

Figure 389(NWA-2/70.5MPa – Rebars of beam sample without strengthening - Explicit Dynamic Analysis)

Deformations

Total Deformations

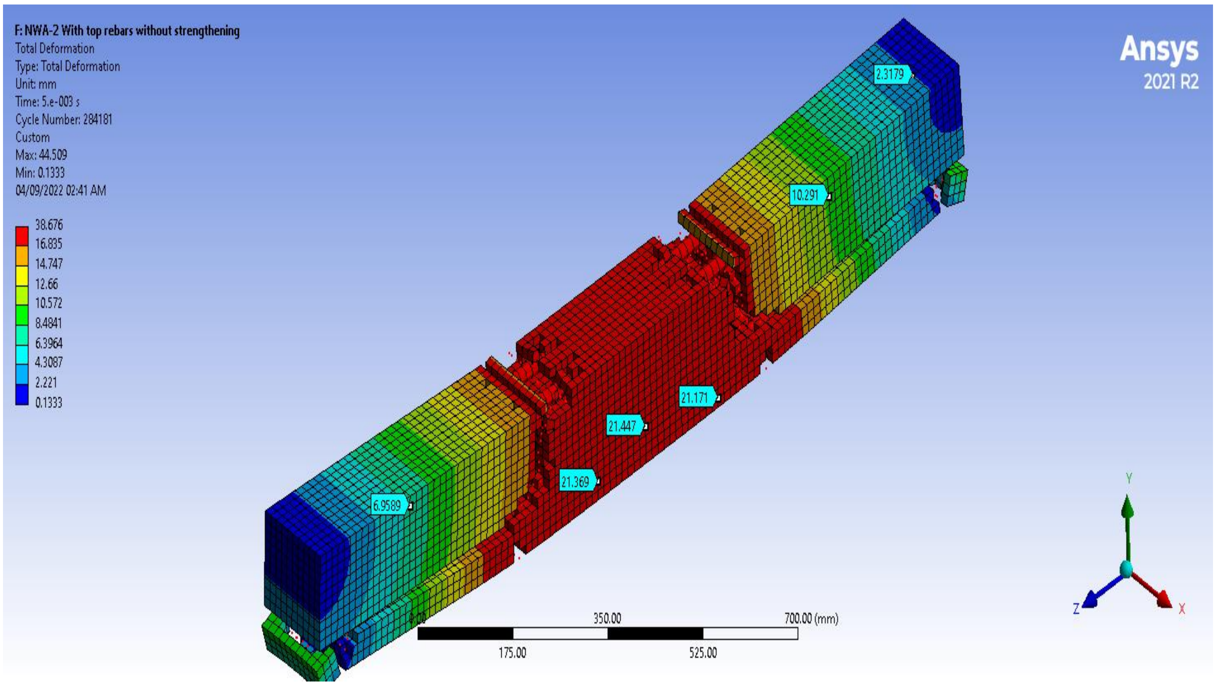

Figure 390(NWA-2/70.5MPa – Total deflections of beam sample without strengthening and with top rebars- Explicit Dynamic Analysis)

The value is 21.447 mm.

Directional Deformation (Y-Direction)-Concrete

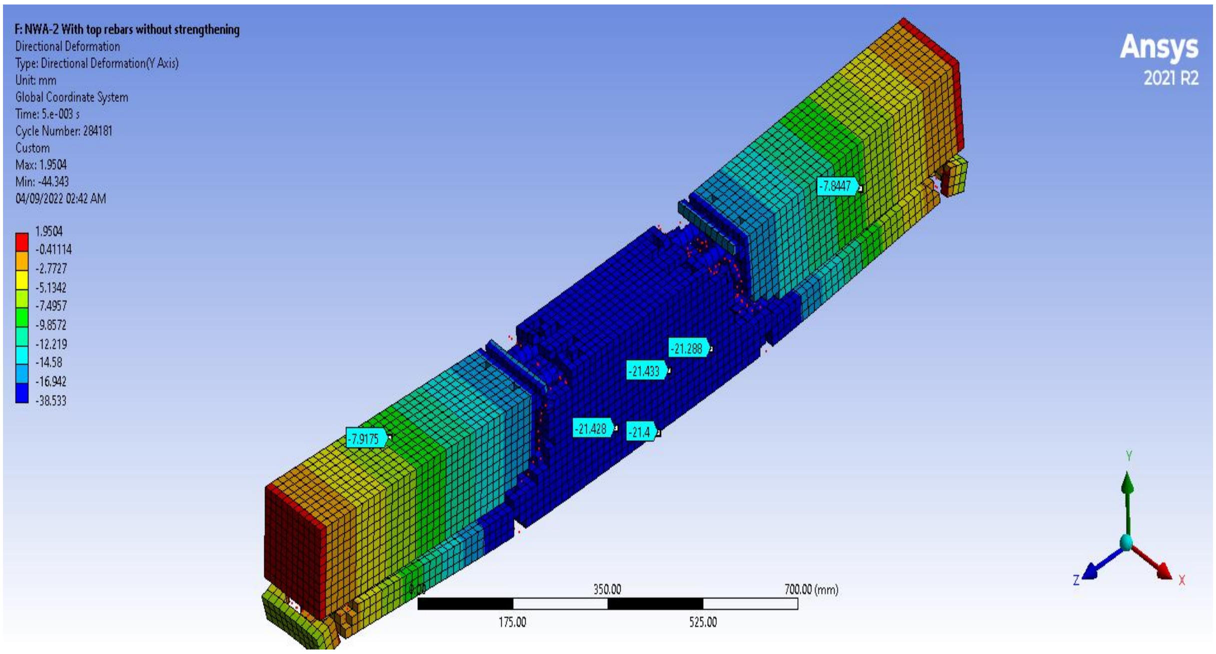

Figure 391(NWA-2/70.5MPa – Directional deflections (Y-Dir.) of beam sample without strengthening and with top rebars- Explicit Dynamic Analysis)

The value is 21.433 mm.

Directional Deformation (Y-Direction)- Rebars

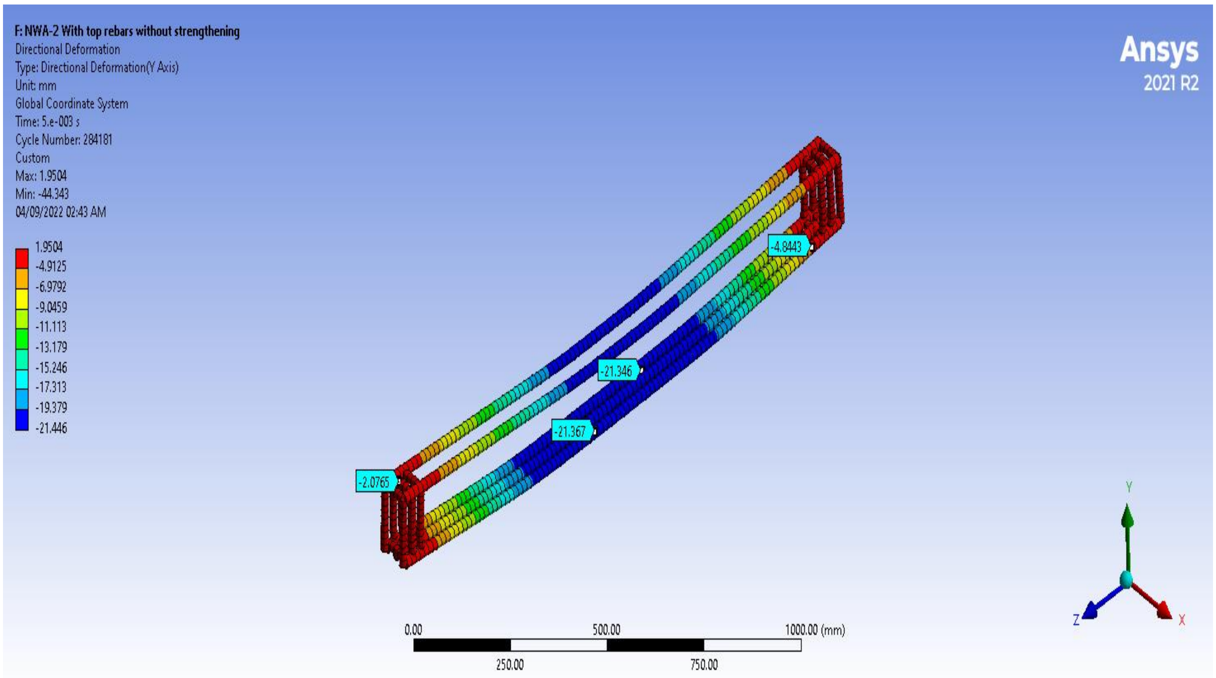

Figure 392(NWA-2/70.5MPa – Directional deflections (Y-Dir.) of beam rebars without strengthening- Explicit Dynamic Analysis)

Normal strain

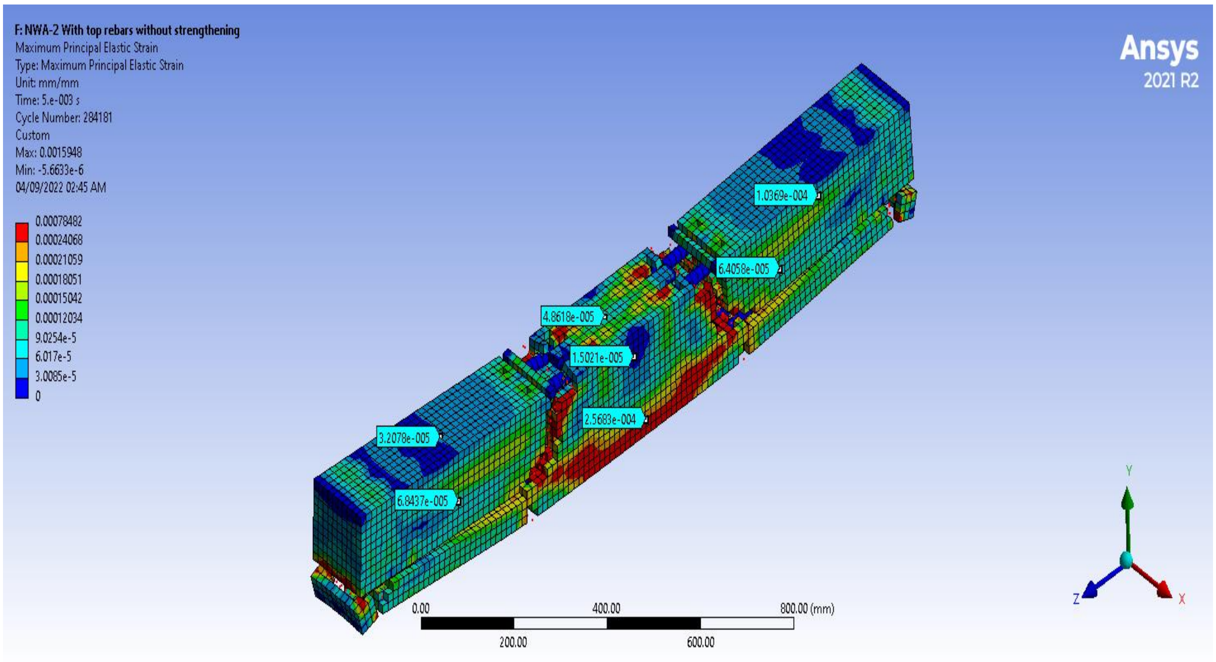

Figure 393(NWA-2/70.5MPa – Normal strain of beam sample without strengthening and with top rebars- Explicit Dynamic Analysis)

Shear Stress

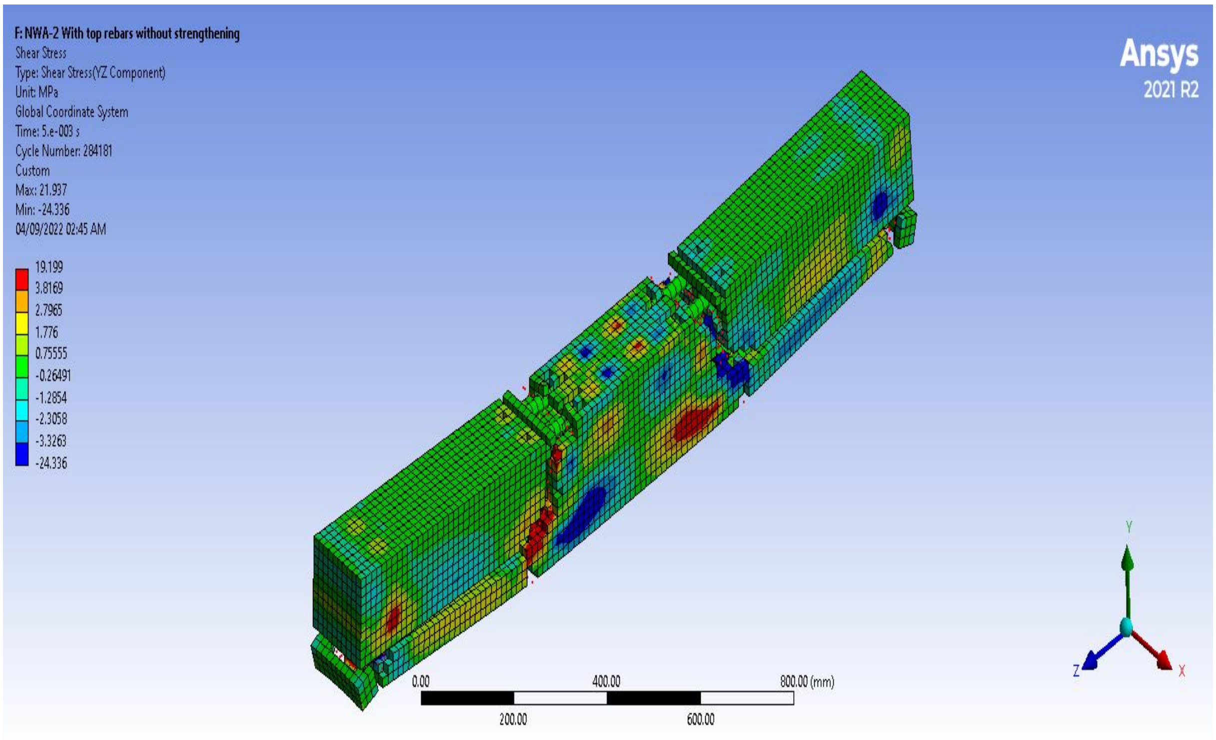

Figure 394(NWA-2/70.5MPa – Shear stress of beam sample without strengthening and with top rebars- Explicit Dynamic Analysis)

Total shape strain

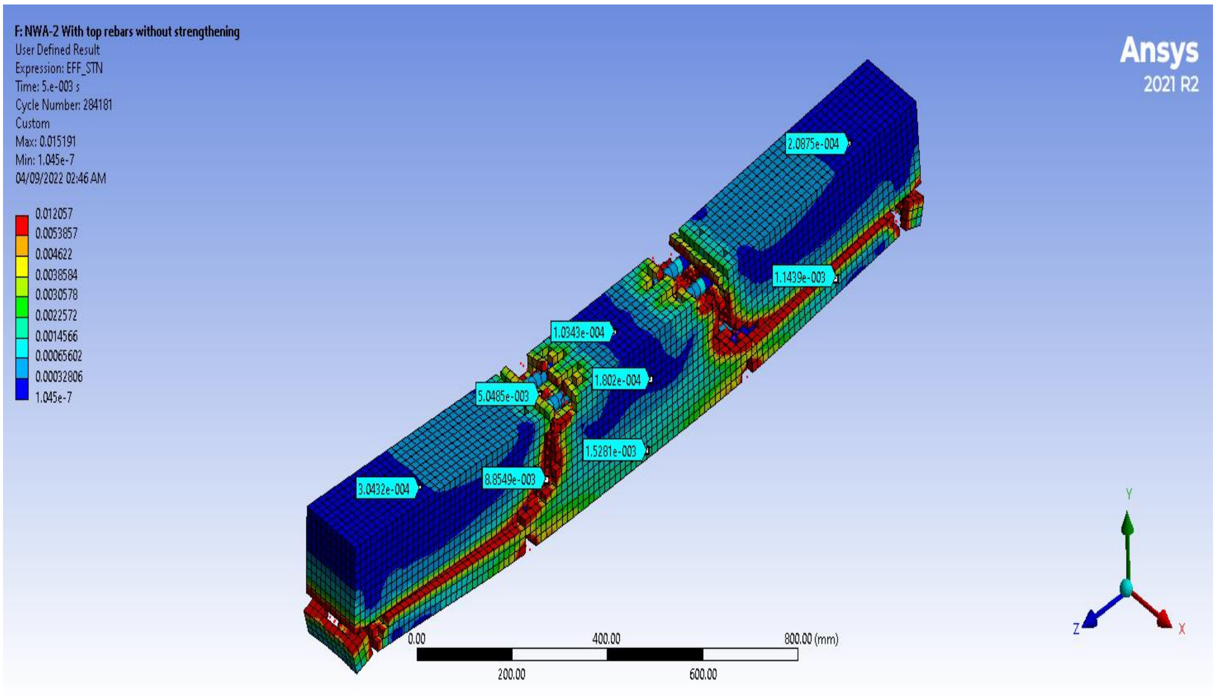

Figure 395(NWA-2/70.5MPa – Total strain of beam sample without strengthening and with top rebars- Explicit Dynamic Analysis)

Maximum Stress

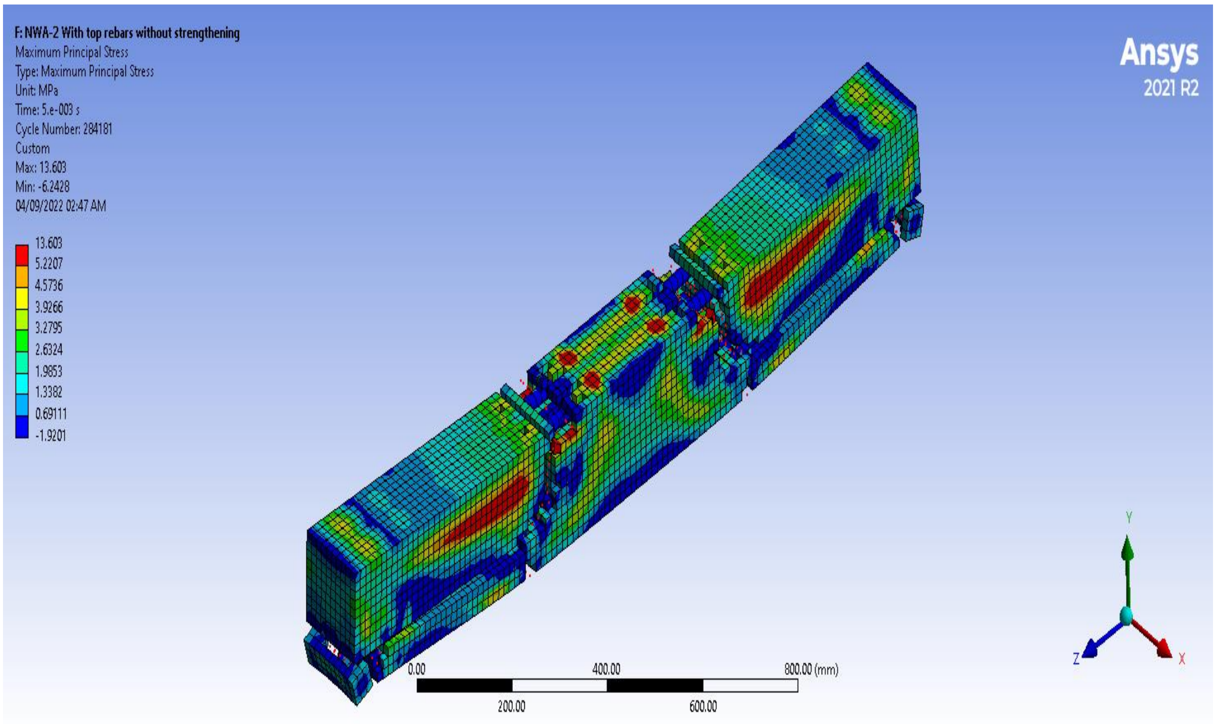

Figure 396(NWA-2/70.5MPa – Maximum stress of beam sample without strengthening and with top rebars- Explicit Dynamic Analysis)

The Damage Pattern

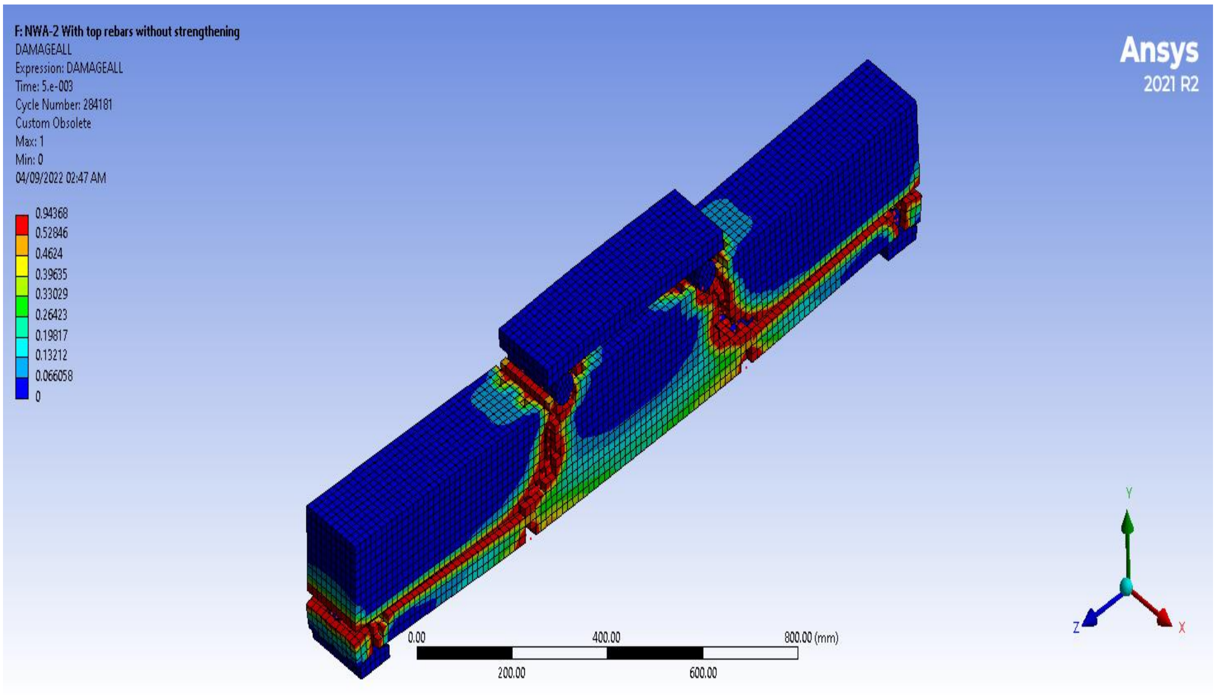

Figure 397(NWA-2/70.5MPa – Damage pattern-1 of beam sample without strengthening and with top rebars- Explicit Dynamic Analysis)

As we can see the shear damage cracks and concrete failures.

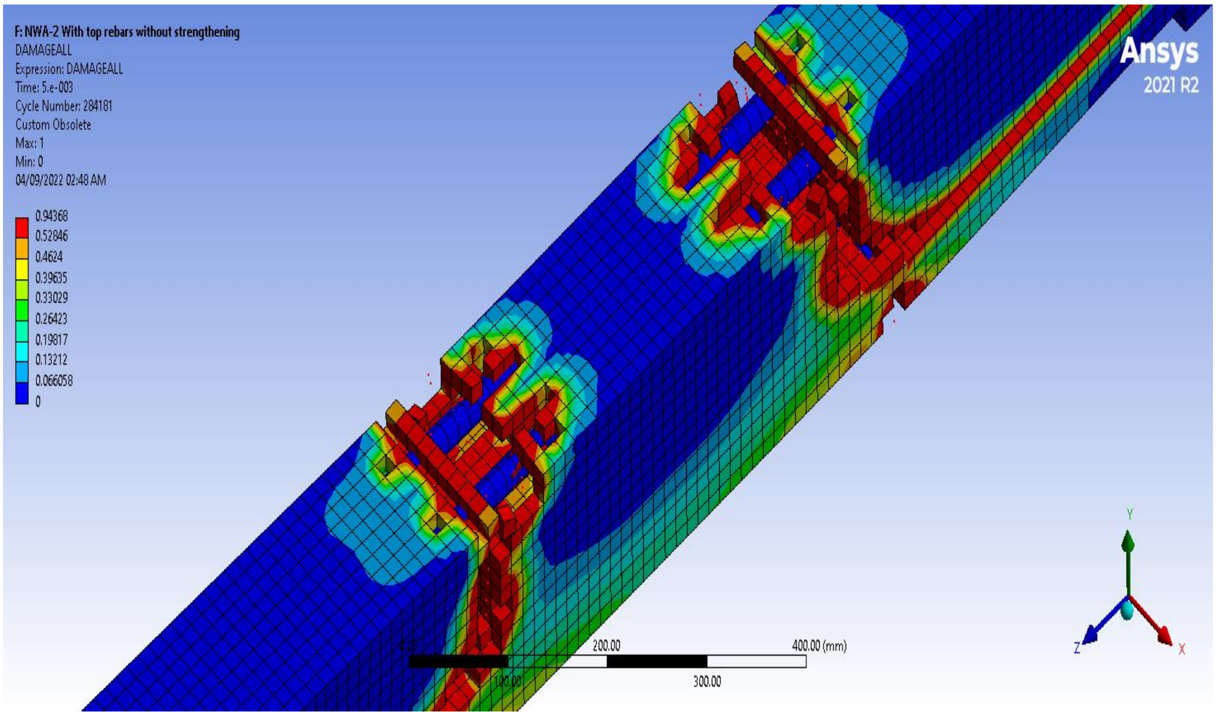

Figure 398(NWA-2/70.5MPa – Damage pattern-2 of beam sample without strengthening and with top rebars- Explicit Dynamic Analysis)

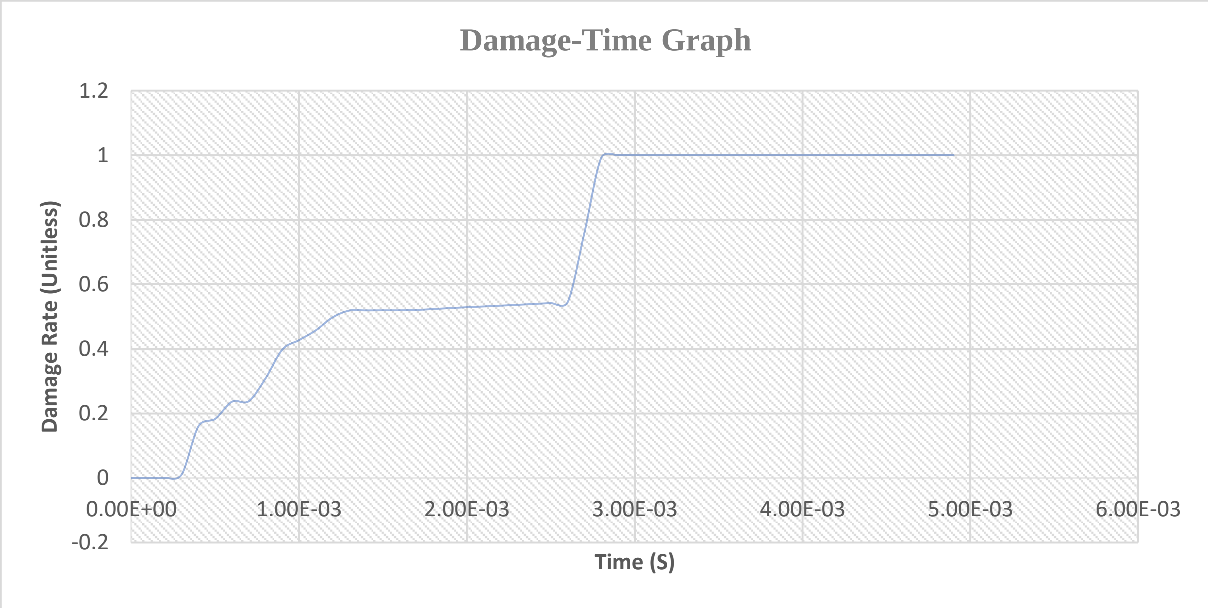

Figure 399(NWA-2/70.5MPa – Damage pattern graph of beam sample without strengthening and with top rebars- Explicit Dynamic Analysis)

28- Static Non-Linear Analysis - Without Strengthening and Top Rebars

Geometry and loads

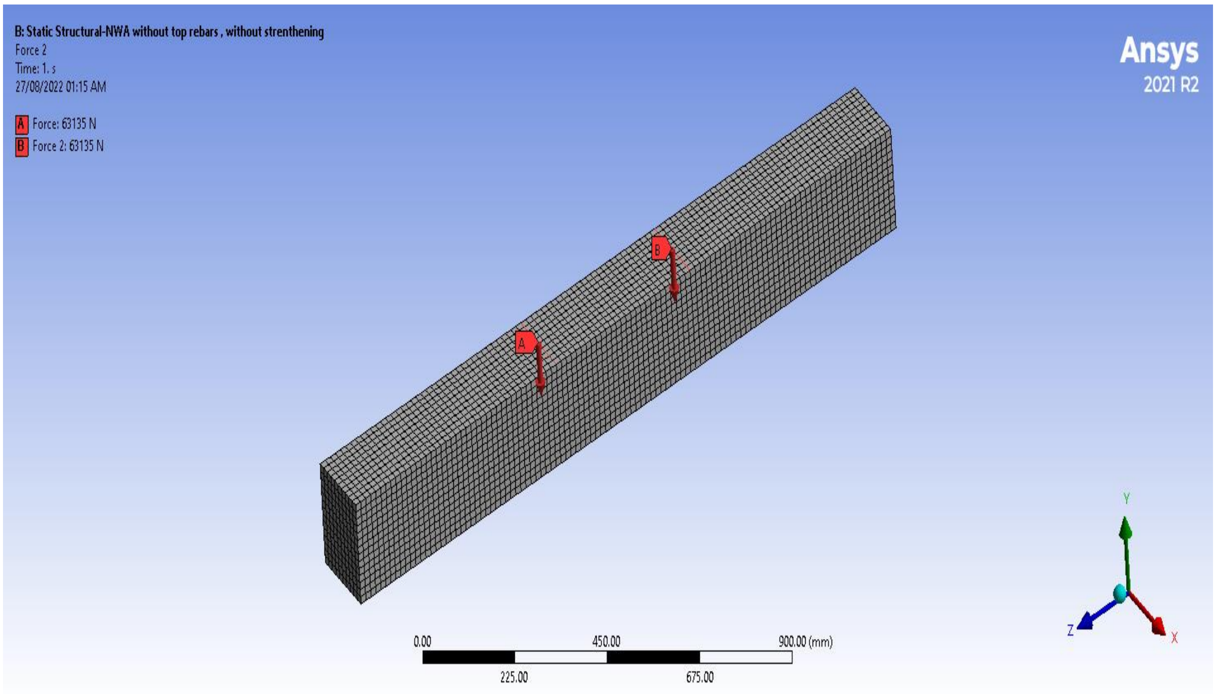

Figure 400(NWA-2/70.5MPa – Geometry & Loads of beam sample without strengthening and top rebars- Static Nonlinear Analysis)

The ultimate load has been divided in to loads which is 126.27/2 =63.135KN.

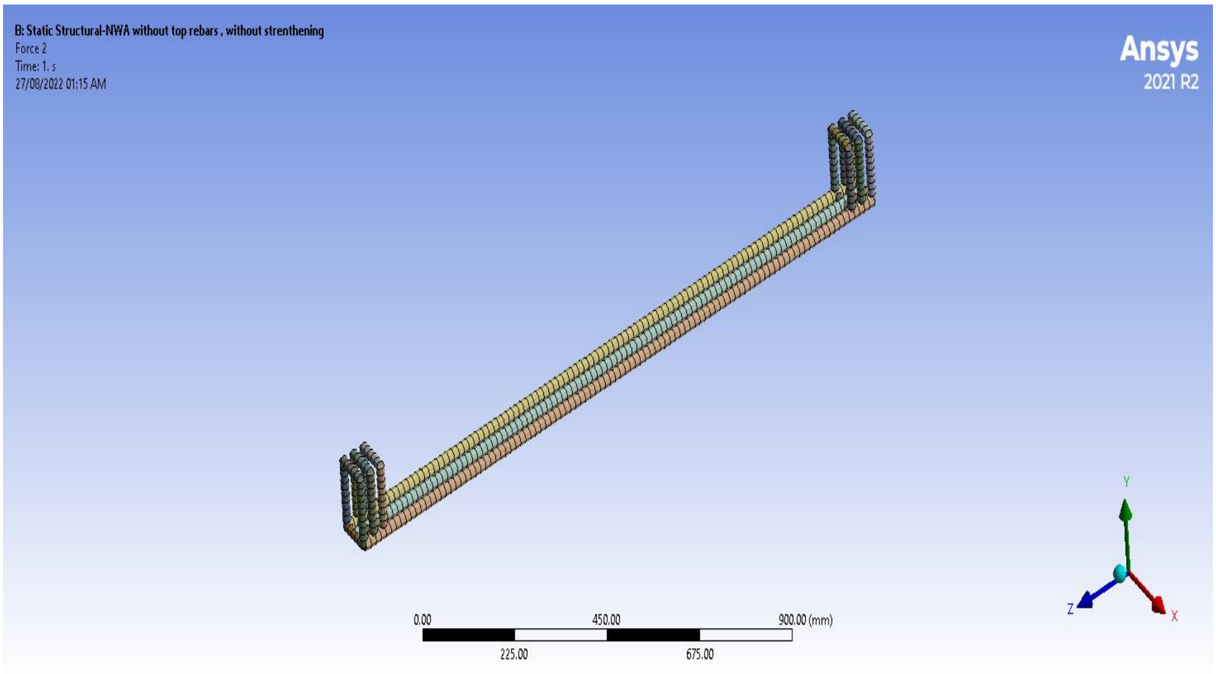

Figure 401(NWA-2/70.5MPa – Rebars of beam sample without strengthening - Static Nonlinear Analysis)

Deformations

Total Deformations

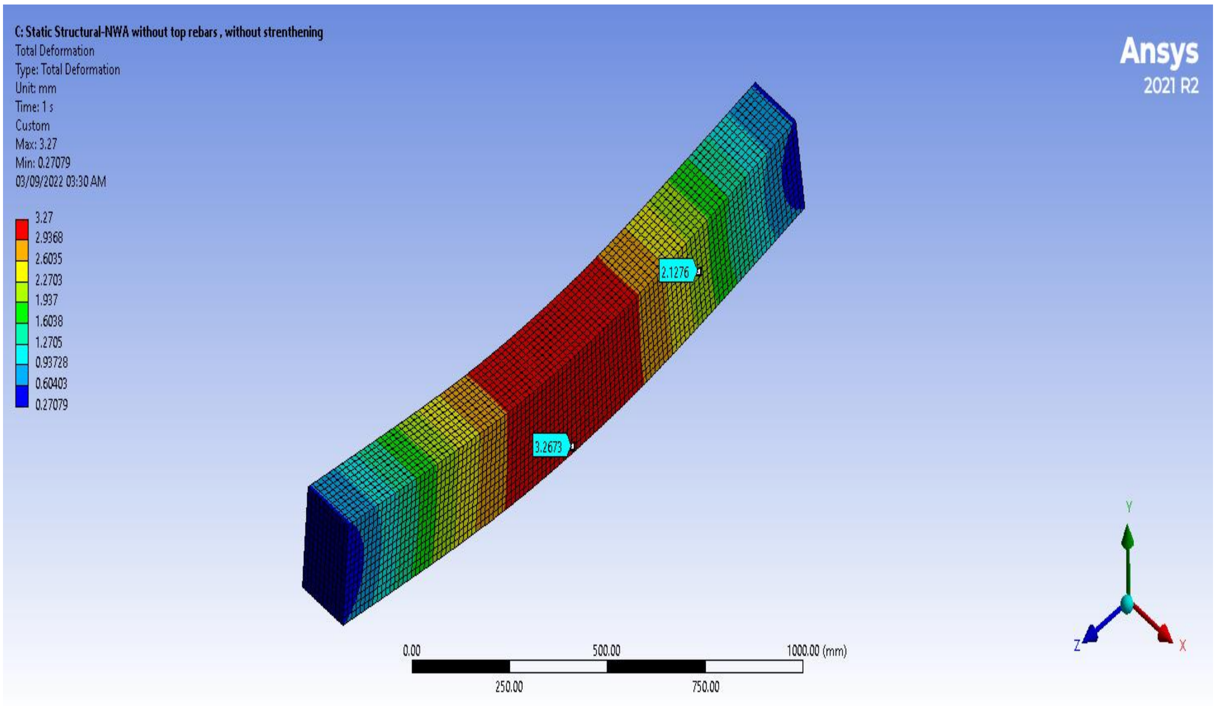

Figure 402(NWA-2/70.5MPa – Total deflections of beam sample without strengthening and top rebars- Static Nonlinear Analysis)

The value is 3.27 mm.

Directional Deformation (Y-Direction)

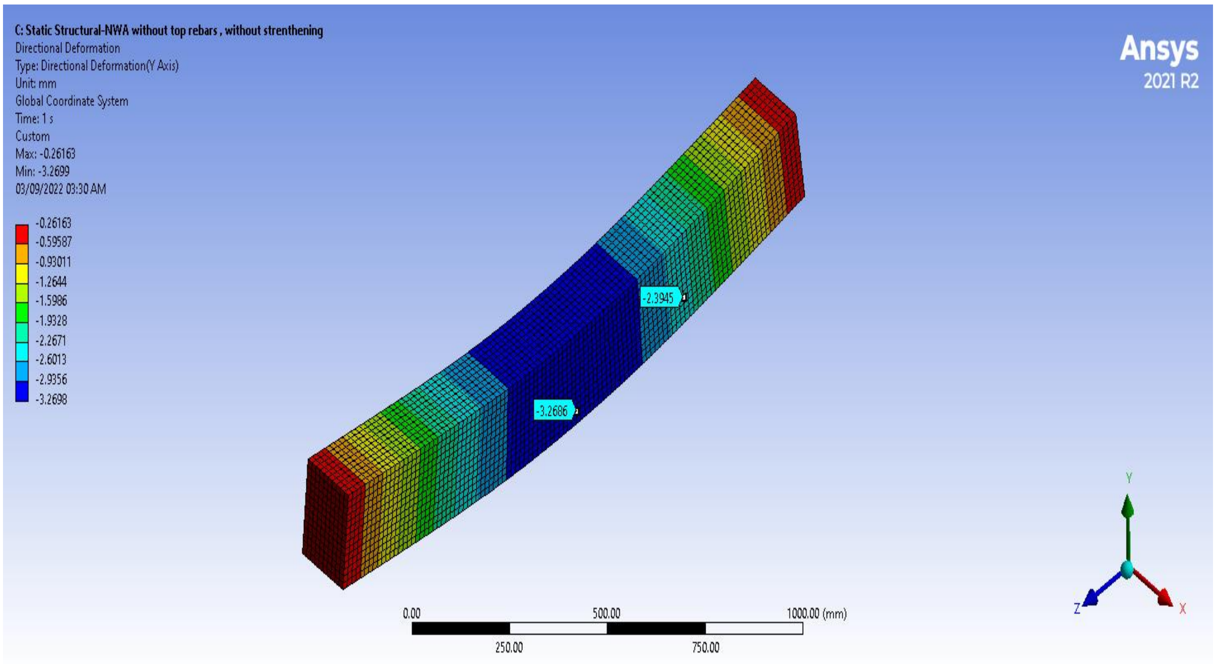

Figure 403(NWA-2/70.5MPa – Directional deflections (Y-Dim.) of beam sample without strengthening and top rebars- Static Nonlinear Analysis)

The value is 3.27 mm.

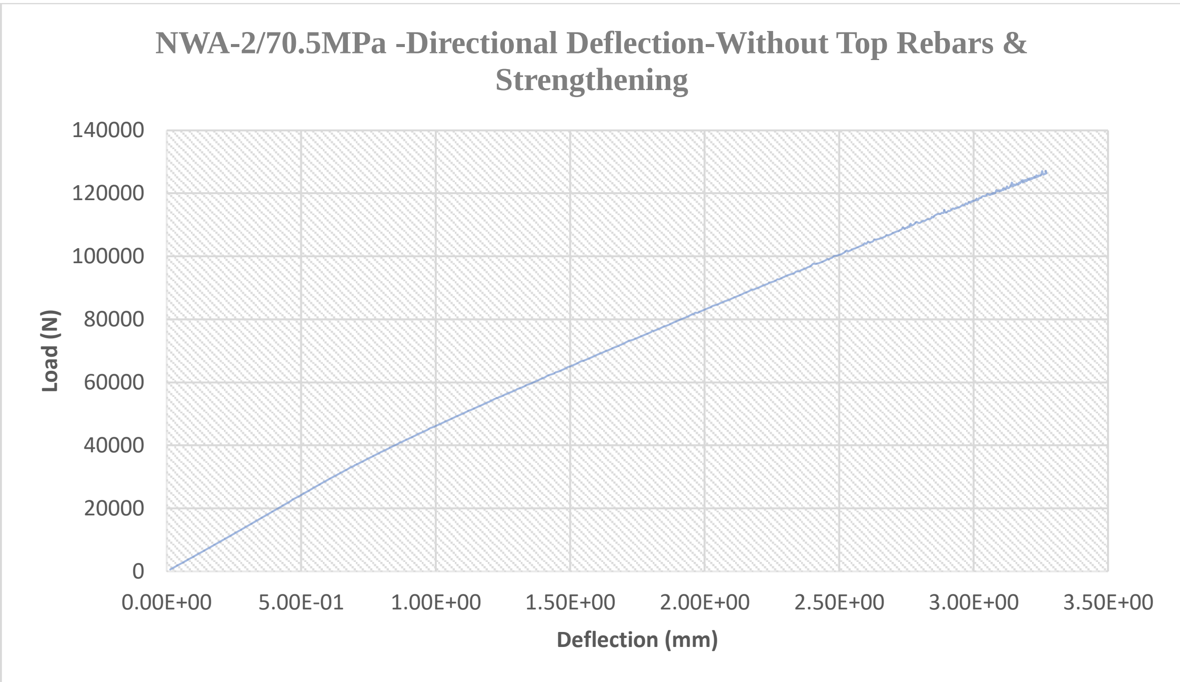

Figure 404(NWA-2/70.5MPa – Directional deflections (Y-Dim.) of beam sample without strengthening and top rebars- Static Nonlinear Analysis)

Normal Stress (Concrete)

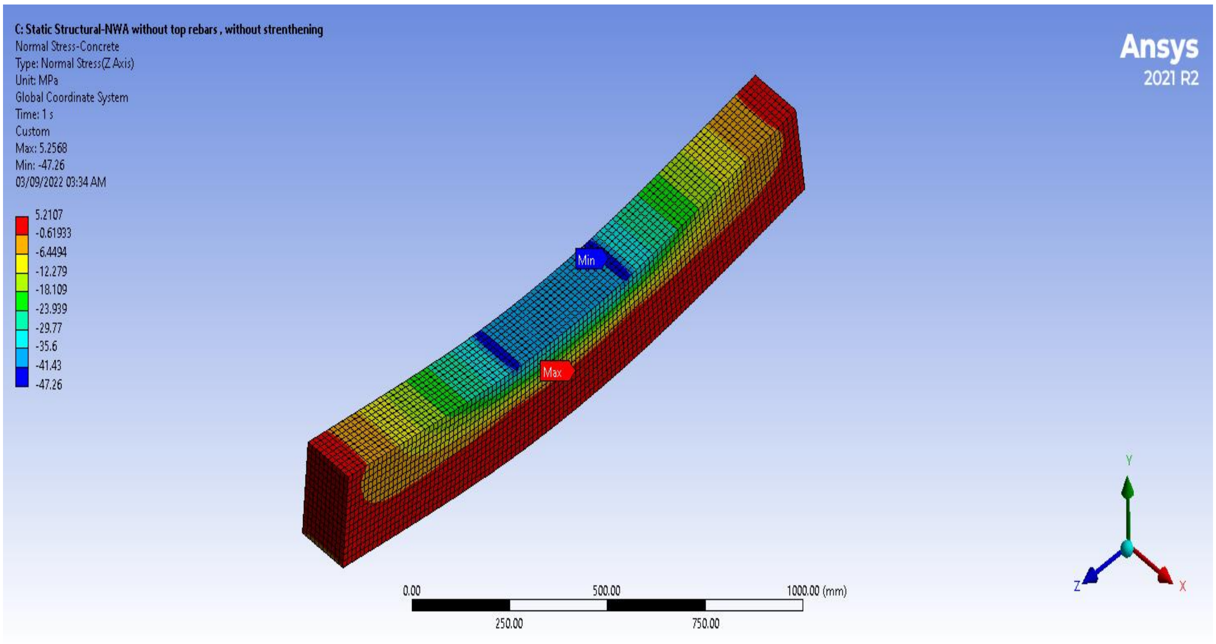

Figure 405(NWA-2/70.5MPa – Normal stress (Concrete) of beam sample without strengthening and top rebars- Static Nonlinear Analysis)

The blue zones show the crushing from loading machine and the maximum value is 47.237MPa, whereas the red zones indicate to tension.

Normal Stress (Rebars)

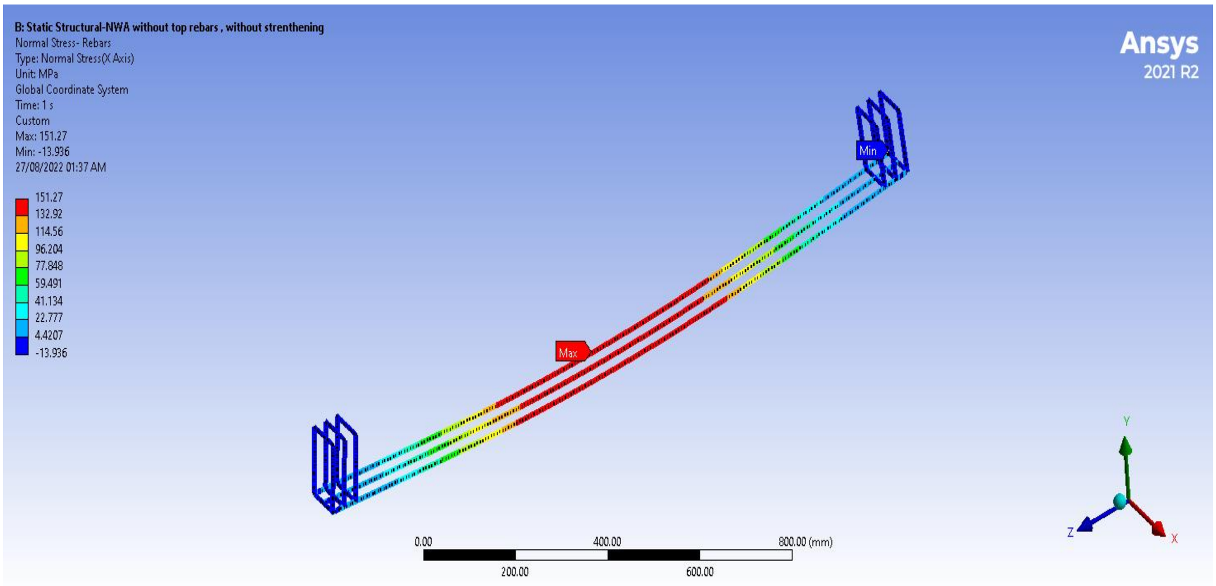

Figure 406(NWA-2/70.5MPa – Normal stress (Rebars) of beam sample without strengthening and with top rebars- Static Nonlinear Analysis)

The red zones show that the rebars is yielding by 151.27 MPa, in the middle span due to tension.

Shear Stress

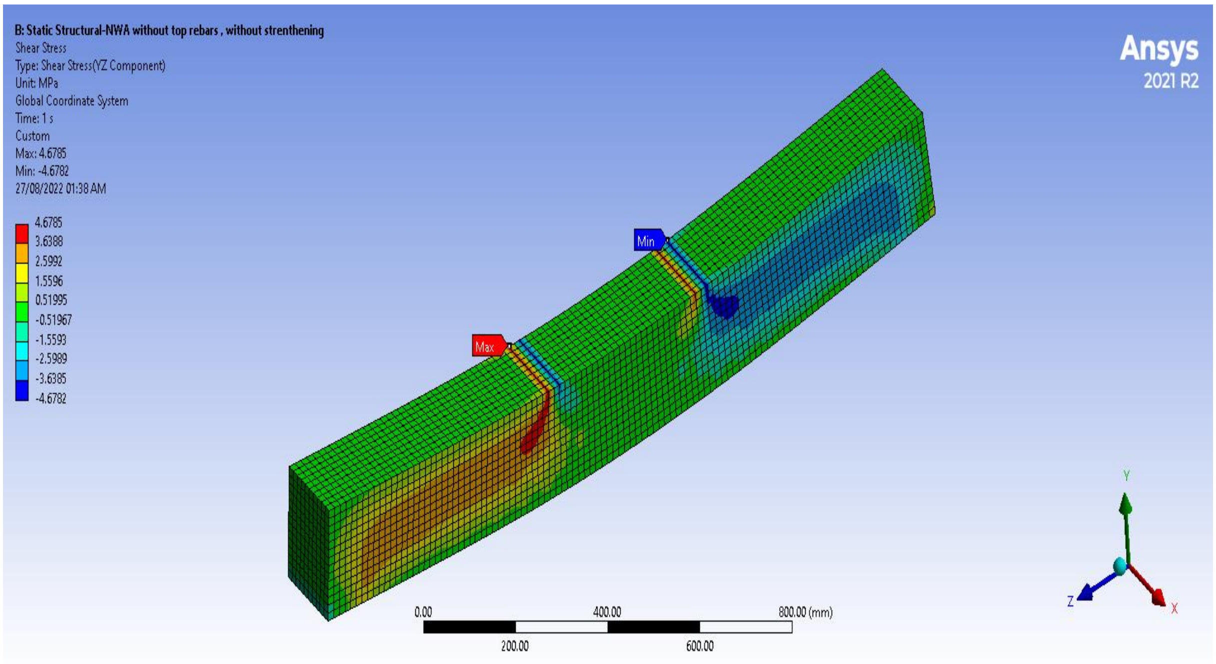

Figure 407(NWA-2/70.5MPa – Shear Stress of beam sample without strengthening and top rebars - Static Nonlinear Analysis)

Elastic Strain

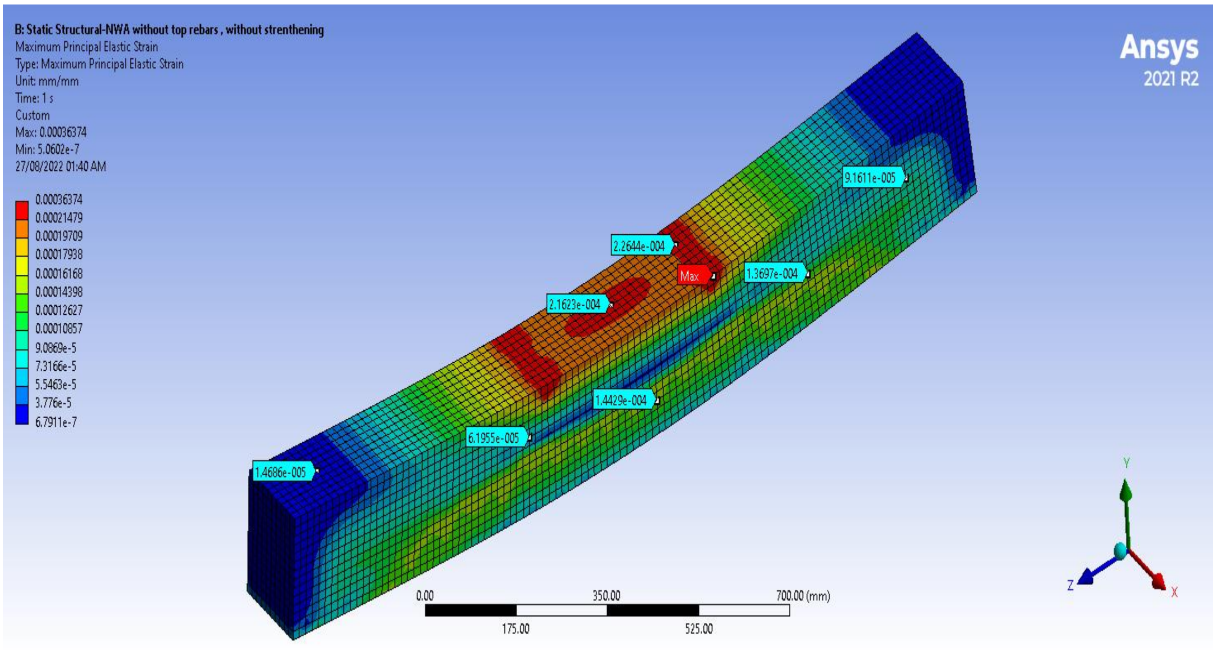

Figure 408(NWA-2/70.5MPa – Elastic Strain of beam sample without strengthening and top rebars - Static Nonlinear Analysis)

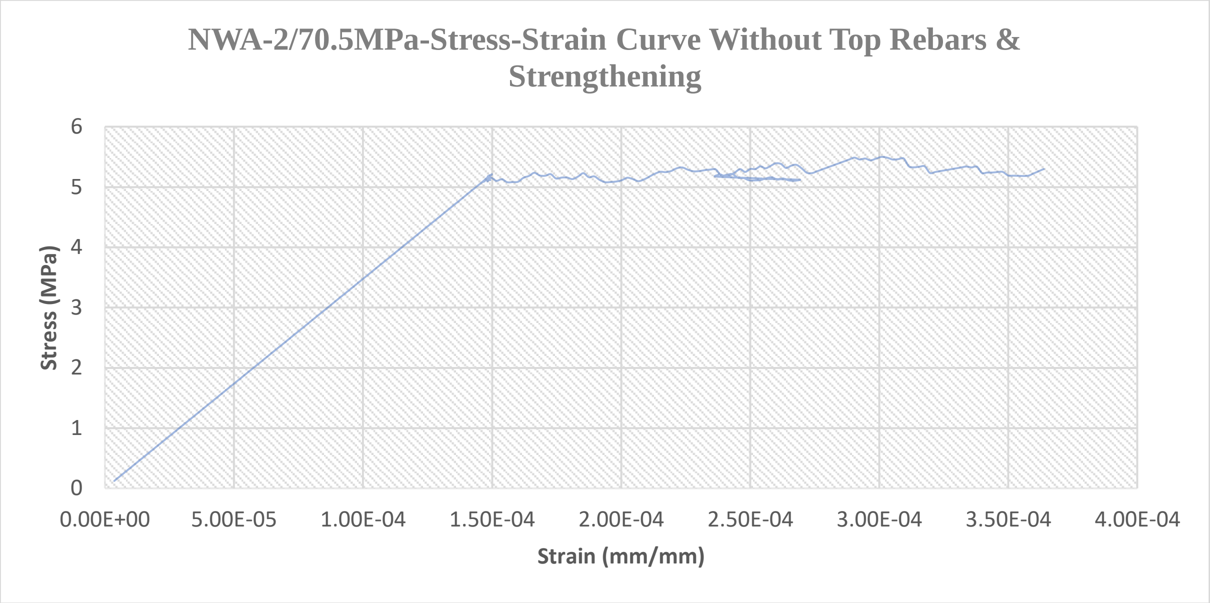

Figure 409(NWA-2/70.5MPa – Stress and Strain graph of beam sample without strengthening and top rebars - Static Nonlinear Analysis)

29- Explicit Dynamics-Without Top Rebars & Strengthening

Geometry and loads

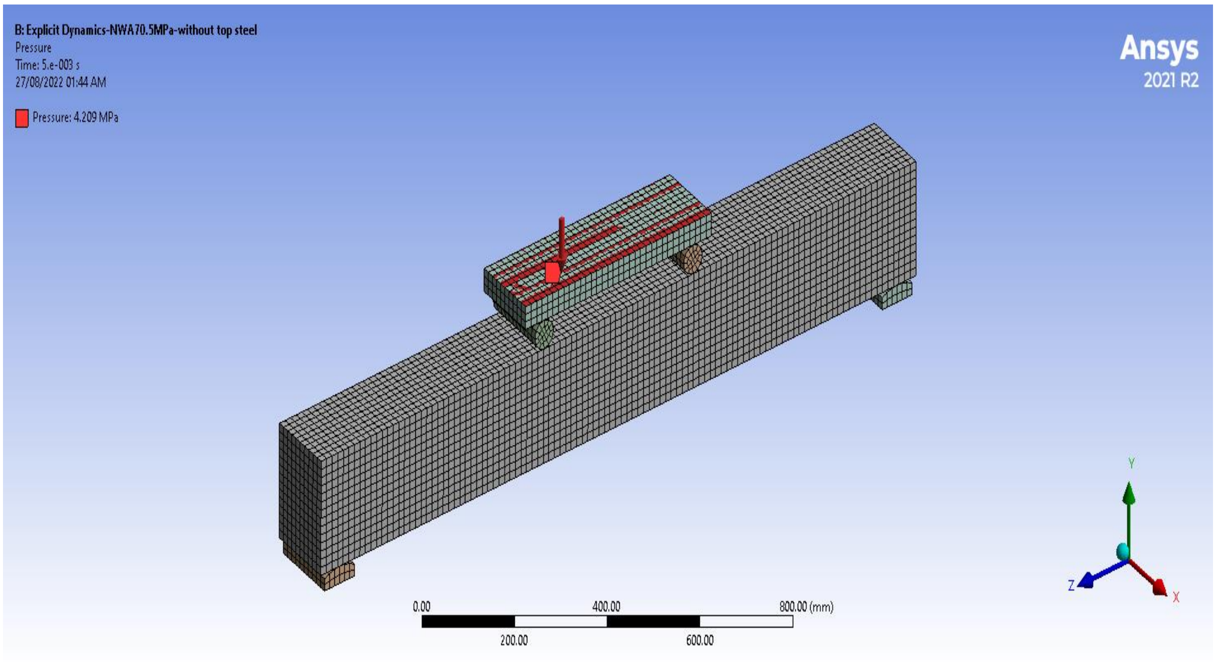

Figure 410(NWA-2/70.5MPa – Geometry & Loads of beam sample without strengthening and top rebars- Explicit Dynamic Analysis)

The ultimate load has been transferred to be as a pressure load which is 4.209 MPa as shown above with rate loading 0.6mm/min.

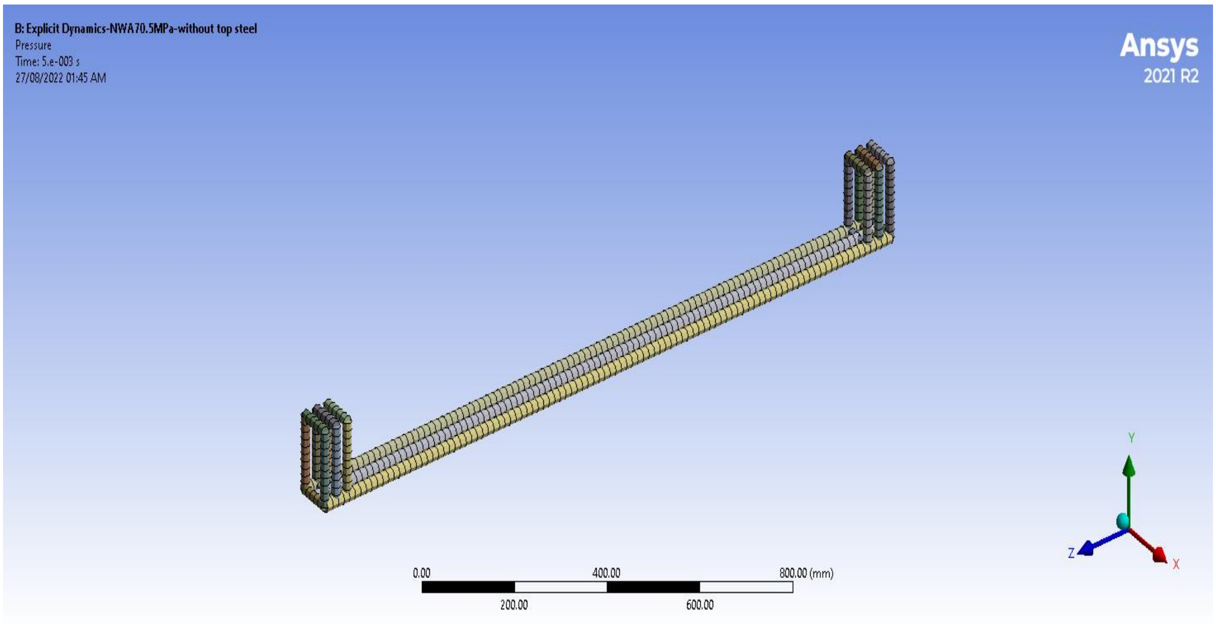

Figure 411(NWA-2/70.5MPa – Rebars of beam sample without strengthening - Explicit Dynamic Analysis)

Deformations

Total Deformations

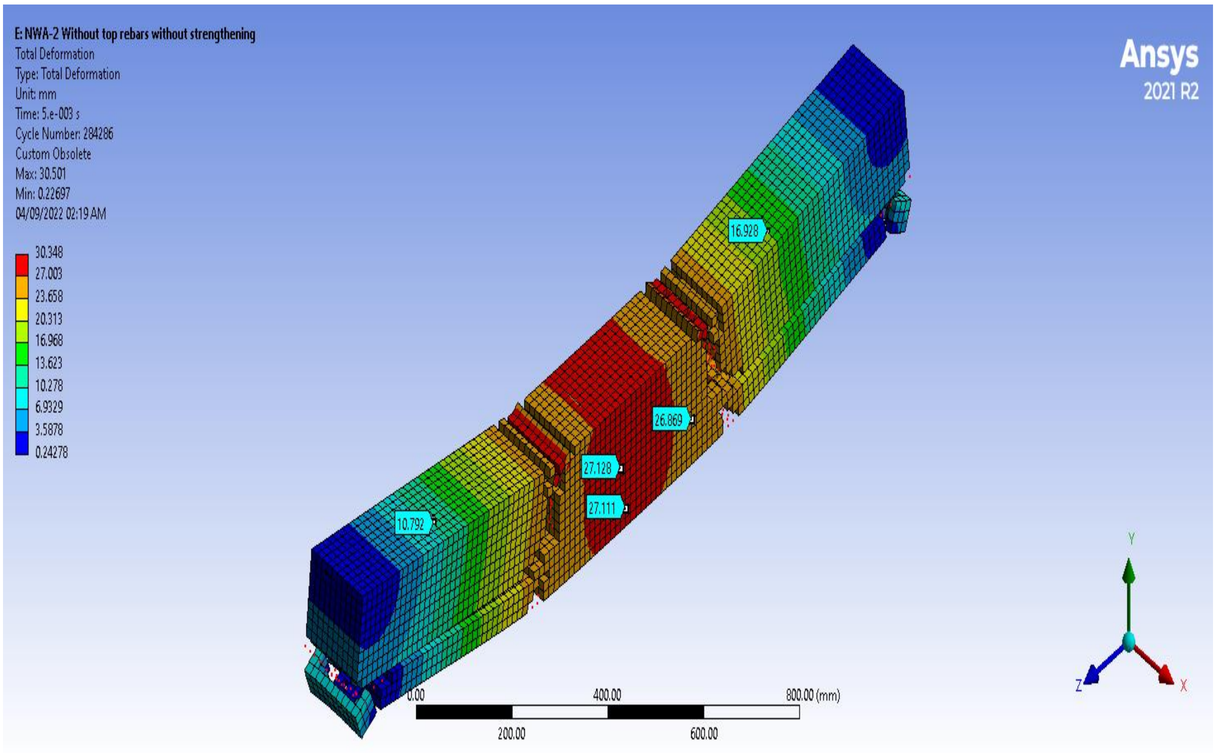

Figure 412(NWA-2/70.5MPa – Total deflections of beam sample without strengthening and top rebars- Explicit Dynamic Analysis)

The value is 27.128 mm.

-Directional Deformation (Y-Direction)-Concrete

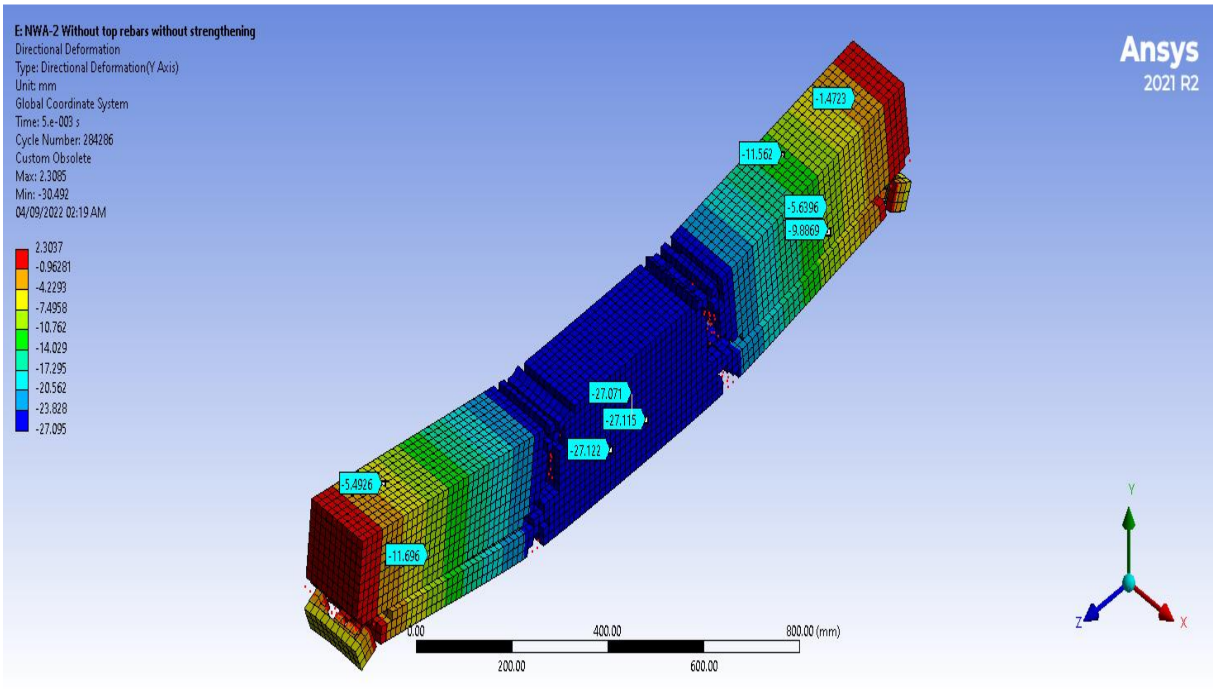

Figure 413(NWA-2/70.5MPa – Directional deflections (Y-Dir.) of beam sample without strengthening and top rebars- Explicit Dynamic Analysis)

The value is 23.35 mm.

Directional Deformation (Y-Direction)- Rebars

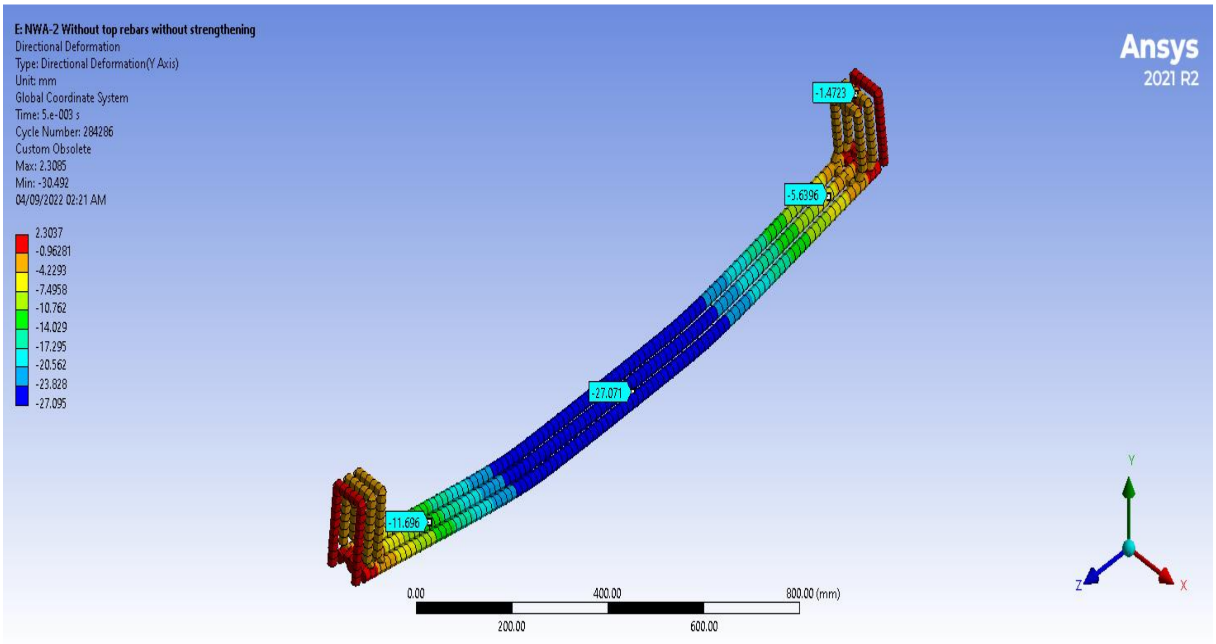

Figure 414(NWA-2/70.5MPa – Directional deflections (Y-Dir.) of beam rebars without strengthening- Explicit Dynamic Analysis)

Normal strain

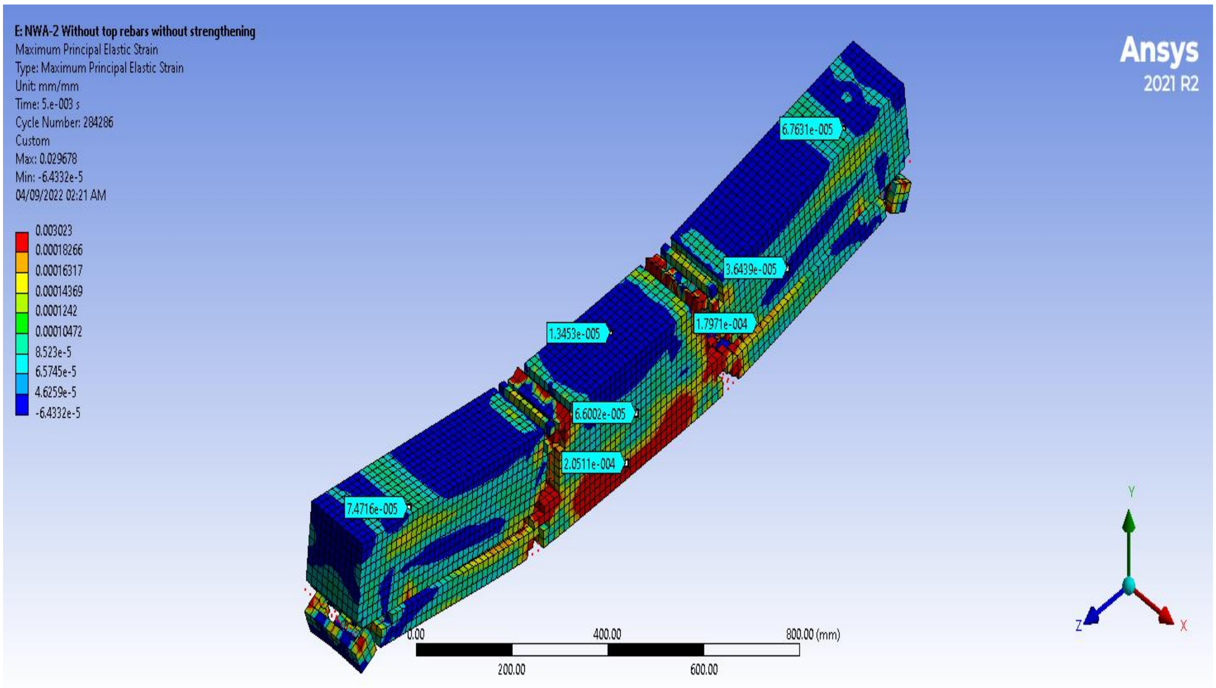

Figure 415(NWA-2/70.5MPa – Normal strain of beam sample without strengthening and top rebars- Explicit Dynamic Analysis)

Shear Stress

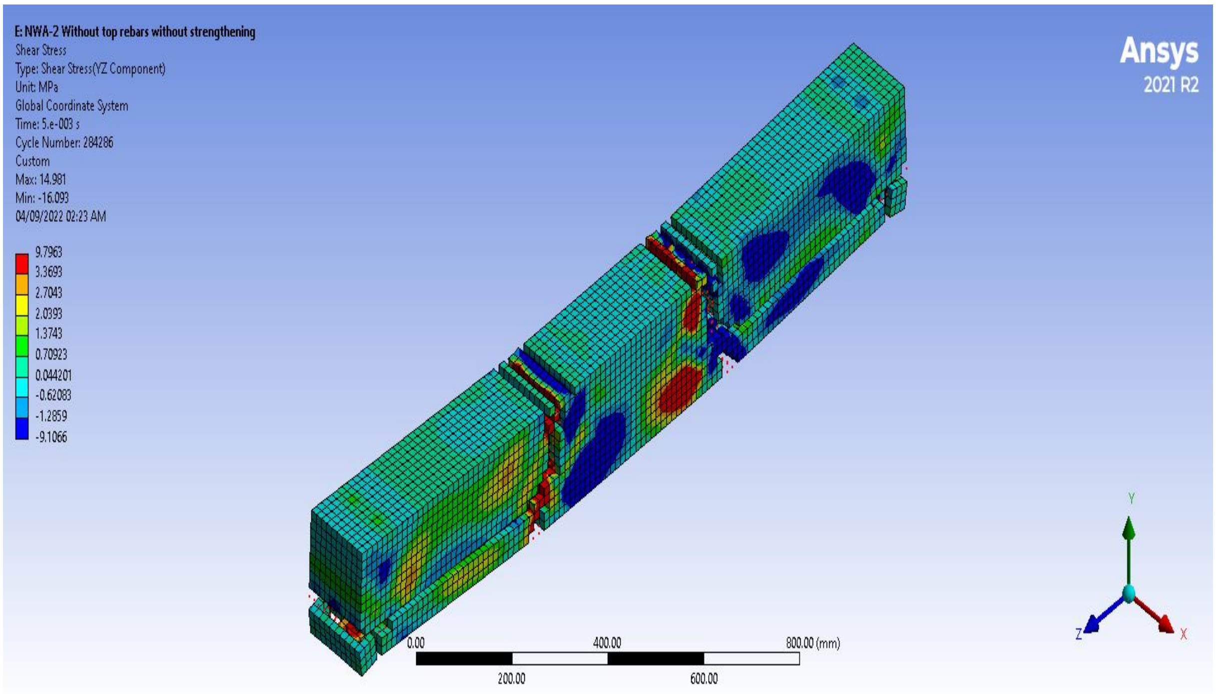

Figure 416(NWA-2/70.5MPa – Shear stress of beam sample without strengthening and top rebars- Explicit Dynamic Analysis)

Total shape strain

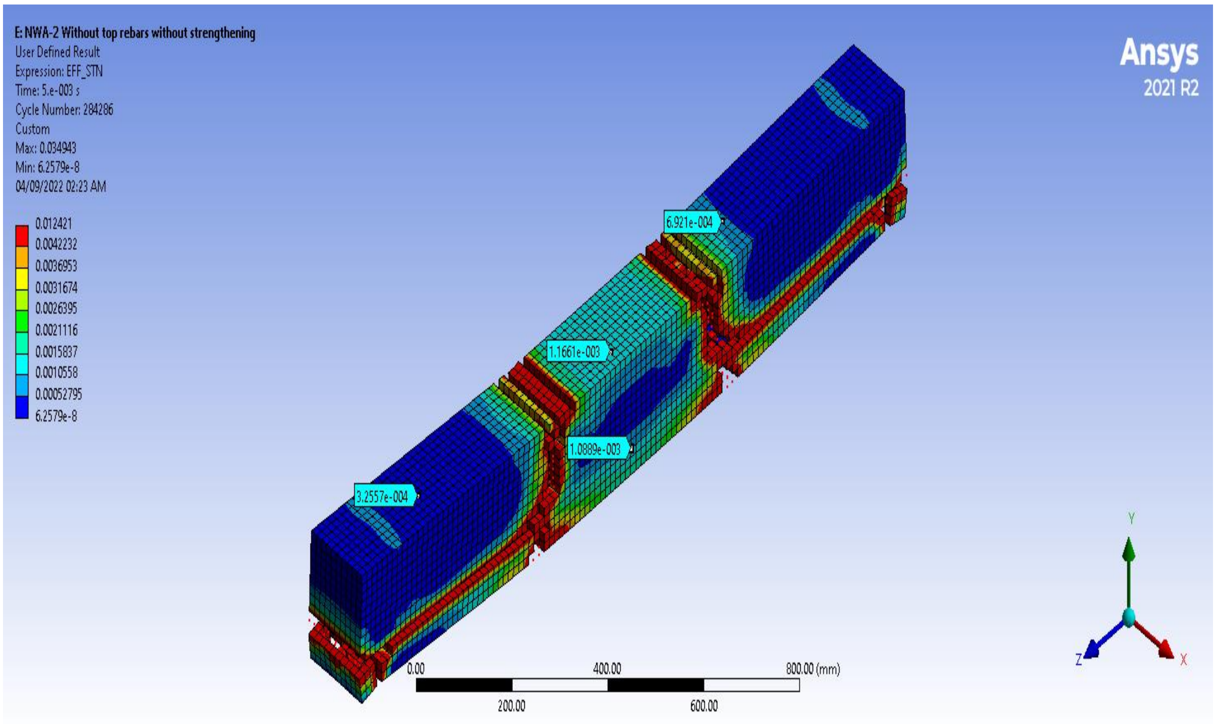

Figure 417(NWA-2/70.5MPa – Total strain of beam sample without strengthening and top rebars- Explicit Dynamic Analysis)

Maximum Stress

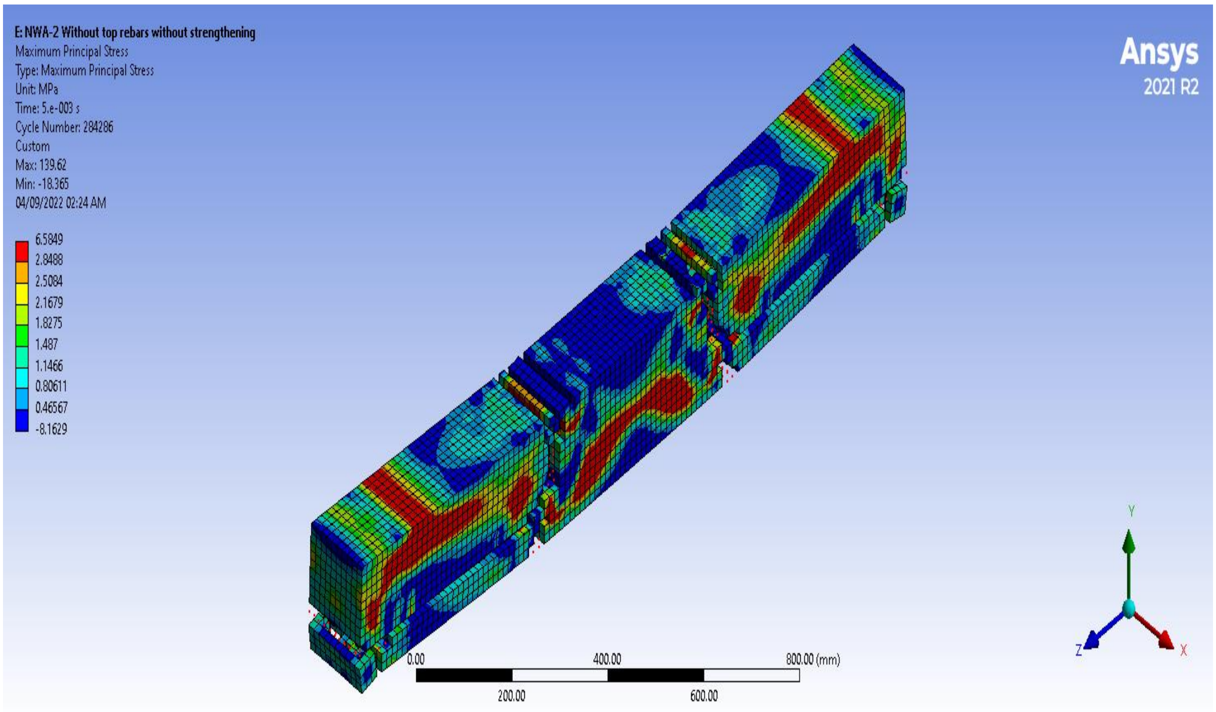

Figure 418(NWA-2/70.5MPa – Maximum stress of beam sample without strengthening and top rebars- Explicit Dynamic Analysis)

The Damage Pattern

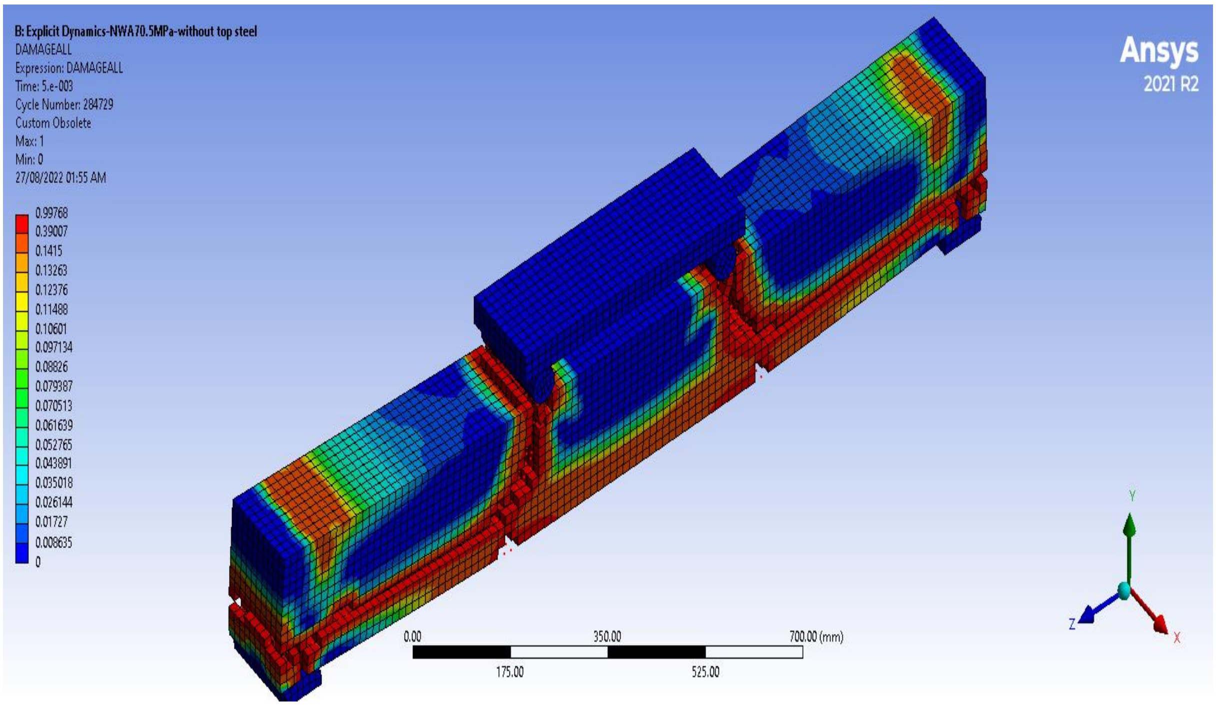

Figure 419(NWA-2/70.5MPa – Damage pattern-1 of beam sample without strengthening and top rebars- Explicit Dynamic Analysis)

As we can see the shear damage cracks and concrete failures.

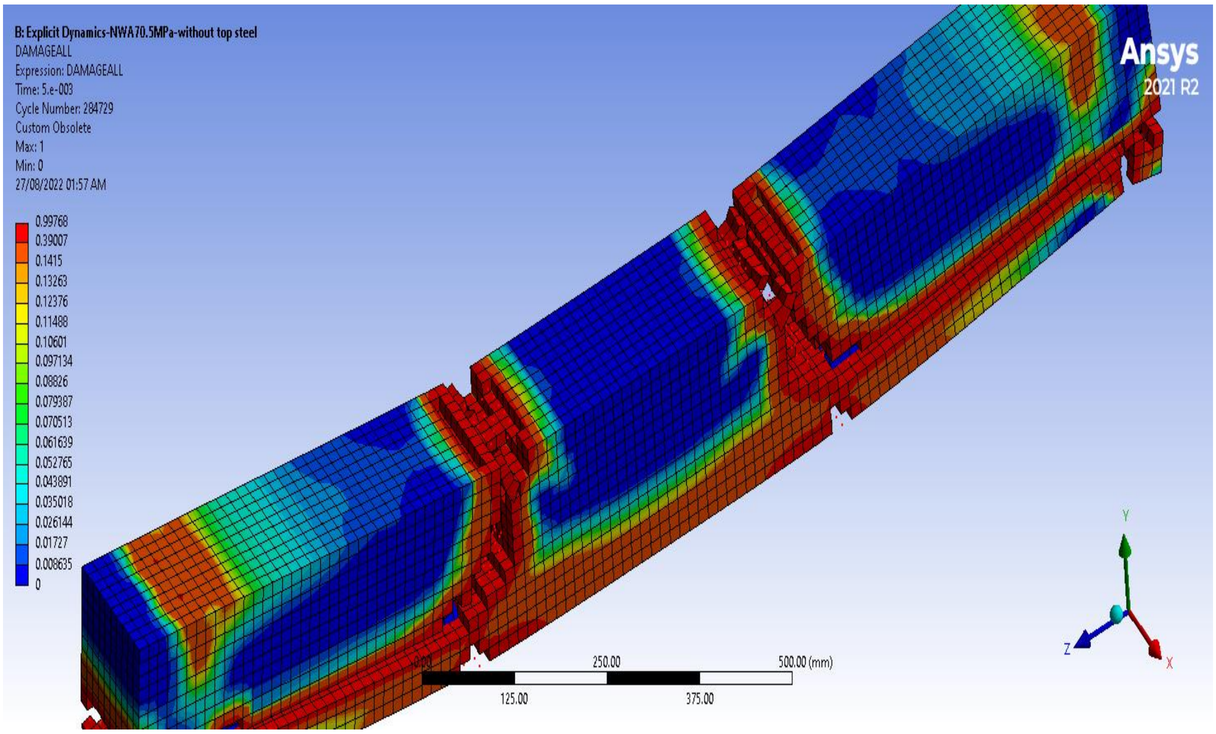

Figure 420(NWA-2/70.5MPa – Damage pattern-2 of beam sample without strengthening and top rebars- Explicit Dynamic Analysis)

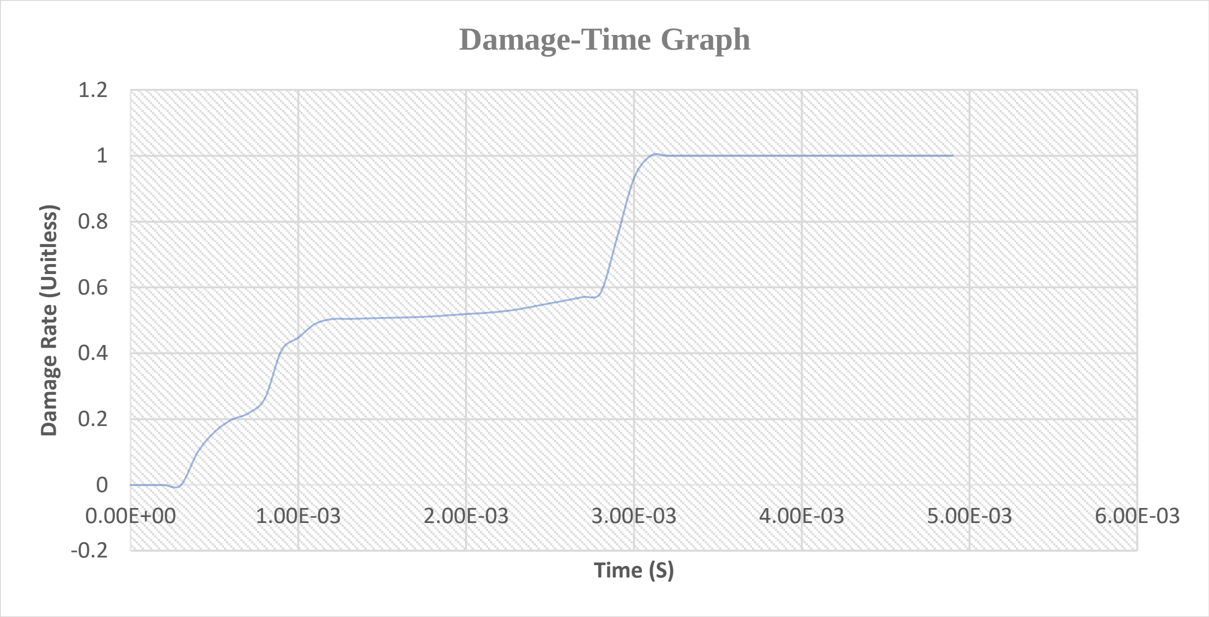

Figure 421(NWA-2/70.5MPa – Damage pattern graph of beam sample without strengthening and top rebars- Explicit Dynamic Analysis)

30- Static Non-Linear Analysis – With Top Rebars and Strengthening

Geometry and loads

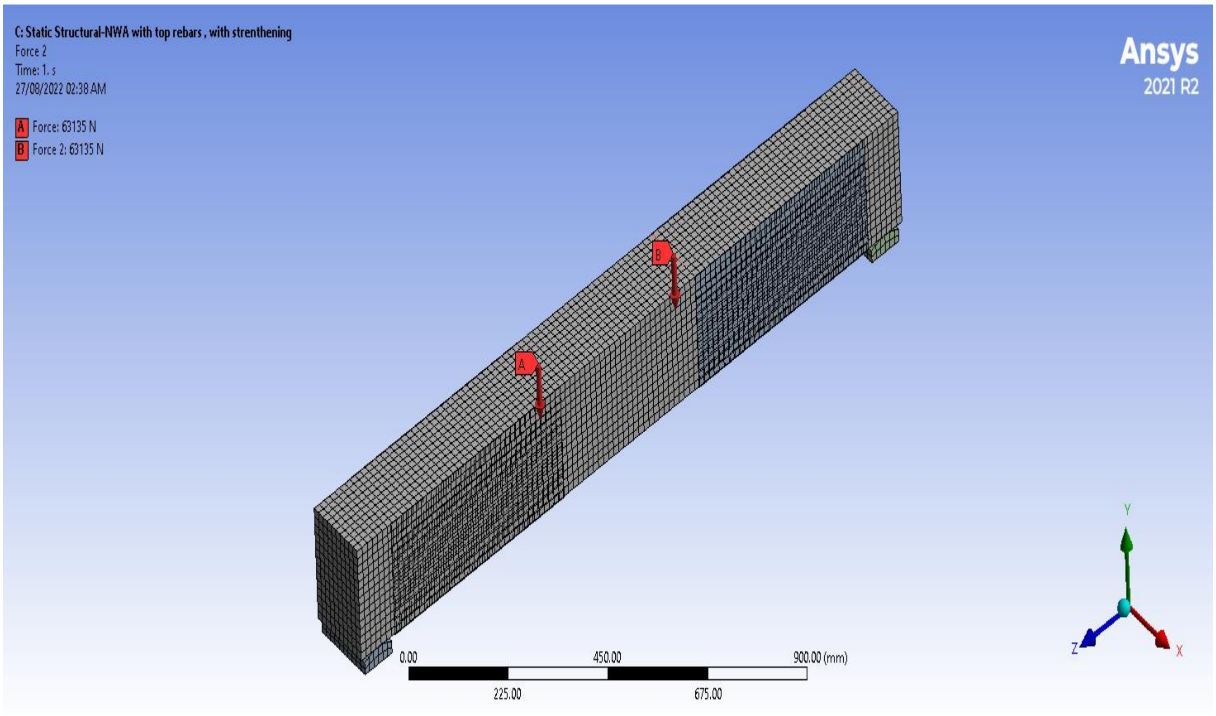

Figure 422(NWA-2/70.5MPa – Geometry & loads of beam sample with strengthening and top rebars- Static Nonlinear Analysis)

The ultimate load has been divided in to loads which is 126.27/2 =63.135KN.

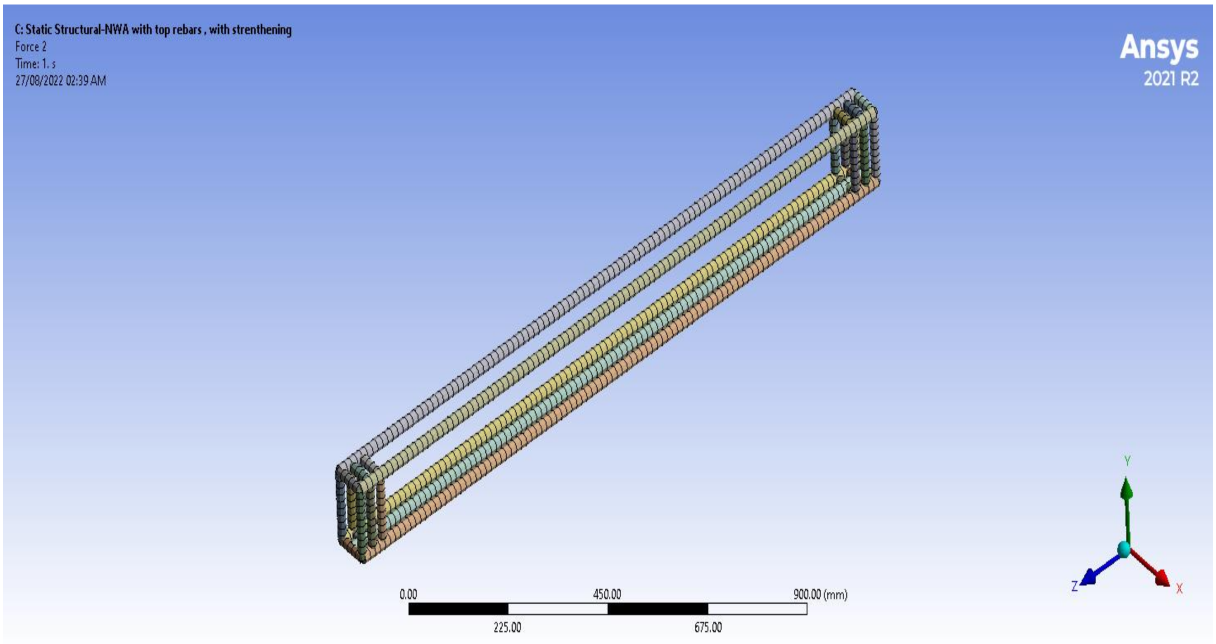

Figure 423(NWA-2/70.5MPa –Rebars of beam sample with strengthening- Static Nonlinear Analysis)

Deformations

Total Deformations

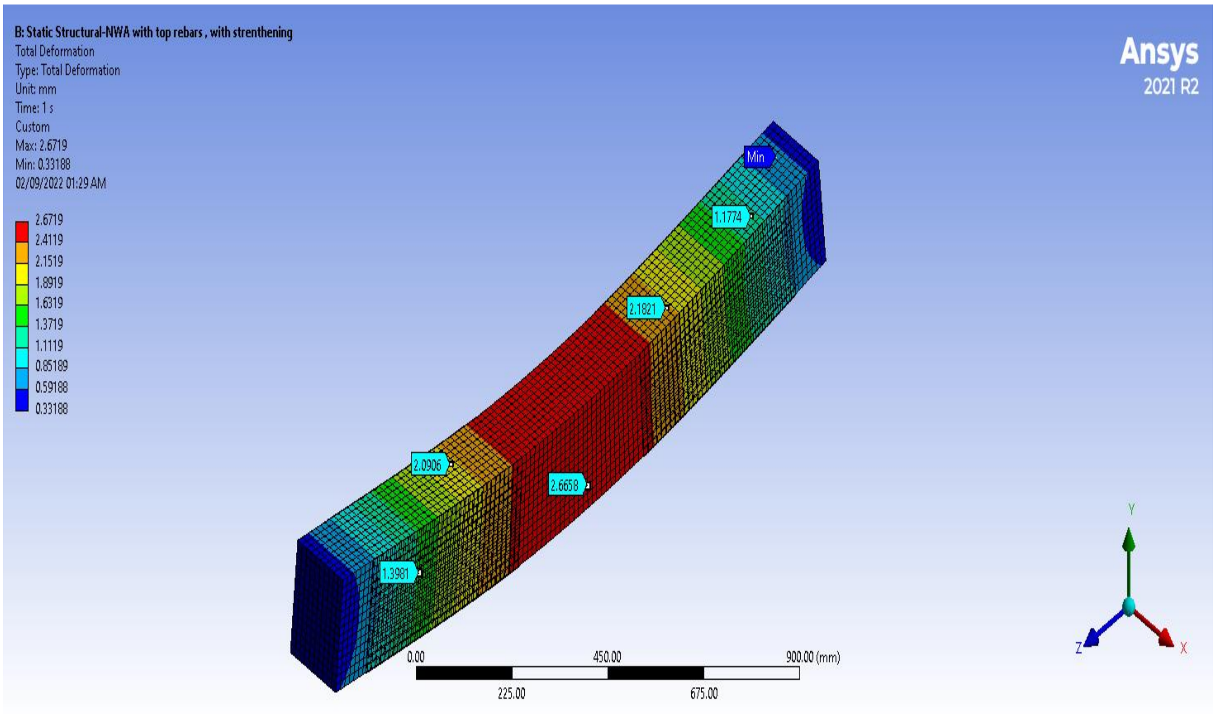

Figure 424(NWA-2/70.5MPa – Total deflections of beam sample with strengthening and top rebars- Static Nonlinear Analysis)

The value is 2.6719 mm.

Directional Deformation (Y-Direction)

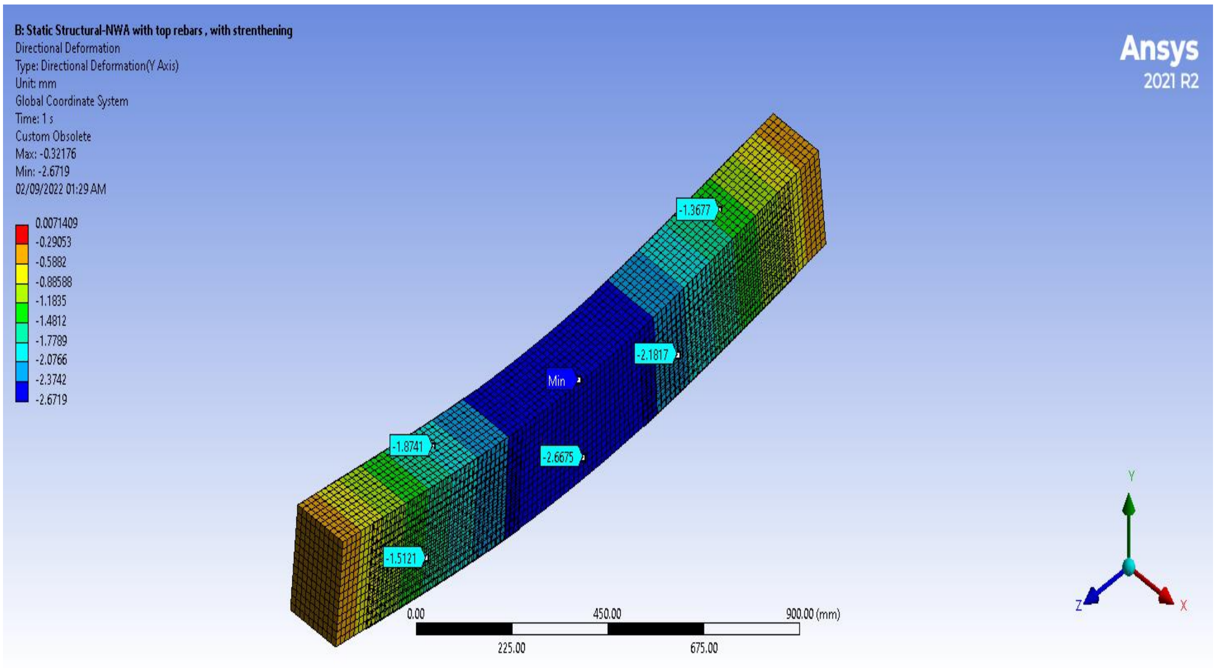

Figure 425(NWA-2/70.5MPa – Directional deflections (Y-Dim.) of beam sample with strengthening and top rebars- Static Nonlinear Analysis)

The value is 2.6719 mm.

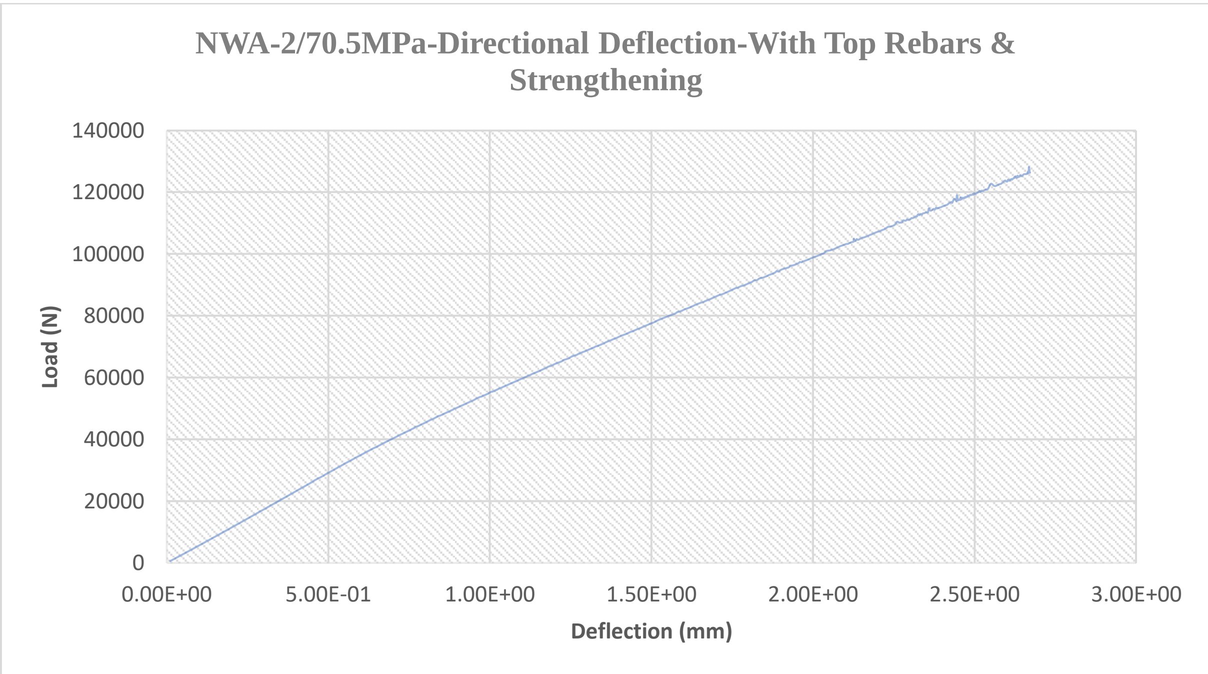

Figure 426(NWA-2/70.5MPa – Directional deflections (Y-Dim.) graph of beam sample with strengthening and top rebars- Static Nonlinear Analysis)

Normal Stress (Concrete)

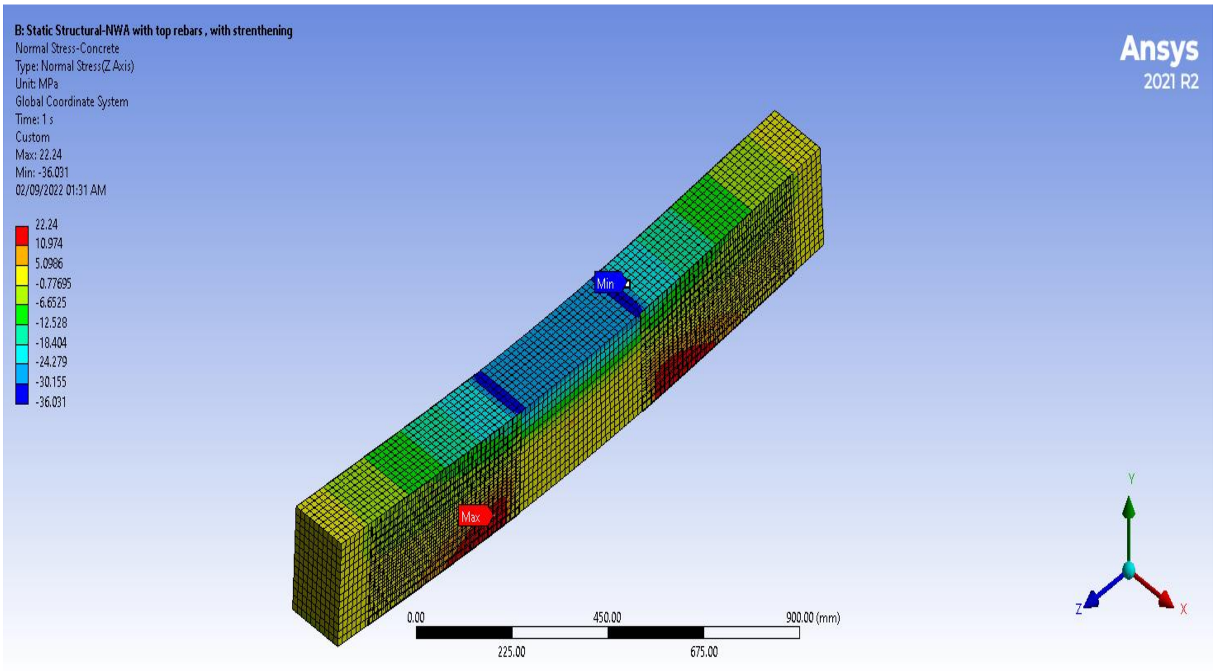

Figure 427(NWA-2/70.5MPa – Normal Stress (Concrete) of beam sample with strengthening and top rebars- Static Nonlinear Analysis)

The blue zones show the crushing from loading machine and the maximum value is 36.031 MPa, whereas the red zones indicate to tension.

Normal Stress (Rebars)

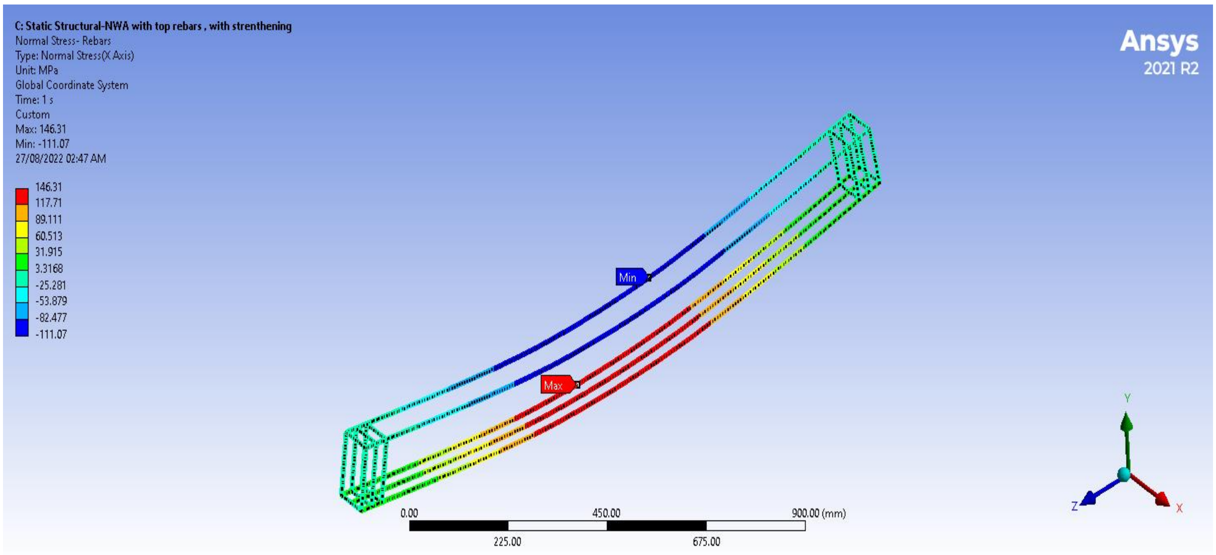

Figure 428(NWA-2/70.5MPa – Normal Stress (Rebars) of beam sample with strengthening and top rebars- Static Nonlinear Analysis)

The red zones show that the rebars is yielding by 146.31MPa, in the middle span due to tension.

Shear Stress

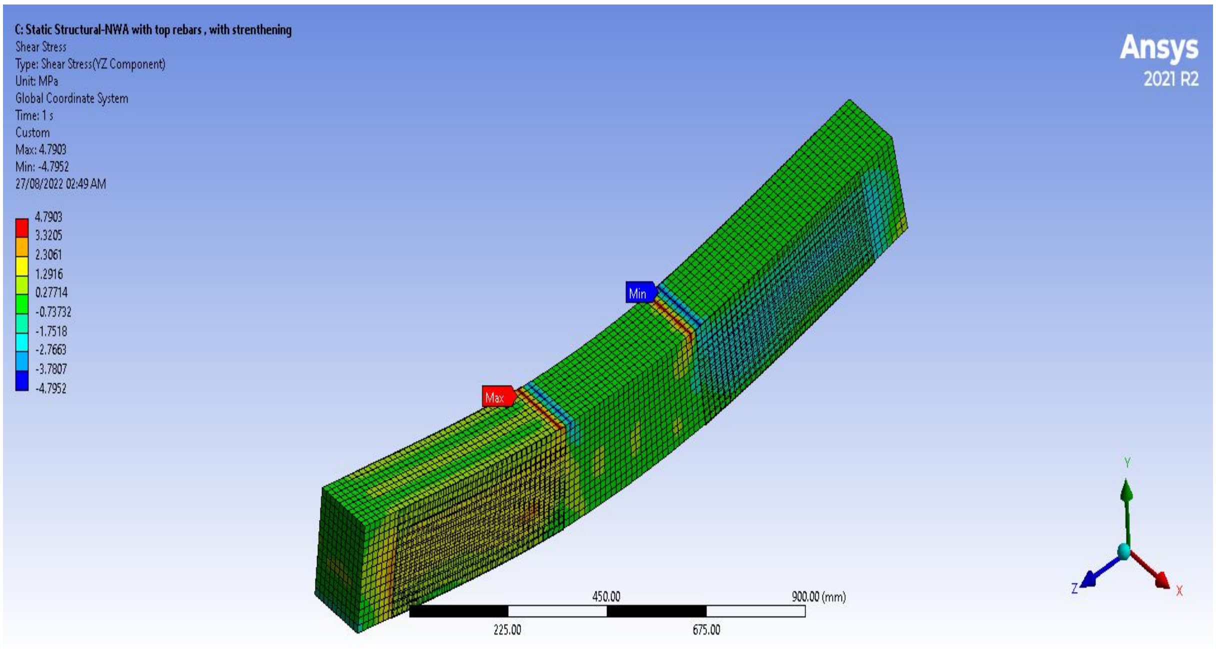

Figure 429(NWA-2/70.5MPa – Shear Stress of beam sample with strengthening and top rebars- Static Nonlinear Analysis)

Elastic Strain

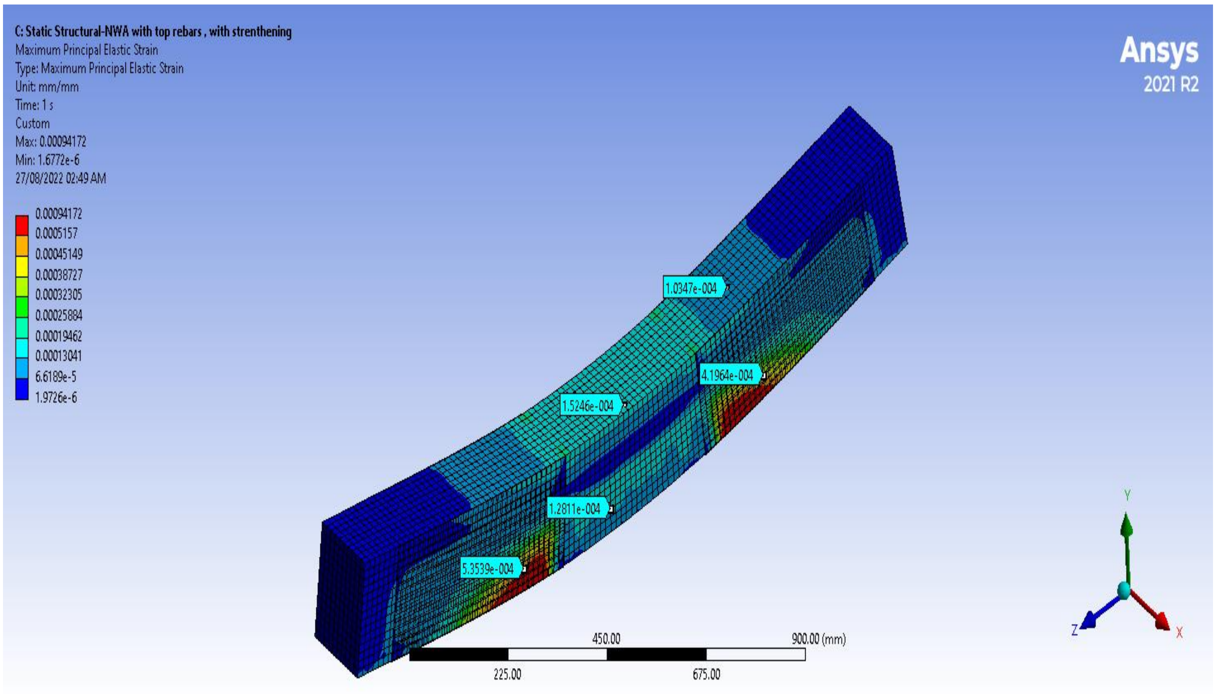

Figure 430(NWA-2/70.5MPa – Elastic strain of beam sample with strengthening and top rebars- Static Nonlinear Analysis)

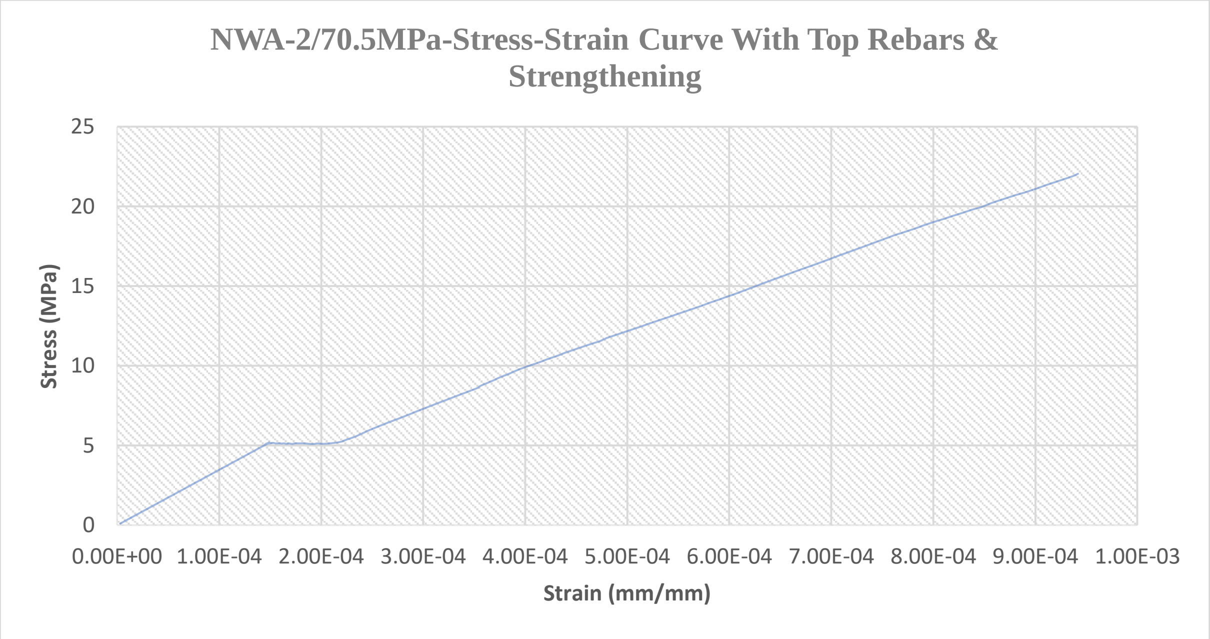

Figure 431(NWA-2/70.5MPa – Stress & Strain graph of beam sample with strengthening and top rebars- Static Nonlinear Analysis)

31- Explicit Dynamic-With Top Rebars & Strengthening

Geometry and loads

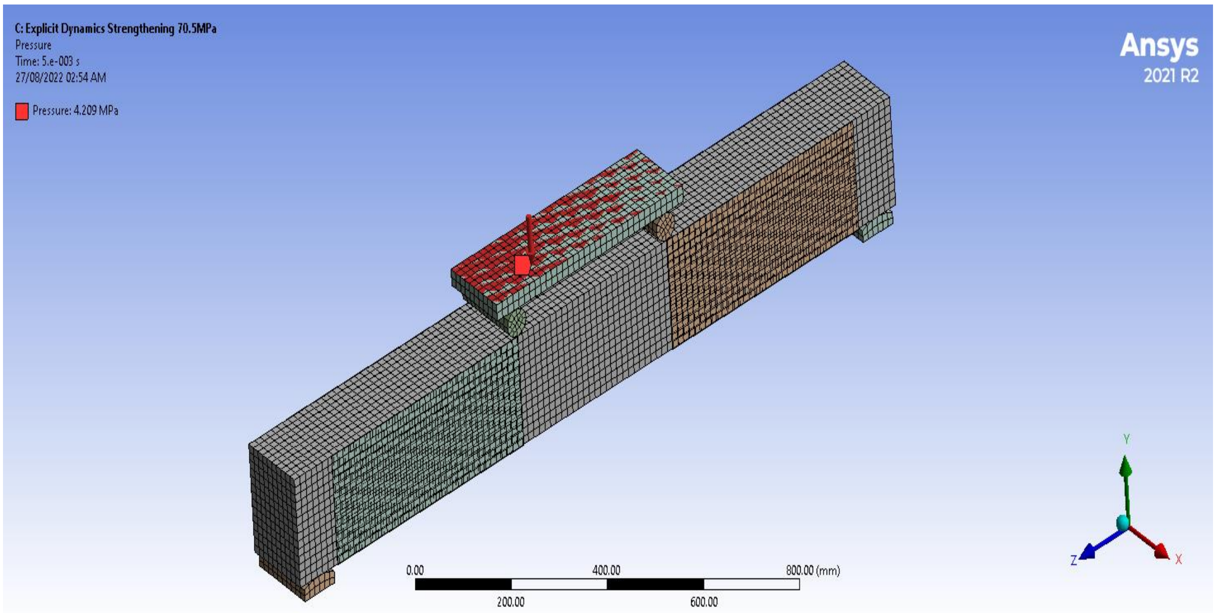

Figure 432(NWA-2/70.5MPa – Geometry & loads of beam sample with strengthening and top rebars- Explicit Dynamic Analysis)

The ultimate load has been transferred to be as a pressure load which is 4.209 MPa as shown above with rate loading 0.6mm/min

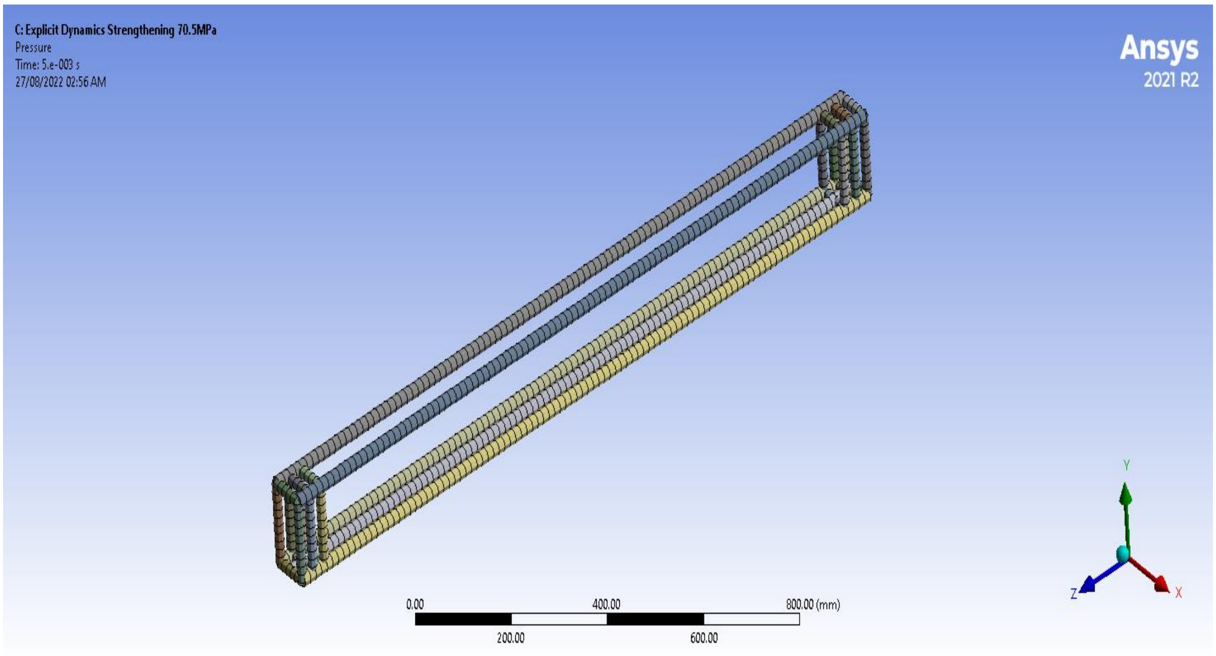

Figure 433(NWA-2/70.5MPa – Rebars of beam sample with strengthening – Explicit Dynamic Analysis)

Deformations

Total Deformations

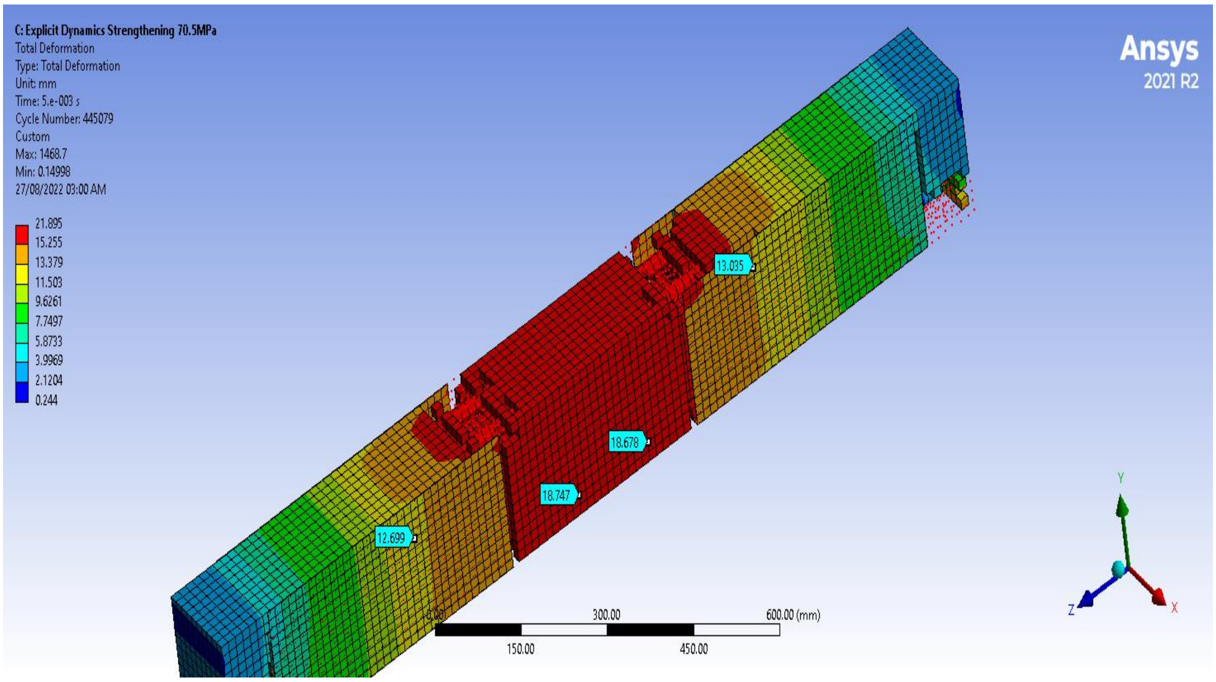

Figure 434(NWA-2/70.5MPa – Total deflections of beam sample with strengthening and top rebars- Explicit Dynamic Analysis)

The value is 18.747 mm.

Directional Deformation (Y-Direction)-Concrete

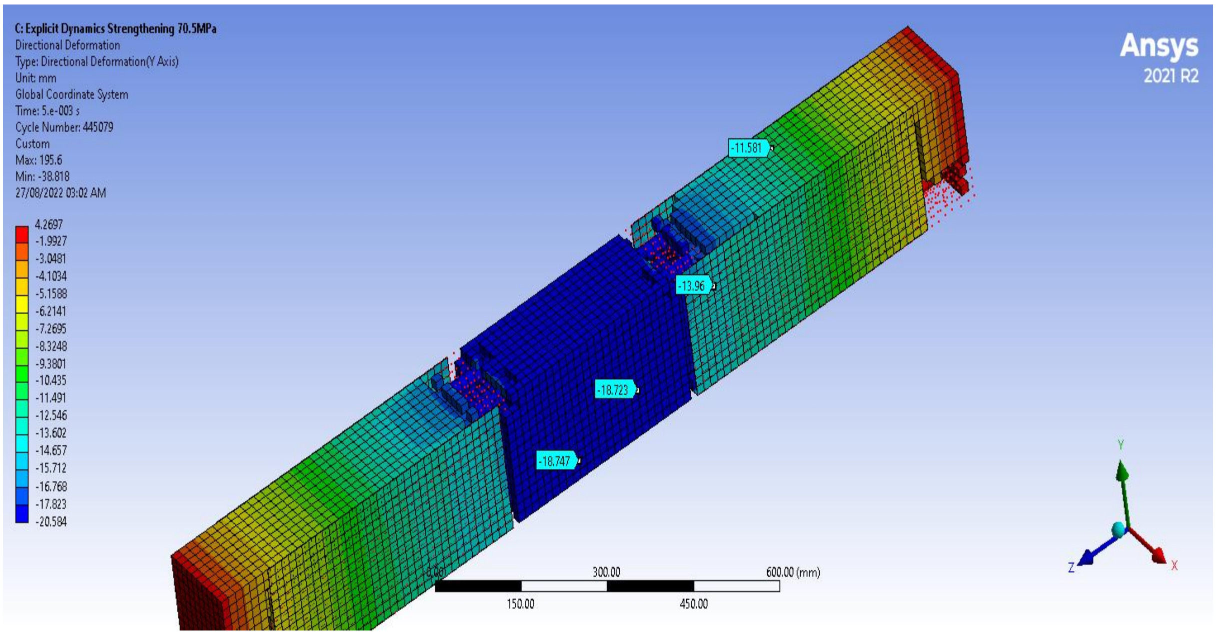

Figure 435(NWA-2/70.5MPa – Directional deflection (Y-Dim.) of beam sample with strengthening and top rebars- Explicit Dynamic Analysis)

The value is 18.747 mm

Directional Deformation (Y-Direction)- Rebars

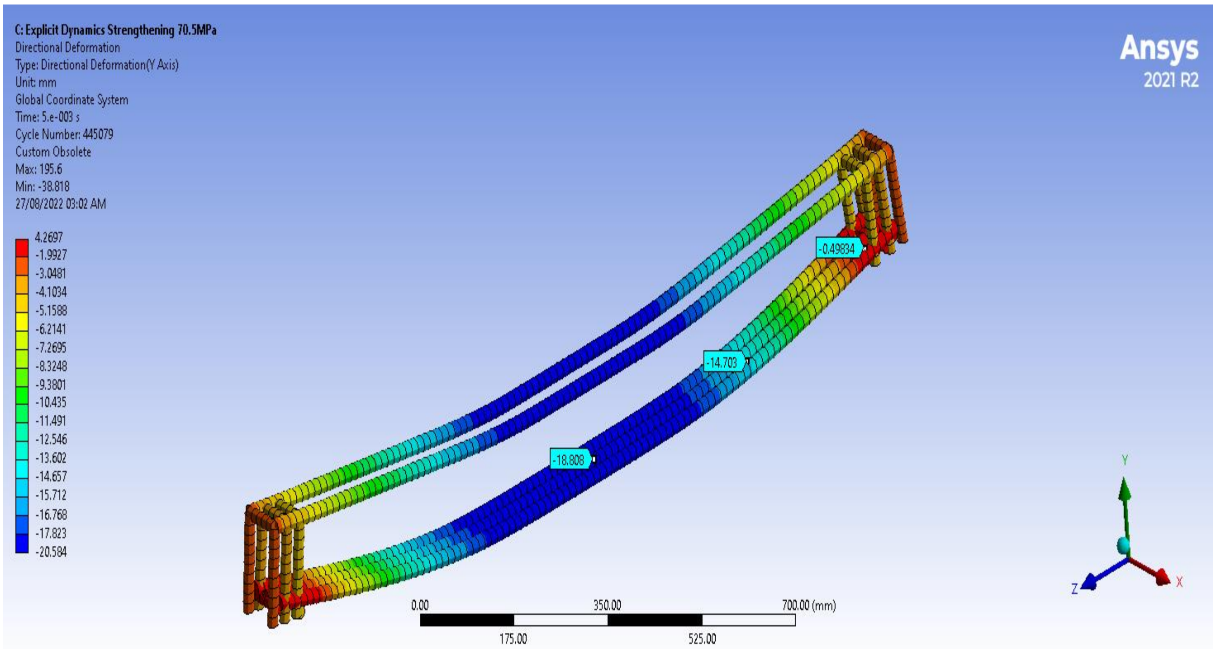

Figure 436(NWA-2/70.5MPa –Directional deflection (Y-Dim.) Rebars of beam sample with strengthening - Explicit Dynamic Analysis)

Normal strain

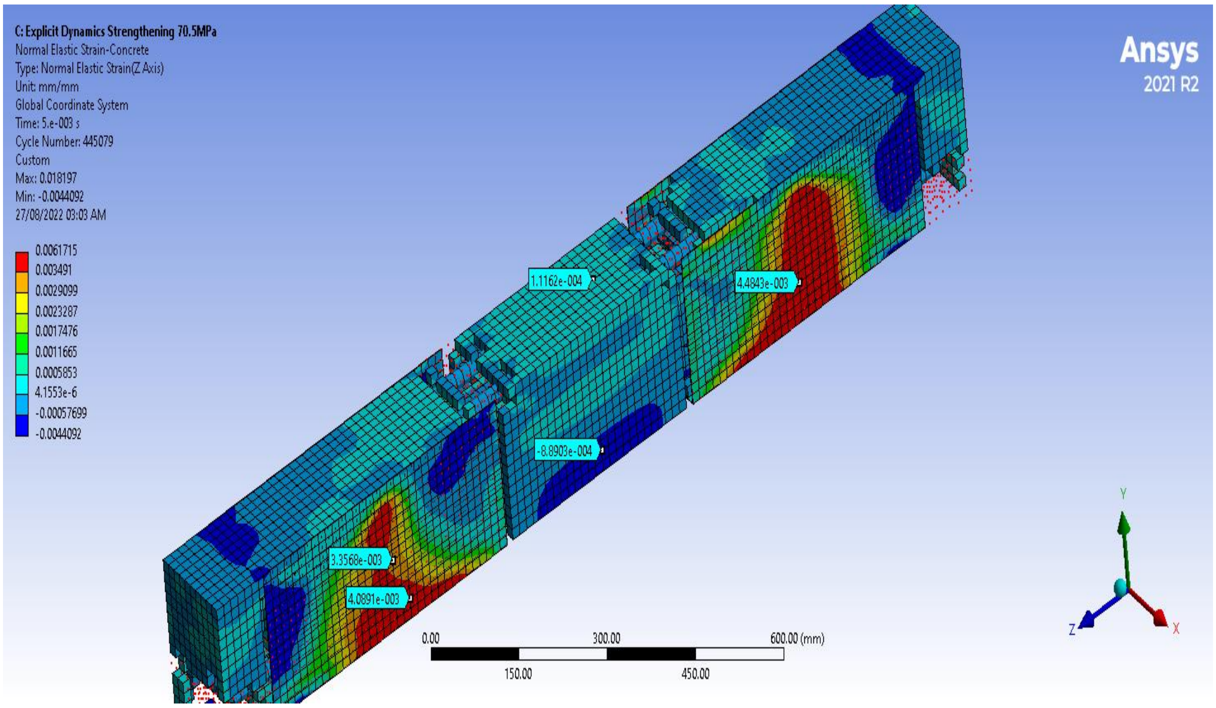

Figure 437(NWA-2/70.5MPa –Normal strain of beam sample with strengthening and top rebars- Explicit Dynamic Analysis)

Shear Stress

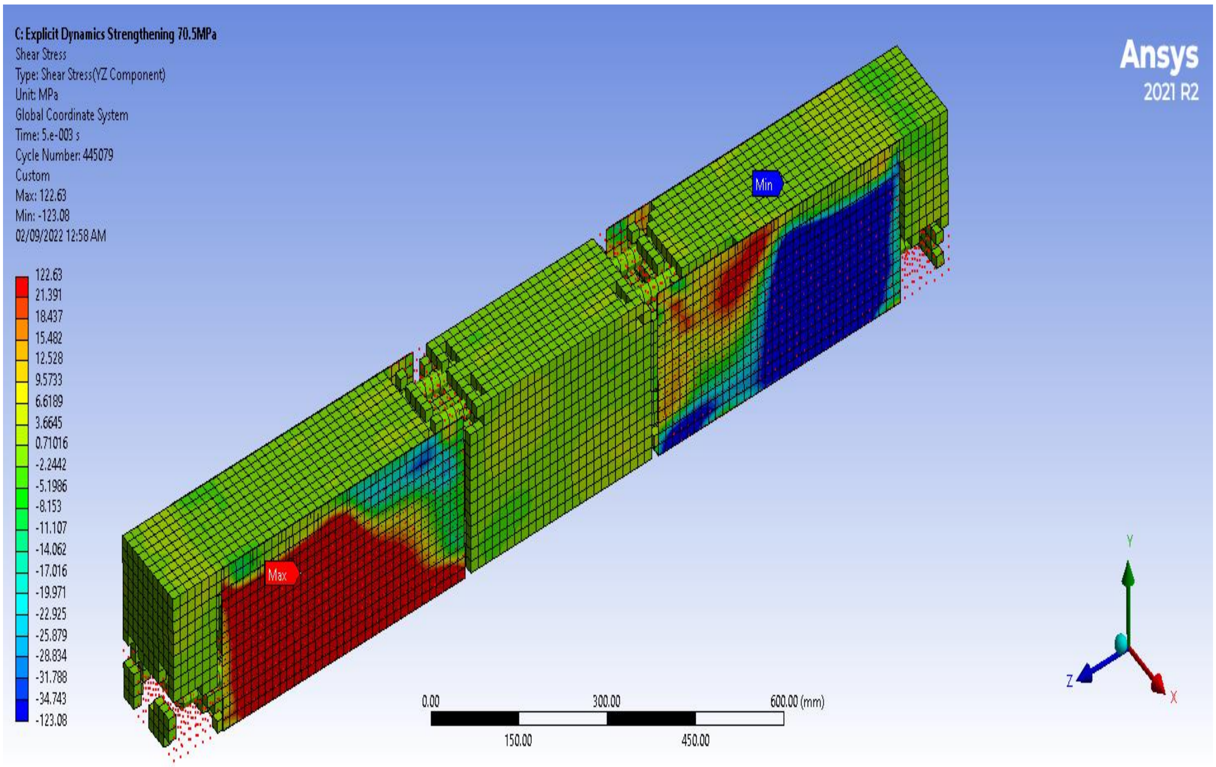

Figure 438(NWA-2/70.5MPa – Shear stress of beam sample with strengthening and top rebars- Explicit Dynamic Analysis)

Total shape strain

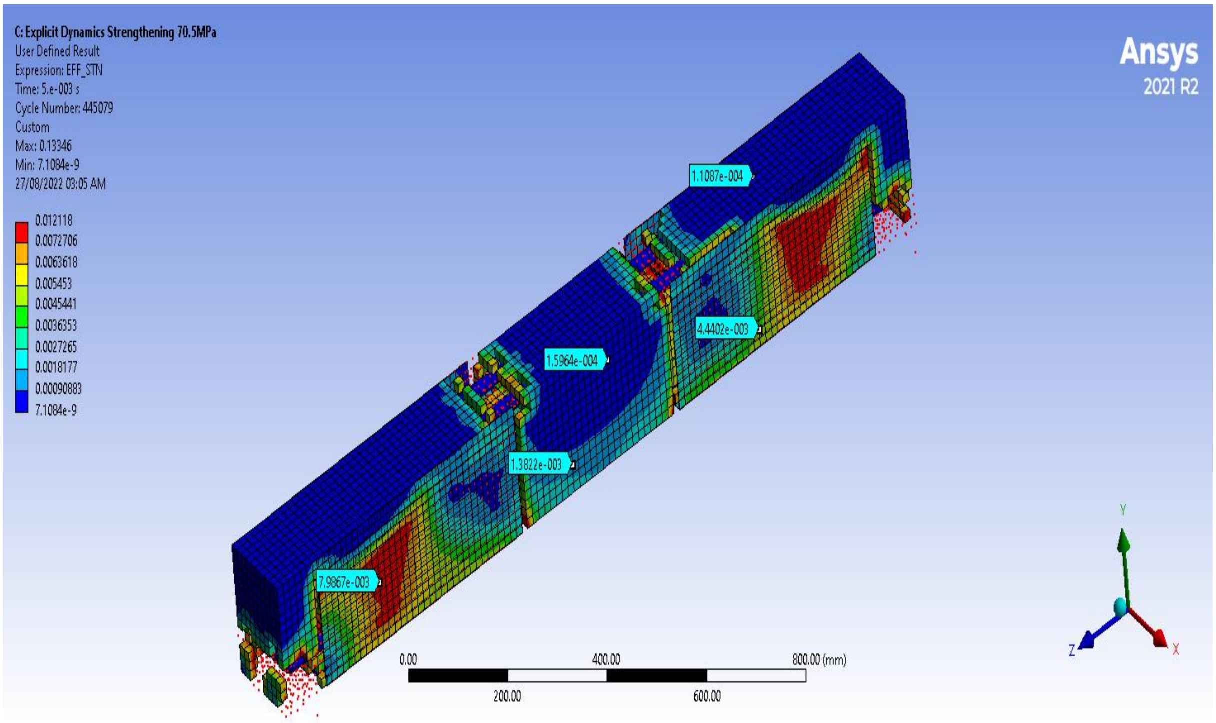

Figure 439(NWA-2/70.5MPa – Total strain of beam sample with strengthening and top rebars- Explicit Dynamic Analysis)

Maximum Stress

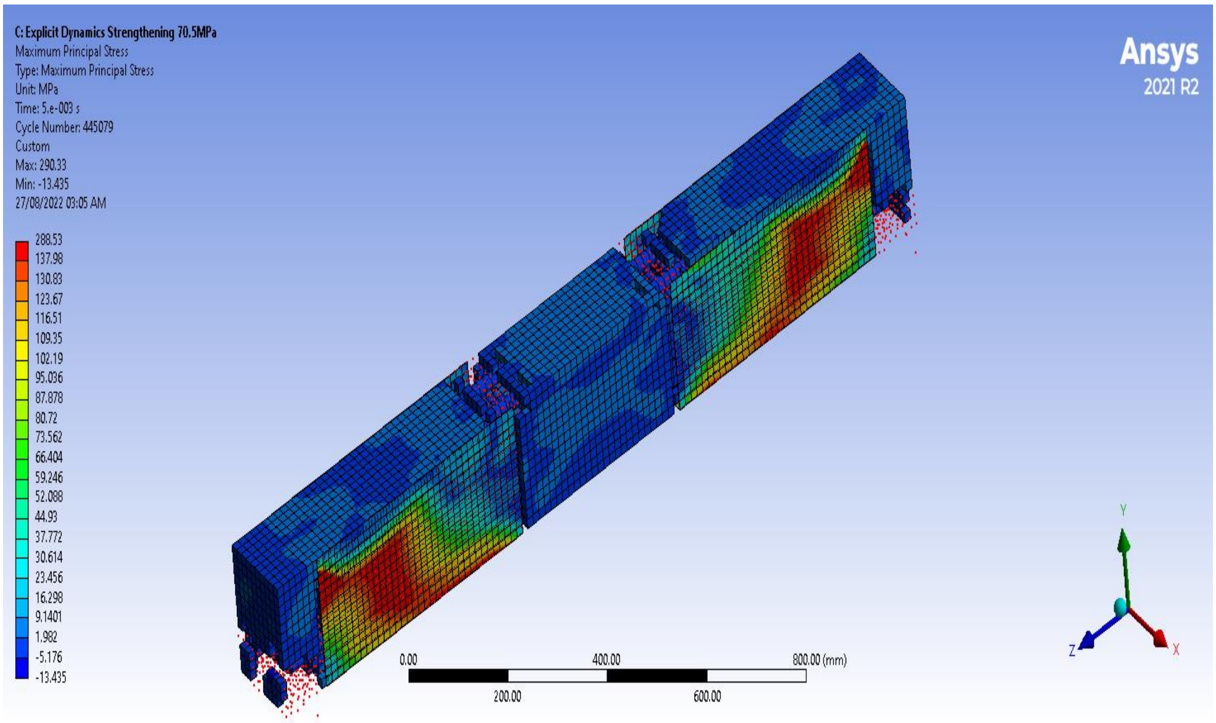

Figure 440(NWA-2/70.5MPa – Maximum stress of beam sample with strengthening and top rebars- Explicit Dynamic Analysis)

The Damage Pattern

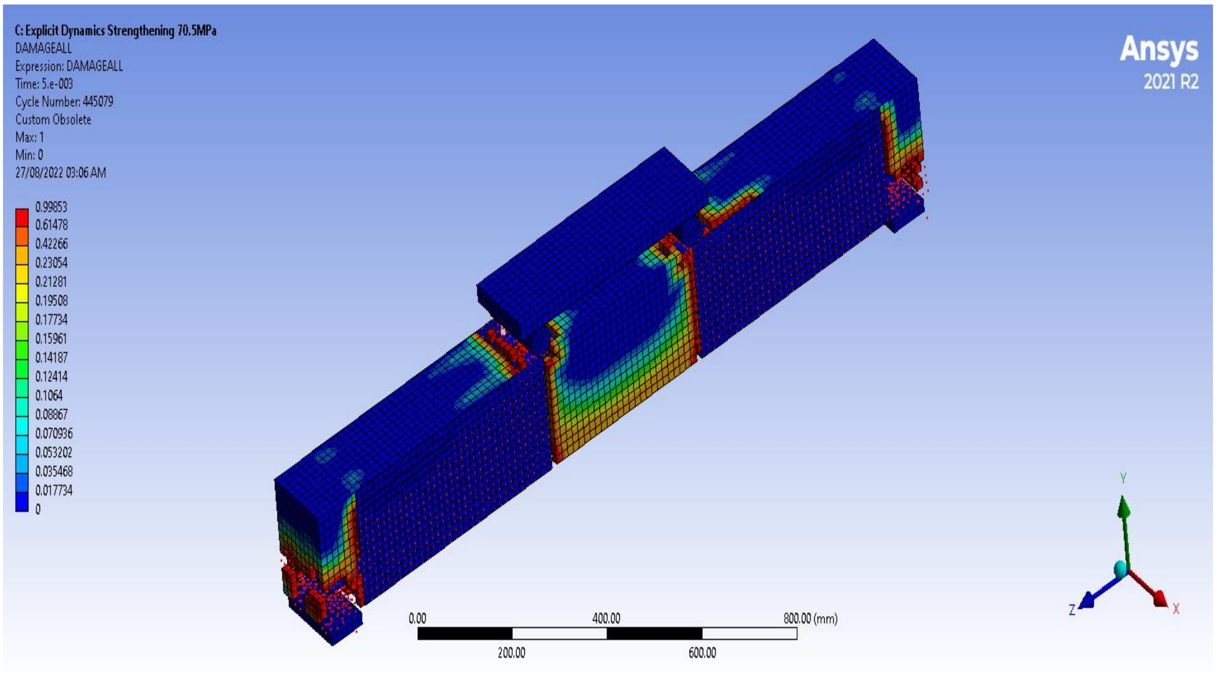

Figure 441(NWA-2/70.5MPa – Damage pattern-1 of beam sample with strengthening and top rebars- Explicit Dynamic Analysis)

As we can see the shear damage cracks in red and CFRP debonding on edges of concrete failure.

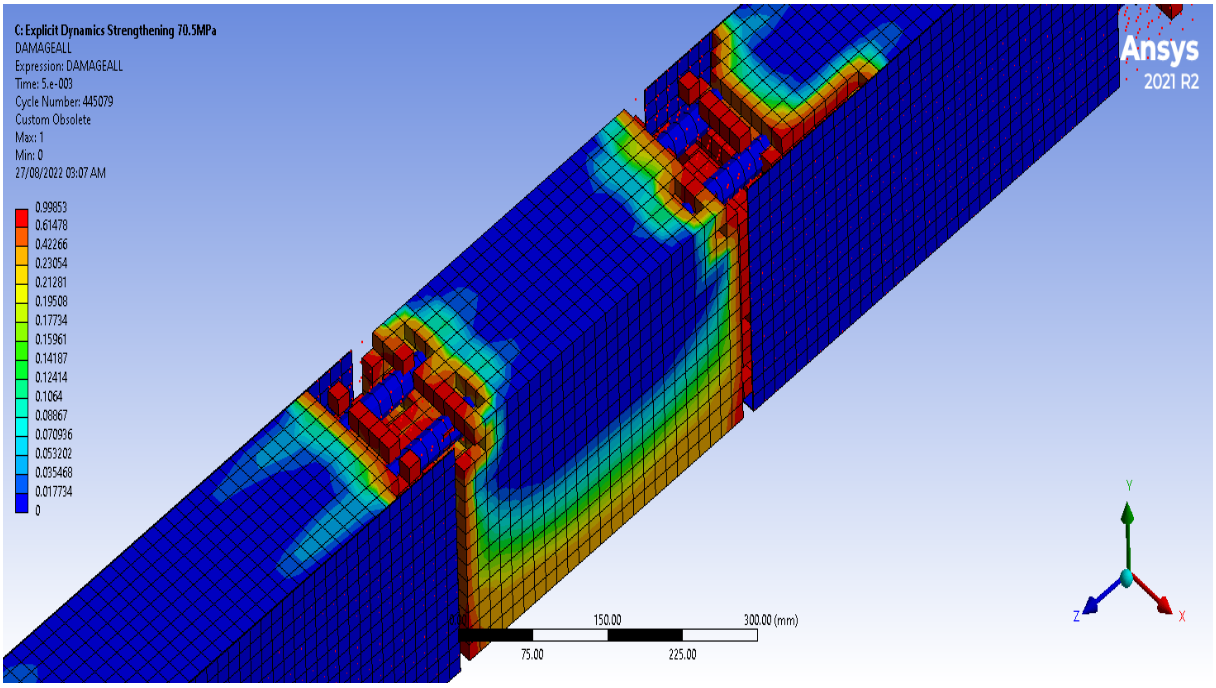

Figure 442(NWA-2/70.5MPa – Damage pattern-2 of beam sample with strengthening and top rebars- Explicit Dynamic Analysis)

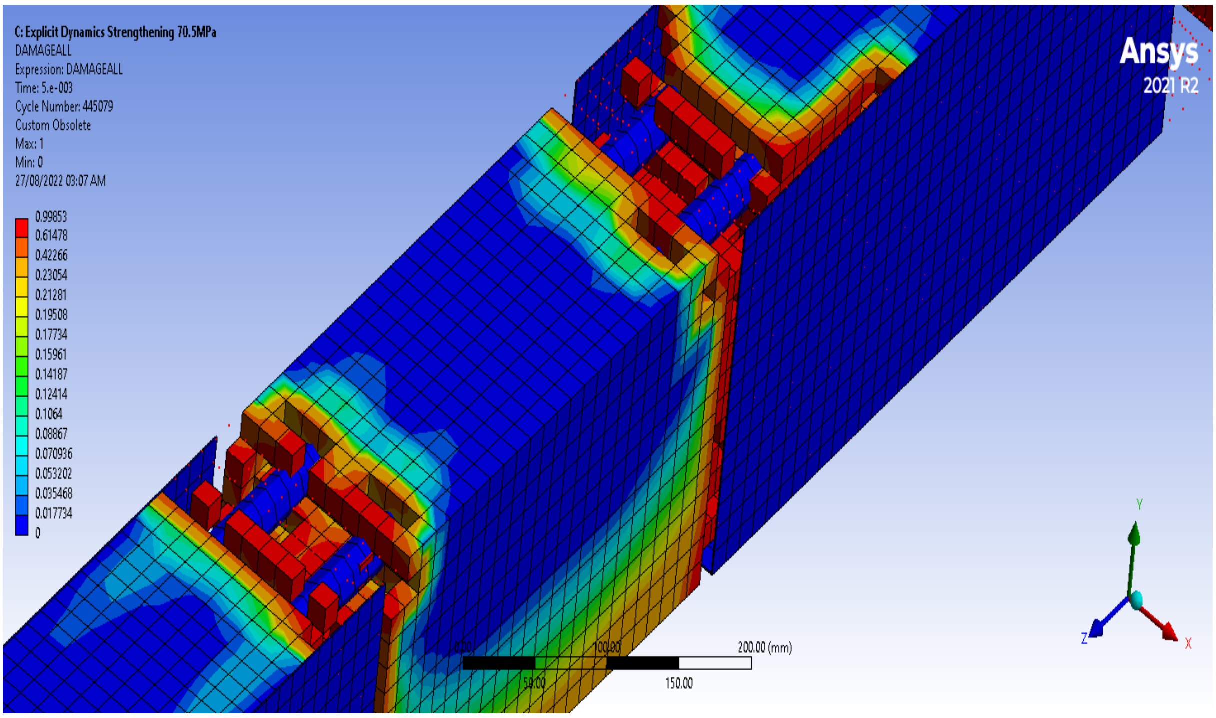

Figure 443(NWA-2/70.5MPa – Damage pattern-3 of beam sample with strengthening and top rebars- Explicit Dynamic Analysis)

CFRP laminates due to ultimate load has been debonding as shown in images above

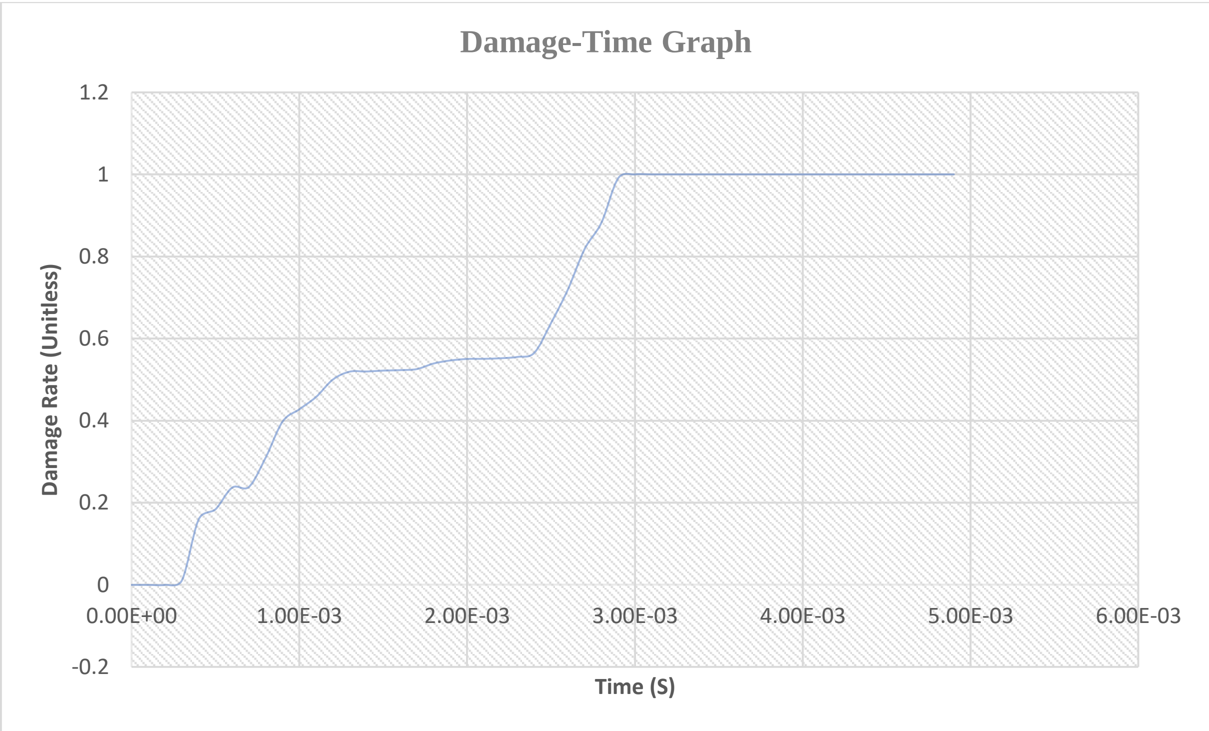

Figure 444(NWA-2/70.5MPa – Damage pattern graph of beam sample with strengthening and top rebars- Explicit Dynamic Analysis)

32- Static Non-Linear Analysis – Without Top Rebars and With Strengthening

Geometry and loads

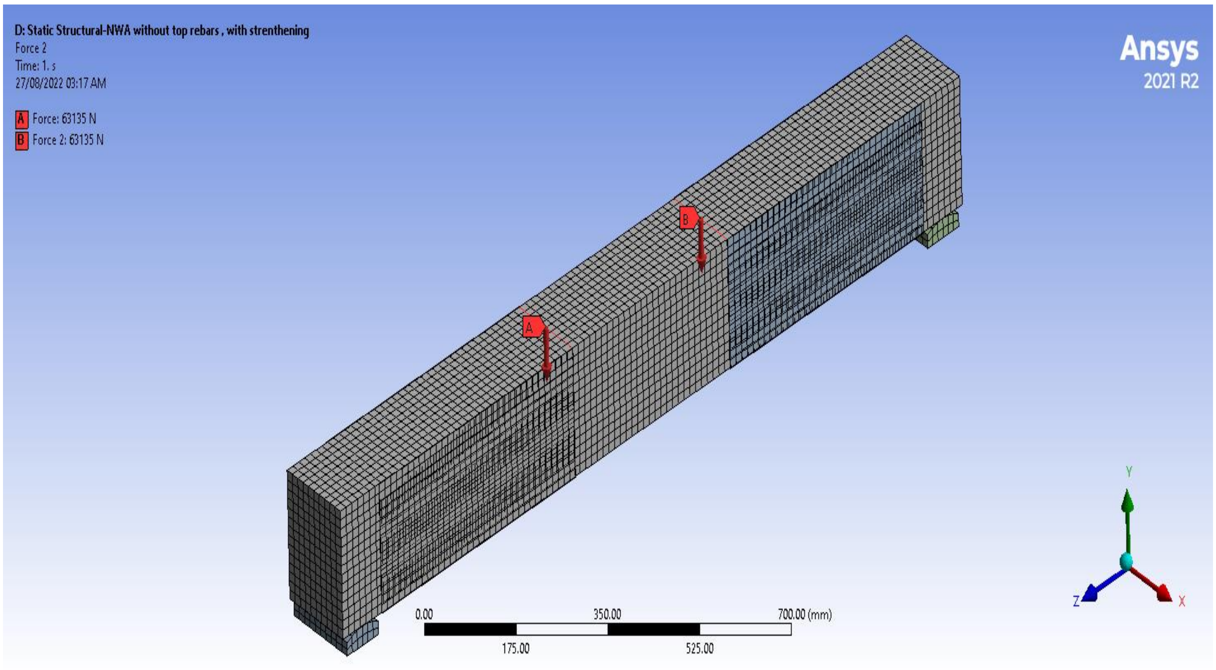

Figure 445(NWA-2/70.5MPa – Geometry & Loads of beam sample with strengthening and without top rebars- Static Nonlinear Analysis)

The ultimate load has been divided in to loads which is 126.27/2 =63.135KN.

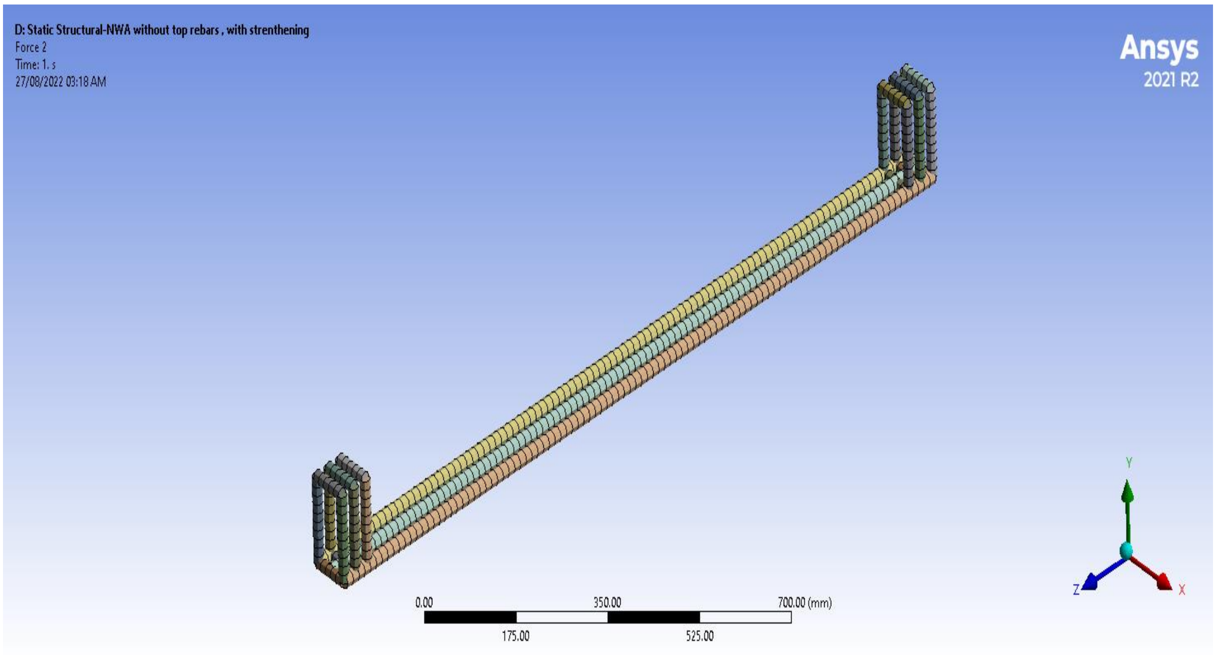

Figure 446(NWA-2/70.5MPa – Rebars of beam sample without strengthening - Static Nonlinear Analysis)

Deformations

Total Deformations

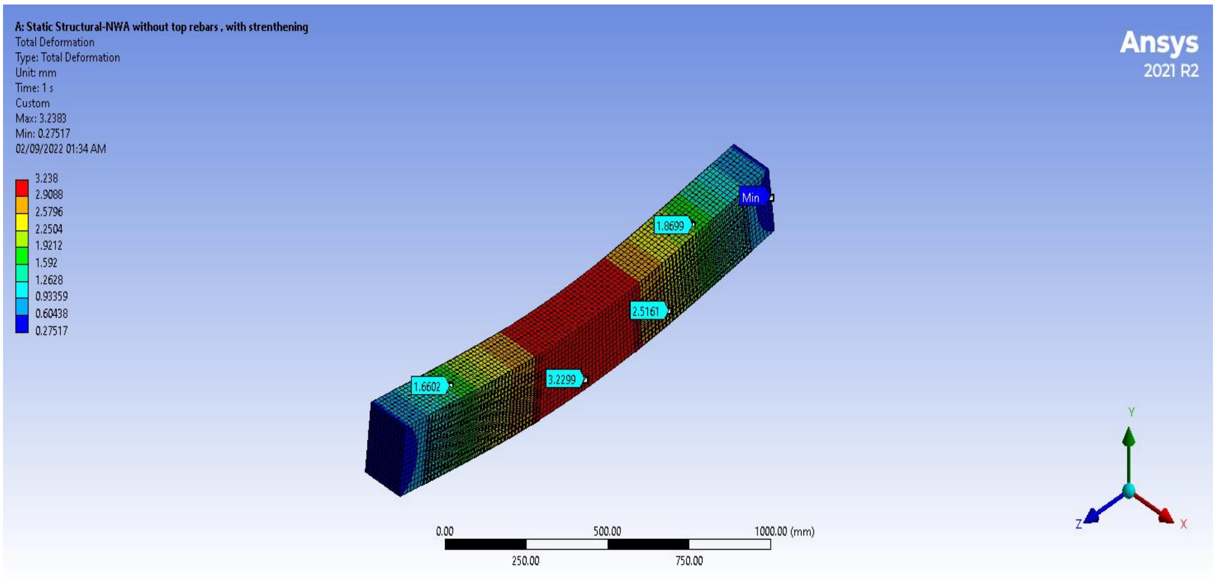

Figure 447(NWA-2/70.5MPa – Total deflections of beam sample with strengthening and without top rebars- Static Nonlinear Analysis)

The value is 3.238 mm.

Directional Deformation (Y-Direction)

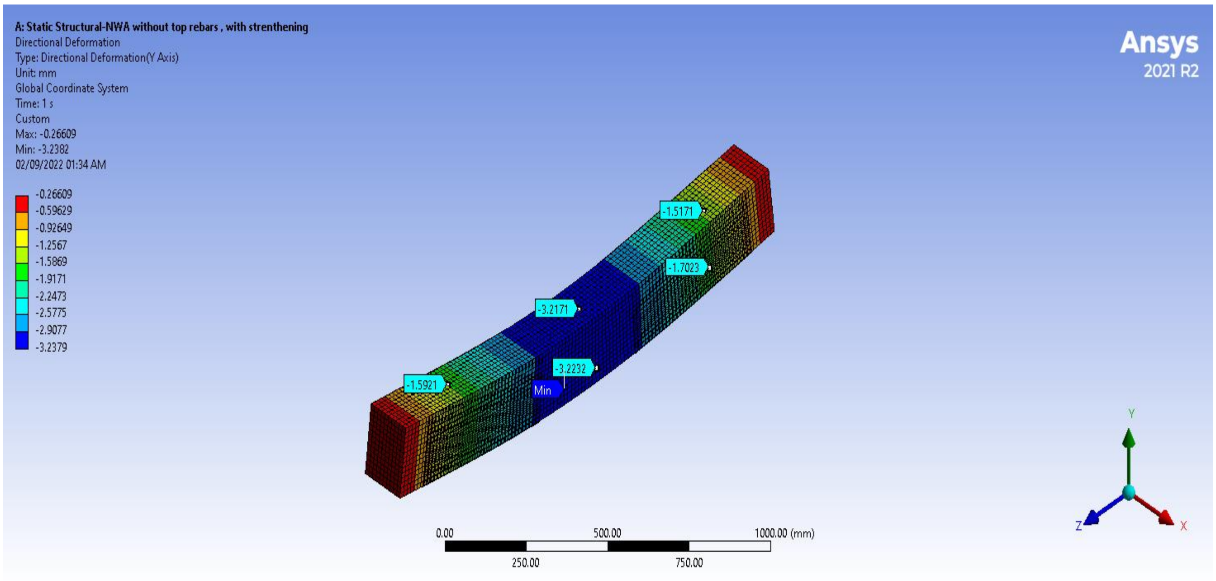

Figure 448(NWA-2/70.5MPa – Directional deflections (Y-Dim.) of beam sample with strengthening and without top rebars- Static Nonlinear Analysis)

The value is 3.238 mm.

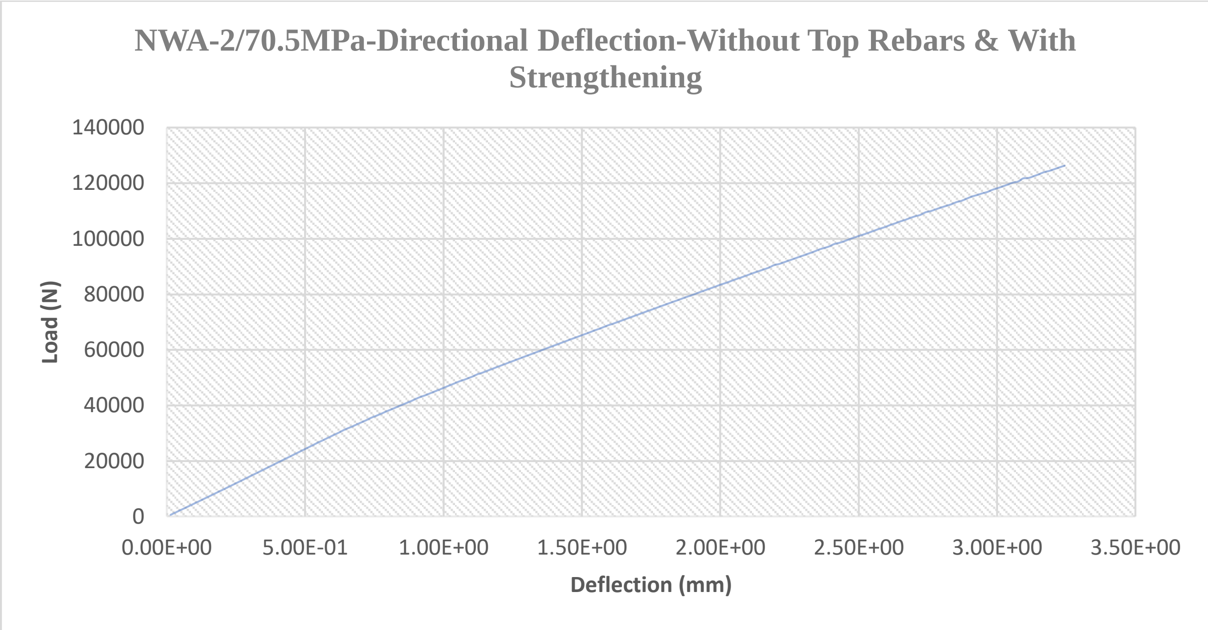

Figure 449(NWA-2/70.5MPa – Directional deflections (Y-Dim.) of beam sample with strengthening and without top rebars- Static Nonlinear Analysis)

Normal Stress (Concrete)

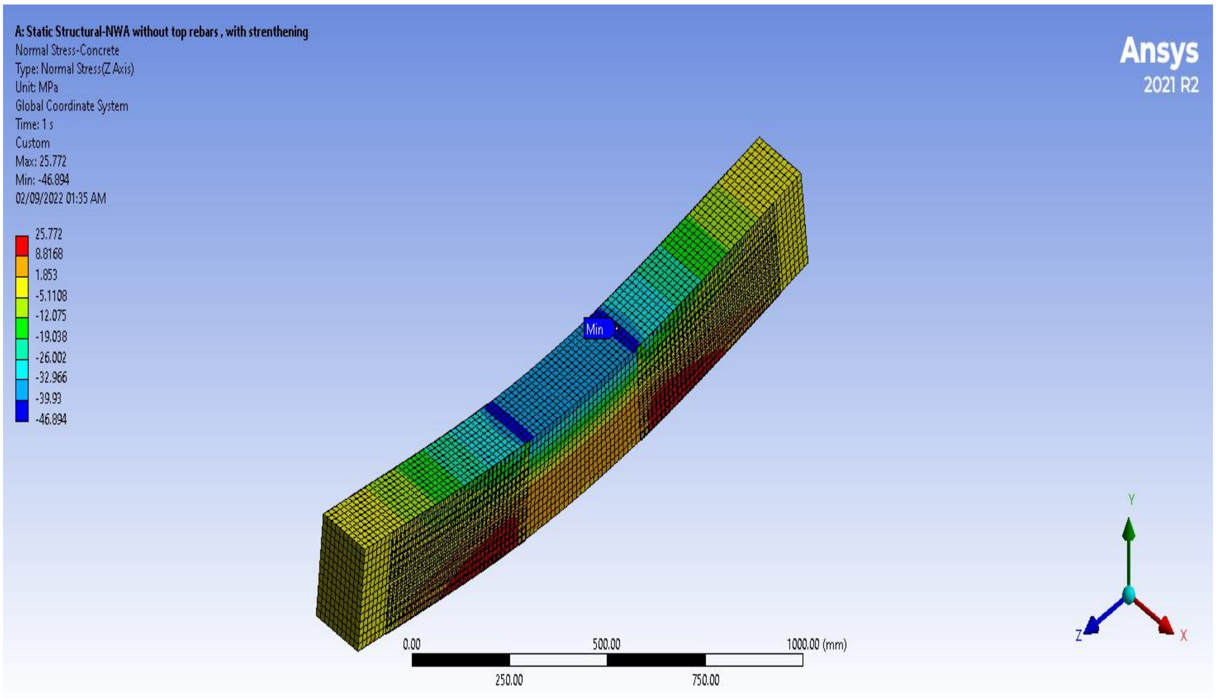

Figure 450(NWA-2/70.5MPa – Normal stress (Concrete) of beam sample with strengthening and without top rebars- Static Nonlinear Analysis)

The blue zones show the crushing from loading machine and the maximum value is 46.894 MPa, whereas the red zones indicate to tension.

Normal Stress (Rebars)

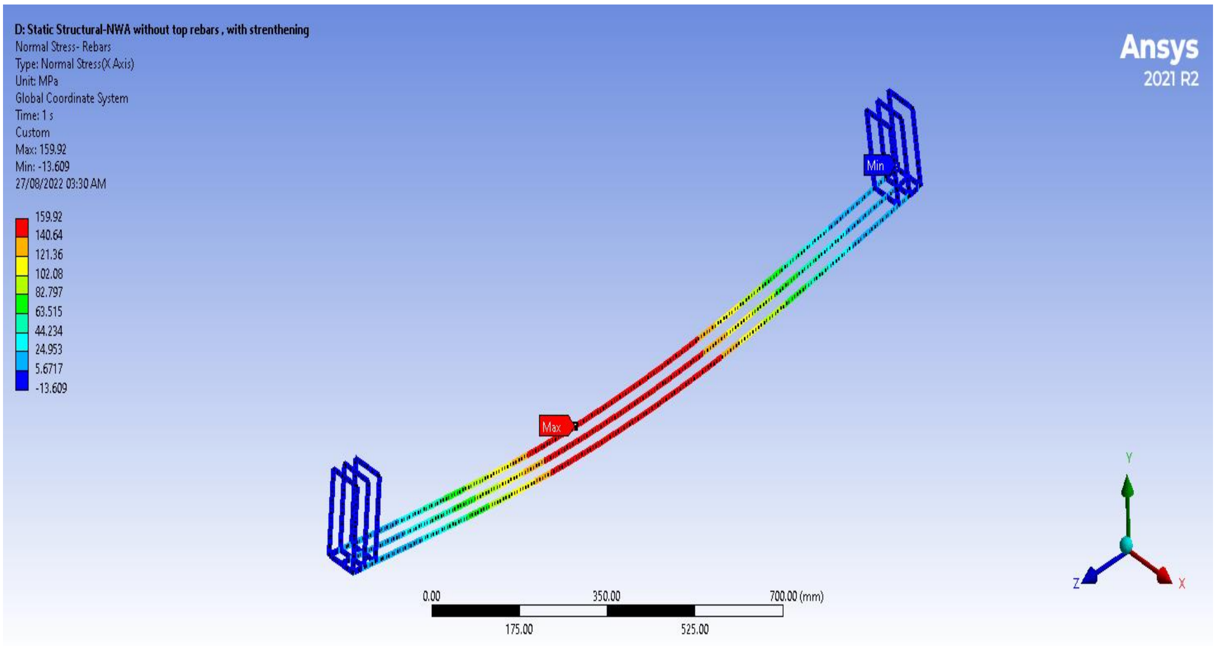

Figure 451(NWA-2/70.5MPa – Normal stress (Rebars) of beam sample with strengthening and without top rebars- Static Nonlinear Analysis)

The red zones show that the rebars is yielding by 159.92MPa, in the middle span due to tension.

Shear Stress

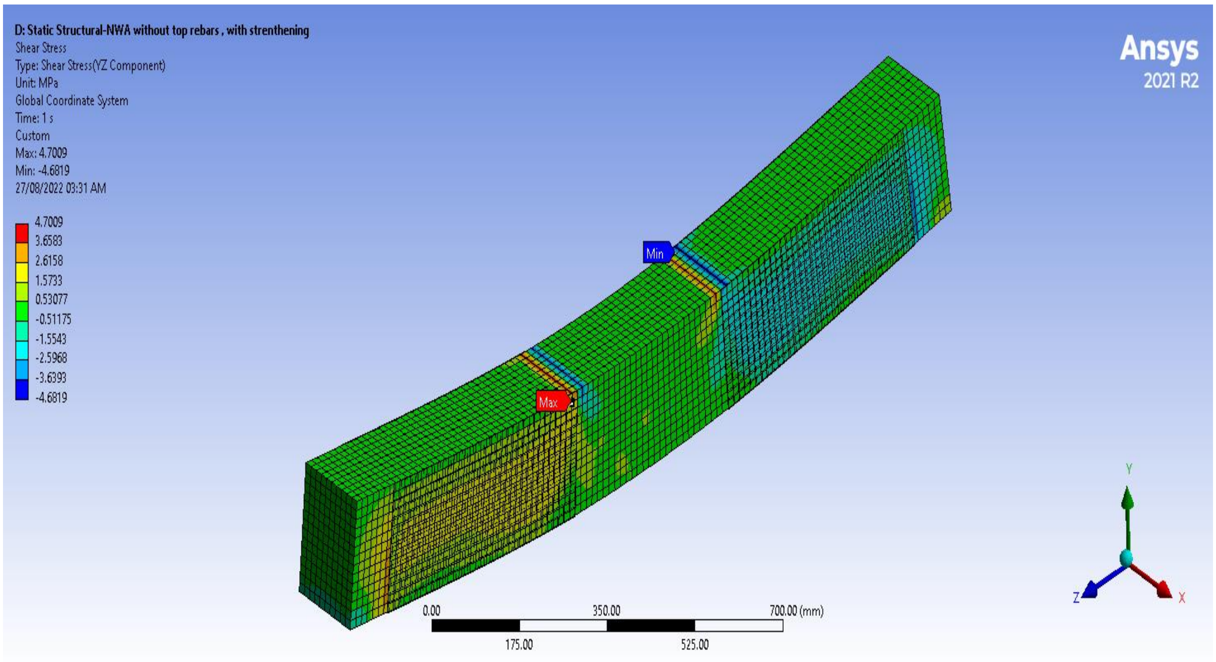

Figure 452(NWA-2/70.5MPa – Shear stress of beam sample with strengthening and without top rebars- Static Nonlinear Analysis)

Elastic Strain

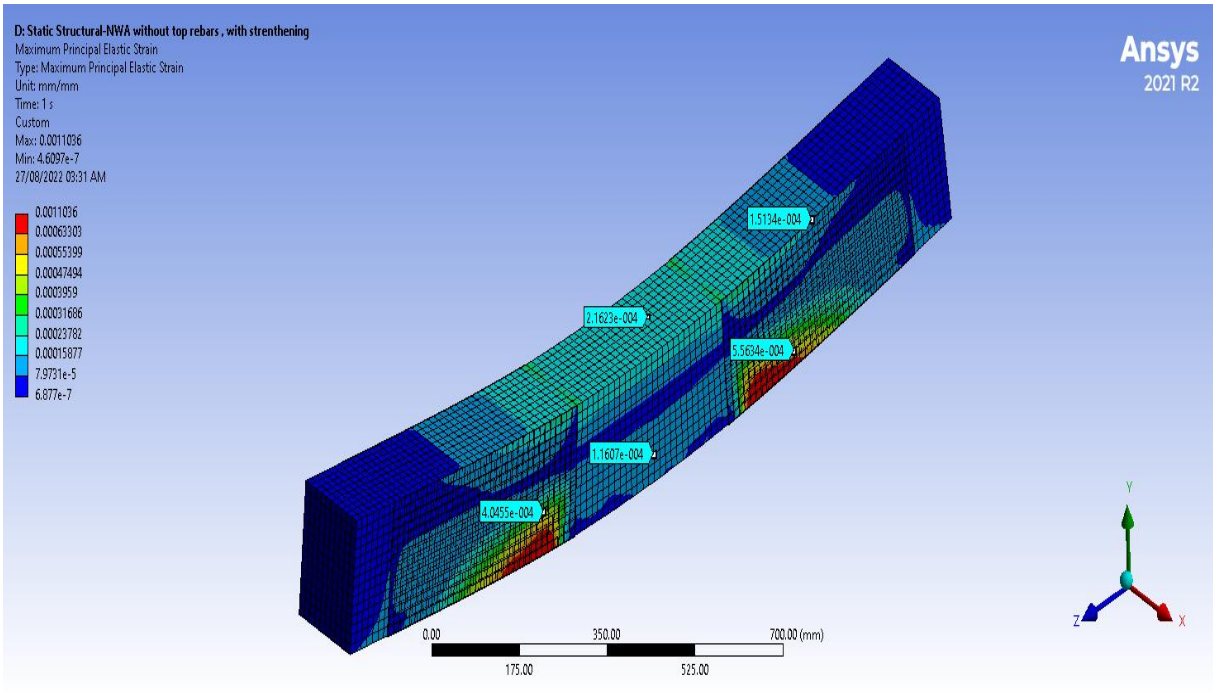

Figure 453(NWA-2/70.5MPa – Elastic strain of beam sample with strengthening and without top rebars- Static Nonlinear Analysis)

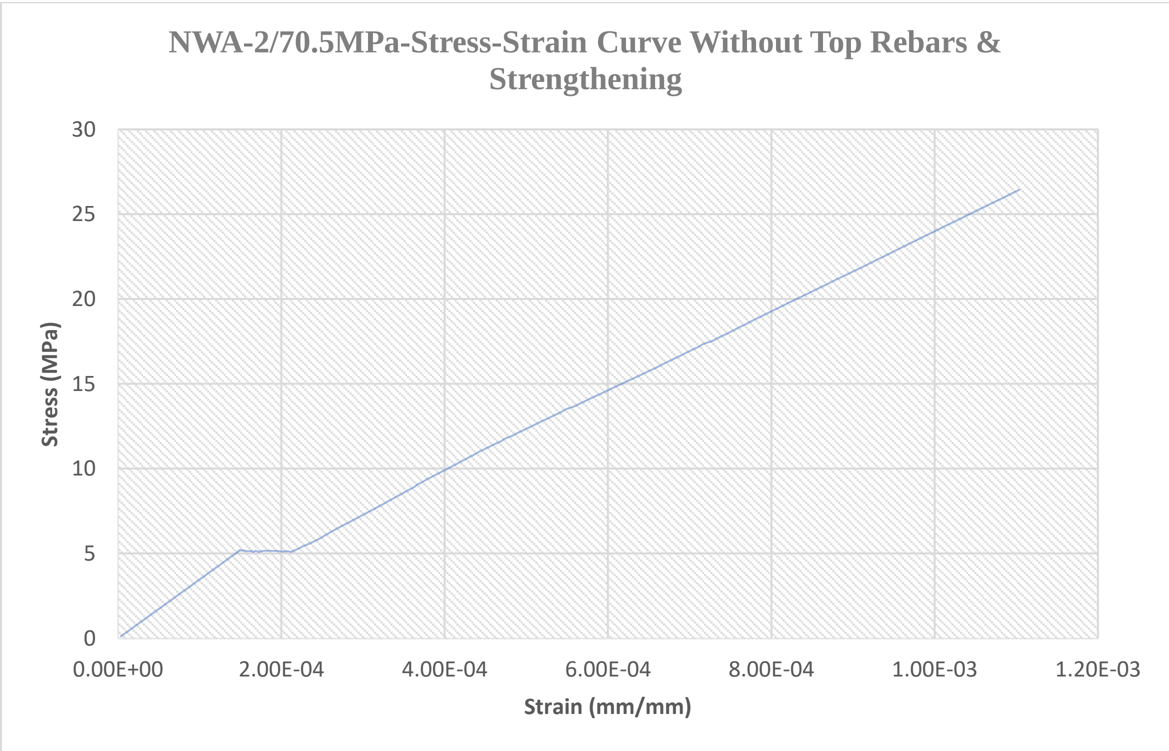

Figure 454(NWA-2/70.5MPa – Stress & Strain graph of beam sample with strengthening and without top rebars- Static Nonlinear Analysis)

33- Explicit Dynamic-Without Top Rebars & With Strengthening

Geometry and loads

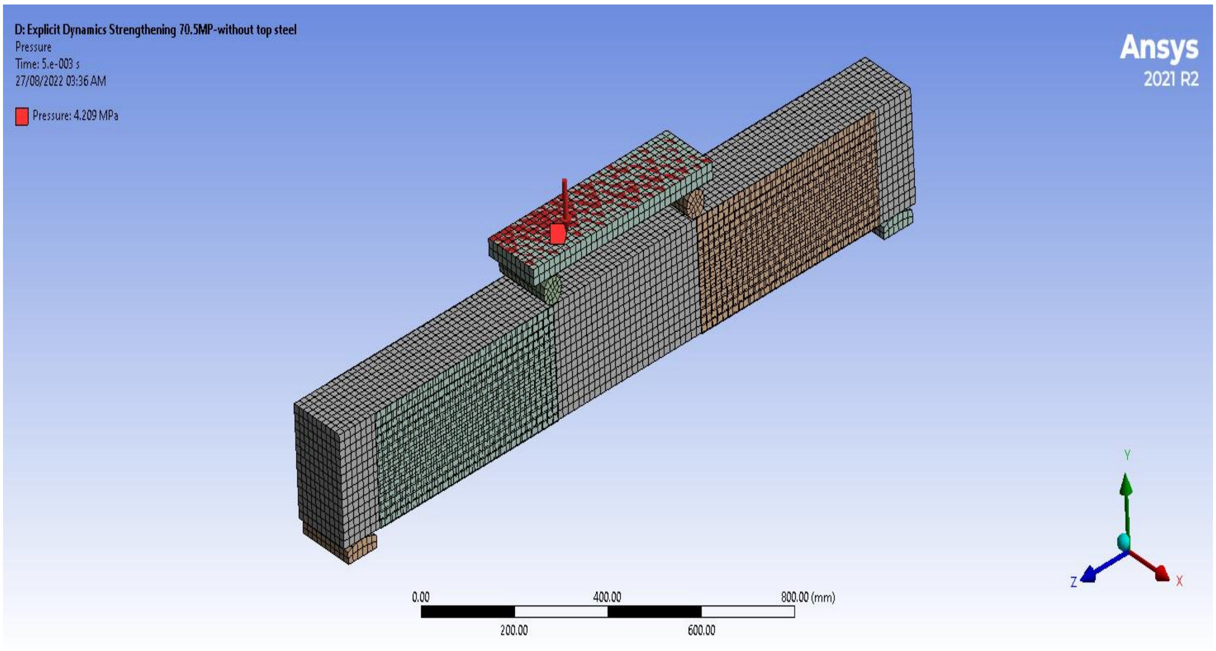

Figure 455(NWA-2/70.5MPa – Geometry & Loads of beam sample with strengthening and without top rebars- Explicit Dynamic Analysis)

The ultimate load has been transferred to be as a pressure load which is 4.209 MPa as shown above with rate loading 0.6mm/min

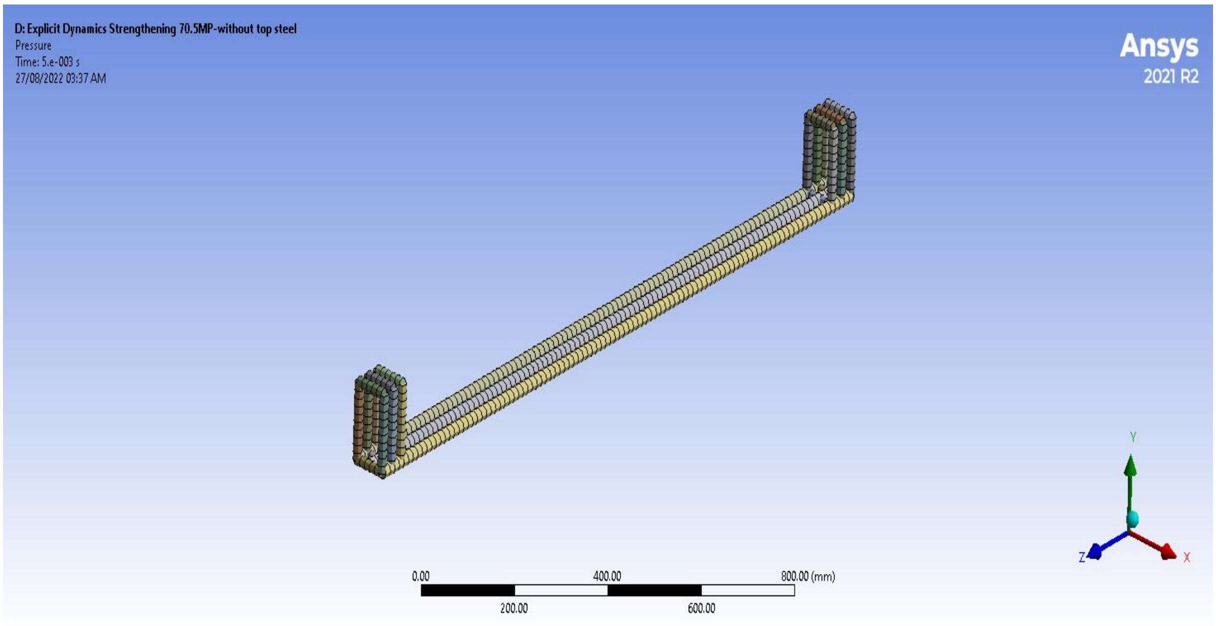

Figure 456(NWA-2/70.5MPa – Rebars of beam sample with strengthening - Explicit Dynamic Analysis)

Deformations

Total Deformations

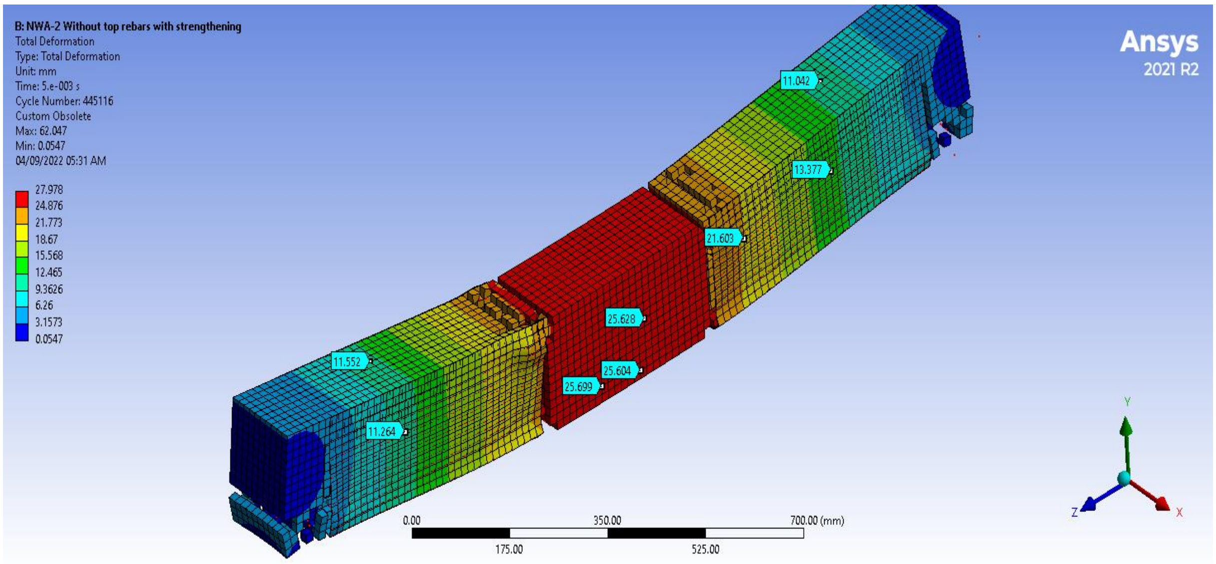

Figure 457(NWA-2/70.5MPa – Total deflections of beam sample with strengthening and without top rebars- Explicit Dynamic Analysis)

The value is 25.699 mm.

Directional Deformation (Y-Direction)-Concrete

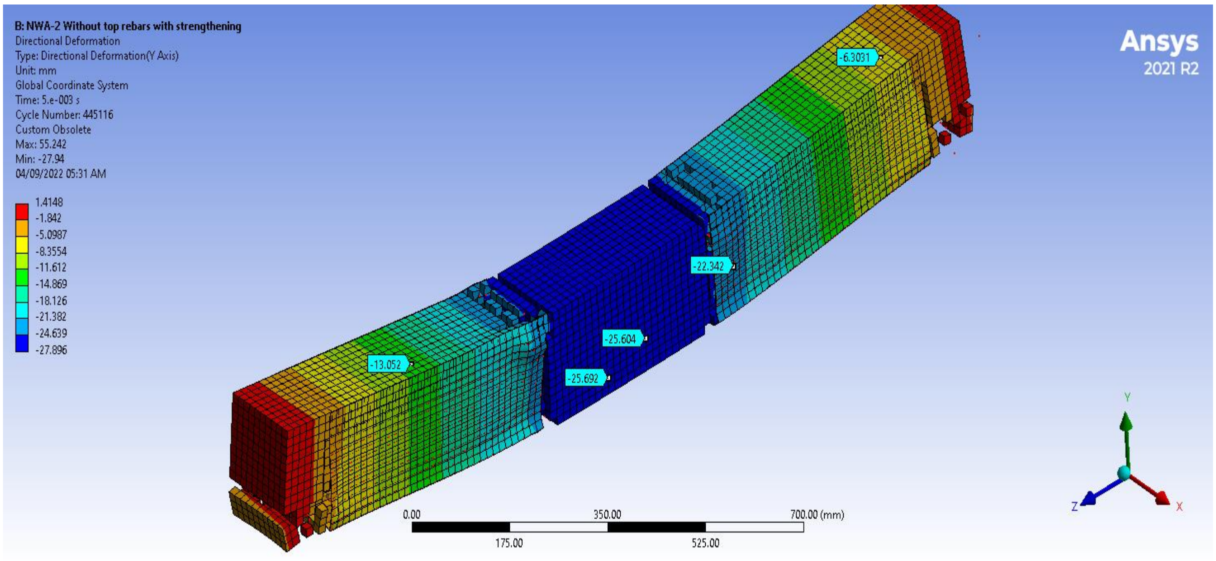

Figure 458(NWA-2/70.5MPa – Directional deflections (Y-Dim.) of beam sample with strengthening and without top rebars- Explicit Dynamic Analysis)

The value is 25.699 mm

Directional Deformation (Y-Direction)- Rebars

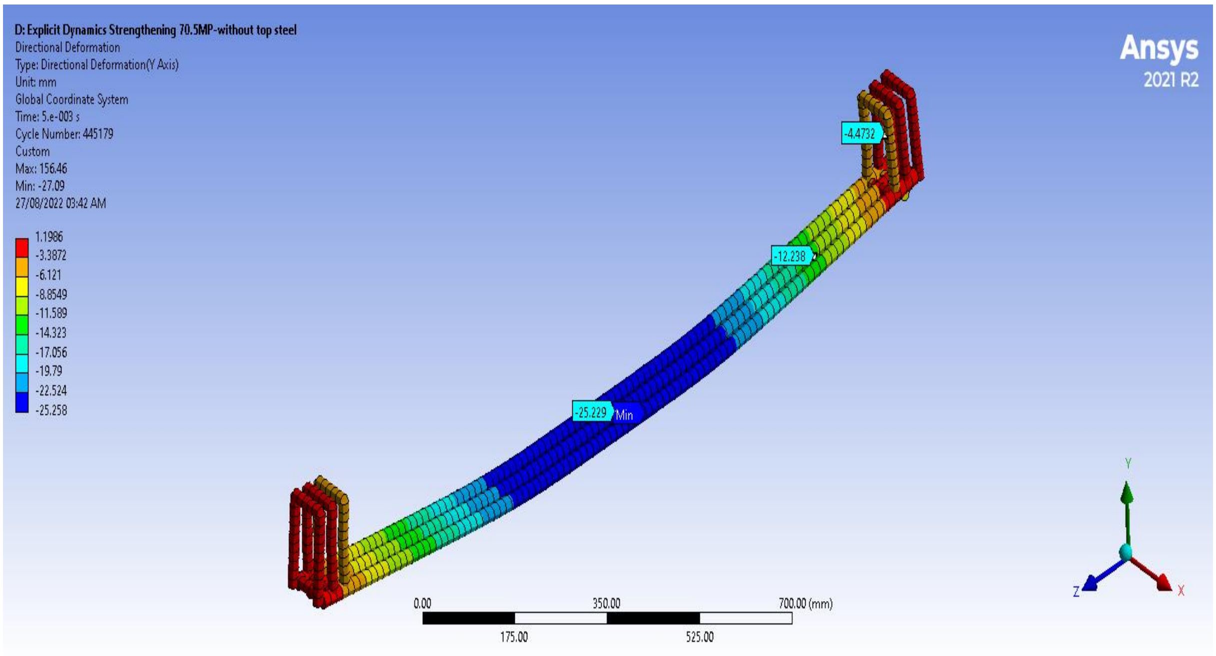

Figure 459(NWA-2/70.5MPa – Directional deflections (Y-Dim.) Rebars of beam sample with strengthening and without top rebars- Explicit Dynamic Analysis)

Normal strain

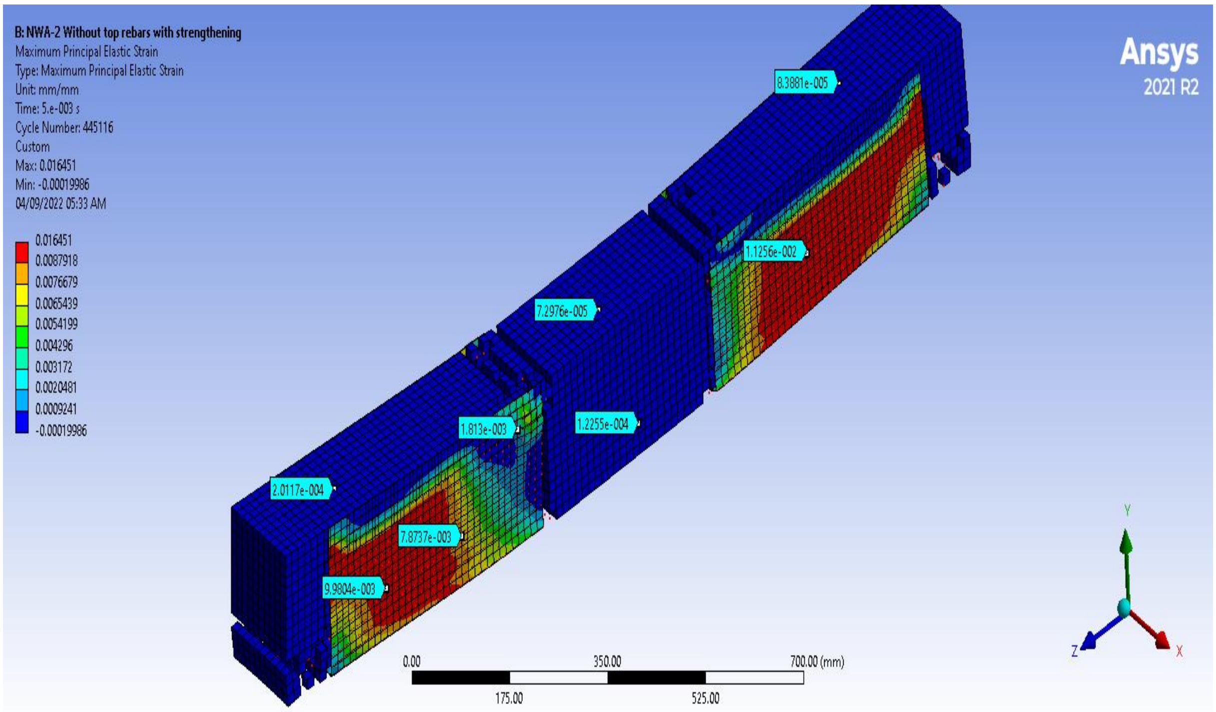

Figure 460(NWA-2/70.5MPa – Normal strain of beam sample with strengthening and without top rebars- Explicit Dynamic Analysis)

Shear Stress

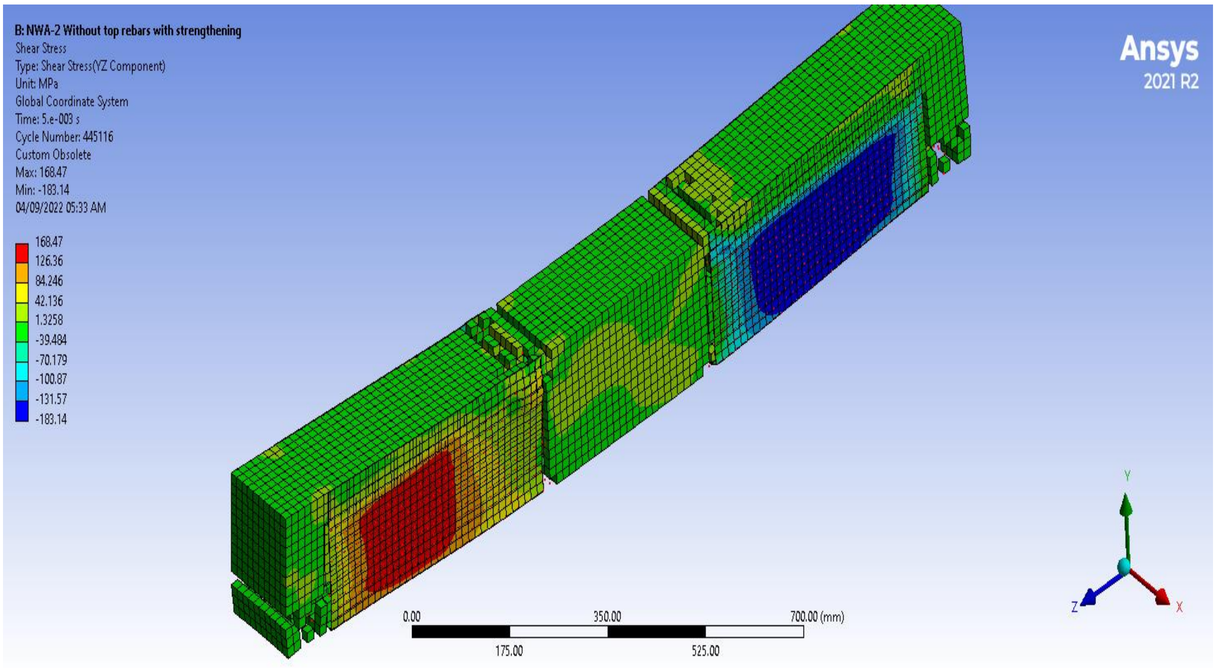

Figure 461(NWA-2/70.5MPa – Shear stress of beam sample with strengthening and without top rebars- Explicit Dynamic Analysis)

Total shape strain

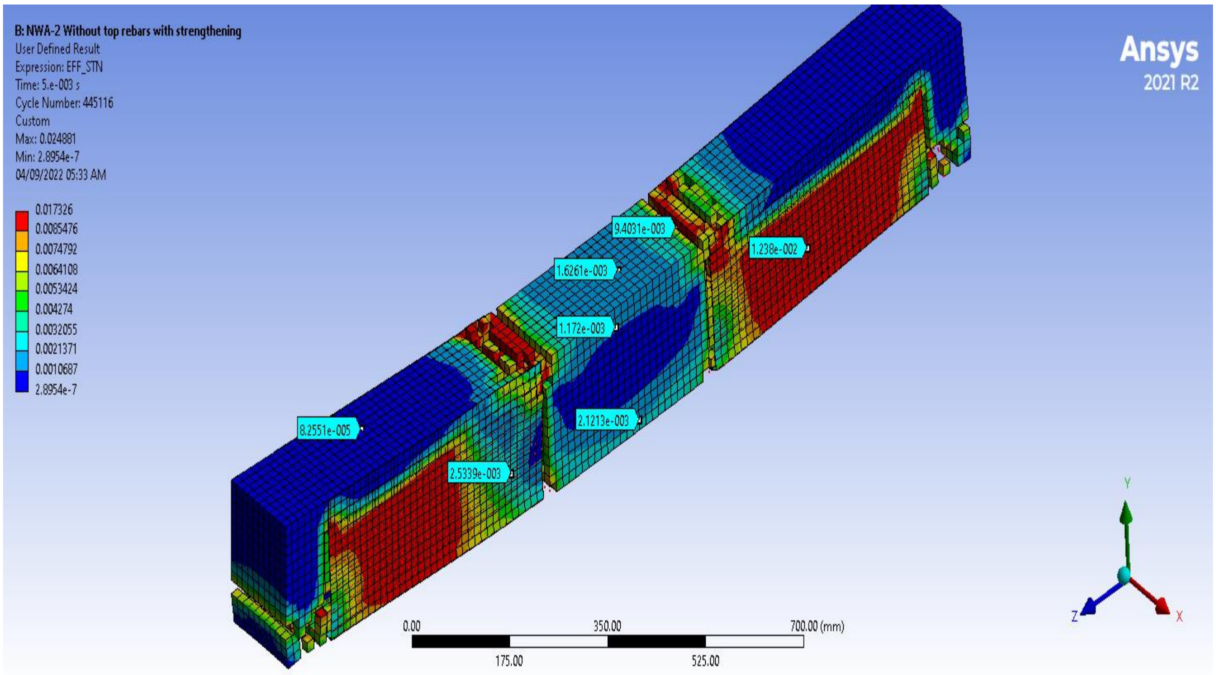

Figure 462(NWA-2/70.5MPa – Total strain of beam sample with strengthening and without top rebars- Explicit Dynamic Analysis)

Maximum Stress

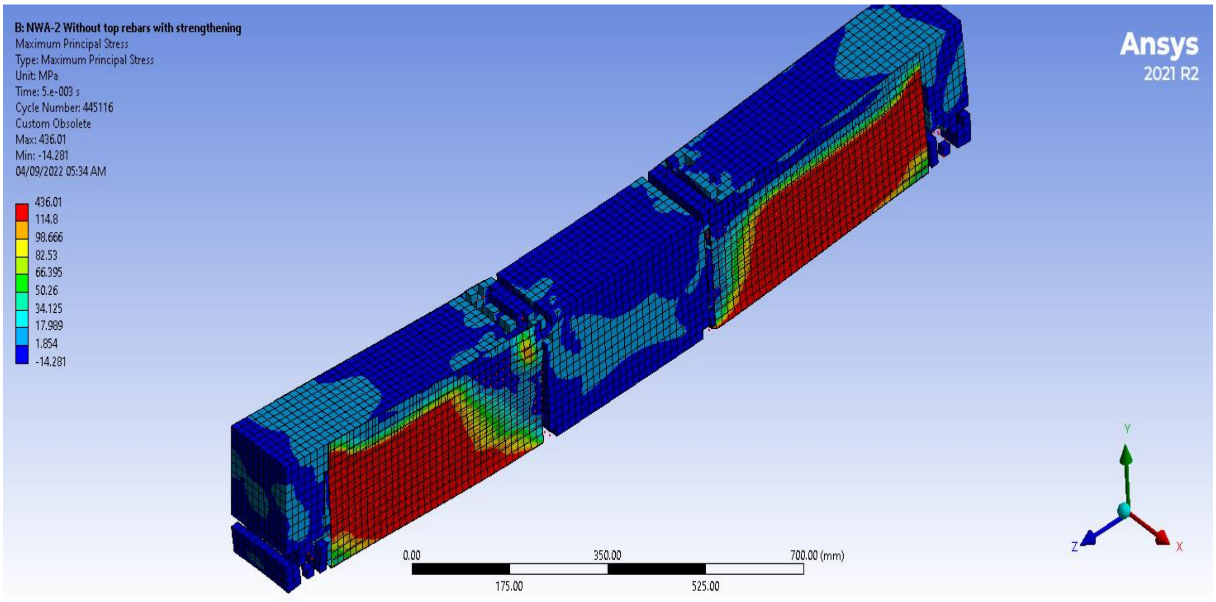

Figure 463(NWA-2/70.5MPa – Maximum stress of beam sample with strengthening and without top rebars- Explicit Dynamic Analysis)

The Damage Pattern

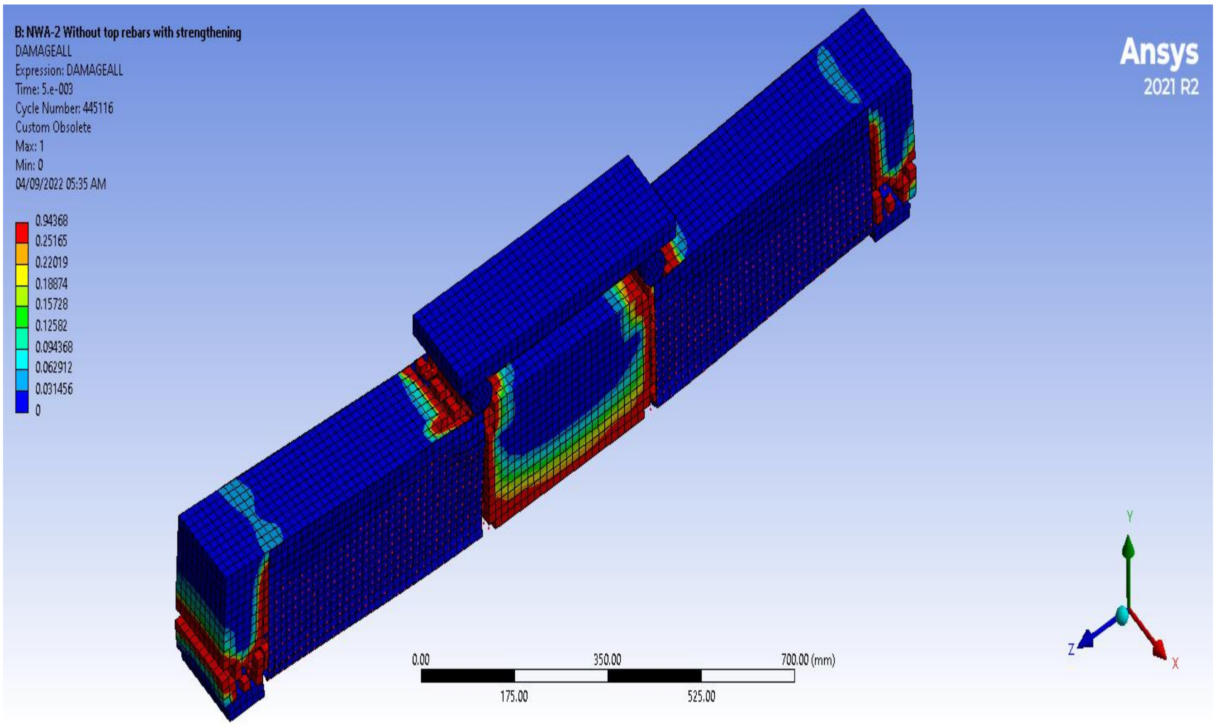

Figure 464(NWA-2/70.5MPa – Damage pattern-1 of beam sample with strengthening and without top rebars- Explicit Dynamic Analysis)

As we can see the shear damage cracks in red and CFRP debonding on edges of concrete failure.

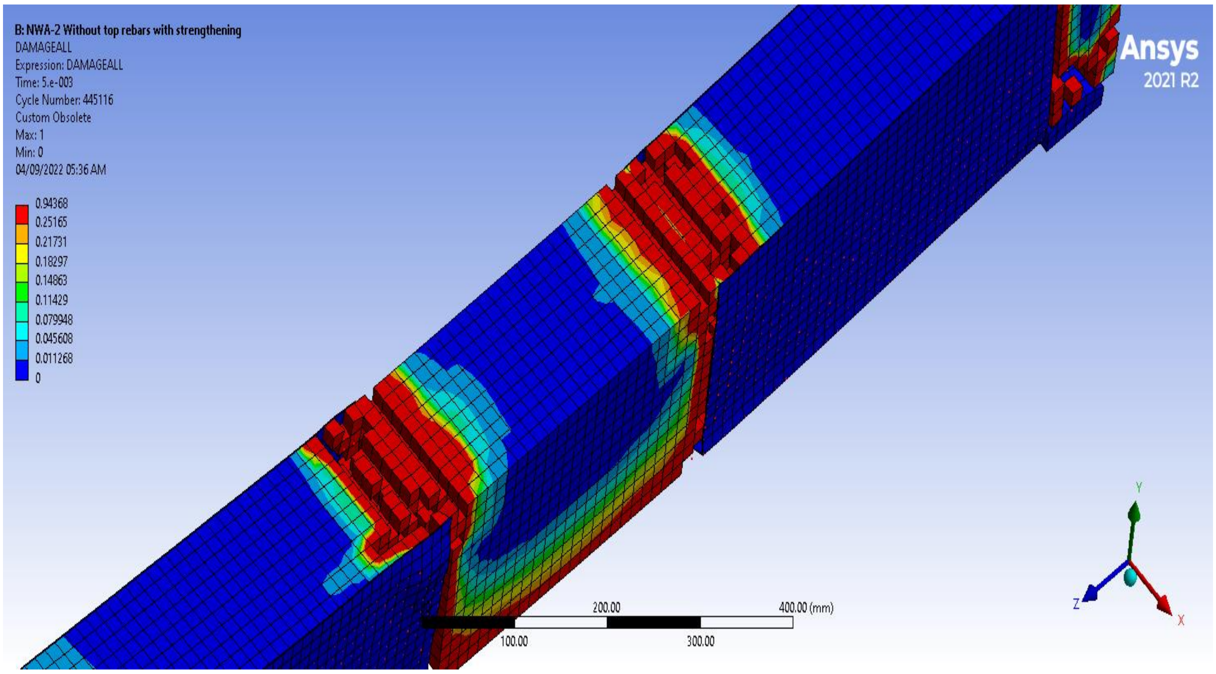

Figure 465(NWA-2/70.5MPa – Damage pattern-2 of beam sample with strengthening and without top rebars- Explicit Dynamic Analysis)

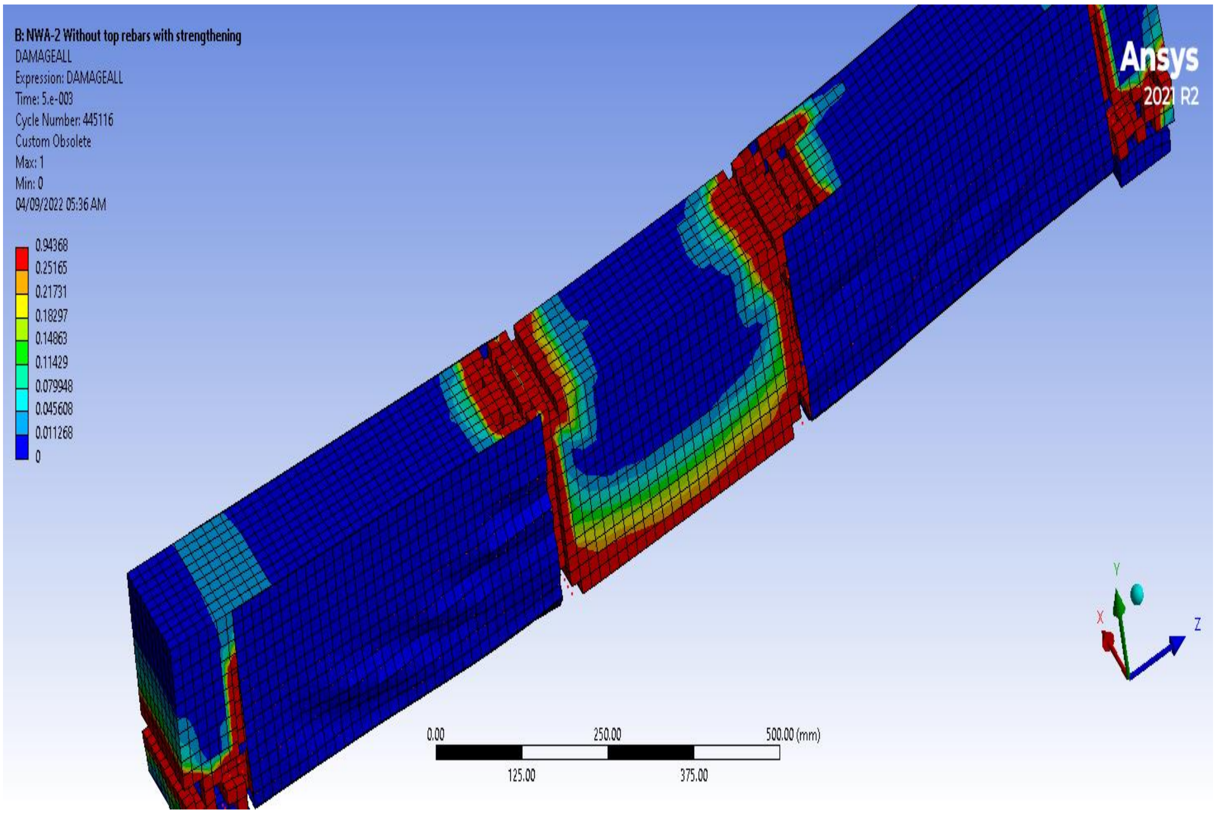

Figure 466(NWA-2/70.5MPa – Damage pattern-3 of beam sample with strengthening and without top rebars- Explicit Dynamic Analysis)

CFRP laminates due to ultimate load has been debonding as shown in images above

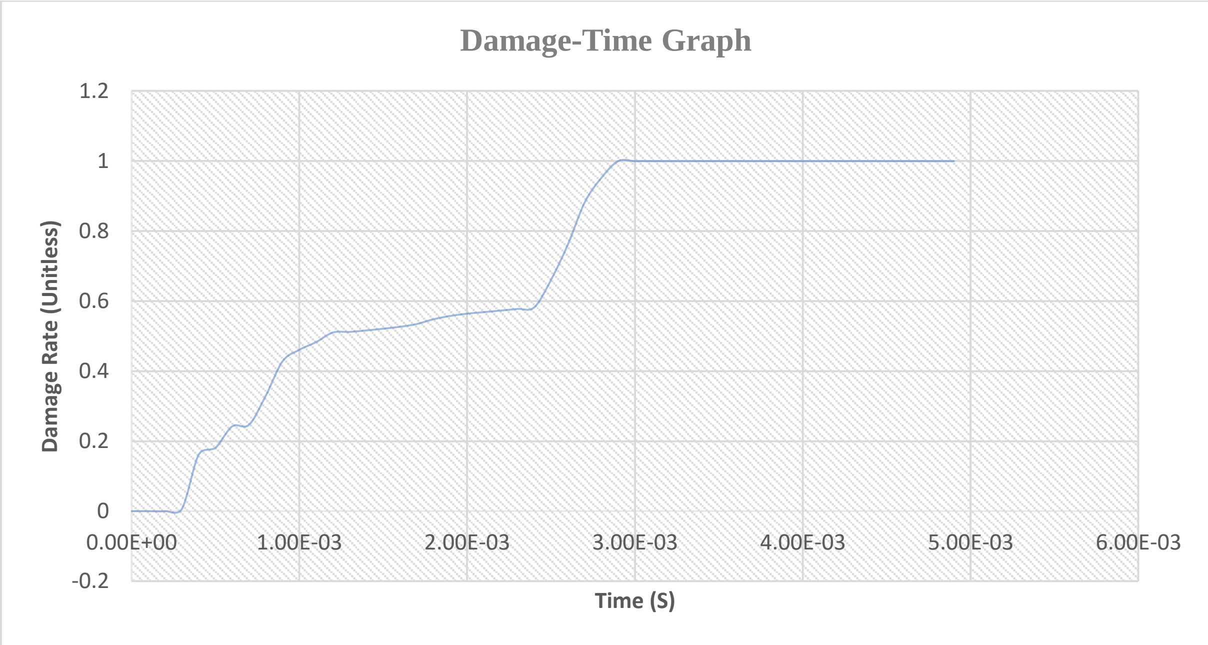

Figure 467(NWA-2/70.5MPa – Damage pattern graph of beam sample with strengthening and without top rebars- Explicit Dynamic Analysis)

Appendix B

1- Normal Weight Aggregate Sample (NWA-1).

Loads and Reactions

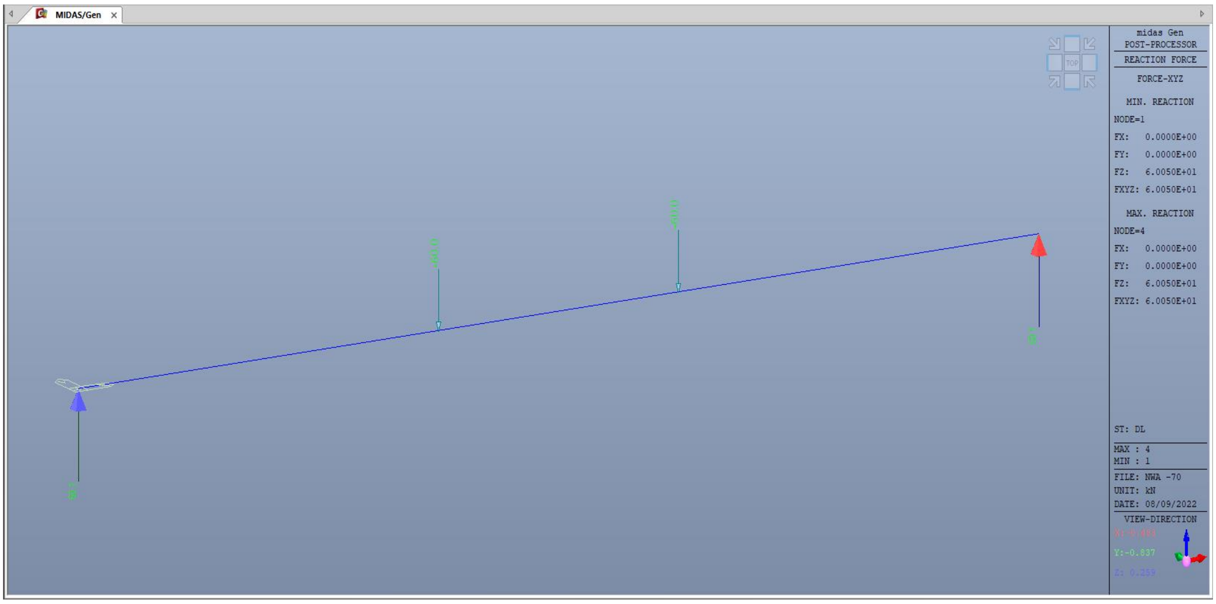

Figure 468(NWA-1/70.5MPa Loads and Reactions-Midas Gen)

Deformations

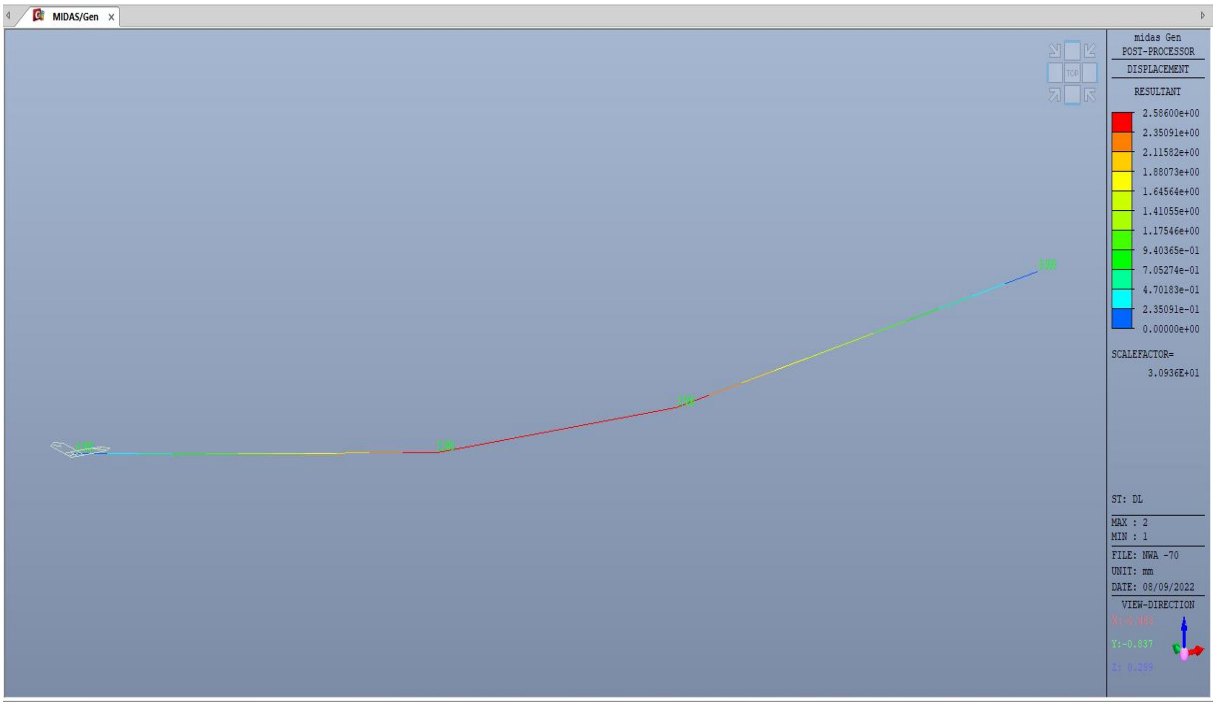

Figure 469(NWA-1/70.5MPa Deformations-Midas Gen)

-Shear

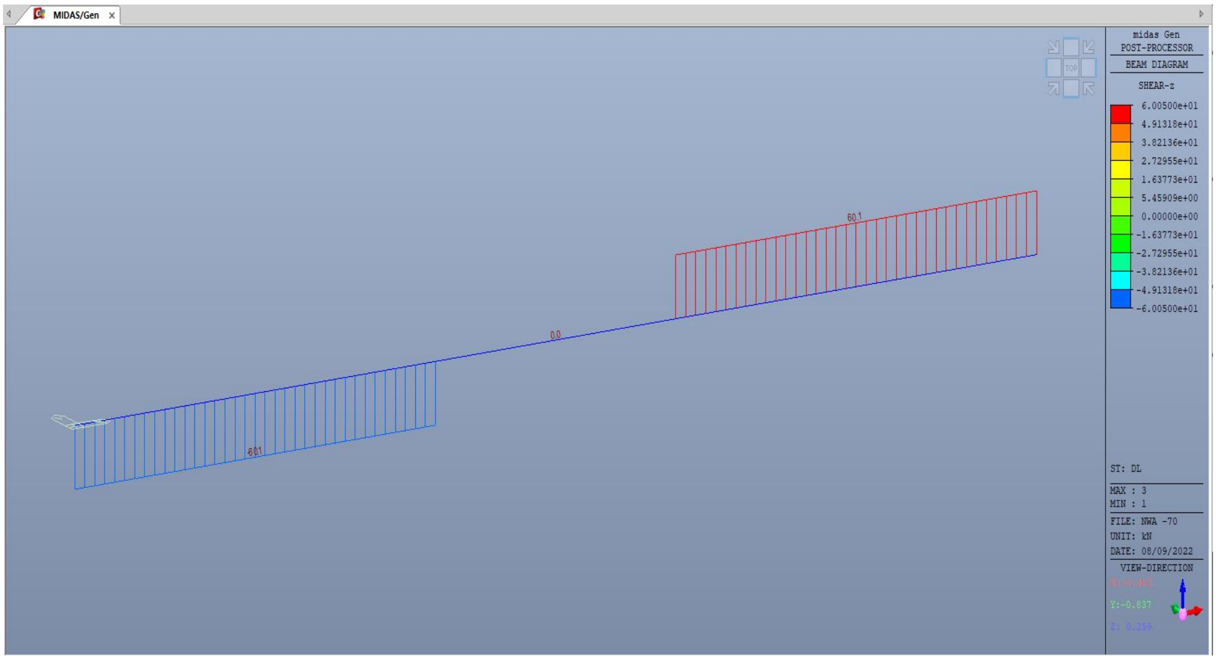

Figure 470(NWA-1/70.5MPa Shear Values-Midas Gen)

-Moment

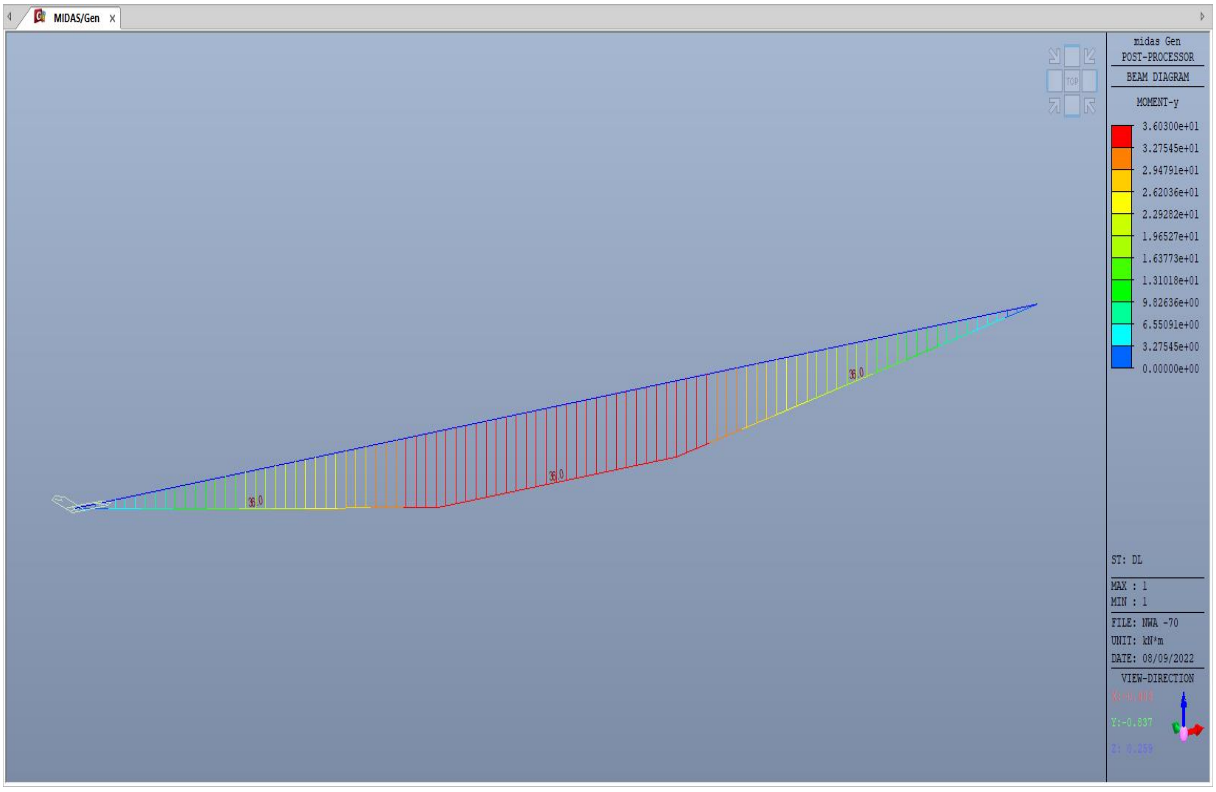

Figure 471(NWA-1/70.5MPa Moment Values-Midas Gen)

2- Recycled Aggregate Concrete with Self Consolidating Concrete Sample (RCA).

Loads and Reactions

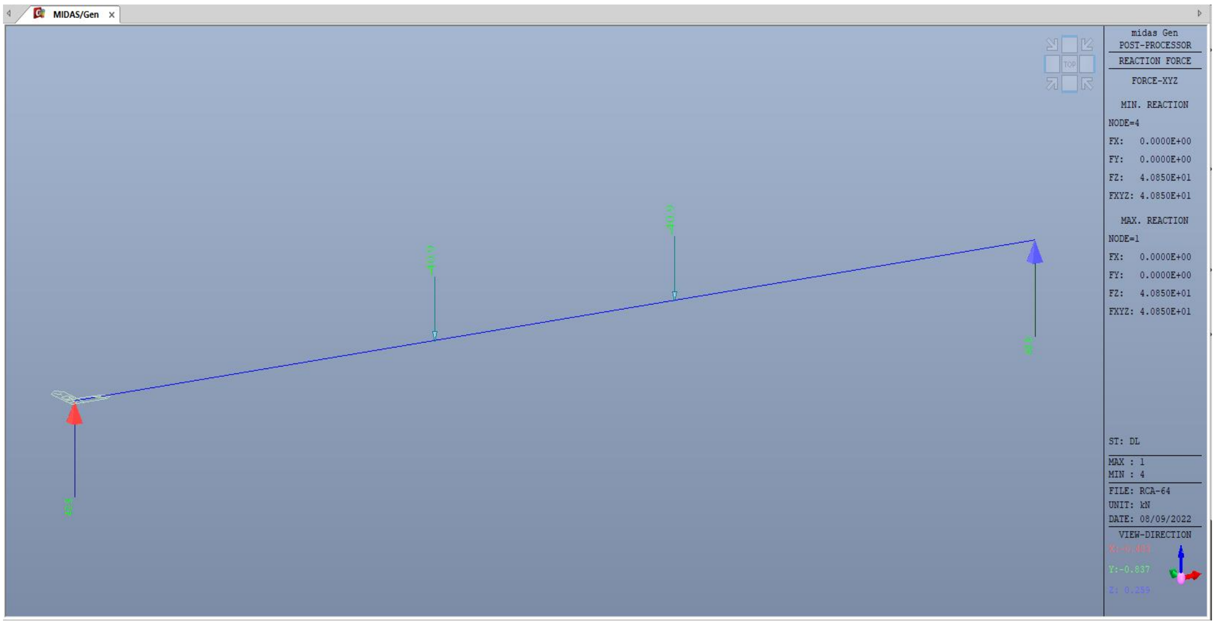

Figure 472(RCA-64.50MPa Loads and Reactions-Midas Gen)

Deformations

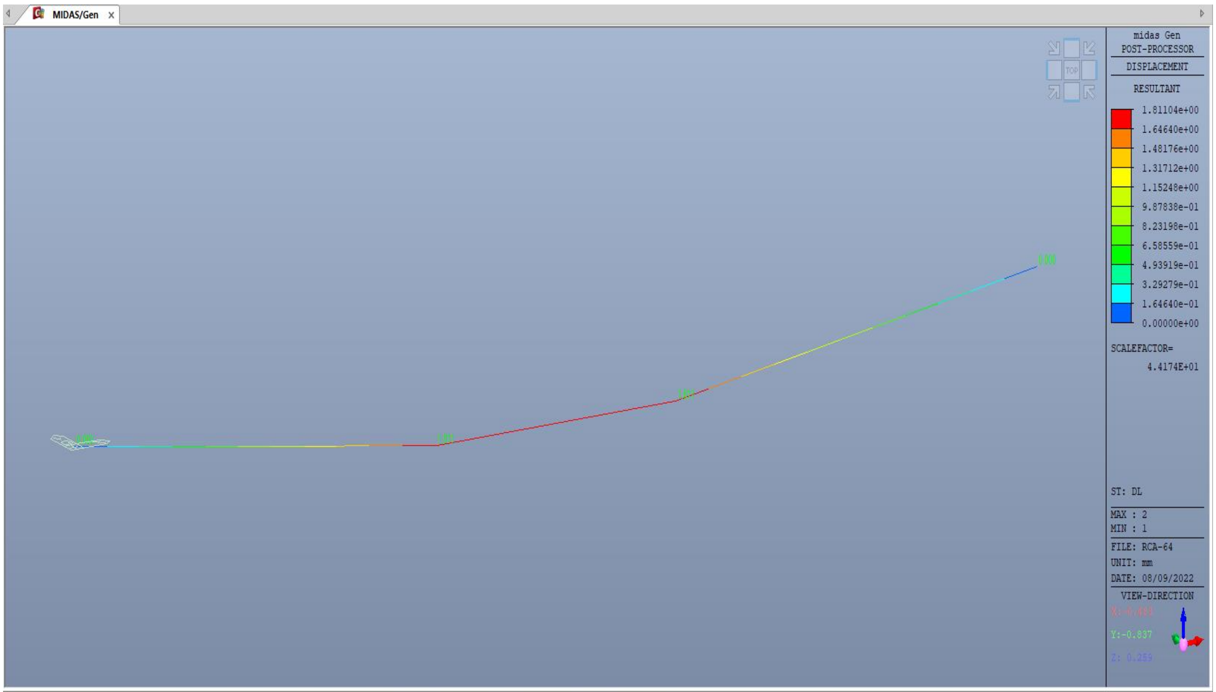

Figure 473(RCA-64.50MPa Deformations-Midas Gen)

-Shear

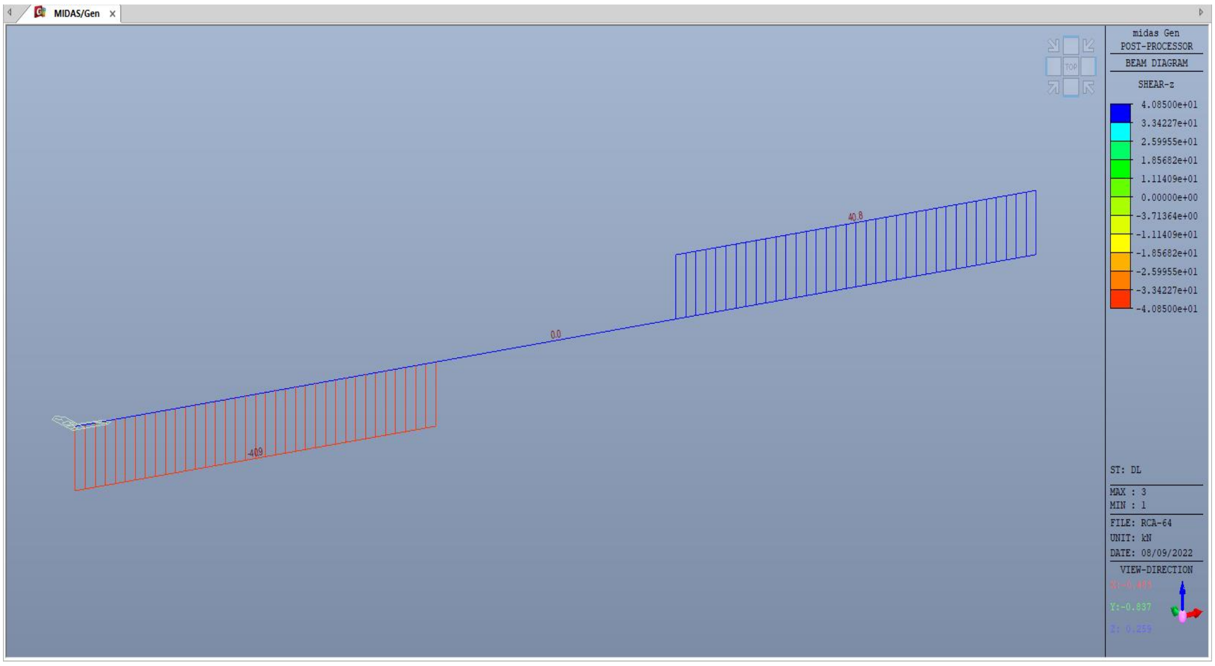

Figure 474(RCA-64.50MPa Shear Values-Midas Gen)

-Moment

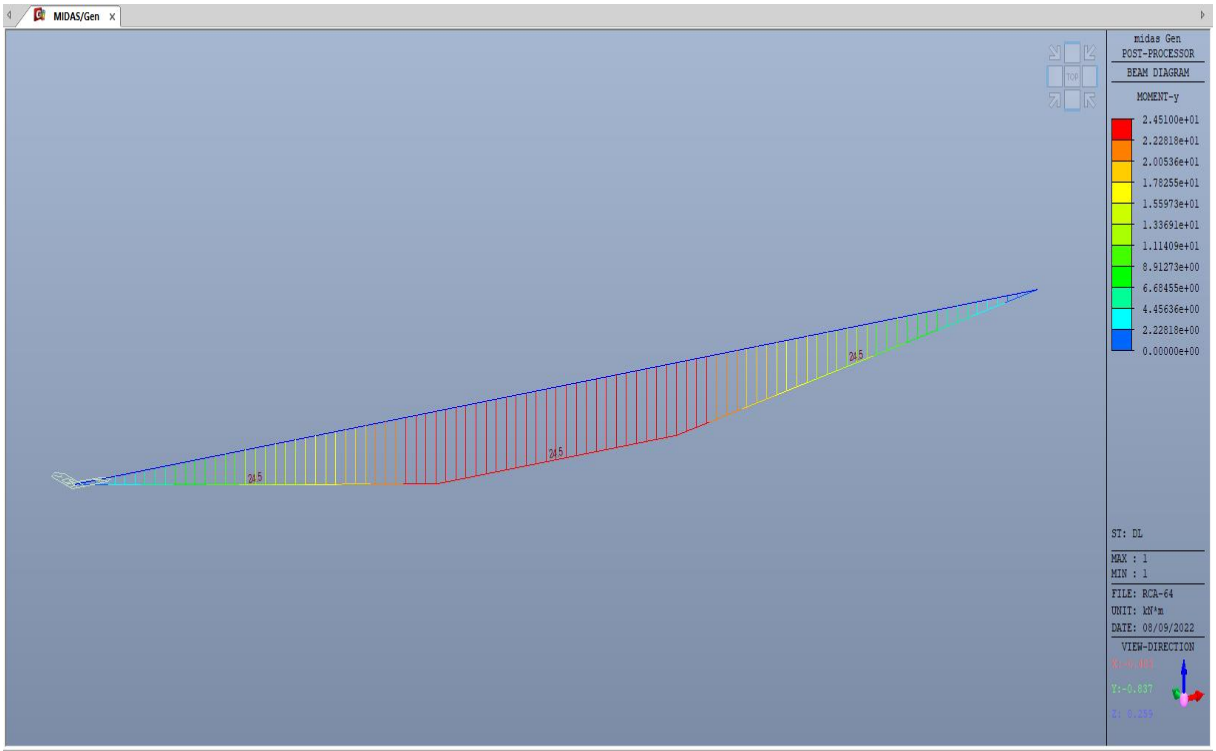

Figure 475(RCA-64.50MPa Moment Values-Midas Gen)

3- Recycled Aggregate Concrete with Self Consolidating Concrete Sample (RCA-5D), Not Strengthened

Loads and Reactions

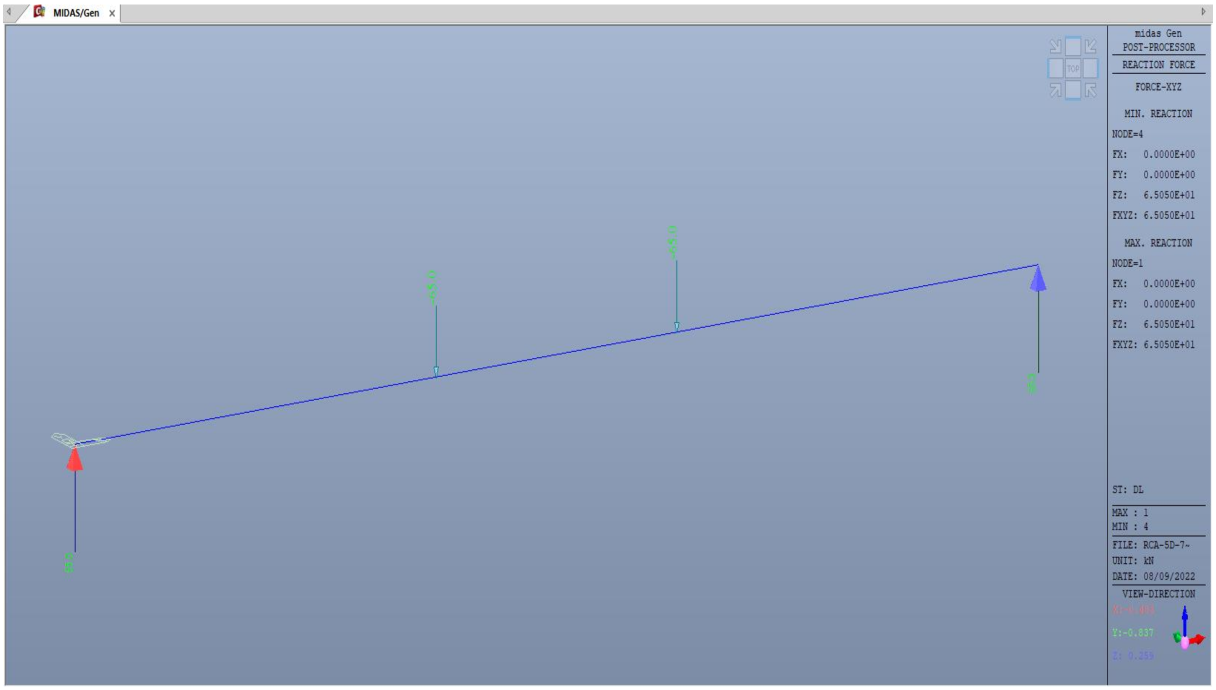

Figure 476(RCA-5D $_{Fibers}$- 77.0MPa Load and Reactions-Midas Gen)

Deformations

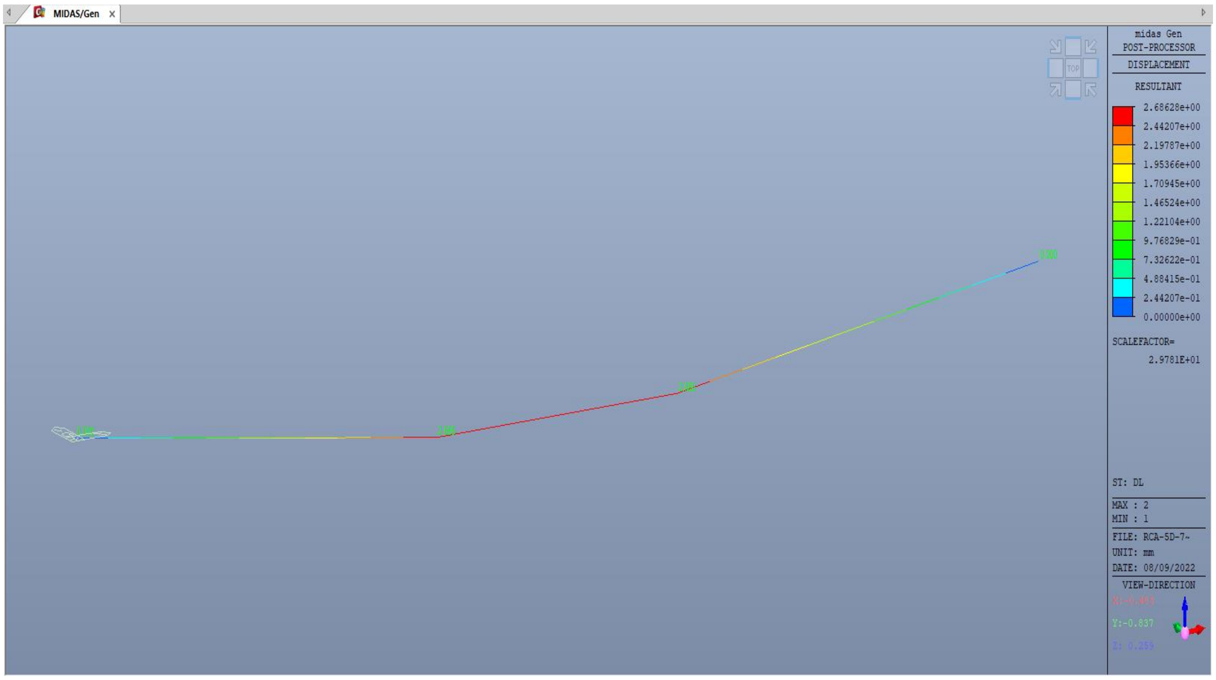

Figure 477(RCA-5D $_{Fibers}$- 77.0MPa Deformations-Midas Gen)

-Shear

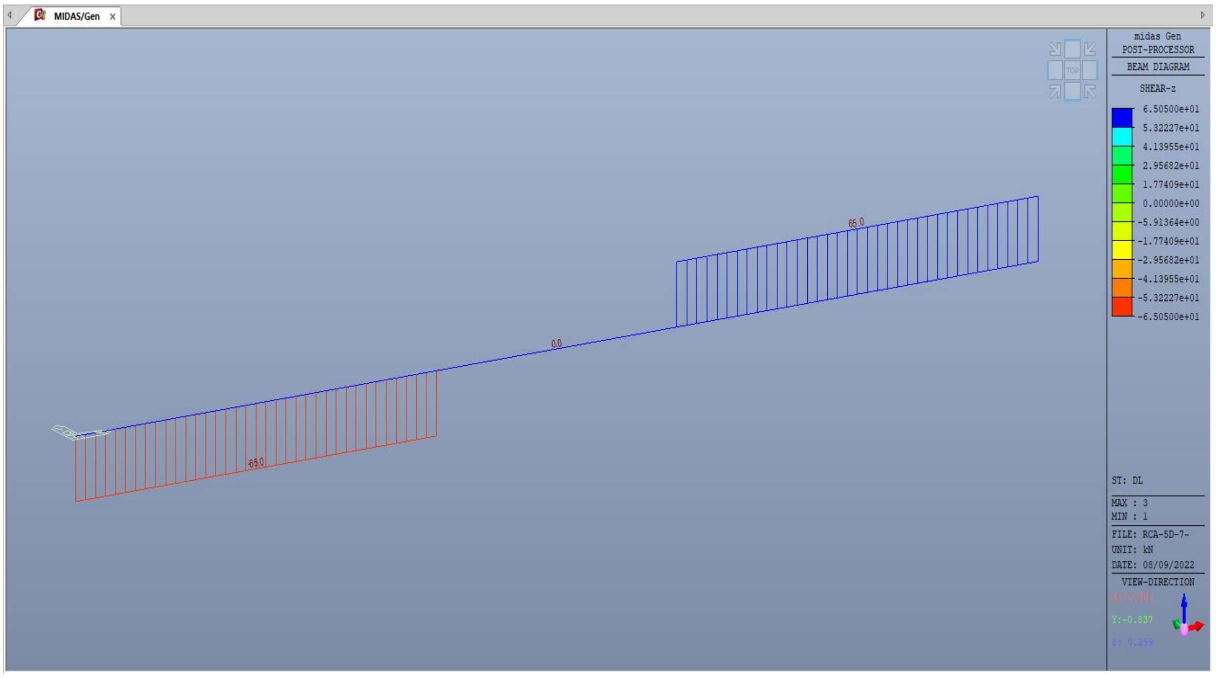

Figure 478(RCA-5D Fibers- 77.0MPa Shear Values-Midas Gen)

-Moment

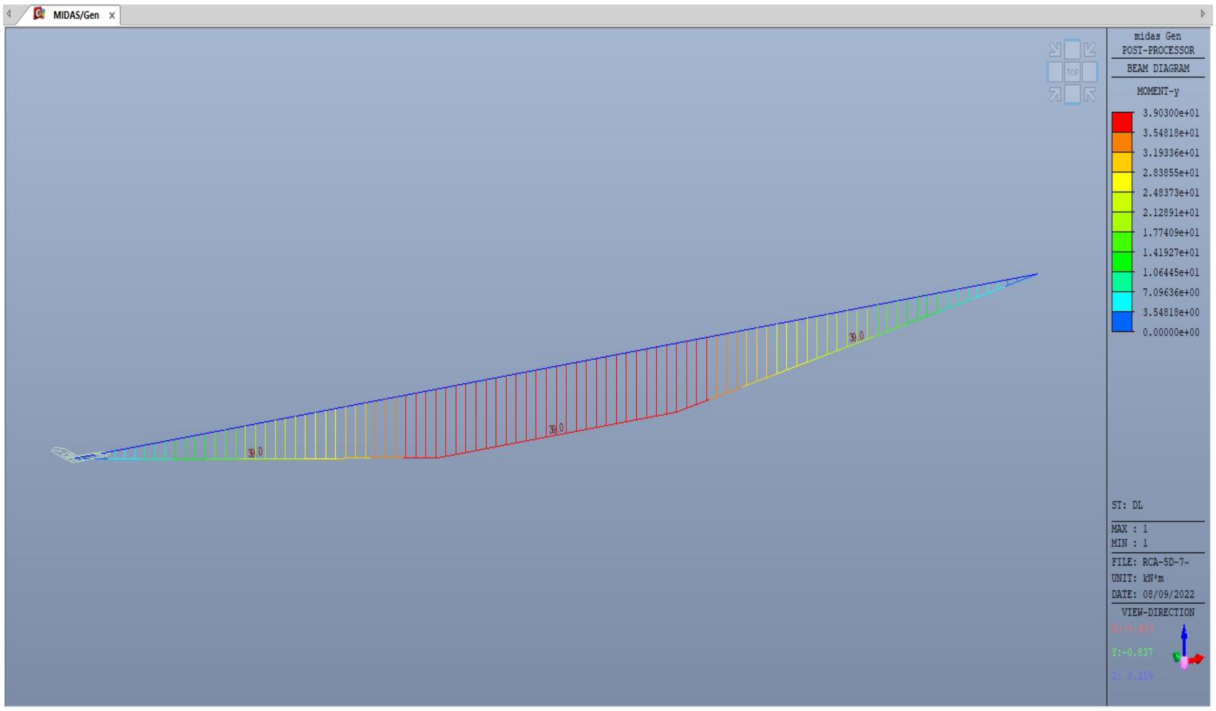

Figure 479(RCA-5D Fibers- 77.0MPa Moment Values-Midas Gen)

4- Normal Weight Aggregate Sample (NWA-2)- Strengthened

Loads and Reactions

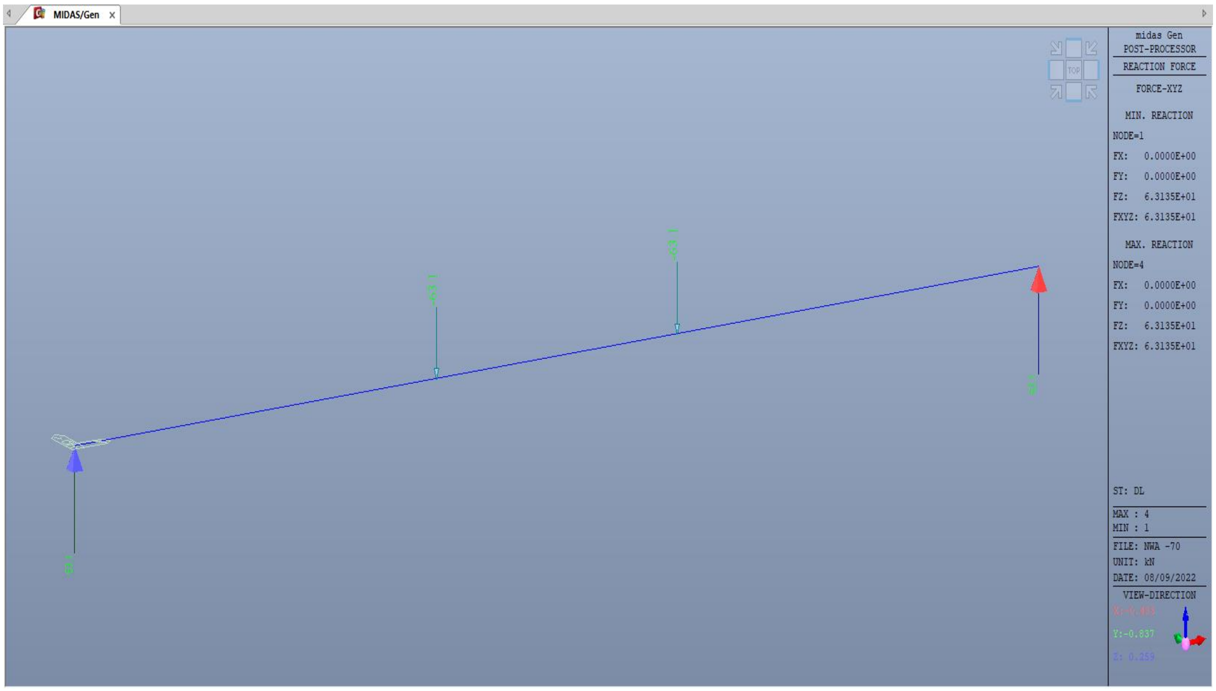

Figure 480(NWA-2/70.5MPa Load and Reactions-Midas Gen)

Deformations

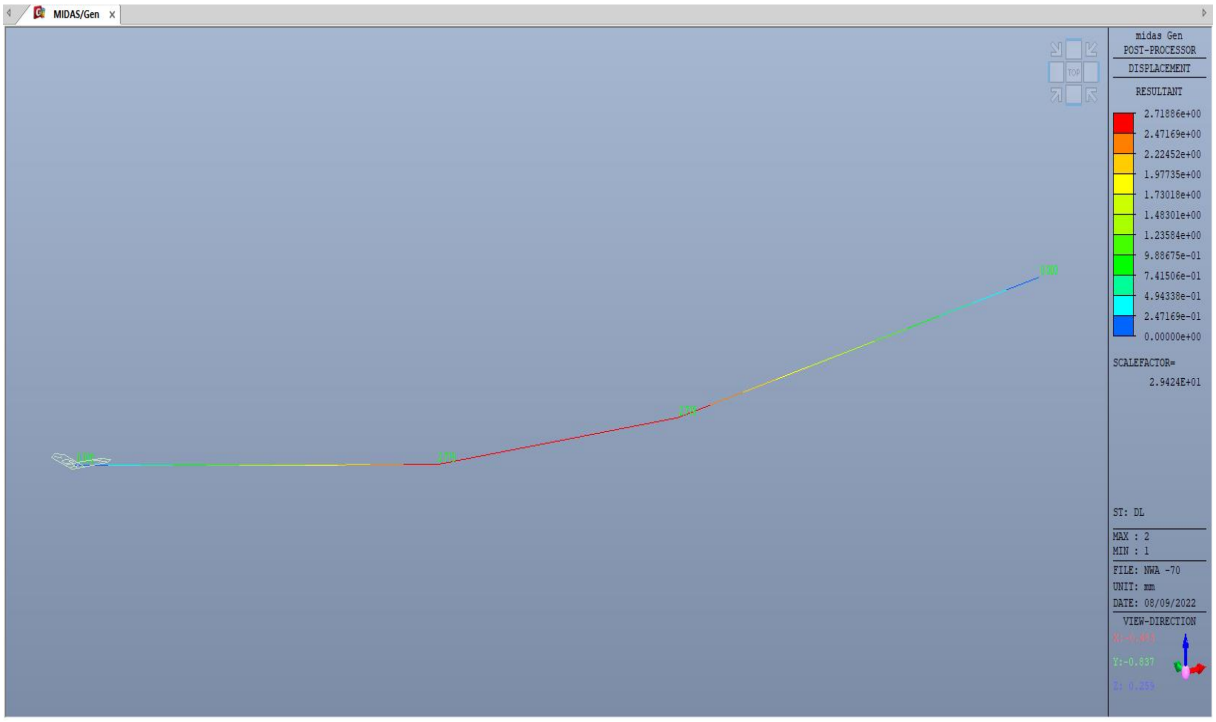

Figure 481(NWA-2/70.5MPa Deformations-Midas Gen)

-Shear

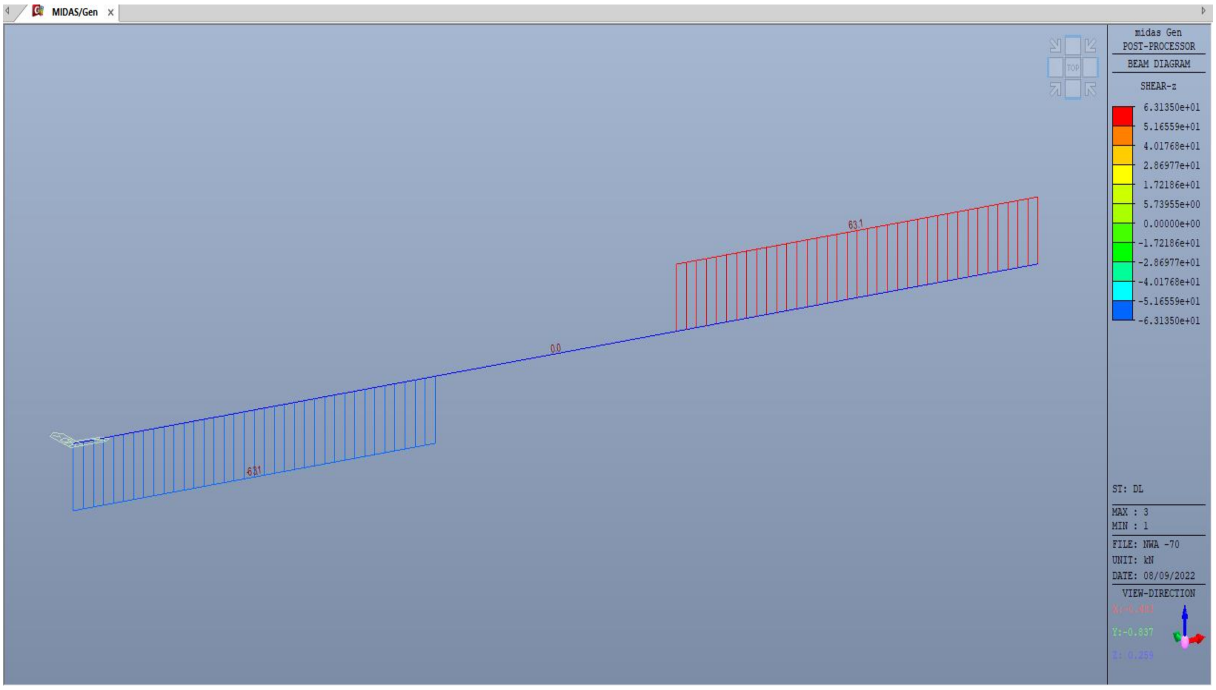

Figure 482(NWA-2/70.5MPa Shear Values-Midas Gen)

-Moment

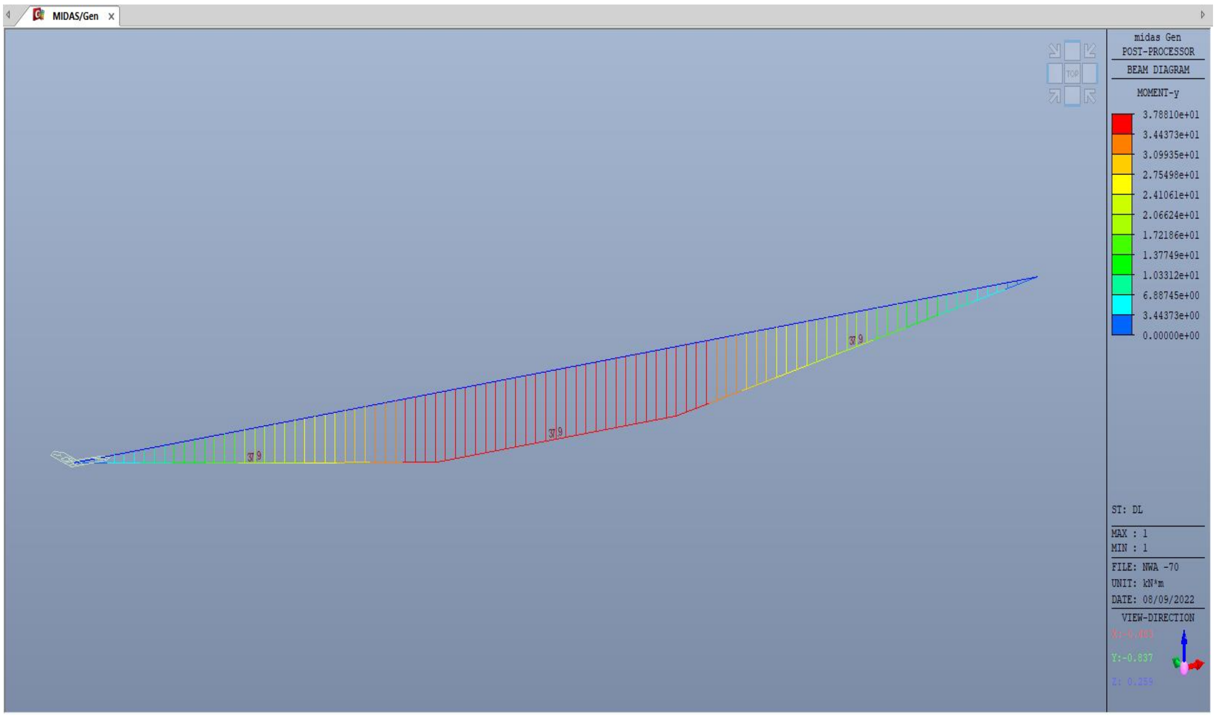

Figure 483(NWA-2/70.5MPa Moment Values-Midas Gen)

Appendix C

Case 1- FRP Strengthening Detailed Calculations-Midas Design Plus 2021

MEMBER NAME : Model No.1- Normal Weight Aggregate Sample (NWA).

General Information
Design Code : ACI318M-14
Reference Code : ACI 440.2R-08
[Guide for Design and Construction of Externally Bonded FRP System for Strengthening Concrete Structures.]
Code Unit : N, mm

Material
Concrete
f_{ck} : 70.50MPa
E_c : 39,463MPa
Rebar
f_y : 460MPa
f_{ys} : 420MPa
E_s : 200,000MPa
FRP / Carbon (MasterBrace FIB 600/50 CFS)
f^*_{fu} : 3,500MPa
E^*_{fs} : 230,000MPa
t_f : 0.337mm
ε^*_{fu} : 0.021000
Fiber Type : Carbon

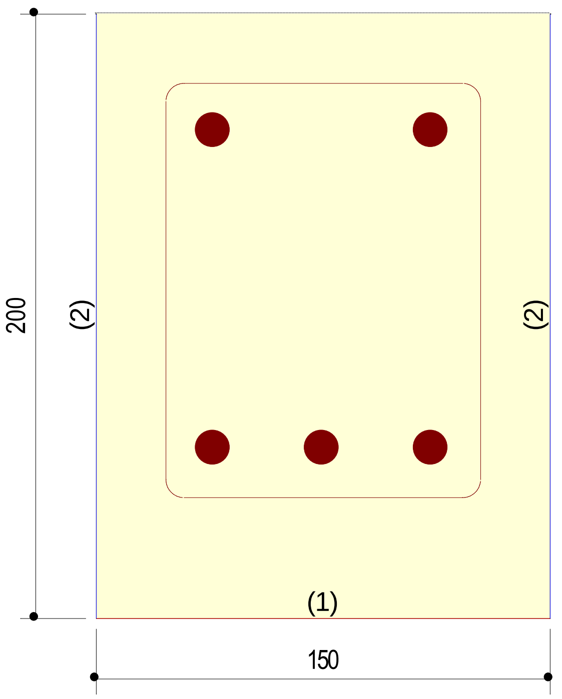

Section
Beam
Section Size : 150 x 200mm
Cover : 23.00 / 40.00mm
Compression : Not Considered
Splicing Limit : 50%
FRP / Carbon

POS.	Apply	Size(mm)	Pieces	Description
(1)	Yes	150	1	Bottom of Beam
(2)	Yes	200	1	Side of Beam (Shear)
(3)	No	120	1	Side of Beam (Bottom)
(4)	No	120	1	Side of Beam (Top)
(5)	No	100	1	Bottom of Slab
(6)	No	150	1	Top of Beam

FRP / Carbon (Shear / U-Wraps (3 Sides Bonded))
w_f : 500mm
s_f : 400mm

Rebar

Top Bar : 2-P12 (A_s = 226mm²)
Layer 1 : 2 EA (C_c = 39.00mm)
Bot Bar : 3-P12 (A_s = 339mm²)
Layer 1 : 3 EA (C_c = 56.00mm)
Stirrup : 2-P10@300 (A_s = 157mm²)

Design Force

Design Force
$M_{u.DL}$: 0.000kN·m
$M_{u.LL}$: 0.000kN·m
M_{ux} : 36.03kN·m
V_{uy} : 60.05kN

Design Data

Exposure Conditions : Exterior Exposure

Calculate the Design Material Properties

[ACI 440.2R-08 / 9.4 - Design material properties]
Calculate the Design Material Properties
$C_E = 0.850$
$f_{fu} = C_E\ f^*_{fu}$ = 2,975MPa
$\varepsilon_{fu} = C_E\ \varepsilon^*_{fu}$ = 0.017850
$E_f = f_{fu} / \varepsilon^*_{fu}$ = 230,000MPa

Check Bending Moment Capacity (RC Section Only)

Calculate design parameter
$\beta_1 = 0.650$
Check space of rebar

$s_{max1} = 380 \left(\frac{280}{f_s} \right) - 2.5c_c$, $\quad s_{max2} = 300 \left(\frac{280}{f_s} \right)$

$s_{max} = \min (s_{max1} , s_{max2})$ = 222mm, $N_{req} = 2$
s = 19.00 < 222mm → O.K
Calculate required ratio of reinforcement

$\rho_{min.11} = \frac{0.25 \sqrt{f'_c}}{f_y}$, $\quad \rho_{min.12} = \frac{1.4}{f_y}$

$\rho_{min.1} = \max (\rho_{min.11} , \rho_{min.12}) = 0.0046$

$\rho_{min.2} = \frac{4}{3} \frac{M_u}{ø\ f_y\ bd(d-a/2)} = 0.0424$

$\rho_{min} = \min (\rho_{min1} , \rho_{min2}) = 0.0046$

$\rho_{\varepsilon t} = 0.85\ \beta_1 \left(\frac{f'_c}{f_y} \right) \left(\frac{\varepsilon_c}{\varepsilon_c + 0.004} \right) = 0.0363$

$\rho_{max} = \rho_{et} = 0.0363$
Check ratio of tensile reinforcement

$\rho = \frac{A_s}{b_w\ d} = 0.0157$

$\rho_{min} < \rho < \rho_{max}$ → O.K
Calculate moment capacity

$a = \frac{A_s\ f_y}{0.85\ f'_c\ b_w}$ = 17.36mm

ø = 0.900

$M_n = A_s f_y (d - a/2) = 21.14\text{kN·m}$
$øM_n = 19.02\text{kN·m}$
Calculate ratio of moment capacity
$M_u / øM_n = 1.894 \rightarrow$ N.G

Check Shear Capacity (RC Section Only)
Calculate shear strength by concrete
$ø = 0.750$ $d = 144\text{mm}$
$øV_c = ø\ 0.17 \sqrt{f'_c}\ b_w d = 22.87\text{kN}$
$V_u > øV_c \rightarrow$ Shear reinforcement is required
Calculate required shear strength by shear reinforcement
$V_{s.req} = (V_u - øV_c) / ø = 49.57\text{kN}$
$V_{c1} = 0.33 \sqrt{f'_c}\ b_w d = 59.20\text{kN}$ Refer to [11.4.5.3]
$V_{c2} = 0.66 \sqrt{f'_c}\ b_w d = 118\text{kN}$
$V_{s.req} < V_{c2} \rightarrow$ O.K
$A_{v.min1/s} = 0.062 \sqrt{f'_c}\ \frac{b_w}{f_{yt}}$, $A_{v.min2/s} = 0.35 \frac{b_w}{f_{yt}}$
$A_{v.min} /s = \max [A_{v.min1} /s , A_{v.min2} /s] = 0.184\text{mm}^2/\text{mm}$
$A_{v.req0} /s = \frac{V_{s.req}}{f_{yt} \cdot d} = 0.819\text{mm}^2/\text{mm}$
$A_{v.req} /s = \max [A_{v.min} /s , A_{v.req0} /s] = 0.819\text{mm}^2/\text{mm}$
Calculate shear strength by stirrup
$N_{leg} = 2$ $A_{v1} = 78.54\text{mm}^2$ (P10)
$øV_s = ø \frac{A_v f_{yt} d}{s} = 23.77\text{kN}$
Calculate ratio of shear capacity
$øV_n = øV_c + øV_s = 46.64\text{kN}$
$V_u / øV_n = 1.287 \rightarrow$ N.G
Calculate spacing limits for reinforcement
$s_{max.0} = \min [d/2, 600\text{mm}] = 72.05\text{mm}$
$s_{req} = \frac{N_{leg} A_{v1}}{A_{v.req} /s} = 192\text{mm}$
$s_{max} = \min [s_{max.0} , s_{req}] = 72.05\text{mm}$
$s = 300\text{mm} > s_{max} = 72.05\text{mm} \rightarrow$ N.G

Check the Strengthening Limit Criteria
[ACI 440.2R-08 / 9.2 - Strengthening limits]
Bending Moment Strength without FRP
$ø = 0.900$
$M_{ns} = 21.14\text{kN·m}$
$øM_{ns} = 19.02\text{kN·m}$
Check the Strengthening Limit Criteria
$M_{u.new} = 1.1M_{DL} + 0.75M_{LL} = 0.000\text{kN·m}$
$M_{u.new} / øM_{ns} = 0.000 < 1.000 \rightarrow$ O.K

Calculate Moment of Inertia of Cracked Section Transformed to Concrete
Calculate Modulus of Rupture
$f_r = 0.63 \sqrt{f_{ck}} = 5.206\text{MPa}$
$n = E_s / E_c = 5.068$
Calculate Moment of Inertia of Cracked Section Transformed to Concrete
$d = 144\text{mm}$
$d' = 39.00\text{mm}$
$A_s = 339\text{mm}^2$
$A'_s = 226\text{mm}^2$
$\gamma = \frac{(n - 1) A'_s}{n A_s} = 0.535$
$B = b / n A_s = 0.0872$
$kd = 46.37\text{mm}$
$k = 0.322$
$I_g = b h^3 / 12 = 100{,}150{,}075\text{mm}^4$
$I_{cr} = \frac{b (kd)^3}{3} + nA_s (d\text{-}kd)^2 + (n\text{-}1) A'_s (kd\text{-}d')^2 = 21{,}459{,}190\text{mm}^4$

Search Neutral Axis

Calculate the Design Strain of the FRP System

$n_f = 1$

$t_f = 0.337mm$

$\varepsilon_{fd.cal} = 0.410 \sqrt{f_{ck} / n\ E_f\ t_f} = 0.012365$

$\varepsilon_{fd.max} = 0.90\ \varepsilon_{fu} = 0.016065$

$\varepsilon_{fd} = 0.012365$

Calculate the Existing State of Strain

$d_f = 200mm$

$$\varepsilon_{bi} = \frac{M_{DL}\ (\ d_f - kd\ )}{I_{cr}\ E_c} = 0.000000$$

Estimate the Depth to the Neutral Axis

$c = 41.39mm$

Calculate the Effective Level of Strain in the FRP Reinforcement

$\varepsilon_{cu} = 0.003000$

$$\varepsilon_{fe.cal} = \varepsilon_{cu} \frac{d_f - c}{c} - \varepsilon_{bi} = 0.011517$$

$\varepsilon_{fe.max} = \varepsilon_{fd} = 0.012365$

$\varepsilon_{fe} = 0.011517$

Calculate the Concrete Strain

$$\varepsilon_c = (\ \varepsilon_{fe} + \varepsilon_{bi}\ ) \left(\frac{c}{d_f - c} \right) = 0.003000$$

Calculate the Stress Level in the Reinforcing Steel

$d = 144mm$

$$\varepsilon_s = (\ \varepsilon_{fe} + \varepsilon_{bi}\ ) \left(\frac{d - c}{d_f - c} \right) = 0.007445$$

$f_{s.cal} = E_s\ \varepsilon_s = 1{,}489MPa$

$f_{s.max} = f_y = 460MPa$

$f_s = 460MPa$

Calculate the Stress Level in the Reinforcing FRP

$f_{fe.cal} = E_f\ \varepsilon_{fe} = 2{,}649MPa$

$f_{fe.max} = f_{fu} = 2{,}975MPa$

$f_{fe} = 2{,}649MPa$

Calculate the Internal Force Resultants

$\varepsilon'_c = 1.7\ f_{ck} / E_c = 0.003037$

$$\beta_1 = \frac{4\ \varepsilon'_c - \varepsilon_c}{6\ \varepsilon'_c - 2\ \varepsilon_c} = 0.748$$

$$\alpha_1 = \frac{3\ \varepsilon'_c\ \varepsilon_c - (\ \varepsilon_c)^2}{3\ \beta_1\ (\ \varepsilon'_c)^2} = 0.885$$

Verify Force Equilibrium

$A_s = 339mm^2$

$A_f = 50.55mm^2$

$F_s = A_s\ f_s = 156kN$

$F_f = A_f\ f_{fe} = 134kN$

$F_{TENS.} = F_s + F_f = 290kN$

$F_{COMP.} = \alpha_1\ f_{ck}\ \beta_1\ b\ c = 290kN$

Calculate Flexural Strength

Calculate Flexural Strength Components

$M_{ns} = A_s\ f_s\ (\ d - \beta_1\ c / 2\ ) = 20.07kN{\cdot}m$

$M_{nf} = A_f\ f_{fe}\ (\ d_f - \beta_1\ c / 2\ ) = 24.74kN{\cdot}m$

Calculate Design Flexural Strength of Section

$ø = 0.900$

$\psi = 0.850$

$øM_n = ø\ [\ M_{ns} + \psi_f\ M_{nf}\ ] = 36.99kN{\cdot}m$

$M_u / øM_n = 0.974 < 1.000 \rightarrow$ O.K

Check Service Stress in the Reinforcing Steel and FRP

Calculate the Elastic Depth to the Cracked Neutral Axis

$A_s = 339mm^2$

$A_f = 50.55mm^2$

$d = 144mm$

d_f = 200mm
ρ_s = 0.015697
ρ_f = 0.001684
$k = \sqrt{(k_1)^2 + 2\,k_2} - k_1 = 0.352$
$k_1 = \rho_s \dfrac{E_s}{E_c} + \rho_f \dfrac{E_f}{E_c}$
$k_2 = \rho_s \dfrac{E_s}{E_c} + \rho_f \dfrac{E_f}{E_c} \dfrac{d_f}{d}$
kd = 50.65mm
Calculate the Stress Level in the Reinforcing Steel
ε_{bi} = 0.000000
$$f_{s.s} = \frac{[\,M_s + \varepsilon_{bi} A_f E_f\,(d_f - kd/3)\,]\,(d - kd)\,E_s}{A_s E_s\,(d - kd/3)\,(d - kd) + A_f E_f\,(d_f - kd/3)\,(d_f - kd)} = 0.000\text{MPa}$$
$f_{s.s.max} = 0.80\, f_y$ = 368MPa
$f_{s.s} / f_{s.s.max}$ = 0.000 < 1.000 → O.K

Check Creep Rupture Limit at Service of FRP
Calculate the Stress Level in the Reinforcing FRP
$$f_{f.s} = f_{s.s} \left(\frac{E_f}{E_s}\right)\left(\frac{d_f - kd}{d - kd}\right) - \varepsilon_{bi} E_f = 0.000\text{MPa}$$
f_{fu} = 2,975MPa
$f_{f.s.max} = 0.550\, f_{fu}$ = 1,636MPa
$f_{f.s} / f_{f.s.max}$ = 0.000 < 1.000 → O.K

Calculate Shear Strength by FRP
Shear Strength without FRP
ø = 0.750
V_c = 30.50kN
V_s = 49.57kN
$øV_{ns}$ = 46.64kN
$øV_{ns.MAX}$ = 112kN
Calculate the Effective Strain Level
n_f = 1
t_f = 0.337mm
d_{fv} = 144mm
$$L_e = \frac{23{,}300}{(n_f\, t_f\, E_f)^{0.58}} = 34.00\text{mm}$$
$k_1 = (f_{ck} / 27.00)^{2/3} = 1.896$
$$k_2 = \frac{d_{fv} - L_e}{d_{fv}} = 0.764$$
$$\kappa_{v.cal} = \frac{k_1\, k_2\, L_e}{11{,}900\, \varepsilon_{fu}} = 0.232$$
$\kappa_{v.max}$ = 0.750
κ_v = 0.232
$\varepsilon_{fe.cal} = \kappa_v\, \varepsilon_{fu}$ = 0.004139
$\varepsilon_{fe.max}$ = 0.004000
ε_{fe} = 0.004000
Calculate the Contribution of the FRP Reinforcement
ψ_f = 0.850
w_f = 500mm
s_f = 400mm
$A_{fv} = 2\, n\, t_f\, w_f$ = 337mm²
$f_{fe} = \varepsilon_{fe} E_f$ = 920MPa
$$V_f = \frac{A_{fv}\, f_{fe}\, d_{fv}}{s_f} = 112\text{kN}$$
Calculate Shear Strength Ratio
$øV_n = ø\,(V_c + V_s + \psi_f V_f)$ = 112kN
$V_u / øV_n$ = 0.538 < 1.000 → O.K

Calculate Development Length
[ACI 440.2R-08 / 13.1.3 - Development length]
Calculate Development Length

POS.	Apply	Pieces	l_{df} (mm)	Description
(1)	Yes	1	96.08	Bottom of Beam
(2)	Yes	1	96.08	Side of Beam (Shear)

$l_{df} = 1.000 \sqrt{n E_f t_f / (f_{ck})^{1/2}}$

Case 2- FRP Strengthening Detailed Calculations-Midas Design Plus 2021

MEMBER NAME : Model No.1- Normal Weight Aggregate Sample (NWA).

General Information
Design Code : ACI318M-14
Reference Code : ACI 440.2R-08
[Guide for Design and Construction of Externally Bonded FRP System for Strengthening Concrete Structures.]
Code Unit : N, mm

Material
Concrete
f_{ck} : 70.50MPa
E_c : 39,463MPa
Rebar
f_y : 460MPa
f_{ys} : 420MPa
E_s : 200,000MPa
FRP / Carbon (MasterBrace FIB 600/50 CFS)
f^*_{fu} : 3,500MPa
E^*_{fs} : 230,000MPa
t_f : 0.337mm
ε^*_{fu} : 0.021000
Fiber Type : Carbon

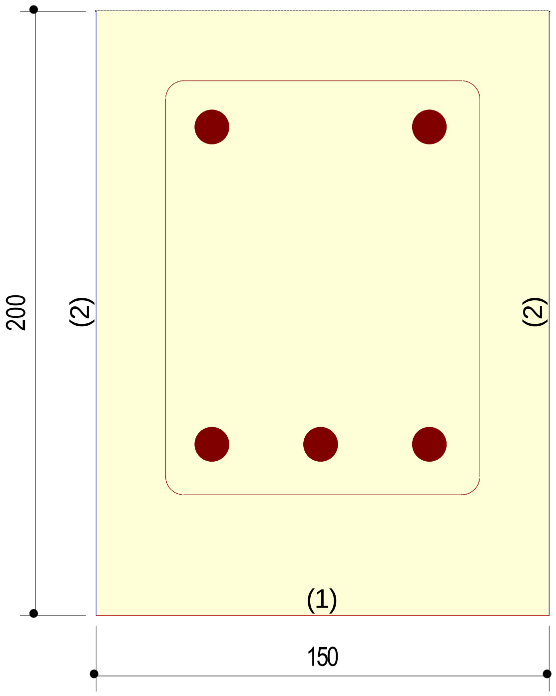

Section
Beam
Section Size : 150 x 200mm

Cover : 23.00 / 40.00mm
Compression : Considered
Splicing Limit : 50%
FRP / Carbon

POS.	Apply	Size(mm)	Pieces	Description
(1)	Yes	150	1	Bottom of Beam
(2)	Yes	200	1	Side of Beam (Shear)
(3)	No	120	1	Side of Beam (Bottom)
(4)	No	120	1	Side of Beam (Top)
(5)	No	100	1	Bottom of Slab
(6)	No	150	1	Top of Beam

FRP / Carbon (Shear / U-Wraps (3 Sides Bonded))
w_f : 500mm
s_f : 400mm

Rebar

Top Bar : 2-P12 (A_s = 226mm²)
Layer 1 : 2 EA (C_c = 39.00mm)
Bot Bar : 3-P12 (A_s = 339mm²)
Layer 1 : 3 EA (C_c = 56.00mm)
Stirrup : 2-P10@300 (A_s = 157mm²)

Design Force

Design Force
$M_{u.DL}$: 0.000kN·m
$M_{u.LL}$: 0.000kN·m
M_{ux} : 36.03kN·m
V_{uy} : 60.05kN

Design Data

Exposure Conditions : Exterior Exposure

Calculate the Design Material Properties

[ACI 440.2R-08 / 9.4 - Design material properties]
Calculate the Design Material Properties
$C_E = 0.850$
$f_{fu} = C_E\, f^*_{fu} = 2{,}975\text{MPa}$
$\varepsilon_{fu} = C_E\, \varepsilon^*_{fu} = 0.017850$
$E_f = f_{fu} / \varepsilon^*_{fu} = 230{,}000\text{MPa}$

Check Bending Moment Capacity (RC Section Only)

Calculate design parameter
$\beta_1 = 0.650$
Check space of rebar

$s_{max1} = 380 \left(\frac{280}{f_s} \right) - 2.5c_c$, $s_{max2} = 300 \left(\frac{280}{f_s} \right)$

$s_{max} = \min (s_{max1} , s_{max2}) = 222\text{mm}$, $N_{req} = 2$
$s = 19.00 < 222\text{mm} \rightarrow$ O.K
Calculate required ratio of reinforcement

$\rho_{min.11} = \frac{0.25 \sqrt{f'_c}}{f_y}$, $\rho_{min.12} = \frac{1.4}{f_y}$

$\rho_{min.1} = \max (\rho_{min.11} , \rho_{min.12}) = 0.0046$

$\rho_{min.2} = \frac{4}{3} \frac{M_u}{ø\, f_y\, bd(d\text{-}a/2)} = 0.0424$

$\rho_{min} = \min (\rho_{min1} , \rho_{min2}) = 0.0046$

$\rho_{\varepsilon t} = 0.85\, \beta_1 \left(\frac{f'_c}{f_y} \right) \left(\frac{\varepsilon_c}{\varepsilon_c + 0.004} \right) = 0.0363$

$\rho_{max} = \rho_{et} = 0.0434$
Check ratio of tensile reinforcement

$\rho = \frac{A_s}{b_w\, d} = 0.0157$

$\rho_{min} < \rho < \rho_{max} \rightarrow$ O.K

Calculate moment capacity

$a = \dfrac{A_s\ f_y}{0.85\ f'_c\ b_w} = 20.67\text{mm}$

$\phi = 0.900$

$M_n = A_s\ f_y\ (\ d - a/2\ ) = 21.76\text{kN}\cdot\text{m}$

$\phi M_n = 19.58\text{kN}\cdot\text{m}$

Calculate ratio of moment capacity

$M_u\ /\ \phi M_n = 1.840 \rightarrow$ N.G

Check Shear Capacity (RC Section Only)

Calculate shear strength by concrete

$\phi = 0.750$ $\qquad d = 144\text{mm}$

$\phi V_c = \phi\ 0.17 \sqrt{f'_c}\ b_w\ d = 22.87\text{kN}$

$V_u > \phi V_c \rightarrow$ Shear reinforcement is required

Calculate required shear strength by shear reinforcement

$V_{s.req} = (\ V_u - \phi V_c\ )\ /\ \phi = 49.57\text{kN}$

$V_{c1} = 0.33 \sqrt{f'_c}\ b_w\ d = 59.20\text{kN}$ Refer to [11.4.5.3]

$V_{c2} = 0.66 \sqrt{f'_c}\ b_w\ d = 118\text{kN}$

$V_{s.req} < V_{c2} \rightarrow$ O.K

$A_{v.min1/s} = 0.062 \sqrt{f'_c}\ \dfrac{b_w}{f_{yt}}\ , \quad A_{v.min2/s} = 0.35\ \dfrac{b_w}{f_{yt}}$

$A_{v.min}\ /s = \max\ [\ A_{v.min1}\ /s\ ,\ A_{v.min2}\ /s\ ] = 0.184\text{mm}^2/\text{mm}$

$A_{v.req0}\ /s = \dfrac{V_{s.req}}{f_{yt}\ \cdot\ d} = 0.819\text{mm}^2/\text{mm}$

$A_{v.req}\ /s = \max\ [\ A_{v.min}\ /s\ ,\ A_{v.req0}\ /s\ ] = 0.819\text{mm}^2/\text{mm}$

Calculate shear strength by stirrup

$N_{leg} = 2 \quad A_{v1} = 78.54\text{mm}^2$ (P10)

$\phi V_s = \phi\ \dfrac{A_v\ f_{yt}\ d}{s} = 23.77\text{kN}$

Calculate ratio of shear capacity

$\phi V_n = \phi V_c + \phi V_s = 46.64\text{kN}$

$V_u\ /\ \phi V_n = 1.287 \rightarrow$ N.G

Calculate spacing limits for reinforcement

$s_{max.0} = \min\ [\ d/2,\ 600\text{mm}\ ] = 72.05\text{mm}$

$s_{req} = \dfrac{N_{leg}\ A_{v1}}{A_{v.req}\ /s} = 192\text{mm}$

$s_{max} = \min\ [\ s_{max.0}\ ,\ s_{req}\ ] = 72.05\text{mm}$

$s = 300\text{mm} > s_{max} = 72.05\text{mm} \rightarrow$ N.G

Check the Strengthening Limit Criteria

[ACI 440.2R-08 / 9.2 - Strengthening limits]

Bending Moment Strength without FRP

$\phi = 0.900$

$M_{ns} = 21.76\text{kN}\cdot\text{m}$

$\phi M_{ns} = 19.58\text{kN}\cdot\text{m}$

Check the Strengthening Limit Criteria

$M_{u.new} = 1.1M_{DL} + 0.75M_{LL} = 0.000\text{kN}\cdot\text{m}$

$M_{u.new}\ /\ \phi M_{ns} = 0.000 < 1.000 \rightarrow$ O.K

Calculate Moment of Inertia of Cracked Section Transformed to Concrete

Calculate Modulus of Rupture

$f_r = 0.63 \sqrt{f_{ck}} = 5.206\text{MPa}$

$n = E_s\ /\ E_c = 5.068$

Calculate Moment of Inertia of Cracked Section Transformed to Concrete

$d = 144\text{mm}$

$d' = 39.00\text{mm}$

$A_s = 339\text{mm}^2$

$A'_s = 226\text{mm}^2$

$\gamma = \dfrac{(\ n - 1\ )\ A'_s}{n\ A_s} = 0.535$

$B = b\ /\ n\ A_s = 0.0872$

$kd = 46.37\text{mm}$

$k = 0.322$
$I_g = b\,h^3 / 12 = 100{,}150{,}075\text{mm}^4$
$$I_{cr} = \frac{b\,(kd)^3}{3} + nA_s\,(d\text{-}kd)^2 + (n\text{-}1)\,A'_s\,(kd\text{-}d')^2 = 21{,}459{,}190\text{mm}^4$$

Search Neutral Axis

Calculate the Design Strain of the FRP System
$n_f = 1$
$t_f = 0.337\text{mm}$
$\varepsilon_{fd.cal} = 0.410\sqrt{f_{ck} / n\,E_f\,t_f} = 0.012365$
$\varepsilon_{fd.max} = 0.90\,\varepsilon_{fu} = 0.016065$
$\varepsilon_{fd} = 0.012365$
Calculate the Existing State of Strain
$d_f = 200\text{mm}$
$$\varepsilon_{bi} = \frac{M_{DL}\,(d_f - kd)}{I_{cr}\,E_c} = 0.000000$$
Estimate the Depth to the Neutral Axis
$c = 41.39\text{mm}$
Calculate the Effective Level of Strain in the FRP Reinforcement
$\varepsilon_{cu} = 0.003000$
$$\varepsilon_{fe.cal} = \varepsilon_{cu}\,\frac{d_f - c}{c} - \varepsilon_{bi} = 0.011517$$
$\varepsilon_{fe.max} = \varepsilon_{fd} = 0.012365$
$\varepsilon_{fe} = 0.011517$
Calculate the Concrete Strain
$$\varepsilon_c = (\varepsilon_{fe} + \varepsilon_{bi})\left(\frac{c}{d_f - c}\right) = 0.003000$$
Calculate the Stress Level in the Reinforcing Steel
$d = 144\text{mm}$
$$\varepsilon_s = (\varepsilon_{fe} + \varepsilon_{bi})\left(\frac{d - c}{d_f - c}\right) = 0.007445$$
$f_{s.cal} = E_s\,\varepsilon_s = 1{,}489\text{MPa}$
$f_{s.max} = f_y = 460\text{MPa}$
$f_s = 460\text{MPa}$
Calculate the Stress Level in the Reinforcing FRP
$f_{fe.cal} = E_f\,\varepsilon_{fe} = 2{,}649\text{MPa}$
$f_{fe.max} = f_{fu} = 2{,}975\text{MPa}$
$f_{fe} = 2{,}649\text{MPa}$
Calculate the Internal Force Resultants
$\varepsilon'_c = 1.7\,f_{ck} / E_c = 0.003037$
$$\beta_1 = \frac{4\,\varepsilon'_c - \varepsilon_c}{6\,\varepsilon'_c - 2\,\varepsilon_c} = 0.748$$
$$\alpha_1 = \frac{3\,\varepsilon'_c\,\varepsilon_c - (\varepsilon_c)^2}{3\,\beta_1\,(\varepsilon'_c)^2} = 0.885$$
Verify Force Equilibrium
$A_s = 339\text{mm}^2$
$A_f = 50.55\text{mm}^2$
$F_s = A_s\,f_s = 156\text{kN}$
$F_f = A_f\,f_{fe} = 134\text{kN}$
$F_{TENS.} = F_s + F_f = 290\text{kN}$
$F_{COMP.} = \alpha_1\,f_{ck}\,\beta_1\,b\,c = 290\text{kN}$

Calculate Flexural Strength

Calculate Flexural Strength Components
$M_{ns} = A_s\,f_s\,(d - \beta_1\,c / 2) = 20.07\text{kN}\cdot\text{m}$
$M_{nf} = A_f\,f_{fe}\,(d_f - \beta_1\,c / 2) = 24.74\text{kN}\cdot\text{m}$
Calculate Design Flexural Strength of Section
$ø = 0.900$
$\psi = 0.850$
$øM_n = ø\,[M_{ns} + \psi_f\,M_{nf}] = 36.99\text{kN}\cdot\text{m}$
$M_u / øM_n = 0.974 < 1.000 \rightarrow$ O.K

Check Service Stress in the Reinforcing Steel and FRP

Calculate the Elastic Depth to the Cracked Neutral Axis

$A_s = 339mm^2$

$A_f = 50.55mm^2$

$d = 144mm$

$d_f = 200mm$

$\rho_s = 0.015697$

$\rho_f = 0.001684$

$k = \sqrt{(k_1)^2 + 2k_2} - k_1 = 0.352$

$k_1 = \rho_s \frac{E_s}{E_c} + \rho_f \frac{E_f}{E_c}$

$k_2 = \rho_s \frac{E_s}{E_c} + \rho_f \frac{E_f}{E_c} \frac{d_f}{d}$

$kd = 50.65mm$

Calculate the Stress Level in the Reinforcing Steel

$\varepsilon_{bi} = 0.000000$

$$f_{s.s} = \frac{[M_s + \varepsilon_{bi} A_f E_f (d_f - kd/3)](d - kd) E_s}{A_s E_s (d - kd/3)(d - kd) + A_f E_f (d_f - kd/3)(d_f - kd)} = 0.000MPa$$

$f_{s.s.max} = 0.80\ f_y = 368MPa$

$f_{s.s} / f_{s.s.max} = 0.000 < 1.000 \rightarrow$ O.K

Check Creep Rupture Limit at Service of FRP

Calculate the Stress Level in the Reinforcing FRP

$$f_{f.s} = f_{s.s} \left(\frac{E_f}{E_s} \right) \left(\frac{d_f - kd}{d - kd} \right) - \varepsilon_{bi} E_f = 0.000MPa$$

$f_{fu} = 2{,}975MPa$

$f_{f.s.max} = 0.550\ f_{fu} = 1{,}636MPa$

$f_{f.s} / f_{f.s.max} = 0.000 < 1.000 \rightarrow$ O.K

Calculate Shear Strength by FRP

Shear Strength without FRP

$\phi = 0.750$

$V_c = 30.50kN$

$V_s = 49.57kN$

$\phi V_{ns} = 46.64kN$

$\phi V_{ns.MAX} = 112kN$

Calculate the Effective Strain Level

$n_f = 1$

$t_f = 0.337mm$

$d_{fv} = 144mm$

$$L_e = \frac{23{,}300}{(n_f\ t_f\ E_f)^{0.58}} = 34.00mm$$

$k_1 = (f_{ck} / 27.00)^{2/3} = 1.896$

$$k_2 = \frac{d_{fv} - L_e}{d_{fv}} = 0.764$$

$$\kappa_{v.cal} = \frac{k_1\ k_2\ L_e}{11{,}900\ \varepsilon_{fu}} = 0.232$$

$\kappa_{v.max} = 0.750$

$\kappa_v = 0.232$

$\varepsilon_{fe.cal} = \kappa_v\ \varepsilon_{fu} = 0.004139$

$\varepsilon_{fe.max} = 0.004000$

$\varepsilon_{fe} = 0.004000$

Calculate the Contribution of the FRP Reinforcement

$\psi_f = 0.850$

$w_f = 500mm$

$s_f = 400mm$

$A_{fv} = 2\ n\ t_f\ w_f = 337mm^2$

$f_{fe} = \varepsilon_{fe}\ E_f = 920MPa$

$$V_f = \frac{A_{fv}\ f_{fe}\ d_{fv}}{s_f} = 112kN$$

Calculate Shear Strength Ratio

$\phi V_n = \phi\ (V_c + V_s + \psi_f\ V_f) = 112kN$

$V_u / \phi V_n = 0.538 < 1.000 \rightarrow$ O.K

Calculate Development Length

[ACI 440.2R-08 / 13.1.3 - Development length]

Calculate Development Length

POS.	Apply	Pieces	l_{df} (mm)	Description
(1)	Yes	1	96.08	Bottom of Beam
(2)	Yes	1	96.08	Side of Beam (Shear)

$l_{df} = 1.000 \sqrt{n\ E_f\ t_f / (\ f_{ck})^{1/2}}$

Case 3- FRP Strengthening Detailed Calculations-Midas Design Plus 2021

MEMBER NAME : Mechanical Properties of Recycled Aggregate Concrete with Self Consolidating Concrete Sample (RCA)

General Information

Design Code : ACI318M-14

Reference Code : ACI 440.2R-08

[Guide for Design and Construction of Externally Bonded FRP System for Strengthening Concrete Structures.]

Code Unit : N, mm

Material

Concrete

f_{ck} : 64.50MPa

E_c : 37,746MPa

Rebar

f_y : 460MPa

f_{ys} : 420MPa

E_s : 200,000MPa

FRP / Carbon (MasterBrace FIB 600/50 CFS)

f^*_{fu} : 3,500MPa

E^*_{fs} : 230,000MPa

t_f : 0.337mm

ε^*_{fu} : 0.021000

Fiber Type : Carbon

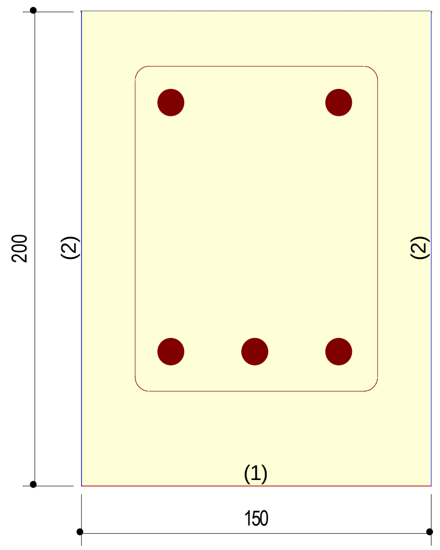

Section

Beam

Section Size : 150 x 200mm

Cover : 23.00 / 40.00mm

Compression : Not Considered
Splicing Limit : 50%
FRP / Carbon

POS.	Apply	Size(mm)	Pieces	Description
(1)	Yes	400	1	Bottom of Beam
(2)	Yes	450	1	Side of Beam (Shear)
(3)	No	120	1	Side of Beam (Bottom)
(4)	No	120	1	Side of Beam (Top)
(5)	No	100	1	Bottom of Slab
(6)	No	150	1	Top of Beam

FRP / Carbon (Shear / U-Wraps (3 Sides Bonded))
w_f : 500mm
s_f : 400mm

Rebar

Top Bar : 2-P12 (A_s = 226mm²)
Layer 1 : 2 EA (C_c = 39.00mm)
Bot Bar : 3-P12 (A_s = 339mm²)
Layer 1 : 3 EA (C_c = 56.00mm)
Stirrup : 2-P10@300 (A_s = 157mm²)

Design Force

Design Force
$M_{u.DL}$: 0.000kN·m
$M_{u.LL}$: 0.000kN·m
M_{ux} : 24.51kN·m
V_{uy} : 40.85kN

Design Data

Exposure Conditions : Exterior Exposure

Calculate the Design Material Properties

[ACI 440.2R-08 / 9.4 - Design material properties]
Calculate the Design Material Properties
$C_E = 0.850$
$f_{fu} = C_E\, f^*_{fu} = 2{,}975\text{MPa}$
$\varepsilon_{fu} = C_E\, \varepsilon^*_{fu} = 0.017850$
$E_f = f_{fu} / \varepsilon^*_{fu} = 230{,}000\text{MPa}$

Check Bending Moment Capacity (RC Section Only)

Calculate design parameter
$\beta_1 = 0.650$
Check space of rebar

$$s_{max1} = 380\left(\frac{280}{f_s}\right) - 2.5c_c\,, \qquad s_{max2} = 300\left(\frac{280}{f_s}\right)$$

$s_{max} = \min(s_{max1}, s_{max2}) = 222\text{mm}$, $N_{req} = 2$
$s = 19.00 < 222\text{mm} \rightarrow$ O.K
Calculate required ratio of reinforcement

$$\rho_{min.11} = \frac{0.25\sqrt{f'_c}}{f_y}\,, \qquad \rho_{min.12} = \frac{1.4}{f_y}$$

$\rho_{min.1} = \max(\rho_{min.11}, \rho_{min.12}) = 0.0044$

$$\rho_{min.2} = \frac{4}{3}\,\frac{M_u}{\phi\, f_y\, bd(d\text{-}a/2)} = 0.0278$$

$\rho_{min} = \min(\rho_{min1}, \rho_{min2}) = 0.0044$

$$\rho_{\varepsilon t} = 0.85\,\beta_1\left(\frac{f'_c}{f_y}\right)\left(\frac{\varepsilon_c}{\varepsilon_c + 0.004}\right) = 0.0332$$

$\rho_{max} = \rho_{et} = 0.0332$
Check ratio of tensile reinforcement

$$\rho = \frac{A_s}{b_w\, d} = 0.0157$$

$\rho_{min} < \rho < \rho_{max} \rightarrow$ O.K
Calculate moment capacity

$a = \dfrac{A_s\ f_y}{0.85\ f'_c\ b_w} = 18.98\text{mm}$

$ø = 0.900$

$M_n = A_s\ f_y\ (\ d - a/2\ ) = 21.01\text{kN·m}$

$øM_n = 18.91\text{kN·m}$

Calculate ratio of moment capacity

$M_u\ /\ øM_n = 1.296 \rightarrow$ N.G

Check Shear Capacity (RC Section Only)

Calculate shear strength by concrete

$ø = 0.750$ $\quad$ $d = 144\text{mm}$

$øV_c = ø\ 0.17 \sqrt{f'_c}\ b_w\ d = 22.13\text{kN}$

$V_u > øV_c \rightarrow$ Shear reinforcement is required

Calculate required shear strength by shear reinforcement

$V_{s.req} = (\ V_u - øV_c\ )\ /\ ø = 24.96\text{kN}$

$V_{c1} = 0.33 \sqrt{f'_c}\ b_w\ d = 57.29\text{kN}$ Refer to [11.4.5.3]

$V_{c2} = 0.66 \sqrt{f'_c}\ b_w\ d = 115\text{kN}$

$V_{s.req} < V_{c2} \rightarrow$ O.K

$A_{v.min1/s} = 0.062 \sqrt{f'_c}\ \dfrac{b_w}{f_{yt}}\ , \quad A_{v.min2/s} = 0.35\ \dfrac{b_w}{f_{yt}}$

$A_{v.min}\ /s = \max\ [\ A_{v.min1}\ /s\ ,\ A_{v.min2}\ /s\ ] = 0.178\text{mm}^2/\text{mm}$

$A_{v.req0}\ /s = \dfrac{V_{s.req}}{f_{yt}\ \cdot\ d} = 0.412\text{mm}^2/\text{mm}$

$A_{v.req}\ /s = \max\ [\ A_{v.min}\ /s\ ,\ A_{v.req0}\ /s\ ] = 0.412\text{mm}^2/\text{mm}$

Calculate shear strength by stirrup

$N_{leg} = 2 \quad A_{v1} = 78.54\text{mm}^2$ (P10)

$øV_s = ø\ \dfrac{A_v\ f_{yt}\ d}{s} = 23.77\text{kN}$

Calculate ratio of shear capacity

$øV_n = øV_c + øV_s = 45.90\text{kN}$

$V_u\ /\ øV_n = 0.890 \rightarrow$ O.K

Calculate spacing limits for reinforcement

$s_{max.0} = \min\ [\ d/2,\ 600\text{mm}\ ] = 72.05\text{mm}$

$s_{req} = \dfrac{N_{leg}\ A_{v1}}{A_{v.req}\ /s} = 381\text{mm}$

$s_{max} = \min\ [\ s_{max.0}\ ,\ s_{req}\ ] = 72.05\text{mm}$

$s = 300\text{mm} > s_{max} = 72.05\text{mm} \rightarrow$ N.G

Check the Strengthening Limit Criteria

[ACI 440.2R-08 / 9.2 - Strengthening limits]

Bending Moment Strength without FRP

$ø = 0.900$

$M_{ns} = 21.01\text{kN·m}$

$øM_{ns} = 18.91\text{kN·m}$

Check the Strengthening Limit Criteria

$M_{u.new} = 1.1M_{DL} + 0.75M_{LL} = 0.000\text{kN·m}$

$M_{u.new}\ /\ øM_{ns} = 0.000 < 1.000 \rightarrow$ O.K

Calculate Moment of Inertia of Cracked Section Transformed to Concrete

Calculate Modulus of Rupture

$f_r = 0.63 \sqrt{f_{ck}} = 4.979\text{MPa}$

$n = E_s\ /\ E_c = 5.299$

Calculate Moment of Inertia of Cracked Section Transformed to Concrete

$d = 144\text{mm}$

$d' = 39.00\text{mm}$

$A_s = 339\text{mm}^2$

$A'_s = 226\text{mm}^2$

$\gamma = \dfrac{(\ n - 1\ )\ A'_s}{n\ A_s} = 0.541$

$B = b\ /\ n\ A_s = 0.0834$

$kd = 47.11\text{mm}$

$k = 0.327$

$I_g = b\,h^3 / 12 = 100{,}150{,}075\text{mm}^4$

$$I_{cr} = \frac{b\,(kd)^3}{3} + nA_s\,(d\text{-}kd)^2 + (n\text{-}1)\,A'_s\,(kd\text{-}d')^2 = 22{,}203{,}709\text{mm}^4$$

Search Neutral Axis

Calculate the Design Strain of the FRP System

$n_f = 1$

$t_f = 0.337\text{mm}$

$\varepsilon_{fd.cal} = 0.410\sqrt{f_{ck} / n\,E_f\,t_f} = 0.011827$

$\varepsilon_{fd.max} = 0.90\,\varepsilon_{fu} = 0.016065$

$\varepsilon_{fd} = 0.011827$

Calculate the Existing State of Strain

$d_f = 200\text{mm}$

$$\varepsilon_{bi} = \frac{M_{DL}\,(d_f - kd)}{I_{cr}\,E_c} = 0.000000$$

Estimate the Depth to the Neutral Axis

$c = 58.35\text{mm}$

Calculate the Effective Level of Strain in the FRP Reinforcement

$\varepsilon_{cu} = 0.003000$

$$\varepsilon_{fe.cal} = \varepsilon_{cu}\,\frac{d_f - c}{c} - \varepsilon_{bi} = 0.007297$$

$\varepsilon_{fe.max} = \varepsilon_{fd} = 0.011827$

$\varepsilon_{fe} = 0.007297$

Calculate the Concrete Strain

$$\varepsilon_c = (\varepsilon_{fe} + \varepsilon_{bi})\left(\frac{c}{d_f - c}\right) = 0.003000$$

Calculate the Stress Level in the Reinforcing Steel

$d = 144\text{mm}$

$$\varepsilon_s = (\varepsilon_{fe} + \varepsilon_{bi})\left(\frac{d - c}{d_f - c}\right) = 0.004409$$

$f_{s.cal} = E_s\,\varepsilon_s = 882\text{MPa}$

$f_{s.max} = f_y = 460\text{MPa}$

$f_s = 460\text{MPa}$

Calculate the Stress Level in the Reinforcing FRP

$f_{fe.cal} = E_f\,\varepsilon_{fe} = 1{,}678\text{MPa}$

$f_{fe.max} = f_{fu} = 2{,}975\text{MPa}$

$f_{fe} = 1{,}678\text{MPa}$

Calculate the Internal Force Resultants

$\varepsilon'_c = 1.7\,f_{ck} / E_c = 0.002905$

$$\beta_1 = \frac{4\,\varepsilon'_c - \varepsilon_c}{6\,\varepsilon'_c - 2\,\varepsilon_c} = 0.754$$

$$\alpha_1 = \frac{3\,\varepsilon'_c\,\varepsilon_c - (\varepsilon_c)^2}{3\,\beta_1\,(\varepsilon'_c)^2} = 0.898$$

Verify Force Equilibrium

$A_s = 339\text{mm}^2$

$A_f = 135\text{mm}^2$

$F_s = A_s\,f_s = 156\text{kN}$

$F_f = A_f\,f_{fe} = 226\text{kN}$

$F_{TENS.} = F_s + F_f = 382\text{kN}$

$F_{COMP.} = \alpha_1\,f_{ck}\,\beta_1\,b\,c = 382\text{kN}$

Calculate Flexural Strength

Calculate Flexural Strength Components

$M_{ns} = A_s\,f_s\,(d - \beta_1\,c / 2) = 19.06\text{kN·m}$

$M_{nf} = A_f\,f_{fe}\,(d_f - \beta_1\,c / 2) = 40.33\text{kN·m}$

Calculate Design Flexural Strength of Section

$ø = 0.752$

$\psi = 0.850$

$øM_n = ø\,[\,M_{ns} + \psi_f\,M_{nf}\,] = 40.12\text{kN·m}$

$M_u / øM_n = 0.611 < 1.000 \rightarrow$ O.K

Check Service Stress in the Reinforcing Steel and FRP

Calculate the Elastic Depth to the Cracked Neutral Axis
A_s = 339mm²
A_f = 135mm²
d = 144mm
d_f = 200mm
ρ_s = 0.015697
ρ_f = 0.004491
$k = \sqrt{(k_1)^2 + 2 k_2} - k_1 = 0.394$
$k_1 = \rho_s \dfrac{E_s}{E_c} + \rho_f \dfrac{E_f}{E_c}$
$k_2 = \rho_s \dfrac{E_s}{E_c} + \rho_f \dfrac{E_f}{E_c} \dfrac{d_f}{d}$
kd = 56.79mm
Calculate the Stress Level in the Reinforcing Steel
ε_{bi} = 0.000000
$f_{s.s} = \dfrac{[\, M_s + \varepsilon_{bi} A_f E_f (d_f - kd/3) \,] (d - kd) E_s}{A_s E_s (d - kd/3)(d - kd) + A_f E_f (d_f - kd/3)(d_f - kd)} = 0.000\text{MPa}$
$f_{s.s.max} = 0.80\, f_y$ = 368MPa
$f_{s.s} / f_{s.s.max}$ = 0.000 < 1.000 → O.K

Check Creep Rupture Limit at Service of FRP
Calculate the Stress Level in the Reinforcing FRP
$f_{f.s} = f_{s.s} \left(\dfrac{E_f}{E_s} \right) \left(\dfrac{d_f - kd}{d - kd} \right) - \varepsilon_{bi} E_f = 0.000\text{MPa}$
f_{fu} = 2,975MPa
$f_{f.s.max} = 0.550\, f_{fu}$ = 1,636MPa
$f_{f.s} / f_{f.s.max}$ = 0.000 < 1.000 → O.K

Calculate Shear Strength by FRP
Shear Strength without FRP
ø = 0.750
V_c = 29.51kN
V_s = 24.96kN
$øV_{ns}$ = 45.90kN
$øV_{ns.MAX}$ = 108kN
Calculate the Effective Strain Level
n_f = 1
t_f = 0.337mm
d_{fv} = 394mm
$L_e = \dfrac{23{,}300}{(n_f\, t_f\, E_f)^{0.58}} = 34.00\text{mm}$
$k_1 = (f_{ck} / 27.00)^{2/3} = 1.787$
$k_2 = \dfrac{d_{fv} - L_e}{d_{fv}} = 0.914$
$\kappa_{v.cal} = \dfrac{k_1\, k_2\, L_e}{11{,}900\, \varepsilon_{fu}} = 0.261$
$\kappa_{v.max}$ = 0.750
κ_v = 0.261
$\varepsilon_{fe.cal} = \kappa_v\, \varepsilon_{fu}$ = 0.004666
$\varepsilon_{fe.max}$ = 0.004000
ε_{fe} = 0.004000
Calculate the Contribution of the FRP Reinforcement
ψ_f = 0.850
w_f = 500mm
s_f = 400mm
$A_{fv} = 2\, n\, t_f\, w_f$ = 337mm²
$f_{fe} = \varepsilon_{fe} E_f$ = 920MPa
$V_f = \dfrac{A_{fv}\, f_{fe}\, d_{fv}}{s_f} = 305\text{kN}$
Calculate Shear Strength Ratio
$øV_n = ø\,(V_c + V_s + \psi_f V_f)$ = 108kN
$V_u / øV_n$ = 0.378 < 1.000 → O.K

Calculate Development Length
[ACI 440.2R-08 / 13.1.3 - Development length]
Calculate Development Length

POS.	Apply	Pieces	l_{df} (mm)	Description
(1)	Yes	1	98.24	Bottom of Beam
(2)	Yes	1	98.24	Side of Beam (Shear)

$l_{df} = 1.000 \sqrt{n\ E_f\ t_f / (\ f_{ck})}\ ^{1/2}$

Case 4- FRP Strengthening Detailed Calculations-Midas Design Plus 2021

MEMBER NAME : Mechanical Properties of Recycled Aggregate Concrete with Self Consolidating Concrete Sample (RCA)

General Information
Design Code : ACI318M-14
Reference Code : ACI 440.2R-08
[Guide for Design and Construction of Externally Bonded FRP System for Strengthening Concrete Structures.]
Code Unit : N, mm

Material
Concrete
f_{ck} : 64.50MPa
E_c : 37,746MPa
Rebar
f_y : 460MPa
f_{ys} : 420MPa
E_s : 200,000MPa
FRP / Carbon (MasterBrace FIB 600/50 CFS)
f^*_{fu} : 3,500MPa
E^*_{fs} : 230,000MPa
t_f : 0.337mm
ε^*_{fu} : 0.021000
Fiber Type : Carbon

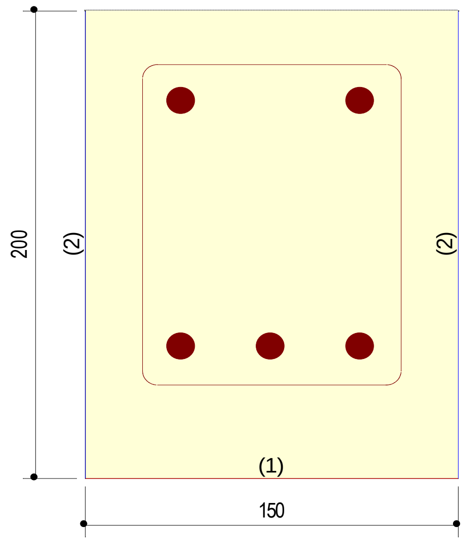

Section
Beam
Section Size : 150 x 200mm
Cover : 23.00 / 40.00mm
Compression : Considered
Splicing Limit : 50%

FRP / Carbon

POS.	Apply	Size(mm)	Pieces	Description
(1)	Yes	400	1	Bottom of Beam
(2)	Yes	450	1	Side of Beam (Shear)
(3)	No	120	1	Side of Beam (Bottom)
(4)	No	120	1	Side of Beam (Top)
(5)	No	100	1	Bottom of Slab
(6)	No	150	1	Top of Beam

FRP / Carbon (Shear / U-Wraps (3 Sides Bonded))

w_f : 500mm

s_f : 400mm

Rebar

Top Bar : 2-P12 (A_s = 226mm²)

Layer 1 : 2 EA (C_c = 39.00mm)

Bot Bar : 3-P12 (A_s = 339mm²)

Layer 1 : 3 EA (C_c = 56.00mm)

Stirrup : 2-P10@300 (A_s = 157mm²)

Design Force

Design Force

$M_{u.DL}$: 0.000kN·m

$M_{u.LL}$: 0.000kN·m

M_{ux} : 24.51kN·m

V_{uy} : 40.85kN

Design Data

Exposure Conditions : Exterior Exposure

Calculate the Design Material Properties

[ACI 440.2R-08 / 9.4 - Design material properties]

Calculate the Design Material Properties

$C_E = 0.850$

$f_{fu} = C_E\, f^*_{fu} = 2{,}975\text{MPa}$

$\varepsilon_{fu} = C_E\, \varepsilon^*_{fu} = 0.017850$

$E_f = f_{fu} / \varepsilon^*_{fu} = 230{,}000\text{MPa}$

Check Bending Moment Capacity (RC Section Only)

Calculate design parameter

$\beta_1 = 0.650$

Check space of rebar

$s_{max1} = 380\left(\frac{280}{f_s}\right) - 2.5c_c$, $\quad s_{max2} = 300\left(\frac{280}{f_s}\right)$

$s_{max} = \min\,(s_{max1} , s_{max2}) = 222\text{mm}$, $\quad N_{req} = 2$

$s = 19.00 < 222\text{mm} \rightarrow$ O.K

Calculate required ratio of reinforcement

$\rho_{min.11} = \frac{0.25\sqrt{f'_c}}{f_y}$, $\quad \rho_{min.12} = \frac{1.4}{f_y}$

$\rho_{min.1} = \max\,(\rho_{min.11} , \rho_{min.12}) = 0.0044$

$\rho_{min.2} = \frac{4}{3}\,\frac{M_u}{ø\, f_y\, bd(d\text{-}a/2)} = 0.0278$

$\rho_{min} = \min\,(\rho_{min1} , \rho_{min2}) = 0.0044$

$\rho_{\varepsilon t} = 0.85\,\beta_1 \left(\frac{f'_c}{f_y}\right)\left(\frac{\varepsilon_c}{\varepsilon_c + 0.004}\right) = 0.0332$

$\rho_{max} = \rho_{et} = 0.0403$

Check ratio of tensile reinforcement

$\rho = \frac{A_s}{b_w\, d} = 0.0157$

$\rho_{min} < \rho < \rho_{max} \rightarrow$ O.K

Calculate moment capacity

$a = \frac{A_s\, f_y}{0.85\, f'_c\, b_w} = 21.68\text{mm}$

$ø = 0.900$
$M_n = A_s f_y (d - a/2) = 21.45kN·m$
$øM_n = 19.30kN·m$
Calculate ratio of moment capacity
$M_u / øM_n = 1.270 \rightarrow$ N.G

Check Shear Capacity (RC Section Only)

Calculate shear strength by concrete
$ø = 0.750$ $d = 144mm$
$øV_c = ø\, 0.17 \sqrt{f'_c}\ b_w d = 22.13kN$
$V_u > øV_c \rightarrow$ Shear reinforcement is required
Calculate required shear strength by shear reinforcement
$V_{s.req} = (V_u - øV_c) / ø = 24.96kN$
$V_{c1} = 0.33 \sqrt{f'_c}\ b_w d = 57.29kN$ Refer to [11.4.5.3]
$V_{c2} = 0.66 \sqrt{f'_c}\ b_w d = 115kN$
$V_{s.req} < V_{c2} \rightarrow$ O.K
$A_{v.min1/s} = 0.062 \sqrt{f'_c}\ \frac{b_w}{f_{yt}}$, $A_{v.min2/s} = 0.35\ \frac{b_w}{f_{yt}}$
$A_{v.min} /s = \max [A_{v.min1} /s , A_{v.min2} /s] = 0.178mm^2/mm$
$A_{v.req0} /s = \frac{V_{s.req}}{f_{yt} \cdot d} = 0.412mm^2/mm$
$A_{v.req} /s = \max [A_{v.min} /s , A_{v.req0} /s] = 0.412mm^2/mm$
Calculate shear strength by stirrup
$N_{leg} = 2$ $A_{v1} = 78.54mm^2$ (P10)
$øV_s = ø\ \frac{A_v f_{yt} d}{s} = 23.77kN$
Calculate ratio of shear capacity
$øV_n = øV_c + øV_s = 45.90kN$
$V_u / øV_n = 0.890 \rightarrow$ O.K
Calculate spacing limits for reinforcement
$s_{max.0} = \min [d/2, 600mm] = 72.05mm$
$s_{req} = \frac{N_{leg} A_{v1}}{A_{v.req} /s} = 381mm$
$s_{max} = \min [s_{max.0} , s_{req}] = 72.05mm$
$s = 300mm > s_{max} = 72.05mm \rightarrow$ N.G

Check the Strengthening Limit Criteria

[ACI 440.2R-08 / 9.2 - Strengthening limits]
Bending Moment Strength without FRP
$ø = 0.900$
$M_{ns} = 21.45kN·m$
$øM_{ns} = 19.30kN·m$
Check the Strengthening Limit Criteria
$M_{u.new} = 1.1M_{DL} + 0.75M_{LL} = 0.000kN·m$
$M_{u.new} / øM_{ns} = 0.000 < 1.000 \rightarrow$ O.K

Calculate Moment of Inertia of Cracked Section Transformed to Concrete

Calculate Modulus of Rupture
$f_r = 0.63 \sqrt{f_{ck}} = 4.979MPa$
$n = E_s / E_c = 5.299$
Calculate Moment of Inertia of Cracked Section Transformed to Concrete
$d = 144mm$
$d' = 39.00mm$
$A_s = 339mm^2$
$A'_s = 226mm^2$
$\gamma = \frac{(n - 1) A'_s}{n A_s} = 0.541$
$B = b / n A_s = 0.0834$
$kd = 47.11mm$
$k = 0.327$
$I_g = b h^3 / 12 = 100,150,075mm^4$

$$I_{cr} = \frac{b\,(kd)^3}{3} + nA_s\,(d\text{-}kd)^2 + (n\text{-}1)\,A'_s\,(kd\text{-}d')^2 = 22{,}203{,}709\text{mm}^4$$

Search Neutral Axis

Calculate the Design Strain of the FRP System

$n_f = 1$

$t_f = 0.337\text{mm}$

$\varepsilon_{fd.cal} = 0.410\sqrt{f_{ck} / n\,E_f\,t_f} = 0.011827$

$\varepsilon_{fd.max} = 0.90\,\varepsilon_{fu} = 0.016065$

$\varepsilon_{fd} = 0.011827$

Calculate the Existing State of Strain

$d_f = 200\text{mm}$

$$\varepsilon_{bi} = \frac{M_{DL}\,(d_f - kd)}{I_{cr}\,E_c} = 0.000000$$

Estimate the Depth to the Neutral Axis

$c = 58.35\text{mm}$

Calculate the Effective Level of Strain in the FRP Reinforcement

$\varepsilon_{cu} = 0.003000$

$$\varepsilon_{fe.cal} = \varepsilon_{cu}\,\frac{d_f - c}{c} - \varepsilon_{bi} = 0.007297$$

$\varepsilon_{fe.max} = \varepsilon_{fd} = 0.011827$

$\varepsilon_{fe} = 0.007297$

Calculate the Concrete Strain

$$\varepsilon_c = (\varepsilon_{fe} + \varepsilon_{bi})\left(\frac{c}{d_f - c}\right) = 0.003000$$

Calculate the Stress Level in the Reinforcing Steel

$d = 144\text{mm}$

$$\varepsilon_s = (\varepsilon_{fe} + \varepsilon_{bi})\left(\frac{d - c}{d_f - c}\right) = 0.004409$$

$f_{s.cal} = E_s\,\varepsilon_s = 882\text{MPa}$

$f_{s.max} = f_y = 460\text{MPa}$

$f_s = 460\text{MPa}$

Calculate the Stress Level in the Reinforcing FRP

$f_{fe.cal} = E_f\,\varepsilon_{fe} = 1{,}678\text{MPa}$

$f_{fe.max} = f_{fu} = 2{,}975\text{MPa}$

$f_{fe} = 1{,}678\text{MPa}$

Calculate the Internal Force Resultants

$\varepsilon'_c = 1.7\,f_{ck} / E_c = 0.002905$

$$\beta_1 = \frac{4\,\varepsilon'_c - \varepsilon_c}{6\,\varepsilon'_c - 2\,\varepsilon_c} = 0.754$$

$$\alpha_1 = \frac{3\,\varepsilon'_c\,\varepsilon_c - (\varepsilon_c)^2}{3\,\beta_1\,(\varepsilon'_c)^2} = 0.898$$

Verify Force Equilibrium

$A_s = 339\text{mm}^2$

$A_f = 135\text{mm}^2$

$F_s = A_s\,f_s = 156\text{kN}$

$F_f = A_f\,f_{fe} = 226\text{kN}$

$F_{TENS.} = F_s + F_f = 382\text{kN}$

$F_{COMP.} = \alpha_1\,f_{ck}\,\beta_1\,b\,c = 382\text{kN}$

Calculate Flexural Strength

Calculate Flexural Strength Components

$M_{ns} = A_s\,f_s\,(d - \beta_1\,c / 2) = 19.06\text{kN·m}$

$M_{nf} = A_f\,f_{fe}\,(d_f - \beta_1\,c / 2) = 40.33\text{kN·m}$

Calculate Design Flexural Strength of Section

$ø = 0.752$

$\psi = 0.850$

$øM_n = ø\,[\,M_{ns} + \psi_f\,M_{nf}\,] = 40.12\text{kN·m}$

$M_u / øM_n = 0.611 < 1.000 \rightarrow$ O.K

Check Service Stress in the Reinforcing Steel and FRP

Calculate the Elastic Depth to the Cracked Neutral Axis

A_s = 339mm²
A_f = 135mm²
d = 144mm
d_f = 200mm
ρ_s = 0.015697
ρ_f = 0.004491
$k = \sqrt{(k_1)^2 + 2\,k_2} - k_1 = 0.394$
$k_1 = \rho_s \dfrac{E_s}{E_c} + \rho_f \dfrac{E_f}{E_c}$
$k_2 = \rho_s \dfrac{E_s}{E_c} + \rho_f \dfrac{E_f}{E_c} \dfrac{d_f}{d}$
kd = 56.79mm
Calculate the Stress Level in the Reinforcing Steel
ε_{bi} = 0.000000
$f_{s.s} = \dfrac{[\,M_s + \varepsilon_{bi} A_f E_f \,(d_f - kd/3)\,]\,(d - kd)\,E_s}{A_s E_s\,(d - kd/3)\,(d - kd) + A_f E_f\,(d_f - kd/3)\,(d_f - kd)} = 0.000\text{MPa}$
$f_{s.s.max} = 0.80\ f_y$ = 368MPa
$f_{s.s} / f_{s.s.max}$ = 0.000 < 1.000 → O.K

Check Creep Rupture Limit at Service of FRP
Calculate the Stress Level in the Reinforcing FRP
$f_{f.s} = f_{s.s} \left(\dfrac{E_f}{E_s} \right) \left(\dfrac{d_f - kd}{d - kd} \right) - \varepsilon_{bi} E_f = 0.000\text{MPa}$
f_{fu} = 2,975MPa
$f_{f.s.max} = 0.550\ f_{fu}$ = 1,636MPa
$f_{f.s} / f_{f.s.max}$ = 0.000 < 1.000 → O.K

Calculate Shear Strength by FRP
Shear Strength without FRP
ø = 0.750
V_c = 29.51kN
V_s = 24.96kN
$øV_{ns}$ = 45.90kN
$øV_{ns.MAX}$ = 108kN
Calculate the Effective Strain Level
n_f = 1
t_f = 0.337mm
d_{fv} = 394mm
$L_e = \dfrac{23{,}300}{(n_f\, t_f\, E_f)^{0.58}} = 34.00\text{mm}$
$k_1 = (f_{ck} / 27.00)^{2/3} = 1.787$
$k_2 = \dfrac{d_{fv} - L_e}{d_{fv}} = 0.914$
$\kappa_{v.cal} = \dfrac{k_1\, k_2\, L_e}{11{,}900\ \varepsilon_{fu}} = 0.261$
$\kappa_{v.max}$ = 0.750
κ_v = 0.261
$\varepsilon_{fe.cal} = \kappa_v\, \varepsilon_{fu}$ = 0.004666
$\varepsilon_{fe.max}$ = 0.004000
ε_{fe} = 0.004000
Calculate the Contribution of the FRP Reinforcement
ψ_f = 0.850
w_f = 500mm
s_f = 400mm
$A_{fv} = 2\ n\ t_f\ w_f$ = 337mm²
$f_{fe} = \varepsilon_{fe}\ E_f$ = 920MPa
$V_f = \dfrac{A_{fv}\, f_{fe}\, d_{fv}}{s_f} = 305\text{kN}$
Calculate Shear Strength Ratio
$øV_n = ø\,(V_c + V_s + \psi_f V_f)$ = 108kN
$V_u / øV_n$ = 0.378 < 1.000 → O.K

Calculate Development Length

[ACI 440.2R-08 / 13.1.3 - Development length]

Calculate Development Length

POS.	Apply	Pieces	l_{df} (mm)	Description
(1)	Yes	1	98.24	Bottom of Beam
(2)	Yes	1	98.24	Side of Beam (Shear)

$l_{df} = 1.000 \sqrt{n\, E_f\, t_f / (f_{ck})^{1/2}}$

Case 5- FRP Strengthening Detailed Calculations-Midas Design Plus 2021

MEMBER NAME : Recycled Aggregate Concrete with Self Consolidating Concrete Sample (RCA-5D).

General Information

Design Code : ACI318M-14

Reference Code : ACI 440.2R-08

[Guide for Design and Construction of Externally Bonded FRP System for Strengthening Concrete Structures.]

Code Unit : N, mm

Material

Concrete

f_{ck} : 77.00MPa

E_c : 41,242MPa

Rebar

f_y : 460MPa

f_{ys} : 420MPa

E_s : 200,000MPa

FRP / Carbon (MasterBrace FIB 600/50 CFS)

f^*_{fu} : 3,500MPa

E^*_{fs} : 230,000MPa

t_f : 0.337mm

ε^*_{fu} : 0.021000

Fiber Type : Carbon

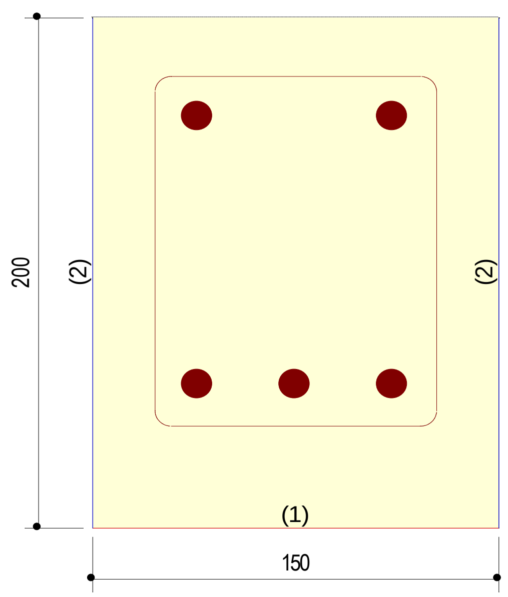

Section

Beam

Section Size : 150 x 200mm

Cover : 23.00 / 40.00mm

Compression : Not Considered

Splicing Limit : 50%

FRP / Carbon

POS.	Apply	Size(mm)	Pieces	Description
(1)	Yes	150	1	Bottom of Beam
(2)	Yes	200	1	Side of Beam (Shear)
(3)	No	120	1	Side of Beam (Bottom)
(4)	No	120	1	Side of Beam (Top)
(5)	No	100	1	Bottom of Slab
(6)	No	150	1	Top of Beam

FRP / Carbon (Shear / U-Wraps (3 Sides Bonded))

w_f : 500mm

s_f : 400mm

Rebar

Top Bar : 2-P12 (A_s = 226mm²)

Layer 1 : 2 EA (C_c = 39.00mm)

Bot Bar : 3-P12 (A_s = 339mm²)

Layer 1 : 3 EA (C_c = 56.00mm)

Stirrup : 2-P10@300 (A_s = 157mm²)

Design Force

Design Force

$M_{u.DL}$: 0.000kN·m

$M_{u.LL}$: 0.000kN·m

M_{ux} : 39.03kN·m

V_{uy} : 65.05kN

Design Data

Exposure Conditions : Exterior Exposure

Calculate the Design Material Properties

[ACI 440.2R-08 / 9.4 - Design material properties]

Calculate the Design Material Properties

$C_E = 0.850$

$f_{fu} = C_E\ f^*_{fu} = 2{,}975\text{MPa}$

$\varepsilon_{fu} = C_E\ \varepsilon^*_{fu} = 0.017850$

$E_f = f_{fu} / \varepsilon^*_{fu} = 230{,}000\text{MPa}$

Check Bending Moment Capacity (RC Section Only)

Calculate design parameter

$\beta_1 = 0.650$

Check space of rebar

$$s_{max1} = 380\left(\frac{280}{f_s}\right) - 2.5c_c\ , \qquad s_{max2} = 300\left(\frac{280}{f_s}\right)$$

$s_{max} = \min(s_{max1}, s_{max2}) = 222\text{mm}$, $N_{req} = 2$

$s = 19.00 < 222\text{mm} \rightarrow$ O.K

Calculate required ratio of reinforcement

$$\rho_{min.11} = \frac{0.25\sqrt{f'_c}}{f_y}\ , \qquad \rho_{min.12} = \frac{1.4}{f_y}$$

$\rho_{min.1} = \max(\rho_{min.11}, \rho_{min.12}) = 0.0048$

$$\rho_{min.2} = \frac{4}{3}\frac{M_u}{\phi\ f_y\ bd(d-a/2)} = 0.0459$$

$\rho_{min} = \min(\rho_{min1}, \rho_{min2}) = 0.0048$

$$\rho_{\varepsilon t} = 0.85\ \beta_1\left(\frac{f'_c}{f_y}\right)\left(\frac{\varepsilon_c}{\varepsilon_c + 0.004}\right) = 0.0396$$

$\rho_{max} = \rho_{et} = 0.0396$

Check ratio of tensile reinforcement

$$\rho = \frac{A_s}{b_w\ d} = 0.0157$$

$\rho_{min} < \rho < \rho_{max} \rightarrow$ O.K

Calculate moment capacity

$$a = \frac{A_s\ f_y}{0.85\ f'_c\ b_w} = 15.90\text{mm}$$

$ø = 0.900$
$M_n = A_s f_y (d - a/2) = 21.25kN·m$
$øM_n = 19.13kN·m$
Calculate ratio of moment capacity
$M_u / øM_n = 2.041 \rightarrow$ N.G

Check Shear Capacity (RC Section Only)

Calculate shear strength by concrete
$ø = 0.750$ $d = 144mm$
$øV_c = ø\ 0.17 \sqrt{f'_c}\ b_w d = 22.87kN$
$V_u > øV_c \rightarrow$ Shear reinforcement is required
Calculate required shear strength by shear reinforcement
$V_{s.req} = (V_u - øV_c) / ø = 56.23kN$
$V_{c1} = 0.33 \sqrt{f'_c}\ b_w d = 59.20kN$ Refer to [11.4.5.3]
$V_{c2} = 0.66 \sqrt{f'_c}\ b_w d = 118kN$
$V_{s.req} < V_{c2} \rightarrow$ O.K
$A_{v.min1/s} = 0.062 \sqrt{f'_c}\ \frac{b_w}{f_{yt}}$, $A_{v.min2/s} = 0.35 \frac{b_w}{f_{yt}}$
$A_{v.min} /s = \max [A_{v.min1} /s , A_{v.min2} /s] = 0.184mm^2/mm$
$A_{v.req0} /s = \frac{V_{s.req}}{f_{yt} \cdot d} = 0.929mm^2/mm$
$A_{v.req} /s = \max [A_{v.min} /s , A_{v.req0} /s] = 0.929mm^2/mm$
Calculate shear strength by stirrup
$N_{leg} = 2$ $A_{v1} = 78.54mm^2$ (P10)
$øV_s = ø \frac{A_v f_{yt} d}{s} = 23.77kN$
Calculate ratio of shear capacity
$øV_n = øV_c + øV_s = 46.64kN$
$V_u / øV_n = 1.395 \rightarrow$ N.G
Calculate spacing limits for reinforcement
$s_{max.0} = \min [d/2, 600mm] = 72.05mm$
$s_{req} = \frac{N_{leg} A_{v1}}{A_{v.req} /s} = 169mm$
$s_{max} = \min [s_{max.0} , s_{req}] = 72.05mm$
$s = 300mm > s_{max} = 72.05mm \rightarrow$ N.G

Check the Strengthening Limit Criteria

[ACI 440.2R-08 / 9.2 - Strengthening limits]
Bending Moment Strength without FRP
$ø = 0.900$
$M_{ns} = 21.25kN·m$
$øM_{ns} = 19.13kN·m$
Check the Strengthening Limit Criteria
$M_{u.new} = 1.1M_{DL} + 0.75M_{LL} = 0.000kN·m$
$M_{u.new} / øM_{ns} = 0.000 < 1.000 \rightarrow$ O.K

Calculate Moment of Inertia of Cracked Section Transformed to Concrete

Calculate Modulus of Rupture
$f_r = 0.63 \sqrt{f_{ck}} = 5.440MPa$
$n = E_s / E_c = 4.849$
Calculate Moment of Inertia of Cracked Section Transformed to Concrete
$d = 144mm$
$d' = 39.00mm$
$A_s = 339mm^2$
$A'_s = 226mm^2$
$\gamma = \frac{(n - 1) A'_s}{n A_s} = 0.529$
$B = b / n A_s = 0.0912$
$kd = 45.64mm$
$k = 0.317$
$I_g = b h^3 / 12 = 100,150,075mm^4$

$I_{cr} = \dfrac{b\,(kd)^3}{3} + nA_s\,(d-kd)^2 + (n-1)\,A'_s\,(kd-d')^2 = 20{,}743{,}035\text{mm}^4$

Search Neutral Axis

Calculate the Design Strain of the FRP System

$n_f = 1$

$t_f = 0.337\text{mm}$

$\varepsilon_{fd.cal} = 0.410\sqrt{f_{ck} / n\,E_f\,t_f} = 0.012923$

$\varepsilon_{fd.max} = 0.90\,\varepsilon_{fu} = 0.016065$

$\varepsilon_{fd} = 0.012923$

Calculate the Existing State of Strain

$d_f = 200\text{mm}$

$\varepsilon_{bi} = \dfrac{M_{DL}\,(d_f - kd)}{I_{cr}\,E_c} = 0.000000$

Estimate the Depth to the Neutral Axis

$c = 39.72\text{mm}$

Calculate the Effective Level of Strain in the FRP Reinforcement

$\varepsilon_{cu} = 0.003000$

$\varepsilon_{fe.cal} = \varepsilon_{cu}\dfrac{d_f - c}{c} - \varepsilon_{bi} = 0.012124$

$\varepsilon_{fe.max} = \varepsilon_{fd} = 0.012923$

$\varepsilon_{fe} = 0.012124$

Calculate the Concrete Strain

$\varepsilon_c = (\varepsilon_{fe} + \varepsilon_{bi})\left(\dfrac{c}{d_f - c}\right) = 0.003000$

Calculate the Stress Level in the Reinforcing Steel

$d = 144\text{mm}$

$\varepsilon_s = (\varepsilon_{fe} + \varepsilon_{bi})\left(\dfrac{d - c}{d_f - c}\right) = 0.007882$

$f_{s.cal} = E_s\,\varepsilon_s = 1{,}576\text{MPa}$

$f_{s.max} = f_y = 460\text{MPa}$

$f_s = 460\text{MPa}$

Calculate the Stress Level in the Reinforcing FRP

$f_{fe.cal} = E_f\,\varepsilon_{fe} = 2{,}789\text{MPa}$

$f_{fe.max} = f_{fu} = 2{,}975\text{MPa}$

$f_{fe} = 2{,}789\text{MPa}$

Calculate the Internal Force Resultants

$\varepsilon'_c = 1.7\,f_{ck} / E_c = 0.003174$

$\beta_1 = \dfrac{4\,\varepsilon'_c - \varepsilon_c}{6\,\varepsilon'_c - 2\,\varepsilon_c} = 0.743$

$\alpha_1 = \dfrac{3\,\varepsilon'_c\,\varepsilon_c - (\varepsilon_c)^2}{3\,\beta_1\,(\varepsilon'_c)^2} = 0.871$

Verify Force Equilibrium

$A_s = 339\text{mm}^2$

$A_f = 50.55\text{mm}^2$

$F_s = A_s\,f_s = 156\text{kN}$

$F_f = A_f\,f_{fe} = 141\text{kN}$

$F_{TENS.} = F_s + F_f = 297\text{kN}$

$F_{COMP.} = \alpha_1\,f_{ck}\,\beta_1\,b\,c = 297\text{kN}$

Calculate Flexural Strength

Calculate Flexural Strength Components

$M_{ns} = A_s\,f_s\,(d - \beta_1\,c / 2) = 20.19\text{kN·m}$

$M_{nf} = A_f\,f_{fe}\,(d_f - \beta_1\,c / 2) = 26.15\text{kN·m}$

Calculate Design Flexural Strength of Section

$\text{ø} = 0.900$

$\psi = 0.850$

$\text{ø}M_n = \text{ø}\,[\,M_{ns} + \psi_f\,M_{nf}\,] = 38.17\text{kN·m}$

$M_u / \text{ø}M_n = 1.022 > 1.000 \rightarrow$ N.G

Check Service Stress in the Reinforcing Steel and FRP

Calculate the Elastic Depth to the Cracked Neutral Axis

A_s = 339mm²
A_f = 50.55mm²
d = 144mm
d_f = 200mm
ρ_s = 0.015697
ρ_f = 0.001684
$k = \sqrt{(k_1)^2 + 2\,k_2} - k_1 = 0.345$
$k_1 = \rho_s \dfrac{E_s}{E_c} + \rho_f \dfrac{E_f}{E_c}$
$k_2 = \rho_s \dfrac{E_s}{E_c} + \rho_f \dfrac{E_f}{E_c} \dfrac{d_f}{d}$
kd = 49.77mm
Calculate the Stress Level in the Reinforcing Steel
ε_{bi} = 0.000000
$$f_{s.s} = \frac{[\,M_s + \varepsilon_{bi}\,A_f\,E_f\,(\,d_f - kd/3\,)\,]\,(\,d - kd\,)\,E_s}{A_s\,E_s\,(\,d - kd/3\,)\,(\,d - kd\,) + A_f\,E_f\,(\,d_f - kd/3\,)\,(\,d_f - kd\,)} = 0.000\text{MPa}$$
$f_{s.s.max} = 0.80\ f_y$ = 368MPa
$f_{s.s} / f_{s.s.max} = 0.000 < 1.000 \rightarrow$ O.K

Check Creep Rupture Limit at Service of FRP

Calculate the Stress Level in the Reinforcing FRP
$$f_{f.s} = f_{s.s}\left(\frac{E_f}{E_s}\right)\left(\frac{d_f - kd}{d - kd}\right) - \varepsilon_{bi}\,E_f = 0.000\text{MPa}$$
f_{fu} = 2,975MPa
$f_{f.s.max} = 0.550\ f_{fu}$ = 1,636MPa
$f_{f.s} / f_{f.s.max} = 0.000 < 1.000 \rightarrow$ O.K

Calculate Shear Strength by FRP

Shear Strength without FRP
ø = 0.750
V_c = 30.50kN
V_s = 56.23kN
$øV_{ns}$ = 46.64kN
$øV_{ns.MAX}$ = 112kN
Calculate the Effective Strain Level
n_f = 1
t_f = 0.337mm
d_{fv} = 144mm
$$L_e = \frac{23{,}300}{(n_f\,t_f\,E_f)^{0.58}} = 34.00\text{mm}$$
$k_1 = (\,f_{ck} / 27.00\,)^{2/3} = 2.011$
$$k_2 = \frac{d_{fv} - L_e}{d_{fv}} = 0.764$$
$$\kappa_{v.cal} = \frac{k_1\,k_2\,L_e}{11{,}900\ \varepsilon_{fu}} = 0.246$$
$\kappa_{v.max}$ = 0.750
κ_v = 0.246
$\varepsilon_{fe.cal} = \kappa_v\,\varepsilon_{fu}$ = 0.004389
$\varepsilon_{fe.max}$ = 0.004000
ε_{fe} = 0.004000
Calculate the Contribution of the FRP Reinforcement
ψ_f = 0.850
w_f = 500mm
s_f = 400mm
$A_{fv} = 2\ n\ t_f\ w_f$ = 337mm²
$f_{fe} = \varepsilon_{fe}\ E_f$ = 920MPa
$$V_f = \frac{A_{fv}\,f_{fe}\,d_{fv}}{s_f} = 112\text{kN}$$
Calculate Shear Strength Ratio
$øV_n = ø\,(\,V_c + V_s + \psi_f\,V_f\,)$ = 112kN
$V_u / øV_n = 0.582 < 1.000 \rightarrow$ O.K

Calculate Development Length

[ACI 440.2R-08 / 13.1.3 - Development length]

Calculate Development Length

POS.	Apply	Pieces	l_{df} (mm)	Description
(1)	Yes	1	93.98	Bottom of Beam
(2)	Yes	1	93.98	Side of Beam (Shear)

$l_{df} = 1.000 \sqrt{n E_f t_f / (f_{ck})^{1/2}}$

Case 6- FRP Strengthening Detailed Calculations-Midas Design Plus 2021

MEMBER NAME : Recycled Aggregate Concrete with Self Consolidating Concrete Sample (RCA-5D).

General Information

Design Code : ACI318M-14

Reference Code : ACI 440.2R-08

[Guide for Design and Construction of Externally Bonded FRP System for Strengthening Concrete Structures.]

Code Unit : N, mm

Material

Concrete

f_{ck} : 77.00MPa

E_c : 41,242MPa

Rebar

f_y : 460MPa

f_{ys} : 420MPa

E_s : 200,000MPa

FRP / Carbon (MasterBrace FIB 600/50 CFS)

f^*_{fu} : 3,500MPa

E^*_{fs} : 230,000MPa

t_f : 0.337mm

ε^*_{fu} : 0.021000

Fiber Type : Carbon

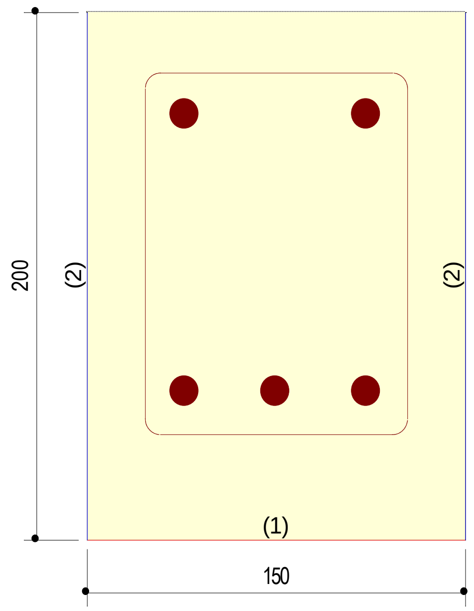

Section

Beam

Section Size : 150 x 200mm

Slab Thickness : 0.100mm

Effective Width : 500mm

Cover : 23.00 / 40.00mm

Compression : Considered

Splicing Limit : 50%

FRP / Carbon

POS.	Apply	Size(mm)	Pieces	Description
(1)	Yes	150	1	Bottom of Beam
(2)	Yes	200	1	Side of Beam (Shear)
(3)	No	120	1	Side of Beam (Bottom)
(4)	No	120	1	Side of Beam (Top)
(5)	No	100	1	Bottom of Slab
(6)	No	150	1	Top of Beam

FRP / Carbon (Shear / U-Wraps (3 Sides Bonded))

w_f : 500mm

s_f : 400mm

Rebar

Top Bar : 2-P12 (A_s = 226mm²)

Layer 1 : 2 EA (C_c = 39.00mm)

Bot Bar : 3-P12 (A_s = 339mm²)

Layer 1 : 3 EA (C_c = 56.00mm)

Stirrup : 2-P10@300 (A_s = 157mm²)

Design Force

Design Force

$M_{u.DL}$: 0.000kN·m

$M_{u.LL}$: 0.000kN·m

M_{ux} : 39.03kN·m

V_{uy} : 65.05kN

Design Data

Exposure Conditions : Exterior Exposure

Calculate the Design Material Properties

[ACI 440.2R-08 / 9.4 - Design material properties]

Calculate the Design Material Properties

$C_E = 0.850$

$f_{fu} = C_E\, f^*_{fu}$ = 2,975MPa

$\varepsilon_{fu} = C_E\, \varepsilon^*_{fu}$ = 0.017850

$E_f = f_{fu} / \varepsilon^*_{fu}$ = 230,000MPa

Check Bending Moment Capacity (RC Section Only)

Calculate design parameter

$\beta_1 = 0.650$

Check space of rebar

$s_{max1} = 380 \left(\dfrac{280}{f_s} \right) - 2.5c_c$, $\quad s_{max2} = 300 \left(\dfrac{280}{f_s} \right)$

$s_{max} = \min (s_{max1} , s_{max2})$ = 222mm, $N_{req} = 2$

s = 19.00 < 222mm → O.K

Calculate required ratio of reinforcement

$\rho_{min.11} = \dfrac{0.25\sqrt{f'_c}}{f_y}$, $\quad \rho_{min.12} = \dfrac{1.4}{f_y}$

$\rho_{min.1} = \max (\rho_{min.11} , \rho_{min.12}) = 0.0048$

$\rho_{min.2} = \dfrac{4}{3} \dfrac{M_u}{ø\, f_y\, bd(d\text{-}a/2)} = 0.0459$

$\rho_{min} = \min (\rho_{min1} , \rho_{min2}) = 0.0048$

$\rho_{\varepsilon t} = 0.85\, \beta_1 \left(\dfrac{f'_c}{f_y} \right) \left(\dfrac{\varepsilon_c}{\varepsilon_c + 0.004} \right) = 0.0396$

$\rho_{max} = \rho_{et} = 0.0468$

Check ratio of tensile reinforcement

$\rho = \dfrac{A_s}{b_w\, d} = 0.0157$

$\rho_{min} < \rho < \rho_{max}$ → O.K

Calculate moment capacity

$a = \dfrac{A_s\, f_y}{0.85\, f'_c\, b_w}$ = 19.76mm

ø = 0.900

$M_n = A_s f_y (d - a/2) = 22.07kN·m$
$øM_n = 19.86kN·m$
Calculate ratio of moment capacity
$M_u / øM_n = 1.965 \rightarrow$ N.G

Check Shear Capacity (RC Section Only)

Calculate shear strength by concrete
$ø = 0.750$ $d = 144mm$
$øV_c = ø\, 0.17 \sqrt{f'_c}\ b_w d = 22.87kN$
$V_u > øV_c \rightarrow$ Shear reinforcement is required
Calculate required shear strength by shear reinforcement
$V_{s.req} = (V_u - øV_c) / ø = 56.23kN$
$V_{c1} = 0.33 \sqrt{f'_c}\ b_w d = 59.20kN$ Refer to [11.4.5.3]
$V_{c2} = 0.66 \sqrt{f'_c}\ b_w d = 118kN$
$V_{s.req} < V_{c2} \rightarrow$ O.K
$A_{v.min1/s} = 0.062 \sqrt{f'_c} \dfrac{b_w}{f_{yt}}$, $A_{v.min2/s} = 0.35 \dfrac{b_w}{f_{yt}}$
$A_{v.min} /s = \max [A_{v.min1} /s , A_{v.min2} /s] = 0.184mm^2/mm$
$A_{v.req0} /s = \dfrac{V_{s.req}}{f_{yt} \cdot d} = 0.929mm^2/mm$
$A_{v.req} /s = \max [A_{v.min} /s , A_{v.req0} /s] = 0.929mm^2/mm$
Calculate shear strength by stirrup
$N_{leg} = 2$ $A_{v1} = 78.54mm^2$ (P10)
$øV_s = ø \dfrac{A_v f_{yt} d}{s} = 23.77kN$
Calculate ratio of shear capacity
$øV_n = øV_c + øV_s = 46.64kN$
$V_u / øV_n = 1.395 \rightarrow$ N.G
Calculate spacing limits for reinforcement
$s_{max.0} = \min [d/2, 600mm] = 72.05mm$
$s_{req} = \dfrac{N_{leg} A_{v1}}{A_{v.req} /s} = 169mm$
$s_{max} = \min [s_{max.0} , s_{req}] = 72.05mm$
$s = 300mm > s_{max} = 72.05mm \rightarrow$ N.G

Check the Strengthening Limit Criteria

[ACI 440.2R-08 / 9.2 - Strengthening limits]
Bending Moment Strength without FRP
$ø = 0.900$
$M_{ns} = 22.07kN·m$
$øM_{ns} = 19.86kN·m$
Check the Strengthening Limit Criteria
$M_{u.new} = 1.1M_{DL} + 0.75M_{LL} = 0.000kN·m$
$M_{u.new} / øM_{ns} = 0.000 < 1.000 \rightarrow$ O.K

Calculate Moment of Inertia of Cracked Section Transformed to Concrete

Calculate Modulus of Rupture
$f_r = 0.63 \sqrt{f_{ck}} = 5.440MPa$
$n = E_s / E_c = 4.849$
Calculate Moment of Inertia of Cracked Section Transformed to Concrete
$d = 144mm$
$d' = 39.00mm$
$A_s = 339mm^2$
$A'_s = 226mm^2$
$\gamma = \dfrac{(n - 1) A'_s}{n A_s} = 0.529$
$B = b / n A_s = 0.0912$
$kd = 45.64mm$
$k = 0.317$
$I_g = b h^3 / 12 = 100,150,075mm^4$
$I_{cr} = \dfrac{b (kd)^3}{3} + nA_s (d-kd)^2 + (n-1) A'_s (kd-d')^2 = 20,743,035mm^4$

Search Neutral Axis

Calculate the Design Strain of the FRP System

$n_f = 1$

$t_f = 0.337\text{mm}$

$\varepsilon_{fd.cal} = 0.410 \sqrt{f_{ck} / n\, E_f\, t_f} = 0.012923$

$\varepsilon_{fd.max} = 0.90\, \varepsilon_{fu} = 0.016065$

$\varepsilon_{fd} = 0.012923$

Calculate the Existing State of Strain

$d_f = 200\text{mm}$

$$\varepsilon_{bi} = \frac{M_{DL}\, (\, d_f - kd\,)}{I_{cr}\, E_c} = 0.000000$$

Estimate the Depth to the Neutral Axis

$c = 39.72\text{mm}$

Calculate the Effective Level of Strain in the FRP Reinforcement

$\varepsilon_{cu} = 0.003000$

$$\varepsilon_{fe.cal} = \varepsilon_{cu} \frac{d_f - c}{c} - \varepsilon_{bi} = 0.012124$$

$\varepsilon_{fe.max} = \varepsilon_{fd} = 0.012923$

$\varepsilon_{fe} = 0.012124$

Calculate the Concrete Strain

$$\varepsilon_c = (\, \varepsilon_{fe} + \varepsilon_{bi}\,) \left(\frac{c}{d_f - c} \right) = 0.003000$$

Calculate the Stress Level in the Reinforcing Steel

$d = 144\text{mm}$

$$\varepsilon_s = (\, \varepsilon_{fe} + \varepsilon_{bi}\,) \left(\frac{d - c}{d_f - c} \right) = 0.007882$$

$f_{s.cal} = E_s\, \varepsilon_s = 1{,}576\text{MPa}$

$f_{s.max} = f_y = 460\text{MPa}$

$f_s = 460\text{MPa}$

Calculate the Stress Level in the Reinforcing FRP

$f_{fe.cal} = E_f\, \varepsilon_{fe} = 2{,}789\text{MPa}$

$f_{fe.max} = f_{fu} = 2{,}975\text{MPa}$

$f_{fe} = 2{,}789\text{MPa}$

Calculate the Internal Force Resultants

$\varepsilon'_c = 1.7\, f_{ck} / E_c = 0.003174$

$$\beta_1 = \frac{4\, \varepsilon'_c - \varepsilon_c}{6\, \varepsilon'_c - 2\, \varepsilon_c} = 0.743$$

$$\alpha_1 = \frac{3\, \varepsilon'_c\, \varepsilon_c - (\, \varepsilon_c)^2}{3\, \beta_1\, (\, \varepsilon'_c)^2} = 0.871$$

Verify Force Equilibrium

$A_s = 339\text{mm}^2$

$A_f = 50.55\text{mm}^2$

$F_s = A_s\, f_s = 156\text{kN}$

$F_f = A_f\, f_{fe} = 141\text{kN}$

$F_{TENS.} = F_s + F_f = 297\text{kN}$

$F_{COMP.} = \alpha_1\, f_{ck}\, \beta_1\, b\, c = 297\text{kN}$

Calculate Flexural Strength

Calculate Flexural Strength Components

$M_{ns} = A_s\, f_s\, (\, d - \beta_1\, c / 2\,) = 20.19\text{kN·m}$

$M_{nf} = A_f\, f_{fe}\, (\, d_f - \beta_1\, c / 2\,) = 26.15\text{kN·m}$

Calculate Design Flexural Strength of Section

$ø = 0.900$

$\psi = 0.850$

$øM_n = ø\, [\, M_{ns} + \psi_f\, M_{nf}\,] = 38.17\text{kN·m}$

$M_u / øM_n = 1.022 > 1.000 \rightarrow$ N.G

Check Service Stress in the Reinforcing Steel and FRP

Calculate the Elastic Depth to the Cracked Neutral Axis

$A_s = 339\text{mm}^2$

$A_f = 50.55\text{mm}^2$

$d = 144\text{mm}$

$d_f = 200\text{mm}$
$\rho_s = 0.015697$
$\rho_f = 0.001684$
$k = \sqrt{(k_1)^2 + 2k_2} - k_1 = 0.345$
$k_1 = \rho_s \dfrac{E_s}{E_c} + \rho_f \dfrac{E_f}{E_c}$
$k_2 = \rho_s \dfrac{E_s}{E_c} + \rho_f \dfrac{E_f}{E_c} \dfrac{d_f}{d}$
$kd = 49.77\text{mm}$
Calculate the Stress Level in the Reinforcing Steel
$\varepsilon_{bi} = 0.000000$
$f_{s.s} = \dfrac{[M_s + \varepsilon_{bi} A_f E_f (d_f - kd/3)](d - kd) E_s}{A_s E_s (d - kd/3)(d - kd) + A_f E_f (d_f - kd/3)(d_f - kd)} = 0.000\text{MPa}$
$f_{s.s.max} = 0.80\ f_y = 368\text{MPa}$
$f_{s.s} / f_{s.s.max} = 0.000 < 1.000 \rightarrow$ O.K

Check Creep Rupture Limit at Service of FRP
Calculate the Stress Level in the Reinforcing FRP
$f_{f.s} = f_{s.s} \left(\dfrac{E_f}{E_s}\right)\left(\dfrac{d_f - kd}{d - kd}\right) - \varepsilon_{bi} E_f = 0.000\text{MPa}$
$f_{fu} = 2{,}975\text{MPa}$
$f_{f.s.max} = 0.550\ f_{fu} = 1{,}636\text{MPa}$
$f_{f.s} / f_{f.s.max} = 0.000 < 1.000 \rightarrow$ O.K

Calculate Shear Strength by FRP
Shear Strength without FRP
$ø = 0.750$
$V_c = 30.50\text{kN}$
$V_s = 56.23\text{kN}$
$øV_{ns} = 46.64\text{kN}$
$øV_{ns.MAX} = 112\text{kN}$
Calculate the Effective Strain Level
$n_f = 1$
$t_f = 0.337\text{mm}$
$d_{fv} = 144\text{mm}$
$L_e = \dfrac{23{,}300}{(n_f\ t_f\ E_f)^{0.58}} = 34.00\text{mm}$
$k_1 = (f_{ck} / 27.00)^{2/3} = 2.011$
$k_2 = \dfrac{d_{fv} - L_e}{d_{fv}} = 0.764$
$\kappa_{v.cal} = \dfrac{k_1\ k_2\ L_e}{11{,}900\ \varepsilon_{fu}} = 0.246$
$\kappa_{v.max} = 0.750$
$\kappa_v = 0.246$
$\varepsilon_{fe.cal} = \kappa_v\ \varepsilon_{fu} = 0.004389$
$\varepsilon_{fe.max} = 0.004000$
$\varepsilon_{fe} = 0.004000$
Calculate the Contribution of the FRP Reinforcement
$\psi_f = 0.850$
$w_f = 500\text{mm}$
$s_f = 400\text{mm}$
$A_{fv} = 2\ n\ t_f\ w_f = 337\text{mm}^2$
$f_{fe} = \varepsilon_{fe}\ E_f = 920\text{MPa}$
$V_f = \dfrac{A_{fv}\ f_{fe}\ d_{fv}}{s_f} = 112\text{kN}$
Calculate Shear Strength Ratio
$øV_n = ø(V_c + V_s + \psi_f V_f) = 112\text{kN}$
$V_u / øV_n = 0.582 < 1.000 \rightarrow$ O.K

Calculate Development Length
[ACI 440.2R-08 / 13.1.3 - Development length]
Calculate Development Length

POS.	Apply	Pieces	l_{df} (mm)	Description
(1)	Yes	1	93.98	Bottom of Beam
(2)	Yes	1	93.98	Side of Beam (Shear)

$l_{df} = 1.000 \sqrt{n E_f t_f / (f_{ck})^{1/2}}$

Case 7- FRP Strengthening Detailed Calculations-Midas Design Plus 2021

MEMBER NAME : Model No.2- Normal Weight Aggregate Sample (NWA-2).

General Information

Design Code : ACI318M-14

Reference Code : ACI 440.2R-08

[Guide for Design and Construction of Externally Bonded FRP System for Strengthening Concrete Structures.]

Code Unit : N, mm

Material

Concrete

f_{ck} : 70.50MPa

E_c : 39,463MPa

Rebar

f_y : 460MPa

f_{ys} : 420MPa

E_s : 200,000MPa

FRP / Carbon (MasterBrace FIB 600/50 CFS)

f^*_{fu} : 3,500MPa

E^*_{fs} : 230,000MPa

t_f : 0.337mm

ε^*_{fu} : 0.021000

Fiber Type : Carbon

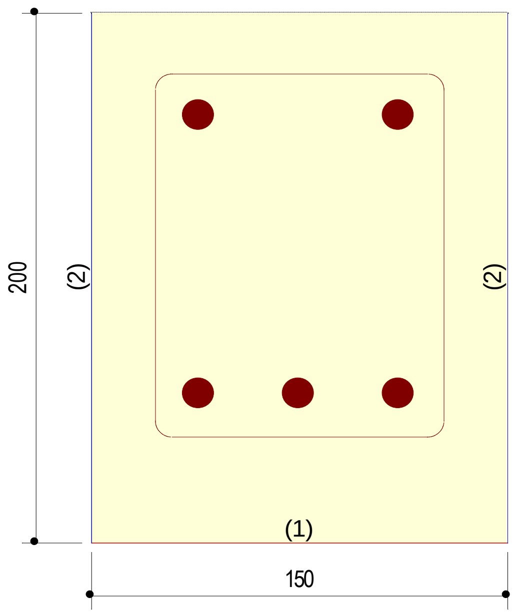

Section

Beam

Section Size : 150 x 200mm

Slab Thickness : 0.100mm

Effective Width : 500mm

Cover : 23.00 / 40.00mm

Compression : Not Considered

Splicing Limit : 50%

FRP / Carbon

POS.	Apply	Size(mm)	Pieces	Description
(1)	Yes	150	1	Bottom of Beam
(2)	Yes	200	1	Side of Beam (Shear)
(3)	No	120	1	Side of Beam (Bottom)
(4)	No	120	1	Side of Beam (Top)
(5)	No	100	1	Bottom of Slab
(6)	No	150	1	Top of Beam

FRP / Carbon (Shear / U-Wraps (3 Sides Bonded))
w_f : 500mm
s_f : 400mm

Rebar

Top Bar : 2-P12 (A_s = 226mm²)
Layer 1 : 2 EA (C_c = 39.00mm)
Bot Bar : 3-P12 (A_s = 339mm²)
Layer 1 : 3 EA (C_c = 56.00mm)
Stirrup : 2-P10@300 (A_s = 157mm²)

Design Force

Design Force
$M_{u.DL}$: 0.000kN·m
$M_{u.LL}$: 0.000kN·m
M_{ux} : 37.88kN·m
V_{uy} : 63.14kN

Design Data

Exposure Conditions : Exterior Exposure

Calculate the Design Material Properties

[ACI 440.2R-08 / 9.4 - Design material properties]
Calculate the Design Material Properties
$C_E = 0.850$
$f_{fu} = C_E\, f^*_{fu} = 2{,}975\text{MPa}$
$\varepsilon_{fu} = C_E\, \varepsilon^*_{fu} = 0.017850$
$E_f = f_{fu} / \varepsilon^*_{fu} = 230{,}000\text{MPa}$

Check Bending Moment Capacity (RC Section Only)

Calculate design parameter
$\beta_1 = 0.650$
Check space of rebar

$$s_{max1} = 380\left(\frac{280}{f_s}\right) - 2.5c_c\ , \qquad s_{max2} = 300\left(\frac{280}{f_s}\right)$$

$s_{max} = \min(s_{max1}, s_{max2}) = 222\text{mm}$, $N_{req} = 2$
$s = 19.00 < 222\text{mm} \rightarrow$ O.K
Calculate required ratio of reinforcement

$$\rho_{min.11} = \frac{0.25\sqrt{f'_c}}{f_y}\ , \qquad \rho_{min.12} = \frac{1.4}{f_y}$$

$\rho_{min.1} = \max(\rho_{min.11}, \rho_{min.12}) = 0.0046$

$$\rho_{min.2} = \frac{4}{3}\frac{M_u}{\o\, f_y\, bd\left(d - a/2\right)} = 0.0450$$

$\rho_{min} = \min(\rho_{min1}, \rho_{min2}) = 0.0046$

$$\rho_{\varepsilon t} = 0.85\,\beta_1\left(\frac{f'_c}{f_y}\right)\left(\frac{\varepsilon_c}{\varepsilon_c + 0.004}\right) = 0.0363$$

$\rho_{max} = \rho_{et} = 0.0363$
Check ratio of tensile reinforcement

$$\rho = \frac{A_s}{b_w\, d} = 0.0157$$

$\rho_{min} < \rho < \rho_{max} \rightarrow$ O.K
Calculate moment capacity

$$a = \frac{A_s\, f_y}{0.85\, f'_c\, b_w} = 17.36\text{mm}$$

$\o = 0.900$

$M_n = A_s f_y (d - a/2) = 21.14kN·m$
$øM_n = 19.02kN·m$
Calculate ratio of moment capacity
$M_u / øM_n = 1.991 \rightarrow N.G$

Check Shear Capacity (RC Section Only)
Calculate shear strength by concrete
$ø = 0.750 \quad d = 144mm$
$øV_c = ø\ 0.17 \sqrt{f'_c}\ b_w\ d = 22.87kN$
$V_u > øV_c \rightarrow$ Shear reinforcement is required
Calculate required shear strength by shear reinforcement
$V_{s.req} = (V_u - øV_c) / ø = 53.69kN$
$V_{c1} = 0.33 \sqrt{f'_c}\ b_w\ d = 59.20kN$ Refer to [11.4.5.3]
$V_{c2} = 0.66 \sqrt{f'_c}\ b_w\ d = 118kN$
$V_{s.req} < V_{c2} \rightarrow O.K$
$A_{v.min1/s} = 0.062 \sqrt{f'_c}\ \frac{b_w}{f_{yt}}, \quad A_{v.min2/s} = 0.35\ \frac{b_w}{f_{yt}}$
$A_{v.min} /s = \max [A_{v.min1} /s , A_{v.min2} /s] = 0.184mm^2/mm$
$A_{v.req0} /s = \frac{V_{s.req}}{f_{yt} \cdot d} = 0.887mm^2/mm$
$A_{v.req} /s = \max [A_{v.min} /s , A_{v.req0} /s] = 0.887mm^2/mm$
Calculate shear strength by stirrup
$N_{leg} = 2 \quad A_{v1} = 78.54mm^2$ (P10)
$øV_s = ø\ \frac{A_v\ f_{yt}\ d}{s} = 23.77kN$
Calculate ratio of shear capacity
$øV_n = øV_c + øV_s = 46.64kN$
$V_u / øV_n = 1.354 \rightarrow N.G$
Calculate spacing limits for reinforcement
$s_{max.0} = \min [d/2, 600mm] = 72.05mm$
$s_{req} = \frac{N_{leg}\ A_{v1}}{A_{v.req} /s} = 177mm$
$s_{max} = \min [s_{max.0} , s_{req}] = 72.05mm$
$s = 300mm > s_{max} = 72.05mm \rightarrow N.G$

Check the Strengthening Limit Criteria
[ACI 440.2R-08 / 9.2 - Strengthening limits]
Bending Moment Strength without FRP
$ø = 0.900$
$M_{ns} = 21.14kN·m$
$øM_{ns} = 19.02kN·m$
Check the Strengthening Limit Criteria
$M_{u.new} = 1.1M_{DL} + 0.75M_{LL} = 0.000kN·m$
$M_{u.new} / øM_{ns} = 0.000 < 1.000 \rightarrow O.K$

Calculate Moment of Inertia of Cracked Section Transformed to Concrete
Calculate Modulus of Rupture
$f_r = 0.63 \sqrt{f_{ck}} = 5.206MPa$
$n = E_s / E_c = 5.068$
Calculate Moment of Inertia of Cracked Section Transformed to Concrete
$d = 144mm$
$d' = 39.00mm$
$A_s = 339mm^2$
$A'_s = 226mm^2$
$\gamma = \frac{(n - 1)\ A'_s}{n\ A_s} = 0.535$
$B = b / n\ A_s = 0.0872$
$kd = 46.37mm$
$k = 0.322$
$I_g = b\ h^3 / 12 = 100,150,075mm^4$
$I_{cr} = \frac{b\ (kd)^3}{3} + nA_s\ (d-kd)^2 + (n-1)\ A'_s\ (kd-d')^2 = 21,459,190mm^4$

Search Neutral Axis

Calculate the Design Strain of the FRP System

$n_f = 1$

$t_f = 0.337\text{mm}$

$\varepsilon_{fd.cal} = 0.410 \sqrt{f_{ck} / n\, E_f\, t_f} = 0.012365$

$\varepsilon_{fd.max} = 0.90\, \varepsilon_{fu} = 0.016065$

$\varepsilon_{fd} = 0.012365$

Calculate the Existing State of Strain

$d_f = 200\text{mm}$

$$\varepsilon_{bi} = \frac{M_{DL}\,(d_f - kd)}{I_{cr}\, E_c} = 0.000000$$

Estimate the Depth to the Neutral Axis

$c = 41.39\text{mm}$

Calculate the Effective Level of Strain in the FRP Reinforcement

$\varepsilon_{cu} = 0.003000$

$$\varepsilon_{fe.cal} = \varepsilon_{cu} \frac{d_f - c}{c} - \varepsilon_{bi} = 0.011517$$

$\varepsilon_{fe.max} = \varepsilon_{fd} = 0.012365$

$\varepsilon_{fe} = 0.011517$

Calculate the Concrete Strain

$$\varepsilon_c = (\varepsilon_{fe} + \varepsilon_{bi}) \left(\frac{c}{d_f - c} \right) = 0.003000$$

Calculate the Stress Level in the Reinforcing Steel

$d = 144\text{mm}$

$$\varepsilon_s = (\varepsilon_{fe} + \varepsilon_{bi}) \left(\frac{d - c}{d_f - c} \right) = 0.007445$$

$f_{s.cal} = E_s\, \varepsilon_s = 1{,}489\text{MPa}$

$f_{s.max} = f_y = 460\text{MPa}$

$f_s = 460\text{MPa}$

Calculate the Stress Level in the Reinforcing FRP

$f_{fe.cal} = E_f\, \varepsilon_{fe} = 2{,}649\text{MPa}$

$f_{fe.max} = f_{fu} = 2{,}975\text{MPa}$

$f_{fe} = 2{,}649\text{MPa}$

Calculate the Internal Force Resultants

$\varepsilon'_c = 1.7\, f_{ck} / E_c = 0.003037$

$$\beta_1 = \frac{4\, \varepsilon'_c - \varepsilon_c}{6\, \varepsilon'_c - 2\, \varepsilon_c} = 0.748$$

$$\alpha_1 = \frac{3\, \varepsilon'_c\, \varepsilon_c - (\varepsilon_c)^2}{3\, \beta_1\, (\varepsilon'_c)^2} = 0.885$$

Verify Force Equilibrium

$A_s = 339\text{mm}^2$

$A_f = 50.55\text{mm}^2$

$F_s = A_s\, f_s = 156\text{kN}$

$F_f = A_f\, f_{fe} = 134\text{kN}$

$F_{TENS.} = F_s + F_f = 290\text{kN}$

$F_{COMP.} = \alpha_1\, f_{ck}\, \beta_1\, b\, c = 290\text{kN}$

Calculate Flexural Strength

Calculate Flexural Strength Components

$M_{ns} = A_s\, f_s\, (d - \beta_1\, c / 2) = 20.07\text{kN·m}$

$M_{nf} = A_f\, f_{fe}\, (d_f - \beta_1\, c / 2) = 24.74\text{kN·m}$

Calculate Design Flexural Strength of Section

$ø = 0.900$

$\psi = 0.850$

$øM_n = ø\, [\, M_{ns} + \psi_f\, M_{nf}\,] = 36.99\text{kN·m}$

$M_u / øM_n = 1.024 > 1.000 \rightarrow$ N.G

Check Service Stress in the Reinforcing Steel and FRP

Calculate the Elastic Depth to the Cracked Neutral Axis

$A_s = 339\text{mm}^2$

$A_f = 50.55\text{mm}^2$

$d = 144\text{mm}$

d_f = 200mm
ρ_s = 0.015697
ρ_f = 0.001684
$k = \sqrt{(k_1)^2 + 2\,k_2} - k_1 = 0.352$
$k_1 = \rho_s \dfrac{E_s}{E_c} + \rho_f \dfrac{E_f}{E_c}$
$k_2 = \rho_s \dfrac{E_s}{E_c} + \rho_f \dfrac{E_f}{E_c} \dfrac{d_f}{d}$
kd = 50.65mm
Calculate the Stress Level in the Reinforcing Steel
ε_{bi} = 0.000000
$$f_{s.s} = \frac{[\,M_s + \varepsilon_{bi}\,A_f\,E_f\,(\,d_f - kd/3\,)\,]\,(\,d - kd\,)\,E_s}{A_s\,E_s\,(\,d - kd/3\,)\,(\,d - kd\,) + A_f\,E_f\,(\,d_f - kd/3\,)\,(\,d_f - kd\,)} = 0.000\text{MPa}$$
$f_{s.s.max} = 0.80\ f_y$ = 368MPa
$f_{s.s} / f_{s.s.max} = 0.000 < 1.000 \rightarrow$ O.K

Check Creep Rupture Limit at Service of FRP
Calculate the Stress Level in the Reinforcing FRP
$$f_{f.s} = f_{s.s} \left(\frac{E_f}{E_s} \right) \left(\frac{d_f - kd}{d - kd} \right) - \varepsilon_{bi}\,E_f = 0.000\text{MPa}$$
f_{fu} = 2,975MPa
$f_{f.s.max} = 0.550\ f_{fu}$ = 1,636MPa
$f_{f.s} / f_{f.s.max} = 0.000 < 1.000 \rightarrow$ O.K

Calculate Shear Strength by FRP
Shear Strength without FRP
ø = 0.750
V_c = 30.50kN
V_s = 53.69kN
$øV_{ns}$ = 46.64kN
$øV_{ns.MAX}$ = 112kN
Calculate the Effective Strain Level
n_f = 1
t_f = 0.337mm
d_{fv} = 144mm
$$L_e = \frac{23{,}300}{(\,n_f\,t_f\,E_f)^{0.58}} = 34.00\text{mm}$$
$k_1 = (\,f_{ck} / 27.00\,)^{2/3} = 1.896$
$$k_2 = \frac{d_{fv} - L_e}{d_{fv}} = 0.764$$
$$\kappa_{v.cal} = \frac{k_1\,k_2\,L_e}{11{,}900\,\varepsilon_{fu}} = 0.232$$
$\kappa_{v.max}$ = 0.750
κ_v = 0.232
$\varepsilon_{fe.cal} = \kappa_v\,\varepsilon_{fu} = 0.004139$
$\varepsilon_{fe.max}$ = 0.004000
ε_{fe} = 0.004000
Calculate the Contribution of the FRP Reinforcement
ψ_f = 0.850
w_f = 500mm
s_f = 400mm
$A_{fv} = 2\ n\ t_f\ w_f$ = 337mm²
$f_{fe} = \varepsilon_{fe}\ E_f$ = 920MPa
$$V_f = \frac{A_{fv}\,f_{fe}\,d_{fv}}{s_f} = 112\text{kN}$$
Calculate Shear Strength Ratio
$øV_n = ø\,(\,V_c + V_s + \psi_f\,V_f\,)$ = 112kN
$V_u / øV_n = 0.565 < 1.000 \rightarrow$ O.K

Calculate Development Length
[ACI 440.2R-08 / 13.1.3 - Development length]
Calculate Development Length

POS.	Apply	Pieces	l_{df} (mm)	Description
(1)	Yes	1	96.08	Bottom of Beam
(2)	Yes	1	96.08	Side of Beam (Shear)

$l_{df} = 1.000 \sqrt{n E_f t_f / (f_{ck})^{1/2}}$

Case 8- FRP Strengthening Detailed Calculations-Midas Design Plus 2021

MEMBER NAME : Model No.2- Normal Weight Aggregate Sample (NWA-2).

General Information

Design Code : ACI318M-14
Reference Code : ACI 440.2R-08
[Guide for Design and Construction of Externally Bonded FRP System for Strengthening Concrete Structures.]
Code Unit : N, mm

Material

Concrete
f_{ck} : 70.50MPa
E_c : 39,463MPa
Rebar
f_y : 460MPa
f_{ys} : 420MPa
E_s : 200,000MPa
FRP / Carbon (MasterBrace FIB 600/50 CFS)
f^*_{fu} : 3,500MPa
E^*_{fs} : 230,000MPa
t_f : 0.337mm
ε^*_{fu} : 0.021000
Fiber Type : Carbon

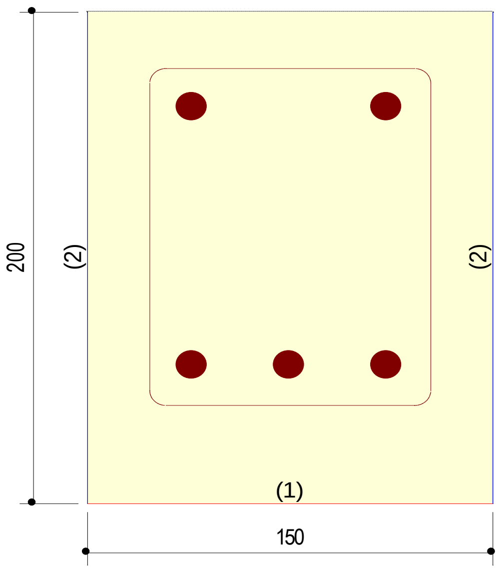

Section

Beam
Section Size : 150 x 200mm
Slab Thickness : 0.100mm
Effective Width : 500mm
Cover : 23.00 / 40.00mm
Compression : Considered
Splicing Limit : 50%
FRP / Carbon

POS.	Apply	Size(mm)	Pieces	Description

(1)	Yes	150	1	Bottom of Beam
(2)	Yes	200	1	Side of Beam (Shear)
(3)	No	120	1	Side of Beam (Bottom)
(4)	No	120	1	Side of Beam (Top)
(5)	No	100	1	Bottom of Slab
(6)	No	150	1	Top of Beam

FRP / Carbon (Shear / U-Wraps (3 Sides Bonded))

w_f : 500mm

s_f : 400mm

Rebar

Top Bar : 2-P12 (A_s = 226mm²)

Layer 1 : 2 EA (C_c = 39.00mm)

Bot Bar : 3-P12 (A_s = 339mm²)

Layer 1 : 3 EA (C_c = 56.00mm)

Stirrup : 2-P10@300 (A_s = 157mm²)

Design Force

Design Force

$M_{u.DL}$: 0.000kN·m

$M_{u.LL}$: 0.000kN·m

M_{ux} : 37.88kN·m

V_{uy} : 63.14kN

Design Data

Exposure Conditions : Exterior Exposure

Calculate the Design Material Properties

[ACI 440.2R-08 / 9.4 - Design material properties]

Calculate the Design Material Properties

$C_E = 0.850$

$f_{fu} = C_E\, f^*_{fu} = 2{,}975\text{MPa}$

$\varepsilon_{fu} = C_E\, \varepsilon^*_{fu} = 0.017850$

$E_f = f_{fu} / \varepsilon^*_{fu} = 230{,}000\text{MPa}$

Check Bending Moment Capacity (RC Section Only)

Calculate design parameter

$\beta_1 = 0.650$

Check space of rebar

$s_{max1} = 380\left(\frac{280}{f_s}\right) - 2.5c_c$, $\quad s_{max2} = 300\left(\frac{280}{f_s}\right)$

$s_{max} = \min(s_{max1}, s_{max2}) = 222\text{mm}$, $N_{req} = 2$

$s = 19.00 < 222\text{mm} \rightarrow$ O.K

Calculate required ratio of reinforcement

$\rho_{min.11} = \frac{0.25\sqrt{f'_c}}{f_y}$, $\quad \rho_{min.12} = \frac{1.4}{f_y}$

$\rho_{min.1} = \max(\rho_{min.11}, \rho_{min.12}) = 0.0046$

$\rho_{min.2} = \frac{4}{3}\frac{M_u}{ø\, f_y\, bd(d\text{-}a/2)} = 0.0450$

$\rho_{min} = \min(\rho_{min1}, \rho_{min2}) = 0.0046$

$\rho_{\varepsilon t} = 0.85\,\beta_1\left(\frac{f'_c}{f_y}\right)\left(\frac{\varepsilon_c}{\varepsilon_c + 0.004}\right) = 0.0363$

$\rho_{max} = \rho_{et} = 0.0434$

Check ratio of tensile reinforcement

$\rho = \frac{A_s}{b_w\, d} = 0.0157$

$\rho_{min} < \rho < \rho_{max} \rightarrow$ O.K

Calculate moment capacity

$a = \frac{A_s\, f_y}{0.85\, f'_c\, b_w} = 20.67\text{mm}$

$ø = 0.900$

$M_n = A_s\, f_y\,(d - a/2) = 21.76\text{kN·m}$

$øM_n$ = 19.58kN·m
Calculate ratio of moment capacity
$M_u / øM_n$ = 1.934 → N.G

Check Shear Capacity (RC Section Only)

Calculate shear strength by concrete
ø = 0.750 d = 144mm
$øV_c = ø\ 0.17 \sqrt{f'_c}\ b_w\ d$ = 22.87kN
$V_u > øV_c$ → Shear reinforcement is required
Calculate required shear strength by shear reinforcement
$V_{s.req} = (V_u - øV_c) / ø$ = 53.69kN
$V_{c1} = 0.33 \sqrt{f'_c}\ b_w\ d$ = 59.20kN Refer to [11.4.5.3]
$V_{c2} = 0.66 \sqrt{f'_c}\ b_w\ d$ = 118kN
$V_{s.req} < V_{c2}$ → O.K
$A_{v.min1/s} = 0.062 \sqrt{f'_c}\ \frac{b_w}{f_{yt}}$, $A_{v.min2/s} = 0.35\ \frac{b_w}{f_{yt}}$
$A_{v.min} /s = \max [A_{v.min1} /s , A_{v.min2} /s]$ = 0.184mm²/mm
$A_{v.req0} /s = \frac{V_{s.req}}{f_{yt} \cdot d}$ = 0.887mm²/mm
$A_{v.req} /s = \max [A_{v.min} /s , A_{v.req0} /s]$ = 0.887mm²/mm
Calculate shear strength by stirrup
N_{leg} = 2 A_{v1} = 78.54mm² (P10)
$øV_s = ø\ \frac{A_v\ f_{yt}\ d}{s}$ = 23.77kN
Calculate ratio of shear capacity
$øV_n = øV_c + øV_s$ = 46.64kN
$V_u / øV_n$ = 1.354 → N.G
Calculate spacing limits for reinforcement
$s_{max.0}$ = min [d/2, 600mm] = 72.05mm
$s_{req} = \frac{N_{leg}\ A_{v1}}{A_{v.req} /s}$ = 177mm
$s_{max} = \min [s_{max.0} , s_{req}]$ = 72.05mm
s = 300mm > s_{max} = 72.05mm → N.G

Check the Strengthening Limit Criteria

[ACI 440.2R-08 / 9.2 - Strengthening limits]
Bending Moment Strength without FRP
ø = 0.900
M_{ns} = 21.76kN·m
$øM_{ns}$ = 19.58kN·m
Check the Strengthening Limit Criteria
$M_{u.new} = 1.1M_{DL} + 0.75M_{LL}$ = 0.000kN·m
$M_{u.new} / øM_{ns}$ = 0.000 < 1.000 → O.K

Calculate Moment of Inertia of Cracked Section Transformed to Concrete

Calculate Modulus of Rupture
$f_r = 0.63 \sqrt{f_{ck}}$ = 5.206MPa
$n = E_s / E_c$ = 5.068
Calculate Moment of Inertia of Cracked Section Transformed to Concrete
d = 144mm
d' = 39.00mm
A_s = 339mm²
A'_s = 226mm²
$\gamma = \frac{(n - 1)\ A'_s}{n\ A_s}$ = 0.535
$B = b / n\ A_s$ = 0.0872
kd = 46.37mm
k = 0.322
$I_g = b\ h^3 / 12$ = 100,150,075mm⁴
$I_{cr} = \frac{b\ (kd)^3}{3} + nA_s\ (d-kd)^2 + (n-1)\ A'_s\ (kd-d')^2$ = 21,459,190mm⁴

Search Neutral Axis

Calculate the Design Strain of the FRP System

$n_f = 1$

$t_f = 0.337\text{mm}$

$\varepsilon_{fd.cal} = 0.410 \sqrt{f_{ck} / n\, E_f\, t_f} = 0.012365$

$\varepsilon_{fd.max} = 0.90\ \varepsilon_{fu} = 0.016065$

$\varepsilon_{fd} = 0.012365$

Calculate the Existing State of Strain

$d_f = 200\text{mm}$

$$\varepsilon_{bi} = \frac{M_{DL}\,(\, d_f - kd\,)}{I_{cr}\, E_c} = 0.000000$$

Estimate the Depth to the Neutral Axis

$c = 41.39\text{mm}$

Calculate the Effective Level of Strain in the FRP Reinforcement

$\varepsilon_{cu} = 0.003000$

$$\varepsilon_{fe.cal} = \varepsilon_{cu} \frac{d_f - c}{c} - \varepsilon_{bi} = 0.011517$$

$\varepsilon_{fe.max} = \varepsilon_{fd} = 0.012365$

$\varepsilon_{fe} = 0.011517$

Calculate the Concrete Strain

$$\varepsilon_c = (\, \varepsilon_{fe} + \varepsilon_{bi}\,) \left(\frac{c}{d_f - c} \right) = 0.003000$$

Calculate the Stress Level in the Reinforcing Steel

$d = 144\text{mm}$

$$\varepsilon_s = (\, \varepsilon_{fe} + \varepsilon_{bi}\,) \left(\frac{d - c}{d_f - c} \right) = 0.007445$$

$f_{s.cal} = E_s\, \varepsilon_s = 1{,}489\text{MPa}$

$f_{s.max} = f_y = 460\text{MPa}$

$f_s = 460\text{MPa}$

Calculate the Stress Level in the Reinforcing FRP

$f_{fe.cal} = E_f\, \varepsilon_{fe} = 2{,}649\text{MPa}$

$f_{fe.max} = f_{fu} = 2{,}975\text{MPa}$

$f_{fe} = 2{,}649\text{MPa}$

Calculate the Internal Force Resultants

$\varepsilon'_c = 1.7\ f_{ck} / E_c = 0.003037$

$$\beta_1 = \frac{4\ \varepsilon'_c - \varepsilon_c}{6\ \varepsilon'_c - 2\ \varepsilon_c} = 0.748$$

$$\alpha_1 = \frac{3\ \varepsilon'_c\ \varepsilon_c - (\,\varepsilon_c)^2}{3\ \beta_1\ (\,\varepsilon'_c)^2} = 0.885$$

Verify Force Equilibrium

$A_s = 339\text{mm}^2$

$A_f = 50.55\text{mm}^2$

$F_s = A_s\, f_s = 156\text{kN}$

$F_f = A_f\, f_{fe} = 134\text{kN}$

$F_{TENS.} = F_s + F_f = 290\text{kN}$

$F_{COMP.} = \alpha_1\, f_{ck}\, \beta_1\, b\, c = 290\text{kN}$

Calculate Flexural Strength

Calculate Flexural Strength Components

$M_{ns} = A_s\, f_s\, (\, d - \beta_1\, c / 2\,) = 20.07\text{kN·m}$

$M_{nf} = A_f\, f_{fe}\, (\, d_f - \beta_1\, c / 2\,) = 24.74\text{kN·m}$

Calculate Design Flexural Strength of Section

$ø = 0.900$

$\psi = 0.850$

$øM_n = ø\,[\, M_{ns} + \psi_f\, M_{nf}\,] = 36.99\text{kN·m}$

$M_u / øM_n = 1.024 > 1.000 \rightarrow$ N.G

Check Service Stress in the Reinforcing Steel and FRP

Calculate the Elastic Depth to the Cracked Neutral Axis

$A_s = 339\text{mm}^2$

$A_f = 50.55\text{mm}^2$

$d = 144\text{mm}$

$d_f = 200\text{mm}$

ρ_s = 0.015697
ρ_f = 0.001684
$k = \sqrt{(k_1)^2 + 2\,k_2} - k_1 = 0.352$
$k_1 = \rho_s \dfrac{E_s}{E_c} + \rho_f \dfrac{E_f}{E_c}$
$k_2 = \rho_s \dfrac{E_s}{E_c} + \rho_f \dfrac{E_f}{E_c} \dfrac{d_f}{d}$
kd = 50.65mm
Calculate the Stress Level in the Reinforcing Steel
ε_{bi} = 0.000000
$f_{s.s} = \dfrac{[\,M_s + \varepsilon_{bi}\,A_f\,E_f\,(d_f - kd/3)\,]\,(d - kd)\,E_s}{A_s\,E_s\,(d - kd/3)\,(d - kd) + A_f\,E_f\,(d_f - kd/3)\,(d_f - kd)}$ = 0.000MPa
$f_{s.s.max} = 0.80\ f_y$ = 368MPa
$f_{s.s} / f_{s.s.max} = 0.000 < 1.000 \rightarrow$ O.K

Check Creep Rupture Limit at Service of FRP
Calculate the Stress Level in the Reinforcing FRP
$f_{f.s} = f_{s.s} \left(\dfrac{E_f}{E_s}\right) \left(\dfrac{d_f - kd}{d - kd}\right) - \varepsilon_{bi}\,E_f$ = 0.000MPa
f_{fu} = 2,975MPa
$f_{f.s.max} = 0.550\ f_{fu}$ = 1,636MPa
$f_{f.s} / f_{f.s.max} = 0.000 < 1.000 \rightarrow$ O.K

Calculate Shear Strength by FRP
Shear Strength without FRP
ø = 0.750
V_c = 30.50kN
V_s = 53.69kN
$øV_{ns}$ = 46.64kN
$øV_{ns.MAX}$ = 112kN
Calculate the Effective Strain Level
n_f = 1
t_f = 0.337mm
d_{fv} = 144mm
$L_e = \dfrac{23{,}300}{(n_f\,t_f\,E_f)^{0.58}}$ = 34.00mm
$k_1 = (f_{ck} / 27.00)^{2/3}$ = 1.896
$k_2 = \dfrac{d_{fv} - L_e}{d_{fv}}$ = 0.764
$\kappa_{v.cal} = \dfrac{k_1\,k_2\,L_e}{11{,}900\,\varepsilon_{fu}}$ = 0.232
$\kappa_{v.max}$ = 0.750
κ_v = 0.232
$\varepsilon_{fe.cal} = \kappa_v\,\varepsilon_{fu}$ = 0.004139
$\varepsilon_{fe.max}$ = 0.004000
ε_{fe} = 0.004000
Calculate the Contribution of the FRP Reinforcement
ψ_f = 0.850
w_f = 500mm
s_f = 400mm
$A_{fv} = 2\,n\,t_f\,w_f$ = 337mm²
$f_{fe} = \varepsilon_{fe}\,E_f$ = 920MPa
$V_f = \dfrac{A_{fv}\,f_{fe}\,d_{fv}}{s_f}$ = 112kN
Calculate Shear Strength Ratio
$øV_n = ø\,(V_c + V_s + \psi_f\,V_f)$ = 112kN
$V_u / øV_n = 0.565 < 1.000 \rightarrow$ O.K

Calculate Development Length
[ACI 440.2R-08 / 13.1.3 - Development length]
Calculate Development Length

POS.	Apply	Pieces	l_{df} (mm)	Description

(1)	Yes	1	96.08	Bottom of Beam
(2)	Yes	1	96.08	Side of Beam (Shear)

$l_{df} = 1.000 \sqrt{n\ E_f\ t_f / (\ f_{ck})^{1/2}}$